AFFDL-TR-68-159

AN INVESTIGATION OF AN INTEGRATED AIRCREW ESCAPE/RESCUE SYSTEM CAPABILITY

R. J. MANZUK

W. R. PECK

ET AL.

FOREWORD

This report was prepared by the Stencel Aero Engineering Corporation, Asheville, North Carolina, and covers the work performed under USAF Contract F33615-68-C-1461, The work reported on herein was accomplished during the time period of 18 March 1968 to 30 December 1968. The contract was initiated under Project No. 6065, "Performance and Design of Deployable Aerodynamic Decelerators", Task No. 606509, "Aerodynamic Deceleration and Recovery System Considerations", and administered by the Recovery and Crew Station Branch, Vehicle Equipment Division, Air Force Flight Dynamics Laboratory, Air Force Systems Command, Wright-Patterson Air Force Base, Ohio. Mr. Reinhold J. Gross, AFFDL (FDFR) Project Engineer, served as technical program manager.

The SAEC program was directed by Mr. Robert J. Manzuk, Staff Engineer. Principal contributors to the technical effort were Messrs. W. R. Peck, C. A. Yost, J. W. Duncan, R. T. Chapin, E. A. Braunlich, L. A. Pond, Jr., and Mrs. Nancy Bentzen.

Special acknowledgment is made by the authors of the significant contributions to the program afforded by Mr. Joe C. Somers, Senior Design Engineer (Preliminary Design), of Continental Aviation and Engineering Corporation.

Also, special acknowledgment is made by the authors to Prof. Edward Seckel, and Messrs. John W. Olcott and Guy G. Williamson, all of Aeronautical Research Associates of Princeton (ARAP), for their crucial contributions in Section IV of this report which contributed significantly to the completeness and overall effectiveness of the feasibility study.

This report was submitted by the authors in December, 1968.
The Contractor's report number is SAEC FTR-419-1.
This technical report has been reviewed and is approved.

GEORGE A. SOLT, JR.
Chief, Recovery and Crew Station Branch
Vehicle Equipment Division
Air Force Flight Dynamics Laboratory

ABSTRACT

A concept was investigated whereby aircrewmembers are given a capability to aid in their own rescue subsequent to emergency ejection from their mission vehicle. The self-rescue capability was achieved by way of integrating a parawing into the ejection-seat escape system to provide an aerodynamic-lift generating surface, and also a twin-turbofan jet engine to provide propulsion for gaining altitude and departing from the emergency site toward a safe area for liaison with allied forces. The escape/rescue system analyses concluded that in the conventional ejection/recovery mode of operation the AERCAB provides a survival capability surpassing that of currently in-service systems. In the self-rescue mode, AERCAB is capable of flight at 10,000 feet (MSL) over a distance of fifty nautical miles at airspeeds approaching 100 knots. The system is manually controllable in both powered and unpowered flight, and it appears feasible to incorporate an automatic homing flight control system. AERCAB is shown capable of adverse weather operation in powered flight provided suitable protective clothing is worn by the occupant. Under all emergency circumstances, the aircrewman using AERCAB retains the capability to descend to terrain level with his personnel parachute. A detailed preliminary design study was accomplished, and it is shown that the system is retrofitable in the existing crewstations of the A-7 and F-4 aircraft with only minor modifications thereto. The investigative program resulted in the generation of specific operational and design criteria for an integrated aircrew escape/rescue system capability; operational and performance limits thereof were defined; and it was analytically shown that the AERCAB concept is feasible, and merits continued study, experimental testing, and development. A full-scale system mockup was prepared during the program, and delivered to the Air Force Flight Dynamics Laboratory integrated in a simulation of the A-7 crewstation.

TABLE OF CONTENTS

LIST OF ILLUSTRATIONS

LIST OF ILLUSTRATIONS (cont.)

LIST OF ILLUSTRATIONS (cont.)

LIST OF ILLUSTRATIONS (cont.)

LIST OF TABLES

NOMENCLATURE

SYMBOL	DEFINITION, UNITS
A	reference area, sq. ft.
A_w	planform area, sq. ft.
b	wing span, ft.
BW	wing structural member weights, lb.
C_D	drag coefficient, D/qS
C_L	lift coefficient, L/qS
C	rolling moment coefficient, $L/qS\ell_k$
C_M	pitching moment coefficient, $M/qS\ell_k$
C_N	yawing moment coefficient, $N/qS\ell_k$
C_t	thrust coefficient, T/qS
C_Y	side force coefficient, Y/qS
C_{D_α}	$\delta C_D/\delta\alpha$, per radian
C_{L_α}	$\delta C_L/\delta\alpha$, per radian
C_{ℓ_β}	effective dihedral parameter, $\delta C_\ell/\delta\beta$, per radian
C_{ℓ_p}	$\delta C_\ell/\delta\left(\frac{pb}{2V}\right)$
C_{ℓ_r}	$\delta C_\ell/\delta\left(\frac{rb}{2V}\right)$
C_{M_α}	static longitudinal stability coefficient, $\delta C_M/\delta\alpha$, per radian
$C_{M_{\dot\alpha}}$	$\delta C_M/\delta\left(\frac{\dot\alpha b}{2V}\right)$
$C_{M_{\dot\theta}}$	$\delta C_M/\delta\left(\frac{\dot\theta b}{2V}\right)$
C_{m_w}	parawing pitching moment coefficient, @ 30% keel point
C_{N_β}	static directional stability coefficient, $\delta C_N/\delta\beta$, per radian

SYMBOL	DEFINITION, UNITS
C_{N_p}	$\delta C_N / \delta\left(\frac{pb}{2V}\right)$
C_{N_r}	$\delta C_N / \delta\left(\frac{rb}{2V}\right)$
C_{Y_β}	$\delta C_Y / \delta \beta$, per radian
CDST	strut drag coefficient
CDSPL	man/seat/engine effective drag area, sq. ft.
D	drag, lb.
D_α	$\frac{1}{m} \frac{\delta D}{\delta \alpha}$, ft. sec.^{2}/rad.
D_V	$\frac{1}{m} \frac{\delta D}{\delta v}$, per second
D_x	damping moment in roll, ft. lb.
D_Y	damping moment in pitch, ft. lb.
D_Z	damping moment in yaw, ft. lb.
d_1^2	squared tube section, I. D.
d_2/d_1	ratio of I. D. to O. D.
DA	density of aluminum, 169 lb./cu.ft.
DF	wing "fabric" density, oz./sq. yd.
DI	density of steel, 487.5 lb./cu. ft.
DT	total drag of system, lbs. (corresponding to L/DT)
DEFL	maximum deflection of L. E.
EA	modulus of elasticity for aluminum, 10×10^6 psi
EM	modulus of elasticity for steel, 30×10^6 psi
EW	engine weight, lb.

SYMBOL	DEFINITIONS, UNITS
EWD	design engine weight, lb.
F_S	stick force, lb.
F_t	thrust, lb.
F_{t_i}	idle thrust of engine, lb.
F_{t_c}	cruise thrust of engine, lb.
FD	fuel density, lb./cu. ft.
FW	fuel weight, lb.
FC_i	amount of fuel consumed, lb.
FTU	ultimate tensile strength of steel, 125,000 psi
FTW	fuel tank weight, lb.
FTFW	fuel tank "fabric" density, lb./sq. yd.
G	stick gearing ratio
g	acceleration of gravity, 32.2 ft./sec.^{2}
h	(1) total height of seat normal to airstream, (2) constant of integration
I_x	moment of inertia about roll axis, slugs-sq.ft.
I_Y	moment of inertia about pitch axis, slugs-sq.ft.
I_Z	moment of inertia about yaw axis, slugs-sq.ft.
i_W	angle of incidence between wing keel and line of thrust, deg. or rad.
I_{xx}	moment of inertia about x stability axis, slug ft.^{2}

SYMBOL	DEFINITIONS, UNITS
I_{xz}	cross product of inertia with respect to stability axes, slug ft.^{2}
I_{yy}	moment of inertia about y stability axis, slug ft.^{2}
I_{zz}	moment of inertia about z stability axis, slug ft.^{2}
ID	tube inner diameter, inches
K_D	pitch-moment damping coefficient
Kd	damping factor
K_W	seat actuator rate, f.p.s.
$K_{\dot{\phi}_W}$	wing bank angle actuator rate, rad./sec.
ℓ_k	wing keel length, ft.
L	lift, lbs. or rolling moment, ft. lbs.
L_a	dimensional lift derivative, $\frac{1}{m}\frac{\delta L}{\delta a}$
L_p	roll damping, $\frac{1}{I_{yy}}\frac{\delta L}{\delta p}$, per sec.
L_r	$\frac{1}{I_{yy}}\frac{\delta L}{\delta r}$, per sec.
L_v	$\frac{1}{I_{yy}}\frac{\delta L}{\delta v}$, per ft. sec.
L_{ϕ_W}	roll control, $\frac{1}{I_{yy}}\frac{\delta L}{\delta \phi_W}$, per sec.^{2}
ℓ	distance from CP to CG of parawing
ℓ_k	keel length, ft.
L/DT	total system lift to drag ratio
L/DW	wing lift to drag ratio

SYMBOL	DEFINITIONS, UNITS
M	elastic coefficient; pitching moment, ft.-lbs.
m	mass, lb.-sec. ^{2}/ft., slugs
M_w	aerodynamic moment
M_x	total moment in roll, ft.-lb.
M_y	total moment in pitch, ft.-lb.
M_z	total moment in yaw, ft.-lb.
M_{ax}	aerodynamic moment in roll, ft.-lb.
M_{ay}	aerodynamic moment in pitch, ft.-lb.
M_{az}	aerodynamic moment in yaw, ft.-lb.
M_v	speed stability derivative, $\frac{1}{I_{yy}} \frac{\delta M}{\delta v}$, rad./ft.sec.
M_α	static stability, $\frac{1}{I_{yy}} \frac{\delta M}{\delta \alpha}$, per sec.^{2}
$M_{\dot{\alpha}}$	$\frac{1}{I_{yy}} \frac{\delta M}{\delta \dot{\alpha}}$, per sec.
$M_{\dot{\theta}}$	$\frac{1}{I_{yy}} \frac{\delta M}{\delta \dot{\theta}}$, per sec.
M_{z_S}	seat position control effectiveness, $\frac{1}{I_{yy}} \frac{\delta M}{\delta z_S}$ per sec.^{2}
N	yawing moment, ft. lbs.; normal load factor; limit load, G's
N_p	$\frac{1}{I_{zz}} \frac{\delta N}{\delta p}$, per sec.
N_r	$\frac{1}{I_{zz}} \frac{\delta N}{\delta r}$, per sec.
N_v	$\frac{1}{I_{zz}} \frac{\delta N}{\delta v}$, per ft. sec.

SYMBOL	DEFINITIONS, UNITS
N_{ϕ_W}	yaw control effectiveness, $\frac{1}{I_{zz}} \frac{\delta N}{\delta \phi_W}$, per sec.^{2}
OD	tube outer diameter, ft.
P	static pressure, psf
P_{Ph}	phugoid period, sec.
p	roll rate about x stability axis, rad./sec.
q	pitch rate, rad./sec. or dynamic pressure, p.s.f.
R	(1) average section radius of wing structural members, inches (2) range
R_{turn}	turn radius
r	seat corner radius
R/C	rate of climb, ft./min.
RHO	mass density of air, lb.-sec.^{2}/ft.^{4}
r	yaw rate about z stability axis, rad./sec.; seat corner radius, ft.
S	wing reference area, ft.^{2}
SFC	specific fuel consumption, lb./hr.
SF	safety factor
SBL	spreader bar length, in.
STW	suspension strut weight, lb.
T	absolute temperature, deg. Rankin or deg. Kelvin
t	time, sec.

SYMBOL	DEFINITIONS, UNITS
T_A/T_R	ratio of time available from initiation to completion of a given sequence (based on ballistic time-in-flight system characteristics unaugmented by performance improvement aids) to total time required for AERCAB to operate from T_i to safe status of flight or descent
t_i	time at initiation of escape
t_{BF}	time lapse in pure ballistic flight (assuming no recovery aids are deployed, nor any augmentive decelerators other than those deployed during launch-propulsion to augment stabilization)
TW	maximum thrust of present engine design at 10,000 ft. pressure altitude
T	thrust, lbs.
T_V	$\frac{1}{m}\frac{\delta T}{\delta V}$, per sec.
$T_{\delta T}$	$\frac{1}{m}\frac{\delta T}{\delta \delta T}$, per sec.^{2}
t_{RBO}	time at launch-propulsion cessation
u	linear velocity component parallel to x-axis, fps
V	flight velocity vector; free stream velocity, fps
v	velocity (true airspeed), ft./sec.; linear velocity component parallel to y-axis, fps
V_e	equivalent airspeed
V_o	steady state value of freestream velocity, fps
W	vehicle gross weight, lb.
w	weight, lb.; linear velocity component parallel to z-axis, fps

SYMBOL	DEFINITION, UNITS
W_1	average cruise gross weight, lb.
W_w	wing weight, lbs.
W/S	wing loading at start of cruise, lbs./sq.ft.
WW	wing "fabric" weight, lbs.
WTC	invariant weight items (man, seat, engine), lbs.
WTW	weight @ start of cruise, lbs.
WTWW	approximate weight of parawing, lb.
X	distance aft of the apex, measured parallel to the keel
x	range, ft.
$\dot{x}$	horizontal component of velocity
x_{ℓ}	the distance from the leading edge of the keel to the intersection of a line normal to the of the keel and passing through the system C.G., ft.
x_{CG}	x component of center of gravity in stability axis system, ft. or in.
x_W	x component of mid-keel point in stability axis system, ft.
Y	lateral displacement, ft.
$\dot{y}$	lateral component of velocity
YSS	yield strength of struts, 35,000 psi
Y_v	$\frac{1}{m}\frac{\delta Y}{\delta v}$ units, per sec.
Y_{ϕ_W}	side force control effectiveness, $\frac{1}{m}\frac{\delta Y}{\delta \phi_W}$, ft./rad.sec.^{2}
Z	pressure altitude, ft.

SYMBOL	DEFINITIONS, UNITS
$\dot{Z}$	sink rate, ft./sec.
$\dot{z}$	vertical component of velocity, ft./sec.
Z_k	perpendicular distance from the system C.G. to the ℄ of the keel, ft.
Z_R	altitude of vehicle above the origin of earth fixed system
Z_t/ℓ_k	distance from the thrust line to c.g. measured perpendicular to the thrust line in percent of keel length
Z_{CG}	z component of center of gravity in stability axis system, ft. or in.
z_S	z component of seat travel in stability axis system, ft.
z_W	z component of mid-keel point in stability axis system

GREEK SYMBOL	DEFINITIONS, UNITS
α	angle of attack (pitch angle plus trajectory angle of load relative to horizon), deg. or rad.
α_p	angle of attack (with reference to relative wind) of payload, deg. or rad.
α_s	seat angles of attack (between thrustline and relative wind) deg. or rad.
α_w	angle of attack (with reference to relative wind) of parawing, deg. or rad.
β	angle of sideslip, deg. or rad.
β_i	angles made by lanyards with local vertical, deg.
β_w	wing angle of sideslip, rad. or deg.
γ	climb angle, deg.; angle between flight path vector and local horizon, deg. or rad.
γ_p	trajectory angle of load relative to horizontal, deg.
γ_w	trajectory angle of wing relative to horizontal, deg.
γ_y	angle between flight path and relative wind vector, deg.
ΔN	change in load
Δt	increment of time (integration increment sec.
Δt_d	time to descend, min.
$\Delta \alpha_{damping}$	longitudinal damping
δ	vertical displacement of the drag vector in the pitch plane, ft.
δ_t	time required for thrust buildup, sec.

GREEK SYMBOL	DEFINITIONS, UNITS
δ_s	toggle switch position controlling wing bank angle
δ_{sw}	toggle switch position controlling seat position
δ_T	thrust lever position
δ_s	linear movement at top of stick, feet
δ_w	wing deflection, radians
$\delta_w - \beta$	angle between flight velocity vector and the product of the pitching velocity and the distance from CP to CG of the parawing (angle between V and $\ell\dot{\theta}$)
ϵ	vertical displacement of the thrust vector in the pitch plane, ft.
θ	pitch angle, deg. or rad.
$\dot{\theta}$	pitching velocity, radians/sec.
θ_p	angle of incidence, deg.
θ_t	deflection of thrust axis, radians
Λ	wing planform sweepback angle, deg.
ρ	density of air, slugs/ft.^{3}
σ	ratio of density of air at altitude to density of air at sea level, ft.
ϕ	bank angle, rad. or deg.
ϕ_w	wing bank angle, rad. or deg.
ψ	angle of yaw, rad. or deg.
T_i	summed unidirectional lanyard tension components
ω	flow rate of fuel, lb./hr.

GREEK SYMBOL	DEFINITIONS, UNITS
ω_{sp}	short period frequency, rad./sec.

SUBSCRIPTS

SUBSCRIPT SYMBOL	DEFINITIONS
A	available (time)
ax	aerodynamic (moment) in roll
ay	aerodynamic (moment) in pitch
az	aerodynamic (moment) in yaw
BF	ballistic flight
c	cruise (conditions)
D	drag
d	(1) descend (conditions) (2) damping
e	equivalent
i	(1) initial (2) idle (conditions)
k	keel
L	lift
ℓ	(1) length of, distance between (2) rolling moment
m	pitching moment
n	yawing moment
p	payload
R	(1) required (time) (2) reference (altitude)
RBO	launch-propulsion cessation
S	stick (force)
s	stick
t	thrust

SUBSCRIPT SYMBOL	DEFINITION
w	parawing
x	roll axis
Y	side force
y	pitch axis
z	yaw axis
1	(1) average cruise (gross weight) (2) outer diameter (tube)
2	inner diameter (tube)
α	per degree angle of attack
β	per degree angle of sideslip

SECTION I - INTRODUCTION

In the relatively brief time lapse of twenty years since their first operational ejection seat installation,[1]* the United States Air Force has oome a long way in provisioning their flying crewmembers with means for safely escaping from their mission vehicle as irreversible emergencies arise. The day is coming in the foreseeable future when ejection under previously deemed "unrecoverable" conditions will become a part of the operational escape envelope. Hence, the percentage of successful ejections/recoveries can reasonably be expected to extend into the high-ninety percentile success rate band. Unfortunately, contemporary combat operations rescue records point out that a successful descent to terrain-level is not enough...the problem remains in many cases of getting the ejectee safely back to his allies. Furthermore, the ejectee in contemporary escape systems has too little (and, often no) control over selection of his landing site. Should the terrain be hostile, in addition to enemy ground forces being in his vicinity, it is obviously desireable to provide the escapee with sufficient maneuverability to discreetly control his landing point and conditions. Rescue of downed crewmembers via fixed-and rotary-winged vehicles has been an operational concept for some time now. It is a well substantiated fact, however, that such rescue missions are in all cases difficult to accomplish, and in many cases can be fulfilled only at great risk to both the downed crewman and the rescue personnel and their support equipment. While retrieval of ejectees in mid-air during their parachute descent is presently under development, such a technique only partially solves the total problem. Recent DOD studies have shown a definite correlation between the probability of rescue-recovery of ejectees, and the distance the ejectee is able to put between the point whereat his irreversable emergency occurs, and his terminal point of return to the earth's surface. It is because the probability of rescue markedly increases with that distance gained, that the "self-rescue" concept evolved.

The primary objectives of the program reported on herein were to investigate a concept wherein the ejectee is provided with both altitude-maintaining (and gaining), and propulsive means which would permit him to assist in his own rescue by flying limited distances toward predetermined sites whereat terminal pickup by allied forces would least jeopardize the safety of all personnel and material involved. Under the investigation, specific operational and design criteria for such a system were established, and realistic performance characteristics thereof were projected. The studies included a determination

*Superscripts refer to the List of References

of modifications required of existing escape systems and operational aircraft (viz., the A-7 and F-4) to provide such a capability to crewmembers.

The Integrated Aircrew Escape/Rescue System, hereafter referred to as AERCAB, was analyzed under this program in its three primary roles as follows.

1. MISSION REQUIREMENTS

a. "The Chair"

First and foremost in consideration of a new escape system in the open ejection seat class is the understanding that the seat acts, during the greater part of its service life, as a platform supporting the crewman from which he performs his mission as an essential integral part of the total flight vehicle system. The operational effectiveness of the aircraft depends largely on the efficiency of its human crew, and their efficiency in turn is highly dependent on the design and functionality of their crewstation, of which the seat is an important part. The seat, as a seat, can serve to minimize crew functional error, minimize fatigue, and serve as a work center from which its occupant has complete access to (and utilization of) his controls and instrumentation. Furthermore, still acting "merely" as a seat, the installation provides a comfortable application of all normal flight loads to the man, protects him against physiologically harmful loads normally induced in ditchings or crash landings; yet while restraining him for safety's sake, still enables the occupant to uninhibitedly reach his controls and read his instruments (and in the pilot's case, enables him to twist about to see his surroundings during both offensive and defensive maneuvering flight).

b. "The Escape Vehicle"

In addition to the physiological comforts above, the ejection seat must also be recognized as a device for providing psychological comfort to its user, enabling the occupant to do his job uninhibited by apprehension, doubt or worry that should an emergency arise, he might not survive. Regardless of the flight-envelope prevailing conditions, the crewman must know, with complete confidence, that upon recognition of an irreversable inflight emergency he can immediately eject without any delay during which prevailing conditions

could further deteriorate. Thus, regardless of the prevailing airspeed, altitude, attitude, and sink-rate conditions, and regardless of the size, shape or weight of the occupant in its confines; the "chair" when called upon to assume its secondary role of escape vehicle, must safely carry the crewman from his station, free and clear of contact with the airframe or its appendages, and provide him with a properly time-sequenced path to the surface below. All the while it is performing in this role, the seat system is protecting its occupant against a potentially hostile dynamic pressure, acceleration, and earth impact environment.

c. "The Self-Rescue Carrier"

The third role, and that which received closest attention under the subject program, is that of secondary flight vehicle. In this role it is required that the escape system provide aerodynamic-suspension to keep the crewman well out of range of contact with hostile ground-based forces; locomotion with which a reasonably rapid departure can be made from the vicinity of the ejection; sufficient fuel for achieving distances traversed in the order of 50 nautical miles; manual control of ascent, descent, and turning maneuvers; onboard instrumentation with which the occupant can monitor his flight conditions, and find and maintain a suitable homing path; adequate protection against flight environments; sufficient life-support provisions for the duration of the self-rescue flight; and means for descent and landing under physiologically tolerable conditions.

The foregoing briefly summarizes the three roles in which AERCAB must be capable of serving its users. The remainder of this introduction is devoted to a description of the performance requirements established early in the concept's evolution, which acted as the basic governing guidelines for the operational, design, and performance analyses made under the subject program.

2. PERFORMANCE REQUIREMENTS

This discussion of AERCAB concentrates on system performance in the latter two of its three above-described roles. The criteria for its performance in its role as a seating platform can be found by the reader through reference to AFSCM 80-1, the "Handbook of Instructions for Aircraft Design (HIAD)"[2]; AFSCM 80-3, the "Handbook

of Instructions for Aerospace Personnel Subsystems Design (HIAPSD)"[3]; and specification MIL-S-9479A (USAF), "Seat: Upward Ejection, Aircraft"[4].

a. "Conventional" Escape

One of the primary performance criteria governing AERCAB's design was "the currently available emergency escape capability from the aircraft and descent by the crewmembers on their personnel type parachute shall not be impaired". Early in the program the term, "currently available", was replaced by, "state-of-the-art", to ascertain that as an escape vehicle, AERCAB could not be outperformed by its peers once it entered into service. Nothing beyond the state of the art was considered during the system investigation, but every attempt was made to judiciously apply the most advanced technology currently within the designer's grasp.

Figure 1 portrays the spectrum of USAF-established critical escape conditions defining the most difficult to combat corners of the overall mission escape envelope.[5]

The equations of motion of the escape system were written as a function of the five prevailing conditions parameters identified in each inset in Figure 1, and consideration was given to those factors in defining the time available to the crewman between his pulling of the ejection handle and his terminal contact with the earth's surface. It was imperative that system weight variation, mass distribution, and inertial/aerodynamic stability characteristics be considered. In addition, man's tolerance to acceleration and deceleration, and the rates of application thereof in any given direction, all played a major role in defining the system's performance limitations. Each factor considered has individual power to determine the success of an escape, recovery and survival attempt. In combination, often these factors conflict seriously with each other in the definition of methods for combating their deleterious effects. The system operating time (or time required, T_R, from initiation of ejection to full parachute inflation) proved to be a hypercritical factor in determining AERCAB's effectiveness as an escape system, when ratioed against the time available under each of the conditions sets in Figure 1.

For the reasons individually discussed in Section III

of this report, the following escape performance requirements were established as system design guidelines:

(1) The pre-ejection functions of restraint haulback and canopy-removal must be accomplished in the minimum practical time, limited only by the physiological tolerance of the occupant to rate-of repositioning in the seat, and to impact with the seating surfaces;

(2) regardless of airspeed (and dynamic pressure) at ejection, empennage clearance must be provided; hence a high-G catapult is required whose characteristics depend on the seat guided-stroke available, and man's tolerance to spinalward acceleration and accelerative-onset;

(3) a sustainer propulsion subsystem is required to provide the altitude gain required under high sink-rate conditions; and to provide a trajectory height compatible with the time-lapse required to decelerate the ejectee (under high-speed ejection conditions) at physiologically acceptable levels and rates of negative acceleration, to velocities at which descent equipment deployment can be tolerated;

(4) the ejection trajectory, through full inflation of the recovery parachute, must be controlled in a prescribable manner along a locus which will not degrade recoverability during ejections at adverse aircraft attitudes; the trajectories relative to the aircraft must be repeatably achieved, and must be not seriously altered by seat occupancy of crewmen ranging from the fifth through ninety-fifth anthropometric/anthropomorphic percentile;

(5) the system must be completely stable and at a prescribable spacial orientation, from ejection through inflation of the recovery parachute;

(6) the event sequencing timing must be designed such that $T_R \leq T_A$ for all ejection conditions;

(7) the personnel parachute must be deployed and inflated in as short a time as possible, as limited only by the structural properties of the recovery system, and physiological tolerance

FIGURE 1 — CRITICAL ESCAPE CONDITIONS SPECTRUM

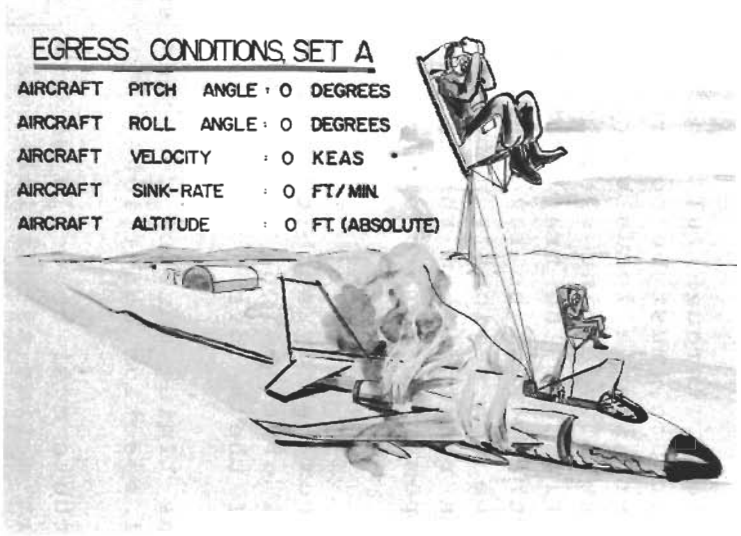

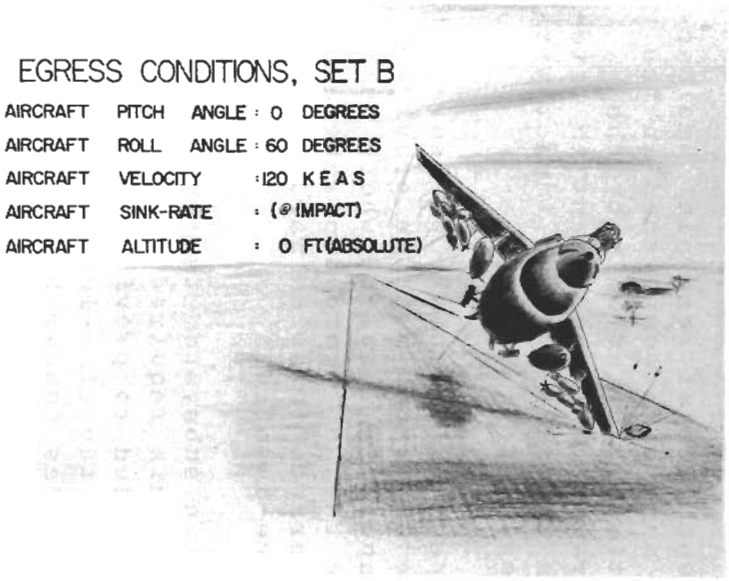

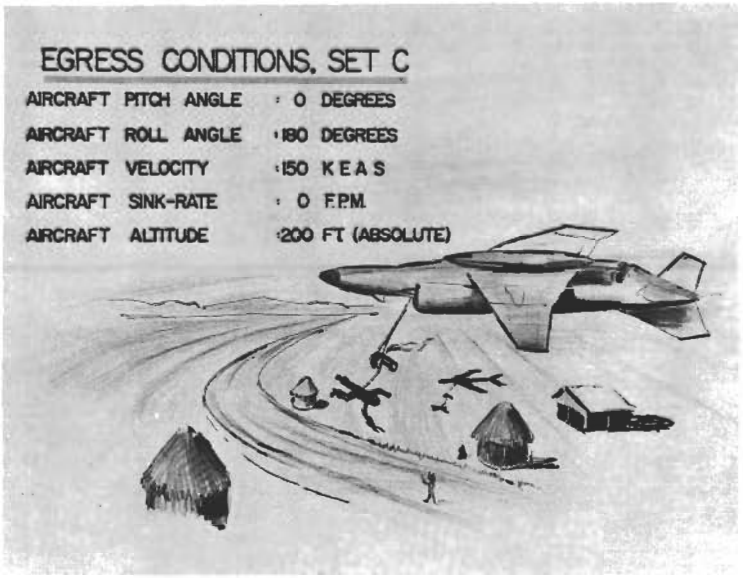

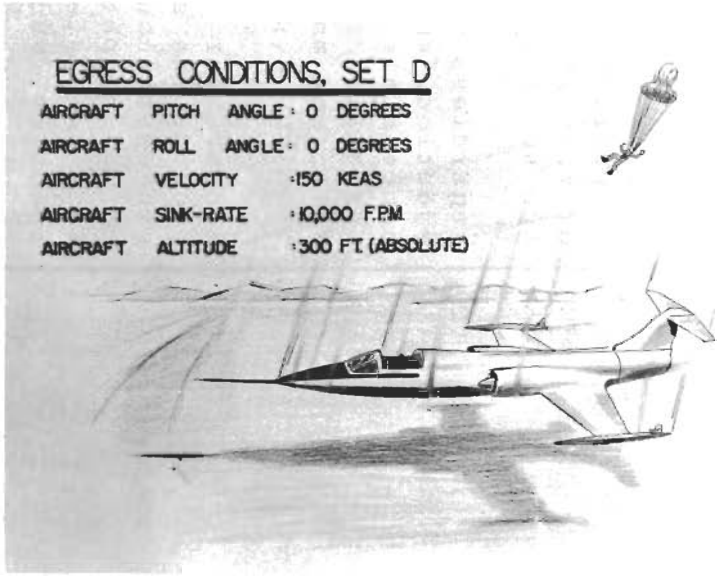

FIGURE 1 (CONCLUDED)— CRITICAL ESCAPE CONDITIONS SPECTRUM

EGRESS CONDITIONS, SET E

AIRCRAFT	PITCH	ANGLE	−60 DEGREES
AIRCRAFT	ROLL	ANGLE	0 DEGREES
AIRCRAFT	VELOCITY		200 K E A S
AIRCRAFT	SINK-RATE		≈17,500 F.P.M.
AIRCRAFT	ALTITUDE		500 FT. (ABSOLUTE)

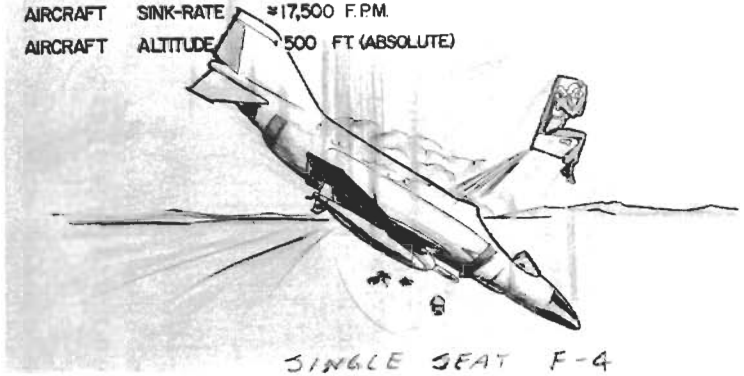

EGRESS CONDITIONS, SET F

AIRCRAFT	PITCH	ANGLE	−60 DEGREES
AIRCRAFT	ROLL	ANGLE	60 DEGREES
AIRCRAFT	VELOCITY		200 KEAS
AIRCRAFT	SINK-RATE		≈17,500 F.P.M.
AIRCRAFT	ALTITUDE		550 FT. (ABSOLUTE)

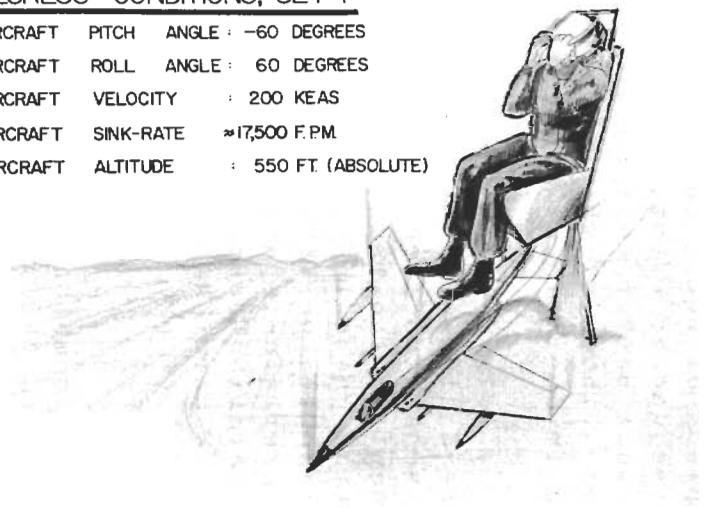

EGRESS CONDITIONS, SET G

AIRCRAFT	PITCH	ANGLE	−45 DEGREES
AIRCRAFT	ROLL	ANGLE	180 DEGREES
AIRCRAFT	VELOCITY		250 K E A S
AIRCRAFT	SINK-RATE		≈18,000 F.P.M.
AIRCRAFT	ALTITUDE		600 FT. (ABSOLUTE)

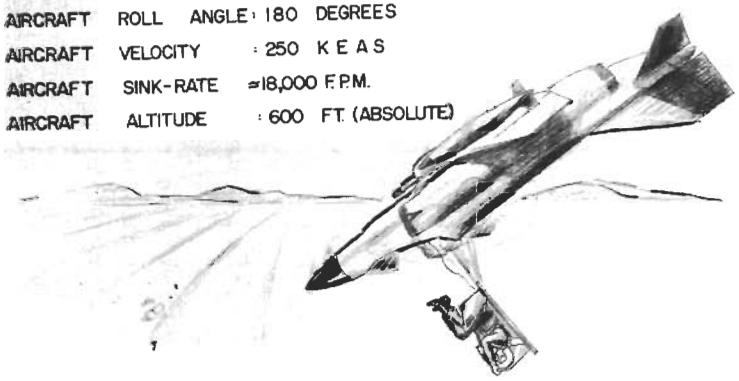

EGRESS CONDITIONS, SET H

AIRCRAFT	PITCH	ANGLE	0 DEGREES
AIRCRAFT	ROLL	ANGLE	0 DEGREES
AIRCRAFT	VELOCITY		600 K E A S
AIRCRAFT	SINK-RATE		0 F.P.M.
AIRCRAFT	ALTITUDE		0 FT. (ABSOLUTE)

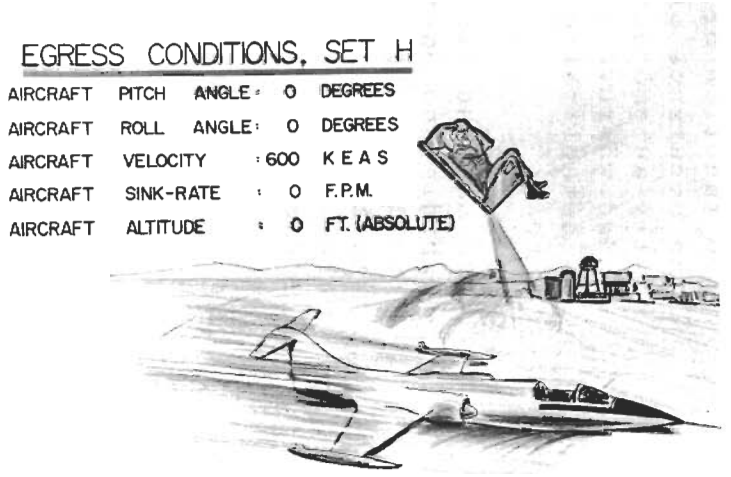

REF: MIL-S-9479A (USAF), 16 JUNE 1967,
TABLE I AND PARA. 3.6.1.

to G and $\dot{G}$ of the man;

(8) the function of every piece of equipment, and the occurance of every sequenced event, must be fully automated; and manual backup must be provided wherever possible; ...both of which aids in establishing a suitable operational confidence level;

(9) the man and his recovery equipment must be rapidly and positively separated from the escape carrier vehicle subsequent to the launch/stabilization/deceleration phase in order to reduce the canopy loading on the parachute, and reduce descent-rates at terrain-impact to tolerable levels; no post-separation contact between man, parachute and seat is permissable, and so their separation paths must be programmed to diverge.

Various propulsion/stabilization combinations were investigated with consideration to AERCAB application, and from the "worst case" conditions shown in Figure 1, the time-available (T_A) was computed. Where adverse attitudes prevailed, a 5-percentile occupant with his CG well above the effective thrustline of the sustainer-rocket was considered, because such a configuration has a resultant predominant velocity vector directed more earthward than other configurations. Similarly for "normal" flight situations, a 95-percentile occupant with a CG significantly below the thrustline was employed as the ejectee.

Table 1 shows the resultant calculated time-available figures for each combination, and Figure 2 portrays the time-required characteristics for the selected AERCAB configuration which governed the time-sequencing performance of the system while operating in its escape mode of operation.

b. Self-Rescue

While operating as a self-rescue system, the contract governing the investigation specified the performance requirements and analyses under the reported program.

(1) All deployables in the system must be capable of operation at altitudes up to 30,000 ft. (MSL), at the maximum velocities and dynamic pressures commensurate with human tolerances to the forces

TABLE I

TIME-AVAILABLE COMPUTATION,

AERCAB ESCAPE MODE,

Ref. No.	PROPULSION METHOD	STABILIZATION METHOD	T_A (sec) for each Condition-SET shown in Figure 1							
			A	B	C	D	E	F	G	H
1	Catapult	None	--	2.30	3.20	2.60	2.34	2.47	2.43	--
2	1200 lb-sec Rocket/Catapult	DART®	6.66	4.40	2.10	3.40	2.25	2.29	2.08	4.50
3	1200 lb-sec Rocket/Catapult	480 lb-sec Vernier-rocket	8.66	5.70	1.80	4.40	2.23	2.35	1.92	5.20
4	2000 lb-sec Rocket/Catapult	DART®	8.50	5.60	1.78	4.20	2.19	2.17	1.92	5.00
5	Catapult	480 lb-sec Vernier-rocket	--	3.50	2.70	2.80	2.33	2.40	2.25	3.20

FIGURE 2

AERCAB ESCAPE OPERATION TIME REQUIRED WITH AIRSPEED

* NOTE THAT THE T_R FUNCTION IS BASED ON THE EIGHT "REQUIREMENTS" EMERGENCIES SPECIFIED IN MIL-S-9479A, ASSUMING ACHIEVEMENT OF "BEST POSSIBLE" SYSTEM OPERATION...

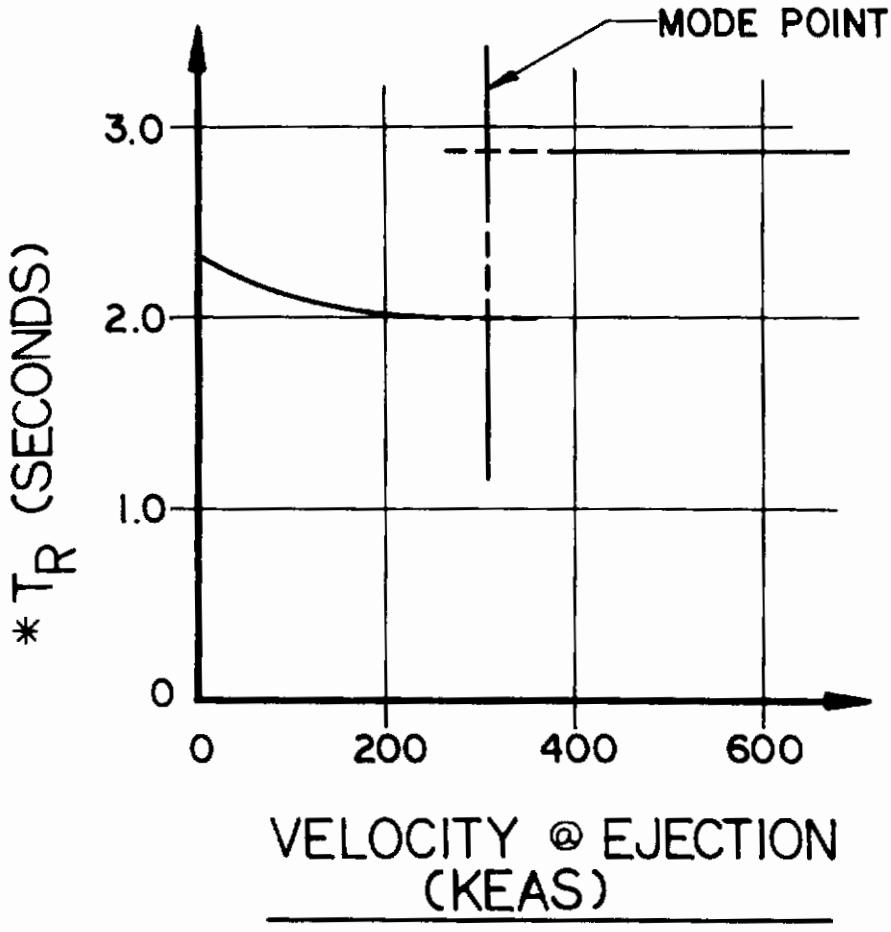

imposed thereby;

(2) The system operational event-sequencing must be fully automatic and pre-established, with all times therein minimized in order to maximize the operational regime of AERCAB's usefulness as a self-rescue carrier;

(3) The current escape envelope will not be compromised by the addition of the self-rescue capability;

(4) The self-rescue vehicle will be configured to provide a maximum-achieveable glide ratio for unpowered flight, limited only to the capabilities of the selected lift-generating surfaces;

(5) The powered system shall have a service ceiling at 10,000 ft. (MSL), and be capable of achieving a range of 50 nautical miles at a minimum cruise velocity of 100 knots;

(6) the system must be capable of climbing at least 4000 ft. (abs.) above the minimum escape altitude from which self-rescue can be achieved;

(7) engine-start must be automatic, taking place after ← μ_o
the rescue vehicle achieves steady-state gliding flight subsequent to ejection and transition from the escape configuration to that of self-rescue;

(8) the direction and altitude of the self-rescue flight-vehicle must be manually controllable (and automatic homing flight control must be considered);

(9) with flight power off, the system must be directionally controllable in gliding descent;

(10) terminal landing conditions must not exceed human tolerances, nor jeopardize the ejectee's well-being during landing on solid terrain or water;

(11) the powered self-rescue vehicle must be capable of adverse weather operation;

(12) under all circumstances, the occupant must be free to descend via his personnel parachute;

3. DESIGN CONSIDERATIONS

In addition to the above performance limits, the design under the subject investigation was dictated by the following requirements:

a. Self-Rescue Reconfiguration

It was required that the erection of lifting surfaces, initiation of system locomotion, and establishment of flight be accomplished prior to reaching terrain-level;

"No SHIT" Dick Tracy

b. Automatic "Lockout"

Above a selected dynamic pressure level, and below a minimum altitude to be defined under the analyses, deployment of self-rescue equipment and ensuing flight must be prohibited if current escape capabilities are compromised thereby;

c. Life-Support

Life-support provisions (e.g. emergency oxygen supply and automatically-actuated (IFF) locator beacon) must be incorporated in AERCAB;

d. System Sizing

It was required that the size of the system to be installed in the aircraft be limited by maintaining the basic cockpit dimensions of AFSCM 80-1, drawings AD1 and AD2. Consideration was given to system integration in the crewstations of the A-7 and F-4 aircraft, which were found to be even more restrictive than the HIAD constraints. Under no circumstances would AERCAB's installation be permitted to compromise the mobility, vision, or access to controls of its occupant;

e. Weight/Volume

Emphasis was required throughout the program on minimizing the weight and volume of the AERCAB installation, while maintaining acceptable levels of expected system reliability;

f. Vulnerability

Consideration was given under the program to the

system's survivability under small arms ground fire conditions. It was required that such factors as target-size minimization, single-hit incapacitation potential, and occupant/critical-component shielding be considered.

With recognition of the foregoing guidelines, this report describes the analysis of the system concept to determine operational and design criteria; and the evaluation of AERCAB with respect to operational feasibility, performance characteristics, ease of system integration and the extent of aircraft modification required to adapt the concept inservice.

SECTION II - COMPREHENSIVE SUMMARY

The objectives of the subject program were identified in Section I. Based on the discussions of the meeting of those objectives throughout the balance of this report, the results of the investigation are summarized below.

The concept of an integrated aircrew escape/rescue system capability (AERCAB) is analytically feasible, subject to verification by testing.

Operational and design criteria for arriving at such a capability have been determined. Its performance characteristics have been calculated. The ease of integrating AERCAB into the A-7 and F-4 aircraft has been shown, and the aircraft modifications required to accommodate the installation have been identified. The system appears to have good potential for future operational in-service adoption.

The system is comprised of an open ejection seat conventionally equipped with necessary life support devices, including a standard personnel parachute upgraded to render improved performance; a stowable, deployable parawing which generates aerodynamic lift to sustain self-rescue flight; a high bypass ratio twin turbofan jet engine for self-rescue flight propulsion; and ancillary subsystems and components which augment and implement the proper functioning of these major elements. The currently available emergency escape capability of crewmembers is enhanced, rather than impaired, through use of AERCAB, in view of the system's inherent advanced capabilities and design features not present in systems in operational service at this writing. The optimized timing sequence is a good example of these advanced features.

The parawing is deployable at relative airspeeds which generate dynamic pressures up to 1.5 times its maximum steady flight "q" (i.e., 50 psf), but is limited to levels more on the order of 18 psf by the time-sequencing subsystem. Deployment of the wing above AERCAB's service ceiling of 10,000 feet (MSL) is prohibited by a barostatic release lockout device in the drogue stabilization parachute's bridle assembly.

The time required for accomplishment of all the events incident to transitioning through the escape and rescue sequences, to the point of safe descent of the crewman to terrain level, has been held to a minimum. The human

tolerances to decelerative magnitude, duration and direction limited the minimum time value. All sequencing in the two-mode operating AERCAB is automatic, and governed by a pre-established time-sequence. The current escape envelope is expanded, rather than compromised, by use of the system.

The AERCAB is configured such that in unpowered (gliding) flight, the system descends at its maximum glide ratio characteristic.

The recommended engine provides sufficient thrust for locomotion over a 50 nautical mile range at cruise speeds in the order of 80 knots, at all altitudes ranging from about 600 feet above terrain to 10,000 feet pressure altitude At the expense of range, flight at nearly 100 knots is possible. The minimum escape altitude in which the self-rescue mode of operation may be implemented is in the order of 600 feet, absolute, with the aircraft in level flight. Hence, the system is capable of rapidly climbing (at a rate of about 1800 ft/min at sea level, to a rate of 100 ft/min at 10,000 feet) to a suitable altitude for terrain-avoidance, reduction of susceptability to small-arms fire, and location of the homing path The engine is automatically started as the seat leaves the troubled parent aircraft, and idle-thrust level is achieved 4 seconds after ejection. In only 6 seconds after escape, full thrust is available to the ejectee for self-rescue flight. It is possible to supply an auxiliary starter in the system, to cover the possibility of flameout, at little or no weight penalty.

The direction and altitude of self-rescue flight with AERCAB are manually controllable; and it appears both feasible and desireable to incorporate an automatic homing flight capability which is independent of manual input.

In the absence of engine thrust, whatever the reason (e.g., fuel-depletion, flameout, etc.), AERCAB's occupant (or the automatic control subsystem) retains the capability for directional maneuvering while in gliding descent. In all cases, terminal descent to the earth's surface is achieved via personnel recovery parachute. Post-landing survival provisions are lowered with the crewman for use as required. Landing impact is attenuated in conventional fashion.

Ten minutes of emergency oxygen are provided onboard AERCAB for use either during descent from ejection at high altitudes, or as a breathing aid during maximum altitude self-rescue flight. An automatically actuated IFF locator

beacon is included to aid allied forces in locating and tracking the AERCAB occupant.

While in powered flight, AERCAB is equipped for self-rescue operation in adverse weather.

When compared to currently in-service emergency escape systems, and considering the added capabilities for self-rescue and improved escape and recovery, AERCAB is recognized as an extremely weight and volume efficient system.

Section VII of this report lists the conclusions drawn as a result of this investigation. The conclusions focus on the fact that the AERCAB concept is deemed feasible from an analytical viewpoint, and because such a system appears to offer a practical and practicable solution to the fundamental problems outlined in Section I, should be further explored in-depth to demonstrate that feasibility; and once proven, should be developed to operational qualified status and adopted by USAF as an advanced life-support system for use by aircrewmen.

Such an in-depth investigation will require continuing detailed contributions from a wide variety of Government and Aerospace Industry specialists in the disciplines of parawinged flight vehicle performance, stability, and control; search and rescue communications; propulsion; navigation; flight and navigation instrumentation; ejection seat technology; and human factors and aeromedical engineering.

SECTION III - SYSTEM DESCRIPTION

Because of the brevity of the overall program, the broad scope of coverage thereunder, and the fact that envelope and weight minimization were major design goals, it was deemed infeasible to attempt to redesign, reconfigure or modify an existing in-service open ejection seat escape system, and strap-on thereto the accommodations for self-rescue. Hence, as a point of departure design, Stencel began with a version of their Company-developed SIIIS escape system previously designed to conform to the form, fit, function and performance requirements of USAF Specification MIL-S-9479A. Correspondingly, under the subject program, the greatest attention could be devoted to the design of the self-rescue equipment envelope, which included the parawing, the twin-fan turbojet engine, fuel containment and management, the flight instrumentation set, the minimum altitude sensing subsystem, the automatic direction finding (navigation) subsystem, the flight control subsystem; and total system dormant packaging and transient deployment concepts.

The initially proposed design, used as a point of departure in system design under the program, was comprised of a hybrid version of Stencel Aero Engineering Corporation's MODPAC and SIIIS escape systems tailored to the self-rescue configuration. The proposed configuration demanded that the seat-shell (which served as both fuel tank and vertical stabilizer during self-rescue flight) be flown in such close proximity to the parawing's undersurface that it was anticipated during concept studies that seat-shell/wing interference effects would seriously degrade the system's aerodynamic performance characteristics. Furthermore, inertial control (or stability) problems were anticipated in deploying that particular arrangement during the configurational transition from the stowed, ejected package to the rescue flight status. Additionally, the deployment dynamics of the proposed arrangement required an excessively complex, difficult to control, train of dependent, in-series, sequential events which would potentially reduce the achieveable reliability; as well as complicating the achievement of desired levels of system performance predictability. Several of the hardware and software elements of that concept were unduly complex (a particularly exemplary item of such complexity was the engine mounting frame which was required to perform a multiplicity of articulative actions which made it heavy as well due to redundant structuring). The redundant structure of the proposed modular seat insert was also shown to be parasitic to weight and space-available for the application and was rejected in favor of a unitary seat approach.

Because of evident deficiencies in the proposed design, an alternate approach to the AERCAB arrangement was taken wherein the system became manually discretionary for usage, in that the crewman was given an in-the-cockpit option to select or reject the system's self-rescue mode of operation (the alternative being conventional ejection and recovery via personnel parachute). The system was provided with an automatic-override capability produced by an on-board prevailing conditions computer which would block-out manual selection of the self-rescue mode if the airspeed, altitude, attitude, and sink-rate conditions at the time of selection are prohibitive to the use of the self-rescue mode because of the extended sequencing time required related thereto. With this approach, then, "conventional" ejection and recovery is the PRIMARY mode of escape; and use of self-rescue is a discretionary option. Initially, the second design approach still involved a modular arrangement wherein all self-rescue equipment was left behind in the crewstation in the PRIMARY mode of operation. With selection of self-rescue, and approval of the conditions computer, the self-rescue module (containing the parawing, engine, fuel, controls, instruments, and auxiliary ejection-propulsion units) was automatically linked to the ejection seat system, and was ejected from the aircraft as a unit. The computer itself was not designed under the subject program, but is believed by the authors to be not only technically feasible, but also the best approach yet conceived at this writing for ascertaining that prevailing conditions are suitable for self-rescue mode implementation. From a practical standpoint, it is recognized that such an item, if placed in the aircraft solely for one potential use during the life of the aircraft, will be difficult to justify. However, similar sensing systems are being currently developed for advanced aircraft to support unique missions (an example of which is tactical terrain-following), and it is altogether conceiveable that the AERCAB conditions computer can be implemented throughout the aircraft's service life for other like tasks. Certainly if a simpler method can be devised, it should be investigated.

That particular configuration was completely designed and used as a base-reference for detailed performance analyses. The results of those analyses indicated that a rigid coupling would be required between wing and vehicle in lieu of the previously selected flexible suspension system because of sensitivity of the decoupled system to relative movement between the wing and vehicle. Such movements were shown to induce instabilities in the system which made it unsafe to fly. The rigidizing of the coupling between wing and vehicle led to the necessity to reorient the seat significantly for steady-state flight because of difficulties with deployment of the wing from its stowed position in the ejected system. While in previously

considered decoupled concepts (flexibly suspended payload) the seated man was in a "normal" upright orientation relative to the horizon, the coupled concept made it necessary to suspend the seated man, in flight, in a face-to-earth position. This did reduce system drag somewhat, further reducing flight-propulsion power required, and greatly simplified the transitional deployment sequence.

As the program progressed, it became apparent that system integration in the A-7 and F-4 crewstations was quite feasible. However, the space available in those cockpits is most meager, and one further design modification was required to "shrink" the AERCAB for those particular installations. It was found impossible to retain the separable self-rescue module and still install the total system in the A-7 and F-4. So the design concept again reverted to a unitary system which was wholly ejected in every case. However, the ejection vs. rescue mode selection concept was retained, and the "intelligence" governing mode selection and system reconfiguration in post-egress flight was programmed to control the post-ejection sequencing subsystem.

The following discussion will pursue the design changes in greater detail, and will describe the form, system elements, operation and sequencing of that concept which ultimately evolved during the reported program. Figure 3 portrays the flying arrangement for the finally selected system configuration.

1. INTEGRATED SYSTEM APPROACH

As envisioned by USAF, AERCAB is a system which, subsequent to its ejection from a disabled aircraft, deploys augmenting lifting surfaces to generate aerodynamic suspension of the crewman and his survival and life-support equipment, and employs an onboard propulsion system to provide locomotion from the ejection site. The system, being fully capable of operating in both the conventional manner (as an escape/recovery system), and as a secondary flight vehicle, must be packaged into the parent aircraft's crewstation, and hence must reconfigure itself while in flight along the egress trajectory into the most favorable configuration amenable with prevailing conditions. Since weight was at a premium, and volume available for crewstation installation was extremely scarce, the AERCAB system as two separate vehicles (one for normal escape, the other for rescue) appeared highly infeasible. Thus it was necessary to come up with an integrated system with sufficient capability to perform both tasks equally well, as the emergency situation demanded.

In order to maximize the ratio of time-available to time-required under extreme emergency conditions, it was recognized early in the program that a pre-ejection selection option should be given the crewman with which he could choose or refuse to utilize the self-rescue provisions. Furthermore, to compensate for the possibility of his making a judgment error under marginal conditions, an automatic override was included to preclude an escape outside the operational performance envelope of his self-rescue system.

Figure 4 is an operational schematic of the integrated system, showing the methods Stencel selected for dual-capability provisioning.

Under circumstances whereunder conditions demand, or the crewmember elects, a mere activation of the leg-brace mounted ejection controls will automatically jettison the cockpit-canopy, restrain the occupant, eject the system from the aircraft, stabilize and decelerate the ejected mass, deploy and inflate the recovery parachute, and separate the man/parachute/survival-gear package from the remainder of the system along divergent paths. This is all done in the shortest time compatible with human and system-structural tolerances.

Under more favorable circumstances, the crewman may elect to depress the MANUAL SELECTOR switch in the cockpit. Closure of that switch activates the airframe-mounted computer which is programmed to receive an instantaneous report of prevailing altitude, attitude, airspeed and sink-rate conditions; compute the time available as a function of those conditions; compare the time-available against the self-rescue system functioning time required (which is stored in its memory); and instantly authorize or reject the use of the self-rescue provisions. With the TA/TR ratio greater than or equal to unity, the computer closes a second switch which in turn activates a valving unit in the time-sequencing system, thereby adjusting the sequencing of events to permit proper deployment of the parawing, and automatic-start of the engine, with corresponding activation of the self-rescue maneuvering controls and flight/navigation avionics and instruments.

The following is a discussion of the AERCAB as a basic escape system.

2 BASIC ESCAPE SYSTEM

Accepting MIL-S-9479A[4] as a minimum design guideline, Stencel

REVISIONS

SYM.	DESCRIPTION	DATE	APPROVED

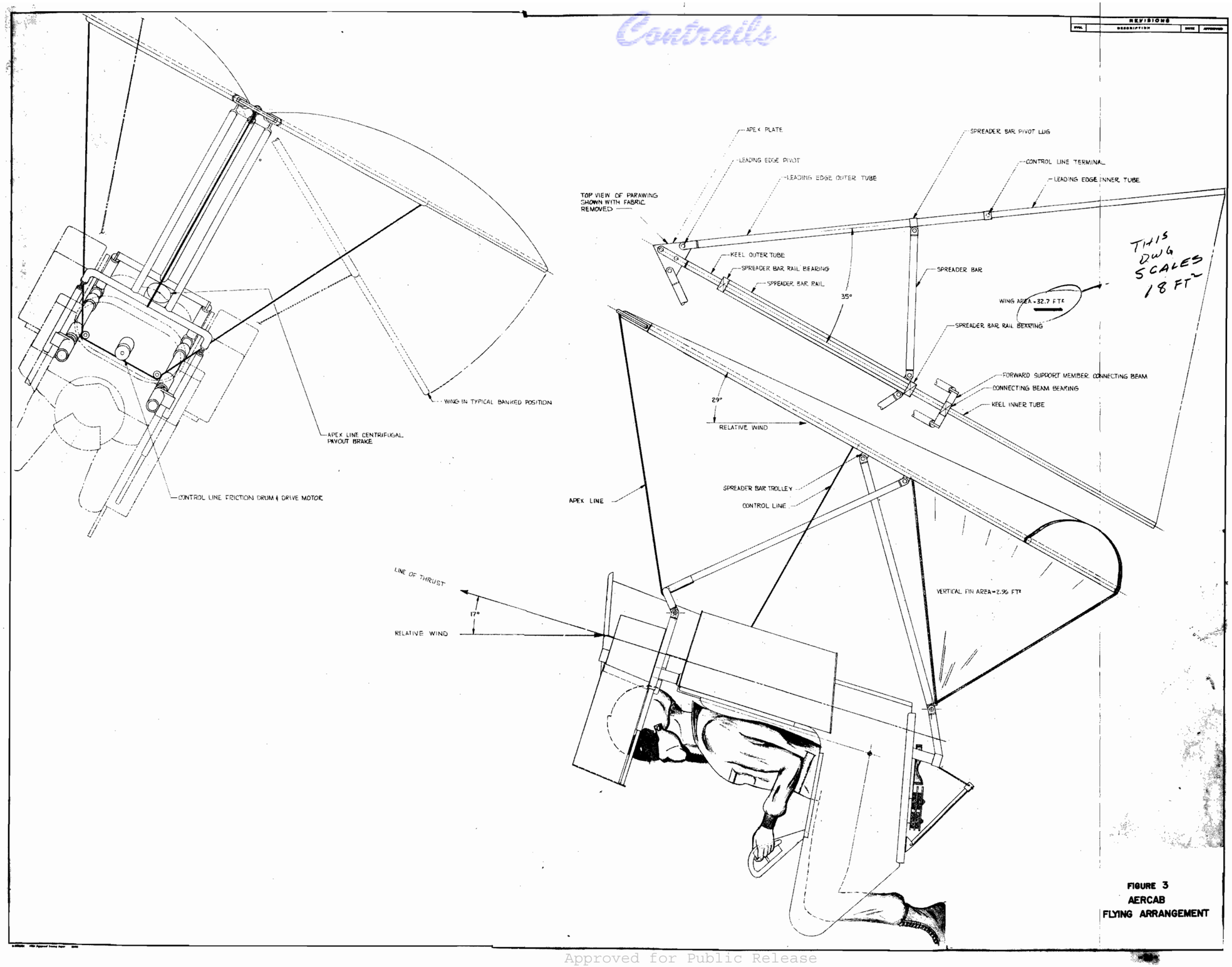

THIS DWG SCALES 18 FT²

FIGURE 3
AERCAB
FLYING ARRANGEMENT

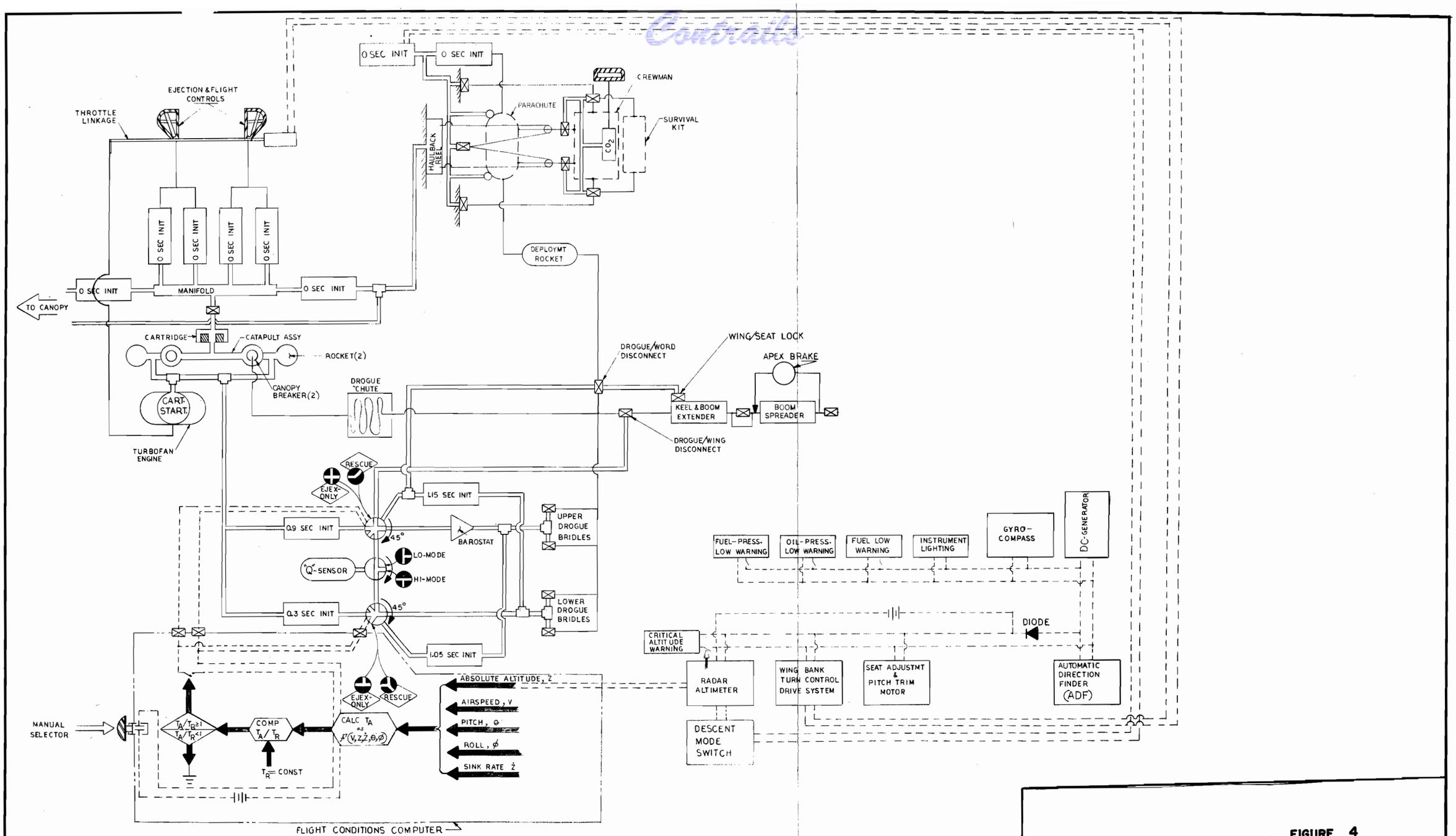

FIGURE 4
AERCAB
SYSTEM SCHEMATIC

Aero has created a basic system felt to offer USAF the best solution to the overall spectrum of escape and recovery related problems. The description below is intended to introduce and familiarize the reader with the SIIIS family of open ejection seats.[5] The series is characterized by its "building-block" assembly which renders the system sufficiently versatile enough to change form and fit (for cockpit tailoring) without effecting function and performance. Remarkably enough, SIIIS's performance capability can be altered by merely adding or deleting the performance-generating "building-block" components and subsystems, with virtually no changes to the foundational (basic) system. With SIIIS, the USAF no longer must sacrifice escape-performance capability because of limits imposed by peculiarities of a crewstation or aircraft. The escape system is tailored to match the mission operational envelope of the parent aircraft with all due consideration given to the emergency situations encounterable in service with that aircraft. While offering this capability however, SIIIS minimizes the penalties in weight, volume, cost, reliability, complexity, availability, comfort, efficiency and safety which heretofore had to be paid to achieve advanced performance capabilities.[5]

a. Form Description

Figure 5 portrays the general arrangement of the AERCAB preliminary design in its final configuration evolved to at the termination of the reported program. Figures 6, 7, and 8 show further sectional views of the system in Figure 5. For sake of future reference the system is depicted as installed in the A-7 and F-4 crewstations.

To aid in minimizing the installation envelope, the SIIIS seat was designed such that the headrest remains at a fixed position in the crewstation, at a location optimized relative to the eye-reference point. During seat adjustment the man in the seat-bucket translates relative to the headrest (hence, proper eye-level maintenance is achieved for all percentile crewmen without compromising the height-dimension of the crewstation). Egress stability is not compromised by so doing, because on SIIIS the rockets for secondary ejection propulsion are affixed to the rear of the seat bucket structure, and move therewith during adjustment, thereby avoiding any CG-thrustline eccentricities beyond those normally encountered in service attributable to mass-distribution variation throughout

the anthropometric spectrum of using crewmen, and the variations in their personal-equipment and its distribution over their person while occupying the seat.

Special tailoring of the structure and relocation of major system bulk elements to fill all available space enabled the envelope to encompass the escape, recovery and rescue equipment and still be installed in minimal-sized crewstations. The separation of catapults and rockets into individual units aided greatly in implementing the evident high-density packaging of the AERCAB's SIIIS-basic system.

b. Escape System Elements

The major AERCAB system elements essential to the system's escape, recovery and survival operations are identified as:

...Seat Bucket Assembly
...Event-Sequencing Subsystem
...Egress-Propulsion Subsystem
...Stabilization Subsystem
...Terminal Descent Subsystem
...Restraint Subsystem
...Survival Equipment

(1) Seat Bucket Assembly

The basic seat bucket is a simplified flat-panel sandwich structure which serves as the seating platform, and on which are mounted the ejection controls, comfort provisions, many of the system sequencing elements, seat adjustment subsystem components and plumbing, the restraint subsystem, and the "working end" of the DART® stabilization unit. The survival kit is housed within the bucket's lower confines. The unit is designed to structurally withstand extreme crash-induced loads of 40/40/10 G's (longitudinal/vertical/lateral). The bucket is strategically attached to the catapult assembly through which all structural loads are transmitted to the airframe. The basic bucket weighs only 31 lbs. The back-tangent plane is inclined 13° aft of vertical (4° forward inclination from the launch catapult thrust-axis), and the seat tangent plane is 103° forward of the back angle (i.e., parallel to the airframe waterline reference system). On the

REVISIONS			
SYM.	DESCRIPTION	DATE	APPROVED
A	CHANGED BULKHEAD ANGLE FROM [illegible] TO [illegible]	[illegible]	R.T.C.

NOTES:

1. THE WL & FS STATIONS ARE FROM McDONNEL DRAWINGS NOS. 53-81050, 53-80002, 53-80003 & 32-82026. THE HEXAGON IS USED FOR LOCATING THESE STATIONS ON THIS DRAWING.
2. THE "X", "Y" & "Z" STATIONS INDICATED BY THE CIRCLE ON THIS DRAWING WERE TAKEN FROM LTV DWG. #214-21135 REV. "A"

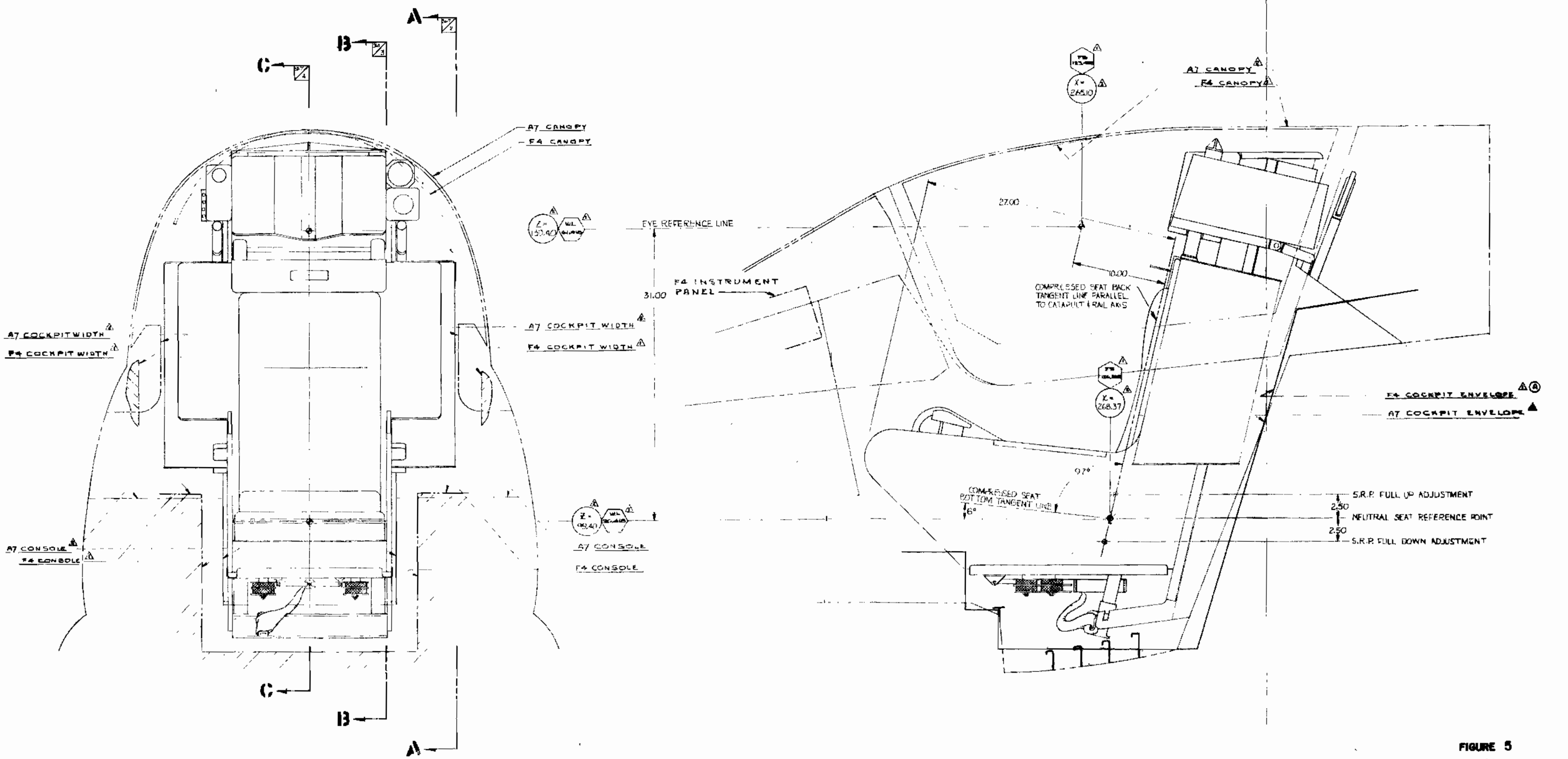

FIGURE 5
AERCAB
PRELIMINARY DESIGN

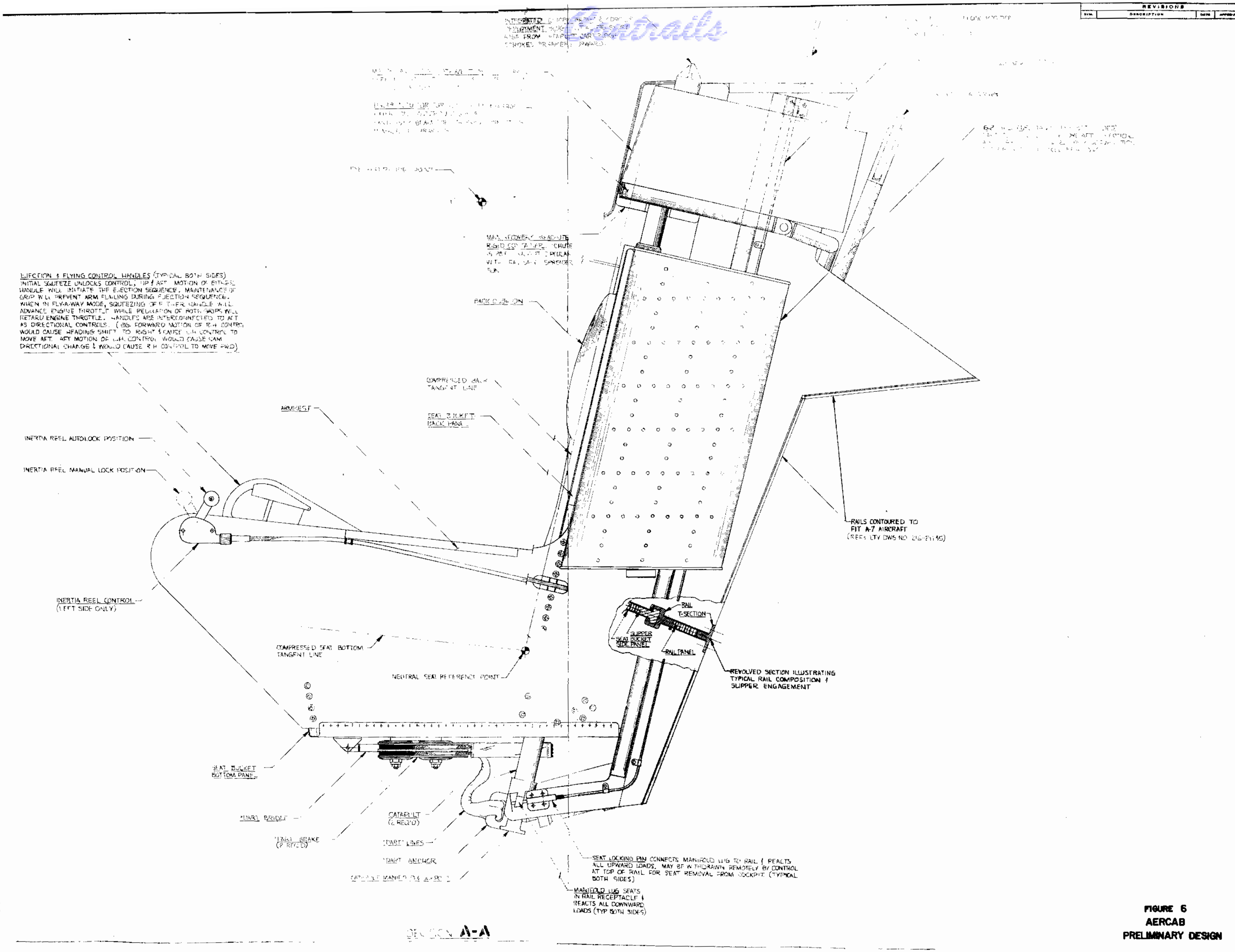

FIGURE 6
AERCAB
PRELIMINARY DESIGN

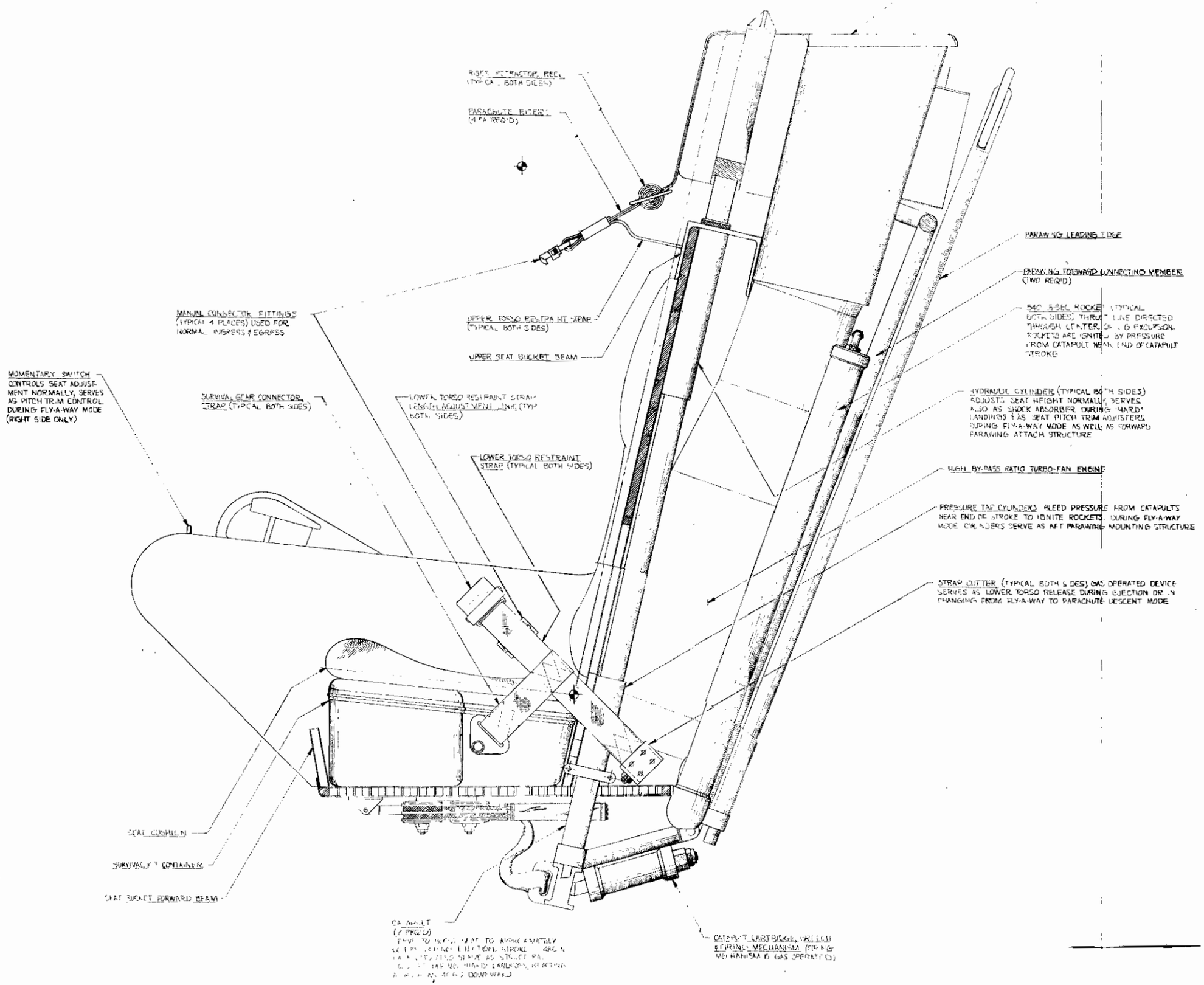

SECTION **B-B**

FIGURE 7
AERCAB
PRELIMINARY DESIGN

REVISIONS			
SYM	DESCRIPTION	DATE	APPROVED

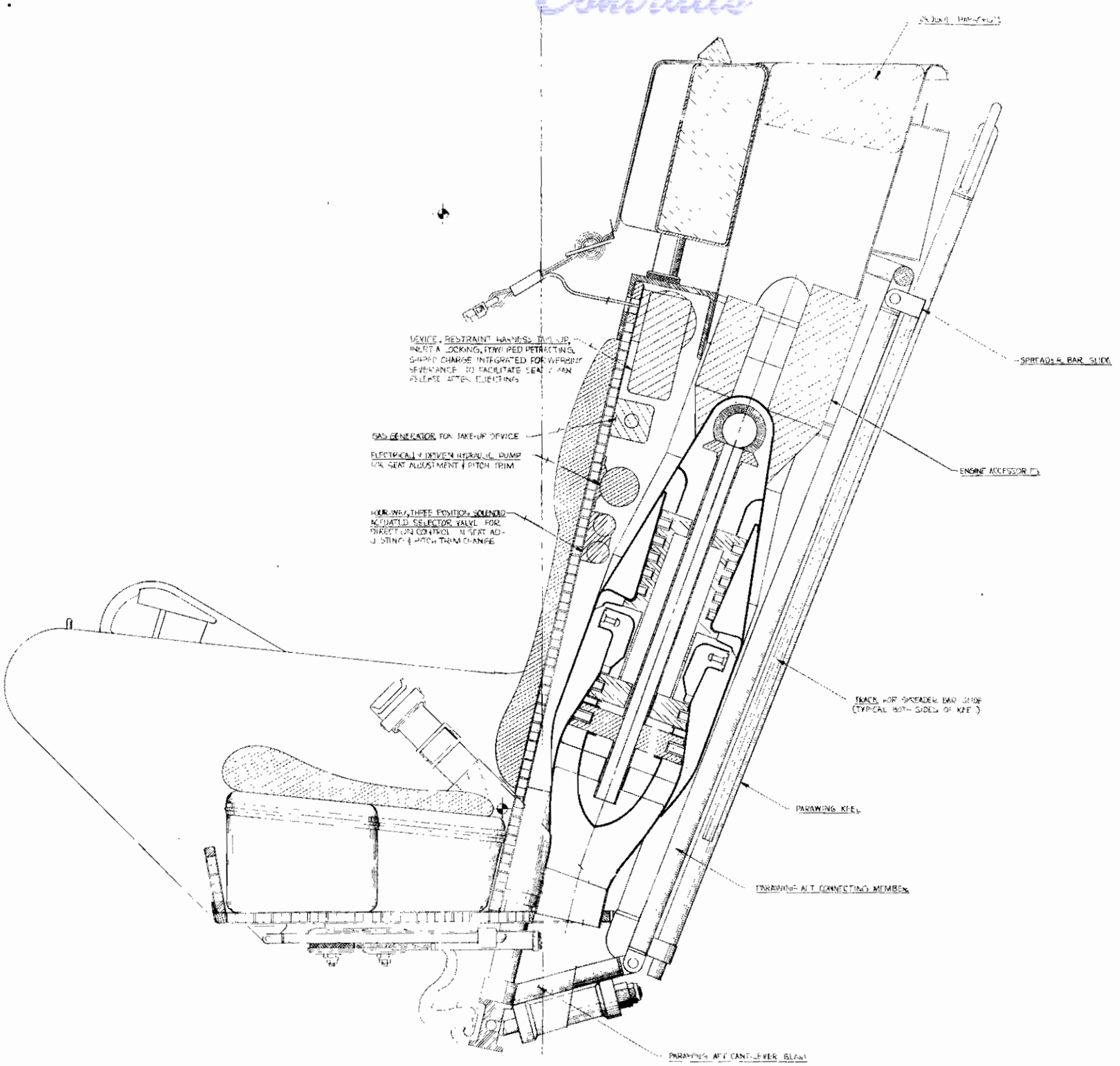

SECTION C-C

FIGURE 8
AERCAB
PRELIMINARY DESIGN

right leg brace is mounted the momentary switch for seat-adjustment actuation (a three-position, momentary-ON, center-OFF switch is used; and the direction of switch action corresponds to the direction of seat movement). To augment lateral leg-support during exposure to high dynamic-pressure windblast, the seat's sides are extended as far forward as the ejection-path clearance envelope permits. Armrests are included as additional comfort provisions. The seat bucket sides extend aftward well beyond the occupant's back tangent plane, and serve as reaction supports for the secondary ejection-propulsion rockets. As the bucket adjusts relative to the catapult assembly, the rockets move with it, thereby maintaining a fixed thrustline relationship with the center of gravity. Figure 6 shows the manner in which the ejection slippers are integrated into the seat bucket side panels, and how the assembly separably mates with the ejection rail-panel assembly. For rescue flight, the fuel reservoirs are mounted on the outboard surfaces of the seat bucket side panels. The slipper assembly is designed so that at the instant the seat separates from the rails during ejection, the catapult tubes simultaneously separate, thereby precluding catapult-induced "tip-off" or tumbling.

(2) Event-Sequencing Subsystem

Figure 4 shows all the elements necessary in the AERCAB system for proper event sequencing. None of the required devices therein are beyond the existing state-of-the-art of development. The time-delay elements (pyrotechnics initiators) can be readily developed to achieve the optimum timing discussed in Section III-2-d of this report. Some willingness to compromise this timing very slightly would enable the user to adapt existing off-the-shelf devices requiring no development. The timing sequence for conventional escape (sans self-rescue) is split into two modes which are entirely airspeed and altitude dependent. A dynamic-pressure sensor onboard the escape system provides the proper mode-selection input by driving a two-position valve in the plumbing system which feeds into the drogue parachute bridle release mechanisms. A barometric lockout device inhibits drogue release above altitudes of 10,000

ft. (MSL). For normal escape the self-rescue sequencing valves are positioned in the EJEX-ONLY orientation which inhibits employment of the self-rescue provisions, and automatically induces immediate reversion to the parachute descent mode of recovery. Section III-2-d describes the event by event sequencing operations, and the timely operation of pertinent elements contributing thereto. In all cases the event sequencing subsystem is designed to function in the shortest possible time consistent with conditions prevailing at the time the ejection is initiated. All pre-ejection functions (canopy-jettisoning and restraint powered haul-back/lock) and the firing of the launch catapults are accomplished merely by rotating the control handles upward and aft to the mechanical stops. Propulsion initiation is provided through simultaneously activated, independent dual and redundant pyrotechnic (0-delay) initiators. As presently configured, the system can be readily adapted to accommodate additional sequencing elements for multicrewmember ejection, regardless of the seating arrangements. Consideration under this program was given only to single-seat installations, however. To accommodate both crewmen in the F-4 aircraft, additional inter-seat sequencing design work is required.

(3) Egress-Propulsion Subsystem

Depending on the operational mission-envelope of the parent-aircraft, a wide variety of propulsion (and stabilization) subsystems could be employed for AERCAB ejection. Analysis of the fundamental requirements led to the selection of a catapult delivering a peak accelerative axial load of 16 G's, giving the ejected mass a velocity of 60 fps at separation from the rails. To accommodate high-density packaging and the building-block concept, the catapults are independently separate units from the rockets. The resulting conservation of volume enabled Stencel to significantly compress the seat along the longitudinal axis (fore-aft). The catapults and rockets are provided in pairs, outboard of the central plane of system symmetry (about which the deployables and self-rescue equipment are stowed in the central volume). The catapults are manifolded together such that neither can

be independently pressurized without the other following suit. A redundant pair of cartridges are provided to energize the catapults. These are delay train (0.300 sec.) cartridges with a Stencel developed, non-indexing, dual-primer ignition element in each.[6] At the head-end (top) of each catapult, an integrated canopy-breaker piston is built-in, which strokes upon pressurization of the catapults, thereby penetrating a "hung-up" canopy ... before first-motion of the ejected mass.[7] The canopy-breaker appendages can be employed either as individual spikes, or as in AERCAB, as a bridged assembly which serves in a dual-capacity as a deployment drogue-mass acting on the stabilization/retardation parachute. This powered canopy-breaker feature adds less than one pound to the system weight when integrated into the catapult assembly in this manner, yet absolutely precludes the seat occupant's having to take initial canopy-penetration forces with his head and shoulders; also, the unit, so-employed, accelerates the drogue parachute into its effective position downstream at the earliest possible time, so that the 'chute is working as the ejected mass separates from the airframe. Hence, at high-speeds, where normal aerodynamic moments on the man/seat system would tend to induce severe "pitch-up" tumbling, the drogue is already acting to combat these moments, thereby maintaining both stability and trajectory control from the very instant the ejected mass becomes an independent "free-flying" object. Just prior to the instant of separation of the inner and outer catapult tubes, the pressurized gases therein are piped off to energize the medium-impulse (840 lb.-sec. each) rockets, the self-rescue engine starter cartridge, and the drogue-bridle upper and lower release delay initiators.

The system's headrest is firmly fixed to the outer tubes of the catapult, and remains stationary during seat-adjustment in order to optimally support the man's head at the required eye-reference level in the cockpit.[7] As a space/weight conserving measure, the seat adjustment mechanism is also integrated into the catapult assembly,[7] and operates as portrayed schematically in Figure 9. Note that a flange is incorporated on the outer surface of catapult tubes, A, and that flange acts as a

FIGURE 9
AERCAB SEAT ADJUSTMENT
LONGITUDINAL TRIM SUBSYSTEM
SCHEMATIC

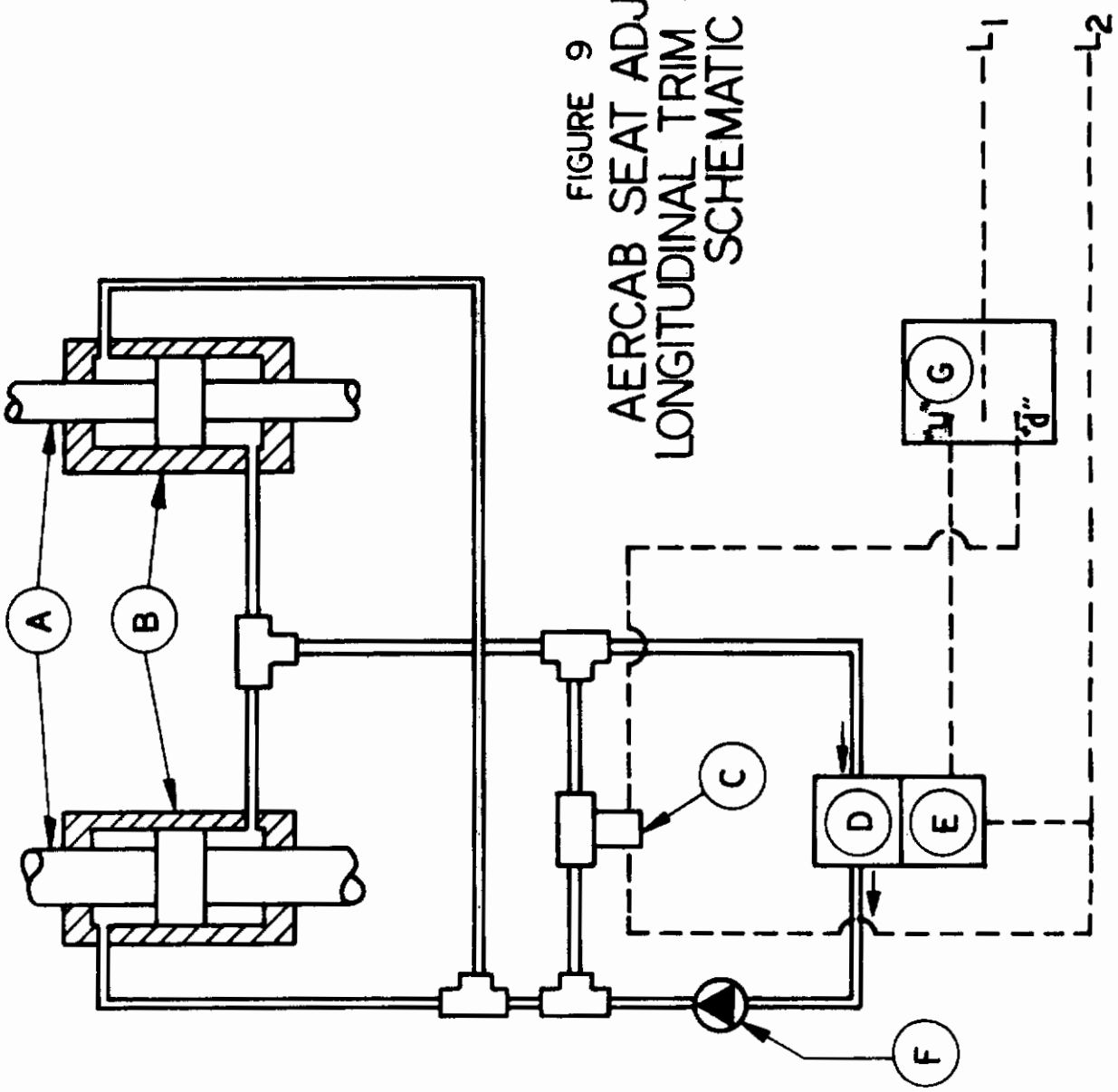

piston in cylinders, B; said cylinders being firmly attached to the seat bucket in which the occupant is seated. Note the recesses above and below the piston into which hydraulic ports are bored. D, is a unidirectional hydraulic pump driven by electric motor, E, causing fluid flow in the direction of the arrows. Check valve, F, prevents flow reversal in the undesired direction. Solenoid valve, C, is employed to permit influx of hydraulic fluid to the lower recess of cylinders, B, whenever downward movement of the seat bucket is desired. G is the three-position momentary switch on the right leg brace which gives the occupant the directionality desired for adjustment. With the seat occupied, the pressure in the upper recess of cylinders B increases. The solenoid valve, C, is in the normally closed position. If the seat is in the desired position, fluid pressure in both recesses keep it stationary. If the seat is too high, the occupant pushes the switch down and L_1 comes in contact with terminal "d", and the solenoid valve opens permitting influx of fluid into the lower recesses of cylinders B. If the seat is too low, the "up" switch is pushed, L_1 comes in contact with terminal "u", in which case the pump draws fluid from the lower recesses of cylinders B, and pumps the fluid into the upper recesses. As the upper recesses fill, the bucket moves upward with the cylinders relative to the airframe-stationary tubes, A. This method of integrating the adjustment device into the catapult assembly weighs only 37% of what an equivalently performing electric screwjack weighs, and contributed positively to the system weight minimization efforts. Note that the rockets used for ejected propulsion sustainers are affixed to the seat bucket, and hence remain essentially at a fixed eccentricity relative to the system CG during their burn period. That eccentricity is not affected by seat position adjustment.

From a standpoint of weight and space savings it would have been preferable to use only the catapults as egress propulsion, but such a system could not be shown to assure tail clearance at airspeeds above 500 knots without exceeding human tolerances (in accord with the USAF Dynamic Response Index, or DRI). With the

selected equipment, AERCAB will assuredly provide full recovery under both "zero/zero" and 600 knots/zero-altitude ejection conditions. The minimum-impulse, forward/vertical oriented rocket sustainer stage also assures optimum performance under adverse dive, bank, sink-rate conditions. The combination of the selected catapults and rockets with DART® contributions was the only system of five combinations considered which affords safe recovery margins under all eight escape conditions shown in Figure 1.

The limiting value for the Dynamic Response Index during catapult action prior to seat/rail separation is given in Paragraph 3.4.2.12.1 of MIL-S-9479A (USAF) as 18.0 at a catapult temperature of 70°F and as 22.2 at a catapult temperature of 200°F. Following seat/rail separation the three-directional expression

$$\sqrt{\left(\frac{DRI_z}{G_{z_L}}\right)^2 + \left(\frac{Gx}{G_{x_L}}\right)^2 + \left(\frac{Gy}{G_{y_L}}\right)^2} \qquad (1)$$

must not exceed unity. The three limiting g levels are:

G_{z_L} = +17g or -12g (for Rise Time $\geq$ 40 millisec)

G_{x_L} = $\pm$35g (for Rise Time $\geq$ 30 milliseconds and duration $\leq$ 30 milliseconds)

= 32.5g (for Rise Time $\geq$ 30 milliseconds and duration $\leq$ 100 milliseconds)

= 20g (for Rise Time $\geq$ 30 milliseconds and duration $\leq$ 1.0 seconds)

G_{y_L} = $\pm$13g (for any Rise Time and duration $\leq$ 100 milliseconds)

= $\pm$7.9g (for any Rise Time and duration $\leq$ 1.0 second)

These limiting values are based upon the trapezoidal/triangular approximation technique described in Paragraph 6.4.2 of MIL-S-9479A (USAF).

A computer program was set up to solve for the DRI based upon the lumped parameter, mechanical model and its describing mathematical equation. This program was used to study the DRI for

several rocket-catapults now commercially available to compare the magnitude during catapult action and during rocket sustainer burning subsequent to seat/rail separation. All values were taken as only the spinal components and the worst case was considered to be the 5% man with the corresponding total system weight during the rocket-catapult action time. A 280 lb.-mass was assumed to correspond to the appropriate thrust-time characteristics of these off-the-shelf motors, since they have not yet produced motors scaled up to handle the added mass of the self-rescue equipment. Table 2 gives the results of the DRI_z calculations for each rocket-catapult considered based on the traces in Figure 10. Here it is evident that the Unit A has the least margin of safety against the DRI_z limit value of 18.0 during the catapult action.

This rocket-catapult also has an insufficient safety margin during rocket burn time since $(15.5/17)^2 = 0.831$; allowing a maximum of $\sqrt{1.0-0.831} * (G_{x_L}) = 0.41 * G_{x_L} \approx 13g$ deceleration resulting from airstream drag. Unit B has the lowest DRI_z values while providing the best safety margin during rocket sustainer burning, and allows a deceleration due to air drag of 23.7 g's. Unit C has the highest DRI_z (16.7) during rocket sustainer burning of all the rocket catapults considered, but is unacceptable because of an insufficient safety margin with respect to the (17.0) limit value allowed subsequent to seat/rail separation. With this value of spinal DRI_z the maximum eye-balls out deceleration resulting from air stream drag which can be allowed is 6 g's. The triangular shape of the sustainer rocket thrust-time trace for this rocket-catapult produces the very high DRI_z value during rocket burning, thus, pointing up the importance of a <u>neutral</u> thrust-time trace for the rocket sustainer.

The DRI_z values for Unit D shows why the parent seat enjoys such a good record of ejections without spine injury. During rocket-sustainer burning the safety margin against the 17.0 limit value of DRI_z allows a maximum eye-balls out deceleration from the airstream drag of about 22 g's.

TABLE 2 - DRI Calculations for Selected Rocket-Catapults
Using the Trapezoidal/Triangular Approximation

Rocket/Catapult	Rocket Impulse lb.-sec.	Trapezoidal/Triangular Approximation			Catapult DRI_z	Rocket DRI_z
		Rise Time Seconds	Dwell Time Seconds	Max.G		
Unit A	2000	0.080	0.155	14.8	17.9	15.5
Unit B	1200	0.087	0	13.1	15.3	11.6
Unit C	1200	0.190	0	15.9	12.5	16.7
Unit D	1200	0.110	0	14.3	15.4	12.6
Unit E	1680	.090	0.026	13.5	15.8	13.5

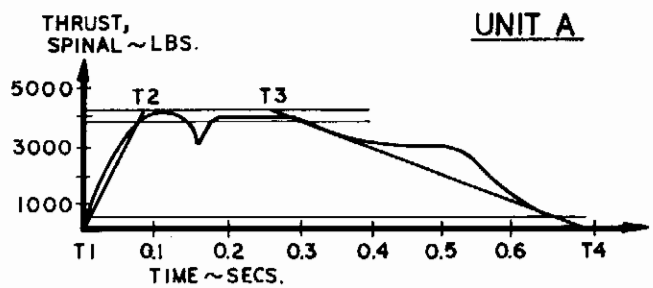

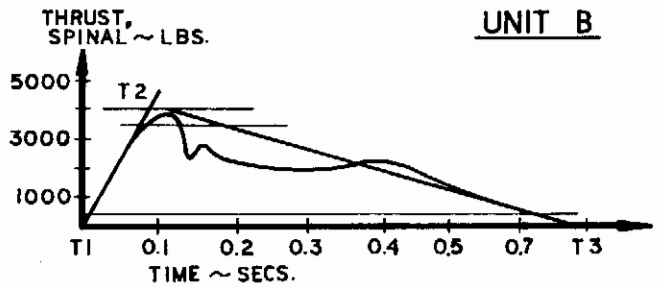

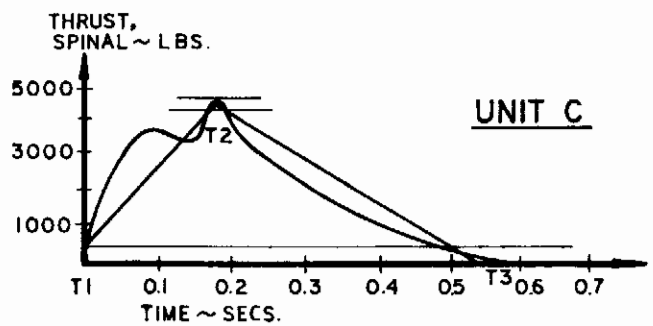

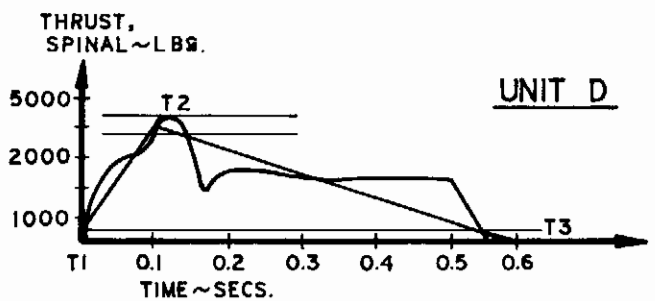

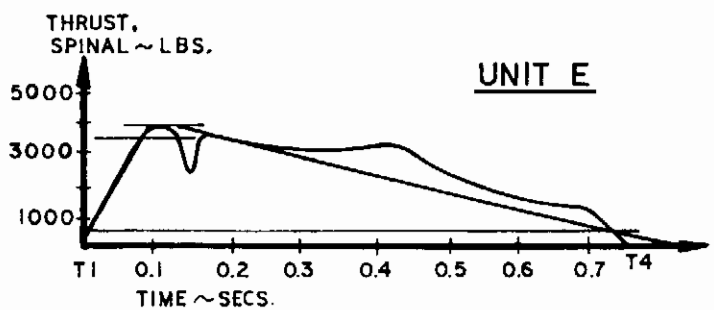

FIGURE 10

ROCKET CATAPULT CHARACTERISTICS USING THE TRAPEZOIDAL TRIANGULAR APPROXIMATION METHOD

The addition to the Unit A rocket-catapult of a seat-bottom mounted vernier rocket[8] with 480 pound-seconds impulse and a 0.5 second action time (Unit E) adds about 3.5 g's spinal acceleration during the vernier rocket burn time. The DRI_z during rocket burning increases from 11.6 to 13.5 and decreases the allowable eye-balls out deceleration due to air drag from 23.7 to 19.7 g's.

The trapezoidal/triangular approximation to the catapult and rocket thrust-time history employed above is valid to obtain the maximum DRI for the complete force-time history; however, if a need exists to obtain the DRI both for the catapult action time and for the rocket burning time, then another straight line method which considers the catapult action time and the rocket action time separately must be used. Rocket-catapult Unit C is a good example. Although the maximum DRI_z during the catapult action time in Table 2 is only 12.5, the catapult action time alone will have a higher DRI_z than the Unit D catapult alone. The fact that the peak spinal thrust occurs during rocket burning for this unit causes the catapult force-time history to be completely over-ridden, reducing the rate of onset unrealistically. Thus, to determine more closely the DRI_z for the catapult action time and the rocket burn time separately, another approximation method was used. Essentially, this method made use of straight line segments to approximate separately the catapult action time and the rocket burn time as shown in Figure 11. Table 3 lists the results obtained using this method, including the catapult rise time, catapult dwell time and the rocket dwell time as well as the catapult DRI_z and the rocket DRI_z. In this table the catapult DRI_z for Unit C compares to that of Unit A, as expected, since the catapult force-time traces for these two rocket-catapults are almost identical. The rocket DRI_z for Unit C (Table 3) increased to 17.6 from 16.7 (Table 2) primarily because of a higher rate of onset of the rocket sustainer thrust following catapult separation.

This method, applying appropriate weight-compensating scaling criteria, enabled Stencel to establish the individual design performance

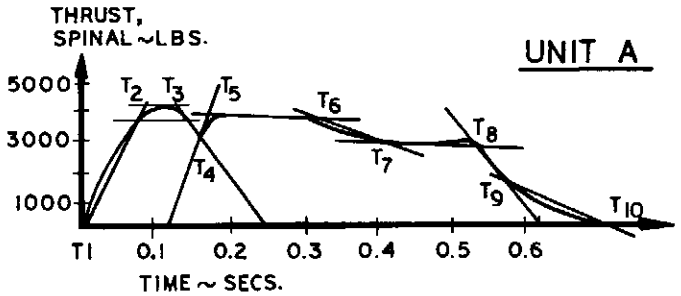

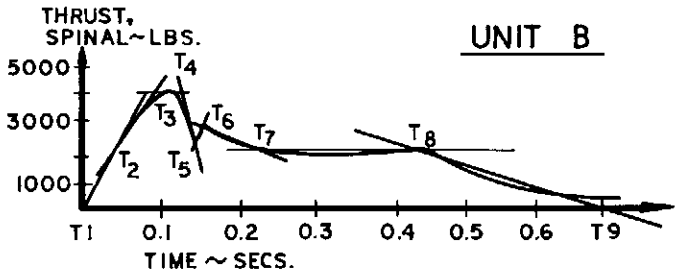

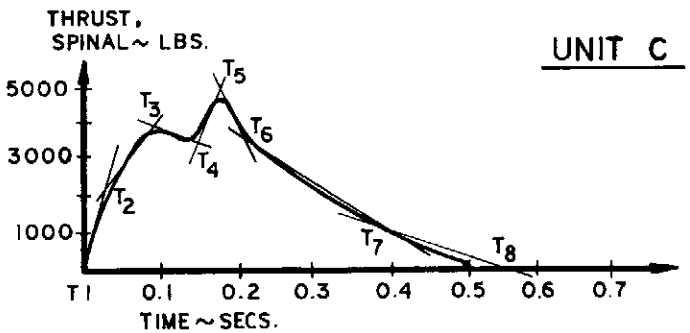

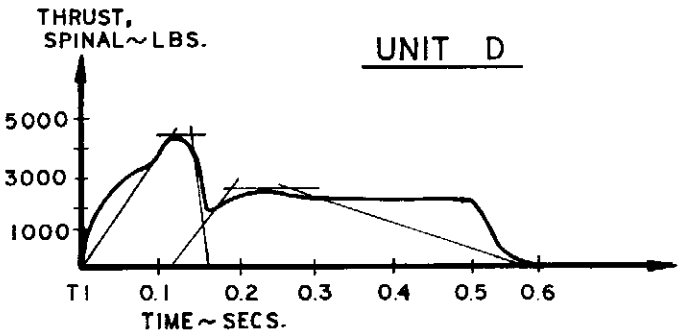

FIGURE 11
ROCKET / CATAPULT CHARACTERISTICS USING THE STRAIGHT-LINE APPROXIMATION METHOD TO SEPARATLY ANALYZE CATAPULT ACTION AND ROCKET SPINAL THRUST

TABLE 3 - DRI Calculations Using Straight Line Approximation to Catapult Action and to Rocket Spinal Thrust Separately

Rocket Catapult	Catapult		Catapult DRI_z	Rocket DRI_z	Rocket Dwell Time, Seconds
	Rise Time, Seconds	Dwell Time, Seconds			
Unit A	.080	.040	17.6	15.4	.112
Unit B	.086	.040	15.3	11.0	0
Unit C	.071	.062	15.4	17.6	0
Unit D	.110	.025	14.8	11.5	0.060

characteristics desired for the AERCAB propulsion subsystem.

(4) Stabilization Subsystem

As previously mentioned, AERCAB employs both Stencel's DART® and a drogue parachute to counteract the moments induced aerodynamically and by CG/Thrust-line eccentricities. The combination properly orients the ejected mass along its trajectory to control the magnitude and sense of deceleration forces applied to the ejectee. The subsystem further sequentially orients the ejected mass along the trajectory at the proper attitude for each forthcoming event (e.g., high-altitude descent, parachute deployment, etc.).

During high speed ejections (e.g., 600 knots) as the ejected occupant enters the air stream with the lowermost slippers still engaged with the guide rails, an angular impulse is imparted to the man/seat combination causing a nose-up pitch rate of 10 to 12 radians per second. It can be shown that this nose-up pitch rate cannot be removed by either a DART stabilization system, or by a gyro-controlled vernier rocket, prior to the time at which the seat has rotated at least 70° backward. At this time the air stream drag of 8 to 12 g's adds to the spinal components of the rocket thrust causing the DRI_z to exceed the 17.0 limit value by as much as 40 percent. Therefore, it is concluded that for high speed stabilization a drag parachute must be rapidly deployed and inflated to assure stabilizing action immediately upon seat/guide rail separation. This drag chute must orient the man's spine nearly perpendicular to the air stream to assure that the air stream drag on the man/seat and on the drag chute is beneficially reduced by the forward rocket-thrust component during the rocket burn time. Approximately 24 g's deceleration, generated by the air stream total drag minus the forward rocket thrust component, are then allowable without having the radical

$$\sqrt{\left(\frac{DRI_z}{G_{z_L}}\right)^2 + \left(\frac{Gx}{G_{x_L}}\right)^2 + \left(\frac{Gy}{G_{y_L}}\right)^2}$$

exceed 1.0. Since G_{y_L} is limited to such small

values ($\approx$10 g's), it is critical that yawing of the seat be prevented. Further, it is important that the air stream drag be felt by the man eye-balls out or eye-balls in and perpendicular to his spine where his tolerance to deceleration is maximum.

To optimize the stabilization parachute it was assumed that the rocket-sustainer thrust-time trace is neutral and very similar to a scaled up version of the previously discussed Unit A's performance, and that the rocket nozzle angle is 45 degrees to the seat back. The C_DS of the man/seat profile for a 5 percentile man was assumed to be approximately 6 square feet. Based upon these assumptions a 1200 pound-per-square-foot q (dynamic pressure) produces 25.7 g's on the man/seat eye-balls out while the forward rocket thrust component produces 9 g's eye-balls in. The net deceleration of 16.7 g's eye-balls out subtracted from the maximum allowable 23.7 g's eye-balls out indicates a 7 g's maximum stabilization chute contribution. Based upon Section 10.1.2 of ASD-TR-61-579, (the USAF parachute manual)[9], it was assumed that the wake of the seat will reduce the drag of the stabilization chute by 1/3. Thus, the stabilization parachute diameter was determined to be 60 inches. A minimum diameter stabilization chute was desired for high speed ejections to reduce the inflation time sufficiently such that seat stabilization is active at seat/guide-rail separation.

Two high speed sled tests were recently performed on Stencel's upgraded A-4 ejection seat. This seat did not have a stabilization chute and in those tests the nose-up pitch rate resulted in a maximum spinal deceleration about 0.15 seconds after catapult separation.

The spinal and fore-aft (eye-balls out or eye-balls in) deceleration traces, as calculated from the test data, showed the contribution of DART in these tests was beneficial not only in taking out the backward (nose-up) pitch rate of the seat/man combination, but also in reducing the spinal acceleration by about 4 g's during DART action time, which covered the period of maximum spinal acceleration. Without DART the spinal acceleration would have been increased significantly.

With spinal accelerations limited to 17 g's maximum for the 5% man (the 95% case was tested in the A-4 high speed sled tests, and is less critical due to increased mass in so far as spinal accelerations are concerned), it is apparent that a stabilization chute is critically needed to prevent backward pitching of the seat/man.

The usefulness of the drogue parachute in event sequencing is emphasized in Section III-3-d, in the discussion of the functioning of the self-rescue mode of AERCAB.

It is important to note that as G_{max} is applied throughout the retardation phase, that this aids in minimizing the time-required to decelerate down to airspeeds compatible with main recovery parachute deployment and inflation, and aids somewhat in overcoming the problem of limb-flailing, since the eyeballs out deceleration tends to cause the limbs to lead rather than trail the torso/seat combination. Also, the man in his ejection seat is clothed for flight in the environs of his crewstation, and he is equipped with a minimum of oxygen in his survival provisions. Thus, if it is necessary that he eject at high-altitudes where it's extremely cold, and little breathable air is available, it becomes necessary to get him down to a minimally suitable environment (about 10,000 MSL) as rapidly as we can. It is also a requirement of USAF that a stable descent from high-altitude be made in a spinal direction. This is, of course, the minimum effective drag profile of the system and so it does meet the rapid descent need. Of course, once main parachute opening altitude is reached, the opening shocks (if in excess of a DRI of 17) cannot be dumped into the man in a spinalward direction. Hence, for the high-altitude descent case the problem becomes one of orienting the parachute load vectors relative to the seated man such that he sees no more than a 17G DRI spinal-compression component, remembering that all other vectorial components must be governed such that

$$\sqrt{\left(\frac{DRI_z^2}{289}\right) + \left(\frac{Gx}{35}\right)^2 + \left(\frac{Gy}{15}\right)^2} \leq 1.0 \qquad (2)$$

(assuming rise times $\geq$ 30 MSEC, and durations of 0-30 MSEC). With a shortening of rise time, or lengthening of duration of force application, of course, the limit values in the x and y terms of this expression will change ——— but the radical expression must be maintained in order to protect the ejectee from serious injury.

The trim-angle of the ejected seat will ideally be at 90° to the airstream because at that angle the forward thrust of the rocket sustainer and the drag of the drogue are virtually cancelling, leaving the DRI loading picture much less complex, with resultant loads directed spinalward. Should the drogue not activate rapidly enough, however, and the seat be allowed to rotate to a 180° trim, then the deceleration due to drag, and the force of the rocket are <u>additive</u> in the spinal direction ——— which <u>can</u> be deleterious, as discussed before. Also, with the seat trimmed at a pitch angle less than or equal to 90°, the flow-field forms a pressure distribution over the upstream-facing area of the ejected mass which inhibits <u>lift</u> on the occupant's legs, and aids in keeping them "pinned" to the seat in a pseudo-restrained fashion. Aft-rotation, at high-speeds, beyond the 90° trim orientation to the flow field <u>augments</u> leg-lift rather than inhibiting it, and incites flailing of the limbs to a dangerous degree.

(5) Terminal Descent Subsystem

The main recovery parachute for the AERCAB occupant is stowed in the headrest, with the risers connected to the restraint harness via manual connector fittings. A retractor reel (comparable in form and operation to standard automotive seat-belt retractors) is incorporated in the riser assembly to permit uninhibited freedom of movement of the crewman in his station.

The subsystem is one conceived and independently developed by Stencel Aero Engineering Corporation[10] to minimize deployment and inflation time without inducing intolerable forces on the crewman, and to maximize the reliability and repeatability of its operation ... characteristics which are not normal to conventional parachutes. During

normal ejections, AERCAB's drogue stabilization/ retardation parachute is released from its seat attachments and is permitted to align and move and align a small deployment rocket a short distance downstream. This movement energizes the rocket, which in turn deploys the main-canopy and suspension lines directly downstream with the canopy-inlet orthogonal to the airflow. The inlet is held closed by the ballistic FAIL-SAFE spreading gun[11] until line-stretch, whereat the gun firing lanyard is tensioned and the gun spreads the inlet for an accelerated inflation.

Initially, SAEC's Ultra-Precision Parachute (UPP) was to be used, but was later rejected because of the inherent restrictions on its use at launch-angles (mortar-deployment) in an upstream direction. In fact, a cross-stream or upstream projection of the spreading-gun equipped UPP can result in a serious delay in inflation if the prevailing dynamic pressure is high enough to prevent spreading gun firing-lanyard stretch until the mortared parachute pack drifts downstream relative to the man/seat payload. Furthermore, a serious collision or entanglement problem exists if the UPP's canopy is spread upstream of the ejectee, and his momentum along his egress trajectory carries him into or through his canopy and/or suspension-lines. Also, if proper control over the system fails, ballistic projection (via mortar) of a ballistically-spread canopy can induce initial inlet spreading with the inlet in a plane parallel with or at an angle askew to the windstream. If the inlet is not very nearly orthogonal to the airflow, a "false apex" may be induced which can structurally damage the canopy by loading it in a fashion for which it was not designed or can induce a "spinnaker"-effect (sail) which collapses the canopy, resulting in reversion to the random, unrepeatable delays in the recovery process common to conventional parachute operation

Stencel's choice of a UPP replacement in AERCAB was a parachute subsystem independently developed by that contractor to eliminate the sensitivity to deployment launch-angle without degrading the rapidity or repeatability of the parachute deployment process. The technique has been

dubbed with the nomer, WORD, signifying Wind Oriented Rocket Deployment (U. S. Patents pending)[10]. During the ejection mode (sans self-rescue), the lower drogue bridles are released prior to the upper bridles, allowing the seat to trim in an eyeballs-up decelerative attitude. At the proper time along trajectory, the upper bridles are released, and after a downstream directed short translation, the tractor rocket (integrated into the drogue assembly) is mechanically actuated via a mechanism analogous to that used for spreading-gun activation. The aerodynamically pre-oriented rocket then applies its impulse to deploy the main canopy from its container in a downstream direction every time. At relatively low airspeeds (relative airspeeds nominally below 150 ft./sec.), the rocket overpowers the drogue input, automatically reefs the drogue, and deploys the canopy and suspension lines of the main 'chute in about 0.400 sec. Such is the anticipated deployment time under "zero/zero" ejection conditions. At higher speeds, then, the rocket merely augments the drogue in deploying the recovery subsystem (about 0.300 sec. to line stretch for the 600 kt./S.L. condition, for example).

Hence, deployment is achieved in a very nearly constant time lapse, regardless of airspeed. The reader will recall that the C-9 canopy is "choke-reefed" by the spreading-gun until the entire subsystem is stretched and aligned with the air-stream. As spreading commences, then, the canopy's inlet is normal to the dynamic-pressure flow field, and a fully-symmetrical filling of the canopy volume occurs. Innumerable tests performed with the spreading-gun as an aid, show the inflation process to also be nearly independent of velocity, with fill times ranging from 0.750 to 0.900 sec. throughout the velocity spectrum from 0 to 300 KEAS.

Adaptation of this parachute subsystem is one more way in which absolute control over the egress/recovery sequence was maintained; and was one in which optimum minimum timing was achieved.

The system schematic in Figure 4 shows that the opposite end of the spreading gun firing lanyard is coupled to the seat in such fashion

that as the line is tensioned by the deployment aids, the sear of a 0-sec. delay initiator is pulled simultaneously with activation of the spreading gun cartridge. That initiator energizes the firing devices in all four of the release mechanisms which previously constrained the occupant and his survival kit within the confines of the seat bucket. Hence, as parachute opening-shock is applied, and the man/parachute ballistic-coefficient (W/C_DS) reduces markedly, and that of the seat alone reduces only slightly, resulting in a net positive differential separation velocity between the two. The ensuing paths of the separated masses are necessarily divergent then, and no post-separation interference is offered.

Throughout parachute deployment and inflation processes, loads imposed on the crewman were computed to ascertain that the Dynamic Response Index radical expression

$$\sqrt{\left(\frac{DRI_z^2}{289}\right) + \left(\frac{Gx}{35}\right)^2 + \left(\frac{Gy}{15}\right)^2} \leq 1.0 \qquad (3)$$

was maintained.

(6) Restraint Subsystem

For escape into high dynamic-pressure flow, full limb-restraint provisions can be made in the portrayed system, although not shown in the drawings herein for purposes of avoiding cluttering up the views of other equipment. Arm and lower-leg restraints are independent of the rest of the system and are considered optional building-blocks in systems subjected to ejections above 400 KIAS, whereat limb-flailing is a known problem. Below 400 knots, the need is not apparent, and incorporation of such restraint would be weight and volume parasitic. The arm restraint is normally stowed flush with the seat-back where it won't interfere with the occupant's access to his consoles in normal flight. During ejection, an inclined plane on the airframe strikes a crank on the arm restraint paddles, and rotates the assembly into a ratchet-locked position wherebetween the ejectee's arms are constrained against lateral or aft displacement. The leg restraint manacles are in a subassembly which is attached underneath the forward portion

of the seat pan. They too are fully automatic, depending on the forces of catapult action to accelerate the crewman's legs aft and down against the buffer-plates which force the manacles into a self-locked position around the lower legs. The manacles inhibit rebound of the feet into contact with the canopy-bow, restrict leg movement due to dynamic pressure lift forces, and preclude "lateral-climb" of the legs over the seat's side-members. At the proper time for sequenced man/seat separation, the manacle assembly is released simultaneously with the torso-restraint in order to permit uninhibited departure of the occupant and his survival equipment on a path that is divergent with that of the then-useless seat and expended ejection/sequencing elements. Upper-arm cuffs can also be attached easily to the seat-back structure to augment arm containment during head-on imposition of dynamic-pressure forces encountered on first entry into the flow-field, while departing the protective confines of the crewstation.

The restraint subsystem also contains a torso garment based on USAF's Dwg. 63J4296, modified to the AERCAB application for reasons discussed in Section III-3-b. During ingress, the crewman is required to be wearing his torso garment, and must manually connect the fittings at shoulder- and hip-level. The upper fittings connect the man to both his parachute risers and his automatic restraint haulback reel. The lower fittings couple him with his survival kit (which in turn couples him firmly with the seat bucket). Provisions for powered haulback of <u>both</u> upper and lower torso can easily be integrated into AERCAB. Automatic release of the subsystem has been described above. In a ditching-situation, the crewman may pull the activation lanyard on his left lower lap strap which releases him completely (in his torso garment) from his parachute, shoulder-restraint, and pelvic restraint. He is then free to climb out over the sill unencumbered by ancillary equipment. Normal egress requires manual disconnect of both shoulder fittings and both leg-strap releases. The system is equipped with a manually controllable takeup reel of the MIL-R-8236 variety. The control is

on the left leg-brace of the seat bucket, just forward of the ejection control handle.

The restraint system protects the crewman against turbulence encountered in-flight, crash-impact, rough-landings and evasive (defensive) maneuvering in combat. The "conventional" inertia-lock reels used in USAF in-service systems are designed to lock during an acceleration period (be it acceleration of the aircraft, or acceleration of the straps from the reel, or both). With such units short-duration, high-peak accelerations that would not cause excessive velocity of the torso approaching contact with aircraft structure (or interfering with flight duties) may in fact lock the reel, while long-duration, low-level accelerations which have a potential for generating deleterious velocities, would not lock the reel to protect the crewman. In our search for a solution to this problem, SAEC found that Space Ordnance Systems, Inc. has devised a powered Restraint Actuator worthy of serious future consideration for AERCAB adaption by USAF. The unit locks with aircraft deceleration in any direction, with acceleration of the restraint straps, and also when strap payout velocity approaches a dangerous magnitude. The SOS restraint actuator is said to give full protection in the 0-3G realm of accelerations encountered during normal aircraft operations; full protection during the "classical" 40G crash; full protection against excessive onsets of acceleration; and full protection during ejection to the point of man/seat separation. In addition to this improved performance, SAEC thinks it valuable for consideration because it is quite simple; does not require manual inputs for lock or unlock, and is lightweight and compact...and cannot fail to lock (as may occur with mechanical locking inertia reels). The ballistic haulback feature incorporates hydraulic buffering which permits haulback forces of sufficient magnitude to retract the crewman under high G's and low upper-torso weight (mass) conditions. For the safety-conscious, it is pointed out that the 4000 psi maximum gas pressure used for power retraction can be confined to a chamber which is easily located in a "buried" locale on the seat structure, away from proximity

with any portion of the crewman's head, body, or limbs. The unit's one apparent deficiency is that the existing device on loan to SAEC for consideration as an SIIIS "building-block" does not have a provision for unlocking (override of the auto-lock) at the crewman's discretion. Using command pilots have expressed a need for such a provision in evasionary combat maneuvering flight, in order to be able to look back over their tail to observe an adversary's "tracking" maneuvers. These airmen are willing to suffer some in-the-cockpit buffeting around, in payment for this additional freedom of movement.

(7) Survival Equipment

USAF, early in the program, established that the AERCAB installation would include provisioning for 1600 cu. in. of survival equipment (weighing approximately 40 lbs.) in the "kit" installed in the seat bucket. Design studies showed this to be practical only in a seat whose dimensions conform entirely with those specified in MIL-S-9479A and AFSCM 80-1. The seating dimensions of AERCAB can be tailored to accommodate these requirements, but not for installation into the A-7 and F-4 crewstations. Section II-6-e of AFFDL-TR-66-150 (Ref. 12) tabulates mandatory, recommended and optional survival items to be packaged in the "kit". Excluded are such items as are normally carried on the crewman's person (i.e., in his clothing), typical of which are the emergency locator beacons and transceivers (e.g , AN/URC-10, for example), pyrotechnic torch distress signals (e.g., the MK-13 MOD O Distress Signal), pencil flares (e.g., the M-131), dye markers, signal mirrors, whistles and revolvers with tracer ammunition. It is noted that the referenced tables cite the following:

Item	Weight	Volume
...Mandatory Survival Equipment	10 lb, 5 oz	242 cu.in.
...Recommended Survival Equipment	12 lb,14 oz	680.8 cu.in.
...Optional Survival Equipment	20 lb, 2 oz	866.8 cu.in.

Assuming the same packing density ($\frac{40}{1600}$ = 0.025 lb/cu.in.),

and noting that AERCAB's kits for the A-7 and F-4 installations respectively have 1250 and 1410 cu.in. of volume available, it is reasoned that all "mandatory" and "recommended" equipment can be carried, along with 328 cu.in. (8.2 lb.) of optional items in the A-7, and 488 cu.in. (12.4 lb.) of optional items in the F-4. The selection of "optional" equipment, of course, depends on the theater of operations.

A miniature transmission beacon (e.g. the AN/URT-21 or URT-27) is housed with the parachute, and is the automatic IFF radio signal generator which is activated by parachute opening.

The above provisions do not include emergency oxygen, and so one must subtract from the above "optional" surplus, a volume of 128 cu.in. (weighing approximately 5.25 lbs.) to provide a 10 minute supply of emergency-0_2 to the AERCAB occupant.

c. Operation

Figures 12 and 13 portray the sequence of events along typical egress trajectories with AERCAB in the PRIMARY ESCAPE MODE. The following narrative describes the operational sequence, and operation of system elements as they function in that mode.

(1) Rotation of either (or both) of the leg-brace mounted ejection actuation control handles mechanically actuates the sears of parallel, independent zero-delay initiators, which in turn generate the pressurized gas transmitted to the primary manifold assembly;

(2) the initiation gases are bled simultaneously into three activity centers. They fire the instantaneous initiators which generate gases which activate the restraint haulback reel and canopy unlock/removal subsystems, and they also energize the dual delay-cartridges in the launch-catapult assembly;

(3) the 0.300 sec delay cartridges in the catapult assembly permit suitable hesitation in sequencing to accommodate complete unlock and removal of the aircraft canopy, and powered repositioning

and restraint of the crewman prior to first motion of the seat/man system;

(4) as the cartridges reach the end of the delay period and generate their gas outputs, the initial pressurization of the catapult tubes causes the integrated pistons to stroke, piercing the canopy if it hasn't properly jettisoned, and deploying the drogue package from its stowed position in the turbofan inlet;

(5) as the canopy-breaker/drogue-slug pistons leave the catapult assembly, the latter automatically seals and unlocks to permit continued pressurization to induce movement between the telescoping inner and outer tubes of the catapults; the ejected package moves upward with the outer tubes, and the inner tubes remain affixed to the airframe;

(6) the ejected mass reaches a translational velocity in the order of 60 ft/sec as the end of guided stroke is reached; just prior to separation of the inner and outer catapult tubes, the stored pressurized gases therein are ported to the sustainer-rocket ignition elements, the turbofan engine starter cartridge, and the drogue bridle release delay initiators; at this time the drogue parachute is considered fully-active in its role as a seat-attitude control aid, and retardation device; the slack-line of the DART® is paying-out at this time, and the seat's angular momentum "error" to be compensated by the stabilization subsystem is beginning to generate as rocket ignition and aerodynamic moments are induced; the cartridge will enable the engine to build up to a negligible idle-thrust output level whereat it will stabilize until throttle inputs are received (approximately 4 seconds are required to reach idle, and the conventional escape mode of operation is completed in less than 3 seconds, so in the primary mode, engine operation produces no useful contribution to system functioning);

(7) the delay elements in the drogue release system burn-off as DART® action controls the seat's attitude and pitch-rate during rocket burning; the dynamic pressure sensor (airframe-mounted)

REVISIONS			
SYM.	DESCRIPTION	DATE	APPROVED

T= 1.48 SECONDS:
SUSPENS ON LINE & CANOPY STRETCH COMPLETED.
DEPLOYMENT ROCKET & DROGUE ARE RELEASED.
FAIL-SAFE SEPARATION GUN IS FIRED, A 0.75 SECOND
DELAY IN VICTOR IS ACTIVATED (FOR SEAT/MAN RELEASE.)
V_x = 50 FPS
V_z = 79 FPS
Z = 87 FT

T= 1.18 SECONDS:
ANGULAR RELATIONSHIP BETWEEN SEAT & DROGUE, PROPER FOR
UPPER DROGUE BRIDLE RELEASE, WHEREAFTER THE MAIN RECOVERY
PARACHUTE PACK IS OPENED & DEPLOYMENT ROCKET IS FIRED,
DROGUE COLLAPSES, MAIN RECOVERY PARACHUTE DEPLOYMENT
BEGINS.

T= 2.23 SECONDS:
MAIN PARACHUTE INFLATED. OCCUPANT RELEASED FROM
SEAT. SURVIVAL GEAR DEPLOYMENT COMPLETED.
V_x = 0.0 FPS
V_z = 0.0 FPS
Z = 109 FT

T= 1.08 SECONDS:
DROGUE INFLATION COMPLETED, DROGUE
DRAG ≈ 82 LBS.
ANGULAR TRANSLATION BEGINS.
V_x = 50 FPS
V_z = 88 FPS
Z = 44.4 FT

T=0.88 SECONDS:
ROCKET BURN-OUT, DROGUE BRIDLES
RELEASED (UPPER BRIDLE CONNECTION
IS MAINTAINED BY A ANGULAR POSITION
LATCH), DART ACTION HAS BEEN
COMPLETED. DROGUE IS STILL IN
THE INFLATION PROCESS.
V_x = 50 FPS
V_z = 93 FPS
Z = 26 FT

T= 0.48 SECONDS:
CATAPULT TUBES SEPARATE. PRESSURE TAP OFF OF CATAPULTS
ACTIVATES ROCKETS, 0.30 SECOND DELAY INITIATORS & 0.90 SECOND
DELAY INITIATORS (FOR LOWER & UPPER DROGUE BRIDLE RELEASES
RESPECTIVELY) PRIOR TO TUBE SEPARATION.

T= 0.0 SECONDS:
EJECTION HANDLE ROTATION ACTIVATES INDEPENDENT ZERO DELAY
INITIATORS WHICH ACTIVATES:
(a) 0.30 SECOND DELAY CATAPULT CARTRIDGE
(b) ZERO DELAY RESTRAINT HAULBACK DEVICE
(c) ZERO DELAY CANOPY JETTISON THRUSTER
AT T= 0.30, RESTRAINT HAULBACK COMPLETED, CANOPY JETTISON CONTINUES,
PRIMARY CATAPULT CARTRIDGE IGNITES, GENERATING PRESSURE TO STROKE
INTEGRATED CANOPY BREAKER/DROGUE MORTAR, UNLOCK CATAPULT TUBES
& BEGIN SEAT MOTION UP RAILS MOUNTED IN AIRCRAFT COCKPIT.
T= 0.32 SECONDS: CANOPY BREAKERS FORCED THRU CANOPY (IF JETTISONING FAILS)
DROGUE DEPLOYMENT BEGINS.

GENERAL NOTES:
EJECTION OCCURS AT ZERO ALTITUDE - ZERO
AIRSPEED.
ROCKET IMPULSE IS 1,680 LB/SEC
CATAPULT VELOCITY = 60 FPS
EJECTED WEIGHT = 530 LBS

FIGURE 12

AERCAB EJECTION
SYSTEM SEQUENCE
LOW SPEED MODE

REVISIONS			
SYM	DESCRIPTION	DATE	APPROVED

T= 0.0 SECONDS:
EJECTION HANDLE ROTATION ACTIVATES INDEPENDENT, DUALLY REDUNDANT, ZERO DELAY INITIATORS WHICH ACTIVATE:
(a) 0.80 DELAY CATAPULT CARTRIDGE.
(b) ZERO DELAY RESTRAINT HAULBACK DEVICE.
(c) ZERO DELAY CANOPY JETTISON THRUSTER.
AT T= 0.30 SECONDS, RESTRAINT HAULBACK COMPLETED, CANOPY JETTISON CONTINUES, PRIMARY CATAPULT CARTRIDGE IGNITES, GENERATING PRESSURE TO STROKE INTEGRATED CANOPY BREAKER/DROGUE MORTAR, UNLOCK CATAPULT TUBES & BEGIN SEAT MOTION UP RAILS MOUNTED IN AIRCRAFT.
T= 0.32 SECONDS, CANOPY BREAKER FORCED THRU CANOPY, (IF IN PLACE), DROGUE DEPLOYMENT BEGINS.

T= 0.82 SECONDS:
ROCKET BURNOUT, LOWER DROGUE BRIDLE RELEASE, V_x HAS DECAYED TO 342 K.E.A.S.
a_x = -15.5 g's, TRANSITION FROM EYEBALL DOWN DECELERATION TO EYEBALL OUT ACCELERATION HAS BEEN COMPLETED.

FROM T= 0.98 SECONDS TO T= 1.98 SECONDS:
V_x DECAYS FROM 342 K.E.A.S.
a_x DECREASES FROM -15.5 g's TO -4.25 g's
ABOVE 14,000 FT., BAROMETRIC OVERRIDE EXTENDS THE DELAY OF THE UPPER DROGUE BRIDLE RELEASE UNTIL 14,000 FT. ALTITUDE IS REACHED. IT IS POSSIBLE FOR V_x & a_x TO BECOME ZERO, & FOR V_z TO BECOME TERMINAL AT 138 K.E.A.S.

T= 1.75 SECONDS:
UPPER DROGUE BRIDLES RELEASE & DROGUE FORCE IS TRANSFERRED TO THE MAIN RECOVERY PARACHUTE.
MAIN RECOVERY PARACHUTE PACK IS OPENED & THE DEPLOYMENT ROCKET FIRES.
DROGUE COLLAPSES DUE TO DEPLOYMENT ROCKET.
MAIN RECOVERY PARACHUTE DEPLOYMENT BEGINS.
60 DELAY INITIATOR IS ACTIVATED FOR SEAT/MAN SEPARATION.

T= 2.28 SECONDS:
SUSPENSION LINE & CANOPY STRETCH COMPLETED, DEPLOYMENT ROCKET & DROGUE RELEASED. SEAT/MAN SEPARATION & SURVIVAL GEAR DEPLOYMENT BEGINS

GENERAL NOTES:
FIGURES SHOWN ARE BASED ON THE FOLLOWING,
EJECTION OCCURS AT 600 K.E.A.S.
CATAPULT VELOCITY 60 FPS
NET ROCKET IMPULSE 1,650 LB/SEC.
EJECTED WEIGHT 330 LBS

FIGURE 13
AERCAB EJECTION SYSTEM SEQUENCE HIGH SPEED MODE

operational requirements. While the "optimum" sensor selected to meet NASA's requirements was an electronic sensor utilizing the Homodyne technique, with a Storable Tubular Extensible Member (STEM) as "backup", SAEC has reviewed the findings and believes that an FM/CW Altimeter utilizes frequency-sweeping of a carrier signal to determine altitude. The frequency difference between transmitted and received (echo) signals is proportional to signal transmit time and is thereby proportional to altitude. One of the primary advantages of the FM/CW device is its long development history which demonstrated remarkably reliable operation. However, current quanticized altimeters (vintage 1963) suffer from inherent "step error" effects at low altitudes. This should not be a significant problem in the anticipated low-altitude operating regime of AERCAB, though. While an FM/CW Non-Quanticized Altimeter would be an improvement due to elimination of step error effects, state-of-the-art devices should apply.

The SAEC studies on radar systems for altitude sensing have encompassed a short-pulse, high range resolution radar system manufactured by the AVCO Space Systems Division of the AVCO Corporation in Lowell, Massachusetts; and a radar altimeter manufactured by Bonzer Incorporation in Shawnee, Kansas.

The AVCO system has an inherent range resolution capability of less than 5 feet even at the desired operating altitude of 200 feet. However the system is designed to sense a given altitude rather than to give a continuous altitude readout. Therefore this unit would be very suitable for switching from the self-rescue flight mode to the terminal-descent (landing) mode but would not be suitable without additional circuitry for giving the ejectee a visual or aural warning signal whenever the AERCAB is approaching within two hundred feet of the altitude of automatic initiation of the terminal-descent mode, or for providing absolute altitude readings for automatic control of AERCAB cruise altitude in the self rescue mode.

The Bonzer absolute altitude radar altimeter

TABLE 7
FLIGHT & NAVIGATION INSTRUMENTATION
WEIGHT AND VOLUME SUMMARY

Item	Envelope	Weight
1) Pressure Altimeter	3" dia. x 4" long	1.40 lb.
2) Gyro. Compass	3.5" x 3.5" x 10"	3.30 lb.
3) ADF-assembly	6.5" x 2.8" x 9.3"	--------
a) 2 Superhet. receivers		6.00 lb.
b) ± Amplifier		1.00 lb.
c) UHF-signal readout		0.50 lb.
d) Keel-Antenna Relation Readout		0.50 lb.
4) Radar Altimeter (with Antenna and Power Supply	2" x 6" x 12"	5.00 lb.
5) Ball-Bank Indicator	½" dia. x 3"	0.25 lb.
TOTAL	10" x 7" x 16" stowed	18.45 lb.

Natick Laboratories, in which terrain proximity sensing activates the retrorocket final descent device. Under N00178-68-C-0174, for the U. S. Navy's Naval Weapons Laboratory, SAEC is performing a research study of a parachute recovery subsystem for helicopter crew module recovery, again employing parachutes and retrorockets for the case of the heavier class of capsules, in which retrorocket ignition depends on sensation of absolute altitude. The findings of both programs contributed to the AERCAB investigation.

The NASA Manned Spacecraft Center was contacted to acquire additional information regarding the absolute-altitude sensing accomplishments at the Houston MSC. The crux of their work was centered about the use of extendable-boom type sensors (up to 18 ft. in length), and variations of a Doppler radar system for the LEM (Lunar Excursion Module). NASA did provide Sylvania Report No. A58-4-5.0-17 (two volumes), "Final Report -- A Study to Select Optimum Altitude Sensing Devices", May 1963, prepared under Contract No. NAS 9-1098 by Sylvania's Electronic Laboratories in Williamsville, New York[19]. Under that study, forty-three sensing devices were explored, and six devices were selected for preliminary design to meet the

is connected either to the visual indicator (needle-dot) for manual access, or to an automatic control system (pulsed servo). Deviation (angular) either right or left of a radial would result in a corresponding "error" output from the amplifier. Because of the angle sensitivity the antennae must be "pointed" at the beacon at all times to home-in.

In cross-wind environments, then, either a relatively inefficient (fuel-consuming) staggered course is flown; or the AERCAB vehicle must fly in "crabbed" fashion (which it doesn't do well) to maintain antennae orientation along a radial; or the antenna assembly can be independently suspended relative to the wing keel and manually-rotated to aim the antennae at the beacon and subsequently align the keel (via appropriate maneuvering flight) with the antenna array. In the latter, slip-rings could be employed to furnish a signal displayed to the pilot to show the angular relation between the keel and antennae.

Figure 5 shows a front view sketch of the instruments as mounted to AERCAB's "airframe". Mirrored panels are extended forward in flight to enable the crewman to see the instruments which remain in their position alongside the headrest.

Table 7, below, gives a summary of size and weight data referenced in the estimates of total system packaging and weight.

(4) Terrain-Sensing Subsystem

Absolute altitude is an entity which must be known both as an input to the conditions-computer which overrides a manual selection of self-rescue under adverse conditions; and as a means for switching from the self-rescue to the terminal-descent (landing) mode at the "end" of self-rescue flight, for whatever reason SAEC has performed under two active contracts inhouse, besides the AERCAB investigation, in which terrain-proximity sensing plays a major role. Under DAAG-17-68-C-0019, SAEC is performing an in-depth investigation of a Parachute-Retrorocket Airdrop System (PRADS) for the U. S. Army's

For navigation purposes, a redundant system is provided. A gyro-stabilized compass, which is coordinated with the aircraft compass at ejection to establish heading reference, is provided to enable a "general direction" heading (magnetically dependent) in the event the ADF unit malfunctions. With the compass, the pilot will be able to direct his flight path at least in a general direction toward friendly forces, and if a map is available to him as a part of his visual aids display, can fairly efficiently navigate to a selected rescue site.

Several automatic direction finding (ADF) subsystem approaches were investigated. These are discussed at greater length in Section V-3 herein.

For system volume and weight estimating purposes, an ADF arrangement suggested by the USAF was used as a base reference. The system was lightweight and not complex, and with some other approaches considered, appears fully feasible for AERCAB use. The concept is one which requires that UHF homing beacon transmitters be located tactfully in low-populated rescue areas within self-rescue range of AERCAB. A pair of antennae are mounted (upwind-directed) on the parawing. These antennae in unison emit a receiving wave pattern characteristic which readily discerns (via signal strength measurement) angular disorientation form a radial of signal transmission with its origin at the beacon and its terminus at the antennae. A pair of superheterodyne receivers are connected between the antennae and a sum-and-difference amplifier, and of course a power source (engine generator).

As the AERCAB is ejected and achieves steady flight, a powered climbing turn would be programmed in to enable the antennae to be exposed to a full 360^{o} spectrum of potential beacon locations if necessary. The climb provides a gain in altitude to let AERCAB "see" a signal from a beacon initially behind a significant obstacle. As the apex of the wing (and the node of the antennae array) aligns with an in-line heading (radial) with the beacon, a steadying signal is produced by the S & D Amplifier which

required that the system give the man an "adverse weather operation" capability. USAF's definition of adverse weather included virtually all possible environments, excluding only severe thunderstorms, tornados, hurricanes, typhoons, or prevailing winds in excess of 30 knots.

Since AERCAB is an emergency flight system, a relatively meager display of instruments was considered acceptable. The fewest possible visual aids were provided to conserve space, weight and electrical power requirements and still enable the pilot to fly "blind". Audio aids could conceivably be developed in the future to replace the instruments, which would considerably simplify the design of the aids-group in so far as getting the proper information to the pilot. Under this program, however, only "conventional", visually perceptable displays were considered.

For flight path monitoring, an altimeter and ball-bank indicator are provided. The altimeter presently in the design is connected to the radar subsystem onboard which measures absolute height above the surrounding terrain. The altimeter can be scrutinized during a turn, in conjunction with the ball indicator, to aid in coordinating a turn with minimum altitude loss. While a pressure altimeter might be employed, it is presently believed that the absolute altimeter will also provide forewarning of approaching obstacles (e.g., mountains) during "blind" flight (at night, through fog or clouds, etc.).

A red critical-altitude warning light is also provided which illuminates whenever the pilot flies within 200 feet of the altitude at which he will be automatically separated from AERCAB and recovered by parachute.

A fuel-low amber warning light illuminates when 5-minutes fuel remains in the tanks to provide the pilot with a chance to select and fly under power to a suitable landing site in the event he has not yet reached his allies.

The optional fuel pressure low, and oil pressure low warning lights were described in the propulsion subsystem discussion.

end to the leading-edge booms of the parawing at approximately their midpoint. As the control handles are deflected and the drum turns, the cable is shortened on one side and correspondingly lengthened on the other such that the wing is rotated about its keel axis, effecting the bank angle needed for the turn. Power for control is provided via generator and battery (see Figure 4).

Because of lack of sufficient stowage space available to accommodate the required section modulus for aluminum structure, the principal members of the wing and support structures are made of high-strength steel. The resulting penalties in total system weight were found to be minimal. The wing's keel and leading-edge booms are of telescoping construction, pinned to the apex plate in rotatable fashion. Lateral spreader bars are used to maintain the proper flying planform. The tripod support articulates into the flight arrangement as guided by integrated bearings which follow the keel-line during deployment. Spreading of the leading edges and erection of the wing assembly occur simultaneously. The vertical fin is a non-porous flexible sail attached along the entire length of its base to the keel, and its apex is attached to the lower-rear lateral support beam in the articulating support assembly. If necessary (subject to future experimentation) additional fin area is easily incorporated into the system.

(3) Flight and Navigation Instrumentation

Subsequent to ejection and achievement of steady-state flight in the self-rescue mode, the AERCAB pilot must be equipped to find and lock onto a homing flight path, and sustain controlled flight for as long a time as fuel available permits, or until he succeeds in mating up with allied rescue forces. A simple means had to be provided for his establishing and maintaining the desired flight path. While an automatic homing flight subsystem is believed to be feasible in AERCAB, the studies concentrated on giving a manual capability which in the future could be replaced or augmented by the automated subsystem. It is noted that it is

discussed in Section IV.

An inertial brake is integrated into the subsystem to control the rate of rotation of the wing and tripod assembly from the stowed to the flying positions. The rate of erection must be retarded to preclude irreversable tumbling which could be thereby induced. The mechanics of this phenomenon were not defined under this investigation, but should be in subsequent analyses of system transitional dynamics.

Limits will also have to be imposed on the rate of application of engine thrust in order to prevent entry into whip-stall maneuvers which also induce subsequent irreversible system tumbling. A rate-limiter on the engine throttle would readily serve this purpose.

Several methods of implementing flight control were investigated. Rotation of the wing about its CG-trim axis for longitudinal control was studied and rejected because of the complexity inherent thereto with the requirement to trim out all moments about the CG simultaneously with maneuvering via wing rotation (in the pitch-plane). Also, that method required trimming of the stick force during change in angle of attack of the wing by shifting the wing's center of rotation.

Attention was given to the use of engine thrust-vectoring (via bending of the exhaust flow with a vane in the tailpipe, or movement of the tailpipe itself). However, the mechanical design complexity of such a method was a system penalty, and since only the jet exhaust, and not the fan exhaust, was available, the required deflection angles were excessively large.

With the seat adjustment mechanism available to implement longitudinal trim, it was finally resolved that control in the pitch plane (ascending and descending powered maneuvers) was best achieved by engine throttling.

Turning control is achieved in AERCAB via an electric-motor driven drum about which is wound a flexible, continuous line which is affixed at each

overshadowed by the easing of installation in the tight confines available.

The wing ultimately selected is shown in the "AERCAB Flying Arrangement" in Figure 3. Its basic characteristics are summarized as:

(a) flat planform sweep angle: 45^{o}
(b) flying sweep angle: 55^{o}
(c) keel length: 81.5 inches
(d) leading-edge boom lengths: 81.5 inches
(e) wing area: 32.68 sq. ft.
(f) cruise angle of attack: 29^{o}
(g) wing-alone lift coefficient: 0.60 @ L/D max
(h) wing L/D: 4.615
(i) wing drag coefficient: 0.13 @ L/D max
(j) maximum wing loading: 16.21 psf
(k) minimum wing loading: 13.77 psf
(l) cruise wing loading: 14.99 psf
(m) support assembly drag coefficient: 0.0334

The characteristically high wing-loading and relatively high dynamic pressure operation has not been previously tested for steady-state flight with conical parawings, and is subject to future experimental verification.

A great deal of care must be taken in tailoring the wing to minimize lobe-assymmetry and trailing edge lufting (sail-flutter).

The wing has an inherently negative pitching moment characteristic[20], hence it is essential that the drogue parachute provide a positive elevation input to the wing during the controlled deployment process (the deployment sequence is described in Section III-3-c, and is illustrated in Figure 17). If the wing were permitted to assume a $+90^{o}$ angle of attack during deployment, system tumbling is expected to result; thus the need for absolute control during the transient period of reconfiguring from the ejected to the flight arrangements.

The vertical fin surface shown in the flight arrangement drawing is included to inhibit adverse sideslip effects encountered in turning flight, and as an aid to lateral stabilization. The need for and sizing of the fin surface is

cylindrical parawing, it was felt that on AERCAB, L/D's in the order of 3.5 could be more reasonably counted on in free-flight. In fact, the data generated by Republic Aviation Corporation's close-coupled Parawing Bomblet was expected to be quite closely matched by SAEC's AERCAB in power-on flight, (Reference 18).

(L/D) maximum for cylindrical wings is much more sensitive to aspect ratio than is that for conical wings. The addition of a small amount of washout (achieved by careful tailoring) also can markedly improve (L/D) maximum, as shown by Bugg (Reference 17). This latter tailoring has been shown to be most effective on cylindrical wings.

The cylindrical parawing had another useful characteristic applicable to AERCAB. C_L max is important to power-off gliding flight, as is a high L/D. But, under power, a high L/D at a low C_L can increase the speed capability of the wing at a given wing-loading (W/S). The higher L/D allows a significant (30%) reduction in thrust-required for forward propulsion of the cylindrical wing, while maintaining acceptable cruise velocity levels. Reference 15 points out, for example, that at a wing-loading of 6 psf, the (propelled) speed of a system could be increased from 65 knots with the conical wing to about 95 knots with the cylindrical wing.

Little is published on the free-flight stability characteristics of cylindrical parawings, and while Sleeman, Croom and Rogallo (Reference 15) feel that dynamic lateral stability problems may arise, SAEC found that lateral control and stability is readily enhanced by the addition of auxiliary surfaces (as was done by Barish on the Sailwing, and by Notre Dame, on Jalbert's Parafoil).

Once the structure and construction of the cylindrical parawing was closely investigated with respect to stowage in AERCAB, and its performance advantages were weighed against the stowing and deployment disadvantages, a decision was made to revert to the conical type wing. The corresponding small apparent degradation in performance characteristics was markedly

where gliding ram-pressure is scarce. This rationale is questionable, however.

(L/D) maximum values demonstrated by the Parafoil to date are equivalent to those of small-L.E. parawings (even though calculated values are much higher...). Packaging, and deployment techniques in a relatively high - q flow field (approaching 30 to 35 psf) were thought to be real problems.

The cellular construction of the parafoil demands use of a lot of material, and packaging space available in the cockpits considered herein is a premium. Hence, since equal performance is achieved by parawings, which are characteristically lower weight and require less volume (being single-membrane devices), and much packaging and deployment work has been accomplished by the NASA (Reference 15) to make them operationally suitable, the decision was made by SAEC to use the small-L.E. parawing on AERCAB in lieu of the parafoil.

Conical parawings have a characteristic high-drag associated with the large variation of aerodynamic twist across the wing span (Reference 15). (For some wings this washout at the tips was as high as 60°.)

Polhamus, Naeseth and Bugg (References 16 and 17) determined that L/D ratios of parawings could be enhanced by eliminating the wing-twist, and adding small, tapered leading-edges. These cylindrical parawings appeared to lend themselves best to the solution of AERCAB's lift problem.

Some compromise was expected to deployment simplicity, wing-loading, packing-volume, wing-weight, and complexity because of the 100 knot target cruise velocity requirement. (Investigation under the program, for example, proved that a rigid frame is necessary, including solid leading-edges and lateral spreader-bars.) However, such compromises were expected to enhance, rather than detract from, overall AERCAB system capability and usefulness.

While tunnel tests have demonstrated L/D's in the order of 17.0 for the small leading-edge

optimum time-sequencing, the "parachute-like" devices (Parasail, Para-Commander, Cloverleaf, Sailwing, and slotted circular wing) were eliminated from contention toward the AERCAB application.

The all-flexible parawing was eliminated from this application because of the problem, repeatedly demonstrated, which Barte (Reference 14) reports as related ... "to the operating lift range between its nose-collapse boundary (for minimum lift) and its stall boundary. This boundary is determined by the construction of the wing, as well as by geometry, since the apex is lightly-loaded. A slight weight increase will require slightly more lift, a disproportionately higher angle-of-attack, and thus a decrease in the usable lift range...". Such a sensitivity to minute variations in weight is hardly acceptable when the 5th through 95th percentile aircrew population must be "hands-off"-recoverable by AERCAB. The nose-collapse problem anticipated under powered-flight further aided in eliminating the all-flexible parawing from contention.

The relatively lower lifting-performance, lack of published quantitative data, and suspected susceptability to incompatible power-on/power-off flight characteristics all contributed to the elimination of Goodyear's "Ram-Air Inflated Wing".

The job of selection then became difficult. The remaining candidates were the "Parafoil" and small leading-edge parawings. The parafoil has been tested extensively in free-flight and wind-tunnels. It is aerodynamically efficient because with ram-air's help, it takes a rigid-wing flying shape, and it employs membranes extending cordwise and spanwise to distribute forces desireably and to channel airflow such that spanwise flow is reduced, tip losses are lessened, and 3-axis stability is enhanced (Reference 14). The operating lift-coefficient range of the Parafoil is very large, and stall is quite gradual, with positive lift available well beyond stall. Based only on limited information on hand, aspect ratio of the Parafoil was thought to be limited to a value near 2.0, by a phenomenon wherein pleating-collapse occurs at certain low angles-of-attack

Of the entire LTA class of devices, Goodyear Aerospace Corporation's Vee-Balloon (TM) appeared to offer the most useful frontal profile for a propelled system ——— and allegedly has a "high L/D". Quantitative data was unavailable, unreliable or incomplete, however, and so some reasonable approximations were made in assessing the Vee-Balloon's value to the AERCAB application.

The construction is basically that of a pair of converging ellipsoidal gas cells adjoined at the upstream end, and spanned by a pressurized "stabilizer" of essentially rectangular planform, mounted near the downstream end. At very best, with such a construction, the weight of the balloon material would be at least twice (or more) that of an equivalent-sized single-membrane device (i.e., planform area) ——— when coupling this conclusion with the additional anticipated difficulties related to the need for rapid deployment and the stowage of high-pressure "buoyant" gases in correspondingly heavy containers, little further attention was paid to LTA; and all attentions were aimed at the compact, lightweight, flexible, deployable "flexiwing" devices.

In support of the study effort, an extensive literature search was accomplished to gather specific, demonstrated performance data of such flexiwing devices as the flexible Parawing, Sailwing, small-leading-edge Parawing, limp paraglider, delta planform conical and delta planform cylindrical parawings, Parasail, Cloverleaf, ram-air inflated wing, Parafoil, slotted circular wing, and Rogallo;s "Flexible Kite" (U. S. Patent Office Number 2,546,078).

As pointed out in Reference 14, flexible wings generate a good L/D for the system penalty paid, and offer maneuvering capability not available from parachutes. The flexiwings permit much wider variation in geometry than do the rigid wings used in aircraft design.

Because of their relatively limited maneuverability, and inherent (and repeatedly demonstrated) problems with deployment, coupled with the fact that certain and immediate deployment is a must for

through use of a parawing. The wing is rigidly coupled to the man/seat payload by way of a deployable, self-locking X-structure of tripod design. Maneuvering control is achieved by banking the wing about its keel axis. The wing, support-structure and control devices make up the parawing subsystem.

Early in (and even prior to) the program reported on herein, Stencel reviewed several lifting-device concepts to seek out the most appropos one for AERCAB integration.

The aspect ratio and thickness of a "conventional", rigid-wing of rectangular, tapered, or elliptical planform which would be required to give AERCAB the desired power-on/power-off lifting characteristics were calculated to be quite large. The structure demanded by a wing of such large aspect ratio, if stowable in cockpits defined by the requirements of this program would be prohibitive from a weight standpoint because of the articulation which would be required to position them relative to the entire system's mass and the thrust vector. The complexity of an articulating rigid wing is similarly considered prohibitive from a servicing and maintenance viewpoint. The thickness resulted in rejection due to space limitations. Further attempts to improve on rigid wing usefulness, for example by implementing the flat-plate sides of the seat as lifting surfaces, were set aside when flat-plate lift-coefficients were determined to be unacceptably low.

As far as the contractor was then concerned, only two avenues of approach remained for investigation in the search for lifting devices: one being lighter-than-air (LTA) devices, and the other being the flexible or semi-rigid devices in the parawing, lifting-parachute, sailwing, or inflatawing class.

Of the LTA class the "aerostat" or balloon type of device was quickly eliminated because of its inherent lack of gliding capability, or controllable transverse flight at the target speeds of 100 knots minimum, without phenomenal power requirements. The required capability for adverse weather operation further refuted the consideration of such high-frontal drag area generators.

may be used for lubrication, cooling and as a generator-actuating fluid. Engine manufacturers were queried to determine if loss of oil pressure constitutes a hazard to the occupant in the form of resultant heating causing the engine to "freeze" and/or throw compressor blades, or start a fire on-board. It has not been determined if this is a problem with this class of engine, and may be found worthwhile in future development to incorporate an oil-pressure-low warning light. Similarly, if the fuel tanks will require pressurization via compressor air to prevent vaporization at altitude, and if such vaporization would constitute an explosion-hazard, then it may be necessary to incorporate a Fuel-Tank Pressure-Low warning light to provide the occupant with sufficient time to leave AERCAB prior to development of a hazardous condition. The need for pressurization has yet to be ascertained.

The engine's calculated thrust-available characteristics are quite phenomenal. It is worth noting in this discussion that such an engine is untypical of "conventional" powerplants because the turbine-inlet temperatures are allowed to be relatively high (in the order of 1950°F) This accounts for the remarkably high by-pass ratio achieved, and is permissable since the engine in the AERCAB application has but a 30 minute useful service life at the maximum output level, and cruise conditions would be less severe.

The primary engine accessories deemed necessary to date are the starter assembly, fuel-pump assembly and generator assembly. The electrical system onboard was analyzed, and the generator was sized accordingly. A 1.0 to 1.1 KVA output is estimated to be quite adequate for system electrification.

The fuel cells on AERCAB each hold up to 6.2 gallons, and are vertically and longitudinally baffled to ease dynamic sloshing effects, and to minimize tank deformation under high G-loading.

(2) Parawing Subsystem

The AERCAB lift-generation capability is provided

effects.

As shown in the preliminary design drawings herein, the onboard fuel is stored in cells mounted on the outboard lateral sides of the seat structure, with the cells projecting above the cockpit consoles into the volume available thereabove. No alternative to fuel location was evident other than remote storage with a surge-transfer system to fill the onboard cells activated by ejection control first-motion. Since only 300 miliseconds are available between ejection initiation and escape system first motion up the rails; and because of the additional weight, bulk and complexity involved, the surge-pump fuel transfer technique was rejected. Toxicity of fumes, fuel flammability and volatility were identified as those properties which make fuel containment in the crewstation potentially dangerous. However, judicious employment of tried-and-proven tank-sealing techniques eliminates the problem of fumes and vulnerability to small-arms fire. Furthermore, proper use of foam, jellies, and perforated macrospheres in the tanks readily suppresses the explosion problem. JP-5, because of its lesser flammability and volatility characteristics (as compared to JP-4) would be preferable, until improved fuels are developed. Fuel leakage into the crewstation prior to rocket ignition will not be tolerated.

In designing the general arrangement, due consideration was given to providing a good inlet which inhibits flow-separation to preclude surging of inlet-air (which could contribute to compressor stall). In reviewing requirements for engine-monitoring visual aids to be provided for the AERCAB pilot, it was decided that an engine fuel-pump failure warning indicator would not be necessary, since loss of fuel merely results in progression into the automatic descent mode induction in any event, whether the pilot knows he's out of fuel or not. The latter does away with the requirements for capacitance type fuel-level probes in each compartment set aside for fuel-containment, and does correspondingly simplify the design task, and overall complexity. Oil under pressure

availability of suitable mounting surfaces, and ended up being mounted to structural supports required for crash integrity even had the engine not been integrated (i.e., redundant structures were unnecessary). However, the engine was "fitted" simultaneously with other major system elements to avoid packaging distribution and interference compromises to the total integrated system.

Engine start can be achieved either by direct impingement of launch-catapult gases on the turbine blades (in which case a manually activated cartridge starter could be redundantly included as a backup); or, the catapult's gases may be ported to the ignition element in the starter cartridge for more "conventional" starting. In the latter case, redundancy would require a second starter cartridge as backup (thereby adding weight and consuming space available).

Preliminary studies by the engine manufacturer indicate that the high accelerative loads encountered during ejection and retardation will have some effect on final engine design. Those forces might be expected to alter the engine bearing support design criteria somewhat, or the rotor clearance criteria. Continental's spring cage supported bearing design methods, however, are expected to allow the bearings to bottom-out under such loading conditions (similar to bearing deflections experienced by an engine running through a critical speed). Because of the small engine size, forced structural deflections throughout the engine will be less than those encountered in larger engines. Hence, mount reactions are expected to be relatively minor, even under high G-loads.

At this writing the only engine components significantly influenced by operating environmental temperatures (0^{o} to 110^{o}F) are those in the cartridge starting system. However, even this influence is considered to be of a minor nature. A quantitative evaluation of the noise generated by the engine has not yet been made. The noise perceived by the occupant however, is quite dependent on other noises to which he is exposed (airflow past his head, for example), the acoustic insulation afforded him by the seat, and his personal equipment (e g., type of helmet). Additional studies would be required to quantify these

to accomplish the same task. Rockets were correspondingly rejected, and an engine in the turbojet class was searched for with suitable characteristics.

In the very earliest design concepts, two different turbojet engines (with single stage compressors, annular burners, and single-stage axial turbines) were considered. The thrust-available characteristics were quite suitable for the AERCAB application. However, several turbofan concepts were simultaneously being considered, and it was found that suitable turbofan engines were even more desireable for adaptation to this application than the turbojets For one thing, the thrust specific fuel consumption of the turbofan is approximately 20% lower than that of the turbojet. The net thrust available with airspeed at all AERCAB operating altitudes is significantly greater from the turbofan. With the fan engine, roughly 30 to 60 percent of the thrust is produced by the fan. The ducting of the fan-exhaust outside the basic engine, rather than totally through the combustion chamber, gives the engine the reduced SFC characteristic. The bypass air further provides a cooling effect which ultimately results in no need for auxiliary insulation on the outer engine surfaces for thermal protection of adjacent subsystems and components. Because the fan engine accelerates much larger quantities of air than does a turbojet, the fan engine is capable of generating greater thrust at lower relative airspeeds. Hence the thrust per unit weight efficiency of the turbofan is quite high. Versatility in fan placement and sizing gave much more freedom in installation and packaging design than could be achieved with a turbojet engine of equivalent power available characteristics. One further distinct advantage to AERCAB was the fact that the velocity of exhaust gases emitted from the fan engine are considerably lower than that of the turbojet (exhaust gas power is extracted to drive the fans via an additional turbine stage), and the lower exhaust velocity inherently means less noise being generated; an important consideration in the concept studied under the subject program.

Engine placement in the AERCAB was dependent on

FIGURE 16

CONTINENTAL MODEL 485 AERCAB HIGH BYPASS RATIO TURBOFAN

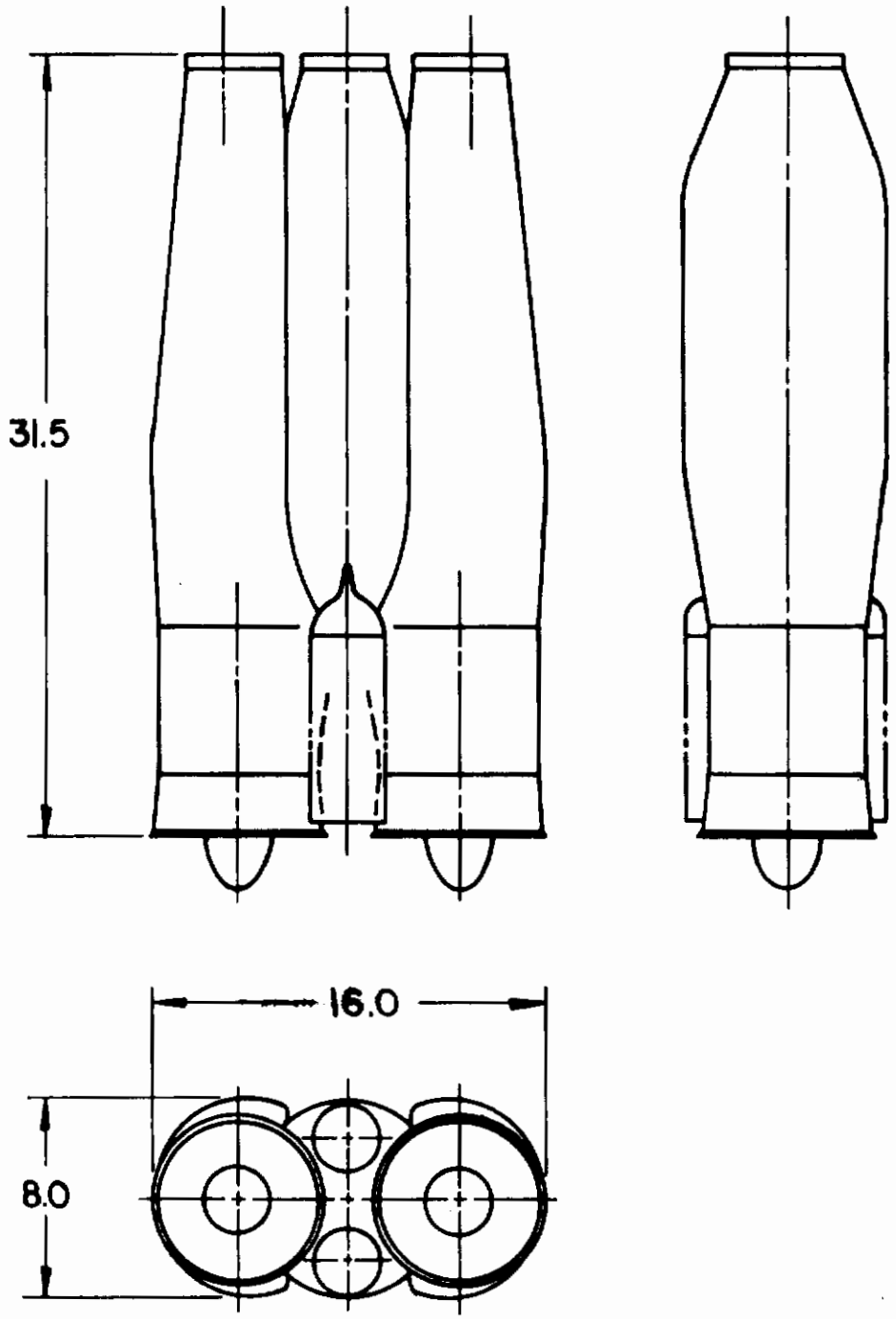

FIGURE 15
AERCAB POWERPLANT
THRUST CHARACTERISTICS

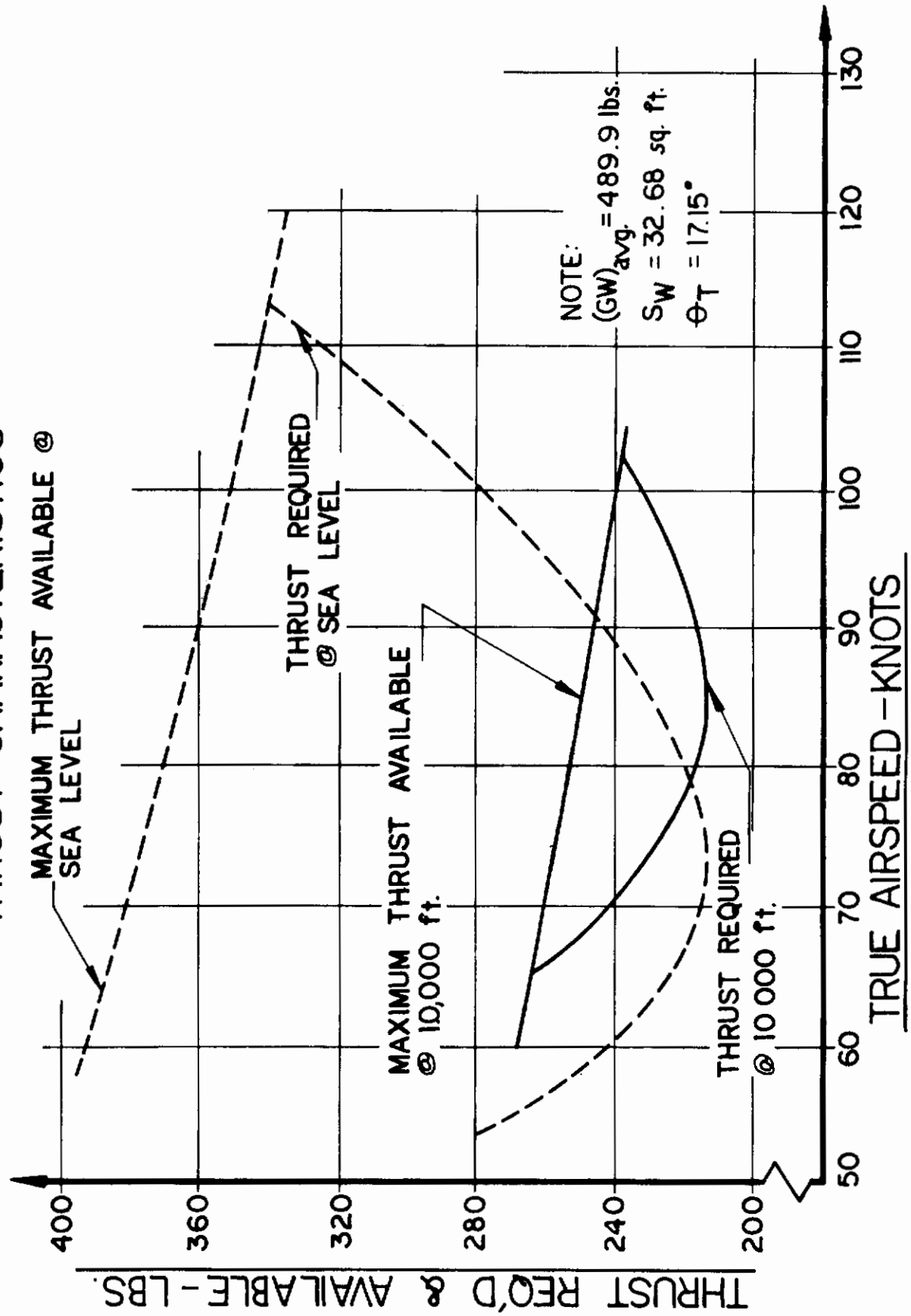

AERCAB in flight, and fuel had to be carried onboard to feed that powerplant. The engine, fuel system, pertinent instruments, controls and accessories make up the flight propulsion subsystem which is completely separate and independent of the egress propulsion subsystem discussed earlier in this report.

Progressively throughout the investigation, as the design of the system changed, the powerplant requirements also changed. Figure 15 portrays the thrust-requirements at sea level and at 10,000 ft. pressure altitude for the finally selected system arrangement shown in this report. Superimposed thereon are the thrust-available characteristics of the Continental Model 485 turbofan engine, shown in the line-sketch of Figure 16, which was the powerplant ultimately selected by Stencel for AERCAB propulsion.

Many state-of-the-art powerplants were investigated prior to and early in the program.[13] Because of inherent danger, noise and vibrations, and apparent installation problems, reciprocating and turboprop engines were discarded from further consideration. The overall efficiency (i.e., the ratio of useful work available to the heat energy of fuel and oxidizers) of the ramjet is virtually zero at the velocities prescribed for AERCAB flight, and so the ramjet was also rejected.

At an average airspeed in the order of 100 kts. (cruise), it can be expected to take approximately 30 minutes to traverse the 50 miles in range until fuel depletion (more exacting figures are presented in Section IV herein). Initial estimates assumed that the system would generate an L/D in the order of 3.0 and would weigh about 525 lbs. It was realized that the specific fuel consumption of a rocket is in the order of 16 lb/hr/lb-thrust. Hence, approximately $\frac{1}{2}(16)(175) = 1400$ lb. of fuel and oxidizer would be required for a half-hour flight with the thrust of the rocket just equal to the then-estimated 175 lb. of aerodynamic drag. Comparitively, known turbojet engines exhibit specific fuel consumption characteristics in the order of 0.8 lb/hr/lb-thrust. Under identical conditions, then, the turbojet would require only 70/1400 = 5% the fuel-required

mechanism, a flight-trim (longitudinal) device, and a main-recovery parachute secondary deployment mortar. The linear-actuators, for deployment of the instrument package into its flight position, serve as a structural beam in support of the forward coupling column of the parawing erection and support assembly (Ref. III-3-b-(3)). The ejection control handles serve dually as flight maneuvering control handles, and engine throttle controls. The catapult manifold serves as a crash-load transferral beam, and as a DART anchor to the airframe. The seat locking pins which made maintenance and servicing a simple task, also serve to react all inflight and crash upward loads. The drogue container serves as an inlet plug to protect the engine against sand and dust accumulation while dormant in the crewstation. The torso-garment serves dually as a flight-restraint means, a parachute-harness, and self-rescue flight "hammock". The seat bucket frame also serves as an ejection slipper assembly. The gas used for launch propulsion (in the catapults) is reused for rocket ignition, sequencing activation, and jet-engine start. The seat adjustment hydraulic cylinders are used as shock absorbers to attenuate hard-landing forces felt by the crewman. All restraint system connectors are also automatic-release devices. The leg-flailing restraints serve as a leg-rest for self-rescue flight.

All such innovations aided markedly in the resultant capability to integrate the system into a minimum envelope.

b. Self-Rescue System Elements

The major AERCAB system elements essential to the system's self-rescue, recovery and survival operations include the escape system elements described in Section III-2-b herein, and additionally:

...Flight propulsion subsystem
...Parawing subsystem
...Flight and navigation instrumentation
...Terrain-sensing subsystem
...Flight conditions assessment computer

(1) Flight Propulsion Subsystem

Because the fundamental self-rescue mission requirements included a climbing-flight and extended range (50 nautical miles) capability, a power-plant had to be selected to overcome the drag of

wherein self-rescue was not required. Increased emphasis on integration of AERCAB into the miniscule cockpits of the A-7 and F-4 aircraft removed that concept from continued study under this program, but the system in modular form remains attractive for application to aircraft having crewstations conforming to AFSCM 80-1 requisites. The size differential between the two approaches is in the order of three-inches in the fore-aft direction (i.e., the modular concept being the larger of the two).

The engine depicted in the drawings incorporated herein is Continental Aviation dual-fan jet engine Model 485, which is preliminary design powerplant configured specially for the AERCAB. Existing powerplants were investigated, and it was found that no "off-the-shelf" engine is available which delivers the power required, has suitable fuel consumption characteristics, and yet fits within the volume available in the integrated system.

As an aid in minimizing the installation envelope many subsystem elements were stowed in space other than that which they would occupy while functioning during self-rescue flight. Typical examples are the drogue parachute, the main-recovery parachute, the instrumentation package, and the parawing assembly. The drogue is stowed in the engine inlet, and is deployed therefrom by the canopy-breaker assembly approximately 200-milliseconds prior to firing of the engine starter cartridge. The main parachute is stowed in the headrest, and remains therein until extracted by either the WORD or the static line. The flight and navigation visual aids are stowed on both sides of the headrest, and are moved to the useful position via linear actuators during wing deployment. The wing and coupling framework is an integrated articulating and telescoping mechanism that permits condensed stowage behind and about the engine in the aft-most compartment of the seat structure. The entire assembly is erected and spread to the flying configuration by drogue parachute action.

Wherever possible, a given subsystem or device was given more than one functional task to perform for the system, again to avoid space consuming and weight-additive "extras". Hence, the catapult assembly serves also as a canopy-breaker launcher, a seat-adjustment

control was finally implemented by banking the wing about the keel axis, and it was resolved that a vertical fin (flexible, deployable) would necessarily be incorporated to enhance turning control and diminish adverse sideslip effects. Longitudinal control depends solely on engine throttling (with "fixed" glide characteristics altered only by trim-adjustment).

Too rapid, or uncontrolled, deployment of the wing from the stowed to the flight configuration was found to be a critical contention from both a structural and stability standpoint, and the decision was made to incorporate a braking mechanism on the flexible keel/boom-apex suspension line connecting the apex to the payload in order to control the rate of wing deployment as a function of the dynamic-pressure prevailing throughout the deployment process.

The effect of the braking mechanism on system stability was not determined under this investigation, but is an important consideration which must be studied during future system development. The sequencing is to be fully automatic as described in Sections III-3-c and -d.

Inhibition of flow-separation and surging of inlet air fed to the engine was found to be an important criterion, and with the finally resolved flight system arrangement it was necessary to include a rigid inlet-extension as an airflow control measure. Initial designs made no such provision.

One design concept investigated in depth under the program was comprised of a modular system in which the escape system was completely separable from the "self-rescue module". The concept had many potential advantages over the unitary design, particularly in the logistics involved. In that concept, the ejection-only mode found only the man/seat/parachute/survival-equipment package being ejected, leaving all self-rescue equipment behind in the aircraft (including fuel, engine, wing, flight instruments, etc.). Only if prevailing conditions were favorable, and the discreet selection were to be made by the crewman prior to egress, would the entire system be ejected and deployed for self-rescue flight. The escape/recovery segment of that concept was separately and independently useful for use in mission-aircraft

have required such a projection (deployment) in any arrangement considered, the UPP type of parachute was rejected in favor of the WORD-concept previously described, which is self-aligning with the airstream. The resultant packaged volume of the selected parachute system was also found to be less than that required for the UPP-assembly.

The system as originally conceived with the wing and payload decoupled (i.e., interconnected by flexible lines) was found to be quite stable in a glide configuration. However, as perturbations were induced as initial conditions in the motion analyses, and propulsive inputs were applied, it was found that the system became extremely sensitive to relative translational and rotational movement between the wing and payload to the extent that a rigid coupling concept had to be designed. The coupled concept introduced major deployment problems if the upright seating orientation of the crewman were to be maintained. Simultaneously with this discovery, it was found that from a weight minimization standpoint the system was still heavy because of the power and fuel onboard necessary to meet speed and range goals. The penalties were directly attributed to the high drag of the payload in its previously selected upright orientation. Thus, to reduce drag and to couple the wing and payload rigidly for stability's sake, the face down flight position of the payload shown in Figure 3 was selected. To alleviate some of the objectionable characteristics of completely horizontal suspension of the crewman, a study was made which resulted in the 17^{o} inclination angle (relative to the airstream) being adapted. The inclination didn't appear to degrade the payload's aerodynamic drag significantly, yet allowed dynamic pressure to relieve and better distribute the suspension loads in the torso-restraint garment as felt by the crewman. Furthermore, the upward inclination of the engine thrust axis contributed to the system lift coefficient, and permitted a further reduction in necessary wing area, which helped from both a weight and volume standpoint as well.

Several control techniques were investigated, including warping the wing tips (analogous to ailerons) for roll induction, and engine thrust vectoring for both turning and pitch control. In all cases, longitudinal trim was achieved via CG-shift implemented through use of the seat-adjustment mechanism. Turning

seat insert suspended below the wing, the seat frame was to be considered as a twin-member vertical stabilizing surface. Three characteristics of that arrangement resulted in its rejection: (1) extreme difficulty in maintaining stability during deployment (all coupling between wing and suspended payload items was flexible); (2) seat-shell/wing aerodynamic interference was expected to deteriorate the wing's performance characteristics; (3) and, the composite aerodynamic drag of the arrangement required excessive propulsion outputs that were incommensurate with volume and weight minimization.

The initial system concept also required ejection in the self-rescue mode in every case. That meant that T_R would have to be penalized under the extreme emergency conditions because of the longer times required to deploy the flight equipment, reposition the system along the trajectory for suitable orientation to the relative wind, and to allow engine thrust buildup to a sufficient level that altitude could be gained in order to implement safe recovery. A dual-mode concept was selected in favor of the single-mode system, to give the crewman a recovery capability under <u>any</u> circumstances, and a rescue capability only as conditions allowed.

The early concepts allowed the engine to start and automatically build-up to full cruise-power output. It was realized that "hands-off" flight was mandatory in order to protect the incapacitated or unconscious occupant. Studies indicated that when under power, inflight anomalies would have to be manually or automatically sensed and corrected to maintain the desired degree of stability and control. Hence, it was decided to retain engine-start at the earliest time possible, but to allow a thrust buildup only to the "idle" level (whereat the power available output is virtually negligible, but the engine is self-sustaining), and then let continued thrust-buildup be dependent on manual or automatic discretionary input once steady-state glide is achieved, and existing conditions permit flight at maintained or varying altitude.

The initially proposed <u>U</u>ltra-<u>P</u>recision <u>P</u>arachutes (UPP's) were determined to be too sensitive to a mortar launch angle in a cross-stream or upstream direction, and since parachute stowage volume allotments would

in generating total systems concept that is in fact an advancement of the state-of-the-art of personnel rescue and survival.

An extensive search was made prior to and early in the program to find a propulsion system providing an optimum array of propulsive efficiency, definable by maximizing power available to power required, minimizing powerplant size to power available, minimizing the powerplant's contribution to system aerodynamic drag, minimizing the weight of the powerplant to a reasonable percentage of system total weight (10% was a target figure), minimizing the specific fuel consumption, and maximizing performance reliability while minimizing maintenance and servicing requirements. The fact that the powerplant is in essence a single-use item which is normally expended after one mission, was given due consideration.

Then, effectively coupled with the powerplant, a lifting device had to be selected which also had to be easily stowed in the crewstation confines, which could be deployed effectively in the maximum encountered dynamic-pressure flow-fields, said deployment (even at reduced "Q") being automatic, rapid, repeatable and reliable. The lift-to-drag generation characteristics of the lifting-device had to be carefully evaluated to ascertain satisfactory glide-range achieving performance in the event of loss of flight power.

The following discussion points out the salient features of AERCAB equipped for and operating as a secondary flight vehicle for self-rescue flight.

a. Form Description

Figures 5, 6, 7, and 8, previously referenced in Section III-2-a herein, show the general arrangement of AERCAB including self-rescue equipment. Figure 3 is added herein to portray the system in its in-flight arrangement with all equipment deployed properly. The system configuration shown is that which had passed through seven stages of design evolution and is that considered best for meeting all the objectives of the program.

Certain significant findings weighed heavily in the resolution of the final configuration. Initially, the seat shell itself was to have been used as a fuel cell, and with the ejectee seated in a modular

TABLE 6
AERCAB ESCAPE PERFORMANCE CAPABILITY

Ref.	Condition	TA/TR
A	Zero airspeed/Zero altitude	6.6/2.49 = 2.65
B	120 kts; 60° Roll; Zero altitude	4.4/1.96 = 2.24
C	150 kts; 180° Roll; 200 ft (abs.)	2.1/1.96 = 1.07
D	150 kts; 10,000 ft/min Sink; 300 ft (abs.)	3.4/1.96 = 1.74
E	200 kts; 60° Roll; 500 ft (abs.)	2.25/1.96 = 1.15
F	200 kts; 60° Roll; 60° dive; 500 ft (abs.)	2.29/1.96 = 1.17
G	250 kts; 180° Roll; 45° dive; 600 ft (abs.)	2.08/1.96 = 1.06
H	600 kts; Zero Altitude	4.5/2.49 = 1.81

and hence predictable and prescribable. Since complete control of the escape, recovery and survival experience was a major objective of the investigation, it can be concluded that the objective was met.

3. SELF-RESCUE SYSTEM

The major problems encountered during the subject program were those related to packaging all essential system elements into the pertinent existing crewstations; deploying those elements in minimum time into the self-rescue flight configuration in order not to jeopardize the envelope of prevailing emergency conditions in which AERCAB might be successfully used to the full extent of its capabilities; whittling-down the system's weight and volume in order to minimize its parasitic impact on the aircraft in which it must be installed; and applying state-of-the-art techniques

TABLE 5

EVENT TIMING

(AERCAB Ejection Sequence Without Self-Rescue, in Low Speed Mode)

Event No.	Event	Timing Seconds	Remarks
0	Ejection Initiation	0.00	Time zero is defined as the instant the zero delay initiator cartridge fires
1	Powered Restraint Haulback Initiation	0.01	Ten millisecond delay allowed for pressure buildup
2	Aircraft Canopy Jettison Initiation	0.01	Ten millisecond delay allowed for pressure buildup
3	Pilot Repositioned and Restrained	0.15	Repositioning time limited by physiological considerations
4	Launch Catapult Fires	0.15	Catapult delay determined by canopy jettison time
5	Aircraft Canopy Clears Ejection Path	0.15	Minimum time for clearance of ejection path in zero speed ejection
6	Canopy Breaker-Drogue Slug Fired	0.15+	Catapult pressure buildup propels the canopy breaker assembly to 100 ft/sec
7	Drogue Parachute Deployment	0.21+	Average deployment velocity is 200 ft/sec; therefore, $T_d \doteq 12/300 \doteq 0.06$ sec
8	Drogue Parachute Inflation	0.36+	$T_f = \frac{8Do}{V^{.9}} = 0.21$ sec, (Do = 5 ft)
9	Catapult Separation	0.34	Catapult separation velocity is approximately 60 ft/sec
10	Sustainer Rocket Ignition	0.34	Dual 840 lb-sec rockets action time = 0.3 seconds
11	DART Start	0.42	DART incorporated to achieve low speed seat stabilization
12	DART End	0.54	
13	Rocket Burnout	0.64	
14	Drogue Parachute Bridles Released	0.71	400 KIAS ejection at 15,000 ft., V_{man} = 290 KIAS at drogue release
15	Main Parachute Container Open	0.71	Simultaneous with 14
16	WORD Firing	0.83	
17	Spreader Gun Firing	1.16	
18	Recovery	1.96	First Full Canopy Inflation

TABLE 4

EVENT TIMING

(AERCAB Ejection Sequence Without Self-Rescue, in High Speed Mode)

Event No.	Event	Timing (Seconds)	Remarks
0	Ejection Initiation	0.00	Time zero is defined as the instant the zero delay initiator cartridges fire
1	Powered Restraint Haulback Initiation	0.01	Ten millisecond delay allowed for pressure buildup
2	Aircraft Canopy Jettison Initiation	0.01	Ten milisecond delay allowed for pressure buildup
3	Pilot Repositioned and Restrained	0.15	Repositioning time limited by physiological considerations
4	Launch Catapult Fires	0.15	Catapult delay determined by canopy jettison time
5	Aircraft Canopy Clears	0.15	Minimum time for clearance of ejection path in zero speed ejection
6	Canopy Breaker-Drogue Slug Fired	0.15+	Catapult pressure buildup propels the canopy breaker assembly to 100 ft/sec
7	Drogue Parachute Deployment	0.19+	In high speed ejections, (above 450 KIAS) the average deployment velocity is 300 ft/sec; therefore, $T_d = 12/300 = 0.04$ sec
8	Drogue Parachute Inflation	0.29+	In high speed ejections, $T_I = \frac{8Dc}{V \cdot g} = 0.10$ sec, (Do = 5 ft)
9	Launch Catapult Separation	0.34	Catapult separation velocity is approximately 60 ft/sec
10	Sustainer Rocket Ignition	0.34	Dual 840 lb-sec rockets, action time = 0.3 seconds
11	DART Start	0.42	DART incorporated to achieve low speed seat stabilization
12	DART End	0.54	
13	Rocket Burnout	0.64	
14	Drogue Parachute Bridles Released	1.24	600 KIAS ejection at 15,000 ft., V_{man} = 310 KIAS at drogue release
15	Main Parachute Container Open	1.24	Simultaneous with 14
16	WORD Firing	1.36	Estimated 2 ft. travel, with 8 g's, to fire rocket
17	Spreading Gun Firing	1.69	
18	Recovery	2.49	First full canopy inflation

FIGURE 14

AERCAB ESCAPE OPERATION VELOCITY DECAY CHARACTERISTICS

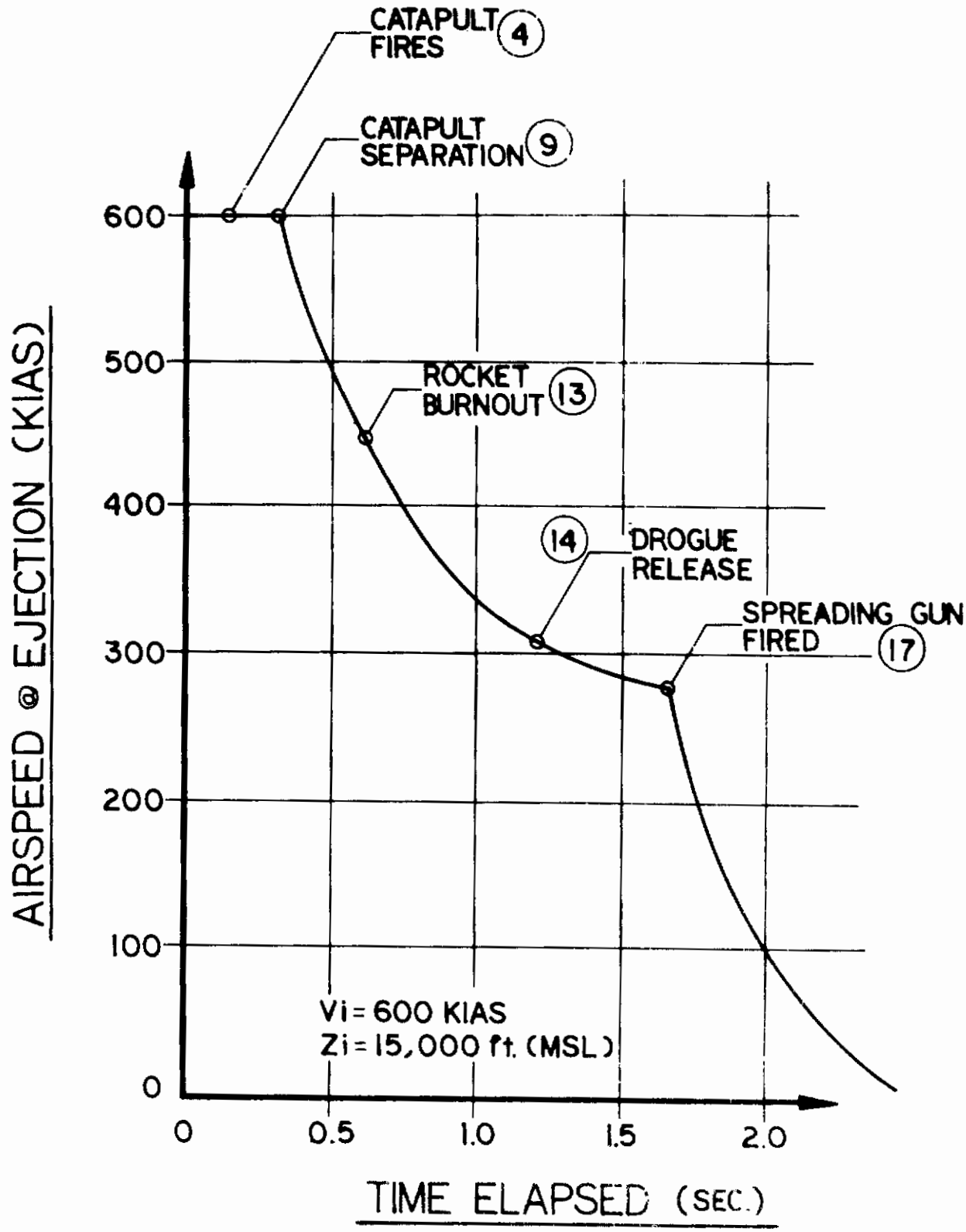

necessary to resort to an automatic time-sequencing change determined through sensing prevailing airspeed and altitude conditions. Hence, the timing for the low-mode of operation was dependent on the extreme zero-altitude/zero-airspeed case; while that for the high-mode was based on the 600 kts. at sea level case.

It was calculated that the best achieveable time required, with all elements functioning as prescribed, is:

Velocity at Ejection	T_R
0 KEAS	2.3 seconds
$<$300 KEAS	2.0 seconds
$>$300 KEAS	2.9 seconds

The estimated target T_R versus airspeed distribution was portrayed in Figure 2. By employing the prescribed effectiveness ratio, T_A/T_R, one can ascertain the acceptability of the AERCAB under any set of emergency conditions merely by showing that $T_A/T_R \geq 1.0$.

Figure 14 shows the calculated velocity decay of the AERCAB operating in the primary ejection, high-speed mode. Table 4 describes the timing of events for sequencing in that mode. Table 5 shows the selected sequence timing for operation in the primary ejection, low-speed mode. Figures 12 and 13 illustrate the system's operation in each of these modes.

e. Escape Performance Assessment

Observing then that from Tables 4 and 5, the time required in each mode of escape operations are at worst

$$T_R = 1.96 \text{ sec for } V < 300 \text{ KIAS} \quad (4)$$

$$T_R = 2.49 \text{ sec for } V > 400 \text{ KIAS} \quad (5)$$

Table 6 was computed for the critical emergency conditions spectrum.

Review of the tabulated performance shows acceptable operation under all the extreme conditions considered. Review of the event timing indicates that some estimates made were conservative, but each is repeatable,

was found that under many of the critical extreme emergency conditions evaluated, the time-available often went below the 3-second plateau. The time-available was found to be not exclusively a function of the ejected mass' ballistic characteristics, since that mass is periodically accelerated and decelerated along its path in space. Instead, T_A was found to be quite sensitive to the particular propulsion and stabilization subsystems being considered. The disadvantages of excessive sustainer-rocket impulse were well demonstrated. The analyses necessarily included consideration giving to magnitude, sense, and rate-of-onset of all forces applied to the occupant, to ascertain that human tolerances, as defined by DRI-criteria, were not violated. It was also found that the AERCAB operating in the escape-only mode had to be capable of "switching" function time-required as prevailing dynamic pressure conditions change. All loads were maximized within physiological limits in order to minimize the T_R characteristic. Load coupling was scrutinized to ascertain that no injury could be imposed on the crewman by combinations of aerodynamic and propulsive forces.

The T_R characteristic (defined as the time required for the escape system to reach suitable terminal descent rates, as measured from first rotation of the ejection controls) is composed of a series of time-increments, each demarcated by onset and completion of an essential event along the escape trajectory. The best way the contractor felt to minimize the total T_R, was to individually minimize each T_{R_N}-increment (where N is the number of essential events). It was known that once propelled from the aircraft, the ejected mass must be slowed to airspeeds suitable for parachute deployment and inflation as rapidly as possible without violating man's or material's structural limits. Man's greatest tolerance to positive and negative acceleration is to G's applied orthogonally to his spine while he is in a seated position (i.e., "eyeballs-out/in"). The minimum allowable deceleration period, then, was computed assuming that the net aerodynamic forces acting on the man/seat combination were at the G_{x_L} limit set forth in MIL-S-9479A, under 600 knot velocities imposed at sea level ambient conditions. Because the delay required to decelerate the mass from high-speed conditions directly conflicted with total time available, it was finally resolved that it was

end, and to a zero-second initiator on the seat at the other end, is tensioned sufficiently to actuate the firing-mechanisms of both devices; the instantaneous cartridge in the gun pressurizes the central manifold therein, and propells the pistons radially to their stops in the cylinder-bores in the main-housing; the pistons drive the canopy skirt-attached slugs radially outward, dispersed normal to the inlet axis, orthogonal to the windstream; the initiator on the seat serves to fire the devices which release the webbing straps linking the man and his survival kit to the seat; the IFF signal generator is also activated by this centerline tensioning;

(12) with the increasing aerodynamic force of the inflating main canopy acting on the man, and not on the seat, separation of the man and seat occurs in positive fashion, with the relative trajectories of each thereafter diverging from that of the other;

(13) as the seat and man separate with a positive differential relative velocity, a lanyard is paid out which is attached at one end to the crewman's torso harness, and at the other end to the survival kit; at tensioning of this lanyard, the kit is extracted from the seat bucket and is thereafter suspended below the ejectee during his parachute descent;

(14) descent rates from 17 to 21 ft/sec are expected since the C-9 canopy is the terminal descent vehicle; upon reaching the surface, the crewman should release his riser fittings to preclude being dragged by the parachute reacting to surface winds; and once unburdened, can retrieve his survival kit via its lanyard, and use its contents to expedite his rescue.

d. Sequencing

During analyses of the sequencing of escape and recovery events, minimization of event-timing was treated as being of paramount importance to meet the system performance criteria in MIL-S-9479A. While investigating the various propulsion/stabilization concepts discussed earlier in this report, it

has already input the LO- or HI-mode signal to the plumbing-system, which will properly transmit the gas pressures to the relevant event-sequencing elements; the EJEX-RESCUE/ valves are in their normal "EJEX-ONLY" position;

(8a) at speeds below 300 KEAS, gases from the 0.3 sec initiator are transmitted to the drogue/wing disconnect (thereby decoupling the fly-away equipment from further action), to the upper drogue bridle releases (through a barometric lockout device which inhibits gas passage therethrough at altitudes above 10,000 ft, MSL), and to the lower drogue bridle releases for immediate disconnect thereof ... hence, at low altitudes (below 10,000 feet) the entire drogue assembly is freed to travel downstream relative to the man/seat mass; and at high-altitudes the upper bridles remain connected to trim the seat in a feet-to-earth stable descent attitude (low drag profile for minimum time of exposure to extreme cold and rarified atmosphere) until 10,000 ft pressure altitude is reached whereat the drogue is then freed to move downstream;

(8b) at speeds above 300 KEAS, the 0.3 sec delay initiator is permitted to release only the lower drogue bridles, allowing the seat to continue decelerating, reorienting into the eyeballs-up trim position; the release of the drogue/wing disconnect and upper drogue bridles must then wait for a pressure pulse from the 0.9 sec delay initiator (and as before, upper bridle release is altitude dependent);

(9) once both groups of drogue bridles are released, a brief translation of the parachute downstream aligns and energizes the WORD-rocket device;

(10) the aerodynamically prealigned rocket pulls on a towline connected to the apex of the main recovery parachute's C-9 canopy, deploying the canopy and suspension lines from the headrest-container, apex-first, and downstream; the inlet of the main canopy is held closed by the spreading-gun assembly;

(11) just prior to suspension line-stretch, the firing lanyard connected to the spreading-gun at one

(e.g., the TRN-70) provides a continuous readout of absolute altitude, and therefore can provide all the altitude data desired in the AERCAB automatic flight control system. This unit has sufficient accuracy for AERCAB purposes, approximately 10 feet out of 200 feet, and has only a weight of 1½ pounds for the radar/antenna package. A visual warning indicator with adjustable height setting (A70-1) is already available. Power requirements are ½ amp at 14 volts D.C. and the unit is compatible in size to the AERCAB system. The radar unit and the antenna are in one package approximately 3 inches high and 4½" in diameter.

Motorola Corporation located in Scottsdale, Arizona, has a ground sensing bomb fuse which is now in production and could be modified for use as the switching means from the self-rescue to the terminal-descent mode with the lowest cost of any unit considered. However this unit would be limited to the same extent as the AVCO short-pulse, high range resolution radar system.

Thus a tentative decision has been reached to incorporate the Bonzer TRN-70 Radar Altimeter with its A70-1 Adjustable Height Warning Indicator (or the equivalent), for the AERCAB flight control system.

c. Operation

Figure 17 portrays the sequence of events along a typical high-speed escape with AERCAB in the SELF-RESCUE MODE. The following narrative describes the operational sequence, and operation of system elements as they function in that mode. The prerequisite for transfer into this mode is depression of the manual selector switch in the cockpit by the crewman <u>prior</u> to operation of the ejection controls (again refer to the system schematic of Figure 4). The flight conditions computer senses prevailing conditions, and in this case closes the switch which repositions the sequencing valves to their RESCUE position. Then,

(1) Rotation of either (or both) of the leg-brace mounted ejection actuation control handles actuates the sears which fire parallel, independent, zero-delay initiators which generate

the pressurized gas transmitted to the propulsion firing manifold.

(2) The manifolded gas travels simultaneously to the initiator which energizes the automatic, powered, restraint haulback device and to both initiators which energize the canopy-jettison subsystem (unlocks and thrusts the canopy from the path of ejection), and also to the dual cartridges which, after a suitable time delay to permit restraint haulback and canopy removal, will energize the ejection-propulsion devices;

(3) Again, for reasons of conservation of installational volume required, the self-rescue module has been assembled in compressed form along the longitudinal axis. Hence, it is reiterated that the launch catapults and rockets are provided in pairs outboard of the engine and parawing stowage volume. The catapults are manifolded together such that neither can be individually pressurized. A pair of cartridges are provided (in redundancy) to energize the catapults. These too are delay train cartridges with a non-indexing, dual-primer ignition element. At the top of the catapult assembly is the integrated dual-piston canopy-breaker which strokes upon initial pressurization of the catapults, thereby penetrating a "hung-up" canopy before first-motion of the ejected mass. The bridged canopy-breaker propelled mass is used as a "drogue-slug" to deploy the system stabilization/retardation drogue parachute, and its container, from its stowed position in the jet-engines' intake duct. This again provides for drogue deployment, downstream orientation and inflation while AERCAB is travelling up the rails, before the ejected mass achieves unconstrained flight. Hence, at high speeds whereat aerodynamic forces would tend to induce severe pitch-up instability problems, the drogue is actively combating those moments, thereby maintaining both stability and trajectory control throughout the flight. Accelerative loading (positive and negative) is controlled within Dynamic Response Index (DRI) limits throughout the operation.

(4) At the instant the slipper group separates from the rails, the catapult tubes simultaneously separate (thereby precluding catapult-induced tipoff moments). Just prior to separation of

T= 0.68 SECONDS:
TURBOFAN IS UP TO FULL THRUST. THE SYSTEM FLIES UNTIL CRITICAL ALTITUDE IS REACHED, WHETHER UNDER POWER OR GLIDING FLIGHT.

T=2.27 SECONDS:
PERISCOPE FULLY SPREAD & ERECTED & LOCKED. ENGINE IS COMPLETELY DISCONNECTED FROM THE SYSTEM. THE INSTRUMENT READING MIRRORS ARE FULLY EXTENDED. AT 4.48 SECONDS, TURBOFAN ENGINE AT FULL IDLE, BY OPENING THE THROTTLE, THE SYSTEM IS READY FOR MAXIMUM RANGE FLIGHT.
ALL CONTROL SYSTEMS ARE NOW OPERABLE.

T=1.57 SECONDS:
DUE TO FORCE EXERTED BY THE DROGUE PARACHUTE, THE PERISCOPE STARTS ITS ERECTION, SPREADING PHASE. AT THIS POINT THE INSTRUMENT READING MIRRORS START EXTENDING.

MAXIMUM RANGE

ONCE CRITICAL ALTITUDE IS REACHED, THE MAIN RECOVERY PARACHUTE IS PROJECTED TO THE FULL LENGTH OF ITS STATIC LINE, & THE OCCUPANT & HIS SURVIVAL GEAR ARE RELEASED FROM THE SEAT.

T= 1.50 SECONDS:
LOWER DROGUE BRIDLES RELEASE, AFTER PROPER ANGULAR RELATIONSHIP HAS BEEN REACHED, DROGUE FORCE IS TRANSFERRED TO THE TELESCOPED SECTIONS OF THE LEADING EDGES & KEEL OF THE PARAWING.
V= 250 KIAS, $\bar{n}$ = -7.3 g's.
AT T= 1.57 SECONDS, LEADING EDGES & KEEL BOOMS ARE EXTENDED & LOCKED. DROGUE RELEASES TO BEGIN SPREADING & ERECTION SEQUENCE.

T= 1.38 SECONDS:
UPPER DROGUE BRIDLES RELEASE, & SEAT BEGINS PITCH FORWARD TRANSITION.
V= 269 KIAS, $\bar{n}$ = -8.3 g's, (IF ABOVE 10,000 FT. AT THIS POINT, THE UPPER BRIDLE RELEASE IS DELAYED BY A BAROMETRIC DEVICE UNTIL THE SYSTEM DESCENDS TO 10,000 FT. ALTITUDE.)

T= 0.88 SECONDS:
ROCKET BURNOUT, V= 385 KIAS, $\bar{n}$ = -17.5 g's.

T= 0.48 SECONDS, PRESSURE TAP FROM CATAPULT TUBES IGNITE ROCKETS, 0.30 & 0.90 SECOND DELAY INITIATORS. CATAPULT TUBES SEPARATE.

T= 0.0 SECONDS:
ROTATION OF EITHER OR BOTH EJECTION CONTROL HANDLES ACTIVATES INDEPENDENT, DUALLY-REDUNDANT ZERO DELAY INITIATORS WHICH ACTIVATE THE FOLLOWING:
(a) .3 SECOND DELAY CATAPULT CARTRIDGE.
(b) ZERO DELAY RESTRAINT HAULBACK DEVICE.
(c) ZERO DELAY CANOPY JETTISONING THRUSTER.
AT T= 0.30 SECONDS, RESTRAINT HAULBACK COMPLETED, CANOPY JETTISONING CONTINUES, CATAPULT CARTRIDGE FIRES, THEREBY UNLOCKING CATAPULT TUBES & PROJECTING CANOPY BREAKER/DROGUE DEPLOYMENT SLUG.

THE RECOVERY PARACHUTE DEPLOYS FROM ITS CONTAINER AS THE OCCUPANT FALLS AWAY, UNTIL FULL LINE & CANOPY STRETCH HAS BEEN REACHED, AT THIS POINT THE SPREADER GUN IS FIRED. THE PARACHUTE CONTAINER REMAINS ATTACHED TO THE SEAT.

GENERAL NOTES:
1. ALL CALCULATIONS ARE BASED ON A 600 KIAS AT TIME OF EJECTION.

FIGURE 17
AERCAB ESCAPE SYSTEM SEQUENCE

the inner and outer tubes of the catapult, the pressurized gases are piped off to energize the sustainer rockets, the engine starter cartridge, and the time delay initiators which will later induce release of the drogue parachute bridle attachment points, and initiate the parawing deployment sequence via release of the trailing-edge drogue attachment point. A direct gas-impingement technique can be employed which would allow us to conserve the cartridge starter for use in the event a midair restart is needed later in the self-rescue flight. The engine is permitted to build to idle RPM, generating insignificant thrust, but ready for throttling up later, immediately upon achieving steady-state gliding flight.

The manual throttle linkage is locked until the wing is positioned relative to the payload satisfactorily for gliding flight. As in the primary ejection sequence, should the prevailing airspeed be greater than the Vmax below which the man may be rotated spine-forward without overloading him (in the eyeballs down direction) during retardation and parawing deployment phases, then the system will function in HI-MODE-2, wherein a longer delay is imposed on the release of the upper drogue bridle release mechanism. In LO-MODE-2, wherein $V < V_{max}$, the time delay initiator is permitted to energize both top and bottom bridle release sets. The lower bridle set releases at a constant delay after rocket firing in both operating modes.

(5) Once the drogue bridles are freed from their connections to the self-rescue module, the initial relative motion of the drogue moving downstream pulls the pins on the parawing container flaps. The wing assembly then is permitted to rotate, spread and erect relative to the seat in such fashion that the system trims out along the trajectory with the seat/man/rescue-module slightly leading the wing, trailed by the drogue. The position sensitive coupler then releases the drogue at the trailing edge (point) of the keel. During this process, at full keel/boom extension, the drogue force is transferred to a point on the spreader-bar slide-knuckle which moves the knuckle along the keel to a self-locking point whereat the bars are most effective

as compression-struts to maintain the proper leading-edge sweepback angle. At this stage, the wing framework forms a trailing delta aligned by the drogue to the windstream so that excessive angles of attack cannot occur.

A rate-sensitive inertial rotary brake controls the payout of the foremost suspension line in such fashion that a gradual, continuous repositioning of the wing takes place relative to the payload. As the wing gains in positive angle of attack to the relative airstream its lifting membranes stabilize into their "natural" dynamically-pressurized lobed shape, and L/D generation begins.

(6) As the wing assumes its proper overhead position relative to the payload, at a (L/D) max glide attitude, the drogue parachute is completely released, and the engine throttle is unlocked.

(7) From this instant, the crewmember has the option of throttling up to his cruise velocity for powered, controlled flight (wherein he may establish and maintain a beacon-guided homing path), or he may fly "hands-off" on a programmed spiral-glide path to a prescribed altitude whereat his absolute altitude sensor will automatically induce his "ejection" from the AERCAB, which will follow the descent sequence previously described.

Should, at any point along his flight path, the crewmember descend to the minimum prescribed altitude, he will be automatically "ejected" and recovered via his personnel parachute.

d. Sequencing

As with the "conventional" sequencing, minimization of time required to allow the system to transition into its flying configuration was of paramount importance. The time-available prerequisite for self-rescue flight allowance will have to be computed in the future as a function of the prevailing conditions at ejection, in order to provide the assessment computer with comparative information to ratio against T_R. The computation of the AERCAB self-rescue limiting envelope under all possible initial conditions was

beyond the scope of the reported program. However, the minimum T_R-characteristics were computed, and are presented in Table 8.

Figure 18 shows the calculated velocity decay of the self-rescue mode from a high-speed launch condition. Figure 17 can be referred to for visualization of each major event.

TABLE 8

EVENT TIMING

(AERCAB Ejection Sequence With Self-Rescue)

Event No.	Event	Timing Seconds	Remarks
0	Ejection Initiation	0.00	Time zero is defined as the instant the zero delay initiator cartridge fires
1	Powered Restraint Haulback Initiation	0.01	Ten milisecond delay allowed for pressure buildup
2	Aircraft Canopy Jettison Initiation	0.01	Ten millisecond delay allowed for pressure buildup
3	Pilot Repositioned and Restrained	0.15	Repositioning time limited by physiological considerations
4	Launch Catapult Fires	0.15	Catapult delay determined by canopy jettison time
5	Aircraft Canopy Clears	0.15	Minimum time for clearance of ejection path in zero speed ejection
6	Canopy Breaker-Drogue Slug Fired	0.15+	Catapult pressure buildup propels the canopy breaker assembly to 100 ft/sec
7	Drogue Parachute Deployment	0.19+	In high speed ejections, i.e., above 450 KIAS, average deployment velocity is 300 ft/sec; therefore, $T_d = 12/300 = .04$ sec
8	Drogue Inflation	0.29+	In high speed ejections, $T_f = \frac{8Do}{V^{.9}} = 0.10$ sec, (Do = 60 inch)
9	Launch Catapult Separation	0.34	Catapult separation velocity is approximately 60 ft/sec
10	Sustainer Rocket Ignition	0.34	Two 840 lbs-sec rockets, action time = 0.3 seconds
11	DART Start	0.42	
12	DART End	0.54	
13	Rocket Burnout	0.64	
14	Upper Drogue Release	1.38	600 KIAS ejection at 15,000 ft., V_{man} = 270 KIAS at upper drogue release
15	Lower Drogue Release and Initiation of Wing Deployment	1.50	600 KIAS ejection at 15,000 ft., V_{man} = 250 KIAS at lower drogue release. Force transfers to wing
16	Wing Booms Extended and Locked & Spreader Bar Locked into Position	1.57	
17	Wing Erection Onset	1.57	Drogue bridle lifts wing working against velocity control brake
18	Wing Deployed	2.57	
19	Mirrors Extended, Engine @ Full Idle, and Drogue Released	4.48	Engine at idle, throttle unlocked, controls operable
20	Stable Glide	4.48	Minimum engine thrust buildup time
21	Full Engine Thrust	6.48	
22	Controlled Flight	30 min.	Cruise conditions

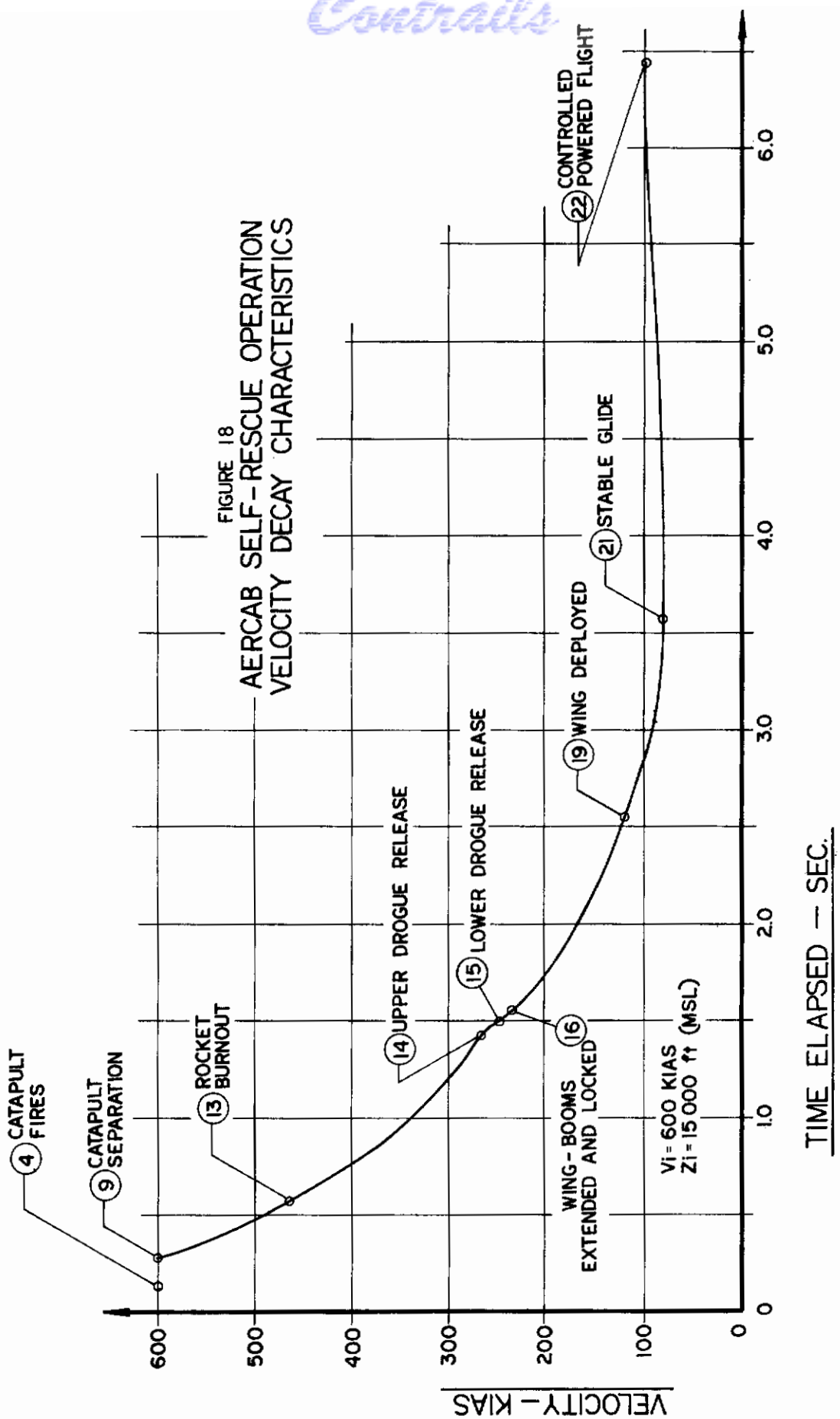

FIGURE 18

SECTION IV - SELF RESCUE FLIGHT SYSTEM DISCUSSION

This discussion of AERCAB concentrates on the material studied during the effort to analytically determine realistic system performance characteristics while operating in the self-rescue mode. Hence, the configuration analysis, performance capabilities analysis, weight and volume minimization studies, streamlining effects and powered/gliding flight profiles are treated herein. An attempt is made to present the information in a fashion which will enable the reader to follow the system's evolution to that ultimately selected and described in detail in other Sections of this report.

1. Configuration Analysis

a. Parawing Selection

The selection of a definite parawing that could be suitably coupled to an ejection seat for stable flight was based upon a comprehensive review of available NASA parawing reports. A conical parawing was selected as a result of that search, having aerodynamic characteristics as presented in NASA TN D-1957. This wing is identified by[20] the listing of characteristics on Page 81 of this report.

The wing keel length (l_k) and wing area (S_o) were determined in an iterative design-performance analysis process until the system design objectives were obtained for range, velocity, rate-of-climb, weight, volume, and powerplant-thrust. The planform reference area (S_o) obtained can be defined as:

$$S_o = l_k^2 \text{Cos } \Lambda_o \qquad (6)$$

The convention of forces and moments used in the parawing aerodynamics analysis is shown in Figure 19.

b. Seat Aerodynamics

The ejection seat aerodynamic reference dimensions were assumed in rectangular frontal planform: 18 inches wide x 54.5 inches high x 33 inches deep, in keeping with the target minimum size design. From these dimensions a seat projected area (S_p) was expressed as a function of the seat back angle (θ_p) as shown in Figure 20.

$$S_p = 4.1 + 3*\text{Sin } \theta \ (ft^2) \qquad (7)$$

AXES SYSTEMS AND CONVENTION USED TO DEFINE POSITIVE SENSE OF FORCES, ANGLES, AND MOMENTS [20]

FIGURE 19

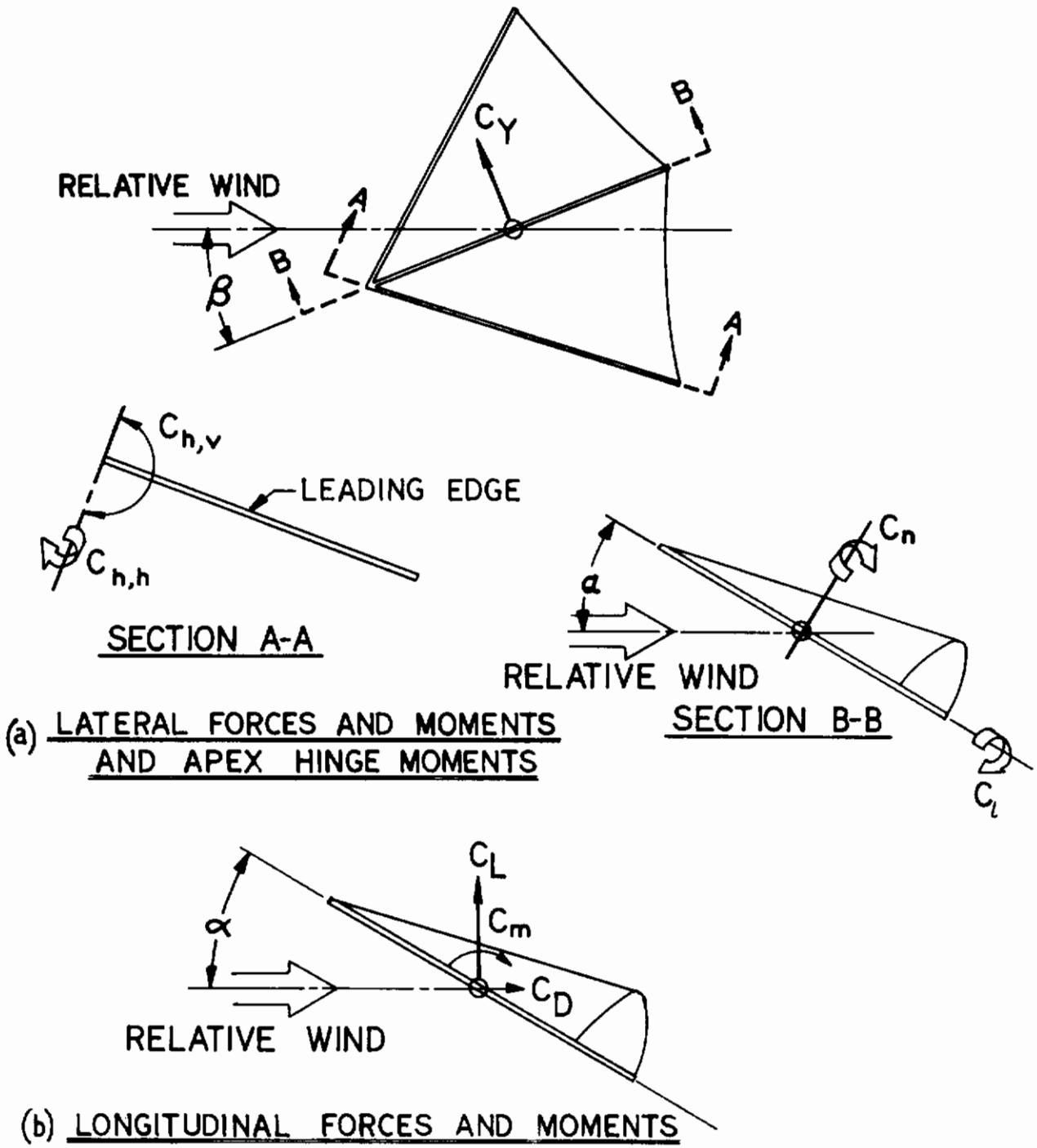

(a) LATERAL FORCES AND MOMENTS AND APEX HINGE MOMENTS

(b) LONGITUDINAL FORCES AND MOMENTS

FIGURE 20

PROJECTED SEAT HEIGHT vs SEAT ANGLE

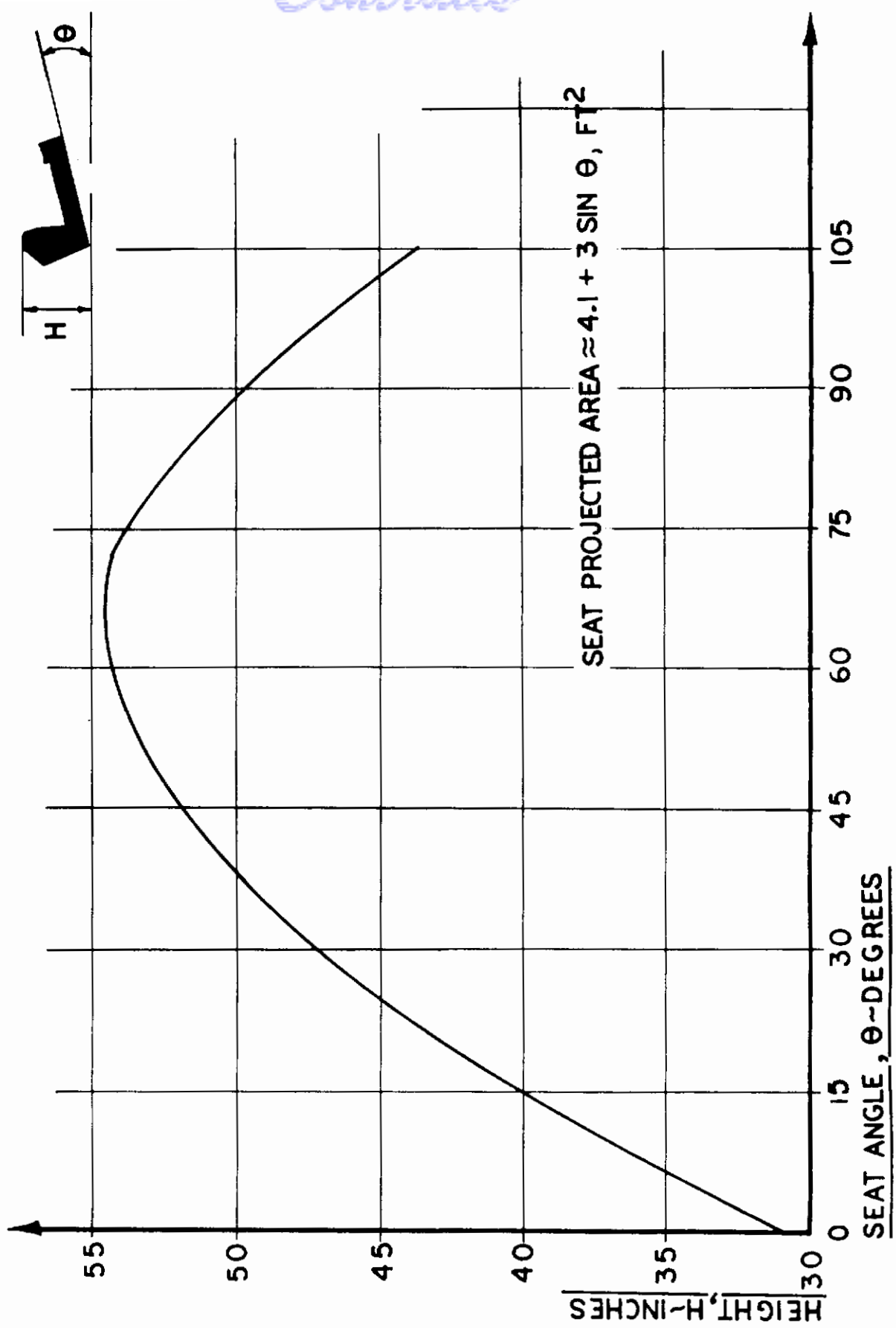

The projected area (S_p) is presented in turn as a seat drag area ($C_D S_p$) in Figure 21; assuming a variation in the C_D as a function of wing angle of attack (α_w) similar to that shown in Figure 22.

The seat was initially assumed to be at a 45 degree back angle attitude, giving a $C_D S_p = 4.2$ ft^2 from Figure 21. The struts joining the seat and wing were given a nominal $C_D S = 1.0$ ft^2.

c. First Estimate of Wing Area & Gross Weight

The initial wing characteristics for a first estimate of design were taken as:

C_L = 0.60

C_d = 0.13

α_w = 28°

L/D max (wing) = 4.6

L/D max (seat + wing) = 2.1

C_L, C_d and α_w were selected for a wing-characteristics set representing a median condition in the useful angle-of-attack range, avoiding use of parameters at either extreme in that range. The values are near, but not at, the maximum wing L/D condition. While $(L/D)_{max}$ was desirable, the compromise was deemed worthwhile in order to have some freedom in both increased and decreased angle-of-attack without having to worry about leaving the useful range of attack-angles.

A wing sizing estimate was made initially for 100 KEAS flight, achieving a 50 mile range at sea level and 10,000 ft MSL. The following expression was employed:

$$G.W. = C_{L_w}\, qSw = 490 + \frac{R * S.F.C.}{V} (5.2q + C_{d_w} qS) \qquad (9)$$

where, in equation (9),

a) 490 lb was the fixed man/seat/engine/wing weight
b) S.F.C. = 0.772 @ S.L. and 0.840 @ 10,000'

FIGURE 21
SEAT DRAG vs SEAT ANGLE

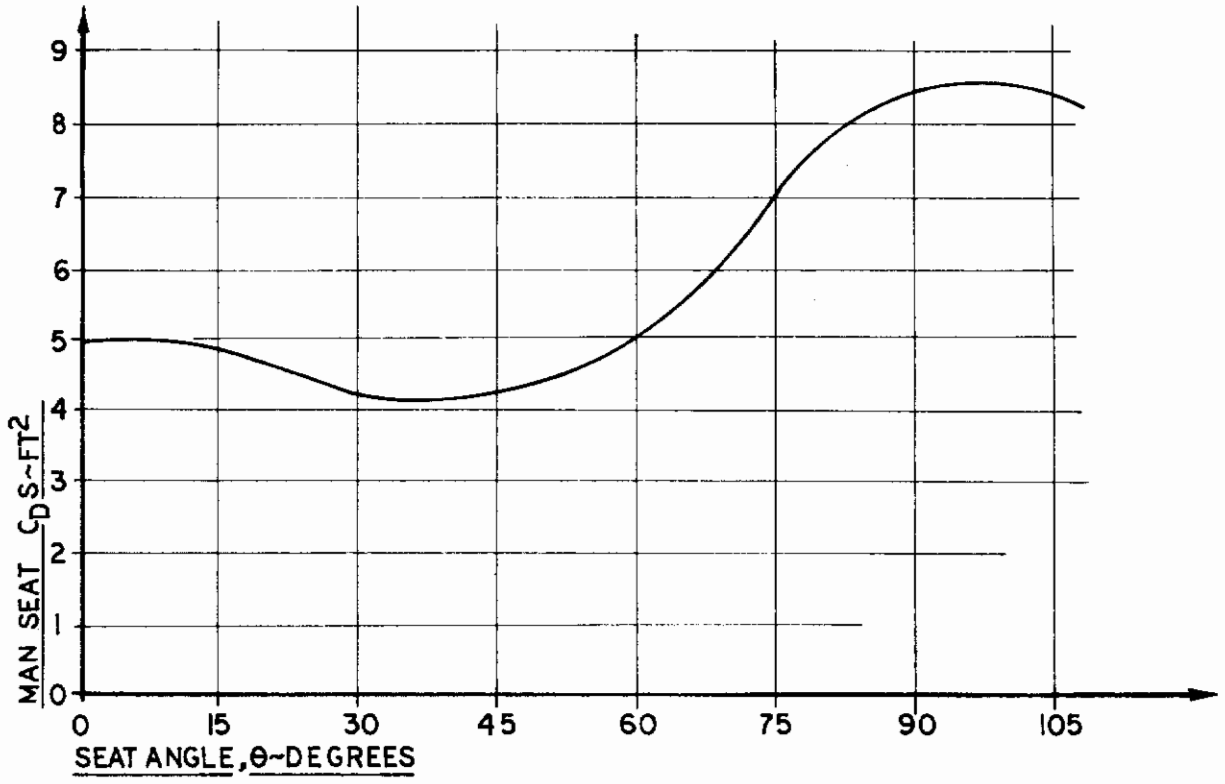

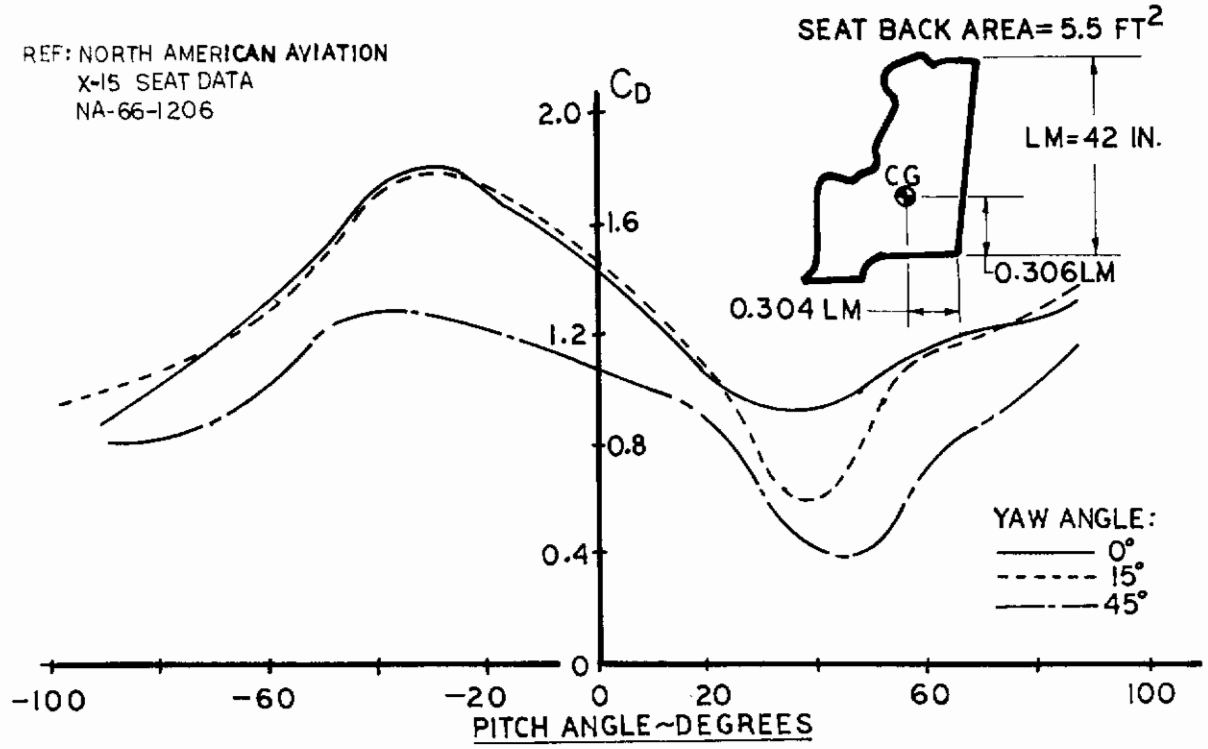

FIGURE 22
SEAT & MAN
ESTIMATED DRAG COEFFICIENT

c) 5.2 sq ft was the drag area estimated from figures 20, 21 and 22, (i.e., 4.2 ft^2, and strut drag area = 1.0 ft^2).

The calculation resulted in a conservative selection of design values as follows:

G.W. = 610 lbs
S_w = 30 sq ft

At that time, the twin turbofan engine had not been "discovered", and the initially proposed turbojet engine's characteristics were being used.

2. Parametric Performance Analysis

In order to optimize the AERCAB design parameters, a parametric analysis was performed involving system weight, thrust, specific fuel consumption, lift/drag ratio, range, velocity and wing area. The previous establishment of a parawing area (30 ft^2) and system gross weight (610 lbs) was used as a baseline from which values could be expected to vary. The parametric study initialized with the assumptions of:

FIXED QUANTITIES:
- ...man/seat/engine weight = 450 lbs
- ...thrust (per engine Mfr's data)
- ...S.F.C. (per engine Mfr's data)
- ...(CdS) man/seat = 4.2 sq ft
- ...(CdS) struts = 1.0 sq ft

INDEPENDENT VARIABLES:
- ...C_L wing
- ...(L/D) wing
- ...range
- ...cruise speed

DEPENDENT VARIABLES:
- ...fuel weight
- ...gross weight
- ...wing area
- ...wing weight (@ a "density" of 1.337 psf)

The results of the initial parametric study are plotted in a series of carpet plots, and are shown here as figures 23, 24 and 25. (Figure 26 depicts the turbojet engine's thrust available estimates used, and is included for reference to these three figures only).

FIGURE 23

EFFECT OF DESIGN CRUISE SPEED
& DESIGN RANGE ON FUEL WEIGHT

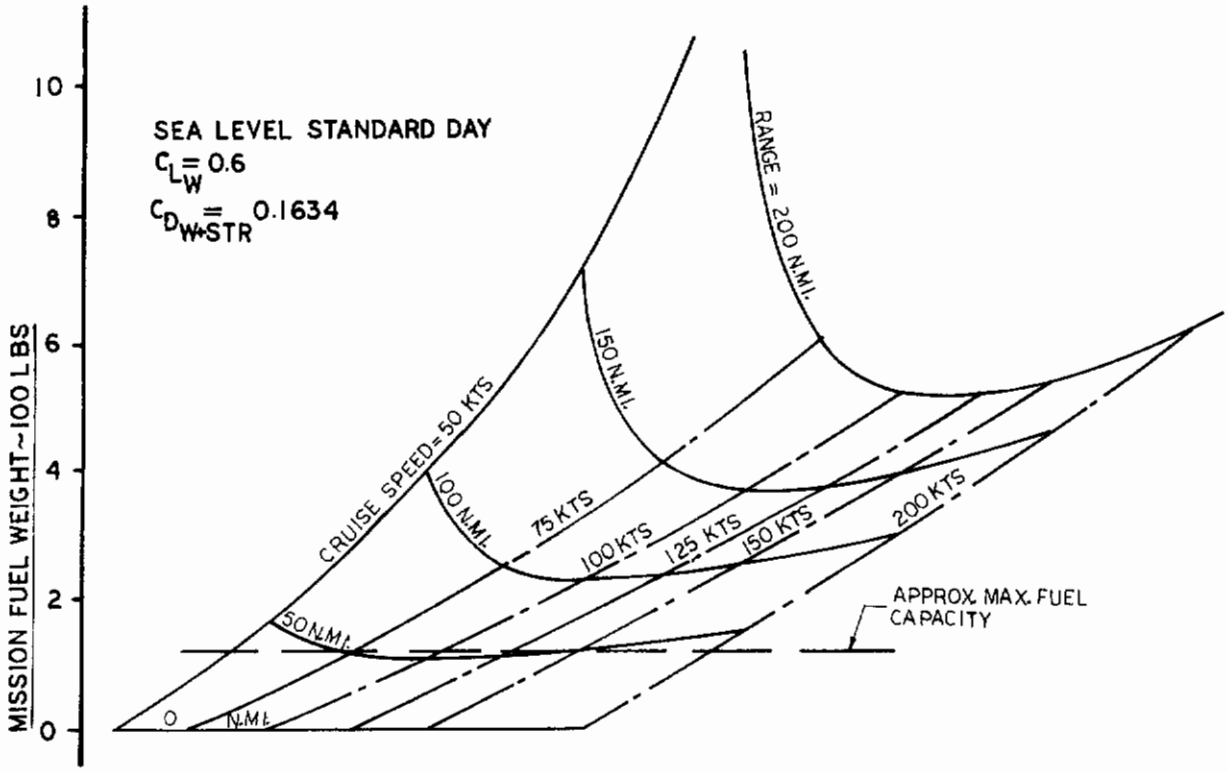

FIGURE 24

EFFECT OF DESIGN CRUISE SPEED
& DESIGN RANGE ON MISSION WEIGHT

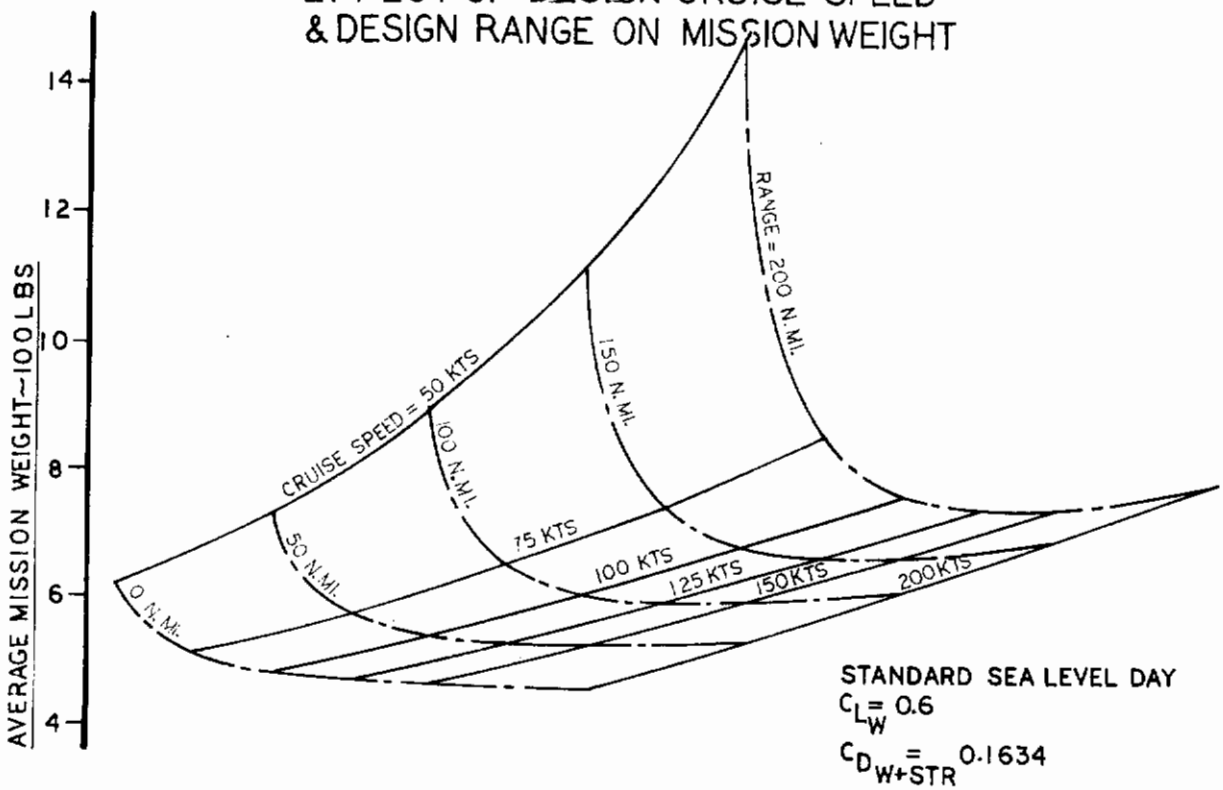

FIGURE 25

EFFECT OF DESIGN CRUISE SPEED & DESIGN RANGE ON WING AREA

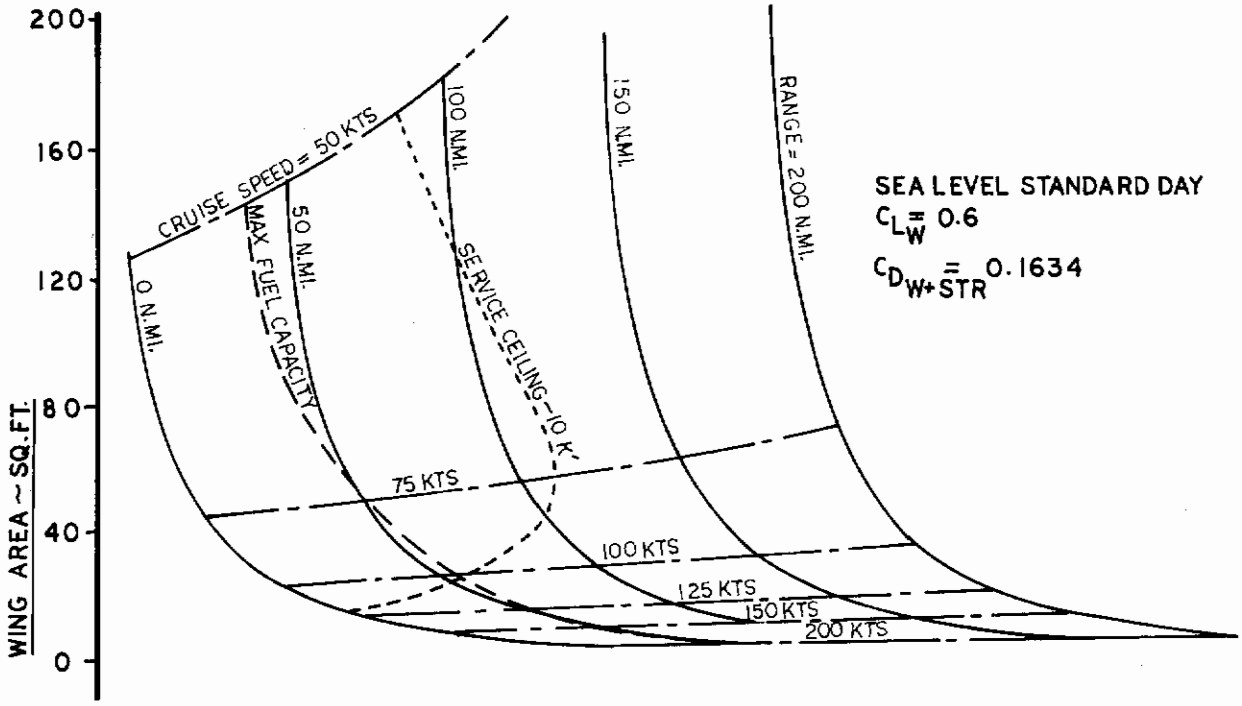

FIGURE 26

MAXIMUM THRUST AVAILABLE* & S.F.C. vs AIRSPEED

*PRELIMINARY TURBOJET ENGINE, STANDARD DAY CONDITIONS

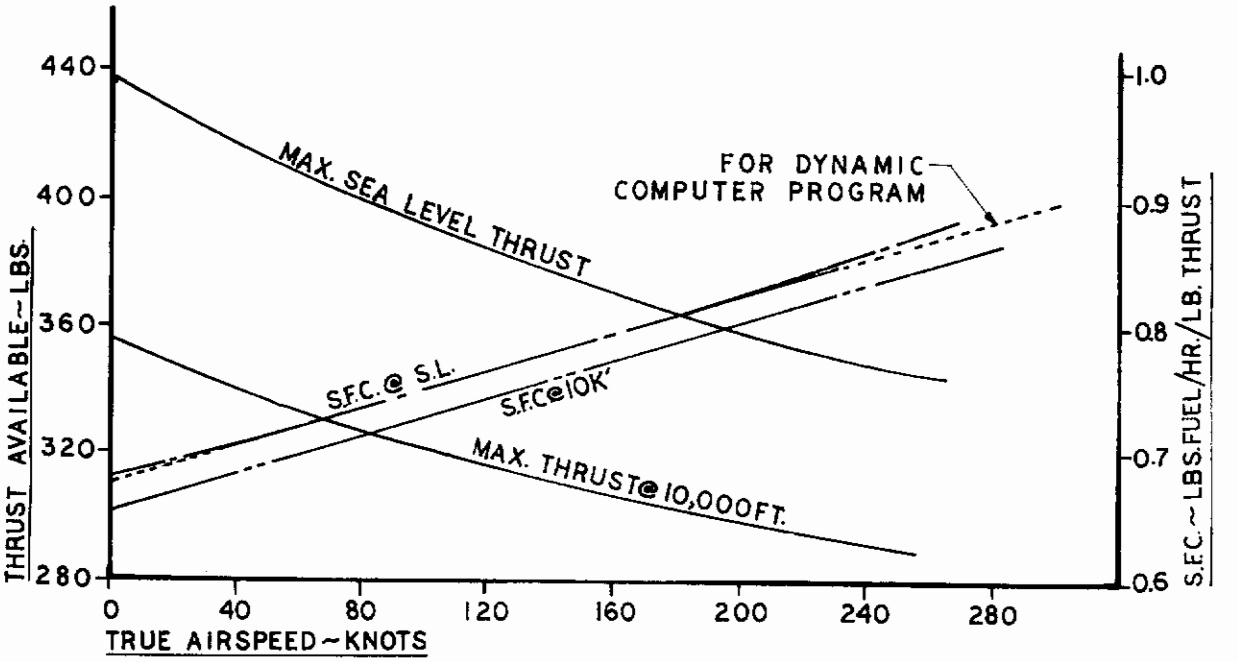

It is noted that the 10,000' service ceiling line and the initially estimated AERCAB maximum fuel capacity line are superimposed on Figure 25

The gross weight of the AERCAB vehicle for the nominal conditions of 100 KEAS cruise and 50 miles range was 595 lbs, as estimated from Figures 23 and 24. This is the sum of a 540 lb average mission weight, and half of the 110 lbs. of fuel, defined by the intersection of range and velocity in the respective figures. The engine data assumed for these results are shown in Figure 26.

The wing area defined by the velocity-range curve intersection in Figure 25 is 26.5 ft^2. This area was somewhat smaller than the first estimate of 30 ft^2. This was because the wing area requirement was based on the average system weight, with half the fuel remaining, which is much more accurate than basing it on maximum weight at mission onset (as was done to determine the preliminary 30 sq.ft. area estimate).

Both the variation of engine fuel and wing weight were considered in the preceding analysis. The importance of the system weight criteria presented the need for a weight parametric evaluation before a final wing area could be established.

It is significant that if the values of C_L and C_D from the NASA wind-tunnel tests of a wing-alone cannot be attained on the full-scale AERCAB vehicle because of manufacturing tolerances and interference effects, the wing area and fuel weight necessary to perform the design mission will increase from the above values. Also, the effects of the limits of a 10,000 ft. service ceiling and a maximum fuel capacity of 120 lbs. (Ref. Figure 25), which would be more critical with decreased C_L and increased C_D, could necessitate a reduction in design cruise speed (or design range, or both). The question of the degree of agreement between the coefficient values used, and the actual system values, must ultimately be determined by full scale testing.

Before going into the weight parameter trade-off; the effects of variations in wing L/D and total system L/D ratios are presented.

Figures 27 through 32 portray the effects of design cruise speed and the wing-alone L/D on wing area, each figure having been plotted for a different lift-coefficient.

FIGURE 27

EFFECT OF DESIGN CRUISE SPEED & WING L/D ON WING AREA

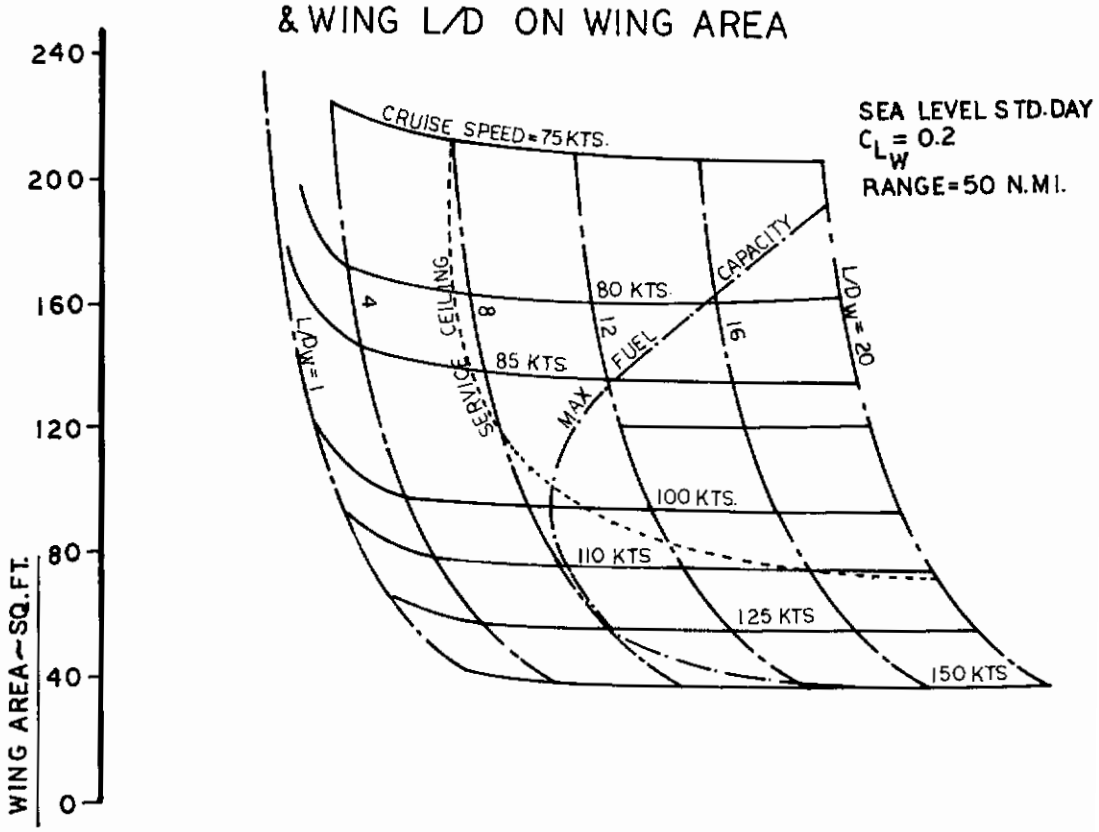

FIGURE 28

EFFECT OF DESIGN CRUISE SPEED & WING L/D ON WING AREA

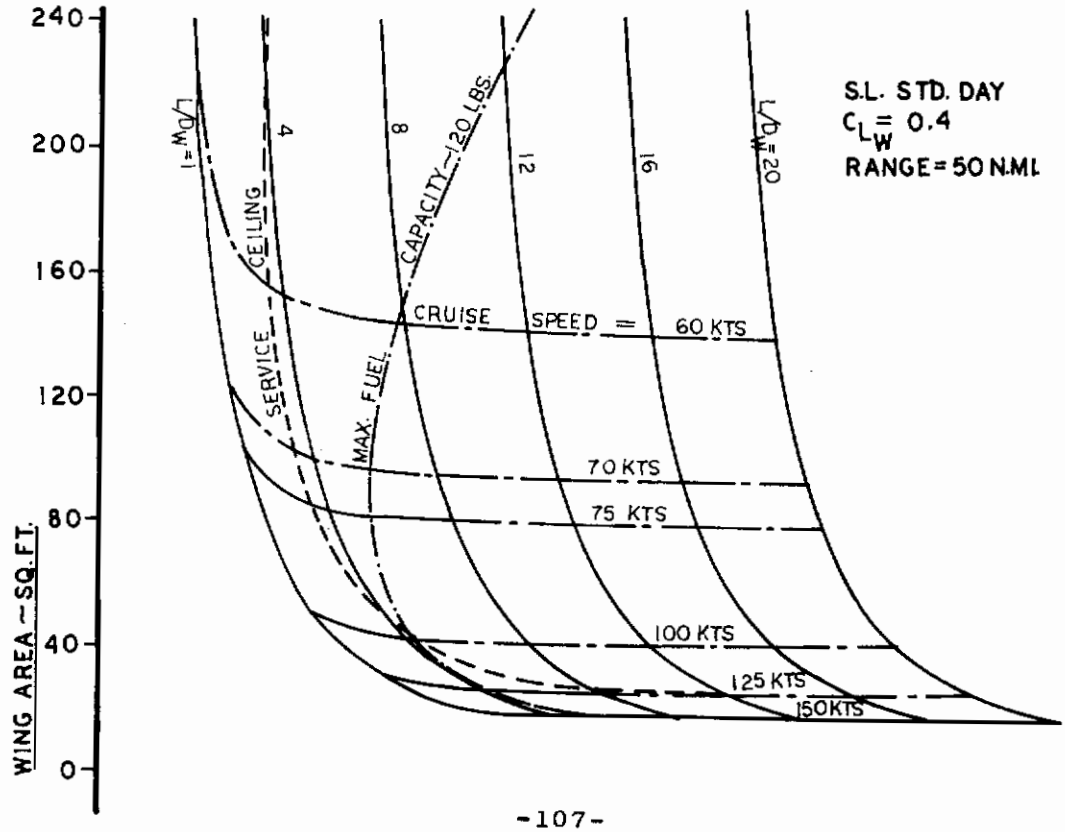

FIGURE 29

EFFECT OF DESIGN CRUISE SPEED
& WING L/D ON WING AREA

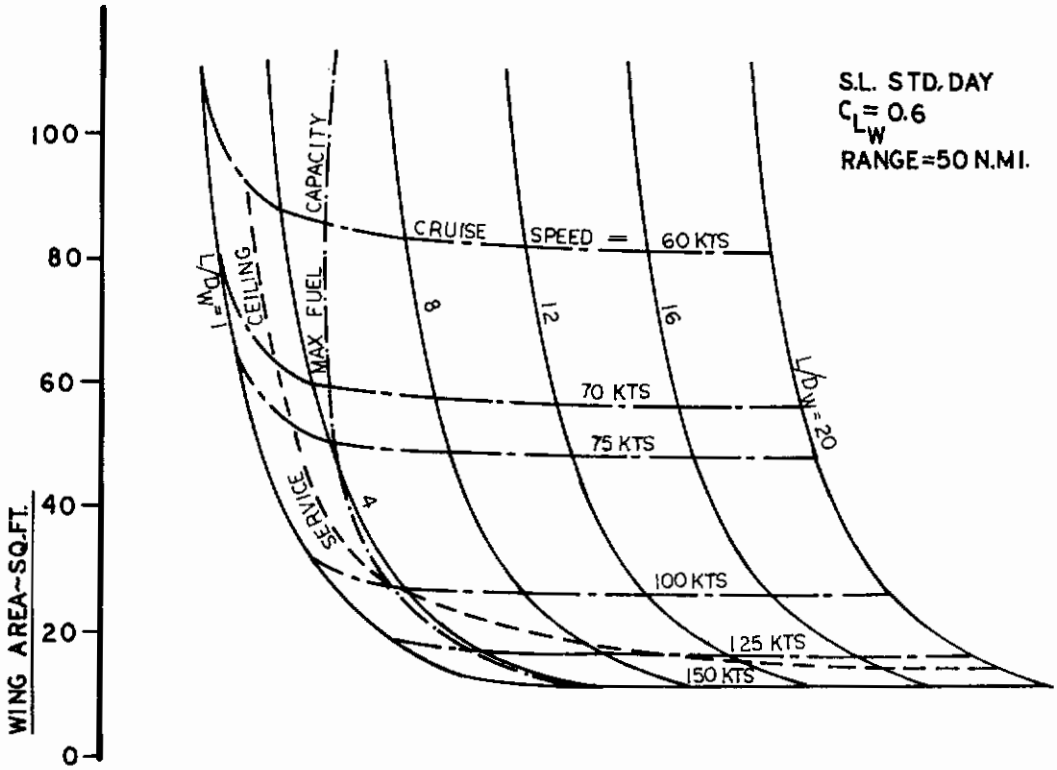

FIGURE 30

EFFECT OF DESIGN CRUISE SPEED
& WING L/D ON WING AREA

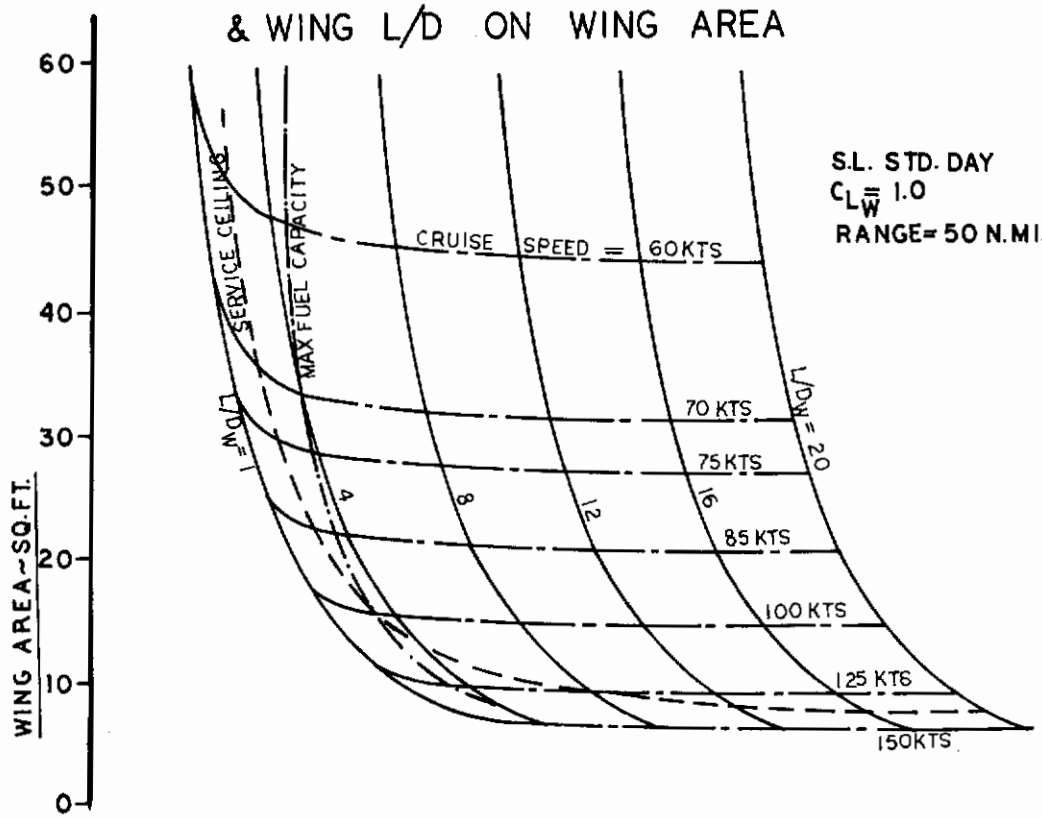

FIGURE 31

EFFECT OF DESIGN CRUISE SPEED & WING L/D ON WING AREA

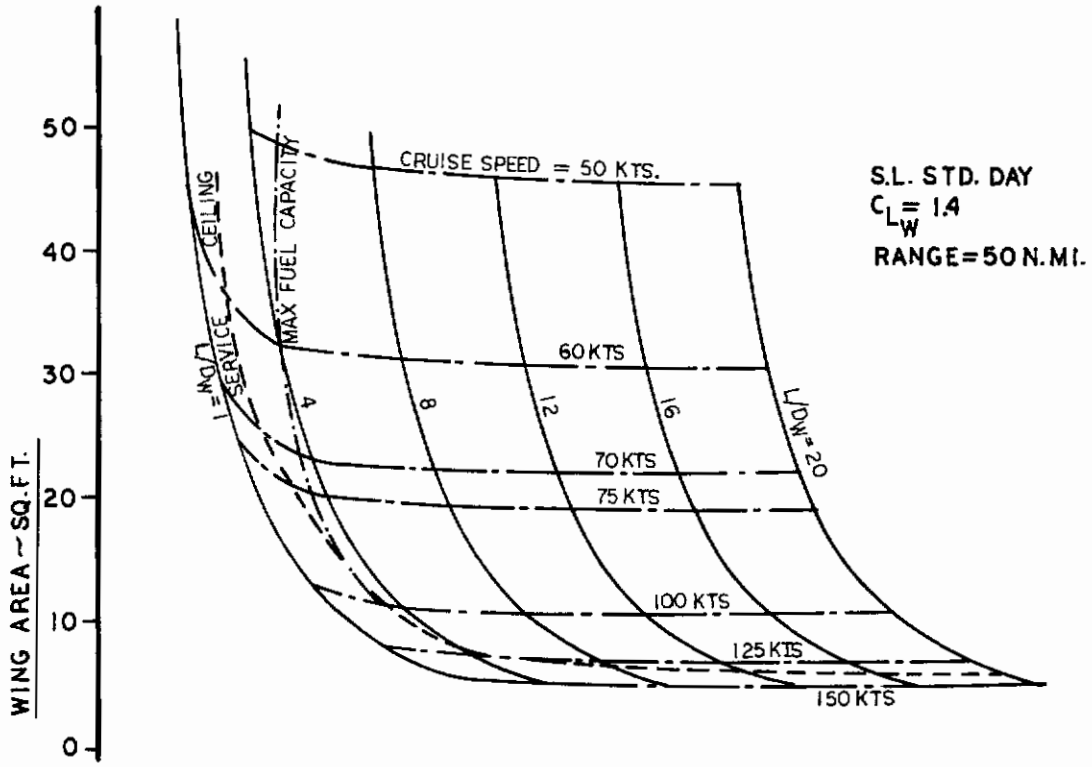

FIGURE 32

EFFECT OF DESIGN CRUISE SPEED & WING L/D ON WING AREA

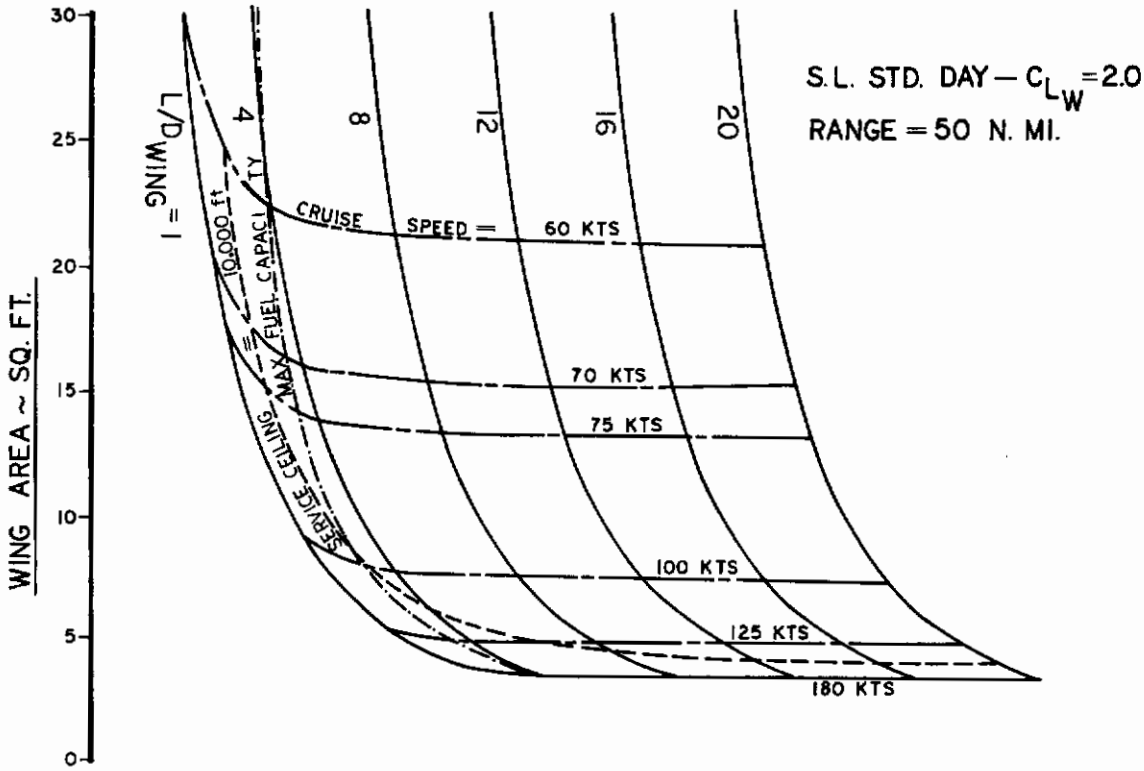

Figures 33 through 38 portray, in like format, the effects of cruise speed and total system L/D on wing area.

It is again noted that these performance variations presume achievement of the required 50 nautical mile range.

A fundamental fact of significance was obviated through this study. In the system arrangements studied, an increase in L/D did not appreciably decrease wing area required beyond an L/D of about 5. This was due to the fact that the fuel required to travel 50 nautical miles is but a very small portion of the total system weight at higher L/D's.

It is noted that the approach used is of relatively general nature, and could be applied, if so desired, to other L/D-generators having the denoted lift-coefficient characteristics.

The equations and definitions of terms used in the generalized parametric performance study are described in Appendices "C" and "D" of this report.

3. Weight Trade-Off Analysis

A predominating criterion in the determination of the wing area to be used for the AERCAB design was the minimization of overall system weight; and thereby, through association, minimized stowage volume.

The approach was to express the total weight of the system as functions of variable wing-weight, engine weight, and fuel weight, and plot the W function against cruise velocity and range. For a fixed range, wing weight decreases with increasing cruise velocity, while the engine plus fuel weight increases therewith. As portrayed in the sketch of Figure 39 below, a minimum W/V-combination can be arrived at by plotting the combine-function as it varies with velocity at cruise.

In this analysis a fixed range of 50 nautical miles was maintained as a fundamental criterion, while the effects of weight variation on cruise velocity were observed.

A computer program (described in Appendix E) was written to determine the optimum cruise velocity for minimum weight.

FIGURE 33
EFFECT OF DESIGN CRUISE SPEED AND TOTAL L/D ON WING AREA

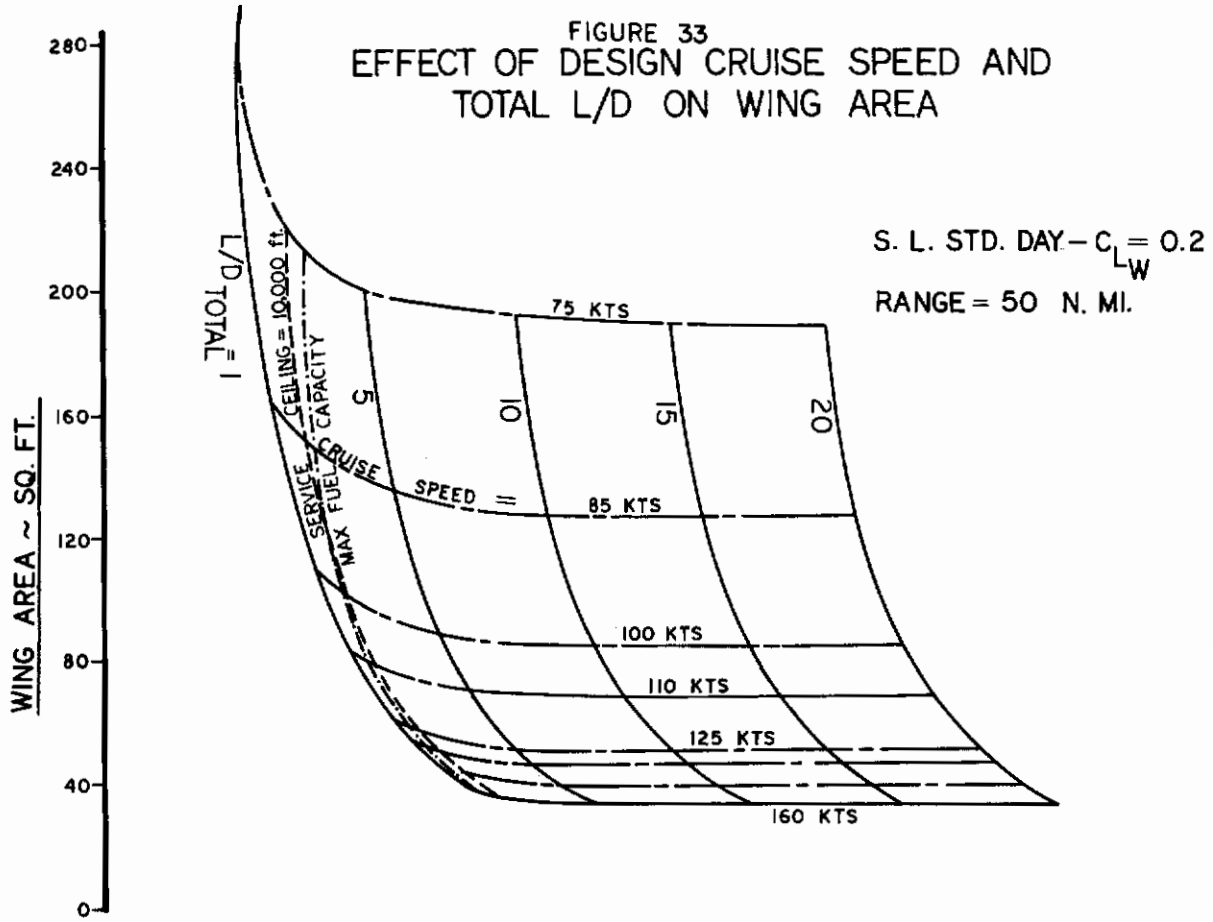

FIGURE 34
EFFECT OF DESIGN CRUISE SPEED & TOTAL L/D ON WING AREA

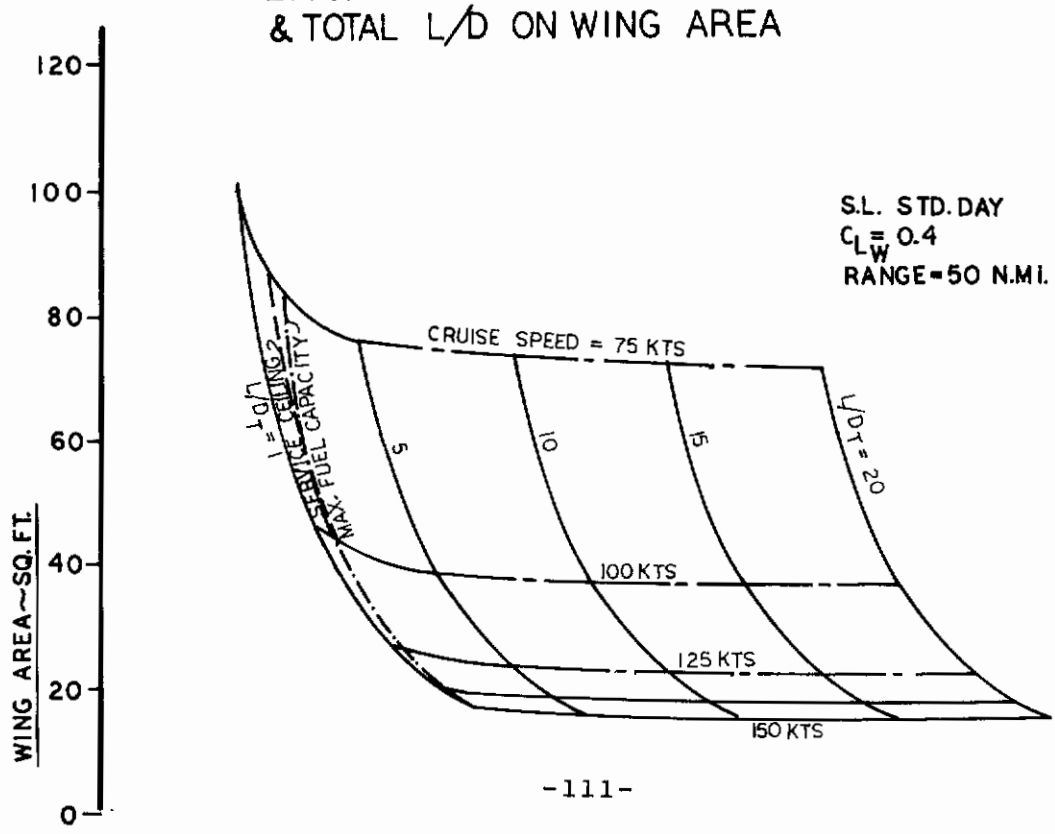

FIGURE 35

EFFECT OF DESIGN CRUISE SPEED & TOTAL L/D ON WING AREA

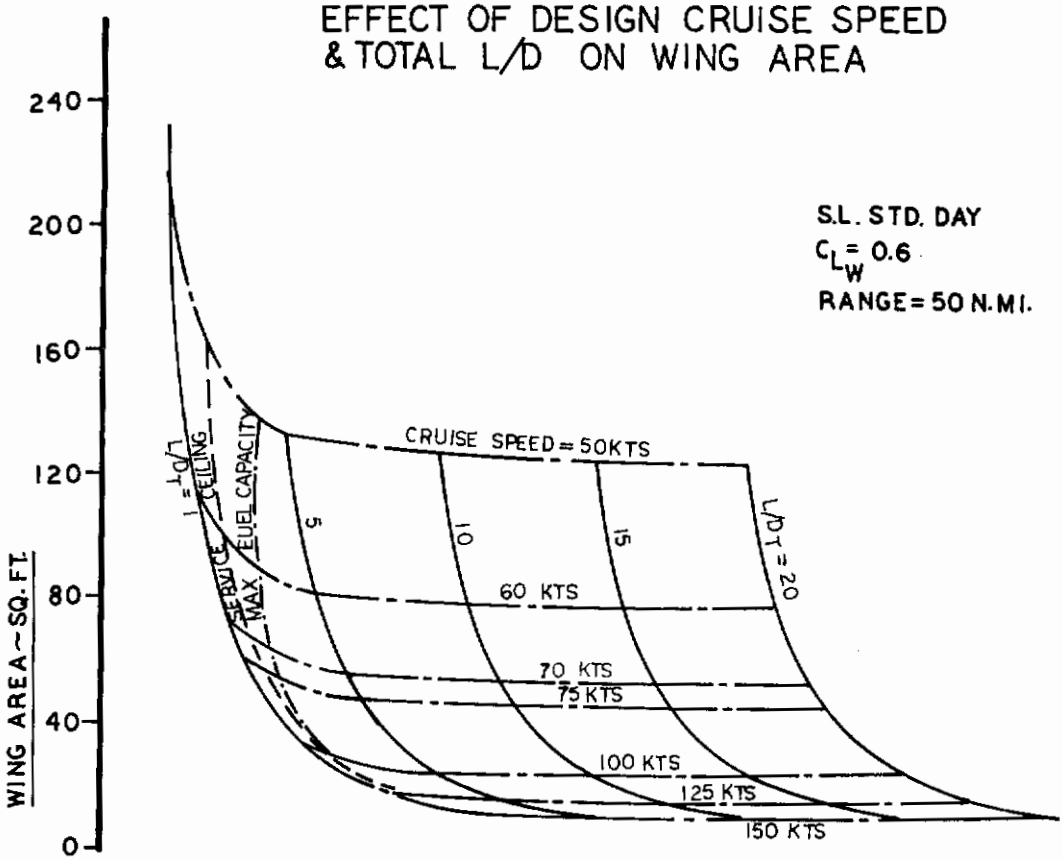

FIGURE 36

EFFECT OF DESIGN CRUISE SPEED & TOTAL L/D ON WING AREA

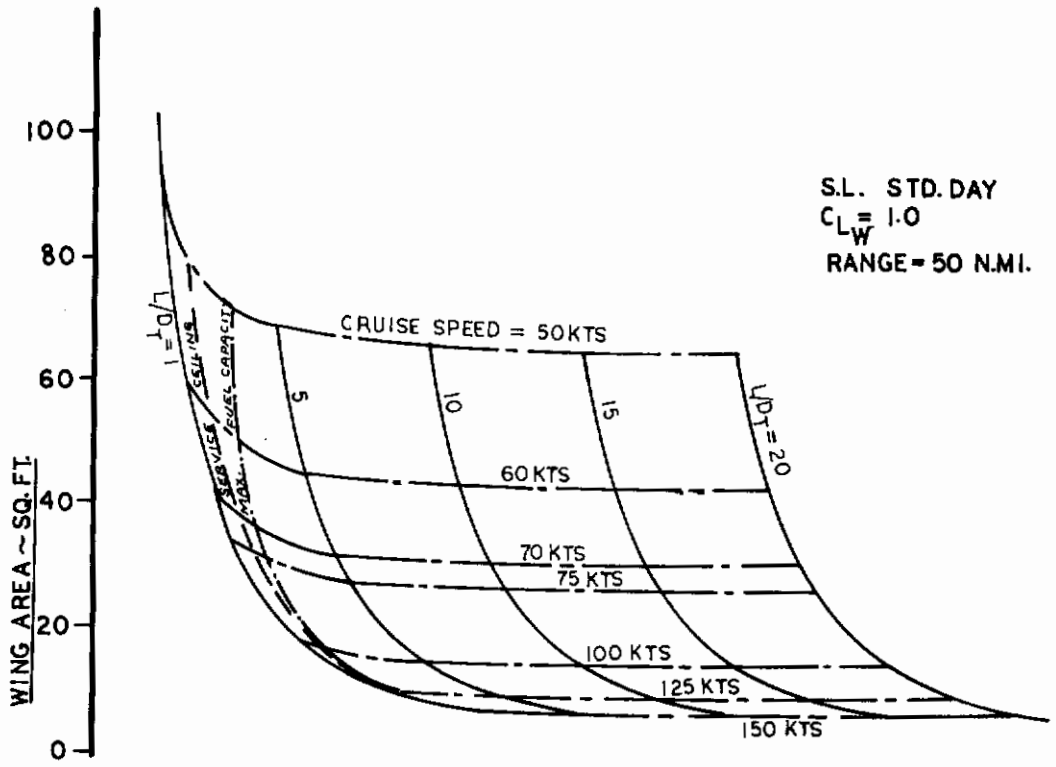

FIGURE 37

EFFECT OF DESIGN CRUISE SPEED & TOTAL L/D ON WING AREA

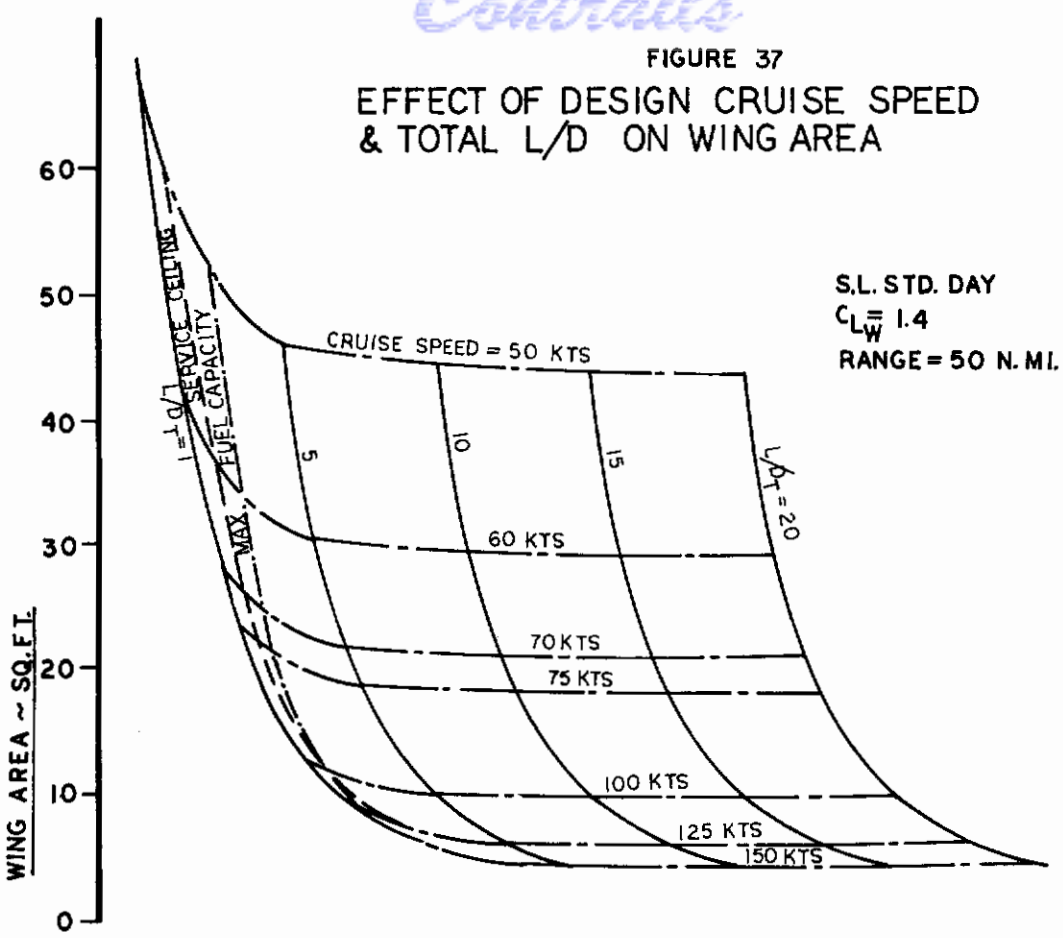

FIGURE 38

EFFECT OF DESIGN CRUISE SPEED & TOTAL L/D ON WING AREA

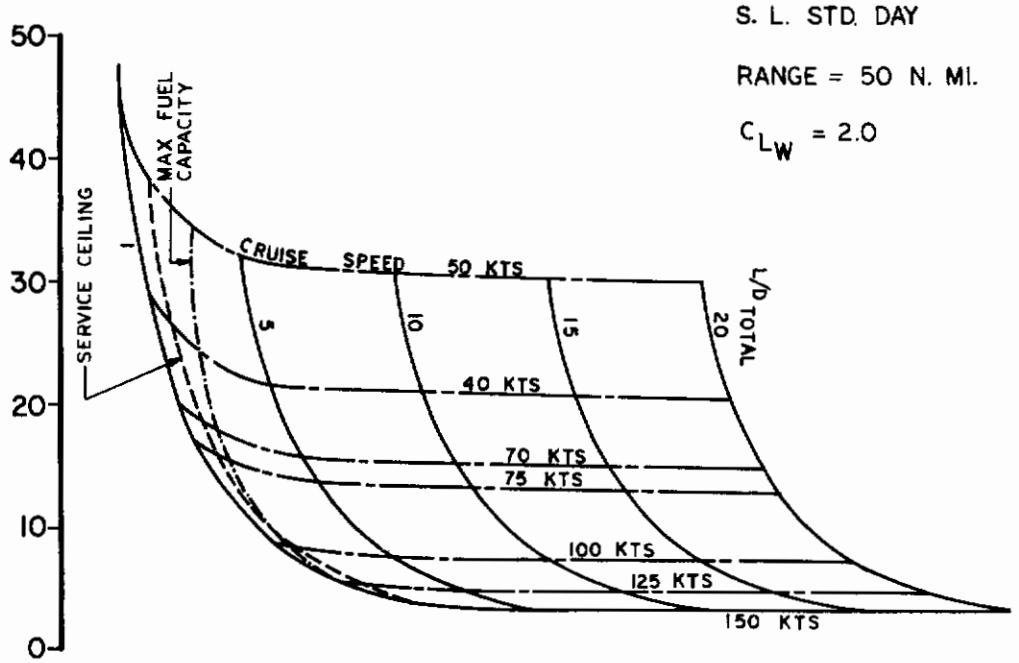

The following were adapted as basic criteria:[20]

$$\left.\begin{aligned} C_{L_W} &= 0.6 \\ (L/D)_W &= 4.615 \\ C_{D\,struts} &= 0.0334 \\ (C_D S)\ \text{Payload} &= 4.2\ \text{sq ft} \end{aligned}\right\} \quad (10)$$

FIGURE 39

TYPICAL SYSTEM WEIGHT VARIATION

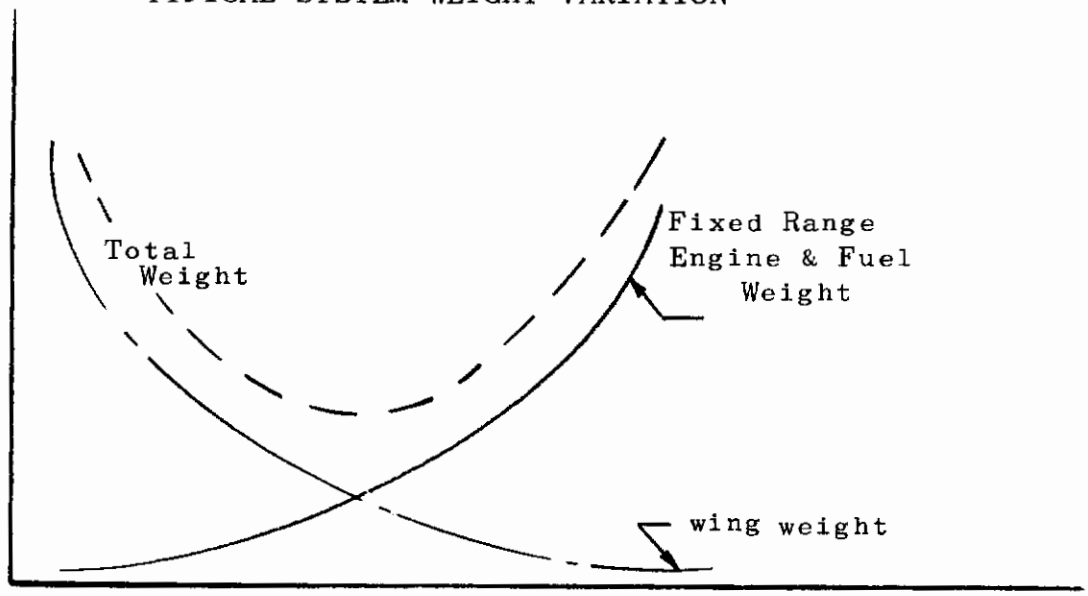

The parameters allowed to vary with cruise velocity were:

Fuel weight
Fuel tank weight
Wing fabric weight
Wing structure weight
Suspension-strut weight
Engine weight

The fuel weight was that needed to cruise 50 miles at the design cruise velocity, assuming fuel flow at the average cruise weight (i.e., half fuel load) held constant for the entire mission.

Fuel tank weight per unit material area was assumed to be 8 oz/sq yd.

The wing structure weight was determined by assuming tubular sections for the keel and booms, and spreader bars, exposed to a 6G ultimate load, deflecting thereunder to the extent of 2% of the keel length. It was assumed that each L.E. boom carried half the total load, and all the aforementioned members were of the same material and section. Where aluminum structure was considered, a uniformly distributed load was assumed, and the spreader bar length varied proportionally to keel length. For the consideration given to steel structure, an isosceles triangular load distribution was assumed, and a 64 inch constant length spreader bar was assumed; and an extra 10% in length was allowed for telescoping and hardware fittings on the L.E. booms and keel. A rigid suspension strut-set weight was computed assuming the 6G ultimate load on aluminum tubes whose length was 75% of that of the keel, loaded tensionally, each of which carried $\frac{1}{4}$ the ultimate load.

Engine weight was allowed to vary as the 3/2 power of the thrust.

The thrust was that required to achieve a 100 ft/min rate of climb at 10,000 ft. (MSL) at the same equivalent airspeed as the design cruise speed.

Engine weight was ratioed from the then current design engine at the same airspeed as that for which the thrust was computed.

Figures E-1 and E-2 in Appendix E depict the results of utilizing the program. Figure E-1 shows that for the unstreamlined configuration having a C_DS of 4.2 sq ft, the optimum cruise velocity was 75 knots. Figure E-2 shows that this corresponds to a wing area of 43.3 sq ft for both the aluminum and steel structured wings.

a. Maximum Velocity

Since the weight minimization studies produced a system configuration which cruised at or about 75-80 knots, even as the design evolved, it was of interest to determine what the V_{max} (dash) capabilities of the system would be at all altitudes (whereat, of course, range would be diminished from the 50 n.mi. achieveable at cruise). Figure 40 shows the results of that computation under standard day conditions. It is noteworthy that the system very nearly achieves the targeted 100 knots airspeed capability in the dash configuration. Figure 40 applies to a configuration

FIGURE 40
MAXIMUM AIRSPEED vs ALTITUDE

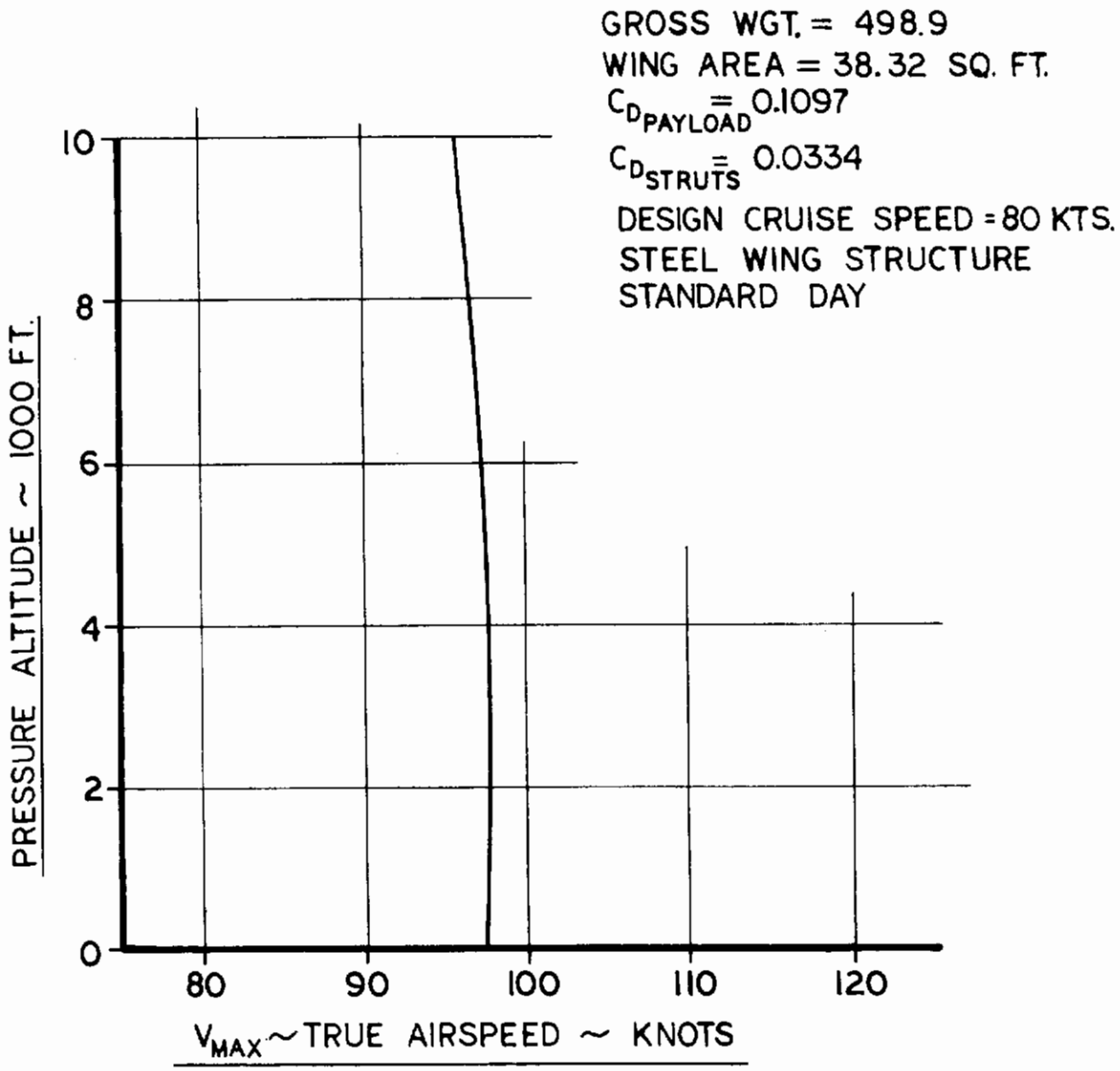

quite close to that settled upon at the program's termination.

b. Engine Cant Angle Effect on System Weight

A revised suspended attitude of the seat dictated that the effects of canting the payload and thrustline to the relative wind on minimum weight be investigated. At the selected cruise angle of attack ($\alpha_w = 29^o$), the tradeoff of wing area (reduction) to compensate for the vertical thrust component was studied; as was the resultant decrease in engine size, fuel required, and wing weight; and the corresponding increase in thrust required due to misalignment in the thrust and drag vectors, and the increase in effective payload drag area were also investigated.

In the "WEIGHT" computer program (Appendix E) a few modifications were made to support this study:

...the term CL was replaced by CL_{total} in all equations of the original program except "F", where,

$$...CL_{total} = CL + CD_{total} * \tan \theta_T \quad (11)$$

$$...CD_{total} = \frac{CL}{(L/D)W} + CDST + \frac{CDSPL}{SW} \quad (12)$$

...θ_T is the deflection of the thrust axis and seat back relative to the windline at an $\alpha_w = 29^o$.

The thrust required for a R/C = 100 fpm at 10,000 ft (MSL) was determined in the program by the following iteration process:

Using as a first approximation,

$$T_{climb} = C*SW+D \quad (13)$$

(where C, SW, & D are from the program); and,

$$T_{climb} = \frac{WTW*R/C}{\left(\frac{V_{e_{climb}}}{V_s}\right)^{*101.3}} + D_{climb} \quad (14)$$

$$\cos \theta_T$$

where,

$$...D_{climb} = C_{D_{total}} * Q_{climb} * SW \quad (15)$$

$$\ldots Q_{climb} = \frac{WTW - T_{climb} * \sin\theta_T}{CL * SW} \qquad (16)$$

$$\ldots V_{e_{climb}} = 17.18 \, (Q_{climb})^{\frac{1}{2}} \qquad (17)$$

The T_{climb} value obtained from equation (14) was then used as the assumed value in the next iteration until calculated and assumed values agreed within 0.01 lb. The iterated value was then used in place of C*SW+D in the program in the equation for computing engine weight, EW.

The program was run for a series of design cruise speeds and thrust deflections, and for two basic different, engine designs. Because engine "W", the initially investigated powerplant, (although having higher specific fuel consumption) had a higher thrust output per pound of engine weight, and was also smaller dimensionally, for the same thrust rating (than the second-choice turbojet engine "C"), engine "W" was selected as the basic powerplant for scaling purposes.

A thrust deflection of 17.15° resulted from the 10.5 inch diameter engine capable of providing an 80 knot cruise velocity. Figures 41 through 44 portray the results of the series of computer runs.

Figure 15 shows a trace of thrust required with airspeed for contemporary weight and wing-area values of the final AERCAB design equipped with the twin turbo-fan engine, with the system so configured such that the engine thrust-line is canted upward relative to the airstream as defined by

$$\alpha_T = \alpha_w - 11.85^{\circ} \qquad (18)$$

where

α_T is the thrust inclination angle to the relative wind

The reader will note that superimposed on Figure 15 are the traces of maximum thrust-available at sea level and 10,000 ft. (MSL) for the subject engine. These traces must be qualified to avoid apprehension concerning the values achieved thereon. Such an engine has a relatively high turbine-inlet temperature approaching 1950°F. The engine has but a 30 minute useful service life at this maximum power output level,

FIGURE 41

EFFECT OF DESIGN CRUISE SPEED
& THRUST INCLINATION ON ENGINE WEIGHT

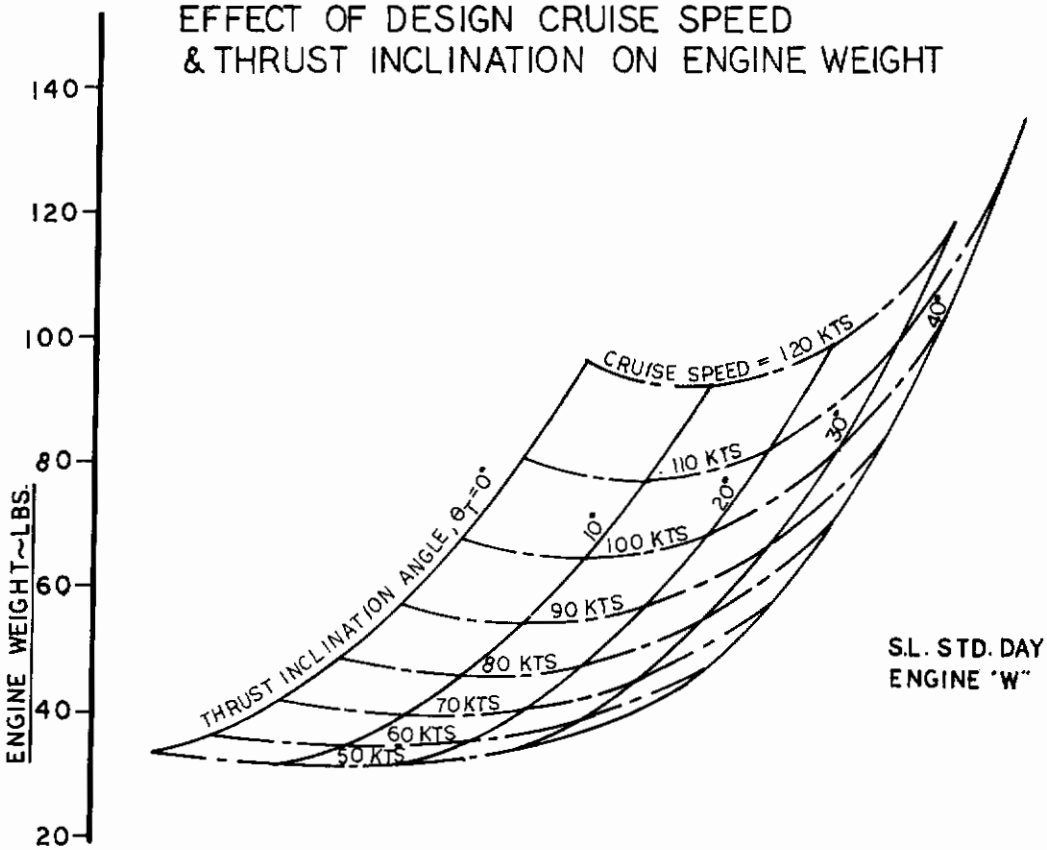

FIGURE 42

EFFECT OF DESIGN CRUISE SPEED
& THRUST INCLINATION ON MAXIMUM
CRUISE WEIGHT

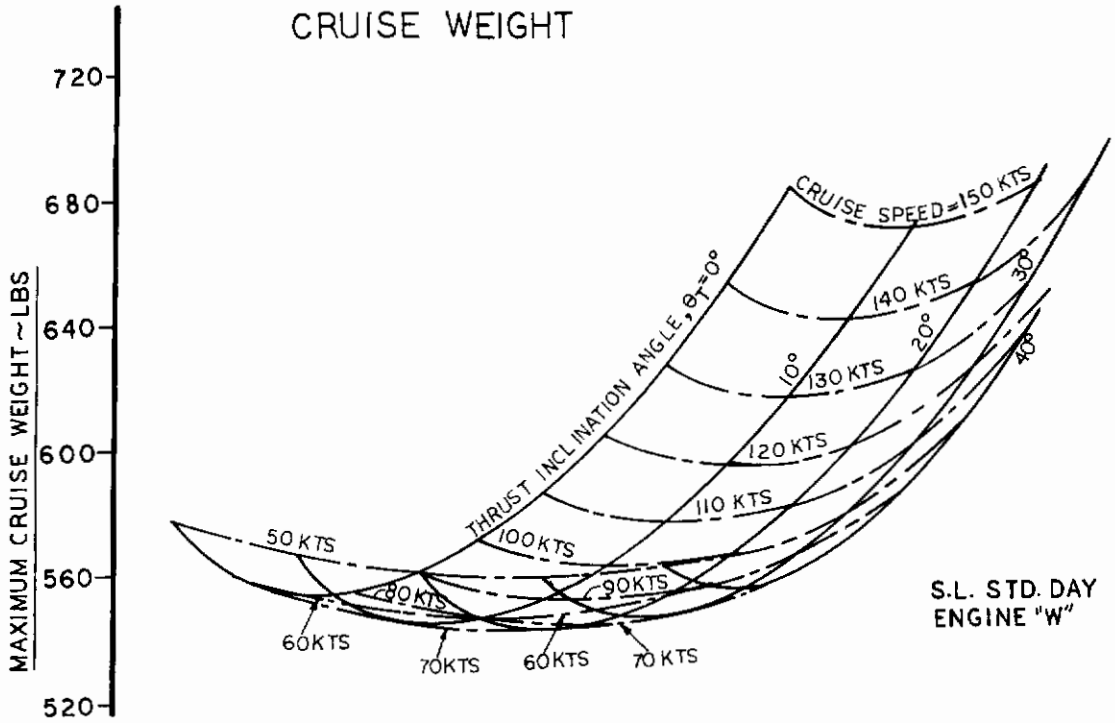

FIGURE 43

EFFECT OF DESIGN CRUISE SPEED & THRUST INCLINATION ON ENGINE WEIGHT

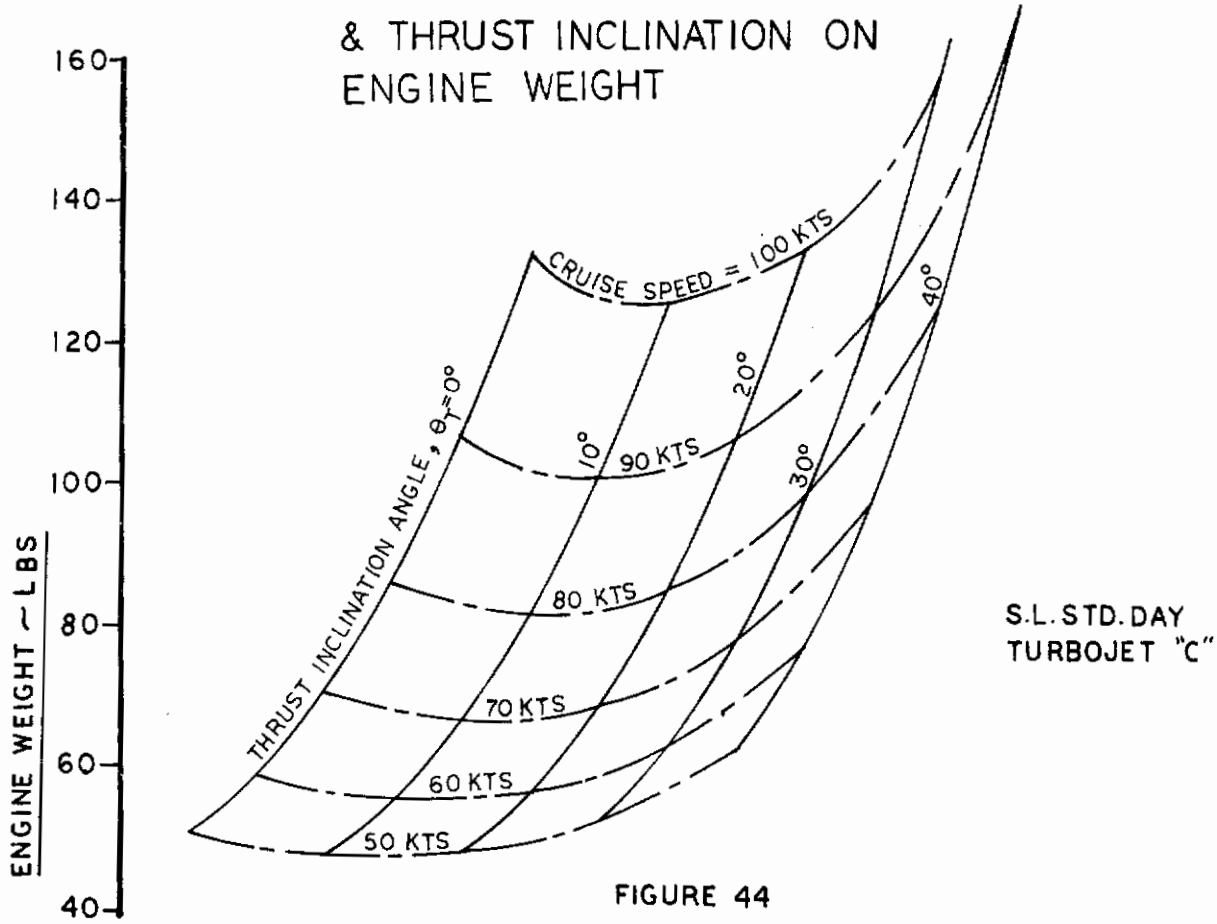

FIGURE 44

EFFECT OF DESIGN CRUISE SPEED & THRUST INCLINATION ON MAXIMUM CRUISE WEIGHT

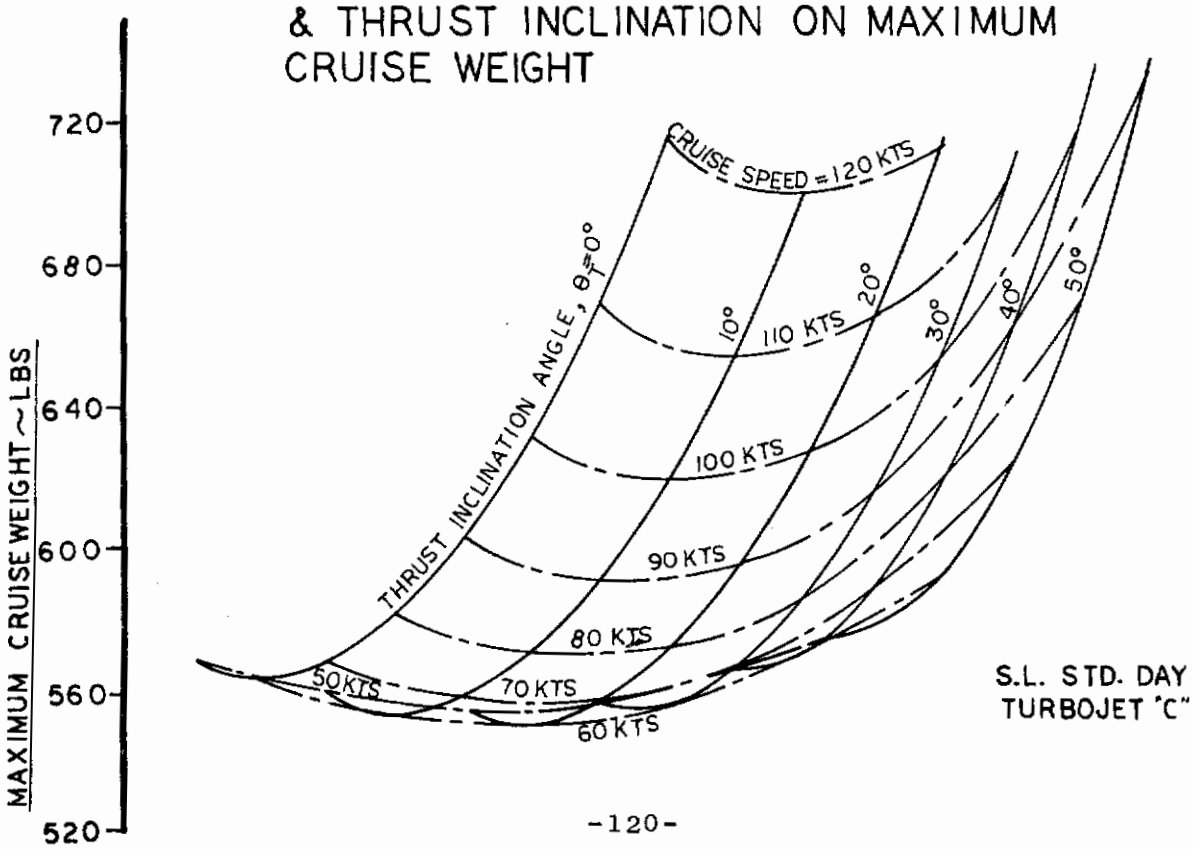

FIGURE 45
(W/I_K) REQUIRED TO TRIM VS. α_W

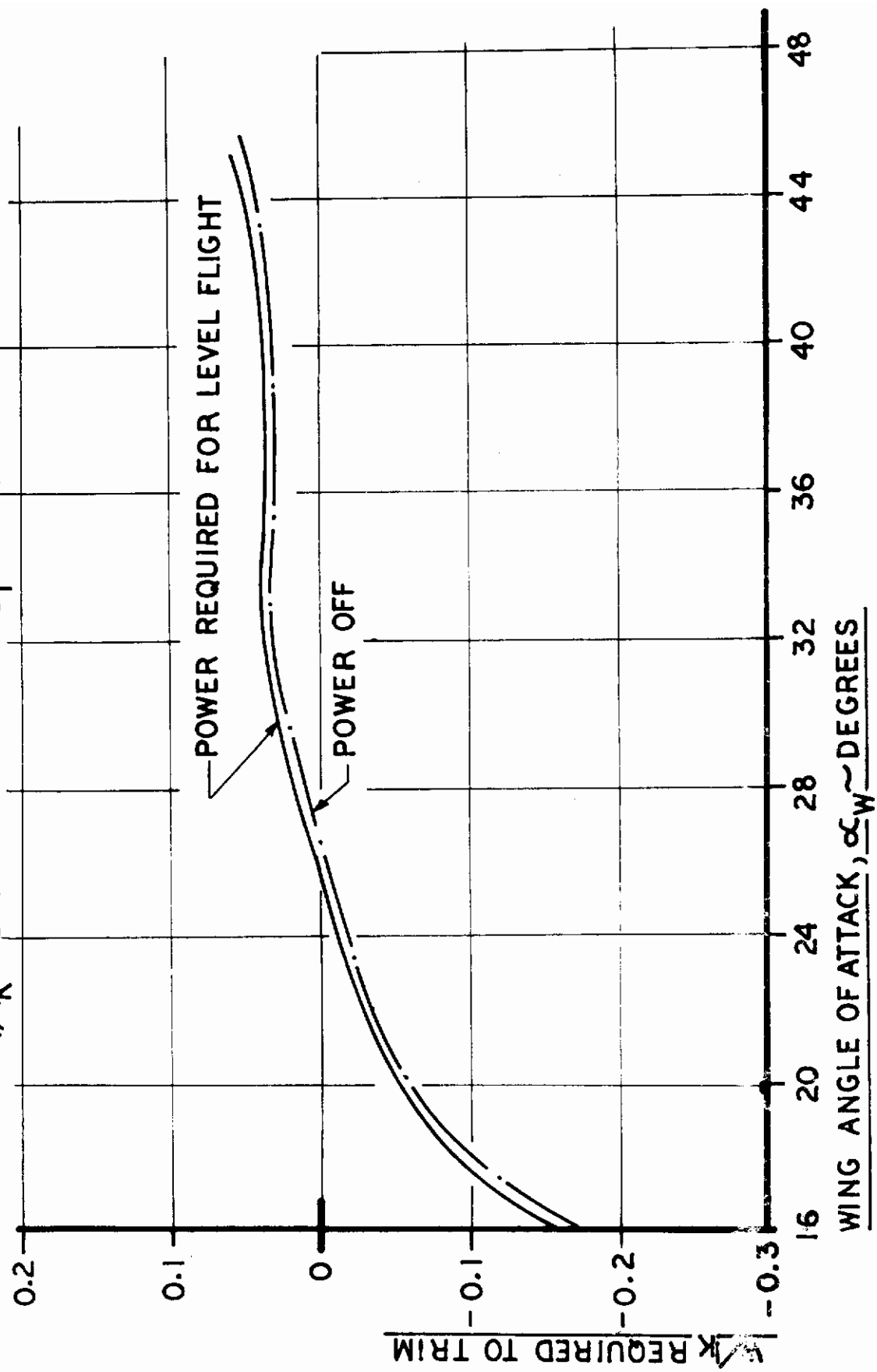

and cruise conditions (75-80 kts) are likely to be less severe. This fact alone allows use of such an engine. Using previously discussed ratioing techniques and assuming a constant S.F.C. of 0.64 lb/lb/hr, the T_A versus airspeed and altitude was estimated.

It is those calculated estimates which you find in Figure 15 showing thrust-availability.

4. Longitudinal Stability and Control

A determination of the stability and control characteristics of the AERCAB configuration was attempted under the subject investigation. Since the design is the result of operational and performance considerations evaluated during the AERCAB program, no attempt was made to alter the design due to purely stability and control considerations, or to conversely evaluate the effect of various configuration changes on the stability and control of the vehicle.

The analysis presented in this report is based on the limited data that exist for parawing configurations, and, unfortunately, those configurations are only similar to the AERCAB design. Since no aerodynamic information for the selected configuration exists in the form of wind tunnel or flight test results, and techniques for extrapolating existing parawing data to new designs have not been perfected, the present effort must be regarded as preliminary in scope. The results presented in this report serve only to identify problem areas which require additional evaluation.

a. Configuration

The AERCAB design analyzed in this report is described fully in earlier sections of this report. The rationale used to develop the design and fix the configuration also is presented earlier. A side view sketch is given in Figure 46, and pertinent details of the configuration are listed in Table 9.

Basically it is recalled that the vehicle consists of an ejection seat modified to house a small dual fan jet engine and a deployable 32.68 square foot parawing with an inflight sweep angle of 55°. In the flying configuration, the seat unit is suspended semi-rigidly below the parawing in such a manner that the parawing center keel is at a 12° angle of inclination to a

reference line extending along the seat back. Since the trim angle of attack for the AERCAB is in the 20° to 40° range, the pilot will fly this vehicle in a head forward, face down position.

The AERCAB is intended for up-and-away flight in VFR and IFR weather conditions. The vehicle is expected to cruise at speeds on the order of 100 knots for 30 minutes, it must be capable of climbing to an altitude of 10,000 feet, and it must be controllable in a descent, power-on and power-off. There is no requirement for take-off or landing. When the pilot wishes to land, he separates himself from the AERCAB and parachutes to the ground.

While no handling qualities have been established for vehicles such as the AERCAB, it seems reasonable to expect that the pilot would not be required to do any precision tracking tasks similar to air to air gunnery or ILS approaches. Presumably, the pilot must be able to maintain an approximate heading and altitude, but he would not be required to do even those simple tasks with any high degree of precision. The handling qualities requirements for an AERCAB vehicle certainly would be far less demanding than the requirements for more conventional flight vehicles.

Longitudinal control is achieved by means of shifting the position of the seat with respect to the parawing, thus changing the relationship between the parawing's center of pressure and the vehicle's center of gravity. A conventional seat up-and-down actuator system is planned to effect the seat shift, and the pilot will control seat position with the same toggle switch he uses to adjust seat height when the AERCAB is employed as a crewstation seat.

The pilot also can achieve some longitudinal control by means of a throttle lever for the jet engine, although the pitch attitude response to power changes was found to be very slow. A subsequent section contains a detailed discussion of how the throttle is an effective flight control when coordinated with the seat positioner.

Lateral/directional control is obtained by lateral rotation of the parawing with respect to the seat unit. The design has a self-centering toggle switch for controlling an actuator drum about which is wound

AXIS SYSTEM FOR LONGITUDINAL STUDY
(Body Axes Aligned with Thrust Axis)

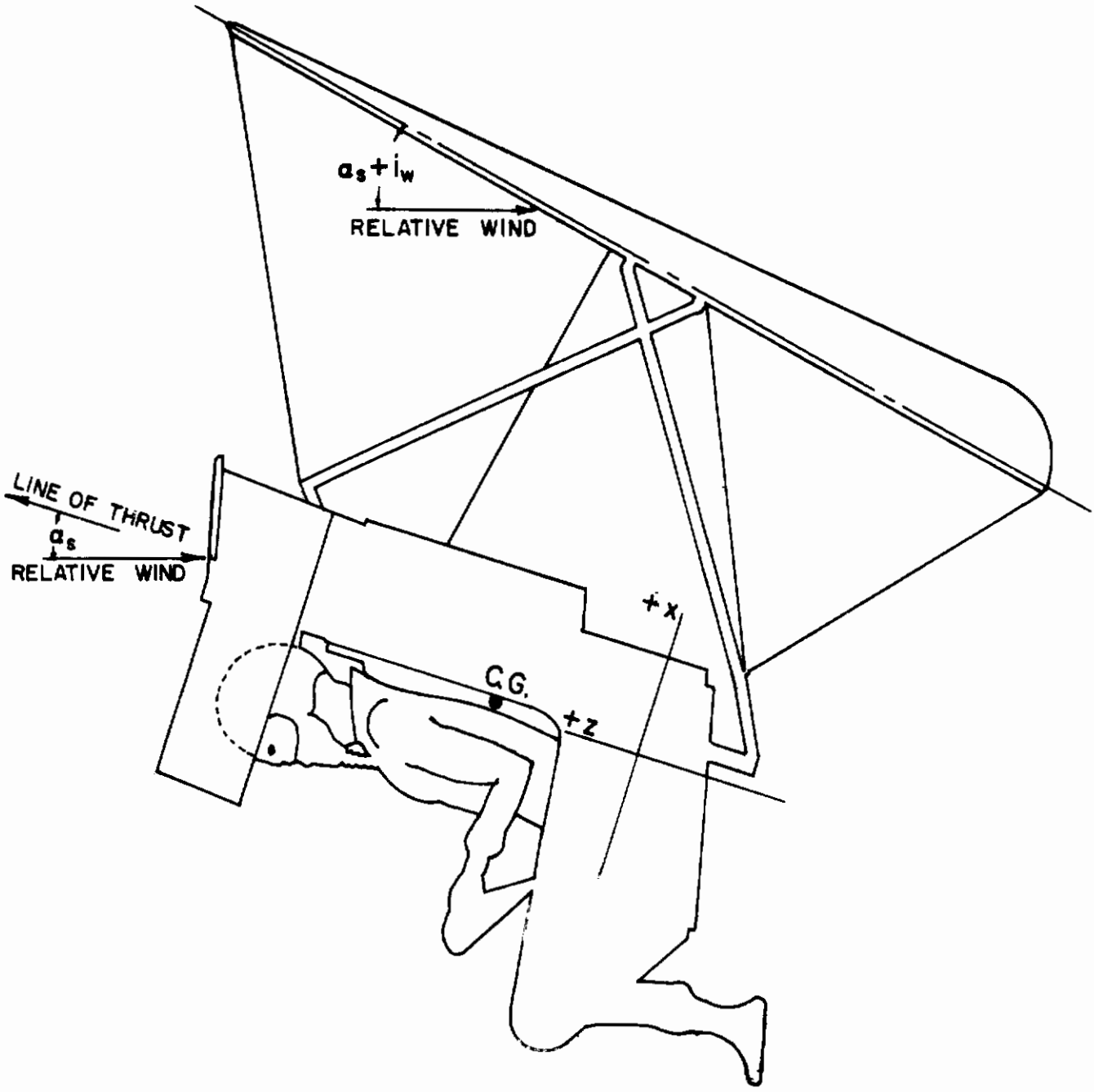

FIGURE 46

TABLE 9

GEOMETRIC PROPERTIES

Wing span, b = 7.80 ft.

Keel length, l_k = 6.81 ft.

Wing reference area, S = 32.68 ft.^{2}

MASS PROPERTIES (SEAT IN NEUTRAL POSITION)

Case	Average Weight	Maximum Weight	Minimum Weight
W, lbs	511	591	441
I yy, slug ft.^{2}	35.1	35.1	35.1
x_{CG}, inches	.804	1.857	.4606
z_{CG}, inches	12.76	14.55	11.41

a continuous line attached at each end to the leading-edge boom of the parawing, approximately at their midpoints. As the drum turns, the cable is shortened on one side and correspondingly lengthened on the other, so that the parawing is rotated about its keel axis, providing the lateral tilt and corresponding rolling moments.

b. Estimation of Aerodynamic Coefficients and Static Longitudinal Stability Derivatives

Numerical estimates of the vehicle's aerodynamic coefficients and static stability derivatives were derived by first developing expressions for the lift, drag, and pitching moment of the Stencel AERCAB. Force and moment data for the wing, which was considered to be the only significant source of lift, were obtained directly from Figure 6 of Reference 20, and are presented in Figure 47 of this report. Strut and seat-man-tanks combination drag values were taken directly without modification from an earlier section of this report.

In the longitudinal analysis presented in this report, all forces and moments were expressed in the axis system of Figure 46. The axis system is conventional for defining coordinates on an ejection seat, but is somewhat unconventional as a reference system for a flying vehicle. So that this report would be consistant with other aspects of the AERCAB analysis the standard ejection seat reference system defined in Figure 46 was used for the longitudinal analysis. The reader should note that when the AERCAB is in the flying position, the Z axis, which is aligned with the back-tangent line of the ejection seat occupant, is orientated nearly into the relative wind much as the longitudinal X axis would be for conventional aircraft notation.

Since the wing force and moment data of reference 20 were with respect to the midpoint of the keel, the pitching moment contribution of the wing with respect to the vehicle's center of gravity was:

$$\Delta C_{M_W} = \left[\left({}^{z}_{W} - {}^{z}_{CG} \right) \left(C_{L_W} \cos \alpha_S + C_{D_W} \sin \alpha_S \right) - \left({}^{x}_{W} - {}^{x}_{CG} \right) \left(C_{L_W} \sin \alpha_S - C_{D_W} \cos \alpha_S \right) \right] \frac{1}{\ell_K} \qquad (19)$$

Figure 47

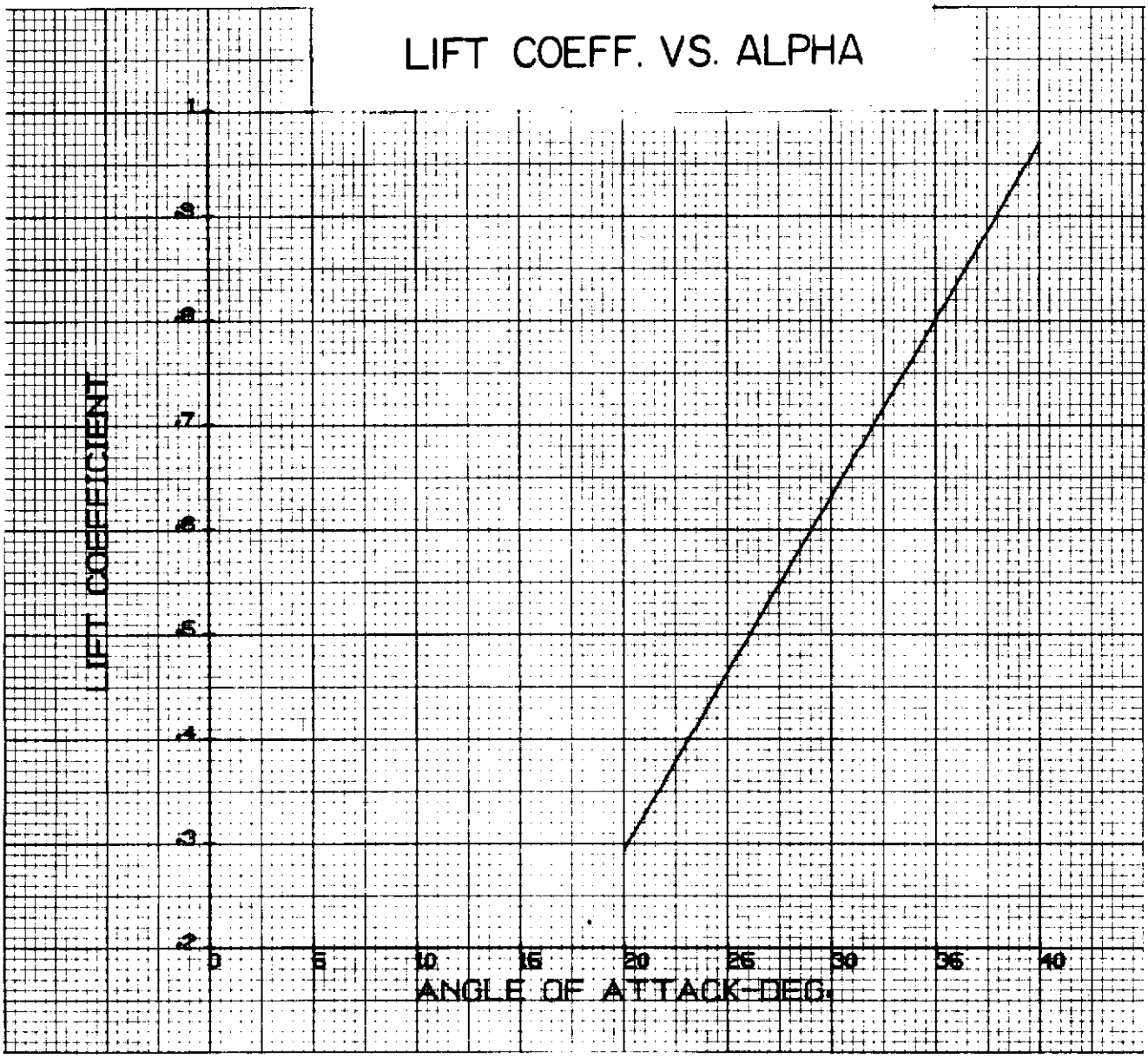

Figure 47, cont.

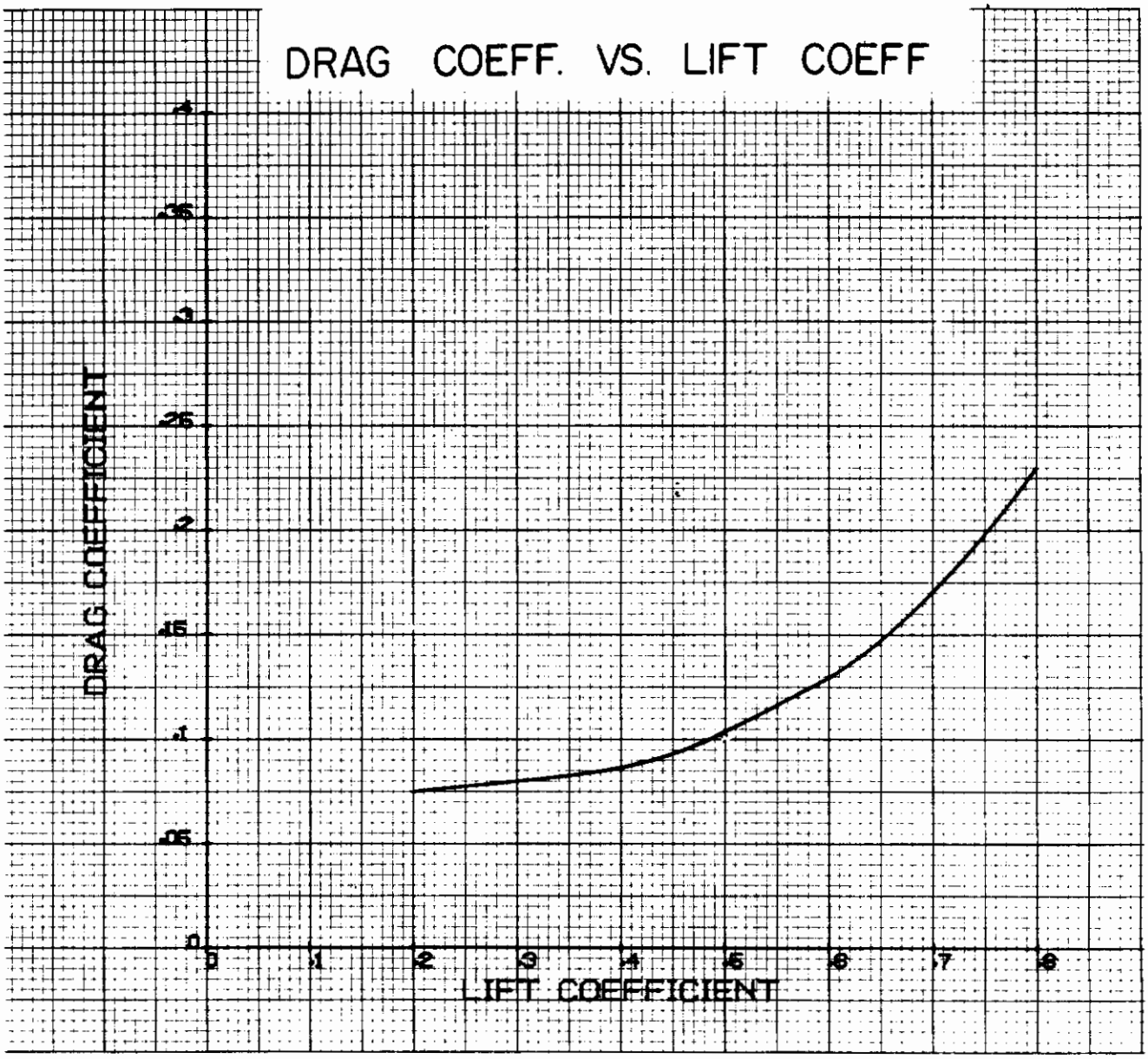

Figure 47, concluded

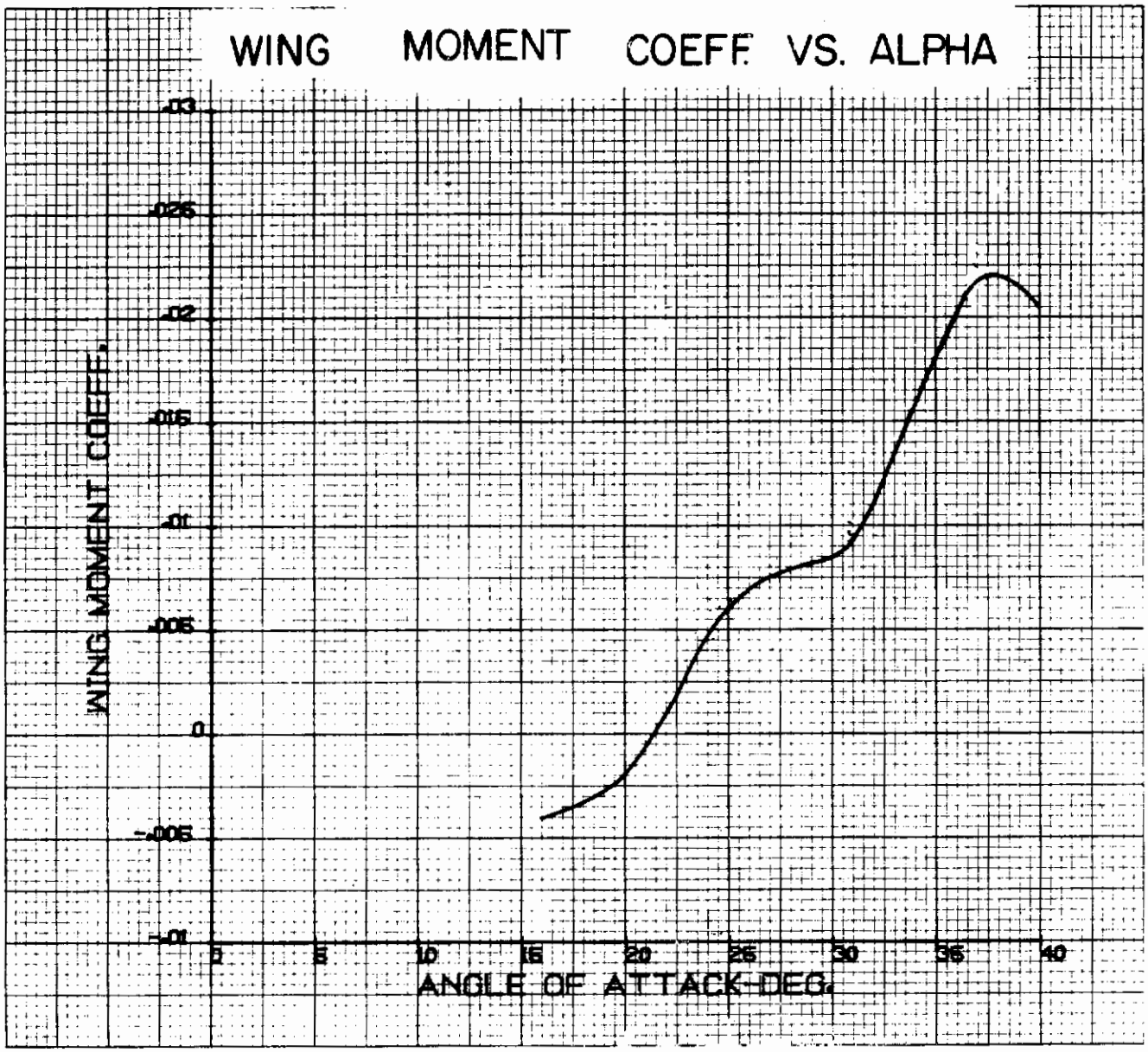

The strut drag was assumed to act parallel to the Z axis and at a point halfway between the seat back and the parawing keel.

Therefore, the X distance between the center of gravity and the centroid of the strut was 2.17 feet and:

$$\Delta C_{M_{STRUT}} = C_{D_{STRUT}} \left(\frac{x_{STRUT} - x_{CG}}{\ell_k} \right) \qquad (20)$$

The drag force associated with the seat-man-tanks combination was assumed to act through the centroid of the frontal projection of those elements. That location of the drag force resulted in a variation of the seat drag moment arm which was an approximately linear function of angle of attack. The seat contribution to the pitching moment coefficient was, therefore:

$$\Delta C_{M_{SEAT}} = \frac{-z_{CG}}{\ell_k} C_{D_{SEAT}} \sin \alpha_S + \left[\left\{ x_o + \dot{x}_o (\alpha_S + i_W) \right\} + \ldots \right.$$
$$\left. \ldots - x_{CG} \right] \left(C_{D_{SEAT}} \cos \alpha_S \right) \frac{1}{\ell_k} \qquad (21)$$

where $x_o = .510$ ft.

$\dot{x}_o = -.033$ ft./rad.

The moment contribution due to engine thrust was

$$\Delta C_{M_{THRUST}} = \frac{T}{qS} \left(\frac{x_{THRUST} - x_{CG}}{\ell_k} \right) \qquad (22)$$

where $x_{THRUST} = .396$ ft.

The engine also contributed a pitching moment due to turning the air through an angle, α_S as it entered the jet intake. Assuming an air to fuel ratio of 20:1, a specific fuel consumption of 0.8 pounds per hour per pound of thrust, and sea level density, that moment contribution was:

$$\Delta C_{M_{JET\ LIP}} = 0.000138\ V\ T\ (z_{JET\ LIP} - z_{CG}) \frac{\sin \alpha_S}{qS\ \ell_k} \qquad (23)$$

where $z_{JET\ LIP} = 3.53$ ft.

Summing up all of the contributions to the pitching moment yielded

$$C_M = C_{M_W} + C_{M_{SEAT}} + C_{M_{STRUT}} + C_{M_{JET\ LIP}} + C_{M_{THRUST}} \quad (24)$$

Numerical values of C_M as shown in static stability graphs contained in Figures 47-62 were obtained using the lift and drag equations shown below

$$\text{Lift:} \quad C_L qS + T \sin \alpha_S - W \cos \gamma = 0 \quad (25)$$

$$\text{Drag:} \quad -C_D qS + T \cos \alpha_S - W \sin \gamma = 0 \quad (26)$$

In addition, the lift and drag coefficients were expressed analytically as

$$C_L = C_{L_\alpha} \alpha_W + C_{L_o} \quad (27)$$

$$C_D = C_{D_o} + C_1 C_L + C_2 C_L^2 \quad (28)$$

where

$$C_1 = d\ C_D / d\ C_L \quad (29)$$

$$C_2 = d\ C_D / d\ C_L^2 \quad (30)$$

First, a given configuration (vehicle weight, wing and CG position) was selected. Secondly, a value of α_W was chosen and C_L and C_D calculated. Then, for level flight, ($\gamma = 0$), the lift and drag equations were solved for q and T. In the climb and glide cases a value of thrust was selected and the equations solved for α_W and q. C_M was then determined as a function of α, q, T, W, $x_W - x_{CG}$, and $z_W - z_{CG}$. Other values of α_W were chosen and the process repeated until enough points were obtained to plot the function $C_M = f(C_L)$ as shown in the static stability graphs.

c. Results and Discussion - Static Longitudinal Stability Analysis

Figures 49, 54, 56, 58, and 61 indicate that the AERCAB is statically stable for the entire center of gravity and weight envelope considered in the original vehicle design. The variations of pitching moment coefficients about the vehicle's center of gravity with lift coefficient for the 'average weight' configuration (511 lbs) in level flight (Thrust = 244 lbs), in a glide (Thrust = 0 lbs), and in a climb (Thrust = 360 lbs) are presented in Figures 49, 54 and 56, respectively. Results for the

'maximum weight' configuration (591 lbs) and the 'minimum weight' configuration (441 lbs), both in level flight, are presented in Figures 58 and 61, respectively. In addition to the design center of gravity range associated with a seat travel of 5 inches, the effects of greater rearward C.G. movement, denoted by larger values of z_s, are shown in Figures 49, 54, and 56.

For the average weight, level flight configuration (Fig. 49), the C_M vs C_L curves have negative slopes throughout their extent for the design extremes of seat position, i.e., $z_s = 0$ and $z_s = 5.0"$. The range of trim airspeeds extends from 112 knots to 96 knots, which corresponds to trim angles of attack between 21^o and 24.25^o. Extending the center of gravity envelope rearward by providing more down travel of the seat (greater values of z_s) causes the static stability to decrease and the range of trim lift coefficients to increase. For the case of $z_s = 6.25$, for example, the vehicle has a trim airspeed of 77 knots ($\alpha = 31^o$), and the static stability is nearly neutral at $C_L = 0.8$. For still more rearward values of C.G., the static stability at trim increases again. The neutral stability at intermediate C.G. values near $C_L = 0.8$ represents a mild pitch-up. The significance or severity of this tendency can only be evaluated by valid simulation of the vehicle and the mission it must perform. The wing alone contribution to static stability for this configuration (Fig. 50) is stable. The effects of the moment contribution due to the seat, struts, and thrust are increased static stability for a given C.G. position, reduced trim airspeed range, and increased trim airspeed magnitude. Comparing curves with identical values of z_s in Figures 49 and 50 demonstrates that dC_M/dC_L becomes more negative, and the trim airspeed range is reduced from 20 knots (between 100 and 80 knots) to 16 knots (between 116 and 96 knots) when the entire vehicle is analyzed. The same effects can be seen in the analysis of a vehicle identical to the basic configuration except that seat drag is greater (Fig. 51). For the same center of gravity positions ($z_s = 7.5$ and 10.0), dC_M/dC_L is more negative for the higher drag case, and the trim airspeed range is reduced from 7 knots (between 71 and 64 knots) to 5 knots (between 103 and 98 knots).

Different values of seat drag appear to have no effect on the static stability for a given trim C_L, however. For example, the static stability at $C_L = 0.4$ for the wing-alone case (Fig. 50) is equal to the static stability

at C_L = 0.4 for both the basic configuration (Fig. 49) and the higher seat drag configuration (Fig. 51). Only at values of $C_L > 0.55$ do the static stabilities for a given value of C_L appear to differ for the two seat drag conditions.

For the configurations analyzed in Figures 49, 50, and 51, the produce of seat drag times its moment arm with respect to the vehicle's center of gravity varies nearly linearly with angle of attack for $0.25 < C_L < 0.55$, and at C_L = 0, the moment due to seat drag is small compared with the moment due to wing drag. Therefore, at a given C.G. location, a change in seat drag effectively alters K, not C_{M_O}, in the following equation for a linear relationship between C_M and C_L:

$$C_M = C_{M_O} + KC_L \qquad (31)$$

Where C.G. position is used for trim, the static stability at trim will only be affected by C_{M_O}, hence, in this case, not by seat drag.

The effect of varying the x-distance between the center of gravity and the parawing keel is presented in Figure 52. Since the x-axis is nearly parallel to the resultant of the wing lift and drag forces for the trim C_L corresponding to $\Delta x_w = 0$ and $z_s = 5.0"$, changes in x_w have little effect on the trim airspeed for this configuration although changes in x_w do alter the vehicle's static stability. Increasing the separation between the parawing and the seat increase the static stability.

Changes in power affect the static stability and the trim speeds of the Stencel AERCAB. The power-off average weight glide (Fig. 54) is stable for the design C.G. envelope, but a mild pitch-up tendency near C_L = 0.85 for certain C.G. locations is present. Compared with the level flight case, the trim range for a 5-inch change in seat position is reduced to 12 knots (between 98.5 and 86.5 knots). The full-power climb at average weight (Fig. 56) is stable for a larger C.G. range than either the glide or level flight conditions. Pitch-up is not apparent for the most rearward C.G. location investigated (z_s = 10.0). The trim airspeed range in the climb is 15 knots (between 113 and 98 knots) which nearly coincides with the level flight trim airspeed range.

The AERCAB also is statically stable for maximum and

Figure 48

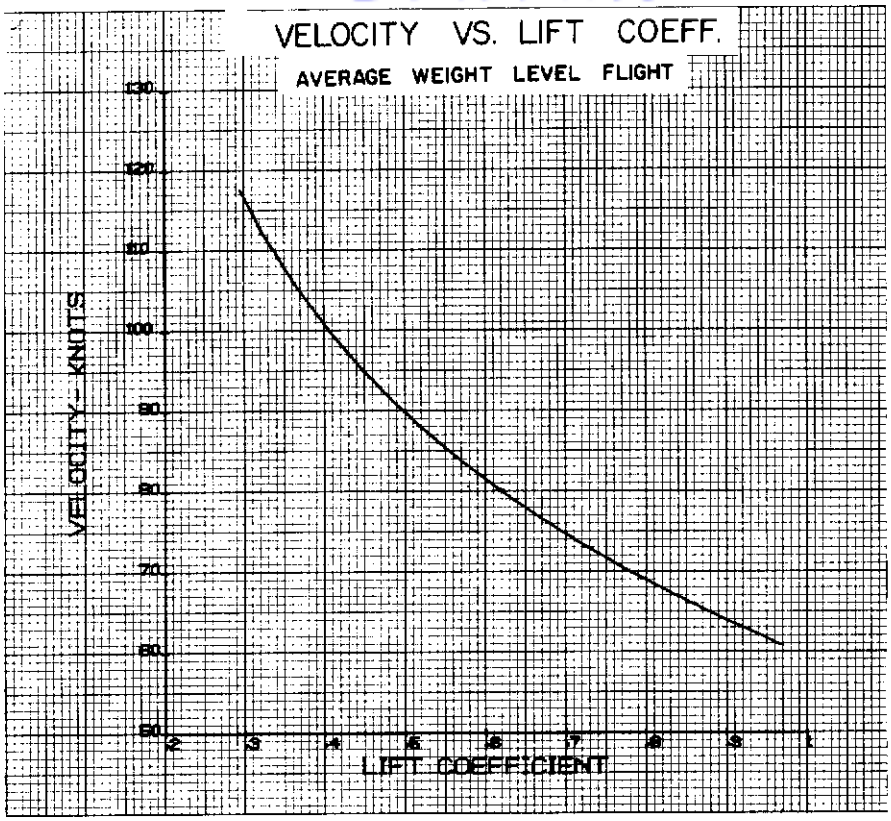

Figure 49

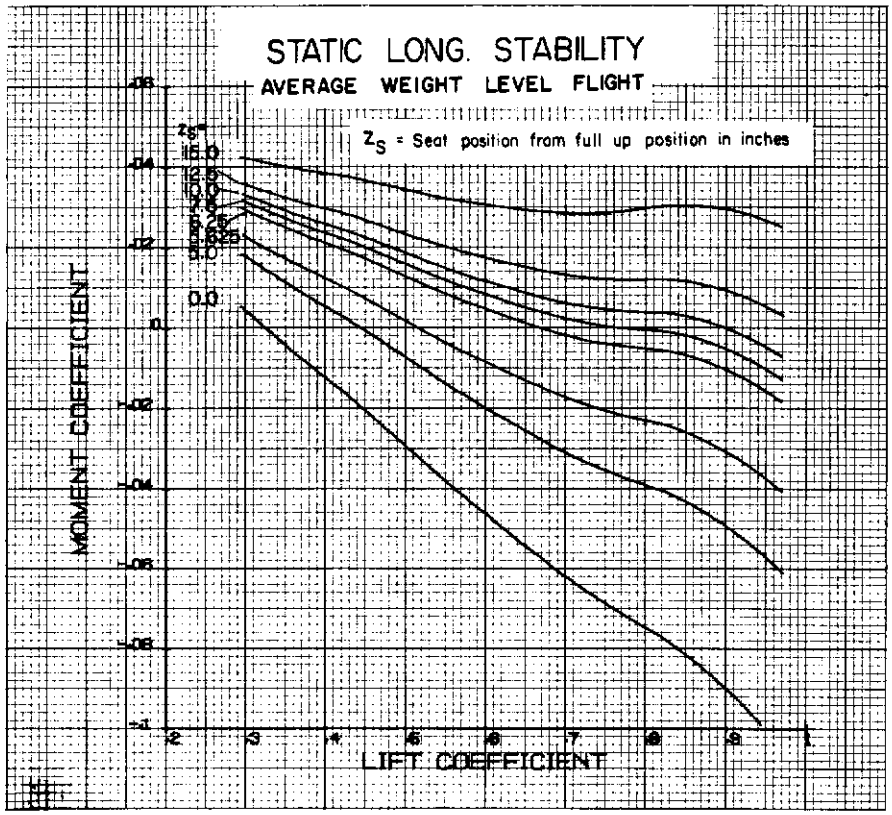

Figure 50

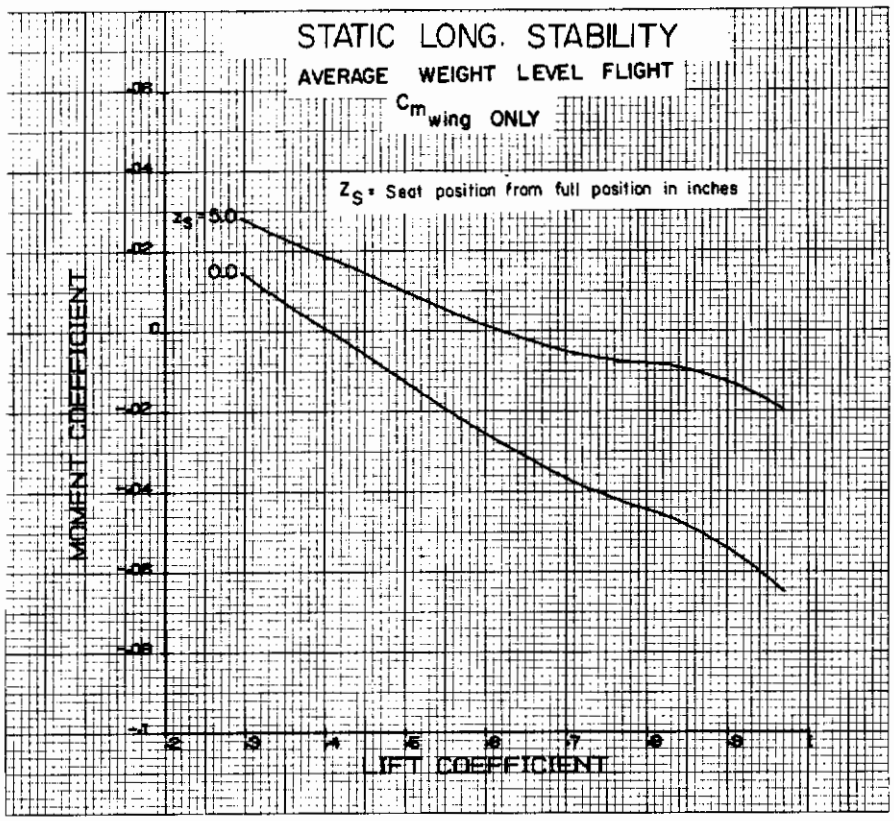

Figure 51

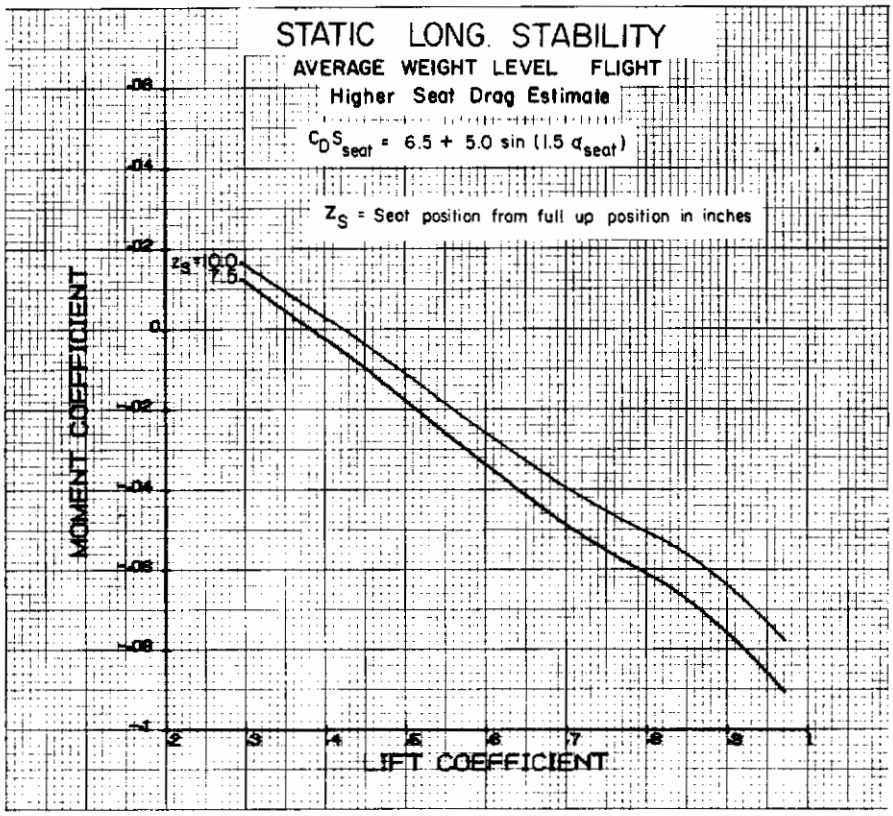

Figure 52

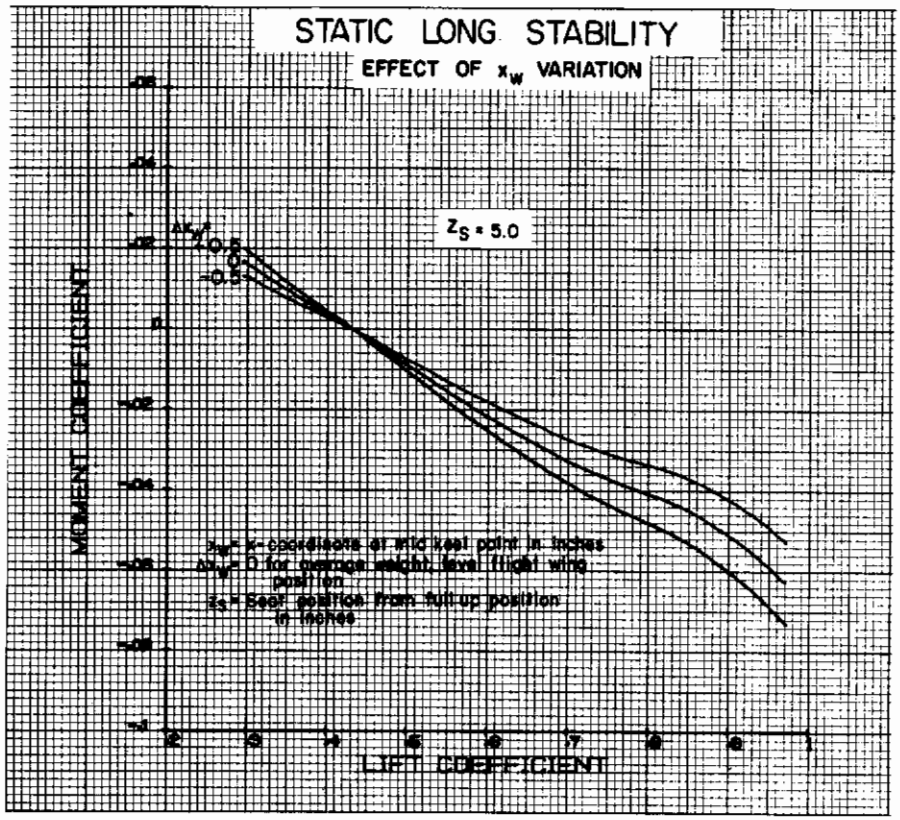

Figure 53

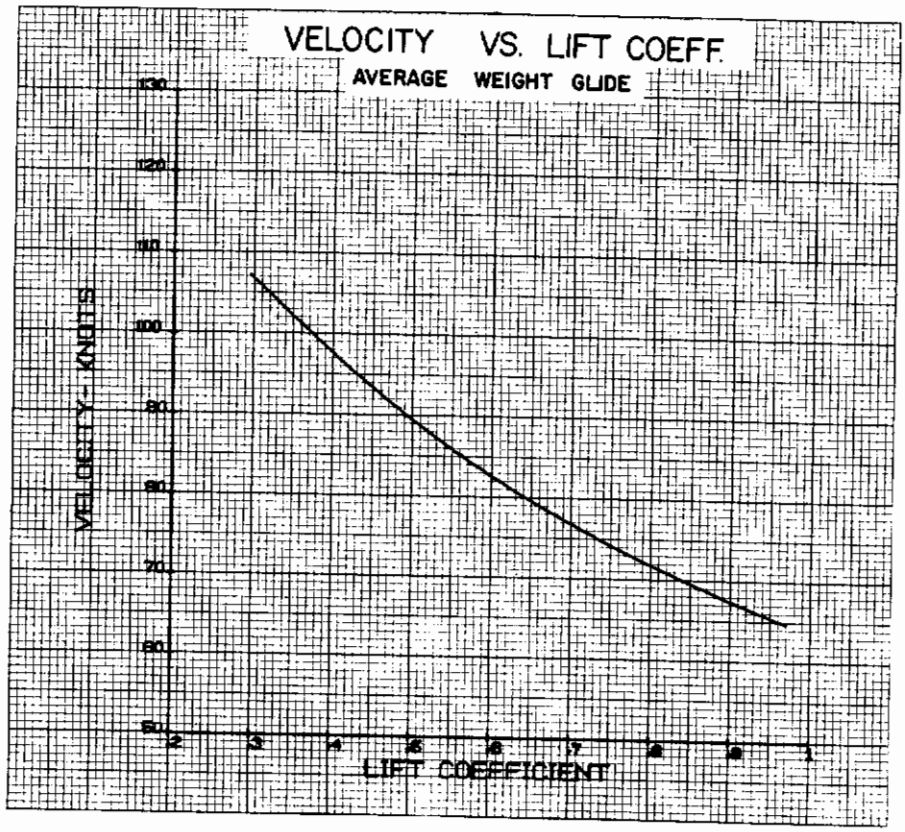

minimum weight level flight conditions, as seen in Figures 58 and 61. The effect of a weight change is nearly identical to a change in C.G. location, as seen be comparing figures 49, 58, and 61. At minimum weight the variation of pitching moment with lift coefficient for the $z_s = 0$ C.G. location is nearly identical to C_M vs C_L at maximum weight for the $z_s = 5.0$ C.G. location. Consequently, the level of static stability for a given trim lift coefficient does not change with changes in vehicle weight. Since weight changes do not affect the static stability of the vehicle at trim C_L's, it is reasonable to assume that power effects at any weight will be similar to the power effects for the average weight case (Figs. 49, 54, and 56).

Weight changes do affect the trim airpseed range. The maximum trim speed is reduced from 131 knots for the maximum weight condition to 100 knots for the minimum weight case. For both maximum and minimum weight conditions, the trim speed range is 15 knots.

The wing-alone contribution to static stability for both the full gross and minimum weight conditions behaves similarly to the average weight, level flight, wing-alone case. For either weight condition, the moment contributions of the seat, engine, and struts increase the static stability for a given C.G. location, but the level of stability doesn't change for a given trim lift coefficient, as seen by comparing figures 58 and 61 with figures 59 and 62. The trim airspeed range is reduced and the magnitude of the trim speeds is increased when the entire vehicle is considered at either weight. For the maximum weight case, the trim range is reduced from 19 knots (between 117 and 98 knots) for the wing-alone case to 15 knots (between 131 and 116 knots) for the complete vehicle. At minimum weight, the trim range is reduced from 26 knots (between 86 and 60 knots) for the wing-alone case to 15 knots (between 100 and 85 knots) for the entire vehicle.

Figures 63 and 64 are summary plots of static stability at trim lift coefficients for the various configurations and flight conditions presented in Figures 49, 54, 56, 58, and 61. Figure 63 indicates that for a given trim C_L, both the full power climb and the power-off glide are more statically stable than the level flight case. The value of dC_M/dC_L for a given trim C_L, however, is the same for all weight conditions. The pitch-up

tendency at high C_L's can also be seen in Figure 63, especially for the power-off glide condition. The static stability for various vehicle configurations can be seen in Figure 64. For level flight at a given trim lift coefficient, the value of dC_M/dC_L is not influenced greatly by the weight of the vehicle or the moment contributions of the seat, engine, or struts.

The AERCAB as presently designed may have an unsatisfactory range of trim lift coefficients. Before a satisfactory flight article can be constructed, the designer must have accurate aerodynamic data for the vehicle and its various components. Performance considerations will place specific demands on the trim C_L of the AERCAB since the vehicle must be trimmable at or near the value of C_L for maximum range. The climb and glide phases of the mission will demand a certain usable range of C_L. With the center of gravity range available in the basic AERCAB design, the designer must be sure that he can achieve specific trim conditions and maintain control at those values of C_L for all the required flight conditions.

An additional factor associated with the trim conditions shown in Figure 58 is the possibility of parawing luffing at low values of C_L. Reference 20 noted the occurrence of this phenomenon at minimum lift coefficients in the C_L = 0.1 to 0.3 range. Since luffing may present a minimum acceptable value of C_L and pitch-up will limit the maximum values of C_L, the designer may have other restraints on trim conditions and C.G. travel in addition to performance and control considerations.

Before the AERCAB's configuration is frozen, therefore, wind tunnel data on the lift, drag, and pitching moment characteristics of the vehicle should be obtained in order to assure that the flight article will be trimmable over the required range of lift coefficients.

d. Estimation of Dynamic Longitudinal Stability Derivatives

(1) Equations of motion.

The longitudinal dynamic stability and dynamic response have been analyzed with perturbation equations in the style of Reference 29. In general, the assumptions and simplifications are the standard ones outlined in that reference; hence, the limitations and qualifications on the

Figure 54

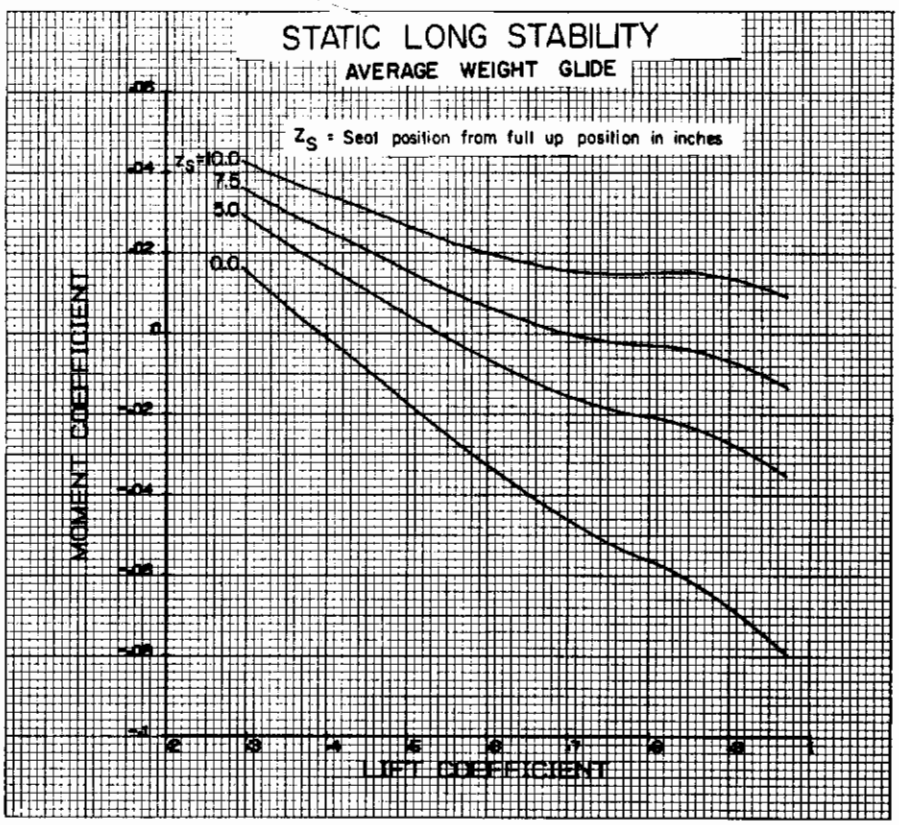

Figure 55

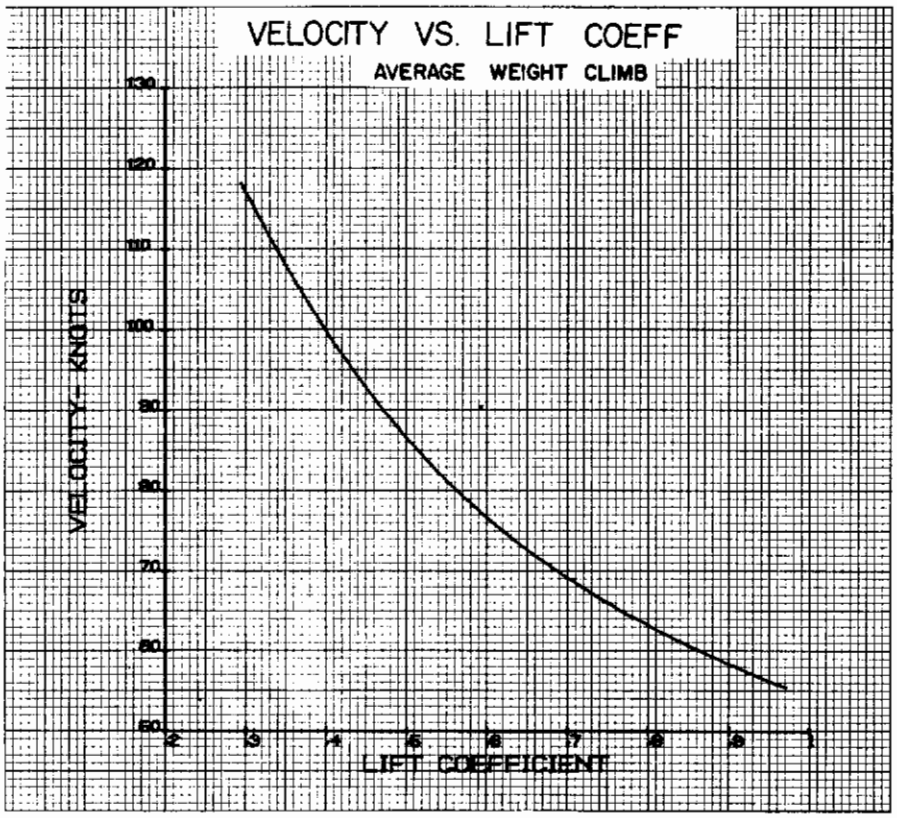

Figure 56

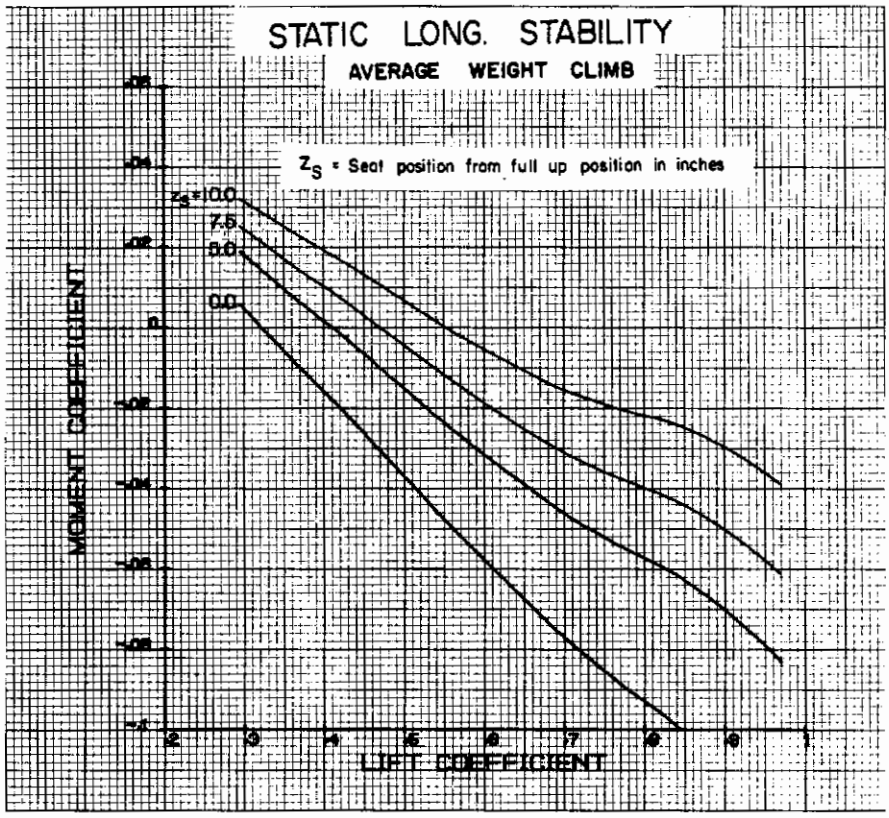

Figure 57

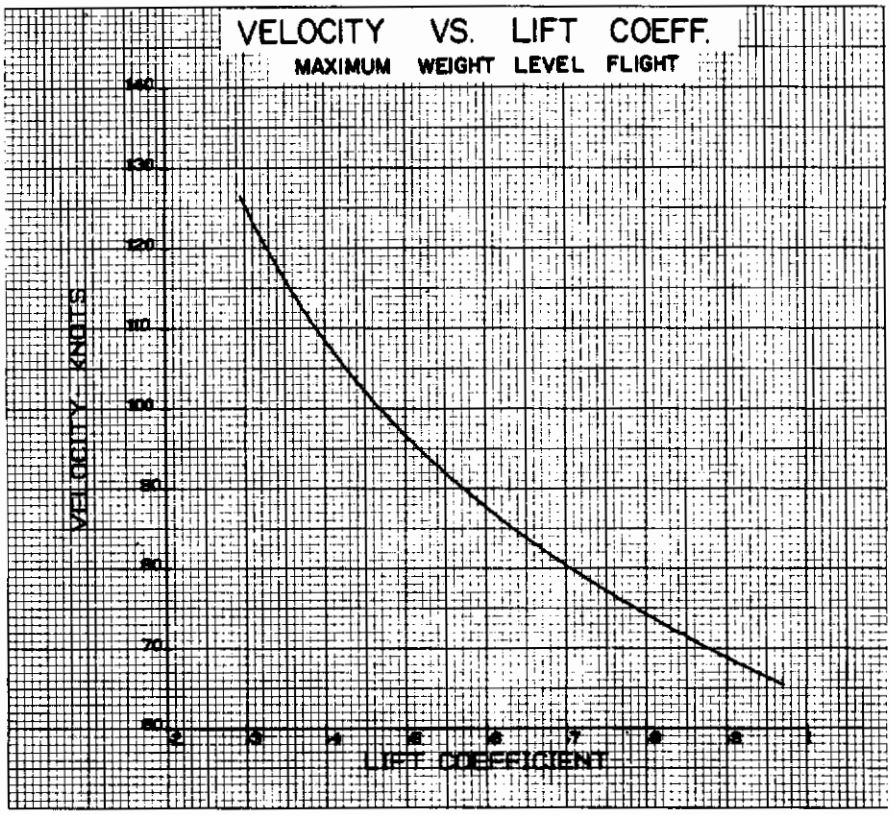

Figure 58

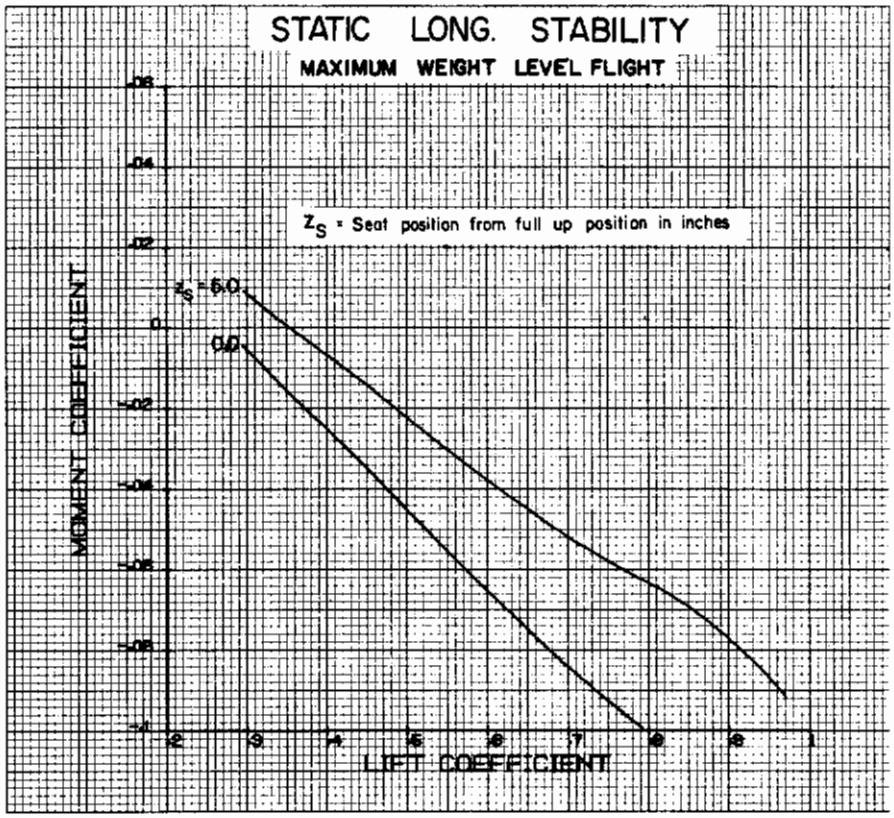

Figure 59

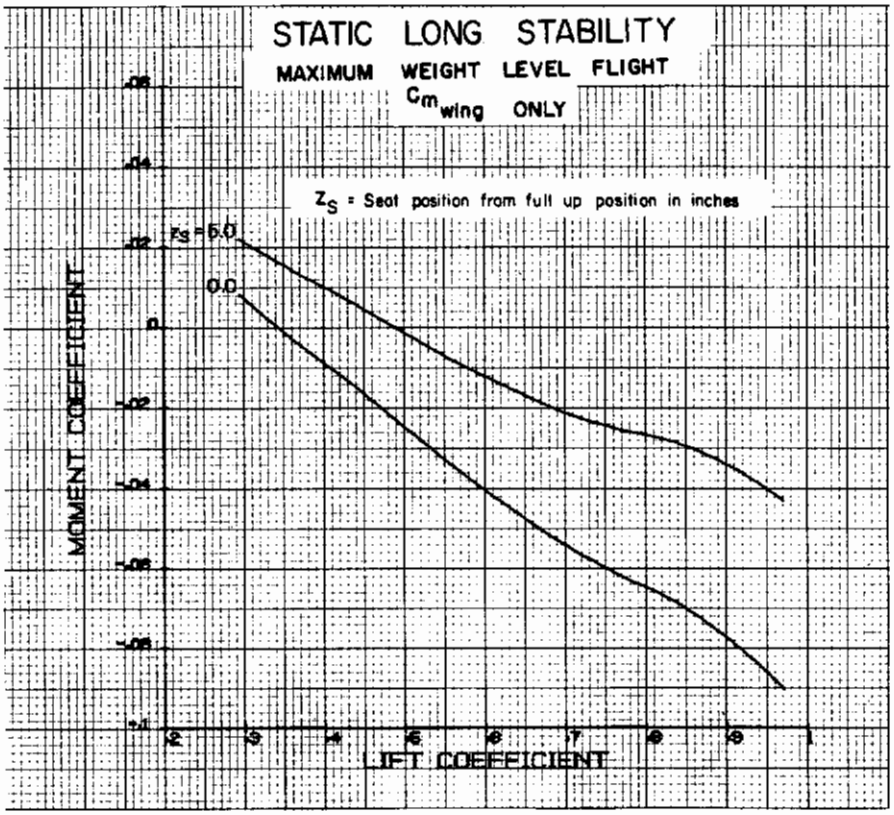

Figure 60

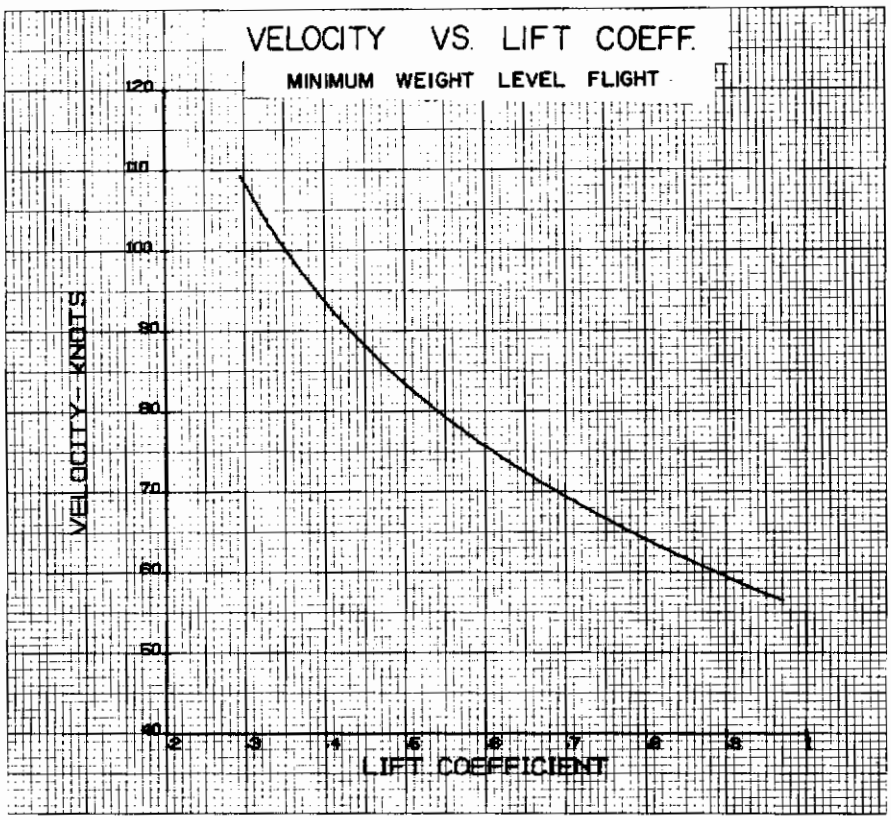

Figure 61

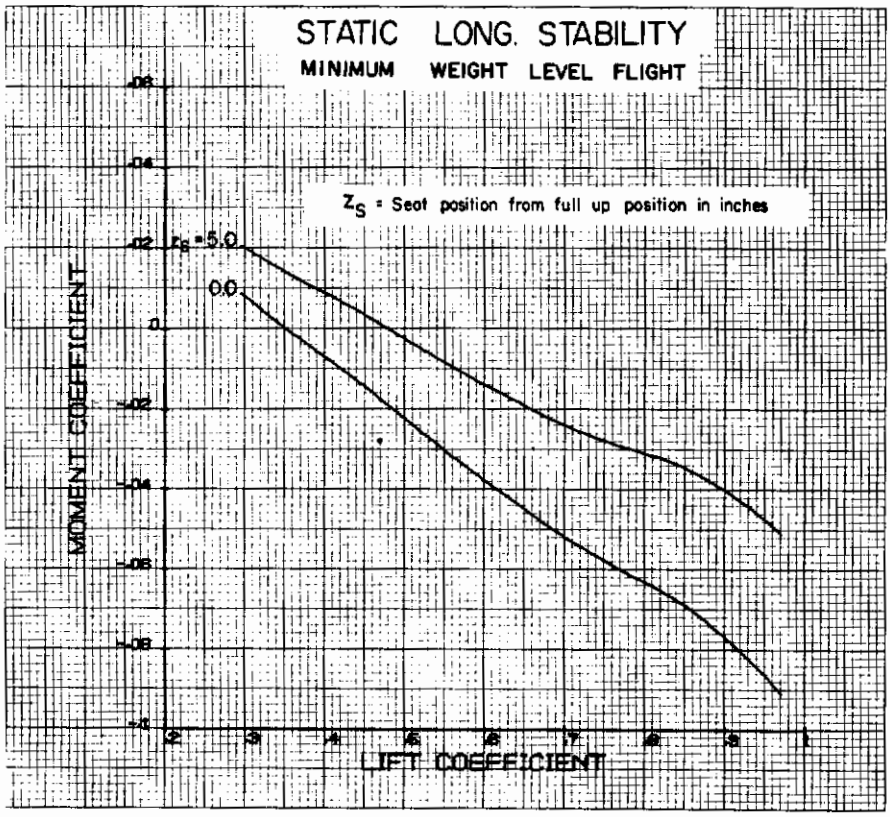

Figure 62

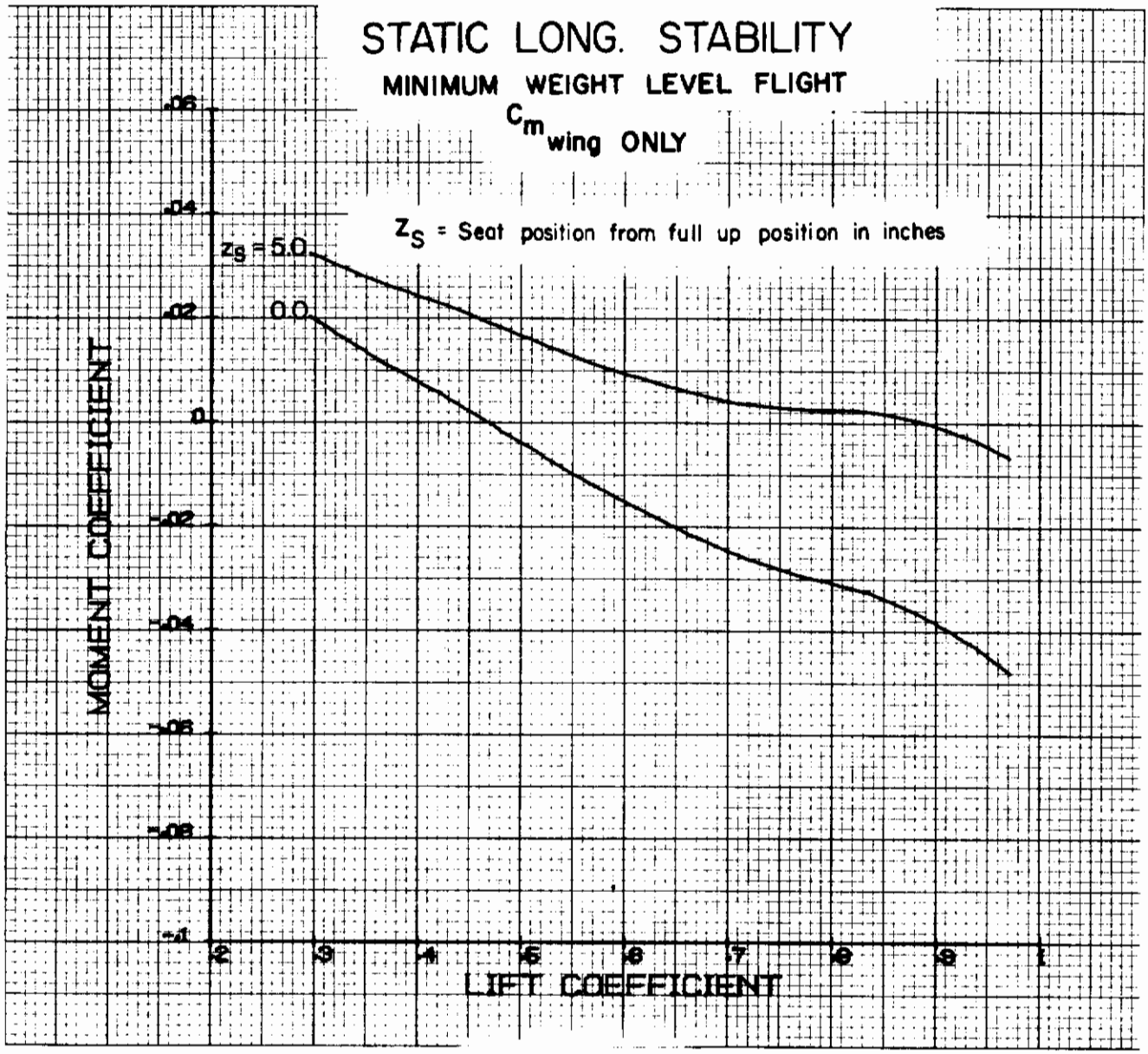

Figure 63

Static Longitudinal Stability for Trim Versus Trim Lift Coefficient

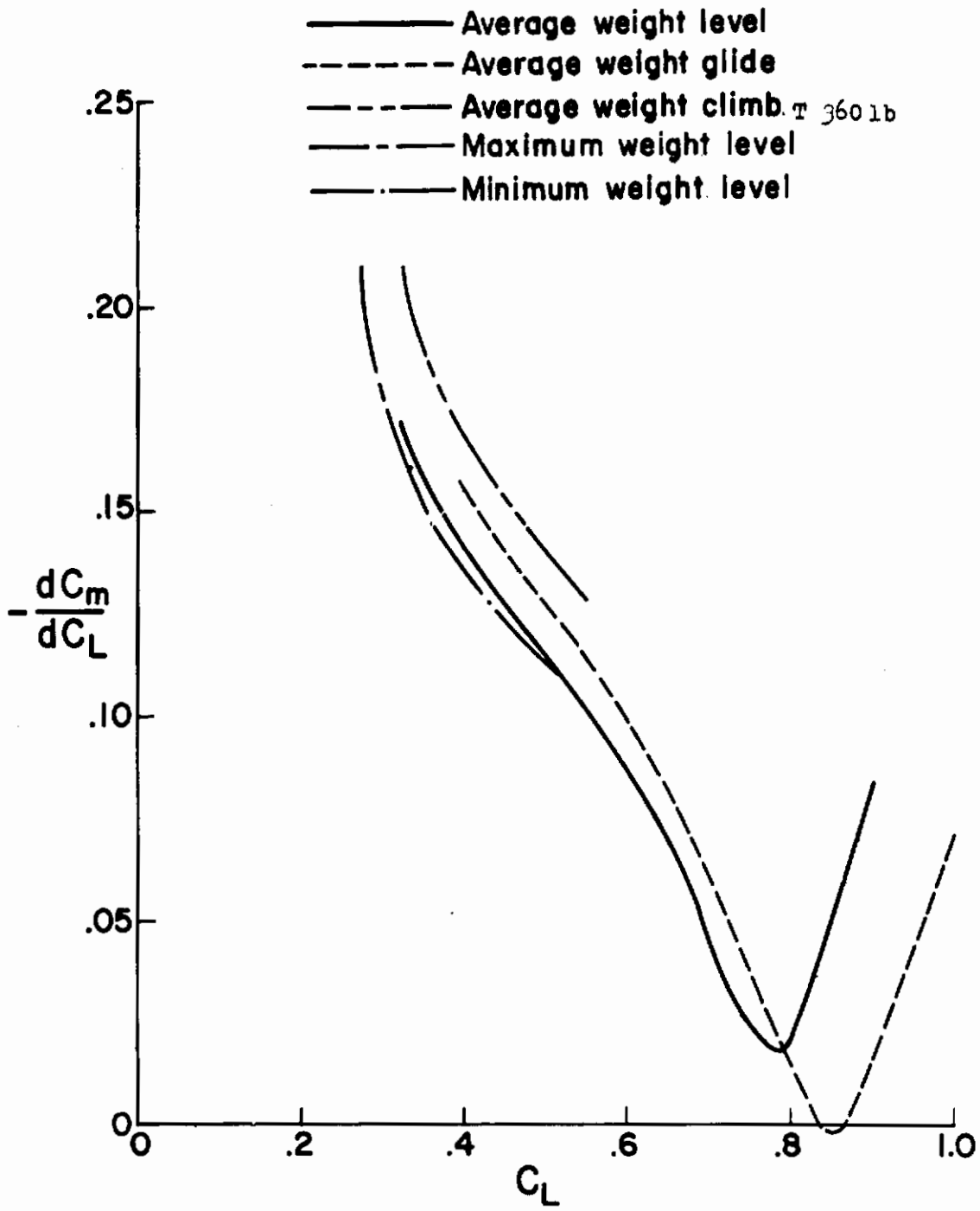

Figure 64

Static Longitudinal Stability for Trim Versus Trim Lift Coefficient

(EFFECTS OF SEAT DRAG AND PITCHING MOMENT ESTIMATES)

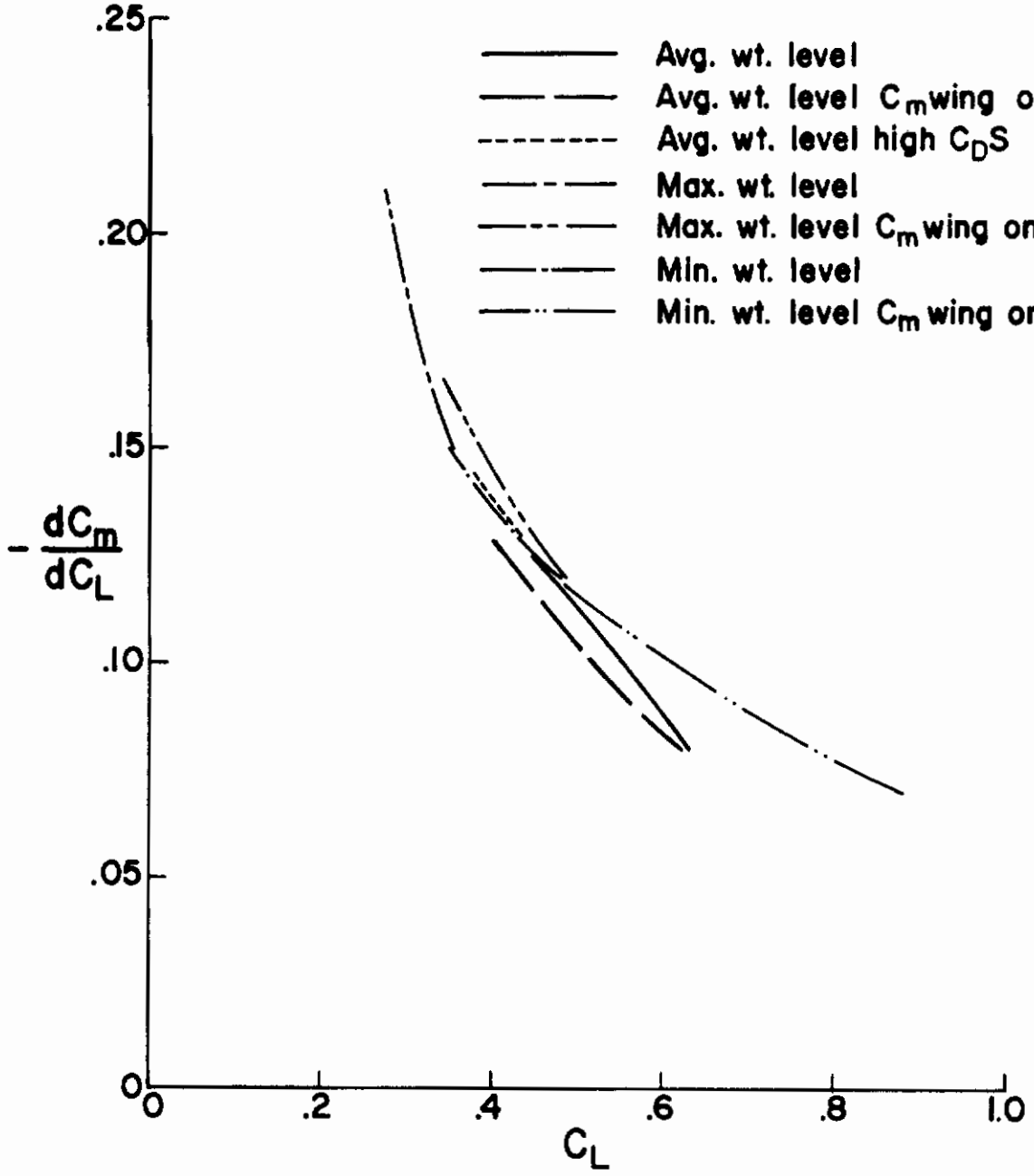

results are the ones familiar in the field of airplane dynamics. There are no particular features of the AERCAB configuration, or the parawing, which require any novel procedures for small perturbation response estimation.

The qualification to small perturbations should be emphasized for a vehicle like the AERCAB. The results herein apply only to the approximately steady, almost level, flight condition after the transients of deployment have subsided. No attempt has been made here to study the deployment phase of the AERCAB mission profile.

The longitudinal equations are:

Drag: $$\left[s + (D_V - T_V)\right]\Delta V + \left[D_\alpha - g\right]\Delta\alpha + g\Delta\theta = T_{\delta_T}\Delta\delta_T \qquad (32)$$

Lift: $$\frac{L_V}{V_O}\Delta V + \left[s + \frac{L_\alpha}{V_O}\right]\Delta\alpha - s\Delta\theta = 0 \qquad (33)$$

Moment: $$-M_V\Delta V - \left[M_{\dot\alpha}s + M_\alpha\right]\Delta\alpha + s\left[s - M_{\dot\theta}\right]\Delta\theta = M_{z_s}\Delta z_s \qquad (34)$$

In the above equations, there are terms on the right-hand side for changes of throttle position and seat (C.G.) actuator position. These are the two controls over longitudinal motion available to the pilot. He has a lever connected to the throttle for controlling thrust, and a three-position switch for controlling the seat-position actuator motor. The switch commands actuator drive-motion in bang-bang fashion, forward or backward, and is spring-loaded to center-off. A small inertia effect associated with the seat control has been omitted for simplicity. It would produce a small impulse of drag and moment whenever the switch was operated. The seat position actuator is thus represented by the auxiliary equation

$$\Delta\dot z_s = K_W\Delta\delta_{sw} \qquad (35)$$

where K_W is the velocity constant of the actuator, and $\Delta\delta_{sw}$ is switch position: either +1 (forward), 0 (center), or -1 (backward).

(2) Coefficients and stability derivatives.

The following formulas and aerodynamic constants

are used in the longitudinal equations. Only one loading configuration is considered for these dynamic calculations, corresponding to the average-weight pilot plus full fuel load (511 lbs). Two flight conditions are considered:

Steady level flight; $C_L = .565$, $V = 142$ fps, $q = 24$ psf,

$T = 244$ lbs

and $C_L = .763$, $V = 119$ fps, $q = 17.0$ psf,

$T = 229$ lbs

The former is close to the nominal, or design, operating point. The latter is included to see the effect of reduced static stability at higher angle of attack.

Starting with the Drag equation:

$$D_V = \frac{2g}{V} \frac{C_D}{C_L} \qquad (36)$$

for $C_L = .565$, $C_D = .30$, $D_V = .208$;

and $C_L = .763$, $C_D = .38$, $D_V = .221$

$$\text{also, } T_V = \frac{1}{m} \frac{\partial T}{\partial V} \qquad (37)$$

$$\frac{\partial T}{\partial V} = .592 \frac{\text{lbs}}{\text{ft/sec}} \quad ; \quad T_V = .037$$

$$\text{and, } D_\alpha = \frac{g}{C_L} \frac{\partial C_D}{\partial \alpha} \qquad (38)$$

$$\text{for } C_L = .565 \text{ , } \frac{\partial C_D}{\partial \alpha} = .63/\text{rad} \text{ , } D_\alpha = 31.1$$

$$C_L = .763 \text{ , } \frac{\partial C_D}{\partial \alpha} = 1.05/\text{rad} \text{ , } D_\alpha = 36.7$$

$T\delta_T$ - This control sensitivity does not enter into the characteristic motions of the vehicle. In the simulation experiments, being in no sense critical, it was simply set to a convenient value.

Considering the Lift equation terms:

$$\frac{L_V}{V_O} = \frac{2g}{V_O^2} = 0.00374 \tag{39}$$

$$\frac{L_\alpha}{V_O} = \frac{g}{V_O C_L} \frac{\partial C_L}{\partial \alpha} \tag{40}$$

for $C_L = .565$; $\frac{\partial C_L}{\partial \alpha} = 1.92/\text{rad}$; $\frac{L_\alpha}{V_O} = .665$

and $C_L = .763$; $\frac{\partial C_L}{\partial \alpha} = 1.92/\text{rad}$; $\frac{L_\alpha}{V_O} = .563$

Considering the Moment equation terms:

$$M_V = \frac{2qS\ell_k}{I_{yy}} \left(- Cm_T + q\frac{\partial C_m}{\partial q} \right) \tag{41}$$

The first effect above, due to engine thrust, is toward positive M_V. Its outside value, for maximum power, allowing for both the direct thrust effect and inlet forces, was estimated to be

$$\Delta_1 M_V = + .063 \tag{42}$$

The second term, for aeroelasticity, cannot really be estimated with any validity. A crude, but possibly reasonable, assumption is that the AERCAB would have elastic properties similar to the vehicle tested in Reference 31. Using the same value of $q \frac{\partial C_m}{\partial q}$:

$$\Delta_2 M_V = - .026 \tag{43}$$

Velocity stabilities, M_V, of this order of magnitude were quickly found to be of no significance to the pilot; and so, for most of the calculations and simulation, it has been assumed $M_V = 0$.

$$M_{\dot{\alpha}} = \frac{qS\ell_k}{I_{yy}} \frac{\partial C_m}{\partial \dot{\alpha}} \tag{44}$$

This angle-of-attack damping derivative is evaluated by the formula in Reference 30 for low aspect-ratio triangular wings. This estimate is considered

in the theory. From this Reference:

$$\frac{\partial C_m}{\partial \frac{\dot{\alpha} \ell_k}{2V}} = -.53 \qquad (45)$$

and for $C_L = .565$; $M_{\dot{\alpha}} = -1.85$

and $C_L = .763$; $M_{\dot{\alpha}} = -1.63$

$$M_\alpha = \frac{qS\ell_k}{I_{yy}} \frac{dC_L}{d\alpha} \frac{dC_m}{dC_L} \qquad (46)$$

This important static stability parameter is evaluated from the static trim analysis preceding. dC_M/dC_L is taken from Figure 63 for the particular lift coefficients:

for $C_L = .565$; $\frac{dC_M}{dC_L} = .088$; $M_\alpha = -25.7$

and for $C_L = .763$; $\frac{dC_M}{dC_L} = -.02$; $M_\alpha = -4.15$

$$M_{\dot{\theta}} = \frac{qS\ell_k}{I_{yy}} \frac{\partial C_m}{\partial \dot{\theta}} \qquad (47)$$

The basic value of the pitch damping, $M_{\dot{\theta}}$, is evaluated, like $M_{\dot{\alpha}}$, from Reference 30. The formula is

$$\Delta_1 \frac{\partial C_m}{\frac{\partial \dot{\theta} \ell_k}{2V}} = -\pi A \left(\frac{3}{16} + \frac{1}{12} + \frac{1}{36} \right) = -1.08 \qquad (48)$$

There are two additional contributions due to separation of the pitching axis (through the C.G.) from the wing axis of the reference report. These are associated with the u and w velocity components at the wing reference axis due to rotation about the C.G.

$$\Delta M_{\dot{\theta}_1} = -2(x_w - x_{CG}) \frac{qS\ell_k}{VI_{yy}} \left[C_L \frac{(z_w - z_{CG})}{\ell_k} + C_{D_W} \frac{(x_w - x_{CG})}{\ell_k} + C_{M_W} \right] \qquad (49)$$

$$\Delta M_{\dot{\theta}_2} = -(z_w - z_{CG}) \frac{qS\ell_k}{VI_{yy}} \left[C_{L_\alpha} \frac{(z_w - z_{CG})}{\ell_k} + C_{D_{\alpha_W}} \frac{(x_w - x_{CG})}{\ell_k} + C_{M_{\alpha_W}} \right] \qquad (50)$$

These latter contributions are on the order of only 5 percent of the first, and so their accuracy is not crucial. For simplification of the analog computer configuration, it was further assumed that angle of attack rate $\dot{\alpha}$ and pitch rate $\dot{\theta}$ were approximately equal. The above two derivatives, $M_{\dot{\alpha}}$ and $M_{\dot{\theta}}$, were then combined to act as an equivalent pitch damping derivative. The totals for the two flight conditions are:

for $C_L = .565$, $M_{\dot{\alpha}} + M_{\dot{\theta}} = -5.4$

and for $C_L = .763$, $M_{\dot{\alpha}} + M_{\dot{\theta}} = -5.0$

$M_{\delta_{sw}}$ - The seat positioner control effectiveness can be specified in terms of its full travel and the time to traverse full throw in response to the ON-OFF control switch. Corresponding to a total seat travel of $\pm$ 2.5 inches, from center, the pitching acceleration would be

$$\Delta M = \frac{W(\Delta z_s - \Delta z_{CG})_{max}}{I_{yy}} = 2.2 \text{ rad/sec}^2 \qquad (51)$$

The actuator rate, in the AERCAB design, is tentatively 5 in./sec. Thus, the time to full travel, from center, is 0.5 sec.

e. Results and Discussion - Dynamic Stability

The equations of motion presented in Section IV-d-(1) were programmed on a digital computer and also, for brief simulation studies, on an analog computer. The characteristic modes, short-period and phugoid, are visible in the various responses displayed in Figures 65 through 71. Consider first the response to initial angle of attack shown in Figures 69 to 71.

The short-period mode is best seen in the angle-of-attack transients (Fig. 69). In configuration No.1, with damping ($M_{\dot{\alpha}} + M_{\dot{\theta}}$) arbitrarily reduced, it is the lightly damped oscillation of about one second period. This corresponds to a natural frequency by the single-degree-of-freedom approximation of

$$\omega_{Sp} = \sqrt{-M_\alpha} = 5.07 \text{ rad/sec} \qquad (52)$$

The residual damping is, of course, due to the vertical damping, L_α/V_0. With the damping derivatives ($M_{\dot{\alpha}} + M_{\dot{\theta}}$) restored, the mode is quite well damped, shown by configuration No. 2. The damping ratio is the order of

0.6. For a conventional piloted airplane, these values would be quite favorable.

At the lower speed (higher C_L) represented by configuration No. 3, the short-period frequency is lower due to the smaller static stability M_α. The natural frequency is presumably about

$$\omega_{Sp} = \sqrt{-M_\alpha - \frac{L_\alpha}{V_0} M_{\dot{\theta}}} = 2.5 \text{ rad/sec} \qquad (53)$$

The damping derivatives are of the same order as at the higher speed so that the damping ratio is large. The mode is overdamped and hard to identify in the transient of Figure 69. In a conventional airplane, this frequency would be on the low side, but without simulation, it is hard to say how serious this would be for the AERCAB with its type of mission.

The phugoid mode can be seen easily in the velocity transients of Figure 70. It exhibits a period of about 20 seconds, which checks pretty well the approximation

$$P_{Ph} = .137V = 19.5 \text{ sec} \qquad (54)$$

The damping, as phugoids go, is relatively heavy for all cases.

In Figure 71 are shown some effects of velocity stability, M_V, for values on the order of what might be reasonable for the AERCAB. There are three effects: on the period of the phugoid, on the damping of the phugoid, and on the steady-state ΔV displacement. In none of these respects, however, is the M_V effect very pronounced, and, as might be expected, it turned out in the simulation that this level of M_V is of no consequence to the piloting task. In the other responses and simulation, therefore, the derivative was set to zero.

Of much greater significance to the flying qualities are the responses to control. Pitch attitude and velocity responses to seat movement are shown in Figures 65 and 66. The control function is a short pulse of activator button depression, producing, in effect, a step change of pitching moment. For the higher speed (no. 2), the response is like that of a conventional airplane to a step of elevator deflection. The attitude quickly responds to a new (quasi) steady state.

This response (no. 2) looks very favorable, and, in fact, with a conventional controller, it would be. But the ON-OFF control of seat position rate is not a particularly good way to control an aircraft, from a piloting point of view. In effect, a dynamic lag is inserted between the pilot and his application of moment to the aircraft. Besides that, the ON-OFF mode of operation will be unfamiliar and requires a somewhat special technique which will have to be learned. The consequences of this control scheme are discussed in the section on the piloted analog simulation.

At the lower speed (no. 3), the small static stability virtually eliminates the quasi-steady state. In this case, the ultimate response of the vehicle will not be predictable, and with the low static stability both θ and V responses in the phugoid are very large. These flaws, with the probable difficulties of the ON-OFF rate control, might make this case practically unflyable. A preliminary examination of this configuration is discussed in Section IV-f.

The attitude and velocity responses to a throttle movement are shown in Figures 67 and 68. They are all perfectly typical of the throttle responses of ordinary aircraft, containing only the phugoid with the short-period mode essentially unexcited. It is easy to see in these responses (Fig. 67) why attitude, θ, cannot be controlled effectively by throttle. A large initial lag in θ is inevitable, and the very large steady-state θ is not reached for roughly one-half of the phugoid period.

The velocity does, however, respond quickly to throttle deflection, as shown in Figure 68. This characteristic is, of course, desirable. In some cases, even the lag due to engine acceleration can interfere with longitudinal control. The throttle, as represented, should be useful and easy to coordinate with moment control for modulation of flight path and airspeed.

f. Piloted Analog Simulation - Longitudinal Mode

The characteristics of the pitch attitude and velocity responses to various control and atmospheric gust (changes in angle of attack due to turbulence) inputs will have a significant effect on the success with which the AERCAB can be flown by a pilot. In order to investigate in a qualitative manner the handling

Figure 65

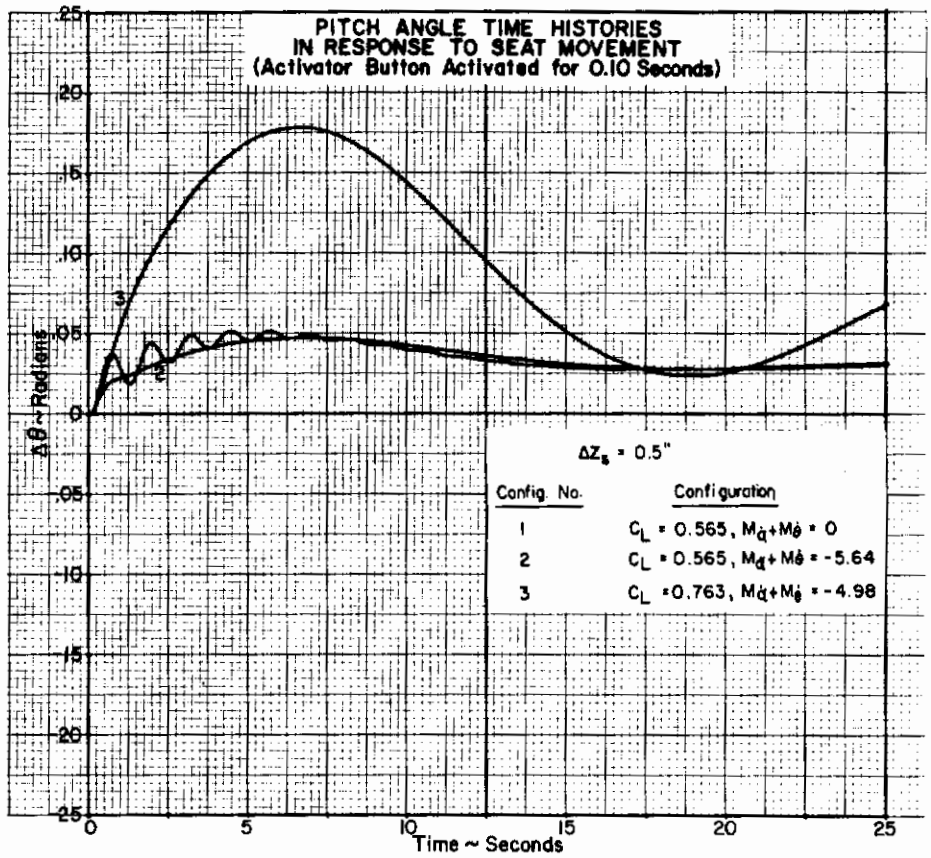

Figure 66

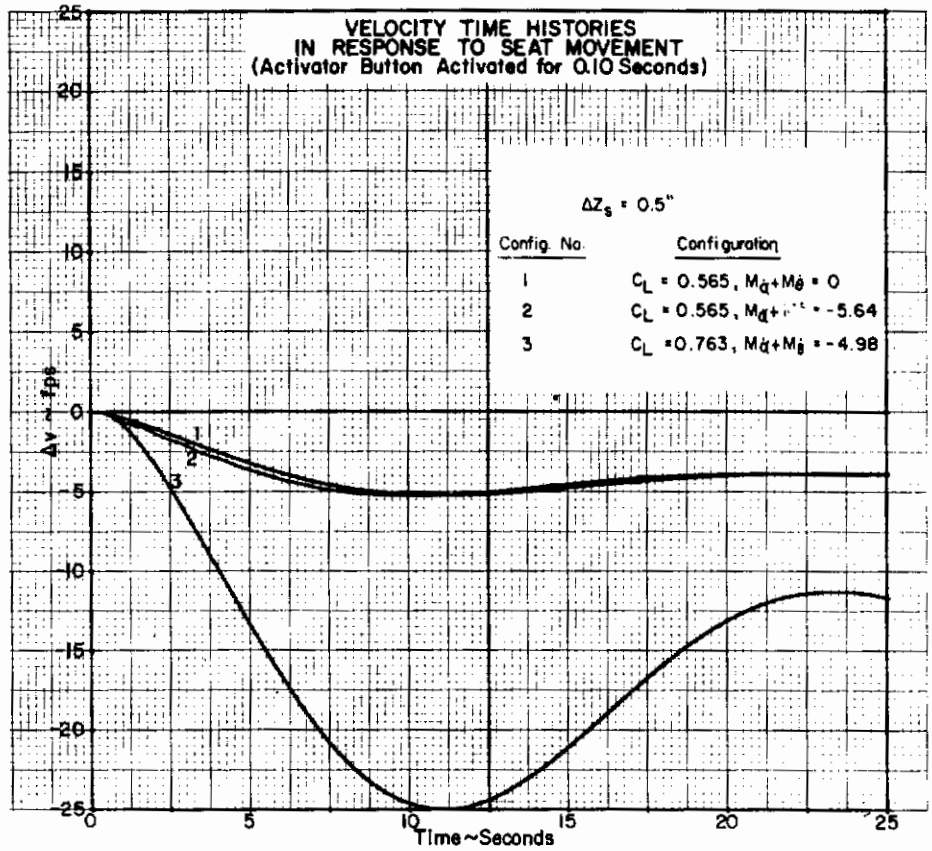

Figure 67

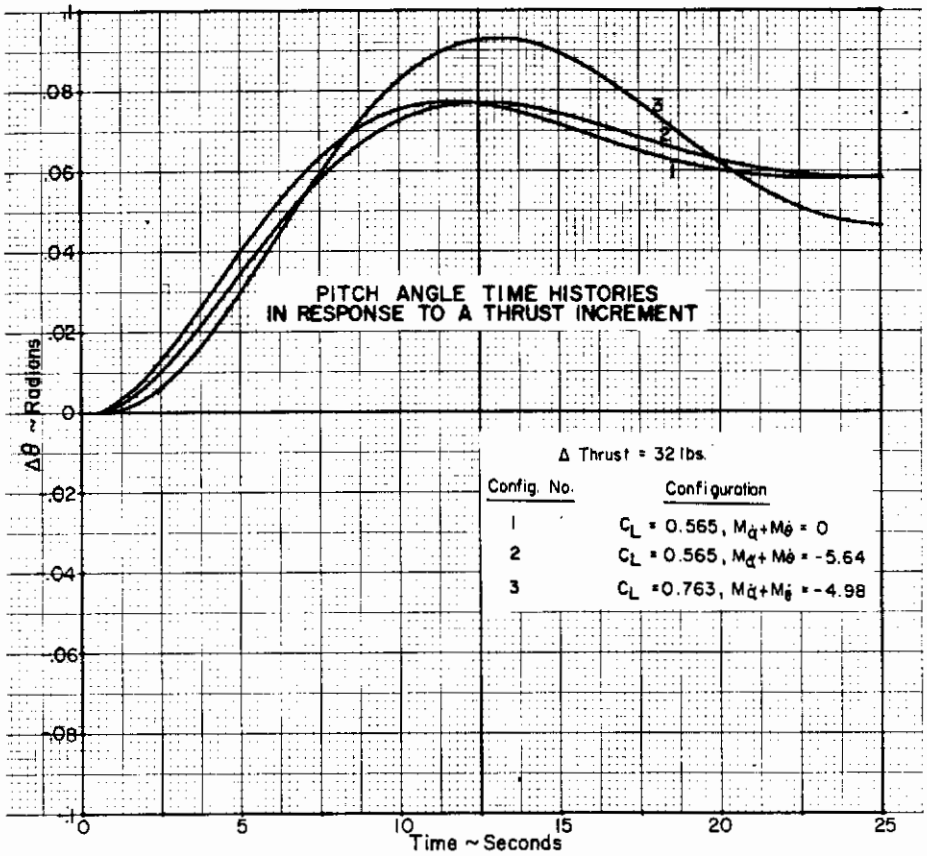

Figure 68

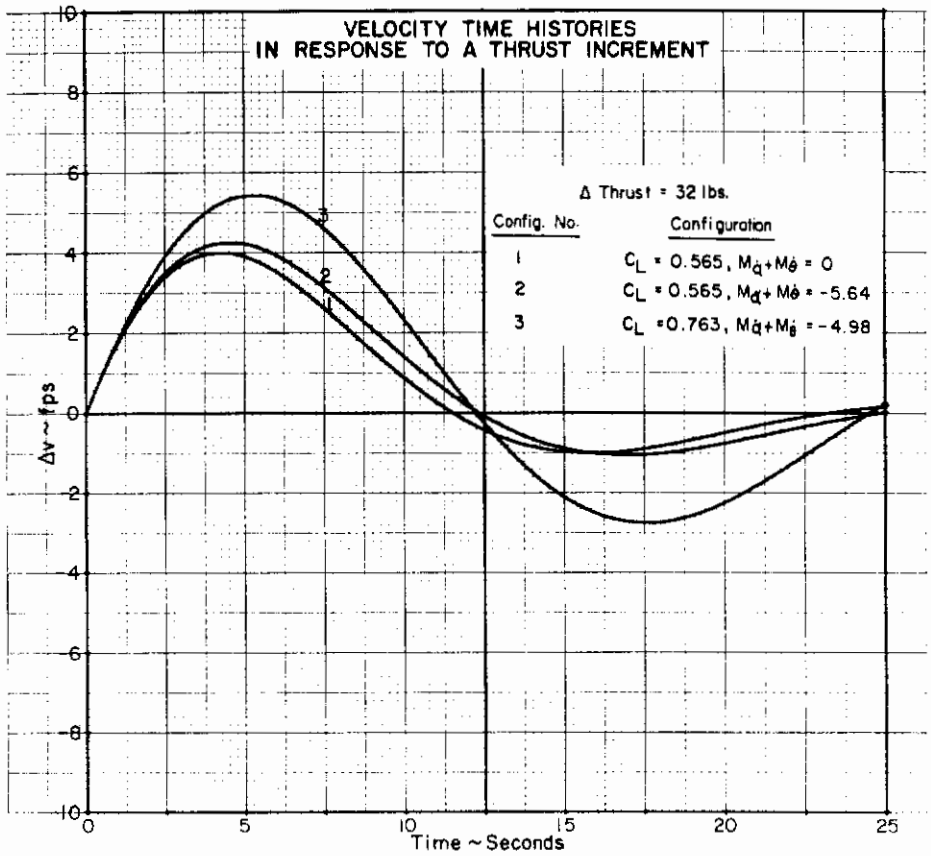

Figure 69

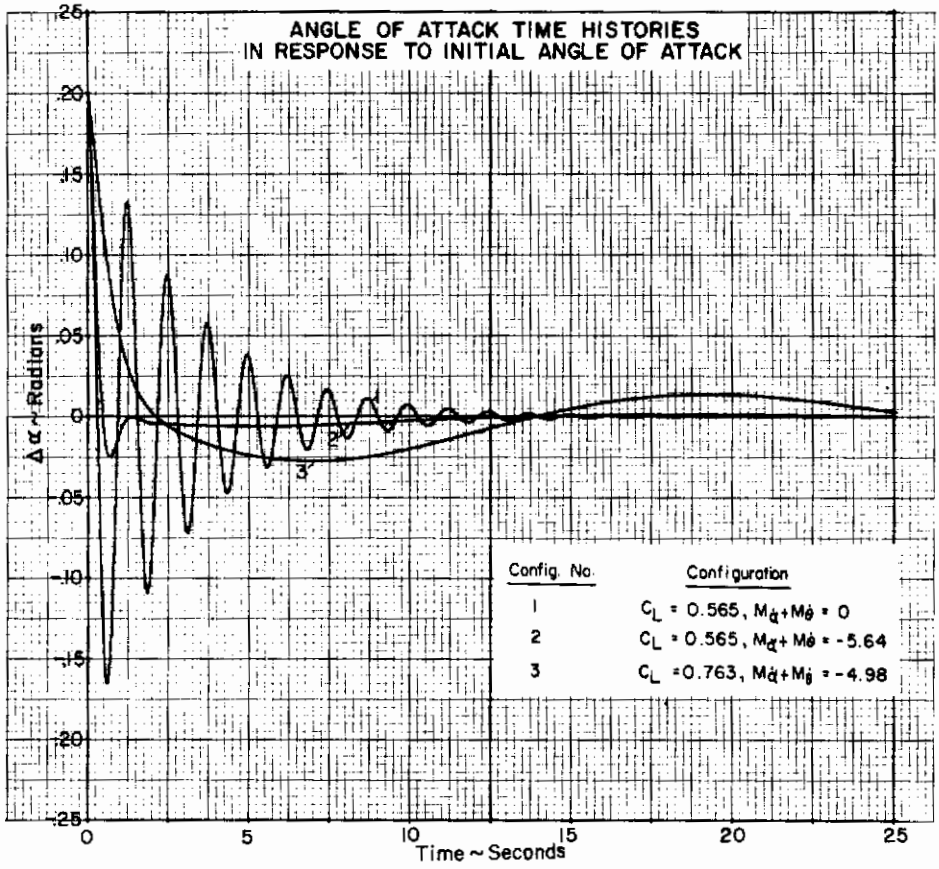

Figure 70

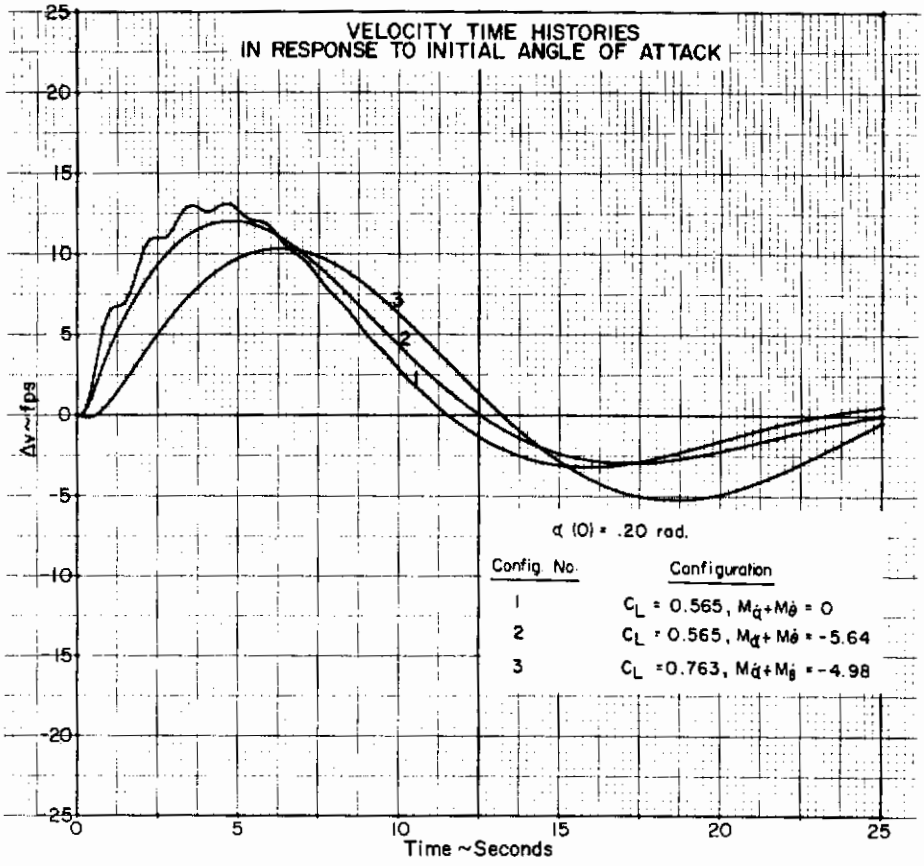

Figure 71

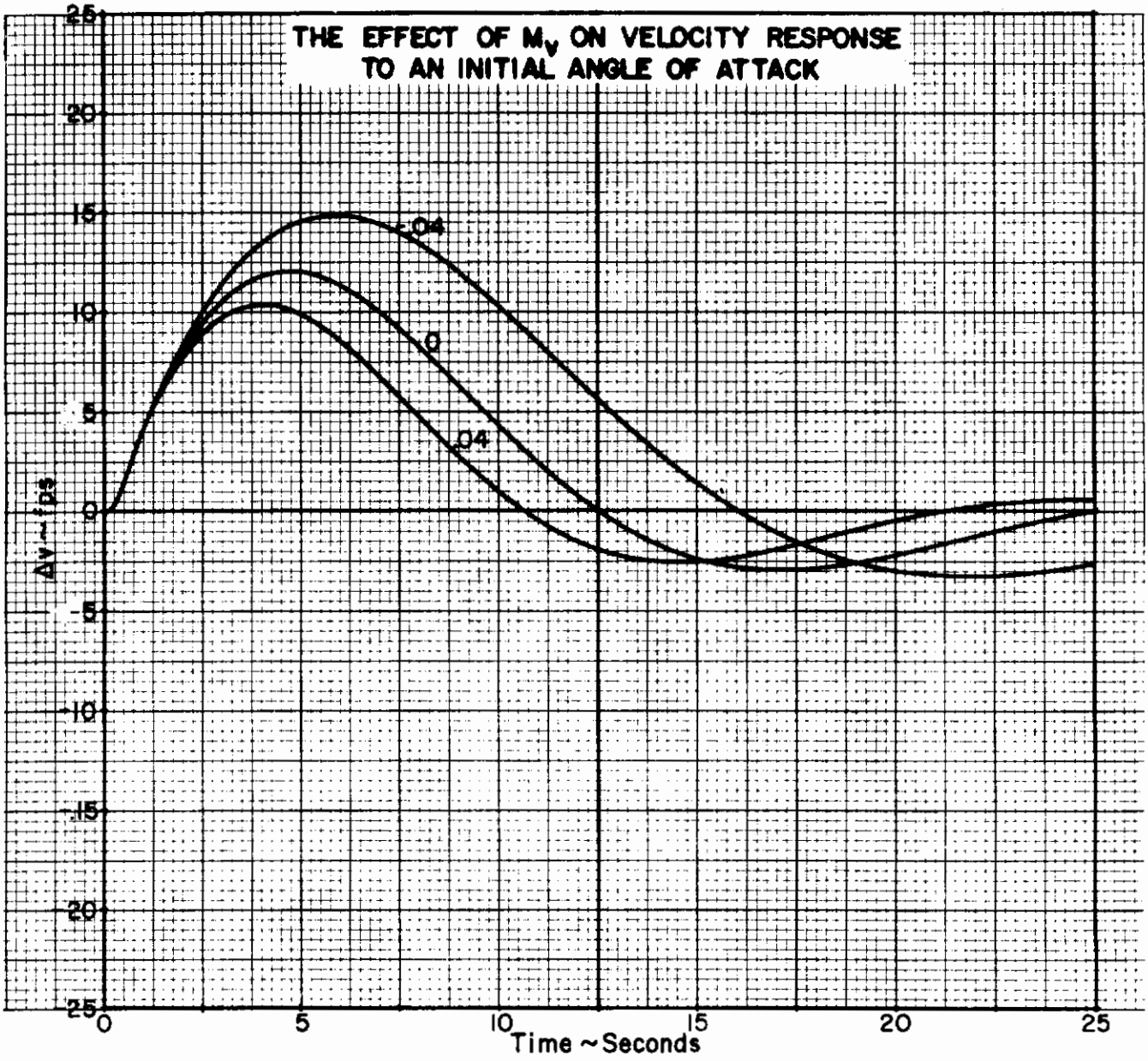

qualities of the AERCAB, a simplified analog simulation capable of being piloted by a human operator was constructed using ARAP's PACE 221-R analog computer, a simple control switch arrangement, and readouts of pitch attitude, velocity, and altitude. Responses generated with the analog computer were identical with those generated on ARAP's IBM 1130 computer and presented in Figures 65 through 71. Thus, comments based upon the ARAP-piloted simulation apply directly to the responses described in Section IV-e of this report.

Pilot comments confirm what should be obvious from inspecting the pitch attitude and velocity responses to seat motion and throttle inputs (Figs. 65, 66, 67, and 68). The sluggish θ response to a throttle input resulted in poor θ control with the throttle, while the relatively quicker θ response to a seat input yielded a significantly better pitch attitude control. The velocity response to a seat input was sluggish. Consequently, it was difficult to achieve good control over velocity using only the seat controller. Throttle inputs, however, provided quicker initial velocity responses.

If the throttle were used as a pitch attitude controller and the seat positioner were used as a velocity controller, the pilot would experience a considerable lag in vehicle response to either a commanded pitch attitude change or a commanded velocity change. Lag of the magnitude shown in either Figure 67 or Figure 66 results in extremely poor handling qualities, and the pilot must develop some compensatory technique for vehicle control. Particularly in the presence of turbulence, a vehicle with the response characteristics shown in Figures 65 through 69 would be extremely difficult to fly if the throttle were used to control attitude and the seat positioner were used to control velocity.

The most satisfactory scheme devised for controlling the simulation of the AERCAB consisted of using the seat positioner as a pitch attitude controller and using the throttle as an airspeed controller. While the frequency of the short period pitch attitude response to a seat motion input was fairly low compared with conventional aircraft, the pilot was able to use the seat positioner as a pitch attitude controller without experiencing much difficulty. The relatively low frequency did require the pilot to activate the seat positioner in an impulsive manner to compensate for a tendency to

overcontrol. Using the seat positioner to command attitude as observed on the attitude voltmeter, and maintaining the desired airspeed with the throttle, attitude tracking was possible even in the presence of gusts (Fig. 72). The use of relatively high-frequency impulsive control inputs also can be observed in Figure 72.

For the reduced static stability, associated with $C_L = 0.763$, the rate of change of seat travel had to be reduced in order to prevent overcontrolling (Figure 77). With full seat travel in two seconds, the pilot was unable to operate the positioner fast enough to achieve proper control. The task took an excessive amount of concentration and any distraction resulted in reduced task performance. Occasionally, the pilot became confused with the control switch orientation and operated the seat positioner opposite to the desired pitch attitude command. By increasing the seat full travel time to four seconds, the level of task difficulty was reduced and the attitude tracking performance became comparable to the $C_L = 0.565$ case. The difference in tracking performance can be seen in a comparison of the traces shown in Figure 77.

Altitude tracking was accomplished by closing an inner loop on attitude. Velocity tracking was done by commanding airspeed changes with the throttle, then coordinating the use of the seat positioner to maintain the desired attitude with the new throttle setting. If the coordination of seat position with throttle application was satisfactory, velocity changes without changes in altitude could be accomplished after a short practice period.

Using the control techniques described above resulted in handling qualities that were considered adequate for the limited mission of the AERCAB. It should be noted, however, that the AERCAB's mission provides a latitude in acceptable handling qualities that might not be considered appropriate for conventional aircraft.

Control of the AERCAB was attempted for several simple attitude, velocity, and altitude tracking tasks which were considered typical of the basic requirements for a self-rescue vehicle. Each task was piloted with and without the presence of random angle of attack disturbances which were generated as part of the simulation in order to represent atmospheric turbulence. The

presence of such atmospheric gusts always increased the level of difficulty of the tasks and emphasized the need to use the seat positioner as a pitch attitude controller and the throttle as a velocity controller.

Before specific tracking tasks were attempted, however, the pilot was given sufficient practice to become completely familiar with the simulation. He then was asked to evaluate the effect of varying the value of the dynamic stability derivatives M_v, $M_{\dot{\alpha}}$, and $M_{\dot{\theta}}$.

The value of M_v, the speed stability derivative, had no noticeable effect on the pilot's ability to control the AERCAB, particularly in the presence of turbulence. Thus, M_v was not considered a parameter of interest in the piloted simulation portion of the analysis and it was set equal to zero for all tasks.

The combined value of $M_{\dot{\alpha}}$, the angle of attack damping and $M_{\dot{\theta}}$, the pitch damping, did effect the pilot's opinion of the simulated vehicle's handling qualities. A zero value for $M_{\dot{\alpha}}$ and $M_{\dot{\theta}}$ caused short period pitch attitude oscillations during the initial phases of the pitch attitude response to seat position control inputs. Those oscillations were distracting to the pilot, and they caused him to downgrade his opinion of the AERCAB's handling qualities for the particular task under evaluation. A zero value for $M_{\dot{\alpha}}$ and $M_{\dot{\theta}}$, however, did not cause the pilot-vehicle system to become unstable. It was decided to evaluate all tasks with the estimated value of $M_{\dot{\alpha}} + M_{\dot{\theta}}$ indicated in Figures 65 through 70.

The results of pitch attitude, altitude, and velocity tracking with and without turbulence are shown in Figures 72 through 81. Figures 72 and 77 indicate that the human operator can maintain a desired attitude at constant airspeed within a range of ± 0.02 radians in the presence of gusts that would cause pitch attitude variations in the order of ± 0.06 radians. The importance of seat positioner rate and impulsive control inputs also are shown in those figures. In Figure 77, the large attitude spikes at 67 seconds and 230 seconds are the result of pilot disorientation with regard to the control sense required for the desired attitude change. Since the pilot must control attitude through impulsive actuation of seat position, attention must be directed to providing a suitable self-centering control switch that operates with a sense of direction that seems

appropriate with regard to the resulting pitch change of the vehicle.

The effect of gusts on an altitude tracking task can be observed by comparing Figures 73 and 74 for the C_L = .565 case, and by comparing Figures 78 and 79 for the C_L = .763 case. For these tasks, the pilot attempted to track a given altitude for approximately 60 seconds, then increase his altitude + 35 feet and track that new altitude until t = 150 seconds, then reduce his altitude -70 feet and track that new altitude until t = 240 seconds, at which time he returned to and tracked the original altitude. While the presence of gusts does reduce task performance, the effect is not large considering the probability of lax altitude tracking requirements for the AERCAB mission. The pilot was able to accomplish a desired altitude change on command, and he could track the commanded altitude without excessive concentration or compensation. Neither the requirement to track a given altitude nor to change altitude caused the pilot-vehicle system to become unstable.

The altitude variations associated with velocity tracking while attempting to maintain a constant altitude are shown in Figure 75 for the C_L = 0.565 case. For velocity tracking, the pilot attempted to track a given velocity for 60 seconds, then increase his velocity + 4 feet per second and track that new velocity until t = 180 seconds in Figures 75 and 76 and t = 150 seconds in Figures 80 and 81, at which time he would reduce his velocity -8 feet per second. In Figures 75 and 76, the pilot continued to track that new velocity until t = 360 seconds. In Figures 80 and 81, he returned to and tracked the original velocity after t = 240 seconds. Gusts detract from task performance, but the overall results are satisfactory. Velocity variations for the velocity tracking task with and without gusts are shown in Figure 76 for the C_L = 0.565 case and in Figures 80 and 81 for the C_L = 0.763 case. The velocity tracking tasks were accomplished without excessive difficulty, and the results are satisfactory even though precision tracking in the presence of gusts does not seem possible.

Provided there is no requirement for precision control and provided the pilot receives some previous training in flying an AERCAB, the results of the simulation indicate the vehicle is controllable, and loose tracking is possible. Several important points must be observed,

Figure 72

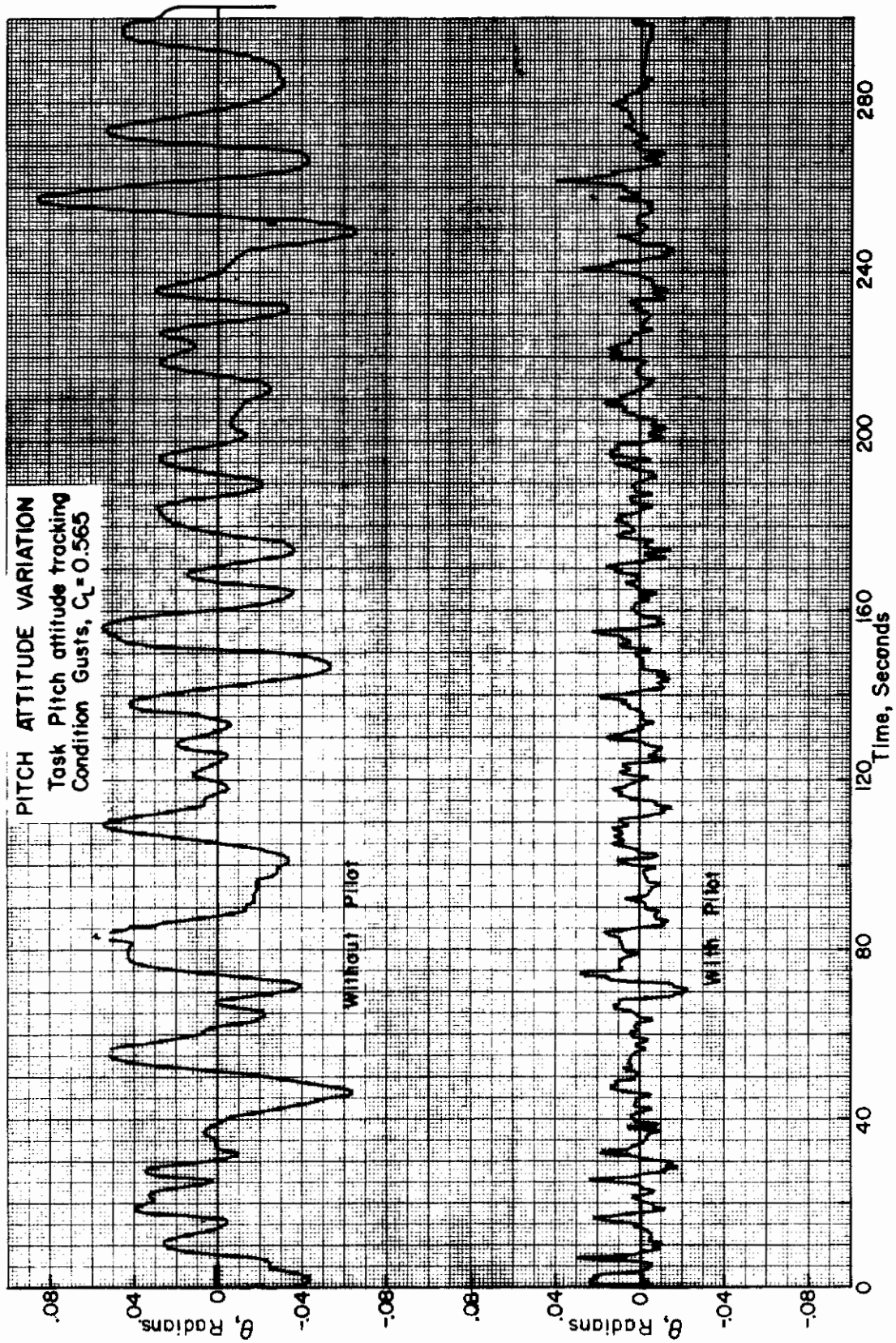

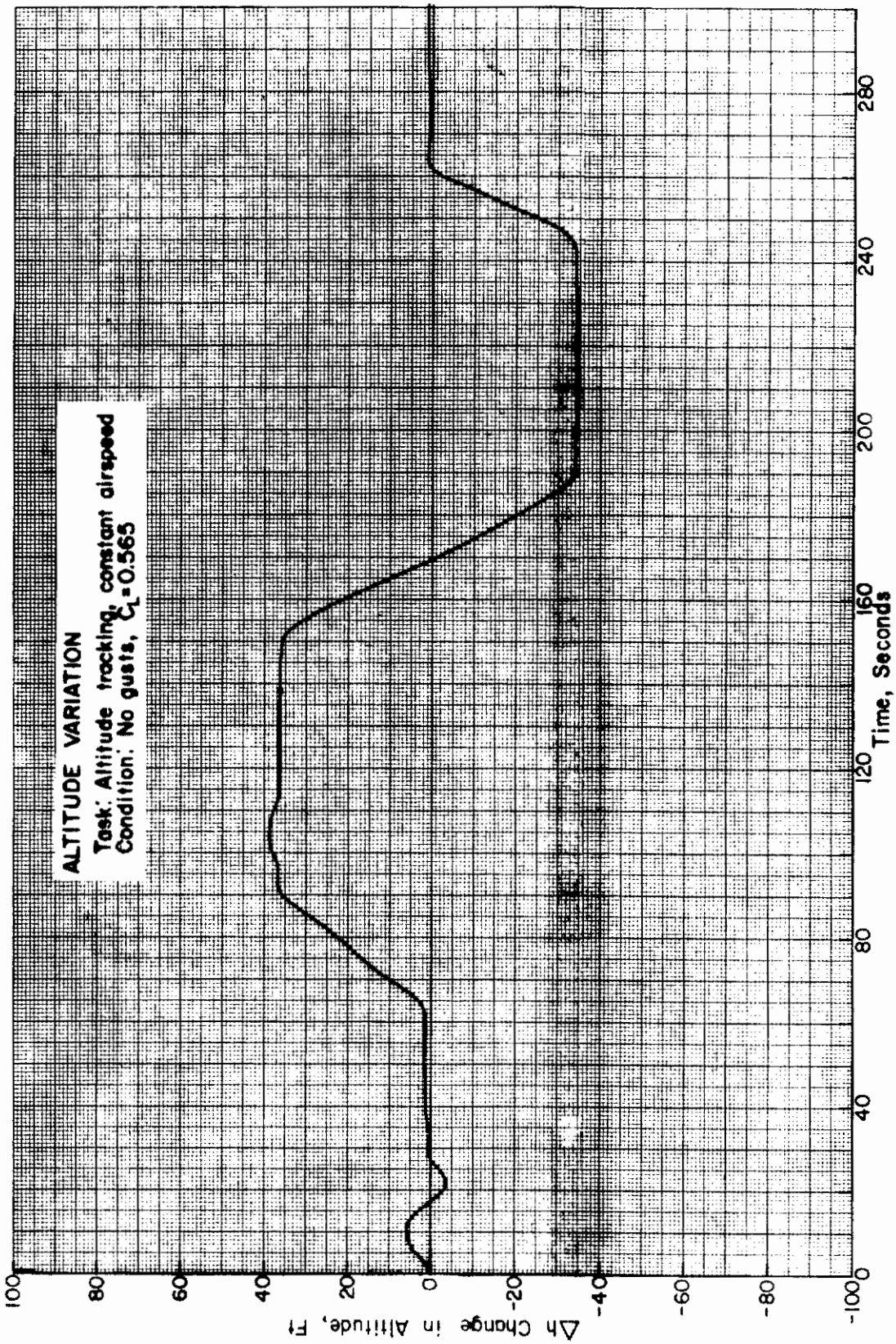

Figure 73

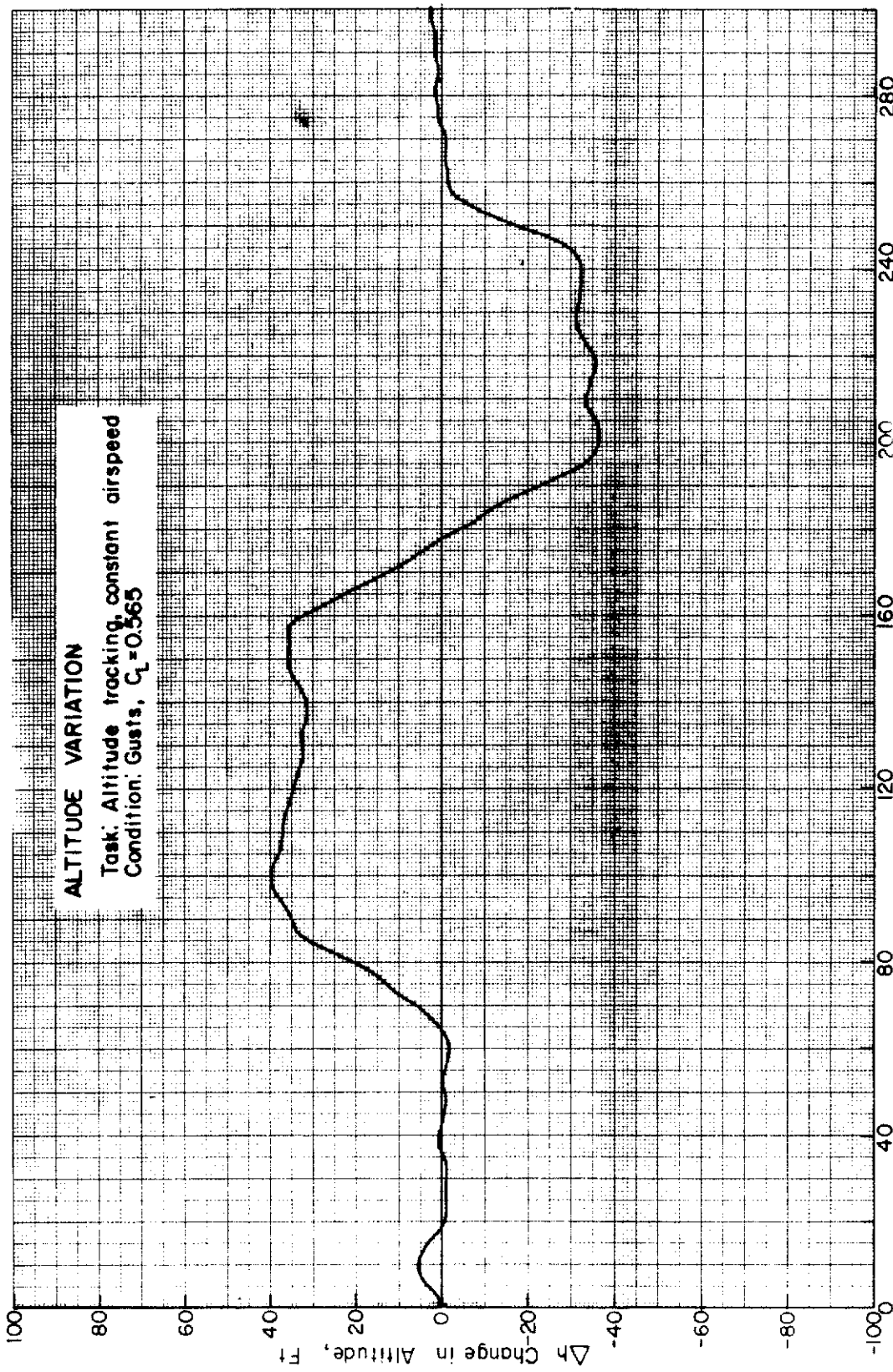

Figure 74

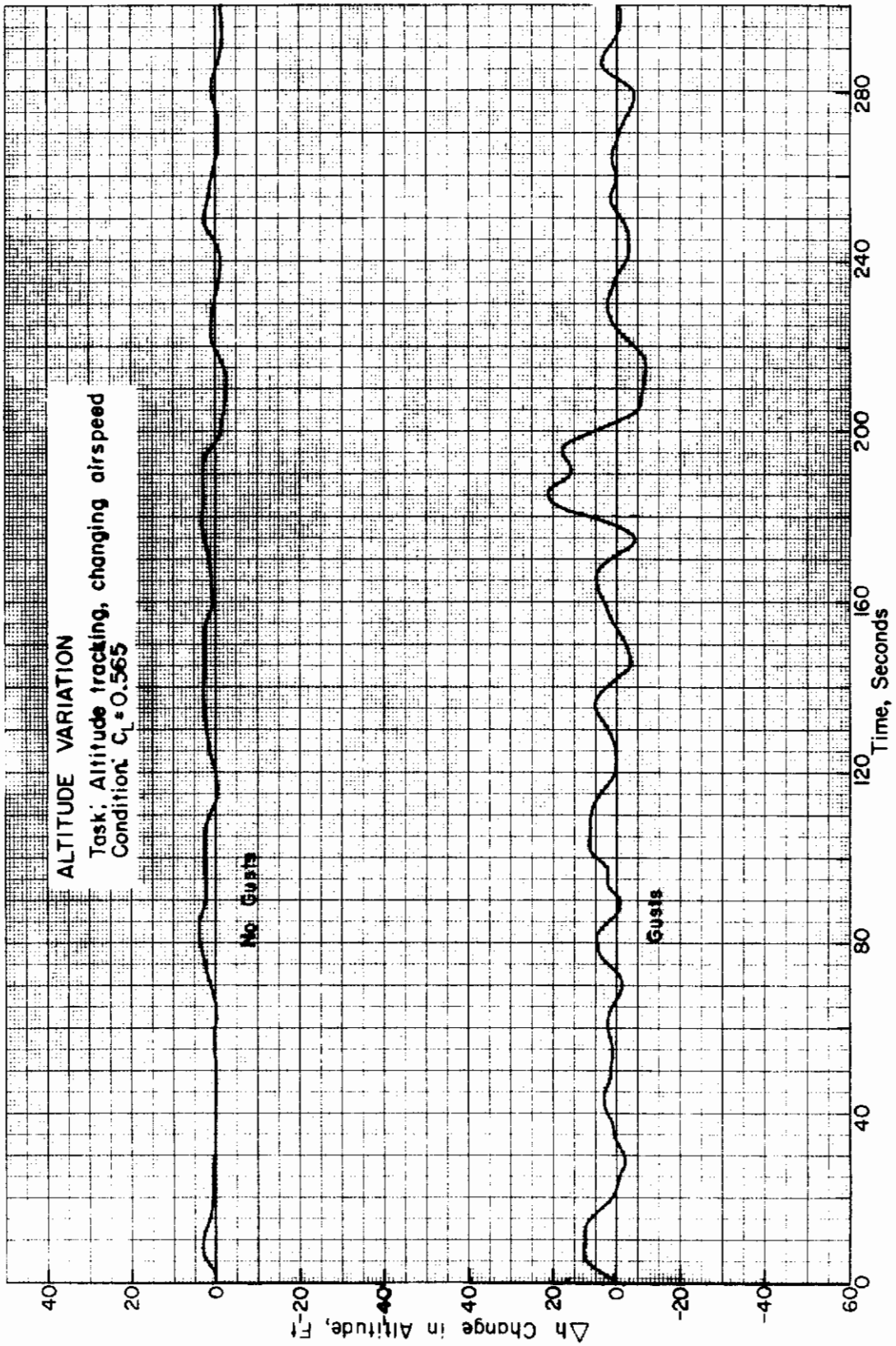

Figure 75

Figure 76

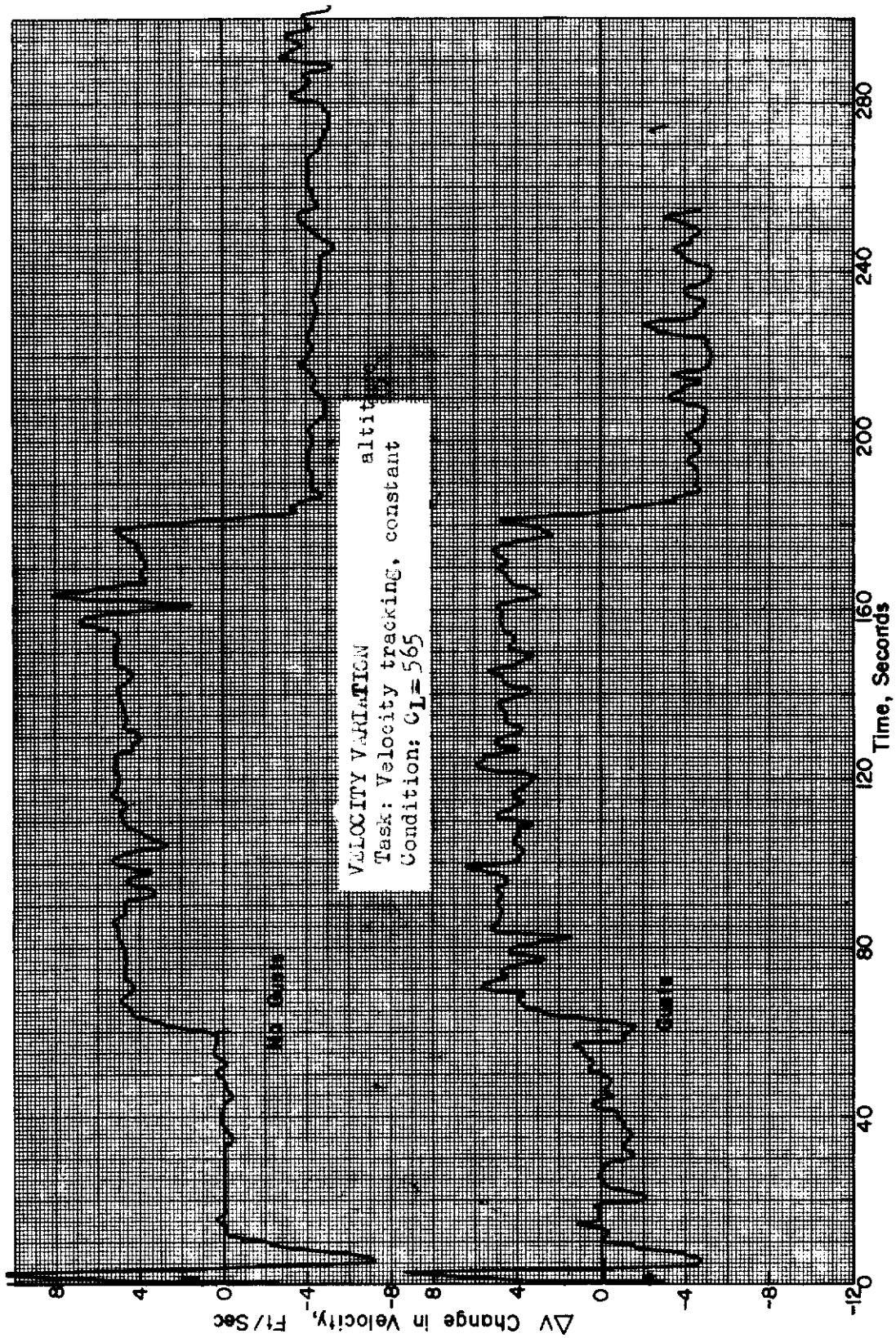

Figure 77

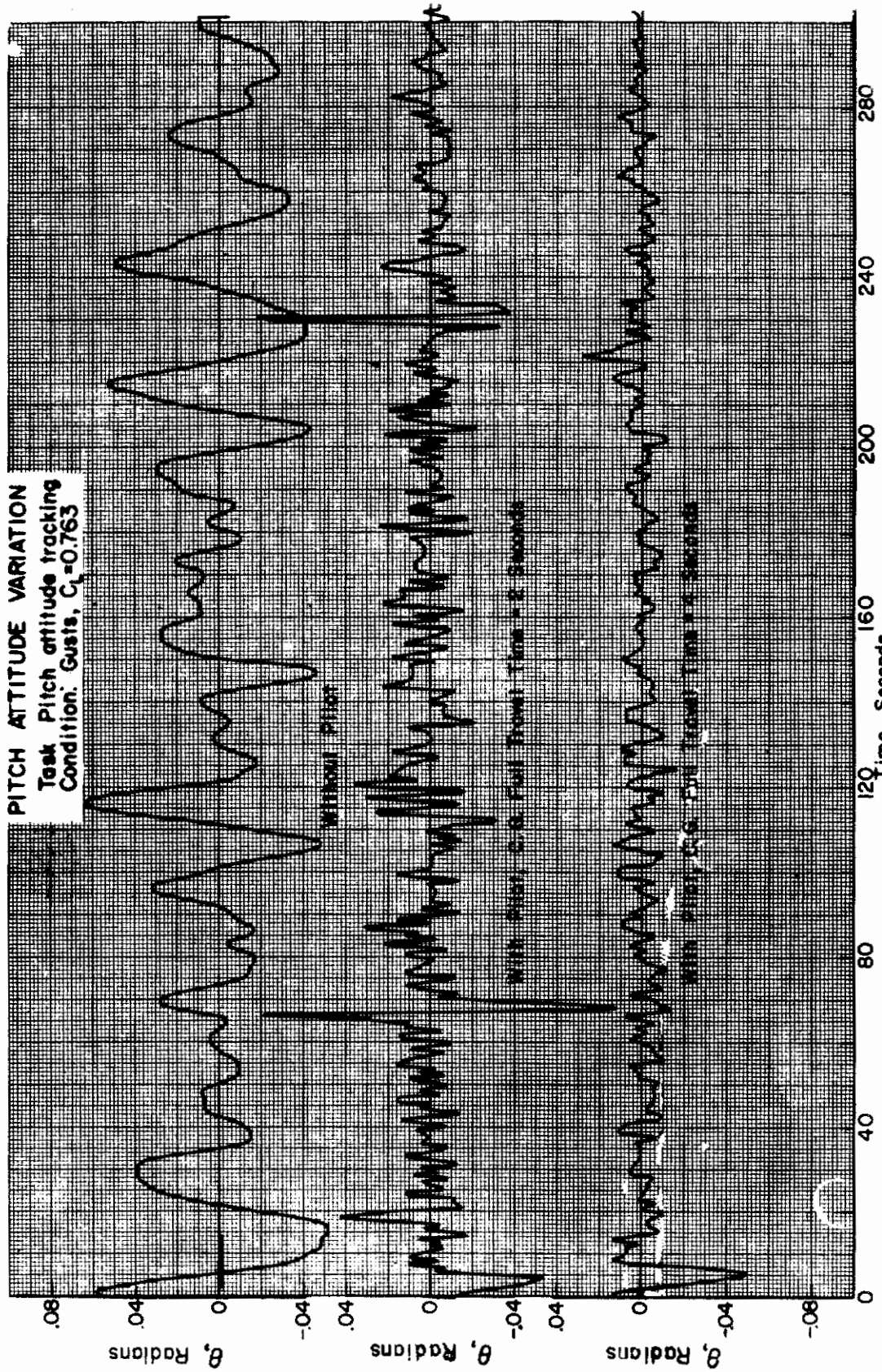

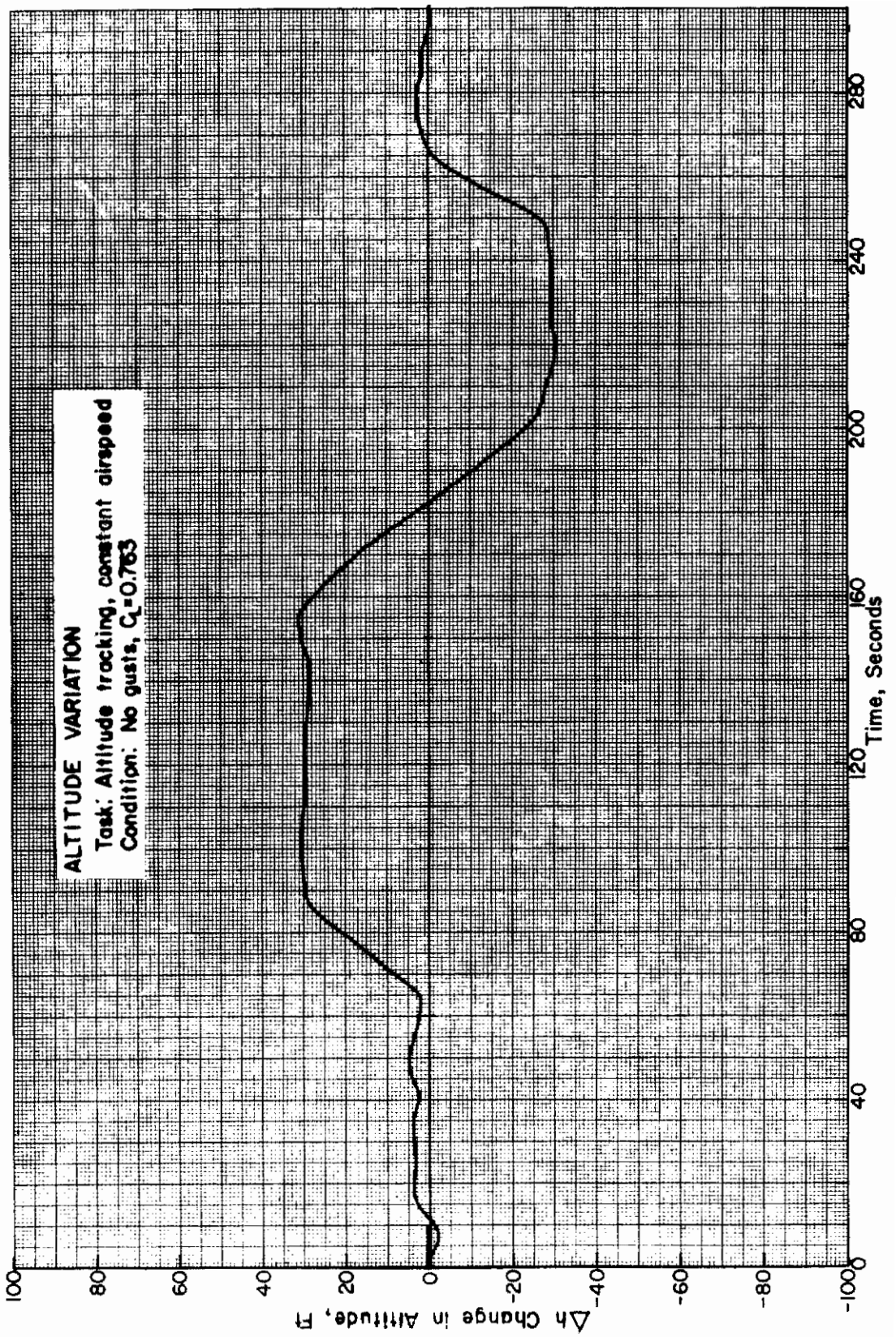

Figure 78

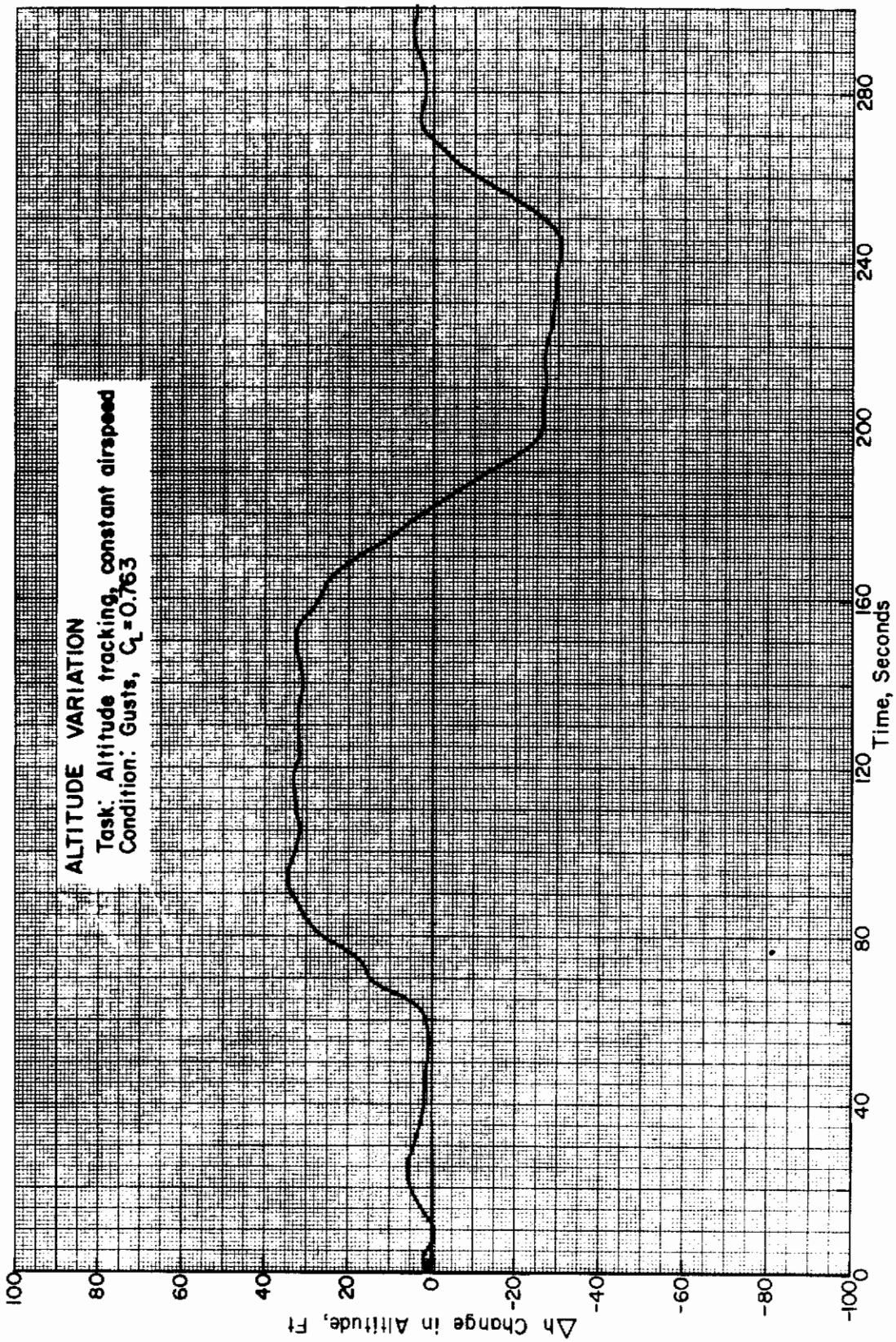

Figure 79

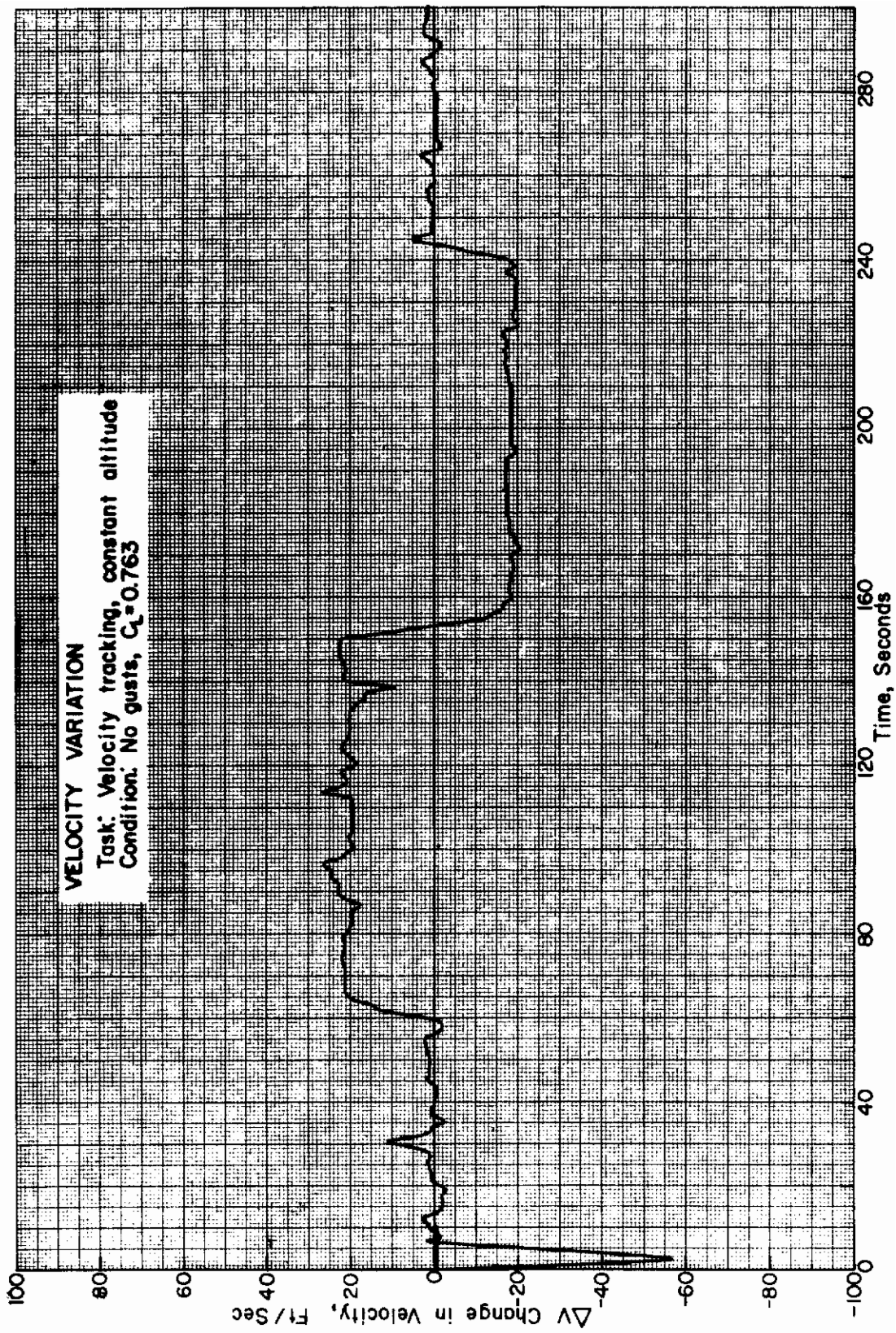

Figure 80

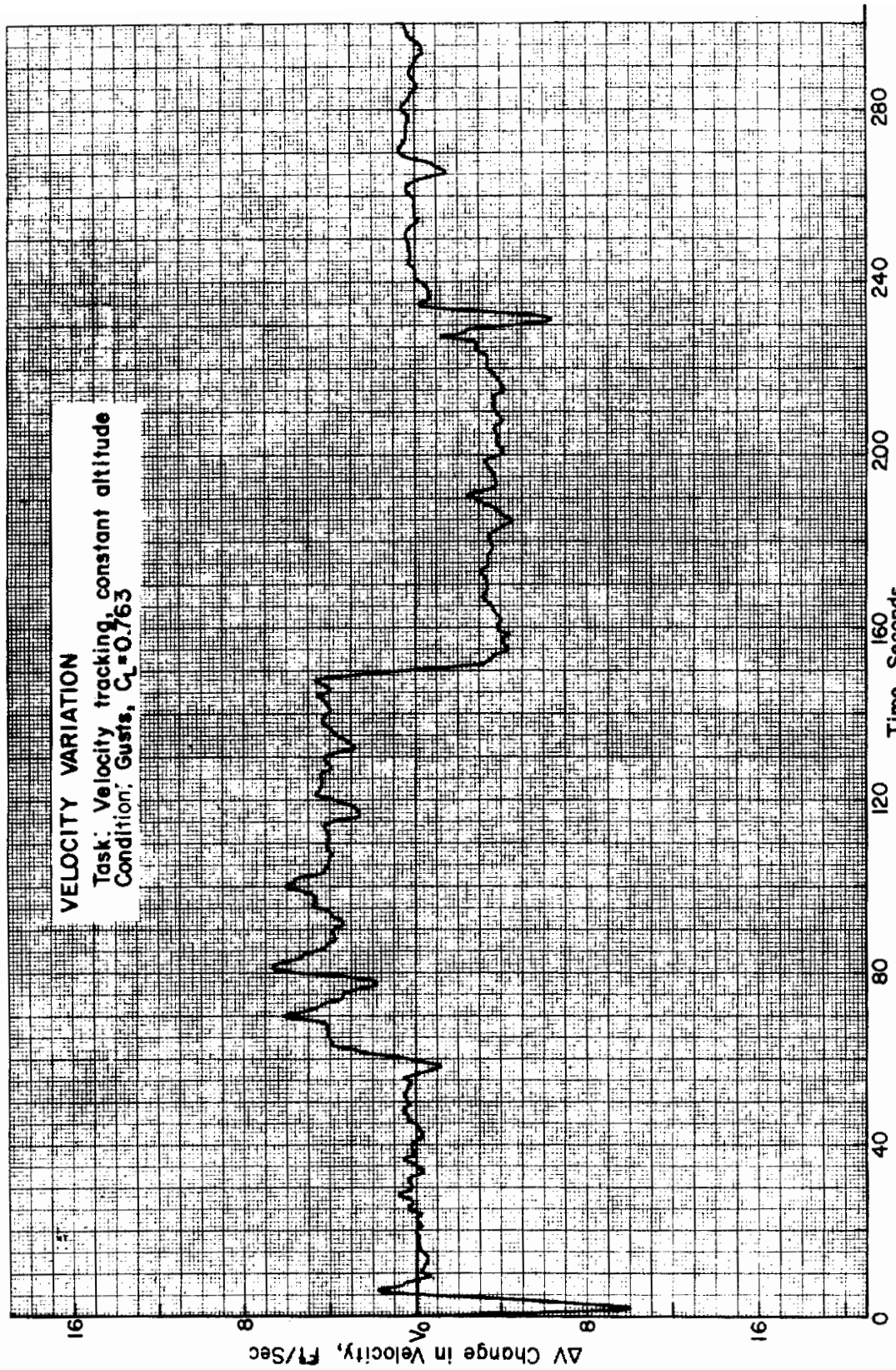

Figure 81

however. The pilot should be given a seat controller that is easy to use in an impulsive manner, and the sensing of the controller should bear some rational relationship to the resulting response of the vehicle. The rate of seat movement must be slow enough to prevent overcontrolling. The pilot definitely will require some prior training before he is exposed to actual flight in the AERCAB, and the logical method of training would appear to be some form of simulation. The degree of sophistication required, however, would be much greater than was available in the simple piloted analog simulation used for this analysis.

5. Stability Analysis - Lateral/Directional Mode

a. Equations of Motion and Estimation of Directional Stability Derivatives

Lateral-directional motions of the AERCAB have been analyzed in a style equivalent to the preceding longitudinal section. The equations are basically those of Reference 29, as follows:

$$\text{Side Force} \qquad (s - Y_v)\Delta v + V\Delta r - g\Delta\phi = Y_{\phi_W}\Delta\phi_W \tag{55}$$

$$\text{Roll Moment} \qquad -L'_v\Delta v - L'_r\Delta r + s(s - L'_p)\Delta\phi = L'_{\phi_W}\Delta\phi_W \tag{56}$$

$$\text{Yaw Moment} \qquad -N'_v\Delta v + (s - N'_r)\Delta r - N'_p s\Delta\phi = N'_{\phi_W}\Delta\phi_W \tag{57}$$

The reference axes here are the usual "stability axes" through the vehicle's center of gravity (Fig. 82). The product of inertia has been eliminated from its explicit appearance in the roll and yaw equations, so that it is implicit instead in each of the primed coefficients above. The latter are defined by:

$$L'_{()} \equiv \frac{L_{()} + \frac{I_{xz}}{I_{xx}} N_{()}}{1 - \left(\frac{I_{xz}}{I_{xx}}\right)\left(\frac{I_{xz}}{I_{zz}}\right)} \tag{58}$$

AXIS SYSTEM FOR LATERAL-DIRECTIONAL STUDY
(Stability Axes with Origin at C.G.)

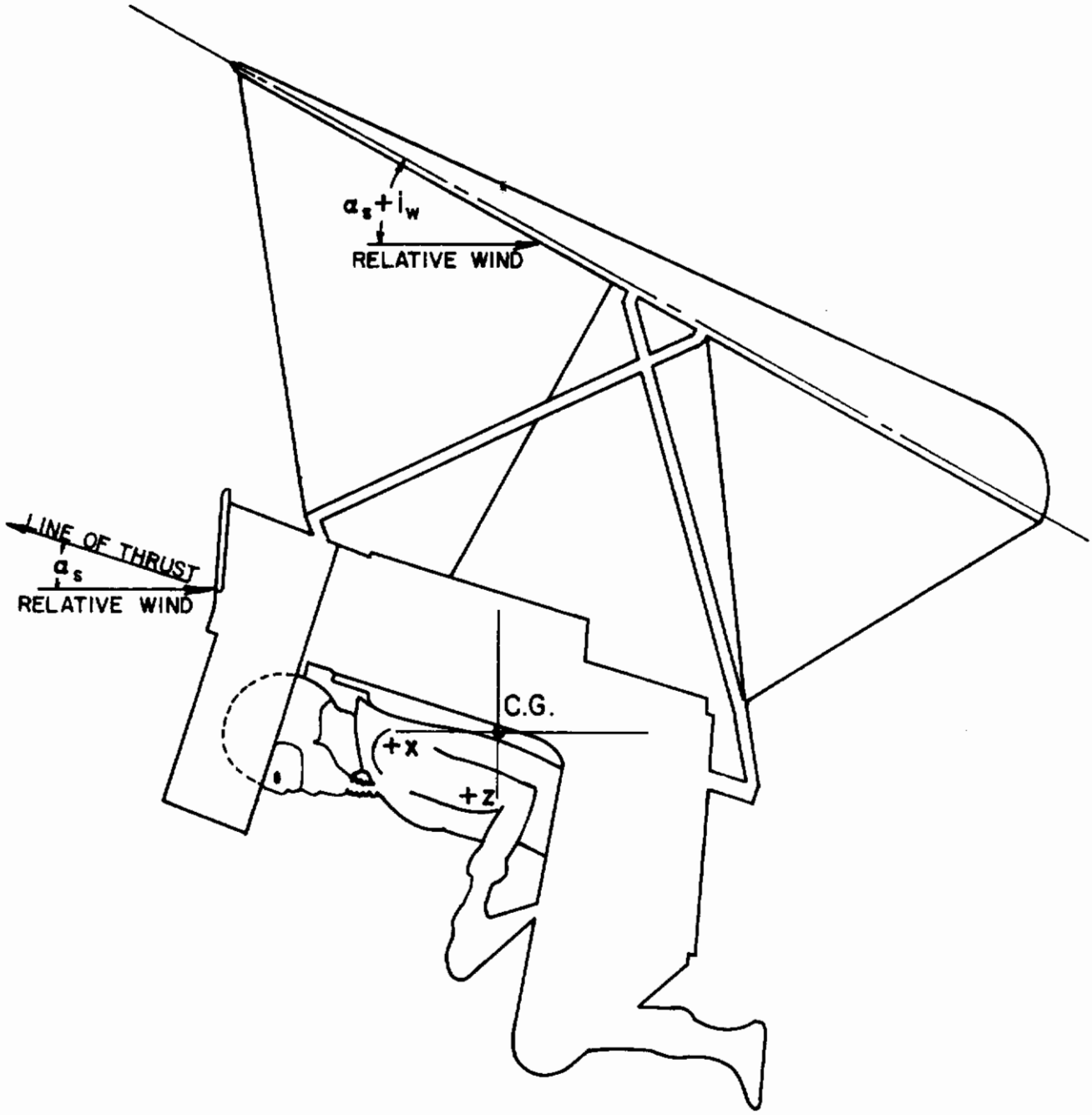

Figure 82

and

$$N'_{(\,)} \equiv \frac{N_{(\,)} + \frac{I_{xz}}{I_{zz}} L_{(\,)}}{1 - \left(\frac{I_{xz}}{I_{xx}}\right)\left(\frac{I_{xz}}{I_{zz}}\right)} \tag{59}$$

Besides this detail about the product of inertia, control over the vehicle by banking the parawing requires some explanation. This is done by an actuator which pulls in the lateral shroud line on one side and lets out the other. In the preliminary design, the actuator is controlled by an ON-OFF switch similar to the one for pitching control. In the simulation, then, the wing bank, $\Delta\phi_W$, is derived from the pilot's control switch, according to

$$\Delta\dot{\phi}_W = K_{\dot{\phi}_W}\Delta\delta_s \tag{60}$$

where $K_{\dot{\phi}_W}$ is the actuator rate, and $\Delta\delta_s$ is $\pm$ 1 or 0, for the ON-OFF control.

The parawing rotates, due to lateral control, about the keel which is inclined by an angle 24° to the stability axes for the case investigated. In the wing system, therefore, $\Delta\phi_W$ results in sideslip, according to

$$\sin\beta_W = \sin\alpha_W \sin\phi_W \tag{61}$$

The control derivatives in the lateral directional equations contain the wing sideslip derivatives, according to

$$Y_{\phi_W} = (C_{Y_\beta}\sin\alpha + C_L)\frac{qS}{m} \tag{62}$$

$$L_{\phi_W} = \left[C_{l_\beta}\sin\alpha - \frac{z_W}{b}(C_{Y_\beta}\sin\alpha + C_L)\right]\frac{qS\ell_k}{I_{xx}} \tag{63}$$

$$N_{\phi_W} = \left[C_{N_\beta}\sin\alpha + \frac{x_W}{b}(C_{Y_\beta}\sin\alpha + C_L)\right]\frac{qS\ell_k}{I_{zz}} \tag{64}$$

It was decided that, for this preliminary investigation of the lateral-directional motions of the AERCAB, the aerodynamic constants of the parawing vehicle of Reference 32 would be used. While this vehicle differs slightly from the basic configuration, it is, in fact, very similar to the AERCAB, and it is doubtful whether the accuracy and validity of aerodynamic data would justify recomputation of the aerodynamic coefficients specifically for the basic design. The following values of the aerodynamic derivatives are derived directly from Reference 32, Figure 8, for the C.G. location of the AERCAB, thus:

$$\frac{-z_w}{b} = .42$$

$$\left.\begin{array}{llll}
C_{Y_\beta} = -.256 & Y_v = -.103 & & \\
C_{\ell_\beta} = -.190 & L_v = -.400 & L'_v = -.462 & \\
C_{N_\beta} = .078 & N_v = .152 & N'_v = .257 & \\
C_{\ell_p} = -.14 & L_p = -1.15 & L'_p = -1.22 & \\
C_{N_p} = .035 & N_p = .265 & N'_p = .553 & \\
C_{\ell_r} = .042 & L_r = .345 & L'_r = .408 & \\
C_{N_r} = -.022 & N_r = -.167 & N'_r = -.257 & \\
C_{Y_{\phi_W}} = .338 & Y_{\phi_W} = 22.3 & & \\
C_{\ell_{\phi_W}} = -.0056 & L_{\phi_W} = 21.7 & L'_{\phi_W} = 23.4 & \\
C_{N_{\phi_W}} = .0628 & N_{\phi_W} = -1.78 & N'_{\phi_W} = -7.07 &
\end{array}\right\} \quad (65)$$

In these, the estimated moments and products of inertia with respect to stability axes for the AERCAB have been used, as follows

$$\left.\begin{array}{l}
I_{zz} = 25.57 \text{ slug ft}^2 \\
I_{xx} = 23.61 \\
I_{xz} = -5.78
\end{array}\right\} \quad (66)$$

In the interest of simplicity, consistent with the use of aerodynamic data directly from Reference 32, only one angle of attack is considered. Hence; for this analysis

$$\alpha = 24 \text{ deg}$$

$$C_L = .44$$

$$V = 97 \text{ knots}$$

b. Results and Discussion - Dynamic Stability

The equations described in all the above have been solved on a digital computer, and they have also been programmed on an analog computer for limited simulation studies.

The Dutch roll motions are displayed in Figures 83 and 85, with and without a small vertical tail. The oscillation period, without tail, is one second. This corresponds to a moderate level of directional stability which in itself would be quite favorable. The vertical tail increases the weathercock stability slightly, but for this flight condition, it is really not needed.

The damping of the lateral oscillation is marginal. For a conventional airplane, its value, $\zeta = .07$, would be on the light side, but for the AERCAB mission it might be adequate. The "vertical tail" does not help since it does not have enough tail length to produce appreciable damping.

Of much more relevance to the flying qualities are the responses to lateral control shown in Figures 84 and 86. The roll rate response of Figure 84 shows two outstanding features: a long roll-time constant and a substantial Dutch-roll excitation. In a conventional airplane, both of these would be substantial defects.

The roll-time constant is about 1.7 seconds. This is definitely on the long side for any sort of precision lateral control, but for the AERCAB mission, it may be acceptable. The time constant, of course, mostly depends on the damping-in-roll derivative, L_p, which for the low aspect ratio parawing is bound to be rather low.

The substantial excitation of the Dutch roll in the

response to lateral control would be a definite nuisance to the pilot. It relates mostly to the dihedral effect derivative L'_v and the two adverse yaw derivatives $N_{\phi W}$ and N_p. The dihedral effect of the AERCAB is very large, at a level that will lead to extreme sensitivity to turbulence and to excessive excitation of the Dutch roll. The yaw derivatives $N_{\phi W}$ and N_p are also large; one can see from the numerical values of $N'_{\phi W}$ and $L'_{\phi W}$ that lateral control produces about one-third as much yawing acceleration as rolling acceleration. This, of course, is what excites the Dutch roll. The responses of Figure 87 show that the whole effect is extremely sensitive to the derivative $N_{\phi W}$. The response shown for the arbitrarily increased value, -10, might well be practically unflyable.

The spiral stability is about neutral in the responses of Figures 84, 86 and 87. This would be quite acceptable for a conventional aircraft, but may not be for the AERCAB. In the real flight situation, the head-down pilot position and unfamiliar controller might make it essential to have at least a moderate level of sprial stability.

It must be emphasized again that the validity of all this discussion of lateral/directional characteristics is severely limited by four factors. They are

1) The aerodynamic data do not exactly apply to the AERCAB configuration;

2) The AERCAB was considered only as a rigid vehicle where no coupled motion between the parawing and the seat arrangement was allowed;

3) Only a relatively high-speed flight condition has been investigated. The characteristics might well be quite different at lower speed;

4) The meaning of the different features of response for the flying qualities of the AERCAB is largely unknown. The perspective of airplane handling is helpful but not decisive, so that valid, realistic simulation will be required at an early date.

c. Piloted Analog Simulation-Lateral/Directional Mode

The analog computer previously described was programmed to investigate qualitatively the lateral/directional

characteristics of the AERCAB. The pilot was able to control vehicle roll rate by means of a toggle switch which controlled the wing bank angle, ϕ_W, and he could observe vehicle roll angle and yaw angle. The AERCAB is not equipped with a rudder or any other means of lateral/directional control other than the wing bank angle controller.

Since the toggle switch controls wing bank angle and does not control vehicle roll rate directly, the pilot must compensate for the fact that the neutral position of the switch does not correspond to a zero or nearly zero roll rate such as the neutral position of a conventional aircraft lateral control does. Rather, the neutral position of the wing bank angle toggle switch corresponds to a nearly constant roll rate which is equal to zero only if the wing bank angle happens to be zero at the time the switch is neutralized. The longer the toggle switch is activated, the greater is the roll rate which must be stopped by reversing the switch for an equal length of time instead of merely neutralizing it. Consequently, the toggle switch roll rate controller designed for the AERCAB is somewhat unconventional, and a certain amount of learning is required before a pilot feels comfortable with such a scheme.

As seen in Figures 84 and 86, the roll mode time constant with or without a vertical tail is in the order of 1.5 to 2 seconds which is longer than conventional aircraft roll rate responses. Consequently, the pilot must learn to compensate by applying some lead with his control inputs. This required compensation is complicated further by the non-conventional roll rate control scheme described in the preceding paragraph. The most successful control technique consisted of learning what lead was required, and then applying very short impulsive control inputs with the wing bank toggle switch.

Figure 88 presents the results of a bank angle tracking task in the presence of gusts. Control inputs are denoted on that trace by sharp spikes that were caused by superimposing an additional voltage in the $+\phi$ direction whenever the wing bank angle controller was activated. The sharpness of the spikes is an indication that the controller was used in an impulsive manner. The frequency with which the pilot activated the controller can be observed by counting the number of spikes

required to track a desired bank angle. Since the control of bank angle is not very precise with the wing bank controller and the vehicle's bank angle variations in the presence of gusts are not large, the best tracking results were obtained by neglecting the gust induced variations and using the controller only to make gross changes in roll rate.

The technique resulted in loose tracking, as seen in Figure 88. The pilot attempted to track $\phi = 0$ radians for 65 seconds, then track $\phi = -.10$ radians until $t = 210$ seconds, and then track $\phi = 0$ until $t = 300$ seconds. The pilot was able to make bank angle changes on command and he was able to loosely track the commanded bank angle. The task did not result in the pilot/vehicle system becoming unstable, although considerable practice was required before reasonable tracking results were obtained. While no heading time histories were recorded, the bank angle tracking was sufficient to produce heading control which probably would be acceptable for the AERCAB mission.

Bank angle tracking would be easier to accomplish if the roll rate controller were more conventional with the neutral position of the controller corresponding to roughly a zero roll rate. Such a control scheme might be possible by means of a feedback system that neutralized the wing bank angle as the lateral controller was neutralized. The controller should be easy to operate in an impulsive manner. Possibly it should be part of the longitudinal controller so that the pilot can operate the AERCAB's flight controls with one hand while he operates the throttle with the other. Even with a more piloted-orientated control scheme, however, the lateral/directional handling qualities of the AERCAB for a bank angle tracking task, might be marginal due to the relatively long roll mode time constant.

Effects of varying the control term, N_{ϕ_W}, were evaluated as part of the piloted simulation analysis. For values of N_{ϕ_W} approaching -10, the control of bank angle was very difficult and tracking was not possible due to the extremely large Dutch roll excitation. Since the pilot did not have a rudder with which to control yaw angle, he was unable to prevent or dampen the Dutch roll with the result that he had great difficulty in controlling bank angle without causing large oscillations of the

vehicle for the case of $N_{\phi_W} = -10$, the pilot/vehicle system was unflyable by means of the wing bank controller, and no figures of those negative results are presented.

In the development of the final AERCAB configuration, wind tunnel or similar data should be utilized to determine the values of N_ϕ and the derivatives which effect the Dutch roll mode. An adequate simulation of the finalized vehicle should be used to evaluate the resulting handling qualities and to investigate suitable means of control. Training probably will be required before a pilot can fly the AERCAB, and the most efficient way to obtain such training will be through simulation.

6. Rejection of the Decoupled Concept

At the onset of the reported investigation it was believed that an all-flexible coupling would be necessary between wing and payload in order to be capable of stowing the AERCAB system in an acceptably small crewstation occupancy volume. It was believed also, however, based on the contractor's past experience with flexibly coupled systems, that the system with the decoupled suspension means would be too readily susceptible to aerodynamically or inertially induced relative motion between the wing and payload. Such relative motion, it was postulated, was characterized by a high potential of onset of irreversible divergent translational and rotational displacements which could result in a non-recoverable flight situation which would obviate the value of having a self-rescue vehicle in the first place. In an attempt to alleviate this adverse potential, design efforts were intensified to develop a useful, packageable rigid coupling framework which kept the wing at a known position relative to the payload throughout the transient wing-deployment phase as well as during self-rescue flight. The arrangement portrayed earlier in this report evolved from those design studies, appeared feasible, and thus stood as just cause for rejection of the decoupled concept.

7. System Performance Considerations

a. Drag Reduction Studies

The inherent drag generated by the man/seat payload overshadows any potential benefits which might be expected to be gained through an increase in L/D of the wing. Also, this drag significantly influences

Figure 83

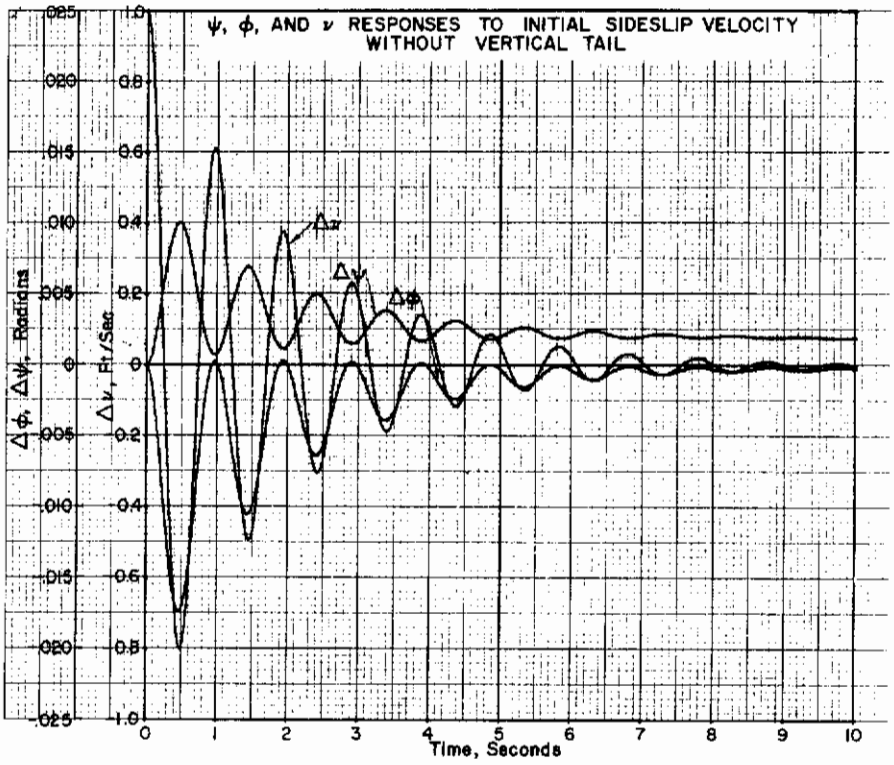

Figure 84

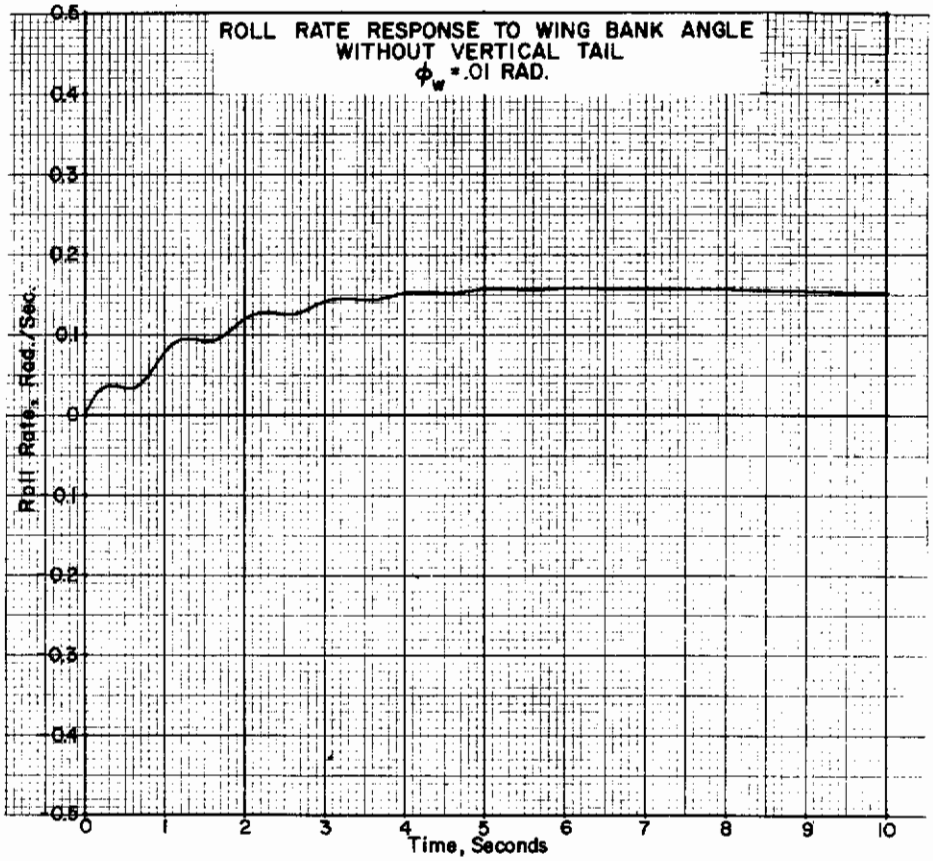

Figure 85

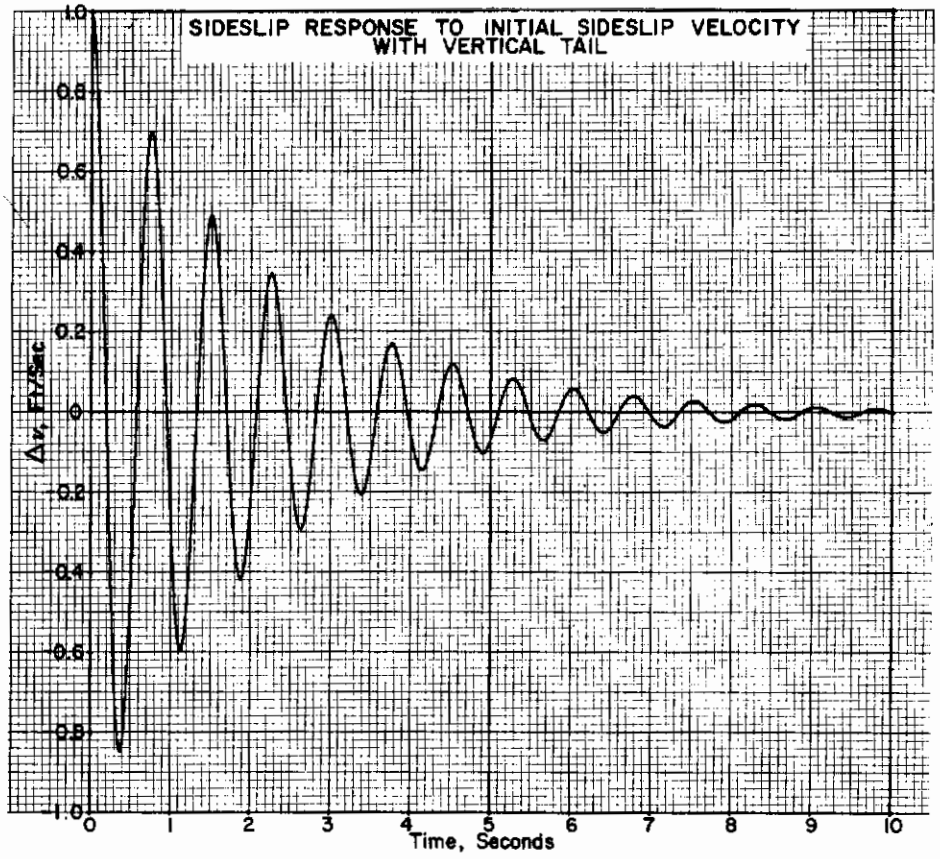

Figure 86

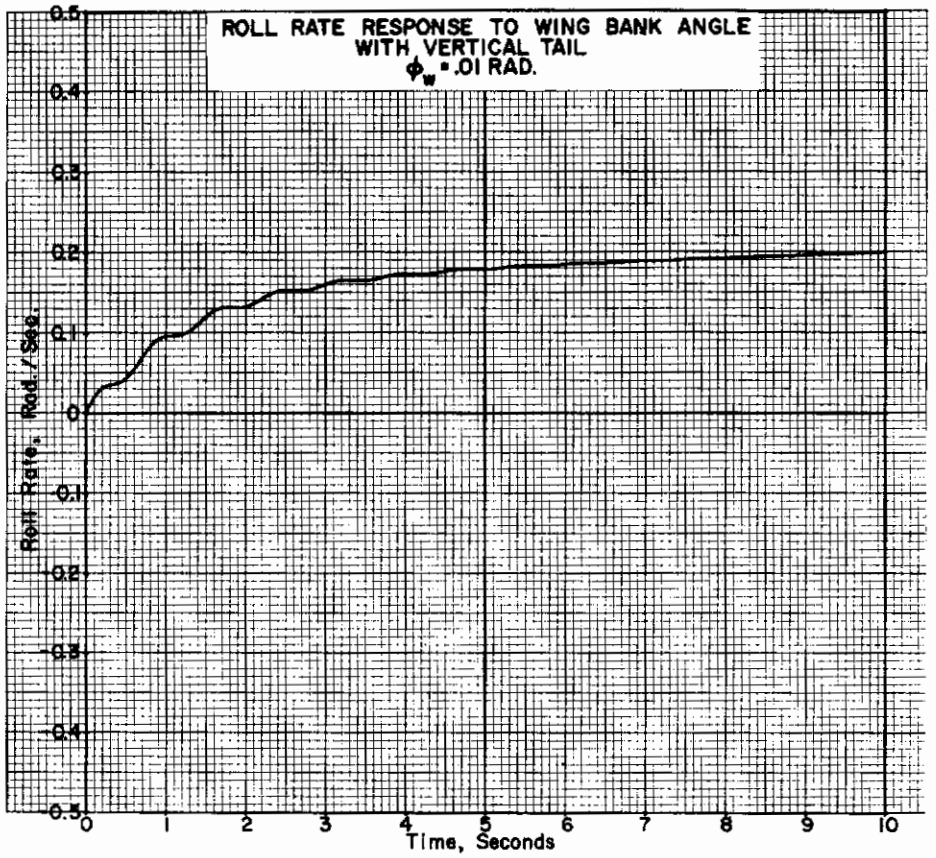

Figure 87

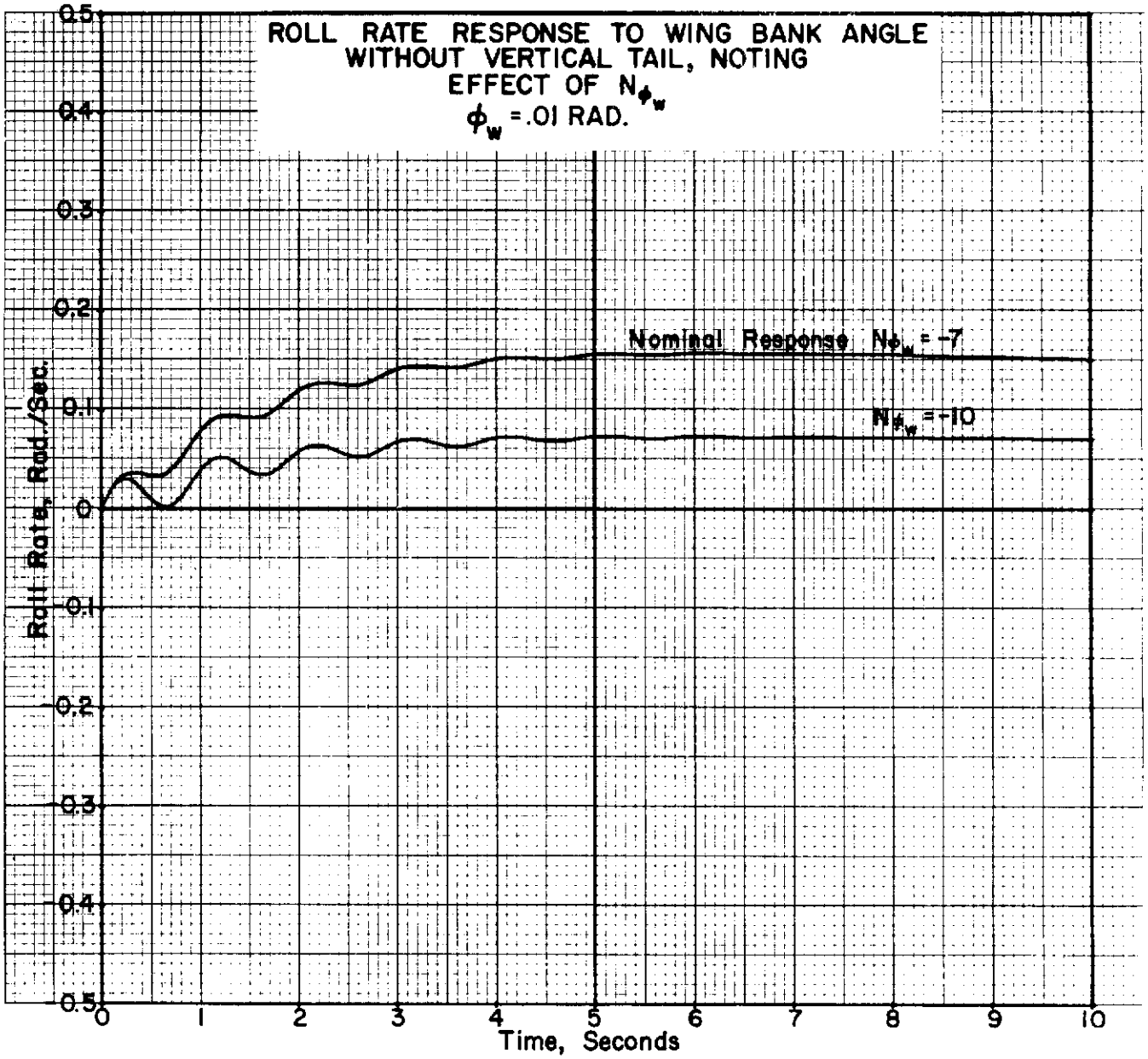

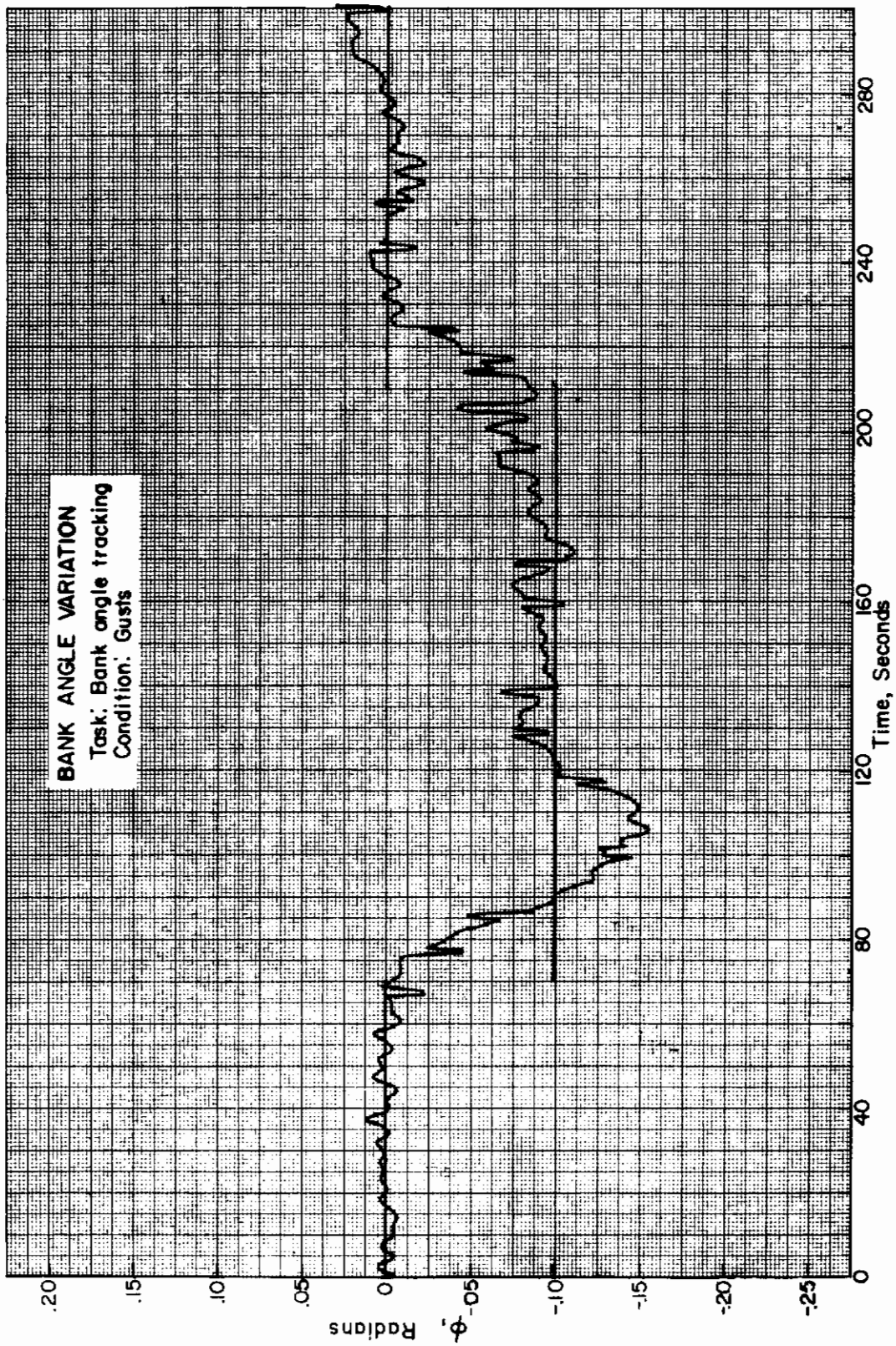

Figure 88

the level of thrust required to achieve target performance goals, and correspondingly effects the amount of fuel which must be carried on board the self-rescue vehicle.

With the initial design in which the upright payload domineered, an investigation into the degree of AERCAB payload drag reduction achieveable was completed, giving consideration to using inflatable bags around the rear, top and bottom of the seat. Estimates were based on Reference to the 1958 edition of Fluid Dynamic Drag by Hoerner.[23] Referring to Figure 23, p. 3-13 thereof, for the curve of his Reference 28 (a) and (b), for three-dimensional rectangular shapes having an r/h = 0.2 (where r is the corner radius, and h is the total height normal to the airstream), it is seen that:

$$\frac{(C_D)\ r/h = 0.2}{(C_D)\ r/h = 0} = \frac{0.17}{0.75} = 0.2266 \qquad (67)$$

Comparing this value to that for a shape more closely approximating the AERCAB upright payload, (but two-dimensional), it is seen that at an r/h = 0.2 for the curve of Hoerner's Ref. 27 (solid square symbols), the drag ratio is:

$$\frac{(C_D)\ r/h = .2}{(C_D)\ r/h = 0} = \frac{0.33}{1.43} = 0.2306 \qquad (68)$$

Using a value of 0.23 (and multiplying by 2.0, since only the aft section of the payload can be streamlined, while the forward face and the man must remain unstreamlined), we have a useful factor of 0.46. This factor multiplied with the unstreamlined payload drag area of 4.2 sq.ft., renders an effective streamlined area of only 1.931 sq. ft.

Thus it is seemlingly possible to reduce the payload's effective drag area to slightly less than two square feet, by streamlining with inflatable bags at the top, bottom and rear in a virtual "boattailing" effect, which by design could also aid in improving the flow conditions at the engine inlet.

Had not the seat been deemed unstable in the initial design, ultimately resulting in a complete reorientation of the seat relative to the wing while in flight, the streamlining would have been more rigorously pursued, and an attempt would have been made to integrate "boattailing" into the design. The minimum weight performance

benefits are superimposed in Appendix E on Figures E-1 and E-2 to indicate potential advantages of streamlining. Some benefits may be gained by further considering streamlining of the reoriented payload in the selected system design.

b. Calculation of Thrust Required for Level Flight

For purposes of completeness and continuity, the following discussion of the calculation of thrust requirements is presented.

Over a range of wing angles-of-attack (α_w) from 20 through 45 degrees, the thrust required for steady-state level flight was determined for a broad band of equivalent airspeeds.

For AERCAB, it is seen from the drawings submitted herewith that the angle-of-attack of the turbofan engine's thrustline (relative to the airstream) is defined by the expression

$$\alpha_T = \alpha_w - 11.85^o \tag{69}$$

The system drag coefficient was taken as

$$C_{D_{TOT}} = C_{D_W} + C_{D_{PL}} + C_{D_{STRUTS}} \tag{70}$$

where

C_{D_W}, the wing drag-coefficient was taken from page 25 of NASA TND-1957 at a value of C_{L_W} from p. 24 therein corresponding to the particular α_w being considered.

$C_{D_{STRUTS}} = 0.0334$

and

$C_{D_{PL}} = \frac{(C_D S)PL}{S_W}$, where $(C_D S)_{PL}$ can be found from Figure 89 herein.

The system lift coefficient is found from

$$C_{L_{TOT}} = C_{L_W} + C_{D_{TOT}} * \text{Tan}\,\alpha_T \tag{71}$$

Where the term $C_{D_{TOT}} * \text{Tan}\,\alpha_T$ is the lift coefficient increment due to that component of the thrust orthogonal to the relative wind. This term can be seen to be

equal to the term $C_T * \sin \alpha_T$,

where

C_T, the "thrust coefficient", = T/qS

since

$$C_{D_{TOT}} = C_T * \cos \alpha_T \tag{72}$$

and

$$C_T = \frac{C_{D_{TOT}}}{\cos \alpha_T} \tag{73}$$

then

$$C_T * \sin \alpha_T = \frac{C_{D_{TOT}} * \sin \alpha_T}{\cos \alpha_T} = C_{D_{TOT}} * \tan \alpha_T \tag{74}$$

Also, from the expression for system gross weight,

$$GW = C_{L_{TOT}} * q * S_W \tag{75}$$

it is seen that

$$q = \frac{G.W.}{S_W * C_{L_{TOT}}} \tag{76}$$

It is known that the true airspeed is defined by

$$V_{TRUE} = \frac{Ve}{\sqrt{\sigma}} \tag{77}$$

$Ve = 17.18\sqrt{q}$ in knots ($17.18 = \frac{1}{1.6889}\sqrt{2/\rho_o}$), from $\rho_o/2\ Ve^2$, where ρ_o is defined on the next page and, where $\sqrt{\sigma}$ is found in the ICAO Standard Atmosphere tables; and Ve is the equivalent airspeed.

The total system drag force is

$$D_{SYS} = C_{D_{TOT}} * q * S_W \tag{78}$$

And the <u>thrust required</u> to combat that drag is

$$T_R = \frac{D_{SYS}}{\cos \alpha_T} \tag{79}$$

It is noted that values of drag and airspeed at any wing loading and gross weight (at the same wing angle of attack) may be obtained merely by multiplying a reference value of system drag by the ratio, $\frac{GW_{new}}{GW_{ref}}$,

FIGURE 89

PAYLOAD DRAG AREA FLUCTUATION WITH THRUST ANGLE OF ATTACK

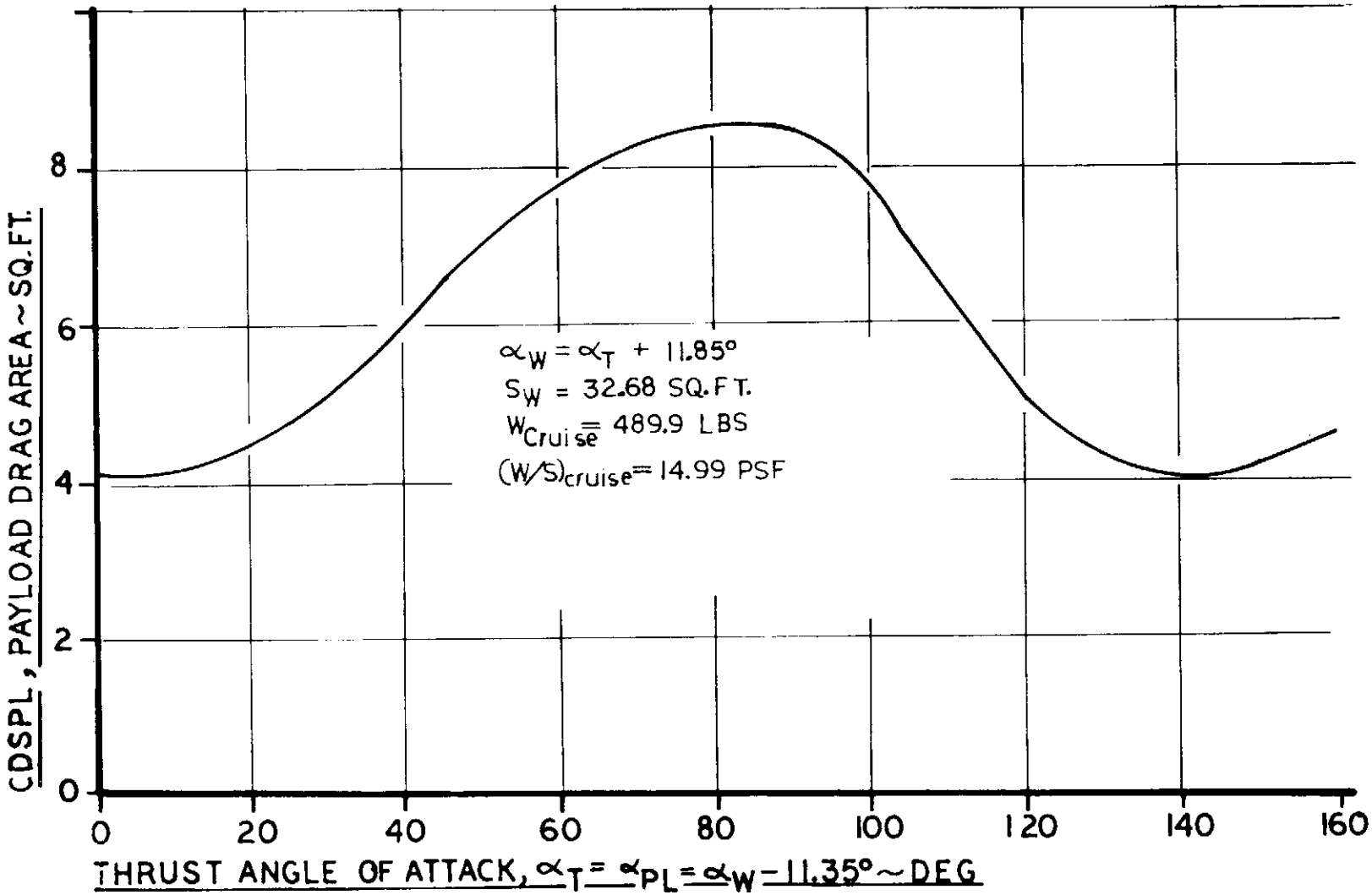

and by multiplying the reference value of equivalent airspeed, Ve, by the term

$$\left[\frac{(W/S)_{new}}{(W/S)_{ref}} \right]^{\frac{1}{2}}$$

Because the drag is calculated as a function of equivalent airspeed, the values hold for all altitudes and temperatures. For comparison to true velocities, one has but to employ the above conversion equation. Since σ is a standard day ratio in the above, it too must be converted for other than standard day temperatures from the expression

$$\sigma = \delta / \theta \tag{80}$$

where

$$\sigma = \rho / \rho_o$$
$$\delta = P/P_o \tag{81}$$
$$\theta = T/T_o$$

the subscript, "o", denotes sea level standard day conditions

ρ is the density

P is the static pressure

T is the absolute temperature (i.e., ^{o}Rankine or ^{o}Kelvin)

Figure 90 shows, in carpet format, the thrust available with equivalent velocity and altitude. The next subsection describes the construction thereof.

c. Mission Profile Computation

A pair of representative AERCAB mission profiles were calculated to give a picture of the system's self-rescue flight performance. A table of the results is presented below. Before looking at these end results, however, let's first discuss the methods employed in their computation.

Fundamentally, MISSION 1 was defined by the AERCAB achieving a steady state flight at 2000 ft MSL,

FIGURE 90
THRUST AVAILABLE
VS. V_E AND ALTITUDE

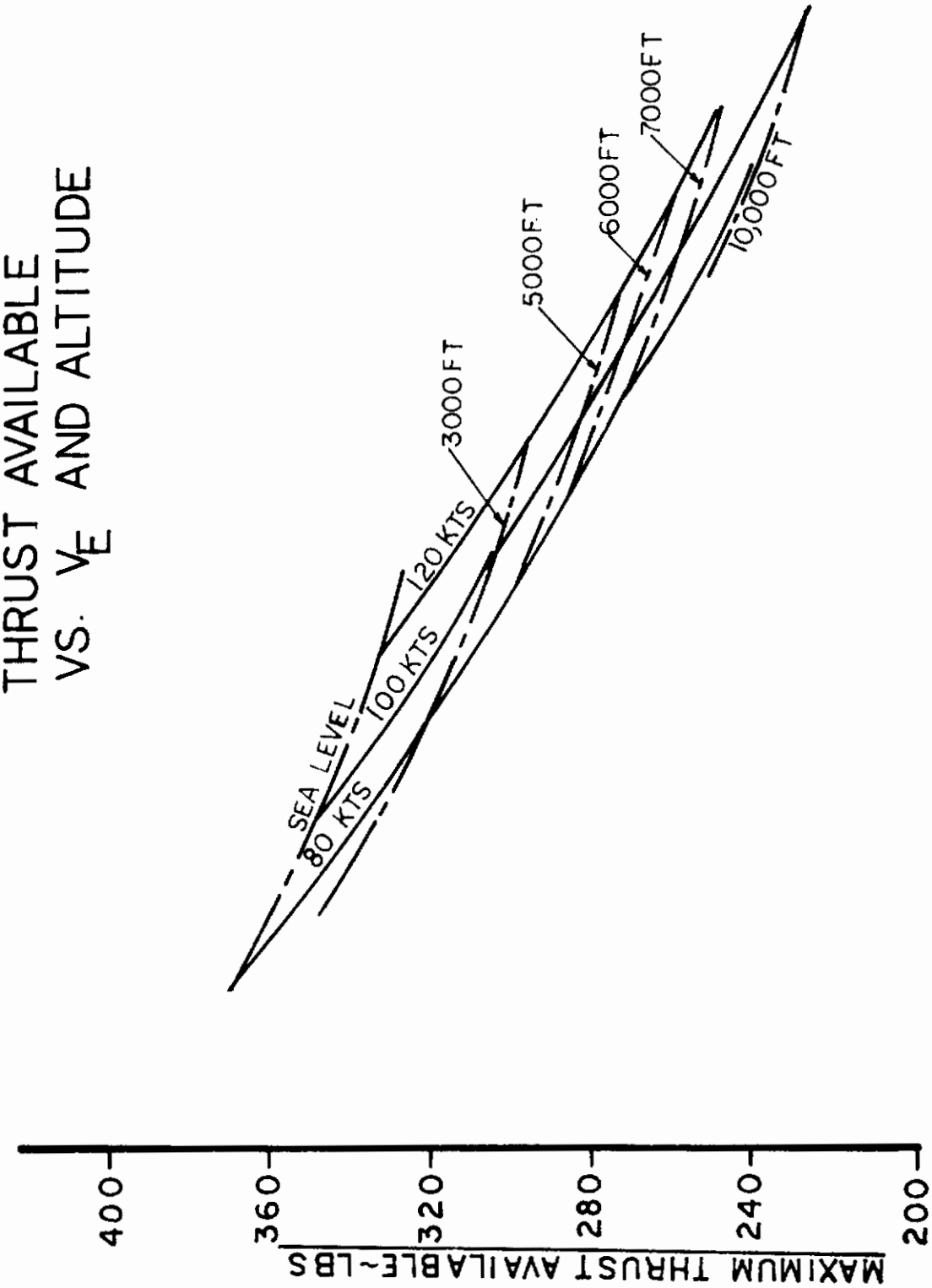

and proceeding to climb to 6000 ft. MSL, whereat the occupant maintained a trim, level flight (unidirectionally) until fuel depletion; whereafter he descended in glide to the altimeter induced separation and subsequent recovery.

MISSION 2 also involved a climb from 2000 to 6000 ft. MSL, whereat straight and level flight resumed for about 15 minutes. At an arbitrarily selected point near the midpoint of the time available for powered flight, a 180° level turn was made (still at 6000 ft. MSL) and the vehicle retraced essentially his former path to the time whereat fuel was depleted, and gliding descent to recovery altitude resumed.

(1) Climb from 2000 to 6000 Ft., MSL

The system having a gross weight of 529.7 lbs., a wing area of 32.68 sq-ft, and the occupant's back tangent line inclined 17.15° upward from horizontal was assumed to be at a trimmed wing angle of attack of 29° at the 2000 ft. altitude set out as conditions for time = zero. For the climbing portion of the mission, the time, distance and fuel expended to climb were calculated from:

$$t = \sum_{h=2000}^{h=6000} \Delta t \tag{82}$$

$$t = \frac{\Delta h}{(R/C)\ avg.} \tag{83}$$

$$\text{Fuel Expended} = \sum_{h=2000}^{h=6000} W_{F\,avg} * \frac{\Delta t}{60} \tag{84}$$

$$\text{Distance Covered} = \sum_{h=2000}^{h=6000} (V \cos\gamma)_{avg} * \frac{\Delta t}{60} \tag{85}$$

where

h = altitude, ft.
t = time, min
R/C = rate of climb, ft/min
fuel = fuel used, lbs
W_f = fuel flow, lbs/hr.
distance is in nautical miles
γ = climb angle, between relative wind and horizon; deg.

The average R/C was calculated at the average altitude for each of the two step calculations (i.e., @ 3000 and 5000') from the expression

$$R/C = \frac{(T*\text{Cos}\ \alpha_T - D)}{GW} * V_T * 101.33,\ \text{fpm} \qquad (86)$$

where

T is the maximum thrust available in lbs., as drawn from Figure 90.

The Drag, D, was ratioed using the gross weight ratioing technique described above, referencing the T_R computation tables at a value of $\alpha_w = 29^o$ (you will recall that angles of attack from 20 to 45 degrees were encompassed in that computation...)

Also V_e was ratioed and V_T was calculated for an altitude of 3000 ft. (first step-calculation) using the previously described methods.

The maximum thrust available, as shown in Figure 90, at 10,000 ft. MSL was calculated from the expression:

$$T = \frac{250}{183} \left(\frac{48.54}{53.0}\right)^{2/3} (0.00173V_T^2 - 0.833V_T + 249.0) \qquad (87)$$

where the 250 lbs. is the guaranteed thrust at V = 100 knots @ 10,000 ft. for the 52 lb. (weight) twin-fan engine with increased bypass ratio;

183 lbs. is the basic twin-fan thrust issued by the low bypass ratio engine for which initial performance data was provided;

48.54 is the computer ("WEIGHT" program) calculated engine weight;

52 lbs. is the basic twin-fan engine weight;

The weight expression is ratioed to the 2/3 power, which is the inverse of the thrust ratio, used for weight scaling;

The remainder of the equation is an expression fitted to the thrust vs. V_T curve for the basic engine at 10,000 ft.

Then, at constant Mach numbers the thrust was ratioed at various altitudes directly with standard atmospheric pressure. The carpet plot Figure 90 resulted.

For the first mission computation step, the average gross weight (@ 3000') was assumed to be the estimated maximum design gross weight (i.e., 529.66 lbs.) as output from the "WEIGHT" computer program. Then the fuel required for the first climb step was calculated from the "Fuel-Expended" equation above wherein $W_F = SFC * T_{3000'}$ (where SFC = $0.001634 * V_T$ - 0.000004* (altitude in ft.) + 0.480). Half of this fuel was subtracted from the initial weight to obtain a more accurate average gross weight, and then the calculation was repeated to get a more accurate value of Δt and Δfuel.

The final iterated value of Δt was input into the "Distance Covered" equation to obtain the range expended in climb. In that equation, the climb angle was determined from the expression:

$$\gamma = \text{Arcsin}\left(\frac{T-D}{GW}\right) \qquad (88)$$

The second climb step was similarly calculated using average values at 5000 ft. MSL.

Obviously greater accuracy could have been achieved by increasing the number of step calculations made, but for purposes of this presentation, the results are felt to be sufficiently close with the two step iterations made.

(2) Cruise @ 6000 Ft., MSL

The cruise segment of the mission profile was then assumed (for MISSION 1) to use all remaining fuel. The "WEIGHT" computer printout for the tested configuration gave a total design fuel weight of 79.59 lbs.

The average cruise gross weight is

$$(GW)_{avg.cruise} = (GW)_{max.dsgn.} - W_{fuel\ climb} - \frac{W_{cruise\ fuel}}{2} \qquad (89)$$

Values of Ve and D were ratioed at the average cruise weight and a 29° angle of attack (as was done for climb) and V_T was calculated from the conversion equation.

The thrust relationship used was

$$T = D/\cos\alpha_T, \tag{90}$$

and the SFC and W_F were calculated in identical fashion to those for climb. Then, the cruise range was determined from

$$X = \left(\frac{V_T}{W_F}\right) * W_{cruise\ fuel} \tag{91}$$

The time in cruise was determined from

$$t_{cruise} = \frac{Range * 60}{V_t}, \text{ minutes} \tag{92}$$

(3) Descent to Recovery Level

The descent from flight level (6000' MSL) was assumed to be trimmed at $\alpha_w = 29°$. A table of glide speeds was prepared for angles of attack ranging from 22 to 38 degrees.

Descent speed was calculated from

$$Ve = 17.18 \left(\frac{W*\cos\gamma}{S*C_{L_W}}\right)^{\frac{1}{2}} \tag{93}$$

where

$$\gamma = \text{Arctan}\ (C_{D_{TOT}}/C_{L_W}) \tag{94}$$

The time to descend was obtained from

$$t_d = \sum_{h\ =\ 6000}^{h\ =\ 1000} \left(\frac{\Delta h}{V_T \sin\gamma * 101.3}\right) \tag{95}$$

Figures for the minimum time to glide descend from altitudes ranging from 10,000 ft. to sea level had been calculated for the gross weight configuration of 529.7 lbs. From that data, the value of descent time from 6000 ft. to 1000 ft. was obtained by interpolating linearly between S.L. and 2000 ft., subtracting that

value from the value for 6000 ft., and ratioing the resultant inversely by the Ve ratio,

The average descent rate was found by dividing the change in altitude by the total time required to make the change.

The average descent speed was found by dividing the average descent rate by the term, sin *101.334.

The range covered during descent was

$$X = \frac{\Delta h}{\tan \gamma * 6080} \qquad (96)$$

(where 6080 is the number of ft. per N.Mi.

(4) MISSION 1 Results

Table 10 contains the values of ΔFuel, ΔTime and ΔRange corresponding to each MISSION 1 segment. The Fuel was summed negatively by subtracting from the gross weight. The table also shows the altitude at the beginning and end of each profile segment, as well as the average true airspeed and wing angle of attack during each segment.

(5) MISSION 2

As previously mentioned, MISSION 2 was identical to MISSION 1 with the single exception that, after half the fuel remaining after the climb was burned during cruise, a 180° level turn (@ α_w=32°) at maximum thrust available was performed.

It was necessary to determine a true airspeed at 6000 ft. at maximum thrust in order to compute the turning (bank) characteristics while maintaining trim. The true airspeed was obtained from Figure 65.

Ve and q were calculated from $Ve = V_T\sqrt{\sigma}$, and $q = 0.00339Ve^2$.

In the turn, the cosine of the angle of bank is $\frac{GW}{C_{L_{TOT}} * q * S_W}$, wherein $C_{L_{TOT}}$ is calculated for $\alpha_w = 32°$ in the same manner as previously described.

TABLE 10
AERCAB MISSION 1 PROFILE

Alt. ft.	Mission Segment	$\triangle$Fuel lbs.	GW lbs.	$\triangle$t min.	t_{tot} min.	$\triangle$X n.mi.	X_{TOT} n.mi.	Avg. V_T KTAS	α_w deg
2000	onset	----	529.7	----	0	----	0	---	---
----	climb	10.1	----	3.21	---	14.95	---	89.9	29
6000	---	----	519.6	----	3.21	----	14.95	---	---
----	cruise	69.5	----	32.27	---	46.81	---	87.1	29
6000	----	----	450.1	----	35.48	----	61.76	---	---
----	descent	0	----	1.39	---	1.68	---	80.6	29
1000	----	----	450.1	----	36.87	----	63.44	---	---

TABLE 11
AERCAB MISSION 2 PROFILE

Alt. ft.	Mission Segment	ΔFuel lbs.	GW lbs.	Δt min	t_{tot} min	ΔX n.mi.	X_{tot} n.mi.	Avg. V_T KTAS	α_w deg
2000	onset	----	529.7	----	0	----	0	----	---
----	climb	10.1	----	3.21	----	14.95	----	89.9	29
6000	----	----	519.6	----	3.21	----	14.95	----	---
----	cruise	34.8	----	15.51	----	22.90	----	88.6	29
6000	----	----	434.8	----	18.72	----	37.85	----	---
level	180°turn	0.8	----	0.28	----	0.44	----	92.8	32
6000	----	----	484.0	----	19.00	----	38.79	----	---
----	cruise	33.9	----	16.43	----	23.39	----	85.4	29
6000	----	----	450.1	----	35.43	----	61.68	----	---
----	descent	0	----	1.39	----	1.68	----	80.6	29
1000	----	----	450.1	----	36.82	----	63.36	----	---

The turn radius was calculated from

$$R = \frac{V_T}{\tan \phi * g} \text{ , ft.} \quad (97)$$

where $g = 32.2$ ft./sec.^{2}

The time consumed in the turn is

$$\Delta t_{Turn} = \frac{\pi R}{60\ V_T} \text{ , minutes} \quad (98)$$

SFC was calculated using previously described expressions, and the thrust, T was obtained from Figure 69.

$$W_F = T*SFC \quad (99)$$

$$\Delta Fuel = W_F * \frac{\Delta t_{Turn}}{60} \quad (100)$$

Range (in the turn) is $X = \frac{\pi R}{6080}$, n.mi. (101)

Table 11 contains the values of ΔFuel, ΔTime and ΔRange corresponding to each MISSION 2 segment. The ΔFuel was again negatively summed to the gross weight figure. The table also includes values of altitude, average true airspeed and wing angle of attack during each segment.

SECTION V - COMPATIBILITY AND PRACTICALITY CONSIDERATIONS

The tradeoffs between lift-generating, drag-reducing, and propulsion subsystem candidates for AERCAB integration to obtain a minimum weight, minimum volume, highly reliable system capable of operating within the established performance spectrum have been discussed at length earlier in this report. Those tradeoffs markedly influenced the practicality of the system for future USAF use. However, other factors influence the system's practicality, and these too were investigated under the subject program. Among these influential factors were AERCAB's compatibility with HIAD, A-7 and F-4 aircraft crewstations; operating characteristics in adverse weather flight; human factors implications; and navigation requirements. This section discusses these additional practicality considerations.

1. CREWSTATIONS COMPATIBILITY

It was required that the design of the system be governed by reference to the following:

a) AFSCM 80-1 (HIAD)[2]
b) AFSCM 80-3 (HIAPSD)[3]
c) AFSC DH 1-6 (System Safety)[24]
d) MIL-S-9479A (USAF)[4]
e) LTV A-7 Crewstation Drawings[25]
f) McDonnell-Douglas F-4 Crewstation Drawings[26]

Quite often one or the other of these basic references demanded compromise of the requirements of one or more of the others. As the program matured, the emphasis on integration into the A-7 and F-4 crewstations intensified (once basic feasibility was identified) and these installations presented the greatest degree of compromise of all. The resulting deviations from 80-1 and 9479A are correspondingly discussed and justified in the following paragraphs.

Your attentions are invited to Figure 5, herein, which portrays the AERCAB preliminary design as installed in both the A-7 and F-4 cockpits.

a. Installation in the A-7 Aircraft Crewstation

(1) Deviation 80-1.1 (A-7) (Ref. Dwg. AD1, Sheet 1 of 5):

The design philosophy was adapted, based on the contractor's judgment, whereunder the Pilot Eye Position was maintained at its existing

coordinates in the A-7 crewstation, and the Neutral Seat Reference Point (NSRP) was located relative thereto in complete accord with HIAD, AD1 specifications (i.e., NSRP lies 10" aft of and 31" below the Pilot Eye Position) which resulted in a 2.23 inch forward shift of the NSRP. This resulted in a NSRP 9" above the "heel rest line" (in lieu of 8.5" in 80-1); a distance of 17.875" from NSRP forward to the neutral Stick Reference Point (in lieu of 20" in 80-1); a distance of 11.375" from the NSRP upward to the neutral stick reference point (in lieu of 13.50" in 80-1). The rudder pedal in the mean adjustment neutral position has been changed from 34.7 to 32.47 inches forward of the neutral seat reference point (in lieu of 36.25 in 80-1). The throttle control was changed from 16.32 to 14.09 inches forward of the neutral seat reference point (in lieu of 20 inches in 80-1). It is emphasized that these irregularities are amplified by a lack of conformity of the A-7 crewstation to HIAD, and were well beyond control of this investigation. All other AD1 specified dimensions were maintained.

As a result, the occupant is moved closer to the instrument panel, stick, throttle, and rudder pedals, which limits the space available for 50th through 95th percentile crewmen. It appears, also, that moving the seat forward and locating the fuel tanks on the sides of the seat will impair aftward arm movement for throttle operation if no changes to the throttle control or its location were made.

(2) Deviation 80-1.2 (A-7) (Ref. Dwg. AD2):

Superimposing the AERCAB installation onto the A-7 cockpit drawing reveals that if the 30" minimum distance for ejection path clearance forward of the NSRP is to be maintained per 80-1, Dwg. AD2, then approximately 4.15" of the bottom of the existing instrument panel will have to be arcuately removed; and approximately 2.5" will have to be trimmed from the hood (or cowl) that appends rearwardly above and over the instrument panel, presumably as a glare inhibition shield. These are the only apparent modifications required forward of the seat back tangent line in order to maintain the 30 inch ejection path clearance. For last resort ejection through the canopy to

be possible, either the parawing will have to be altered or restowed, or the aircraft canopy would have to be redesigned with the glass extended further aft to prevent the apex of the stowed wing from colliding with metal canopy structure.

(3) Deviation 9479A.1 (A-7):

Paragraphs 3.4.1.4 and 3.4.2.6.1 require that seat/man separation be effected by the deployment and inflation of the recovery parachute. During AERCAB operations in the normal escape mode (i.e., sans self-rescue), this feature is provided. However, under self-rescue operations, at termination of flight, seat/man separation is effected by the net differential forces acting as lift on the seat, and gravity-acceleration on the man. Should the need be proven during later experimentation, auxiliary separation aids (e.g. the rotary actuator type) may be added to augment the rapidity and positiveness of separation. Presently, however, this is not deemed necessary since a positive differential in separation forces acting on man and seat appears to exist in calculations made during system studies.

(4) Deviation 9479A.2 (A-7):

Paragraph 3.4.2.2 of the referenced specification demands that the basic ejection seat shall consist of the seat bucket structure with a fixed headrest (i.e., headrest fixed to the bucket structure). Since installation envelope minimization was paramount to the AERCAB design, this requirement was deviated from, resulting in an overall savings of at least 2.5 inches in height. This saving stems from the fixity (relative to the airframe) of the AERCAB headrest as different sized crewmen adjust the bucket height in the cockpit to achieve their proper mission eye-level seated height, and does not jeopardize mission accomplishment.

(5) Deviation 9479A.3 (A-7):

Paragraph 3.4.2.2.1 of the referenced specification demands that the "interior seating width shall be a minimum of 18 inches". The AERCAB is designed such that it can be given a shape having the

required width-dimension with virtually no tooling cost to the USAF to implement the change. However, to accommodate installation in the A-7, it was necessary to design the bucket such that the seating width is 16.625". USAF should recognize, however, that as crewstation space available permits, AERCAB can readily be enlarged to any width, (said space is available in the F-4).

(6) Deviation 9479.4 (A-7):

Paragraph 3.4.2.2.4 of the referenced specification demands that "ejection seat adjustment shall be accomplished by a positive-action, electrically powered screwjack". However, SAEC has determined that AERCAB, which also uses seat-adjustment for trimming longitudinal self-rescue flight, is more weight and volume efficient if the SAEC-developed "infinite-position", hydraulically-actuated, electrically operated adjustment system is integrated into the catapult assembly structure. Comparisons made with "off-the-shelf" screwjacks indicate that the hydraulic system weighs but 37% of what an equivalently performing screwjack weighs. Additionally, the integrated system requires no additional volume for stowage, while the screwjack demands considerable space in a region in tight cockpits that is extremely critical. The hydraulic actuator can also be used as a shock attenuator in "hard" landing situations.

(7) Deviation 9479.5 (A-7):

With reference to Figure 4 of MIL-S-9479A, the following dimensional deviations have been made in designing AERCAB to fit the A-7 and F-4 installations:

(1) as mentioned above, the seating width has been reduced to 16.625" in lieu of the 18" min.

(2) the dimensions related to the parachute cavity in Figure 4 (viz., 14.75" R; 24.5" length; and 5" depth) are not applicable to AERCAB since the recovery parachute in the latter is stowed in the headrest area rather than between the man and seat...

(3) the space available for survival gear has been reduced from Spec MIL-S-9479A requirements by direction of the USAF for this investigation only, and is not to be construed by the reader as a sanction of such a reduction for this or other applications.

(8) Additional Deficiencies (A-7):

With the portrayed installation, it was discovered late in the program that in the event the canopy failed to jettison and the system should have to eject through it, the apex of the parawing would contact metalic portions of the canopy rather than the plexiglas. There are three possible solutions: (1) adding a shaped-charge system to cut out the metal section in the event of canopy jettisoning failure; (2) redesign of the canopy wherein the plexiglas portion is extended aft 3.25 inches; (3) redesign of the parawing to incorporate hinges on the booms to allow the apex portion to stow forward of its present position. It is also possible that changing the general arrangement of the system design would allow a stowed parawing configuration that would eliminate the interference.

b. Installation in the F-4 Aircraft Crewstation

As shown in Figure 5, the AERCAB design configuration as evolved under this investigation was superimposed on available crewstation information related to the F-4 installation. This made several integration problems obvious. It is emphasized that the HIAD and MIL-S-9479A discrepancies described herein are subject to the peculiarities of the F-4 crewstation, and reflect in no way on AERCAB's suitability for integration in other contemporary or future generation aircraft.

(1) Deviation 80-1.1 (F-4):

In the F-4, the AERCAB pilot's eye position was maintained at its existing height, and moved 1.25 inches aft in the crewstation such that the Neutral Seat Reference Point (NSRP) was located relative thereto in complete accord with the HIAD dwg. AD1, sheet 1 specifications (10" aft and 31" below the eye reference point); hence the AERCAB NSRP

coincides with that of the encumbant seat. Thus, as shown in Figure 5, the F-4 NSRP lies 12.3" above the "heel rest line"; the distance between the NSRP and the neutral Stick Reference Point lies 10.4" above the Neutral Seat Reference Point. All other ADl specified dimensions were maintained.

With that configuration the most apparent interference lies with the bulkhead and metal canopy structure aft of the seat, and probably with the canopy actuator as well. Note that these interferences arise because of the NSRP coincidence, and the fact that the installation so located did not appear to change the occupant's relation to his crewstation provisions, instruments and controls was noted. However, the ejection path angle relative to vertical during catapult stroke is 13° for AERCAB versus 19.5° for the existing seat, so the ejection clearance envelope was modified, although not to the extent of introducing any evident or immediately apparent interferences forward of the NSRP.

(2) Deviation 80-1.2 (F-4):

With the above installation constraints (coincident NSRP's), there exists an interference between the front edge of the seat and the control stick pedestal when the seat is adjusted downward. This is easily corrected however by merely changing the shape of the leg-braces on the seat bucket and the location of the seat bucket front panel; neither of which involve very extensive design changes to the seat itself.

(3) Deviation 80-1.3 (F-4):

The fuel tanks projecting laterally outward from the seat prevent access to that portion of the consoles below the tanks, and might present a problem, as in the A-7, with aftward articulation of the aircraft throttle control.

(4) Deviation 80-1.4 (F-4):

As presently configured and shown herein, the fixed or stationary portion of the seat-rails and catapult manifold assembly interferes with the aircraft control torque tube in the forward cockpit of the

F-4. This would require reconfiguration of the seat's stationary assembly arrangement, or relocation of the control tube.

(5) MIL-S-9479A Deviations (F-4):

Because of the operational and functional identity of the AERCAB A-7 and F-4 installations, the deviations spelled out in paragraphs V-1-a-(3) through V-1-a-(7) apply equally to the F-4. It is noted that because the width between the consoles in the F-4 is 23", there is no problem whatever in that installation in providing the full-width (22") seat bucket as specified by MIL-S-9479A. The changes therein would be principally in the slightly heavier seat bucket, and the added volume which would likely be filled with added survival equipment.

c. Closing Rationale

The cockpit installations shown in Figure 5 were based on the assumption that it would be economically better to modify the control stick, throttle, instrument panel, glare shield and rudder controls rather than moving the aft pressure bulkhead further aft. This matter was not considered in detail and consequently it may be more desirable to either move the bulkhead or add a "plug" section in the fuselage.

2. ADVERSE ENVIRONMENT OPERATIONS

In studying the operational suitability characteristics of the AERCAB configuration, limited time was expended in analyzing the influence of adverse environment operation. The following is a brief commentary on the findings related to system performance effects. Consideration was given to the flight regime bounded by a maximum of 10,000 ft. pressure altitude, a maximum relative airspeed of 100 knots true airspeed, and prevailing conditions of icing, rain, snow, clouds, turbulence, hail, thunderstorm activity in the vicinity of the flying man/seat, night-flying, cold and hot weather flying.

Icing of lifting (control) surfaces adds parasitic weight and drag-area to the flying self-rescue configuration, thereby either reducing achievable range at a given thrust setting; or requiring additional thrust either to maintain velocities required for lift, or to achieve the desired range. At a given specific

fuel consumption rating (lb-fuel/lb-thrust/hr) the added thrust requirement would demand that more fuel be carried to achieve the same airspeed and range capabilities of the "non-iced" configuration. This becomes quite evident with a quick reference to the "carpet" plots in Section IV showing the relationships of mission weight, cruise speed and range, knowing that ice @ 32°F weighs 57.5 lbs. per cu. ft., and our preliminary wing has a "wetted surface" of 32.68 sq. ft., (i.e., a 1/8-inch thick homogeneous, evenly-distributed buildup on the wing alone would weigh 19.6 lbs.). Uneven buildup of ice could effect the wing's lifting characteristics as well as those of drag, and could be expected to reduce the control effectiveness and resulting system maneuverability. No quantitative experimental evidence has been found in the literature dealing with icing influence on the aerodynamic performance characteristics of parawings, but local buildups will effect local airflow and separation in a manner similar to that experienced on fixed wings, so that similar performance degradation may be anticipated. Some relief in this area of concern lies in the possibility that the "flagging" of the flexible wing surface in a high dynamic pressure flow field experienced in powered cruising flight may inhibit the buildup sufficiently to enable the occupant to maneuver to a regime wherein icing is no longer a problem. Since the wing has rigid leading edges, however, such relief thereon probably cannot be expected.

The most probable regime in which free air icing occurs varies from 25°F @ S.L. to -12°F @ 20,000 ft. MSL, in very nearly linear fashion.

Icing of the engine and intake duct can result in at least two known types of harm: ice buildup on the inlet guide vanes can result in a restriction of inlet airflow which leads to a measurable loss of thrust, a rapid rise in exhaust gas temperature, and a high potential of compressor stall; also, intake duct ice breaking loose in relatively large fragments can be ingested into the compressor section of the engine, doing structural damage in that section.

In the rain, the wing fabric will likely become saturated with moisture and be slightly on the heavy side, possibly even going out of trim. It is not known, however, if the high moisture content of the air will result in a change in lift and drag which might contribute to detrimming the system.

Turbulence encountered in regions near thunderstorm areas

(often found to contain hail, also) can structurally damage hard- and soft-structures through imposition of shock-type (gust) loads, often oriented in directions for which the system's structure hasn't been designed. While this would possibly result in a loss of self-rescue capability, the terminal descent made under parachute is effected to a lesser degree as borne out by experience (on record) of parachute descents through thunderstorms. Often in this case, the slow terminal descent rate of the parachute does prolong the crewman's exposure to hail impact and to very uncomfortable "coning" oscillatory motion.

At higher altitudes in areas around thunderstorms, ice crystals form in the air which don't settle at the inlet duct, but rather go into the engine with intake air, and then are heated during compression, thereby becoming ingested water. The resulting phenomenon is often referred to as "ice crystal compressor stall". Also in thunderstorm areas, the turbulence can induce violent changes of inlet angle of incidence which results in surging of inlet airflow conditions and corresponding marginal engine performance. Of course, the high liquid content of cumulus cloud buildups, as well as the icing of intake ducts or inlet guide vanes therein, all could contribute to the engine flameout. AERCAB can readily be given a mid-air restart capability, but even if restart failed, flameout would only terminate any further self-rescue departure flight beyond that achievable in gliding.

Cold weather effects on system function and operation are not expected to introduce significant performance problems, although the physiological problems related thereto could be significant, and are discussed below.

To aid in combating the effects of inlet-surging and moisture-ingestion, and to enhance overall safety, a constant ignition feature on the engine would prove most desirable.

During operation in desert areas and locations where high temperatures prevail, a reduction in lift achievable at a given thrust setting is anticipated. Sand and dust in the engine, fuel system, aerodynamic sensors, navigation equipment and controls could create attendant problems worthy of designed-in protection before-the-fact.

3. NAVIGATION (HOMING)

a. Requirement

The requirement for automatic navigation means in AERCAB is considered firm since those crewmen ejecting over enemy held territory, and therefore most urgently needing the AERCAB fly-away departure capability, are those most likely to have suffered injury or to be in a confused state of shock; which could preclude accurate manual navigation. In addition, crewmen such as radar-observers or special-equipment operators need to be recovered by AERCAB without requiring excessive and expensive special flight and navigation training.

b. Systems Considered

During the course of this study program, and in discussion with Air Force flight-navigation specialists, several systems for providing automatic navigation were considered. The most promising of the systems considered utilizes UHF homing beacon transmitters located in the preassigned rescue area, with a homing-receiver for controlling the AERCAB flight path located on the seat. Another system which is almost universally considered chronologically first as the solution to the AERCAB navigation problem, is the use of an on-board compass (preferrably a gyro-compass) to maintain flight on a predetermined compass setting. The most sophisticated system would utilize data from computers on-board the parent aircraft to establish a position and a homing flight vector to the nearest rescue area, at time of ejection. Subsequent to ejection, the AERCAB flight vector would be oriented via a gyro-compass on-board the seat in the direction prescribed by the parent aircraft computers at the instant of ejection.

c. Comparison of Homing Beacon Mode and Fixed Compass Heading

To realize the advantages realized through use of the homing beacon mode, the trajectories of Figure 91 were plotted assuming the homing beacon to be located at the rescue area. The AERCAB flight velocity was considered to be 100 knots and the point of departure was assumed to be 50 nautical miles due north of the rescue area. Wind from the west was considered to be 10, 20, 30, 40 and 50 knots (the circled dots in this figure show the AERCAB position after 30 minutes of

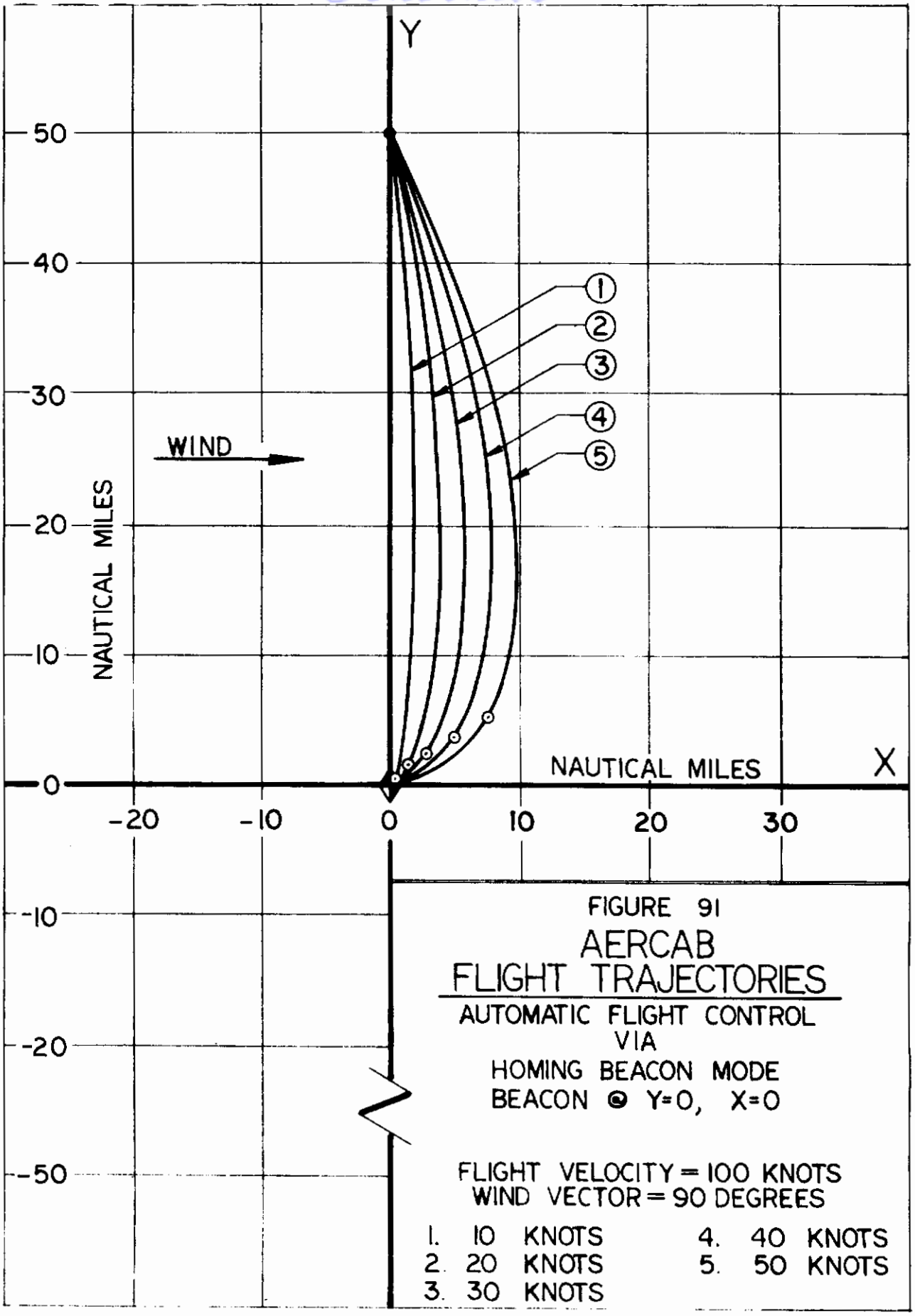

FIGURE 91

AERCAB
FLIGHT TRAJECTORIES

AUTOMATIC FLIGHT CONTROL
VIA
HOMING BEACON MODE
BEACON @ Y=0, X=0

FLIGHT VELOCITY = 100 KNOTS
WIND VECTOR = 90 DEGREES

1. 10 KNOTS
2. 20 KNOTS
3. 30 KNOTS
4. 40 KNOTS
5. 50 KNOTS

flight). From these curves it is clear that with a homing beacon at the rescue area, if the eject point is within the prescribed 50 mile range capability of AERCAB, then, even in a 30 knot side wind the rescue area can be reached in gliding unpowered flight after total fuel depletion. Also it is clear that for an initial distance of less than fifty nautical miles, even in a cross wind of 50 knots, successful flight to the rescue area would be achieved.

In Figure 92, five trajectories are plotted with identical conditions to those of Figure 91, but assuming that navigation was by a fixed compass heading (flight direction of AERCAB was due south). Here it is clear that any side wind is very detrimental, and a 30 knot side wind introduces a 15 nautical mile error into the flight trajectory even for a perfect compass heading for the AERCAB flight. If the ejection point was less than 50 nautical miles from the rescue area, the error of the flight termination point to the rescue area would be increased unless, through some additional intelligence, the flight was terminated as the AERCAB reached the X-axis. Thus, the advantage of a homing beacon is evident.

In Figures 93 and 94, the starting point for the AERCAB flight is shown to have an X-error of -10, +10, +20 nautical miles. This could arise either by an error in the preset compass heading of -11.3^{o}, $+11.3^{o}$ or 21.8^{o}; or ejections at points -10, +10, or +20 nautical miles from the expected ejection point (e.g., the attacked target) for which the preset compass heading was established. Again the advantage of the homing beacon mode is obvious.

Comparing Figure 95 to Figure 91 it is seen how important it is to locate the homing beacon at the rescue area. In Figure 95 the homing beacon was assumed to be 50 miles beyond the rescue area directly opposite the eject point. With a 30 knot side wind the terminal point for powered flight is 10 nautical miles downward of the rescue area, and clearly indicates that the homing beacon must be located in the rescue area to realize the full benefits attendant thereto.

d. Recommended Automatic Navigation System

It is believed that the following automatic navigation

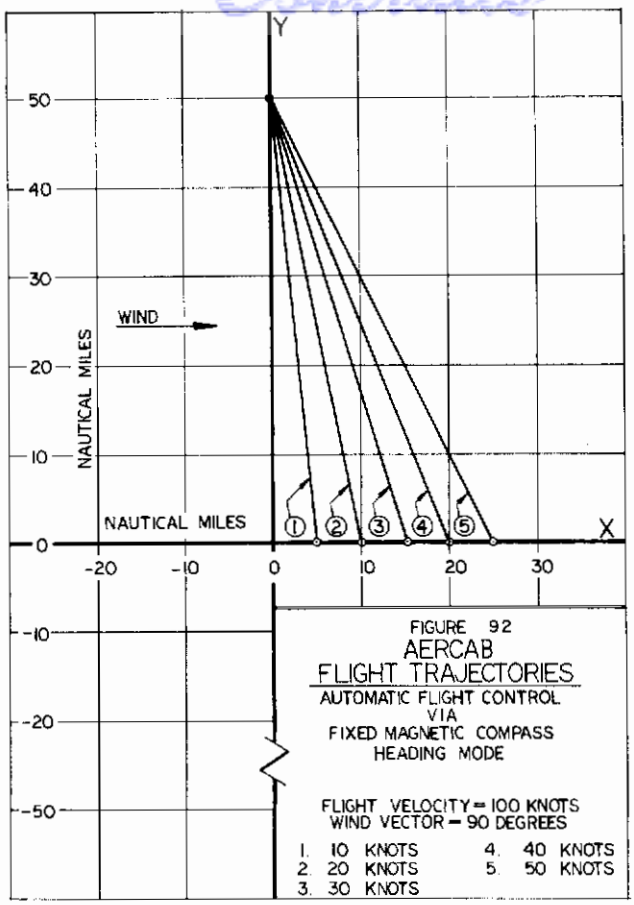

FIGURE 92
AERCAB
FLIGHT TRAJECTORIES
AUTOMATIC FLIGHT CONTROL
VIA
FIXED MAGNETIC COMPASS
HEADING MODE

FLIGHT VELOCITY = 100 KNOTS
WIND VECTOR = 90 DEGREES

1. 10 KNOTS
2. 20 KNOTS
3. 30 KNOTS
4. 40 KNOTS
5. 50 KNOTS

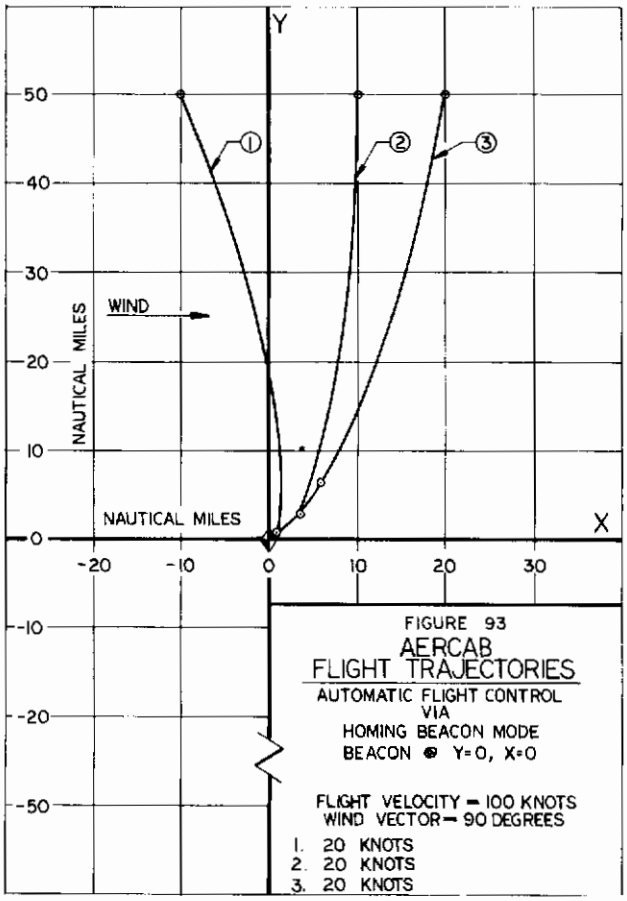

FIGURE 93
AERCAB
FLIGHT TRAJECTORIES
AUTOMATIC FLIGHT CONTROL
VIA
HOMING BEACON MODE
BEACON @ Y=0, X=0

FLIGHT VELOCITY = 100 KNOTS
WIND VECTOR = 90 DEGREES

1. 20 KNOTS
2. 20 KNOTS
3. 20 KNOTS

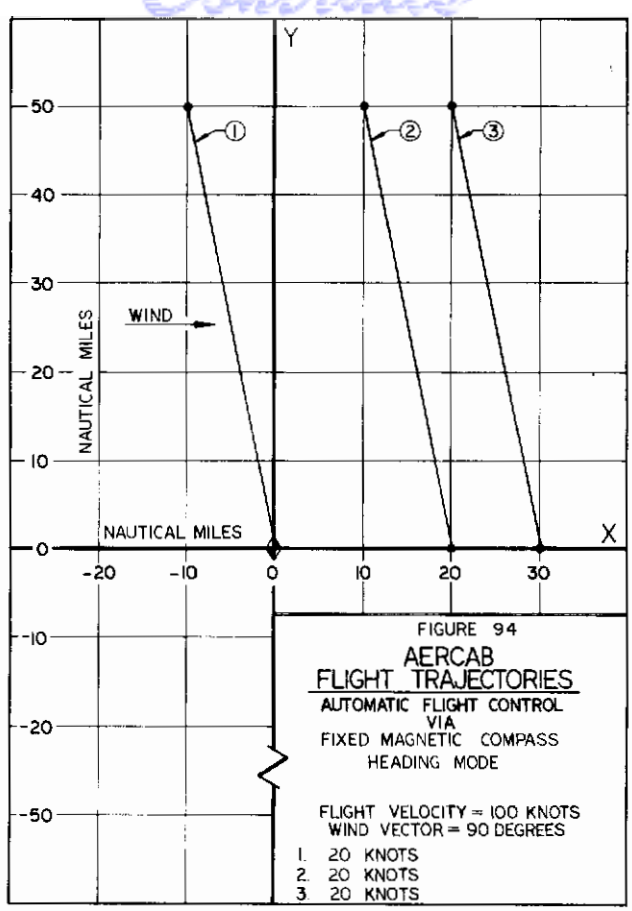

FIGURE 94

AERCAB
FLIGHT TRAJECTORIES

AUTOMATIC FLIGHT CONTROL
VIA
FIXED MAGNETIC COMPASS
HEADING MODE

FLIGHT VELOCITY = 100 KNOTS
WIND VECTOR = 90 DEGREES

1. 20 KNOTS
2. 20 KNOTS
3. 20 KNOTS

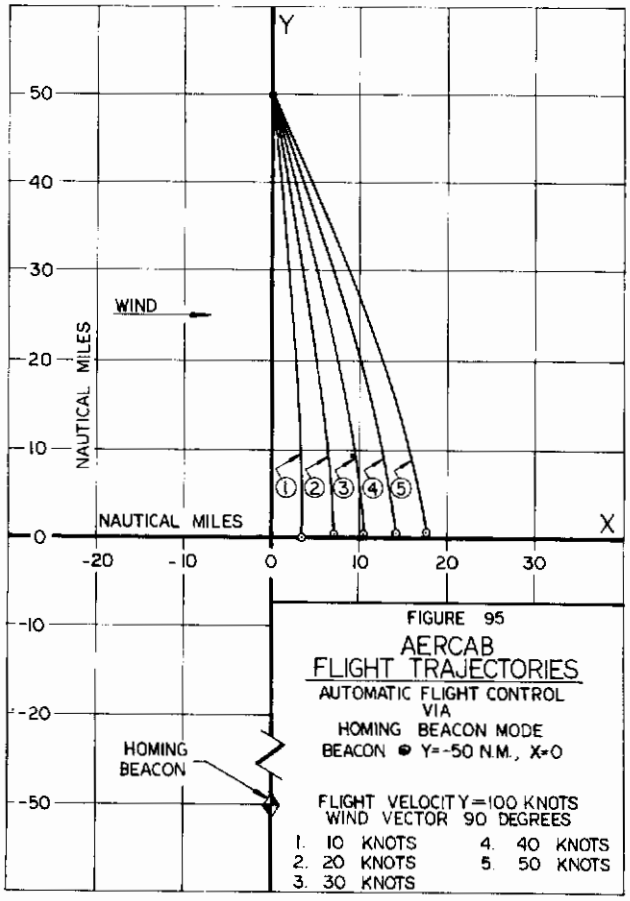

FIGURE 95

AERCAB
FLIGHT TRAJECTORIES

AUTOMATIC FLIGHT CONTROL
VIA
HOMING BEACON MODE
BEACON @ Y=-50 N.M., X=0

FLIGHT VELOCITY=100 KNOTS
WIND VECTOR 90 DEGREES

1. 10 KNOTS
2. 20 KNOTS
3. 30 KNOTS
4. 40 KNOTS
5. 50 KNOTS

system would offer the optimum rescue capability for an unconscious or seriously incapacitated pilot. This system concept requires that a UHF homing beacon transmitter be located tactfully in the rescue area, operating in the frequency range of 243 MC. Mounted to the apex of the AERCAB parawing are two simple, single element antennae, spring-loaded to snap into their operating position upon parawing deployment. The electronics package on AERCAB includes a phase discriminator and power amplifiers to operate the flight controls in such a manner that AERCAB is turned until the signals received in the two antennae are in phase. A fail-safe relay integrated into the receiver will function to switch, in the absence of any received homing beacon signal, to a gyro-compass signal which will cause the AERCAB to turn to a preset compass heading. At any time during the self-rescue flight, upon receipt of the proper homing beacon signal, the fail-safe relay would switch to the antennae coupled phase discriminator for automatic navigation control. The absolute altitude sensor (radar altimeter) included for automatic initiation of the final parachute descent phase can be integrated into the automatic flight control system to permit automatic flight at presetable absolute altitudes. Upon ejection, automatic climb (or descent) to the desired absolute altitude will occur provided a homing beacon signal is received. In the absence of the homing beacon signal, the AERCAB would automatically climb on the prescribed compass heading to the maximum service ceiling, or to that altitude whereat the homing beacon signal is received. This feature will account for those instances where a mountain ridge or range between the eject point and the homing beacon in the rescue area has blocked the UHF homing beacon signal.

e. Alternate or Rejected Approaches

A pair of fishbone antennae for the parawing mounted receiving antennae were considered. However, the complexity of this type of antennae in addition to its length requirements (3 to 5 times the signal wave length), the problems associated with its deployment, and the signal distortion produced by the parawing keel and leading edge booms have indicated that the proposed dual single-element, dipole type antenna array is definitely optimum because of its inherent simplicity.

Higher frequencies in the UHF band could be used, however greater signal directivity will result. Thus, signal blockage by mountain ranges would be much more pronounced and an unnecessary deterioration in the automatic navigation system performance results. Additionally, the homing beacon in generally mountainous terrain should not be located down in a valley due to the signal blockage that could result. However, low lying and more level valley floor areas would be preferred over mountain tops for the rescue area both for ease of equipment installation and for safety of the pilot descending under a parachute.

One serious problem in the homing beacon system is the need for distinguishing false homing signals generated by an enemy beacon. It appears feasible to design the system to eliminate all homing signals outside a prescribed angle from the pre-determined and preset fixed compass heading, thereby eliminating all homing signals which would otherwise direct the AERCAB flight path away from the "friendly" rescue area.

A concept which was rejected because of its weight and bulk might be feasible in those aircraft already using on-board computers of sufficient capacity to provide position data to AERCAB continuously prior to ejection. The on-board computer would then feed continuously the true compass heading of the rescue area into the auto gyro in the fixed compass heading section of the automatic navigation system. This system would offer more potential for recovery in the rescue area of pilots ejecting at points quite distant from the mission target area in the fixed compass heading mode.

4. HUMAN FACTORS

Thus far, AERCAB's compatibility with existing and future aircraft has been validified analytically and design-wise. The system is compatible with its mission performance requirements as well. The obvious remaining compatibility consideration is, then, ...is the system wholly compatible with its occupant? Referring back to Section I, it is seen that AERCAB must complement the crewman's workstation, and since no extraordinary changes have been made outside of convention in that respect, certainly it can be concluded that AERCAB is at least as good as any crewstation "chair" and work-center presently in service. The restraint

subsystem might even prove more comfortable than the bulky shoulder-harness/lap-belt types now in service. The hydraulic seat adjustment subsystem's shock absorbitive characteristics might be expected to make the system more comfortable and safe during abnormally hard landings of the mother ship. In any event, as a chair, AERCAB appears wholly compatible with its occupant.

But, what of its human compatibility during escape, self-rescue flight, and terminal recovery? The discussion below limitedly treats what were felt to be critical areas related to AERCAB's compatibility with its occupant (viz., accelerative loading and environmental protection). Each factor is subject to further study, but is definitely an AERCAB design criterion.

a. Accelerative Loading

The man seated in AERCAB is routinely subjected to triaxial accelerations and decelerations throughout his normal flight and emergency escape and rescue missions. Hence, throughout the entire period of AERCAB occupancy, specific levels of protection are required.

The seat, when in normal use, if HFE designed to be compatible with access to (and utilization of) work-station controls and instrumentation, as well as being comfort-oriented (i.e., distribute normal flight loads over the entire body to remove or minimize pressure point application; give the occupant freedom to shift about to alter this distribution; and provide vertical articulation of the seat where potentially exhausting missions of long tenure are to be accomplished). For access to controls and instruments, and for ability to twist about in the seat to see downstream (whereat a hostile aircraft may be attempting to position for a strike), and for general defensive (avoidance) flying, it is essential that the seated occupant be provided with the freedom of movement found only with a loose restraint subsystem. Of course, the restraint is provided to protect the occupant during exposure to accelerative and decelerative loads encountered in flight through turbulence, aerobatic maneuvering flight, crashing into the earth's surface, ejection, retardation, and recovery. Hence, we encounter the problem of a loose restraint which must, often cyclically, automatically impose constraint on torso and limb movement under potentially perilous conditions. Negative-G

(eye balls-up) restraint must be maintained even with comfortable slack in the rest of the restraining provisions. Manual override of automatic inputs is a must for missions involving flight maneuvers in turbulent air or in aerial combat.

The ejection seat is designed basically for the injured crewman who has only the capacity to initiate egress by actuating his ejection-control handle, and then is assumed to be incapacitated for any further input. Hence, the escape system takes over once activated, and is completely automatic to the point of return to the earth's surface. Because the crewman has been allowed, up to the time of emergency, complete freedom in the cockpit, the escape system must accomplish three things for him before he can be allowed to exit. He is brought into a position relative to the seat whereat his head and limbs are positioned for encountering the airstream, and his torso is aligned to best withstand the onset and application of forces needed to separate man and seat from the parent vehicle. Once positioned, he must be restrained there, securely enough to preclude excessive relative movement between man and hardware, regardless of the direction he will be ejected in relative to the earth's gravitational field. Of course, as an additional pre-ejection measure, his egress path must be cleared--hence, any inhibiting structures must be moved from his path of travel. It is well within the state-of-the-art to haulback and restrain the crewman's legs and torso. It is an advancement to the state-of-the-art to do so practically to his head and arms (...at least, automatically). It is well within the state-of-the-art to jettison the hatch or canopy to clear his way, or to destroy the canopy so that he can pass through it without injury. However, the time required to accomplish these tasks detracts from the man's overall recoverability--and to minimize these times for haulback, restraint and path-clearance is of essence.

For those flight vehicle systems which can get themselves into all of the conditions A through H (Figure 1), it becomes immediately obvious that no matter how the escape system is propelled and stabilized, 3.0 seconds after ejection will find too many ejectees in "premature contact" with the terrain. The T_A values previously listed further demonstrate the disadvantage of excessive available ejection propulsion impulse under all conditions, but serve to prove also that <u>some</u> impulse over and above

that afforded by the catapult alone is needed to combat tail clearance problems at high-speed, and straight-and-level sink-rate situations. In determining impulse-levels for optimum performance, of course, the problem must also entail considerations of magnitude, sense and onset-rate of accelerations imposed spinalward on the occupant (DRI limits). In any event, to encompass the entire emergency envelope, one problem confronted is that of performing within the envelope (time vs. air-speed).

It becomes clearly evident that the seat must be capable of quite a versatility in that it must be able to "switch" function-time in accordance with prevailing dynamic pressure conditions. This was evidenced in a previous discussion herein of the problems encountered during deceleration and stabilization. However, it is important to note that, out of necessity due to the peculiarities of seat installations in cockpits, the propulsive elements must apply their accelerative loads on the man/seat combination in a spinalward direction. These loads are maximized (within physiological limits) in order to minimize total time for egress. However, depending on the airspeed and altitude (affecting aerodynamic loading), a component of the aero-loads may couple with propulsive loads to a degree which could be injurious or even fatal to the ejectee. This coupling during ejection is a problem which must be overcome.

For those weapons systems having a multiplicity of personnel to perform mission tasks as a coordinated team, provisions must be made for simultaneous ejection of all team-members in order to preclude jeopardizing any individual's chances for survival through programmed time delays. Because post-ejection interference must be prohibited by induction of divergence of all trajectories scribed by the aircraft, all ejectees, and all seats, with sufficient separation allowed so that no contact takes place even after full inflation of all recovery parachutes occurs. This assures that the T_R min ingrained in each seat will be fully taken advantage of by each escapee.

Measures must be taken to protect the ejectee from windblast effects. His attire (helmet, mask, flight-suit, gloves) may well protect him against the abrasive effects of the wind, but the dynamic pressure acting over his head, torso and limbs can wrench, tear and

distort to the point of serious injury or fatality. Statistics contain cases wherein ejectees have had serious trauma (to the point of hemhorrage) induced by "buffet" of the helmeted head against the headrest's surface. Compound fractures induced by flailing during the ejection have been known to be fatal, because they enabled the ejectee to bleed to death during his descent under a perfectly operating parachute. The problem related thereto is one of effective positioning and restraint in and to the seat during the initial period of exposure to the dynamic-pressurized flow field outside the cockpit. To assure the man of egress regardless of inputs from airframe-fixed subsystems, provisions must be made for an ingrained capability to eject through the canopy in the event of failure of the canopy removal equipment. Correspondingly, the seat must be configured such that seat-structure itself receives the onset and application of canopy-penetrating loads, rather than the crewman's head or extremities (even though it has been demonstrated as permissible to permit the latter to "carry away the pieces" once penetration is accomplished). Serious cervical vertebraic damage can be imposed by the helmeted head's contacting the inner-mold-line of the canopy's surface prior to satisfactory fracturing thereof, especially when the head is bent forward under the acceleration induced by stroking of the catapult. Even retention of good head position against the rear supportive surface of the headrest can result in injury to the spine of compressive-nature if the ejectee, rather than the seat, makes initial contact and penetration of the canopy.

And, directing discussion to the catapult's thrusting, it is noteworthy that the design must be such as to maximize the stroke-length of the catapult as limited only by height available within the confines of the crewstation interior. This maximization in length allows one to achieve the highest practical egress-boost velocities without unduly jeopardizing the ejectee's well-being, by controlling the force levels and onset rates to well within tolerable limits. The DRI (Dynamic Response Index) limits set forth in MIL-S-9479A must be religiously adhered to in designing the propulsive subsystem's output. SAEC has established a computer program for DRI calculation based on inputs of a given force-time history. The accelerative characteristics of the rocket-catapults integrated into existing escape systems was already discussed.

Of particular interest therein is the strong limiting influence of the spinal loading allowed, on the magnitude of deceleration allowable to slow the system to airspeeds suitable for parachute deployment and opening. Assuming complete yaw-stability, so that planar induction of loads takes place, it is interesting to note that since one must maintain the expression

$$\sqrt{\left(\frac{DRI_z}{G_{z_L}}\right)^2 \quad \left(\frac{G_x}{G_{x_L}}\right)^2} \leq 1.0, \qquad (102)$$

that a rocket of the high-impulse type permits little margin of safety for spinal loading, and no room for a longitudinally-directed deceleration (not even that which is unavoidable due to the inherent drag of the man/seat combination). Interestingly enough, the low-impulse type of rocket sustainer, because of its good thrust-time characteristic, at least allows 24G to be input for deceleration in an eyeball's out direction. Previous discussion also points out one weakness in the trapezoidal/triangular approximation method presented in MIL-S-9479A when applied to the problem of computing DRI values for the coupled catapult-rocket thrust-time history. However, the alternate approximation technique presented appears to overcome the shortcoming of the prescribed method.

From the above it is seen that selection of the propulsive elements of the system becomes a problem of weighing the need for sink-rate compensation and tail-clearance against the physiological limits of the ejectee coupled with the system's need for retardation to velocities at which the recovery system (or self-rescue system) can be effectively utilized.

Before departing from this brief discussion on ejection problems, one should note the importance of being able to restrain and contain the occupants legs as well as his arms. During catapult stroking, the crewman's legs are drawn back off the control pedals very rapidly, and inertial forces tend to "tuck" the legs in a toes down, heels-back position. However without suitable means for containment and retention, the legs can slam into the resilient calf-guard plate on the fore-end of the seat bucket, and rebound with sufficient energy stored to position the feet in a dangerous proximity with the bow (frame) of the windscreen (forward canopy section). "Hooking" the canopy bow can

result in leg damage as well as serious perturbation to the egress trajectory, neither of which are acceptable for a model seat. Hence, the problem is one of prevention of rebound of the legs through suitable restraint.

For those emergencies wherein the crew is unable to eject (e.g., G loads are such as to prohibit reaching controls in time), the AERCAB seat must afford all personnel on board with protection against crash effects. Again restraint and containment become problem areas. Crash loads must be distributed suitably over the seat occupant, and dumped into the airframe through points of sufficient strength in order to prevent separation of man, seat, or equipment from each other or from the vehicular supportive structure. G-limiters must be included if crash load application is anticipated which could violate DRI criteria. Once a post-crash steady state condition is reached, MIL-S-9479A criteria are quite explicit; they state fundamentally that the occupant must be enabled to release himself from any bonds to parachute, survival equipment and seat--and get out and away from the troubled vehicle as rapidly as he is physically able. To release himself, he should only have to actuate a single-motion control which is released from its neutral locked position by squeezing.

In the past, policies have differed widely in regard to providing a means for the occupant to either "bail-out" in flight with his parachute and survival gear, or to "ditch" over the side (subsequent to a forced landing) taking only his survival gear with him. Because SAEC anticipates that there will be USAF Using Commands in the future who will be faced with missions wherein emergencies will be encountered warranting such provisions, SAEC believes the AERCAB seat should be versatile enough to provide these means if needed without necessitating a major development or retrofit program (which is expensive in both time and dollars). It's understood that such provisions are <u>not</u> required in MIL-S-9479A, but they are recognized as important nonetheless.

With his troubled vehicle on the ground traveling at speeds of less than 10-15 KEAS, the crewman's chances of going over the side and surviving are pretty good. Given just a bit of altitude or additional airspeed, though, his chances are nil unless he uses his assisted

egress provisions. In his AERCAB must be a means for both slowing him down, and for gently lowering him to terrain level from whatever height he may leave the cockpit. Parachutes are normally employed to do the lowering job. Some pretty poor performance has been demonstrated by parachutes in the past. Most of that was attributable to an absence of reliability in their operation...they functioned...sporadically and randomly... and could <u>hardly</u> be used in a system whose total performance must be both predictable and repeatable. However, in the past few years some pretty remarkable advancements to the state of the art of parachute technology have entered the picture; and reliable, repeatable, predictable performance is now achievable (and being achieved in-service through upgrading retrofits). But, the parachute canopies themselves have changed very little--hence, they are still limited in strength (which limits the dynamic pressure flow field into which they can be deployed); and still exhibit a "spike" type of loading (Force vs. Time) characteristic which limits their use even further (in so far as deployment and inflation "g" is concerned) because of man's relatively low tolerance to such generally spinalward shock loadings. Because of both these limitations, if ejection takes place at an airspeed above that which is survivable, a means must be provided for delaying the deployment of the main recovery parachute, and for retarding the ejected mass's flight speeds during that delay period.

We cannot forget, however, the importance of the <u>time</u> commodity as previously reviewed herein. Because the function, T_R (required system total time to reach suitable terminal descent rates), is composed of a series of time-increments demarcated by onset and completion of essential events along the trajectory, the only effective way of minimizing total T_R is to minimize each T_{R_N} increment. Thus, the ejected package must be slowed down to parachute deployable airspeeds in as short a time period as we can without violating physiological or structural limits. Man's greatest tolerance to acceleration (positive and negative) is to G's applied orthogonally to his spine (while in a seated position) in what has been termed an "eyeballs-in" or "eyeballs-out" direction. The minimum allowable deceleration period, then, is computed by inducing an aerodynamic drag on the man/seat combination in an eyeballs-out direction at a magnitude of G_{X_L} under 600 knot airspeeds at sea-level ambient conditions.

The drag can be effectively applied by augmenting normally induced man/seat drag with that induced by a flexible, deployable, aerodynamic decelerator. To date, a "drogue" parachute has best met this need--but the problem remains of getting that drogue out of its container and into its fully-effective shape early enough to prevent aerodynamic moments on the man/seat to rotate the package aftward into a less-favorable orientation for drag-induction and G-onset.

It is readily shown that the time delay needed for protection at high-speeds, is consistently in conflict with the time available (T_A) under extreme low-speed or adverse attitude and sink-rate emergencies. Because of this conflict, quite often (but, here we must emphasize--not always), it is necessary to resort to automatic induction of a time-sequencing change as determined through sensation of airspeed and altitude prevailing conditions. Multimode time-delay magnitudes are determined by evaluating the extreme emergency conditions. Hence, the lowest-mode time is based on the zero-altitude/zero-airspeed ejection case, while the highest-mode timing is based on the sea-level 600 knot ejection.

It is of interest, of course, to note that application of G_{max} to the ejected mass not only enables one to achieve T_{Rmin}, but also aids somewhat in combating the flailing of the ejectee's unrestrained limbs because the eyeballs-out deceleration tends to permit the limbs to "lead" rather than "trail" the man/seat mass.

State-of-the-art stabilization devices such as DART are incapable of adequately controlling 600 knot pitching moments, and the retardation drogue becomes a helpful aid in augmenting such devices in high-speed stabilization and trajectory control. The man in his ejection seat is clothed for flight in the environs of his crewstation, and he is equipped with a minimum of oxygen in his survival provisions. Thus, if it is necessary that he eject at high-altitudes where it's plenty cold, and little breathable air is available, it becomes necessary to get him down to a minimally suitable environment (about 15,000 MSL) as rapidly as we can. USAF requirements demand that a stable descent from high-altitude be made in a spinal direction. This is, of course, the minimum effective drag

profile of the system and so it does meet the rapid descent need. Of course, once main parachute opening altitude is reached, the opening shocks (if in excess of a DRI of 17) cannot be dumped into the man in a spinalward direction. For the high-altitude descent case the problem becomes one of orienting the parachute load vectors relative to the man such that he sees no more than a 17G DRI spinal-compression component, remembering that all other vectorial components must be governed such that

$$\sqrt{\left(\frac{DRI_z^2}{289}\right) + \left(\frac{Gx}{35}\right)^2 + \left(\frac{Gy}{15}\right)^2} \leq 1.0, \qquad (103)$$

(assuming rise times $\geq$ 30 MSEC, and durations of 0-30 MSEC). With a shortening of rise time, or lengthening of duration of force application, of course, the limit values in the x and y terms of this expression will change--but the radical expression must be maintained in order to protect the ejectee from serious injury.

The flying trim-angle of the ejected seat during launch will ideally be at 90° to the airstream because at that angle the forward thrust of the rocket sustainer and the drag of the drogue are virtually cancelling, leaving the DRI loading picture much less complex, with resultant loads directed spinalward. Should the drogue not activate rapidly enough, however, and the seat be allowed to rotate to a 180° trim, then the deceleration due to drag, and the force of the rocket are additive in the spinal direction--which can be dangerous, as discussed before. Also, with the seat trimmed at a pitch angle less than or equal to 90°, the flow-field forms a pressure distribution over the upstream-facing area of the ejected mass which inhibits lift on the occupant's legs, and aids in keeping them "pinned" to the seat in a pseudo-restrained fashion. Aft-rotation, at high-speeds, beyond the 90° trim orientation to the flow field augments leg-lift rather than inhibiting it, and incites flailing of the limbs to a dangerous degree.

Because one can take no chances of post-ejection interference between the ejectee, his seat and parachute, and his aircraft from which he's ejected, a positive means was provided to propel him from that aircraft. Similarly, once the seat has succeeded in carrying the man from his crewstation, and has helped him withstand the loads to which he is exposed during deceleration and parachute opening, then the seat can be considered only as

"excess baggage" which adds mass to the descent package, thereby increasing its terminal velocity. It is desirable to get rid of the seat and all ancillary equipment in preparation for landing on the earth's surface. But one cannot permit any contact, collision, or interference between the seat and the man/parachute combination once they've separated. Hence, the separation must be positively induced, and the trajectories of the separated elements of the system must be divergent. Thus, it becomes necessary to release the seat from the man subsequent to onset of parachute opening shock, and depend on either the resultant mass-to-drag ratio differential to induce separation, or to rely on some augmentive devices to do the job. The C-9 canopy has repeatedly proven its value; the descent rates it produces are well within tolerable limits. Oscillatory characteristics are not severe--so the C-9 is satisfactory. At terrain contact, a natural roll of the man to distribute the impact over a large, continuous and progressive portion of his legs, torso, and shoulders should not be inhibited. Thus, any hard structures should be removed from his person, or be designed to complement his landing. This pertains to parachute pack liners, modular seat backs, backboards, rigid survival equipment containers and any other structure of similar application. Of course, as previously mentioned, once in the water or on land, the man no longer needs his parachute, and retention thereof can create problems for the crewman which he just doesn't need at that time. So it should be easy for him to free himself of his 'chute, but still be able to use the device as a survival aid if the situation warrants it.

Back in an earlier discussion of human tolerance problem areas we saw the importance of maintaining absolute control over both MAGNITUDE and DIRECTION of the forces felt by the crewmember. Also described were the constraints in accelerative and decelerative loading with which one must live in developing AERCAB. Catapult forces are limited by DRI constraints. Similarly, coupled rocket-booster/deceleration-drogue forces are DRI constrained. MIL-S-9479A requires that the parachute be deployed off the seat, and the man in his harness is subjected to opening shock loads transmitted in quite different fashion to those loads he felt during propulsive and retardation events. He is no longer rigidly restrained, so DRI

constraints no longer apply. However, the loading imposition on AERCAB's occupant in his parachute is no different from that in presently in-service systems, so no problems are anticipated.

As shown herein, the AERCAB includes a torso-restraint harness conforming to Dwg. 63J4296 modified to accommodate powered upper (and optionally lower) haulback and restraint as a pre-ejection function. The release of the man in his hybrid restraint/ parachute harness is achieved automatically at onset of parachute inflation; or, in an "over-the-side" ditching situation, an emergency release handle is located on the left lower lap-strap which, if manually pulled, releases the man in his harness, instantaneously. "Normal" egress requires manual disconnect of the shoulder-releases, and the pelvic-release on each leg-strap.

With regard to powered haulback and restraint, the "conventional" inertia-lock reels used in USAF in-service systems are designed to lock during an acceleration period (be it acceleration of the aircraft, or acceleration of the straps from the reel, or both). With such units, short-duration, high-peak accelerations that would not cause excessive velocity of the torso approaching contact with aircraft structure (or interfering with flight duties) may in fact lock the reel; while long-duration, low-level accelerations which have a potential for generating deleterious velocities, would not lock the reel to protect the crewman. In a search for a solution to this problem, SAEC found that Space Ordnance Systems, Inc., has devised a powered Restraint Actuator worthy of serious consideration for AERCAB adaption by USAF. The unit locks with aircraft deceleration in any direction, with acceleration of the restraint straps, and also when strap payout velocity approaches a dangerous magnitude. The SOS restraint actuator gives full protection in the 0-3G realm of accelerations encountered during normal aircraft operation; full protection during the "classical" 40G crash; full protection against excessive onsets of acceleration; and full protection during ejection to the point of man/seat separation. In addition to this improved performance, SAEC thinks it valuable for consideration because it is quite simple; does not require manual inputs for lock or unlock, and is lightweight and compact...and cannot fail to lock (as may occur with mechanical locking inertia reels). The

ballistic haulback feature incorporates hydraulic buffering which permits haulback forces of sufficient magnitude to retract the crewman under high G's, and low upper-torso weight (mass) conditions. For the safety-conscious, it is pointed out that the 4000 psi maximum gas pressure used for power retraction is confined to a chamber which is easily located in a "buried" locale on the AERCAB seat structure, away from proximity with any portion of the crewman's head, body, or limbs. The unit's one apparent deficiency is that the existing device on loan to SAEC for consideration, does not have a provision for unlocking (override of the auto-lock) at the crewman's discretion. USAF pilots have expressed a need for such a provision in evasionary combat maneuvering flight, in order to be able to look back over their tail to observe an adversary's "tracking" maneuvers. These airmen are willing to suffer some in-the-cockpit buffeting around, in payment for this additional freedom of movement.

b. Environmental Protection

To determine design criteria for protecting the AERCAB pilot against potentially severe self-rescue flight environments, limited consideration was given to the flight regime bounded by a maximum pressure altitude of 10,000 ft., a maximum relative airspeed of 100 knots, and prevailing conditions of icing, rain, snow, clouds, turbulence, hail, thunderstorm activity in the vicinity, night-flight, and cold and hot weather effects.

Self-rescue flight in AERCAB at night, in clouds, fog, or heavy rain will be difficult due to the attendant reduction (or elimination) of visibility. If minimal instrumentation were not available, loss of ground-reference could result in spacial disorientation which could lead to the occupant's maneuvering too low toward the terrain, or into irreversible spins, stalls or spiral-descents which would (at best) merely terminate rescue flight, but could induce unfavorable conditions (attitudes and rates of motion) for onset of the terminal descent mode which is dependent only on sensation of absolute altitude. Any flight instruments and navigational aids, then, require lighting for low-visibility conditions, and the type of instrumentation provided the occupant depended on the requirement for IFR capability. System weight and complexity was not seriously effected. High relative humidity will

likely result in fogging of the occupant's visor, and the importance of that visor's being in proper position on his face is emphasized below. Hence, such fogging could hinder or destroy essential visibility.

Perhaps the worst potential physiological hazard encountered in this search was that which relates to "cold-soaking" the seat occupant under flight conditions prescribed as target performance goals under the contract. Two primary effects are worthy of serious concern:

(1) The seated, relatively immobile man is subject to loss of use of his fingers, hands, arms, legs and eyes due to severe exposure to cold; with attendant potential loss of capability to manually input control, establish or maintain headings, correct for inflight anomalies in performance, or induce voluntary emergency measures such as induction of terminal descent, or correction for control subsystem malfunction.

(2) Cold exposure can do permanent harm or even be fatal if carried to the extreme, and it appears that the extreme is achievable in prescribed self-rescue flight in AERCAB, and is just cause for precaution.

During this brief study, extensive reference was made to the following publications:

...AFSCM 80-3; Handbook of Instructions for AEROSPACE PERSONNEL SUBSYSTEMS DESIGN (HIAPSD); First Edition; reprinted 15 Oct. 1966, revised 15 April 1967; Headquarters, Air Force Systems Command; Andrews AFB, Washington, D. C.[3]

...NASA SP-3006; BIOASTRONAUTICS DATA BOOK: August 1964; Webb Associates, Yellow Springs, Ohio.[27]

...NASA CR-878; A DESCRIPTIVE MODEL FOR DETERMINING OPTIMAL HUMAN PERFORMANCE IN SYSTEMS; Volume III; "An Approach for Determining the Optimal Role of Man and Allocation of Functions in an Aerospace System; March 1968; Serendipity Associates, Chatsworth, Calif.[28]

Normally, crewstations are designed thermally to provide an environment which will permit the crew to

function comfortably and efficiently. Since AERCAB is an emergency system, it was assumed that the occupant's environment need be controlled only to the extent that he be capable of finding and maintaining a "homing" flight-path, and perform any emergency tasks required for self-preservation. Hence, he must be capable (even though he may be quite uncomfortable while doing so) of manipulating his flight and engine controls, monitoring his spacial position, and terminating his flight at his discretion. It would be unacceptable to permit him to be exposed to any environment which will cause potentially permanent injury, and certainly not death. Hence, when "tolerances" or "limits" are mentioned below, we are speaking not of "comfort" but of the threshold or onset of physiologic/psychic damage (if only to the loss of use of an extremity, for example--or the loss of decision-making capacity).

The above-listed references explicitly define human tolerance to cold stress in terms of exposure time at various temperatures, the type and amount of clothing (insulation) and the prevailing metabolism or activity-level. AFSCM 80-3 states that..."Prolonged exposure at extremely low ambient temperatures (4°C or 40°F, or below) requires use of electrically heated clothing assemblies, including heated gloves, shoe inserts, and in some cases a face mask..."and also, "...when clothing becomes wet or wind velocity is high, the effective insulation may be significantly reduced." Figures C.4-13 and C.4-14 of AFSCM 80-3 are reproduced in part herewith, as Figure 96, for your convenience of reference, in noting man's tolerance time of exposure to cold. (By definition, one "CLO" is a unit of insulation required to maintain in comfort a sitting-resting subject in a room ventilated at 200 fpm at 70°F with less than 50% humidity. The unit is merely a convenient reference in common use by USAF and NASA.)

Of far more significance to the case at hand is the influence of wind chill on the occupant's tolerance to cold stress. The limits spoken of above were for ambient temperatures under windless conditions. Figure 97 herein is taken from AFSCM 80-3, Figure C.4-15 and NASA SP-3006, Sheet 7-18, and NASA CR-878, Item No. 138; and represents the prescribed flight regime of AERCAB (assuming the temperature vs pressure altitude distributions shown in Figure 98 herewith). Using the NACA standard, it is seen for example that

FIGURE 96

MAN'S TOLERANCE TO COLD WHILE DOING LIGHT WORK

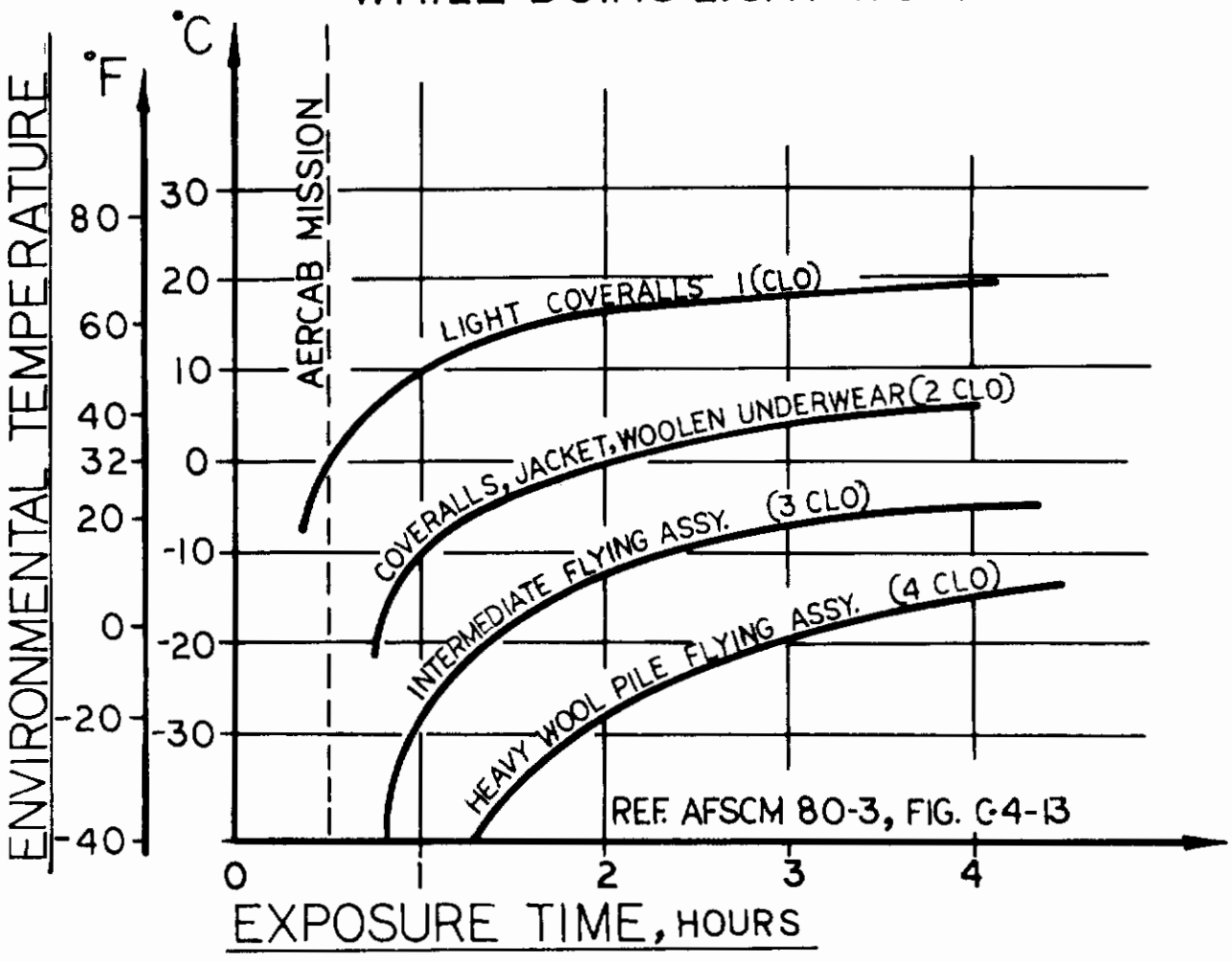

FIGURE 97
WINDCHILL INDEX

REF: AFSCM 80-3, FIG. C.4-15
NOT FOR RIGOROUS USE

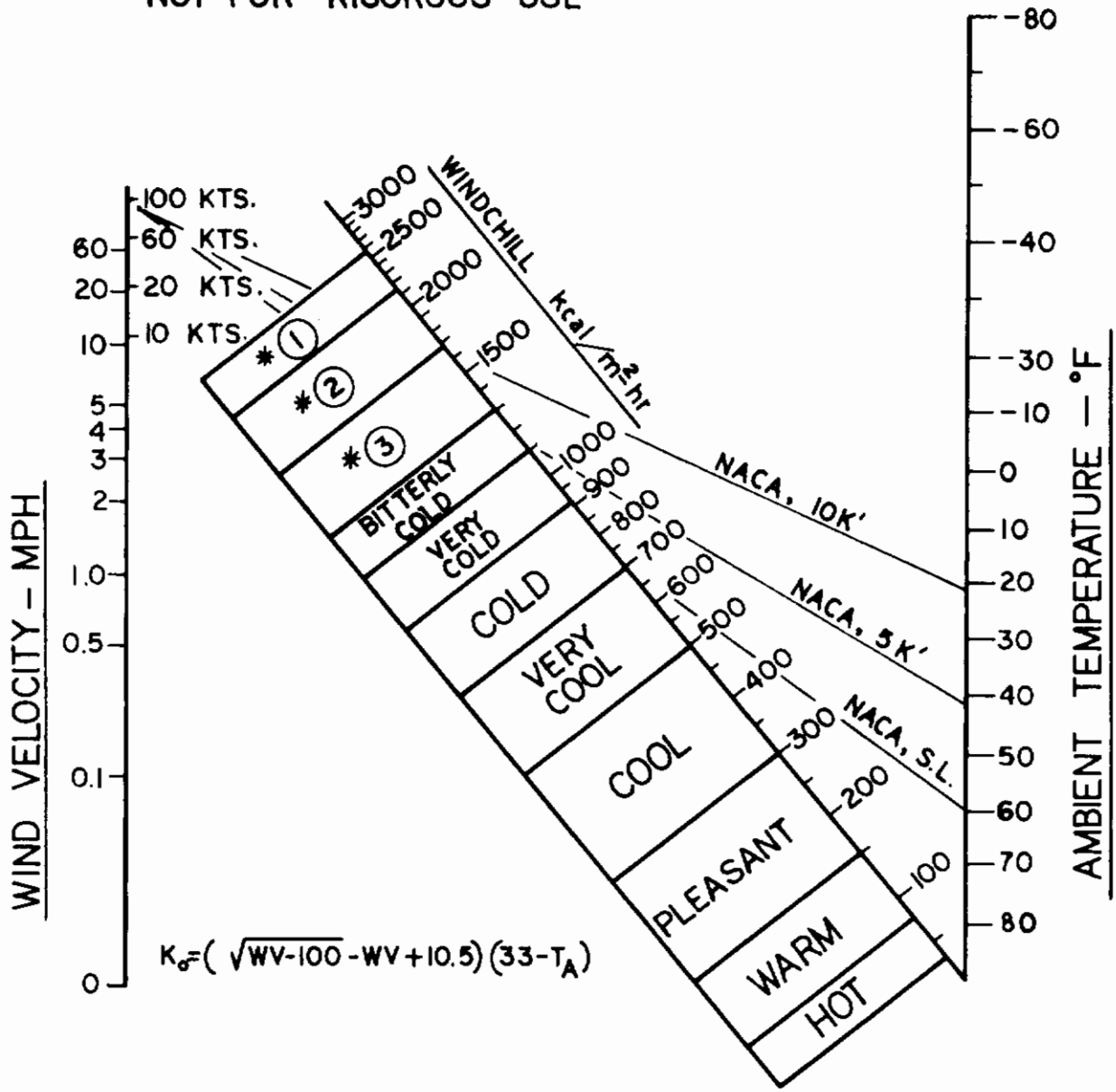

* ① EXPOSED FLESH FREEZES IN 30 SEC.

* ② EXPOSED FLESH FREEZES IN 1 MIN. — TRAVEL DANGEROUS

* ③ EXPOSED FLESH FREEZES — TRAVEL DISAGREEABLE

FIGURE 98

TEMPERATURE VARIATION WITH ALTITUDE IN SELECT REGIONS

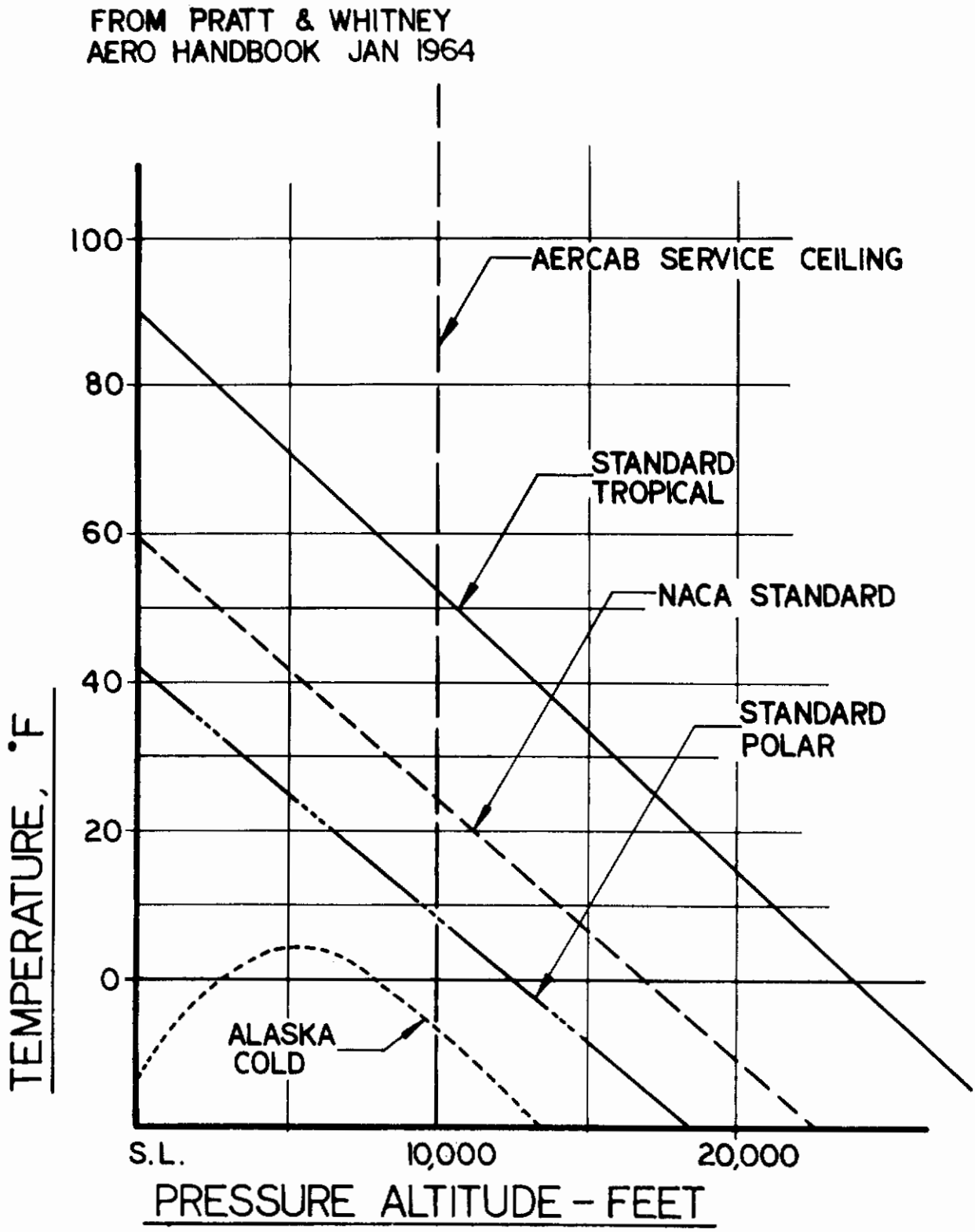

at sea level, $T_A = 60^oF$; at 5000 ft., $T_A = 42^oF$; and at 10,000 ft., $T_A = 24^oF$. With these three points on the temperature scale of Figure 97, a line was drawn from each temperature to the estimated 100 knot wind velocity scale point. It is observed then, that at the prescribed cruise speed of 100 knots with AERCAB, that flight at 10,000 ft. is dangerous (exposed flesh freezes in 1 minute), flight at 5,000 ft. will be bitterly cold (and will be painful at best), and even flight at sea level may be qualitatively described as ranging from "very cool" to "cold". Of course, that pertains to flight in relatively temperate zones. Polar emergencies appear to virtually eliminate self-rescue flight at speeds above 4 or 5 knots, while tropical emergencies appear to proffer no ban to 100 knot self-rescue flight at even 10,000 feet. It must be emphasized that the danger prevails, however, only if suitable precautions are not taken in design of AERCAB.

Protective insulation requirements for the AERCAB occupant can be non-rigorously estimated by assuming a flight speed and an altitude, take the temperature at that altitude and draw a line from that temperature on the nomogram of Figure 97 to the proper point on the velocity scale. Note the intersect on the wind-chill index scale, and draw a second line from the zero velocity point through the intersect to a point on the temperature scale which will, for purposes herein, be called the "equivalency" temperature. Then by referring back to Figure 99 one can use that "equivalency" temperature to estimate clothing requirements.

Example: Assume one provides the AERCAB occupant with only an Intermediate Flying Assembly (3 CLO) which should enable him to withstand -40^oF for 1/2 to 3/4 hours in still air. A line drawn between the 0 mph origin and the -40^oF temperature point gives a windchill index intersect point at about 740 $kcal/M^2$-hr. At that tolerance level, then, one can draw lines from a reference altitude (temperature) point and see what velocities the so-protected man can fly at. It is seen that he is limited to 2 mph at 10,000 ft.; 8 mph at 5,000 ft.; and nearly 100 mph at sea level. (Obviously the system capable of 100 mph flight at sea level, couldn't even sustain flight at altitude at the limiting airspeeds.)

FIGURE 99

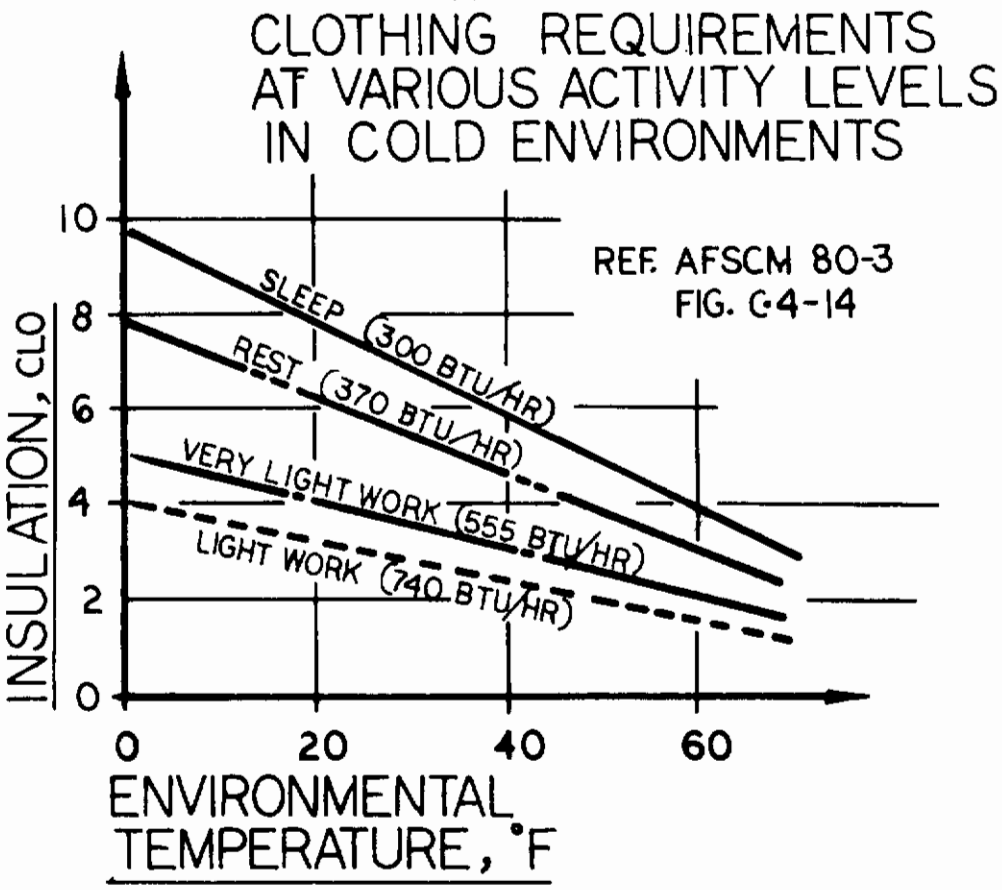

Obviously, then, a set of prescribed flight conditions exists which may demand that additional or improved insulative protection be given the crewman to wear on all his normal flight duties in order to be prepared for the eventuality that he may enter an emergency situation which will ultimately result in his using his AERCAB self-rescue provisions. The problem merits further USAF aeromedical study.

Up until now the "dry-but-cold" man has been considered. Since it is a prerequisite that the self-rescue system fly in "adverse weather", consider the case wherein it is raining or the relative humidity is such that in addition to ambient temperatures being low, a moisture problem exists as well. Figure 100 herewith is taken from AFSCM 80-3, Figure C.4-16, and gives some tolerance limits on cold water immersion based on empirical evidence. The graph in Figure 101 is from NASA CR-878, Item No. 121, and describes quite well man's demonstrated tolerance to cold water exposure. Note that in this later graph, in the MARGINAL category there is a 50% expectancy of loss of consciousness, which could prove catastrophic if it were to occur in fully-powered AERCAB flight. State-of-the-art means for affording some protection in cold water (or rain and wind) seem to be limited to the dry, compression-resistant insulation ("dry suit") and the nonwettable (closed cell) protective anti-exposure clothing which retains effectively its insulative properties while allowing some water to contact the skin (wet suit). Neither typically provides adequate protection to hands, feet and head. Obviously, at the extremes in temperature, protection from frostbite must be provided. It is a matter of observation that conventional clothing will be inadequate for AERCAB self-rescue flight. During high-speed ejections, helmets are sometimes lost, clothing is sometimes shredded or torn and gloves and even boots are often lost. Also, all pilots cannot fly to their own satisfaction with gloves--so they might be expected to discreetly leave them off in the adequately tempered environs of the cockpit. Furthermore, even if the helmet is retained in ejecting, and self-rescue is begun, if visibility is limited, chances are the crewman will have to raise his tinted visor to see his instruments. If his clear, secondary visor is not then in position, he's exposing flesh to airstream--so the windchill index must certainly be kept well below the 1300 kcal/m^2-hr. level. Without auxiliary heating, stored body heat will be discharged

FIGURE 100
MAN'S TOLERANCE LIMITS
TO COLD WATER IMMERSION

REF: AFSCM 80-3, FIG. C.4-16

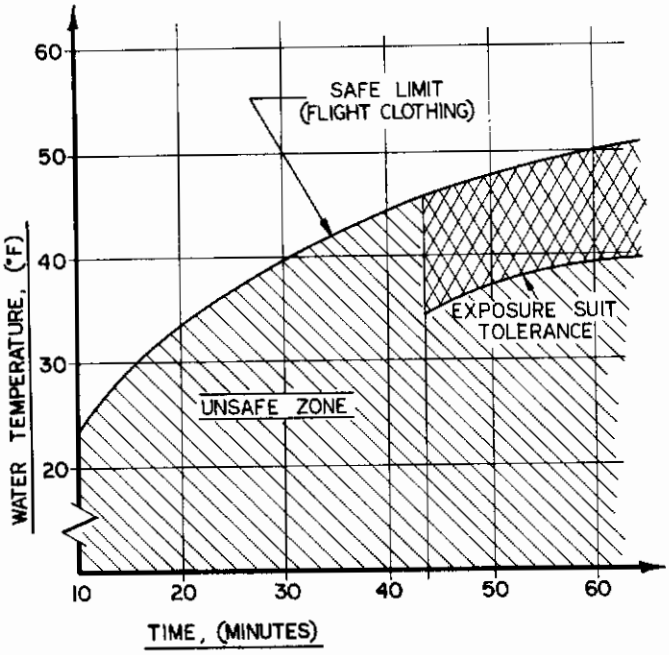

FIGURE 101
MAN'S TOLERANCE TO
COLD WATER EXPOSURE
(WITHOUT EXPOSURE SUIT)

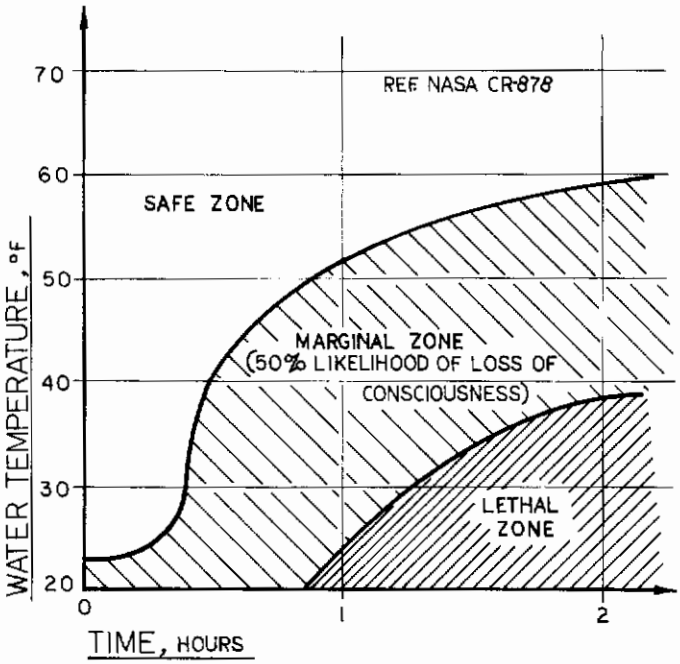

through conduction, convection, evaporation, radiation, and respiration. As the body temperature lowers, NASA SP-3006 points out that:

When the hands reach:	When the feet reach:	They feel:
68°F	73.5°F	Uncomfortably cold
59°F	64.5°F	Extremely cold
50°F	55.5°F	Painful and numb

Another potential problem is that as airspeed is reduced at a given altitude to accommodate the wind-chill index demands, the time of exposure is extended to achieve a given range. Aside from the parasitic effects an extension of time in the air has on system weight and performance, one must realize that prolonged exposure at reduced index levels can be as harmful as brief exposure at extreme levels.

In summary then, achieving prescribed performance levels with the AERCAB self-rescue mode may require that corresponding physiological protection against exposure be given the occupant; or one must alternatively determine rigorously the practical limits of man in flight clothing which won't inhibit his accomplishing his fundamental mission, and reduce the self-rescue flight performance requirements correspondingly. The former solution, in the opinion of the contractor, is the better of the two. Accordingly, it is concluded that more intensive studies by USAF aeromedical specialists are required to quantitatively define practical environmental protective means for AERCAB crewmen.

SECTION VI - DESIGN SPECIFICATIONS

One of the objectives of the reported investigation was to establish design criteria for the integrated aircrew escape/rescue system. Throughout this report the fundamental criteria have been discussed along with offered methods of meeting those criteria. While the AERCAB design generated under the program is certainly to be considered to be of a preliminary nature, certain components therein were categorized as sufficiently well thought out that at least cursory detail design specifications could be written therefor. These specifications are included below, fully recognizing that they are not final or complete in any stretch of the imagination; nor is the list complete, since so very many components and subsystems in AERCAB are subject to continuing future inputs from a wide variety of specialists in the Government and the Aerospace Industry. The specifications are included herein, then, simply to act as a foundation for future work on the system.

1. SEAT BUCKET

The basic structure of the seat bucket shall be panels composed of an aluminum honeycomb core with sheet aluminum facings. The panels shall be reinforced locally with solid aluminum framework of the same thickness as the honeycomb core wherever loads and/or sub-assembly mountings dictate. Upper torso restraint loads shall be distributed to the seat side panels by means of an aluminum extrusion of sufficient section modulus and material properties. The seat bucket shall be structurally capable of withstanding the loads stipulated in paragraph 3.6.2 of MIL-S-9479A with the specified margins of safety.

The seat bucket design shall incorporate the physical features described in paragraph 3.4.2.2 of MIL-S-9479A with the following exceptions:

(a) The headrest is not fixed relative to the seat bucket.
(b) For system installation in the A-7 aircraft, the minimum interior bucket width will be less than 18 inches (16.625 inches maximum).

(c) The entire ejectable portion of the system does not adjust with the seat bucket.

(d) Seat adjustment is not accomplished by means of an electric screwjack.

A more detailed explanation of the deviations and the justifications for them are given in Section V of this report. The assembled weight shall be approximately 31.0 lbs.

2. MAIN RECOVERY PARACHUTE

The main recovery parachute shall meet the requirements given in paragraphs 3.4.1.3 and 3.4.2.6 of MIL-S-9479A. The assembly shall consist of the following subassemblies:

(a) PARACHUTE

The parachute shall be per Air Force Drawing 50E6877-3 modified to SAEC Drawing No. 422S830D001. The basic parachute is a 28 foot diameter flat circular canopy with 28 suspension lines. The modification to the canopy consists of adding loops of nylon line at each suspension line/skirt junction for purpose of attaching the spreader gun slugs.

(b) SPREADER GUN

The spreader gun shall be per SAEC Drawing SK86-0051 which is qualified by the U.S. Navy and is currently being qualified by the U.S. Air Force. This spreader gun is "fail-safe" in that the parachute will inflate normally by means of aerodynamics in the event of a gun-cartridge malfunction.

(c) RISERS

There shall be four risers each of which will connect one of four suspension line links to one of two personnel connectors. Breaking strength of each individual riser shall be 5500 lbs. minimum. The

length of risers shall be sufficient to allow upper torso movement of 18 inches forward minimum. Slack shall be prevented by means of spring retracting reels.

(d) CONTAINER

The container shall be essentially a three-sided fiberglass box with the top closure made of nylon pack cloth. Closure shall be accomplished by normal locking cone/ripcord pin arrangement. The forward side of the container shall be contoured per Figures 2 and 4 of MIL-S-9479A in order to serve as a headrest. Two aluminum cylinders shall be integrated within the fiberglass structure to serve as mounting provisions for the parachute assembly over the upper portion of the catapult tubes, and as the deployment mortars in the descent from self-rescue mode.

The parachute system shall be operable and structurally adequate in the speed range from 30 to 300 keas without producing deceleration histories beyond human tolerances. The parachute system weight shall be approximately 30 lbs.

3. TURBO-FAN ENGINE

The turbofan engine is based on a preliminary design by Continental Aviation and Engineering Corporation, Detroit, Michigan. The engine size shall not exceed that shown in Continental Drawing L8789. The following criteria should be closely approximated:

Thrust at 10,000 ft. at 100 KTAS $\geq$ 250 lbs.
S.F.C. = 0.65 lb/lb of thrust/hr.
By pass ratio = 6.0.
Weight (including accessories) = 54.0 lbs.
Envelope 8 x 16 x 35 inches.

Accessories shall include fuel pump, a 1.0 KVA D.C. generator and a pyrotechnic starter.

4. INERTIA REEL, POWERED, DUAL STRAP

The inertia reel shall meet the requirements of

MIL-R-8236. The reel shall be Pacific Scientific Company, Anaheim, California, P/N 0103182-1, or equivalent. Weight (including gas generator) shall be approximately 3.6 lbs. Envelope (not including gas generator) shall be approximately 3.12 x 5.34 x 5.1 inches. The gas generator shall be gas pressure initiated, 350 psi no fire, 500 psi all fire. All ballistic components shall meet MIL-D-23615 and MIL-C-25918. The inertia reel control shall be manual and shall conform to MIL-R-8236. The control shall be mounted to the forward outboard side of the left-hand side panel.

5. SEAT BACK ROCKETS

The seat back rockets shall be similar in design to Space Ordnance Systems, Inc., El Segundo, California, P/N S04-110961-11 and -12. There shall be two rockets per seat, each having an impulse of approximately 840 lb-sec. Peak thrust shall be approximately 4000 lbs. The rocket nozzles shall direct the thrust through the nominal center of gravity of the ejected mass. The rockets shall be gas pressure initiated and shall conform to MIL-C-25918. Approximate envelope shall be 2.25 dia. x 31 inches long each. The "live" weight shall be approximately 9.5 lbs. each and the inert weight shall be 5.5 lbs. each. A progressive-burning grain shall be used, but the net thrust-time characteristic shall be "neutral".

6. CATAPULTS

The catapults shall be of twin-catapult design with a common cartridge as a pressure source. The canopy breaker/drogue slug shall be integrated within the catapults. The catapults shall be essentially aluminum and shall be structurally adequate to react all vertical crash loads as well as the loads during ejection. The catapult inner and outer tubes shall be mechanically locked together in a manner capable of reacting 6.0 g's upward. The catapult outer tube shall incorporate a pressure tap approximately 6.0 inches from end of stroke for ignition pressure to the seat back rockets and other devices. The catapult design shall incorporate a hydraulic cylinder about each outer tube for seat adjustment. The envelope of each catapult shall be 2.75 dia. x 50 inches long. Total weight including manifold, cartridge and

canopy breaker shall be approximately 8,0 lbs. The following performance criteria shall be closely approximated:

Canopy breaker velocity = 100 fps (1 lb. mass)
Pressure to unlock $\leq$ 300 psi
Stroke = 48 inches
Peak force = 4000 lbs.
Imparted velocity of ejected mass = 60 fps
Pressure at pressure tap $\geq$ 1000 psi
Column load capacity $\geq$ 10,000 lb/each
Pressure to fire cartridge: 400 psi no fire,
500 psi all fire

Entire device to meet requirements of MIL-C-25918.

7. HYDRAULIC PUMP AND MOTOR

The hydraulic pump and motor used to adjust the seat position shall be that manufactured by Eastern Industries, Hamden, Connecticut, P/N 310393 or the equivalent. The weight shall be approximately 2.4 lbs. and the envelope shall be approximately 2 x 3 x 7 inches. The unit shall meet or exceed the following specifications.

(a) Rated flow: 0.5 gal/min @ 600 psia

(b) Voltage: 24 volts D.C.

(c) Duty: Intermediate 10 sec. on, 30 sec. off

(d) Radio interference shall not exceed limits in MIL-I-6181

(e) Fluid: Hydraulic oil per MIL-H-5606

(f) Type: gear pump

(g) Life: 5000 cycles at rated conditions, each cycle to consist of 10 seconds on, 5 minutes off

(h) Ports to be per AND 10050-4

(i) Internal relief valve to relieve at 800 psia

8. HYDRAULIC SELECTOR VALVE

The Selector Valve in the seat-adjustment device shall be per Sterer Engineering and Manufacturing Company, Los Angeles, California, (P/N 40440), or equivalent. The valve shall meet the following specifications:

(a) Weight $\leq$ 1.0 lbs.

(b) Type: 3 position 4 way solenoid operated

(c) Operating pressure 600 psia

(d) Burst pressure 12,000 psia

(e) Flow: 0.5 gal/min @ 600 psia

(f) Fluid: Hydraulic oil per MIL-H-5606

(g) Leakage: External - none
Internal - 1.5 cc/min @ 600 psia

(h) Electrical power: 1.5 amps at 24 VDC and 70°F

(i) Ports per AND 10050-4

(j) Envelope: 2 x 2.5 x 4.5 inches

9. SURVIVAL KIT

The survival kit container shall be per MIL-S-38380 in aircraft cockpits of available space. In the A-7 and F-4 aircraft, the container size shall be reduced, but the construction and functions shall be as set forth in MIL-S-38380.

10. DART® STABILIZATION SYSTEM

The DART brake system shall be similar to the system described by SAEC Drawing No. 46-001-001. The brake force setting and line lengths shall be adjusted for the particular installation. The system weight shall be approximately 6 lbs. The system shall reduce pitching moments due to center of gravity to thrust line eccentricities to 10 rpm forward (max.) and 50 rpm AFT (max.).

11. DROGUE PARACHUTE

The drogue parachute shall be of moderately heavy construction. It shall be a ribbed guide surface of approximately 5 foot nominal diameter. The entire assembly shall be structurally capable of withstanding 600 keas windblast under infinite mass conditions for at least 2.0 seconds. The suspension system shall terminate in four bridles which attach the drogue to the seat. The drogue releases shall be gas operated but shall maintain mechanical connection to the seat until the seat has reached the proper angular alignment with the airstream. The release shall conform to the requirements of MIL-C-25918.

The wind-oriented rocket deployment system (WORD) shall be an integral part of the drogue system. The firing mechanism shall be rigged in a manner such that it is fired only when the main recovery parachute is to be deployed rather than the parawing. The impulse shall be sufficient to completely deploy the main recovery parachute under zero wind conditions in no more than 400 milliseconds. The rocket assembly shall weigh approximately 1.5 lbs. and its envelope shall be approximately 2.0 inches dia. x 15 inches long.

The entire drogue assembly (less bridle fittings) shall weigh approximately 10 lbs. and shall be packaged to approximately 8 x 16 x 4 inches in size.

12. PARAWING

The parawing shall be a conical type with rigid leading edges and keel. The parawing shall have the following physical characteristics:

Area = 32.7 $ft.^2$
Keel length = 6.8 ft. = 81.5 inches
Leading edge length = 81.5 inches
Apex angle in flat pattern = 90^o
Apex angle in flying configuration = 70^o
Vertical stabilizer area = 2.96 $ft.^2$
Leading edge and keel diameter = 1.00 inch
Weight $\leq$ 30 lbs.

The leading edges and keel shall telescope to form a stowed length of 48 inches. The leading edges

shall be hinged at the apex to fold in to become parallel to the keel when stowed. The spreader bars will be hinged to the leading edges and to a sliding member which is guided by the keel.

When deployed the telescoping sections of keel and leading edges shall lock in place when fully extended. The spreader bar sliding member shall lock in position on the keel when fully deployed.

The parawing shall be connected to the seat by three rigid tubes and three flexible cables. All rigid members will be steel, the fabric portions will be constructed of a material found suitable in tests to be conducted in future programs.

13. WING BANK CONTROL MECHANISM

Wing bank will be implemented by a cable drum driven by an electric motor. The motor shall run on 24 volts D.C. with a duty cycle of 10 seconds "on", 20 seconds "off". The assembly shall weigh no more than 3 lbs. and have a maximum envelope of 2.0 dia. x 6 inches long.

14. INITIATORS

All gas initiators shall conform to MIL-C-25918 and be of minimum weight and envelope.

SECTION VII - CONCLUSIONS

As a result of the reported investigation, the following conclusions are drawn:

1. The concept of providing aircrewmen with an Integrated Aircrew Escape/Rescue System Capability (AERCAB), with a high bypass ratio twin turbofan engine for locomotion, and a conical parawing for lift-generation and maneuvering control, is analytically feasible from an operational, design and performance-achievement viewpoint.

2. AERCAB can be integrated into the A-7 aircraft with modifications to the instrument panel and aircraft canopy. The repositioning of the NSRP 2.23 inches forward in the cockpit limits the space available for larger pilots, and must be further evaluated by a representative cockpit/seat mockup.

3. The AERCAB seat would have to be modified fore and aft (as well as widened) to properly fit in the F-4 cockpit; otherwise modifications to the aircraft's canopy, bulkhead, control stick pedestal, control torque tube and consoles would be required.

4. As a separable modular design, logistically useful as either an independent escape/recovery system, or as an integrated escape/rescue system, AERCAB can be installed to operate out of crewstations meeting AFSCM 80-1 (HIAD) sizing requirements.

5. Operating as a "conventional" escape and recovery system, the AERCAB design evolved under the reported program is expected to perform as well as, or better than, contemporary in-service or advertized developmental escape systems in the open ejection seat category.

6. For powered flight with the parawing, and with the engine affixed to the payload, rigid coupling is mandatory between wing and payload in order to preserve stability during unsteady or perturbed flight.

7. Steady-state flight with parawinged vehicles under high-wingloadings and in high dynamic pressure flow fields has not been demonstrated, and hence, AERCAB's predicted performance is subject to experimental validation.

8. Coupling effects of AERCAB's aerodynamic and inertial characteristics were not considered during the subject stability investigations, and must be defined before the system's stability analysis can be considered complete.

9. System performance studies reported on herein were based on estimated aerodynamic and inertial system characteristics which are subject to redefinition based on later experimentally-measured characteristics.

10. Careful tailoring of the parawing is required to avoid asymmetry about the keel-axis which could result in an out-of-trim flying arrangement.

11. Braking of the wing's apex during deployment will be required to retard deployment thereof, and thus achieve deployment rates below those at which irreversable tumbling is induced.

12. Face-downward restraint of the crewman is concluded to be optimum for AERCAB in the fly-away departure mode to optimize the man/seat combination lift to drag ratio, to improve downward visibility, and to reduce to a minimum the problems and time delays associated with exiting from the seat upon initiation of the final descent phase.

13. Face downward restraint of the crewman will be physiologically acceptable for the fly-away departure mode even neglecting the beneficial contribution of the dynamic airpressure upon the man's body and incorporating the presently used parachute harness without any modification. To improve crewman comfort in the fly-away departure mode the harness should be improved to distribute the supporting forces over wider areas to relieve the pressure points resulting from face downward suspension in the existing Air Force harness.

14. The AERCAB concept studied thus far is useful for recovery of crewmen who become incapacitated subsequent to initiating ejection.

15. As long as the use of AERCAB remains discretionary, an automatic override must be interposed to preclude selection of the self-rescue flight mode outside the envelope of the system's capability in that mode.

16. No existing, "off-the-shelf" powerplant is available which meets all of AERCAB's (and its attendant installation) needs. Hence, a propulsion subsystem development is required which is complementary to the development of the complete system.

17. Protection of the AERCAB pilot against environmental exposure effects (e.g., windchill stress and cold water "immersion") requires further aeromedical evaluation in order to quantify the degree of protection required.

18. Manual homing and flight-control appear feasible with AERCAB. Additional studies are required to verify that automation of these functions is feasible, as presently believed to be.

19. Because of the attendant lack of precise control over descent rates and tumbling upon ground contact, landing while seated in AERCAB is considered prohibitive, even if a flare maneuver were automatically induced to minimize impact energy-available. Correspondingly, regardless of the operational mode prevailing, AERCAB's occupant must ultimately land with his conventional recovery parachute providing suitable descent rate and orientation to the terrain surface.

20. The computer programs developed incident to this investigation will be of further use should the AERCAB concept be explored in further depth in future programs. These computer programs are USAF-owned, and may be requested for use in similar applications.

21. To finalize the homing subsystem design requirements, it will be necessary that the USAF determine the rescue radio network to be established, allocate specific available rescue frequencies, determine the type of broadcasting system to be used (fixed-base, transient, mobile, or any combination), and determine methods of prevention of misuse of the network by hostile forces.

22. Any future increase in L/D of the lifting surface will have no appreciable impact on improving overall system performance. The inherent drag generated by the payload overshadows any potential benefits which might be expected to be gained through wing L/D increase.

23. Cursory studies of drag reduction techniques applied to AERCAB showed that marked improvements may be possible by streamlining. Further, more rigorous analysis of the effects of streamlining on system efficiency may be worthwhile, since gains in performance may be achieved thereby with an attendant reduction in total system weight and propulsive power required.

24. The AERCAB system has an optimum cruise velocity of from 75 to 80 knots, at which the full range of 50 nautical miles may be achieved. The system is capable of a maximum velocity of from 96 to 98 knots (TAS), however, at the expense of range.

25. AERCAB's longitudinal stability is significantly sensitive to eccentricity (linear displacement) of the engine thrustline with the system CG, yet is relatively insensitive to the thrust inclination angle, although the latter markedly influences the system's flight-performance.

26. The instrumentation set shown herein was based entirely on the contractor's judgment, and is subject to change on the ultimately determined needs of USAF using commands.

27. The AERCAB potential is sufficient to warrant continued and expedited effort in testing, design and development in order to arrive at an integrated aircrew escape/rescue capability for the using services at the earliest possible date.

28. Within the limitations of this investigation, due particularly to nonavailability of aerodynamic data which relates specifically to AERCAB as described herein, the following conclusions are drawn related to system longitudinal stability:

    a. AERCAB is statically and dynamically stable for the analyzed flight conditions.

    b. The trim airspeed range is limited, and may not be adequate for the AERCAB mission.

    c. A mild pitch-up tendency occurs at high values of C_L for certain rearward CG positions.

    d. The frequency of the short period mode is

typical of conventional aircraft for the high speed configuration, but is relatively low for the low speed, high C_L conditions that exhibit the mild pitch-up tendency.

e. The flying qualities of the vehicle are marginal but they may be adequate for the AERCAB mission. For low speed flight conditions, the control of pitch attitude becomes critical for high rates of seat adjustment travel.

f. The control scheme for the AERCAB is unconventional which detracts from the pilot's ability to control the vehicle. Control of attitude and velocity requires coordination between the seat positioner and the throttle, with the seat positioner basically commanding pitch attitude and the throttle commanding velocity.

g. Rough control of attitude, altitude, and velocity is not difficult, but precision tracking probably is not possible.

h. Detailed aerodynamic wind tunnel and/or in-flight model test data for the forces and moments acting on the AERCAB and its various components should be obtained to provide for valid calculations of trim airspeeds and trim range.

i. Valid simulation of the dynamic characteristics and piloting tasks of the AERCAB will be needed to evaluate the vehicle's handling qualities, to develop a suitable control scheme, and to train pilots.

29. The following observations are based on limited study of the lateral/directional characteristics of the AERCAB in one flight condition. The supporting aerodynamic data were for a vehicle similar, but not identical, to the AERCAB:

a. The Dutch roll mode is rather moderate in frequency, corresponding to a moderate level of directional stability. The Dutch roll damping ratio is light in the order of $\zeta = .07$.

b. The roll mode time constant is about 1.7 seconds. The rather large value interferes with accurate control of bank angle.

c. Excitation of the Dutch roll mode, in response to lateral control, is excessive. Combined with the low damping, long roll-mode time constant and unfamiliar controller, the overall effect on roll control is unfavorable.

d. The dihedral effect is quite large. It contributes to the excessive excitation of the Dutch roll, and will make the vehicle very responsive to turbulence.

e. The spiral mode is about neutrally stable. For the AERCAB piloting task, positive spiral stability may be required.

f. The large roll-mode time constant degrades the vehicle's handling qualities. Rough control of bank angle and flight direction is possible, but precision tracking, even without disturbances, is not possible.

g. The lateral/directional controller is unconventional and somewhat unfavorable. This requires that the pilot develop an unusual flying technique.

h. Additional studies relating to other flight conditions, particularly at low speed, and relating to the specific AERCAB configuration should be made.

i. Aerodynamic data from wind tunnel or in-flight model tests are required to accurately predict the AERCAB's flying characteristics.

j. Adequate and realistic simulation, including presentation of visual and perhaps motion cues, should be used to evaluate the AERCAB's handling qualities, to develop an easy-to-use control scheme, and to train pilots.

APPENDIX A

DECOUPLED AERCAB (FLEXIBLE SUSPENSION) PITCH-MOTION COMPUTER PROGRAM

"AERCAB 1"

APPENDIX A
DECOUPLED AERCAB COMPUTER PROGRAM

In the flexible coupling (between wing and body) program written for AERCAB, all motions are referred to a ground-fixed cartesian coordinate system.

Figure A-1 schematically identifies the major computer model and the symbols used in the equations below. Conventionally, a "w" subscript denotes wing characteristics, while the subscript, "p" references the suspended payload.

Let θ and θp be the local angles of incidence to the horizontal reference, and γ_w and γ_p be the trajectory angles of the wing and load relative to horizontal.

Then,

$$\gamma_w = \arctan \dot{Y}_w/\dot{X}_w \tag{A.1}$$

$$\gamma_p = \arctan \dot{Y}_p/\dot{X}_p \tag{A.2}$$

and the angles of attack (referenced to the relative wind) are:

$$\alpha_w = \theta_w + \gamma_w \tag{A.3}$$

$$\alpha_p = \theta_p + \gamma_p \tag{A.4}$$

The forces on the parawing are:

$$\sum F_{x_w} = L_w \sin \gamma_w - D_w \cos \gamma_w + \tau_{w_x} \tag{A.5}$$

$$\sum F_{y_w} = L_w \cos \gamma_w + D_w \sin \gamma_w - W_w - \tau_{w_y} \tag{A.6}$$

$$M(z_w) = M_w - K_d(V_w * \sin \alpha_w)\dot{\theta}_w + a_2 \tau_{w_{2m}} - a_1 \tau_{w_{1m}} \tag{A.7}$$

and for the payload:

$$\sum F_{x_p} = L_p \sin \gamma_p - Dp \cos \gamma_p - \tau_{p_x} T * \cos \gamma_p + (\theta_p + \epsilon) \tag{A.8}$$

$$\sum F_{y_p} = L_p \cos \gamma_p + Dp \sin \gamma_p + \tau_{p_y} + -Wp + T * \sin (\theta p + \epsilon) \tag{A.9}$$

$$M(z_p) = Mp + E * T * \cos (\theta + \epsilon) \tag{A.10}$$

where:

$$Lw = \tfrac{1}{2}\rho Vw^2 \, Aw * C_D(\alpha_w) \tag{A.11}$$

FIGURE A-1

COMPUTER MODEL, AERCAB, DECOUPLED CONCEPT

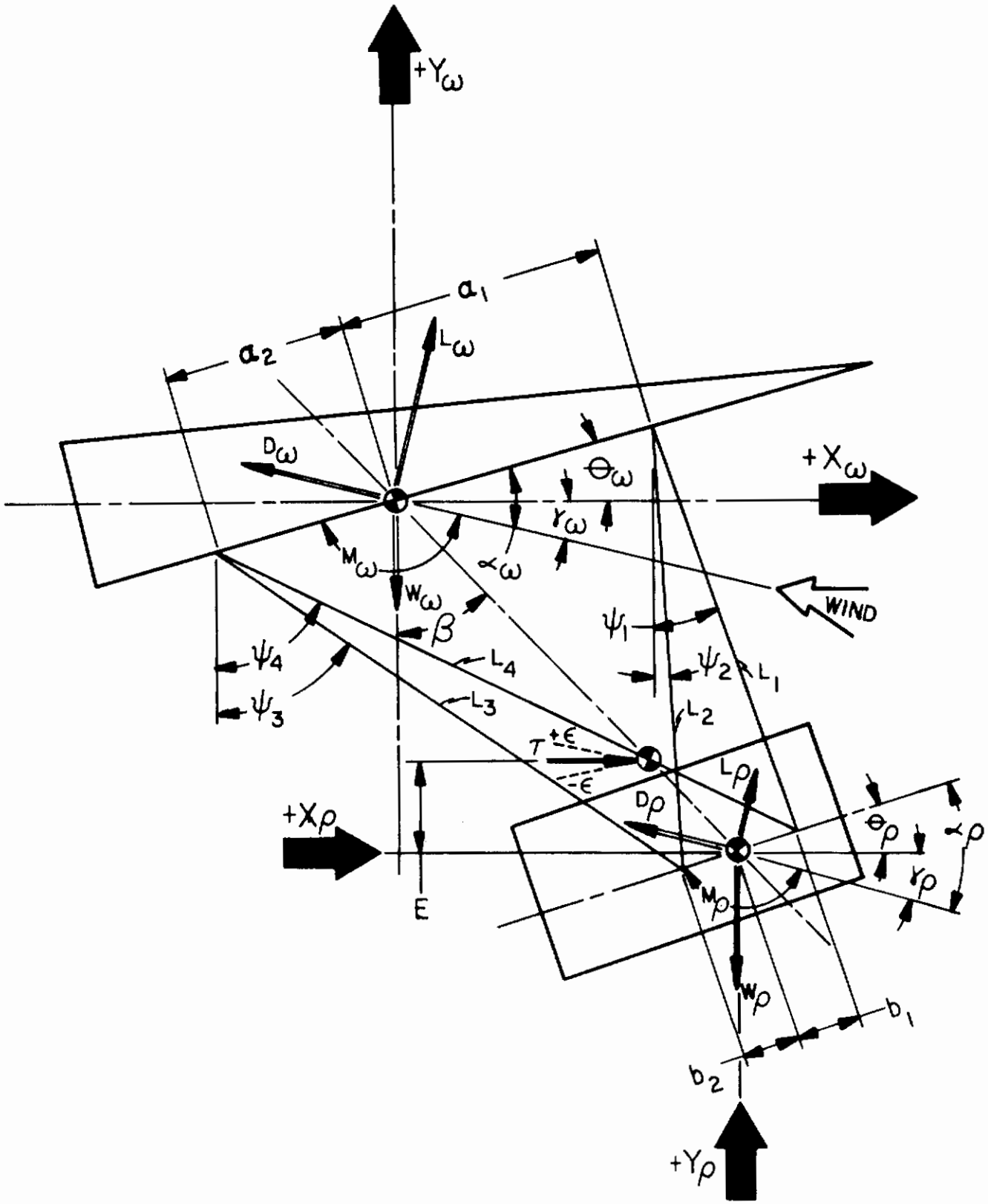

$$Dw = \tfrac{1}{2}\rho\, Vw^2\, Aw * C_D(\alpha_w) \qquad (A.12)$$

$$Mw = \tfrac{1}{2}\rho\, Vw^2\, Aw * Sw * Cm(\alpha_w) \qquad (A.13)$$

$$Lp = \tfrac{1}{2}\rho\, Vp^2\, Ap * C_L(\alpha_p) \qquad (A.14)$$

$$Dp = \tfrac{1}{2}\rho\, Vp^2\, Ap * C_D(\alpha_p) \qquad (A.15)$$

$$Mp = \tfrac{1}{2}\rho\, Vp^2\, Ap * Sp ** Cm(\alpha_p) \qquad (A.16)$$

and, the τ's are the tensile-forces in the suspension lines. They may be computed as follows:

INITIAL (STATIC) LINE LENGTHS & ANGLES

$$L_1 = \left\{ \left[Xp + b_1 \cos\theta p - (Xw + a_1 \cos\theta w) \right]^2 + \ldots \right.$$
$$\left. \ldots + \left[Yw + a_1 \sin\theta w - (Yp + b_1 \sin\theta p) \right]^2 \right\}^{\frac{1}{2}} \qquad (A.17)$$

$$L_2 = \left\{ \left[Xp - b_2 \cos\theta p - (Xw - a_2 \cos\theta w) \right]^2 + \ldots \right.$$
$$\left. \ldots + \left[Yw - a_2 \sin\theta w - (Yp - b_2 \sin\theta p) \right]^2 \right\}^{\frac{1}{2}} \qquad (A.18)$$

$$L_3 = \left\{ \left[Xp - b_2 \cos\theta p - (Xw + a_1 \cos\theta w) \right]^2 + \ldots \right.$$
$$\left. \ldots + \left[Yw + a_2 \sin\theta w - (Yp - b_2 \sin\theta p) \right]^2 \right\}^{\frac{1}{2}} \qquad (A.19)$$

$$L_4 = \left\{ \left[Xp + b_1 \cos\theta p - (Xw - a_2 \sin\theta w) \right]^2 + \ldots \right.$$
$$\left. \ldots + \left[Yw + -a_2 \sin\theta w - (Yp + b_1 \sin\theta p) \right]^2 \right\}^{\frac{1}{2}} \qquad (A.20)$$

$$\psi_1 = \arctan \frac{(Xp \_ b_1 \cos\theta p) - (Xw + a_1 \cos\theta w)}{(Yw + a_1 \sin\theta w) - (Yp + b_1 \sin\theta p)} \qquad (A.21)$$

$$\psi_2 = \arctan \frac{(Xp - b_2 \cos\theta p) - (Xw - a_2 \cos\theta w)}{(Yw - a_2 \sin\theta w) - (Yp - b_2 \sin\theta p)} \qquad (A.22)$$

$$\psi_3 = \arctan \frac{(Xp - b_2 \cos\theta p) - (Xw + a_1 \cos\theta w)}{(Yw - a_1 \sin\theta w) - (Yp - b_2 \sin\theta p)} \qquad (A.23)$$

$$\psi_4 = \arctan \frac{(Xp + b_1 \cos\theta p) - (Xw - a_2 \sin\theta w)}{(Yw - a_2 \sin\theta w) - (Yp + b_1 \sin\theta p)} \qquad (A.24)$$

Now, if δ_i ($i = 1,2,3,4$) is the elongation in the lines due to the applied forces, then the tensile forces may be obtained by Hooke's Law:

$$T_i = M * \delta_i \qquad (A.25)$$

where M is the elastic coefficient.

The accelerations on the parawing and the payload may then be written as:

$$\ddot{X}_w = \sum F_{x_{w/m_w}} \tag{A.26}$$

$$\ddot{Y}_w = \sum F_{y_{w/m_w}} \tag{A.27}$$

$$\ddot{\theta}_w = \sum M(Z_w)/I_{z_w} \tag{A.28}$$

$$\ddot{X}_p = \sum F_{x_{p/m_p}} \tag{A.29}$$

$$\ddot{Y}_p = \sum F_{y_{p/m_p}} \tag{A.30}$$

$$\ddot{\theta}_p = \sum M(Z_p)/I_{z_p} \tag{A.31}$$

and the velocities and displacements are obtained routinely via successive integration.

TABLE A-1

AERCAB 1 COMPUTER PROGRAM

INPUT DEFINITIONS

NOMENCLATURE	DEFINITIONS	UNITS
WGTW	Weight of parawing	lbs.
WGTP	Weight of payload	lbs.
AERAW	Reference area of parawing	sq.ft.
AERAP	Reference area of payload	sq.ft.
KEEL	Length of parawing keel	ft.
LGTH	Characteristics length of payload	ft.
IZW	Mass moment of inertia of parawing	sl.-sq.ft.
IZP	Mass moment of inertia of payload	sl.-sq.ft.
K1	Damping coefficient for tensile forces	
CPD	Payload drag coefficient	---
OTIME	Initial time	sec.
FTIME	Final time	sec.
DELT	Increment of time	sec.
PCOT	Number of integration steps between printouts	---
E	Vertical thrust displacement	ft.
FUEL	Fuel capacity	lbs.
THA	Thrust cant angle (thru P.L. C.G.)	deg.
DTIME	Time required to build up thrust	sec.
ITHR	Idle thrust	lbs.
CTHR	Cruise thrust	lbs.
A1	Distance from wing C.G. to forward lanyard connections	ft.
A2	Distance from wing C.G. to aft lanyard connections	ft.
B1	Distance from payload to forward lanyard connections	ft.
B2	Distance from payload C.G. to aft lanyard connections	ft.
MOD1	Elastic coefficient	lb./ft.
XLK	Ratio (X-system C.G. distance from keel leading edge/keel length)	---
XLKW	Ratio (Distance from leading edge to keel to parawing C.G./keel length)	---
YLK	Ratio (Y-system C.G. distance from keel axis/keel length)	---
YLKW	Ratio (Perpendicular distance from parawing C.G. to keel/keel length)	---
xrwo	Initial range of parawing	ft.

TABLE A-1

NOMENCLATURE	DEFINITIONS	UNITS
YRWO	Initial altitude of parawing	ft.
WTHOD	Angle between wing keel and local horizontal	deg.
XDW	Initial horizontal velocity of parawing	ft./sec.
YDW	Initial vertical velocity of parawing in pitch	ft./sec.
THDW	Initial angular velocity of parawing in pitch	deg./sec.
XRPO	Initial range of payload	ft.
YRPO	Initial altitude of payload	ft.
PTHOD	Angle between P.L. char. length and local horizontal	ft.
XDP	Initial horizontal velocity of payload	ft./sec.
YDP	Initial vertical velocity of payload	ft./sec.
THDP	Initial angular velocity of payload in pitch	deg./sec.

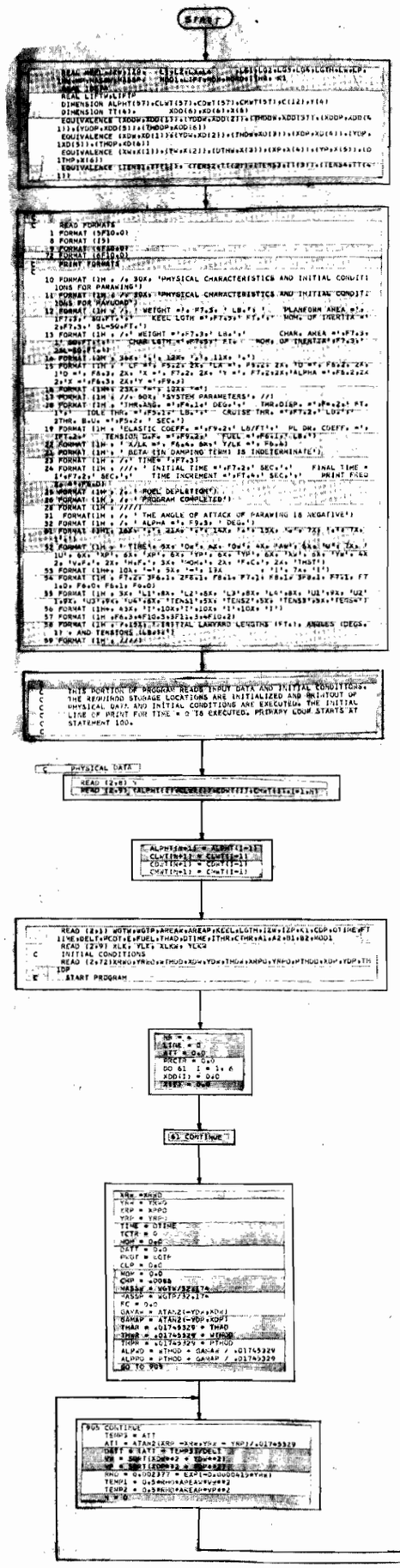

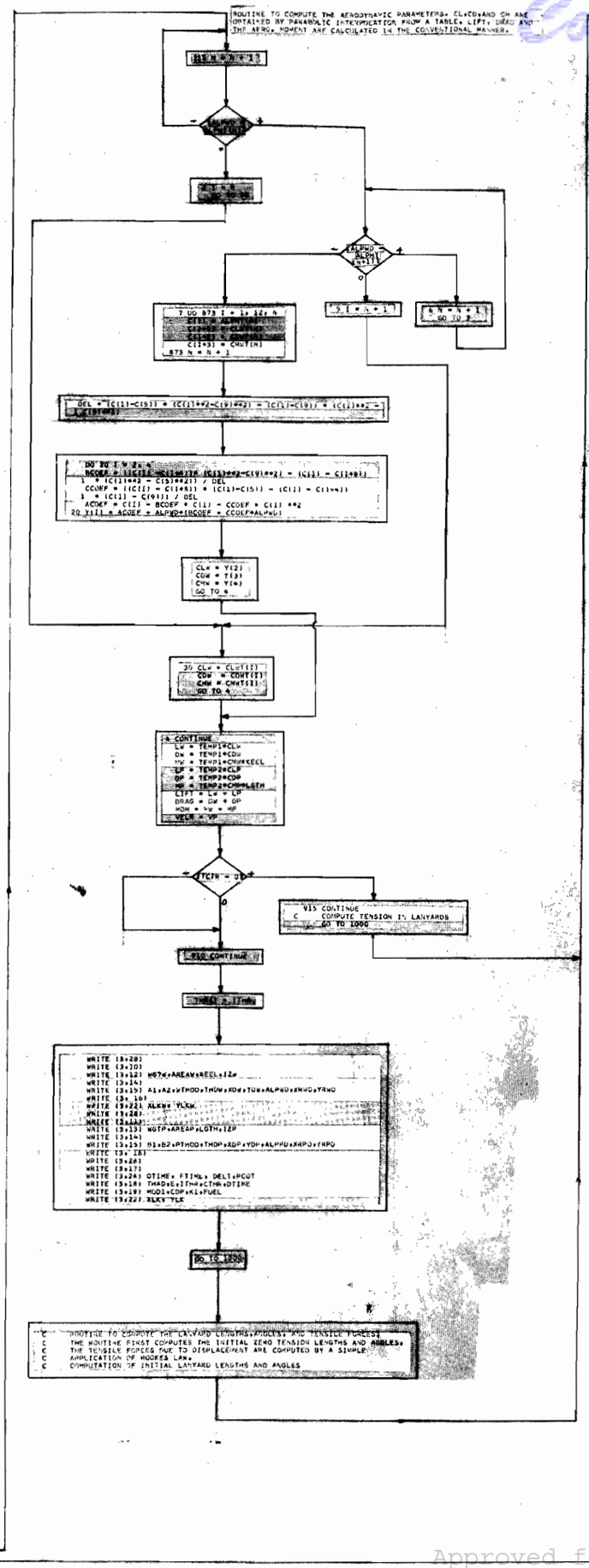

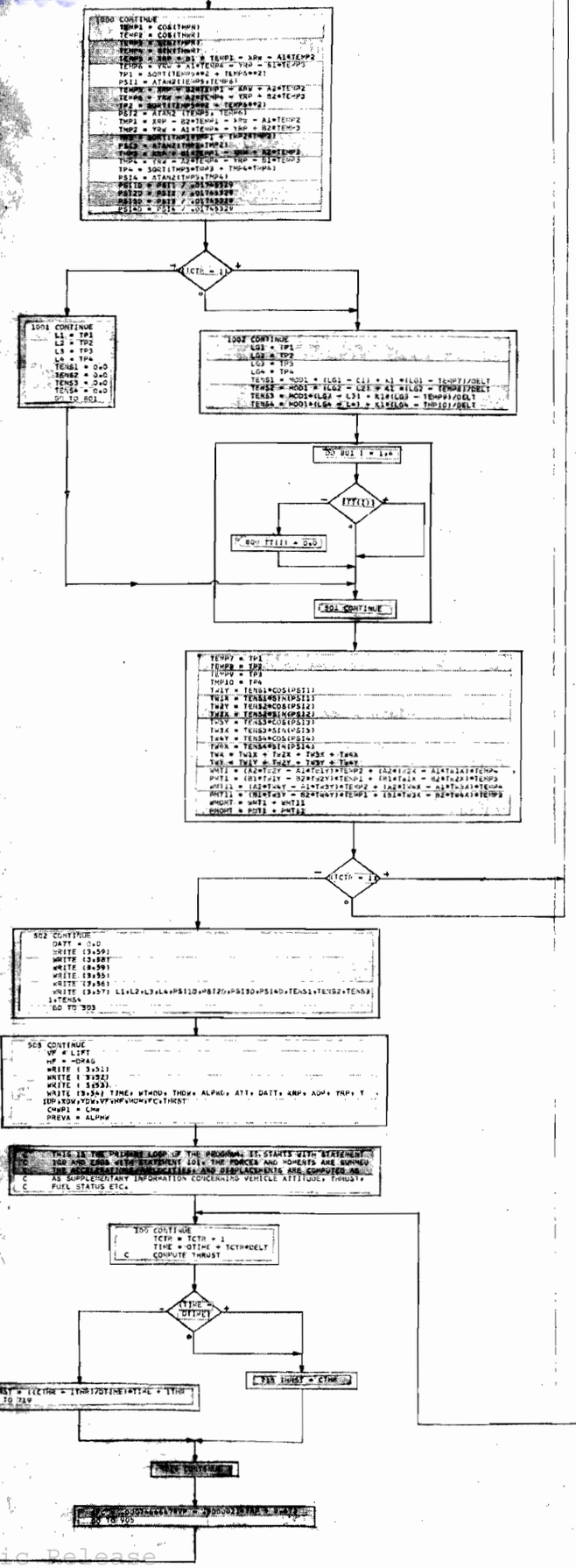

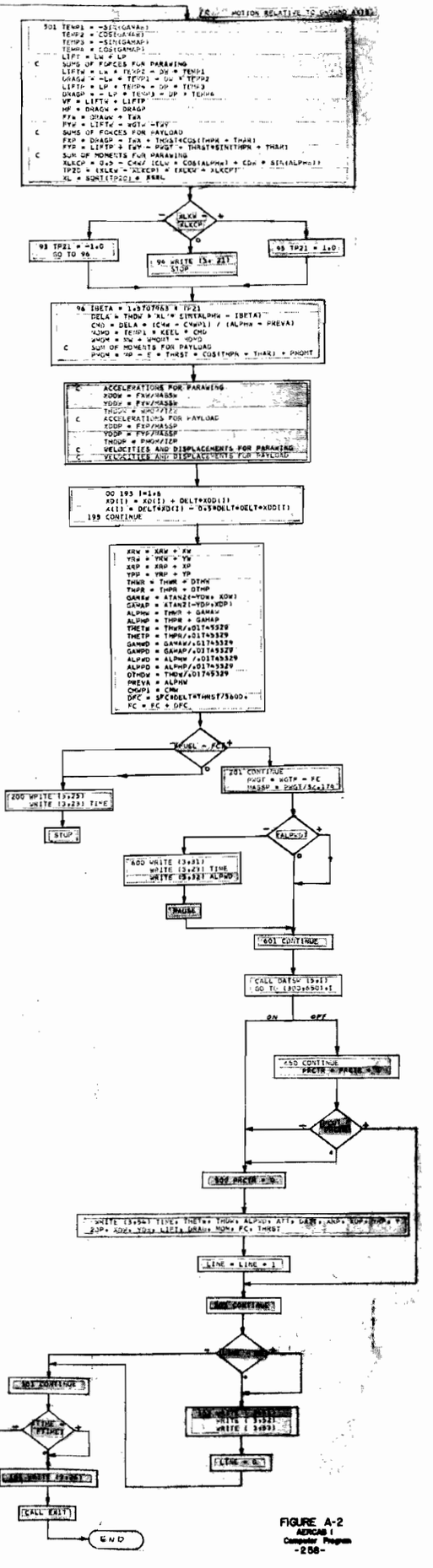

FIGURE A-2
AEROAB I
Computer Program
-258-

SAMPLE PRINTOUT
"AERCAB 1"

```
// JOB
// FOR
*IOCS (CARD, 1132 PRINTER)
*EXTENDED PRECISION
*ONE WORD INTEGERS
*LIST SOURCE PROGRAM
*NAME ARCB1
*TRANSFER TRACE
*ARITHMETIC TRACE
C
C
C                                  INPUT DATA
C
C      THE FIRST 56 DATA CARDS IDENTIFIED BY 'ALPHA, CLW , CDW, CMW' ARE
C      A TABLE OF VALUES OF THE AERODYNAMIC COEFFICIENTS OF THE PARAWING.
C      THE EIGHT DATA CARDS THAT FOLLOW THESE CONTAIN THE INPUT DATA AND
C      INITIAL CONDITIONS AS INDICATED BELOW.
C
C                          ****************************
C
C      CARD NO. 1
C
C      1. WGTW = WEIGHT OF PARAWING (LB.).
C      2. WGTP = WEIGHT OF PAYLOAD (LB.).
C      3. AREAW = REFERENCE AREA OF PARAWING (SQ.FT.).
C      4. AREAP = REFERENCE AREA OF PAYLOAD (SQ.FT.).
C      5. KEEL = LENGTH OF PARAWING KEEL (FT.).
C
C      CARD NO. 2
C
C      1. LGTH = CHARACTERISTIC LENGTH OF PAYLOAD (FT.)
C      2. IZW = MASS MOMENT OF INERTIA OF PARAWING (SL.-SQ.FT.).
C      3. IZP = MASS MOMENT OF INERTIA OF PAYLOAD (SL.-SQ.FT.).
C      4. K1 = DAMPING COEFFICIENT FOR TENSILE FORCES.
C      5. CDP = PAYLOAD DRAG COEFFICIENT.
C
C      CARD NO. 3
C
C      1. OTIME = INITIAL TIME (SEC.)
C      2. FTIME = FINAL TIME (SEC.).
C      3. DELT = INCREMENT OF TIME (SEC.).
C      4. PCOT = NO. OF INTEGRATION STEPS TO BE EXECUTED BETWEEN PRINTOUTS.
C      5. E = VERTICAL THRUST DISPLACEMENT (FT.)
C
C      CARD NO. 4
C
C      1. FUEL = FUEL CAPACITY (LB.)
C      2. THA = THRUST CANT ANGLE (THRU P.L. C.G.)(DEG.).
C      3. DTIME = TIME REQ'D TO BUILD UP FROM IDLE THRUST TO CRUISE THRUST (SEC.
C      4. ITHR = IDLE THRUST (LB.)
C      5. CTHR = CRUISE THRUST (LB.)
C
C      CARD NO. 5
C
C      1. A1 = DIST. FROM WING C.G. TO FORWARD LANYARD CONNECTIONS (FT.).
C      2. A2 = DIST. FROM WING C.G. TO AFT LANYARD CONNECTIONS (FT.).
C      3. B1 = DIST. FROM PAYLOAD C.G. TO FORWARD LANYARD CONNECTIONS (FT.).
C      4. B2 = DIST. FROM PAYLOAD C.G. TO AFT LANYARD CONNECTIONS (FT.).
C      5. MOD1 = ELASTIC COEFFICIENT (LB./FT.)
C
C      CARD NO. 6
C
C      1. XLK = RATIO OF (DIST. FROM LEADING EDGE OF KEEL TO INTERSECTION
C         OF LINE NORMAL TO KEEL AND PASSING THROUGH SYSTEM C.G. TO (THE
```

```
C      KEEL LENGTH).
C   2. YLK = RATIO OF (PERPINDICULAR DISTANCE FROM SYSTEM C.G. TO KEEL)
C      TO (THE KEEL LENGTH).
C   3. XLKW = RATIO OF (DISTANCE FROM LEADING EDGE OF KEEL TO PARAWING
C      C.G.) TO (THE KEEL LENGTH).
C   4. YLKW = RATIO OF (PERPINDICULAR DISTANCE FROM PARAWING C.G. TO
C      THE KEEL) TO (THE KEEL LENGTH).
C
C                              INITIAL CONDITIONS
C
C   CARD NO. 7
C
C   1. XRWO = INITIAL RANGE OF PARAWING (FT.).
C   2. YRWO = INITIAL ALTITUDE OF PARAWING (FT.)
C   3. WTHOD = ANGLE BETWEEN WING KEEL AND LOCAL HORIZONTAL (DEG.)
C   4. XDW = INITIAL HORIZONTAL VELOCITY OF PARAWING (FT./SEC.).
C   5. YDW = INITIAL VERTICAL VELOCITY OF PARAWING (FT./SEC.).
C   6. THDW = INITIAL ANGULAR VELOCITY OF PARAWING IN PITCH (DEG./ SEC.).
C
C   CARD NO. 8
C
C   1. XRPO = INTIIAL RANGE OF PAYLOAD (FT.).
C   2. YRPO = INITIAL ALTITUDE OF PAYLOAD (FT.).
C   3. PTHOD = ANGLE BETWEEN P.L. CHAR. LGTH. AND LOCAL HORIZONTAL (DEG.).
C   4. XDP = INITIAL HORIZONTAL VELOCITY OF PAYLOAD (FT./SEC.).
C   5. YDP = INITIAL VERTICAL VELOCITY OF PAYLOAD (FT./SEC.).
C   6. THDP = INITIAL ANGULAR VELOCITY OF PAYLOAD IN PITCH (DEG./SEC).
C
C                              OUTPUT DATA
C
C   THE FIRST PRINTOUTS EXECUTED WRITE THE INPUT DATA AND ARE SELF EX-
C   PLANATORY
C
C   THE LANYARD LENGTHS (UNDER ZERO TENSION) AND THE ANGLES THEY MAKE
C   WITH THE VERTICAL ARE THEN PRINTED.
C
C   FOR EACH LINE OF PRINT THEREAFTER THE FOLLOWING ARE PRINTED READING
C   FROM LEFT TO RIGHT.
C
C   1. TIME = TIME (SEC.).
C   2. THETW = THE ANGLE THE KEEL MAKES WITH THE HORIZONTAL (DEG.).
C   3. DTHDW = THE ANGULAR VELOCITY OF THE PARAWING IN PITCH (DEG./SEC.).
C   4. ALPWD = THE ANGLE OF ATTACK OF THE PARAWING (DEG.).
C   5. ATT = THE VEHICLE ATTITUDE (DEG.).
C   6. DATT = RATE OF CHANGE OF THE ATTITUDE (DEG./SEC.).
C   7. XRP = THE RANGE OF THE PAYLOAD WITH REFERENCE TO THE GROUND (FT.).
C   8. XDP = THE HORIZONTAL VELOCITY WITH REF. TO GROUND (FT./SEC.).
C   9. YRP = THE PAYLOAD ALTITUDE (FT.).
C   10.YDP = THE VERTICAL VELOCITY OF THE PAYLOAD (FT./SEC.).
C   11.XDW = THE HORIZONTAL VELOCITY OF THE PARAWING (FT./SEC.).
C   12.YDW = THE VERTICAL VELOCITY OF THE PARAWING (FT./SEC.).
C   13.VF = THE SUM OF THE VERTICAL COMPONENTS OF THE AERODYNAMIC FORCES (LB.
C   14.HF = THE SUM OF THE HORIZ. COMPONENTS OF THE AERODYNAMIC FORCES (LB.).
C   15.MOM = THE SUM OF THE AERODYNAMIC MOMENTS (WING + P.L.) (FT.-LB.).
C   16.FC = THE AMOUNT OF FUEL CONSUMED (LBS).
C   17.THRST = THRUST LEVEL (LB.).
C
C
      REAL KEEL,IZW,IZP,   L1,L2,L3,L4      ,LG1,LG2,LG3,LG4,LGTH,LW,LP,
     1MW,MP,MASSW,MASSP,   MOD1,LIFT,MOM,MOMD,ITHR, K1
      REAL IBETA
      REAL LIFTW,LIFTP
      DIMENSION ALPHT(57),CLWT(57),CDWT(57),CMWT(57),C(12),Y(4)
      DIMENSION TT(4),       XDD(6),XD(6),X(6)
```

```
      EQUIVALENCE (XDDW,XDD(1)),(YDDW,XDD(2)),(THDDW,XDD(3)),(XDDP,XDD(4
     1)),(YDDP,XDD(5)),(THDDP,XDD(6))
      EQUIVALENCE (XDW,XD(1)),(YDW,XD(2)),(THDW,XD(3)),(XDP,XD(4)),(YDP,
     1XD(5)),(THDP,XD(6))
      EQUIVALENCE (XW,X(1)),(YW,X(2)),(DTHW,X(3)),(XP,X(4)),(YP,X(5)),(D
     1THP,X(6))
      EQUIVALENCE (TENS1,TT(1)), (TENS2,TT(2)),(TENS3,TT(3)),(TENS4,TT(4
     1))
C
C     READ FORMATS
    1 FORMAT (5F10.0)
    8 FORMAT (I5)
    9 FORMAT (4F10.0)
C
C     PRINT FORMATS
C
   10 FORMAT (1H , /, 30X, 'PHYSICAL CHARACTERISTICS AND INITIAL CONDITI
     1ONS FOR PARAWING')
   11 FORMAT (1H , /, 30X, 'PHYSICAL CHARACTERISTICS AND INITIAL CONDITI
     1ONS FOR PAYLOAD')
   12 FORMAT (1H , /, ' WEIGHT =', F7.3, ' LB.', '    PLANFORM AREA =',
     1F7.3,' SQ.FT.','    KEEL LGTH =',F7.5,' FT.','  MOM. OF INERTIA ='
     2,F7.3,' SL-SQ.FT.')
   13 FORMAT (1H , /,' WEIGHT =',F7.3,' LB.','       CHAR. AREA =',F7.3,
     1' SQ.FT.','    CHAR LGTH =',F7.5,' FT.    MOM. OF INERTIA',F7.3,'
     2SL-SQ.FT.')
   14 FORMAT (1H , 34X, '.', 12X, '.', 11X, '.')
   15 FORMAT (1H , ' LF =', F5.2, 2X, 'LA =', F5.2, 2X, 'O =', F6.2, 2X,
     1'O =', F8.3, 2X, 'X =', F7.2, 2X, 'Y =', F7.2,2X,'ALPHA =',F6.2,2X
     2,'X =',F6.3, 2X,'Y =',F9.3)
   16 FORMAT (1H+, 23X, '-', 10X, '-')
   17 FORMAT (1H , //, 50X, 'SYSTEM PARAMETERS', //)
   18 FORMAT (1H , 'THR.ANG. =',F4.1,' DEG.','   THR.DISP. =',F4.2,' FT.
     1','   IDLE THR. =',F5.1,' LB.','   CRUISE THR. =',F7.2,' LB.','
     2THR. B.U. =',F5.2, ' SEC.')
   19 FORMAT (1H , 'ELASTIC COEFF. =',F9.2,' LB/FT',' PL DR. COEFF. =',
     1F7.2,'    TENSION D.F. =',F9.2,'   FUEL =',F6.1,' LB.')
   22 FORMAT (1H , ' X/LK =', F6.4, 5X,' Y/LK =', F6.4)
   21 FORMAT (1H , ' BETA (IN DAMPING TERM) IS INDETERMINATE')
   23 FORMAT (1H , /,' TIME= ',F7.3)
   24 FORMAT (1H , ///, ' INITIAL TIME =',F7.2,' SEC.','    FINAL TIME =
     1',F7.2,' SEC.','    TIME INCREMENT =',F7.4,' SEC.','    PRINT FREQ
     2. =',F6.0)
   25 FORMAT (1H , /, ' FUEL DEPLETION')
   26 FORMAT (1H , /, ' PROGRAM COMPLETED')
   28 FORMAT (1H , ////)
   31  FORMAT(1H , /, ' THE ANGLE OF ATTACK OF PARAWING IS NEGATIVE')
   32 FORMAT (1H , /, ' ALPHA =', F9.3, ' DEG.')
   51 FORMAT (1H1, 16X, '.', 21X, '.', 14X, '.', 15X, '.', 7X, '.', 7X,
     1'.')
   52 FORMAT (1H , ' TIME', 5X, 'OW', 4X, 'OW', 4X, 'AW', 6X, 'U', 7X, '
     1U', 6X, 'XP', 6X, 'XP', 6X, 'YP', 6X, 'YP', 6X, 'XW', 6X, 'YW', 4X
     2, 'V.F.', 2X, 'H.F.', 3X, 'MOM.', 2X, 'F.C.', 2X, 'THST')
   53 FORMAT (1H+, 10X, '-', 5X, '-', 13X         , 'I', 7X, 'I')
   54 FORMAT (1H , F7.2, 3F6.1, 2F8.1, F8.1, F7.1, F8.1, 3F8.1, F7.1, F7
     1.0, F6.0, F6.1, F6.0)
   55 FORMAT (1H , 3X, 'L1',8X, 'L2',8X, 'L3',8X, 'L4',8X, 'U1',9X, 'U2'
     1,9X, 'U3',9X, 'U4',6X, 'TENS1',5X, 'TENS2',5X, 'TENS3',5X,'TENS4')
   56 FORMAT (1H+, 43X, 'I',10X,'I',10X, 'I',10X, 'I')
   57 FORMAT (1H ,F6.3,4F10.3,3F11.3,4F10.2)
   58 FORMAT (1H , /,15X, ' INITIAL LANYARD LENGTHS (FT.), ANGLES (DEGS.
     1) , AND TENSIONS (LB.).')
   59 FORMAT (1H , ////)
```

```
   72 FORMAT (6F10.0)
C     THIS PORTION OF PROGRAM READS INPUT DATA AND INITIAL CONDITIONS.
C     THE REQUIRED STORAGE LOCATIONS ARE INITIALIZED AND PRINTOUT OF
C     PHYSICAL DATA AND INITIAL CONDITIONS ARE EXECUTED. THE INITIAL
C     LINE OF PRINT FOR TIME = 0 IS EXECUTED. PRIMARY LOOP STARTS AT
C     STATEMENT 100.
C
C     PHYSICAL DATA
      CALL TSTOP
      READ (2,8) N
      READ (2,9) (ALPHT(I),CLWT(I),CDWT(I),CMWT(I),I=1,N)
      ALPHT(N+1) = ALPHT(I-1)
      CLWT(N+1) = CLWT(I-1)
      CDWT(N+1) = CDWT(I-1)
      CMWT(N+1) = CMWT(I-1)
      READ (2,1) WGTW,WGTP,AREAW,AREAP,KEEL,LGTH,IZW,IZP,K1,CDP,OTIME,FT
     1IME,DELT,PCOT,E,FUEL,THAD,DTIME,ITHR,CTHR,A1,A2,B1,B2,MOD1
      READ (2,9) XLK, YLK, XLKW, YLKW
C     INITIAL CONDITIONS
      READ (2,72)XRWO,YRWO,WTHOD,XDW,YDW,THDW,XRPO,YRPO,PTHOD,XDP,YDP,TH
     1DP
C      START PROGRAM
      CALL TSTRT
      NR = 4
      LINE = 0
      MOMD = 0.0
      ATT = 0.0
      PRCTR = 0.0
      DO 61  I = 1, 6
      XDD(I) = 0.0
      X(I) = 0.0
   61 CONTINUE
      XRW =XRWO
      YRW = YRWO
      XRP = XRPO
      YRP = YRPO
      TIME = OTIME
      TCTR = 0
      MOM = 0.0
      DATT = 0.0
      PWGT = WGTP
      CLP = 0.0
      CMP = 0.0
      MASSW = WGTW/32.174
      MASSP = WGTP/32.174
      FC = 0.0
      GAMAW = ATAN2(-YDW,XDW)
      GAMAP = ATAN2(-YDP,XDP)
      THAR = .01745329 * THAD
      THWR = .01745329 * WTHOD
      THPR = .01745329 * PTHOD
      ALPWD = WTHOD + GAMAW / .01745329
      ALPPD = PTHOD + GAMAP / .01745329
      GO TO 905
  910 CONTINUE
      THRST = ITHR
      WRITE (3,28)
      WRITE (3,10)
      WRITE (3,12) WGTW,AREAW,KEEL,IZW
      WRITE (3,14)
      WRITE (3,15) A1,A2,WTHOD,THDW,XDW,YDW,ALPWD,XRWO,YRWO
      WRITE (3, 16)
      WRITE (3,22) XLKW, YLKW
      WRITE (3,28)
```

```
      WRITE (3,11)
      WRITE (3,13) WGTP,AREAP,LGTH,IZP
      WRITE (3,14)
      WRITE (3,15) B1,B2,PTHOD,THDP,XDP,YDP,ALPPD,XRPO,YRPO
      WRITE (3, 16)
      WRITE (3,28)
      WRITE (3,17)
      WRITE (3,24) OTIME, FTIME, DELT,PCOT
      WRITE (3,18) THAD,E,ITHR,CTHR,DTIME
      WRITE (3,19) MOD1,CDP,K1,FUEL
      WRITE (3,22) XLK, YLK
      GO TO 1000
  503 CONTINUE
      VF = LIFT
      HF = -DRAG
      WRITE ( 3,51)
      WRITE ( 3,52)
      WRITE ( 3,53)
      WRITE (3,54) TIME, WTHOD, THDW, ALPWD, ATT, DATT, XRP, XDP, YRP, Y
     1DP,XDW,YDW,VF,HF,MOM,FC,THRST
      CMWP1 = CMW
      PREVA = ALPHW
C     THIS IS THE PRIMARY LOOP OF THE PROGRAM. IT STARTS WITH STATEMENT
C     100 AND ENDS WITH STATEMENT 101. THE FORCES AND MOMENTS ARE SUMMED
C     THE ACCELERATIONS, VELOCITIES, AND DISPLACEMENTS ARE COMPUTED AS
C     AS SUPPLEMENTARY INFORMATION CONCERNING VEHICLE ATTITUDE, THRUST,
C     FUEL STATUS ETC.
  100 CONTINUE
      TCTR = TCTR + 1
      TIME = OTIME + TCTR*DELT
C     COMPUTE THRUST
      IF (TIME - DTIME) 717,718,718
  717 THRST = ((CTHR - ITHR)/DTIME)*TIME + ITHR
      GO TO 719
  718 THRST = CTHR
  719 CONTINUE
      SFC = .0007466667*VP - .0000021*YRP + 0.673
      GO TO 905
  915 CONTINUE
C     COMPUTE TENSION IN LANYARDS
      GO TO 1000
C     MOTION RELATIVE TO GROUND AXIS
  501 TEMP1 = -SIN(GAMAW)
      TEMP2 = COS(GAMAW)
      TEMP3 = -SIN(GAMAP)
      TEMP4 = COS(GAMAP)
      LIFT = LW + LP
C     SUMS OF FORCES FOR PARAWING
      LIFTW = LW * TEMP2 - DW * TEMP1
      DRAGW = -LW * TEMP1 - DW * TEMP2
      LIFTP = LP * TEMP4 - DP * TEMP3
      DRAGP = - LP * TEMP3 - DP * TEMP4
      VF = LIFTW + LIFTP
      HF = DRAGW + DRAGP
      FXW = DRAGW + TWX
      FYW = LIFTW - WGTW -TWY
C     SUMS OF FORCES FOR PAYLOAD
      FXP = DRAGP - TWX + THRST*COS(THPR + THAR)
      FYP = LIFTP + TWY - PWGT + THRST*SIN(THPR + THAR)
C     SUM OF MOMENTS FOR PARAWING
      XLKCP = 0.5 - CMW/ (CLW * COS(ALPHW) + CDW * SIN(ALPHW))
      TP20 = (XLKW - XLKCP) * (XLKW - XLKCP)
      XL = SQRT(TP20)*KEEL
      IF (XLKW - XLKCP) 93, 94, 95
```

```
   93 TP21 = -1.0
      GO TO 96
   94 WRITE (3, 21)
      STOP
   95 TP21 = 1.0
   96 IBETA = 1.5707963 * TP21
      DELA = THDW * XL * SIN(ALPHW - IBETA)
      CMD = DELA * (CMW - CMWP1) / (ALPHW - PREVA)
      MOMD = TEMP1 * KEEL * CMD
      WMOM = MW + WMOMT - MOMD
C     SUM OF MOMENTS FOR PAYLOAD
      PMOM = MP - E * THRST * COS(THPR + THAR) + PMOMT
C     ACCELERATIONS FOR PARAWING
      XDDW = FXW/MASSW
      YDDW = FYW/MASSW
      THDDW = WMOM/IZW
C     ACCELERATIONS FOR PAYLOAD
      XDDP = FXP/MASSP
      YDDP = FYP/MASSP
      THDDP = PMOM/IZP
C     VELOCITIES AND DISPLACEMENTS FOR PARAWING
C     VELOCITIES AND DISPLACEMENTS FOR PAYLOAD
      DO 193 I=1,6
      XD(I) = XD(I) + DELT*XDD(I)
      X(I) = DELT*XD(I) - 0.5*DELT*DELT*XDD(I)
  193 CONTINUE
      XRW = XRW + XW
      YRW = YRW + YW
      XRP = XRP + XP
      YRP = YRP + YP
      THWR = THWR + DTHW
      THPR = THPR + DTHP
      GAMAW = ATAN2(-YDW, XDW)
      GAMAP = ATAN2(-YDP,XDP)
      ALPHW = THWR + GAMAW
      ALPHP = THPR + GAMAP
      THETW = THWR/.01745329
      THETP = THPR/.01745329
      GAMWD = GAMAW/.01745329
      GAMPD = GAMAP/.01745329
      ALPWD = ALPHW /.01745329
      ALPPD = ALPHP/.01745329
      DTHDW = THDW/.01745329
      PREVA = ALPHW
      CMWP1 = CMW
      DFC = SFC*DELT*THRST/3600.
      FC = FC + DFC
      IF (FUEL - FC) 200,200,201
  200 WRITE (3,25)
      WRITE (3,23) TIME
      STOP
  201 CONTINUE
      PWGT = WGTP - FC
      MASSP = PWGT/32.174
      IF (ALPWD) 600,601,601
  600 WRITE (3,31)
      WRITE (3,23) TIME
      WRITE (3,32) ALPWD
      PAUSE
  601 CONTINUE
      CALL DATSW (5,I)
      GO TO (300,650),I
  650 CONTINUE
      PRCTR = PRCTR + 1
```

```
      IF (PCOT - PRCTR) 300, 300, 303
  300 PRCTR = 0
      WRITE (3,54) TIME, THETw,DTHDW, ALPWD, ATT, DATT, XRP, XDP, YRP, Y
     2DP, XDW, YDW,VF ,  HF    , MOM, FC, THRST
      LINE = LINE + 1
  303 CONTINUE
      IF (LINE - 55) 301,302,302
  302 WRITE ( 3,51)
      WRITE ( 3,52)
      WRITE ( 3,53)
      LINE = 0
  301 CONTINUE
      IF (TIME - FTIME) 100,101,101
  101 WRITE (3,26)
      CALL EXIT
C
C     ROUTINE TO COMPUTE THE AERODYNAMIC PARAMETERS. CL,CD,AND CM ARE
C     OBTAINED BY PARABOLIC INTERPOLATION FROM A TABLE. LIFT, DRAG AND
C     THE AERO. MOMENT ARE CALCULATED IN THE CONVENTIONAL MANNER.
C
  905 CONTINUE
      TEMP3 = ATT
      ATT = ATAN2(XRP -XRW,YRW - YRP)/.01745329
      DATT = (ATT - TEMP3)/DELT
      VW = SQRT(XDW**2 + YDW**2)
      VP = SQRT(XDP**2 + YDP**2)
      RHO = 0.002377 * EXP(-0.0000415*YRW)
      TEMP1 = 0.5*RHO*AREAW*VW**2
      TEMP2 = 0.5*RHO*AREAP*VP**2
      N = 0
  111 N = N + 1
      IF (ALPWD -ALPHT(N))111,2,3
    3 IF (ALPWD -ALPHT(N+1)) 7, 5, 6
    5 I = N + 1
   30 CLW = CLWT(I)
      CDW  = CDWT(I)
      CMW = CMWT(I)
      GO TO 4
    6 N = N + 1
      GO TO 3
    7 DO 873 I = 1, 12, 4
      C(I) = ALPHT(N)
      C(I+1) = CLWT(N)
      C(I+2) = CDWT(N)
      C(I+3) = CMWT(N)
  873 N = N + 1
      DEL = (C(1)-C(5)) * (C(1)**2-C(9)**2) - (C(1)-C(9)) * (C(1)**2 -
     1 C(5)**2)
      DO 20 I = 2, 4
      BCOEF = ((C(I) -C(I+4))* (C(1)**2-C(9)**2) - (C(I) - C(I+8))
     1  * (C(1)**2 - C(5)**2)) / DEL
      CCOEF = ((C(I) - C(I+8)) * (C(1)-C(5)) - (C(I) - C(I+4))
     1  * (C(1) - C(9))) / DEL
      ACOEF = C(I) - BCOEF * C(1) - CCOEF * C(1) **2
   20 Y(I) = ACOEF + ALPWD*(BCOEF + CCOEF*ALPWD)
      CLW = Y(2)
      CDW = Y(3)
      CMW = Y(4)
      GO TO 4
    2 I = N
      GO TO 30
    4 CONTINUE
      LW = TEMP1*CLW
      DW = TEMP1*CDW
```

```
      MW = TEMP1*CMW*KEEL
      LP = TEMP2*CLP
      DP = TEMP2*CDP
      MP = TEMP2*CMP*LGTH
      LIFT = LW + LP
      DRAG = DW + DP
      MOM = MW + MP
      VELR = VP
      IF (TCTR - 0) 910, 910, 915
C
C     ROUTINE TO COMPUTE THE LANYARD LENGTHS,ANGLES, AND TENSILE FORCES.
C     THE ROUTINE FIRST COMPUTES THE INITIAL ZERO TENSION LENGTHS AND ANGLES.
C     THE TENSILE FORCES DUE TO DISPLACEMENT ARE COMPUTED BY A SIMPLE
C     APPLICATION OF HOOKES LAW.
C     COMPUTATION OF INITIAL LANYARD LENGTHS AND ANGLES
 1000 CONTINUE
      TEMP1 = COS(THPR)
      TEMP2 = COS(THWR)
      TEMP3 = SIN(THPR)
      TEMP4 = SIN(THWR)
      TEMP5 = XRP + B1 * TEMP1 - XRW - A1*TEMP2
      TEMP6 = YRW + A1*TEMP4 - YRP - B1*TEMP3
      TP1 = SQRT(TEMP5**2 + TEMP6**2)
      PSI1 = ATAN2(TEMP5,TEMP6)
      TEMP5 = XRP - B2*TEMP1 - XRW + A2*TEMP2
      TEMP6 = YRW - A2*TEMP4 - YRP + B2*TEMP3
      TP2 = SQRT(TEMP5**2 + TEMP6**2)
      PSI2 = ATAN2 (TEMP5, TEMP6)
      TMP1 = XRP - B2*TEMP1 - XRW - A1*TEMP2
      TMP2 = YRW + A1*TEMP4 - YRP + B2*TEMP3
      TP3 = SQRT(TMP1*TMP1 + TMP2*TMP2)
      PSI3 = ATAN2(TMP1,TMP2)
      TMP3 = XRP + B1*TEMP1 - XRW + A2*TEMP2
      TMP4 = YRW - A2*TEMP4 - YRP - B1*TEMP3
      TP4 = SQRT(TMP3*TMP3 + TMP4*TMP4)
      PSI4 = ATAN2(TMP3,TMP4)
      PSI1D = PSI1 / .01745329
      PSI2D = PSI2 / .01745329
      PSI3D = PSI3 / .01745329
      PSI4D = PSI4 / .01745329
      IF (TCTR - 1) 1001,1002,1002
 1001 CONTINUE
      L1 = TP1
      L2 = TP2
      L3 = TP3
      L4 = TP4
      TENS1 = 0.0
      TENS2 = 0.0
      TENS3 = 0.0
      TENS4 = 0.0
      GO TO 801
 1002 CONTINUE
      LG1 = TP1
      LG2 = TP2
      LG3 = TP3
      LG4 = TP4
      TENS1 = MOD1 * (LG1 - L1) + K1 *(LG1 - TEMP7)/DELT
      TENS2 = MOD1 * (LG2 - L2) + K1 *(LG2 - TEMP8)/DELT
      TENS3 = MOD1*(LG3 - L3) + K1*(LG3 - TEMP9)/DELT
      TENS4 = MOD1*(LG4 - L4) + K1*(LG4 - TMP10)/DELT
      DO 801 I = 1,4
      IF (TT(I)) 800, 801, 801
  800 TT(I) = 0.0
  801 CONTINUE
```

```
      TEMP8 = TP2
      TEMP9 = TP3
      TMP10 = TP4
      TW1Y = TENS1*COS(PSI1)
      TW1X = TENS1*SIN(PSI1)
      TW2Y = TENS2*COS(PSI2)
      TW2X = TENS2*SIN(PSI2)
      TW3Y = TENS3*COS(PSI3)
      TW3X = TENS3*SIN(PSI3)
      TW4Y = TENS4*COS(PSI4)
      TW4X = TENS4*SIN(PSI4)
      TWX = TW1X + TW2X + TW3X + TW4X
      TWY = TW1Y + TW2Y + TW3Y + TW4Y
      WMT1 = (A2*TW2Y - A1*TW1Y)*TEMP2 + (A2*TW2X - A1*TW1X)*TEMP4
      PMT1 = (B1*TW1Y - B2*TW2Y)*TEMP1 + (B1*TW1X - B2*TW2X)*TEMP3
      WMT11 = (A2*TW4Y - A1*TW3Y)*TEMP2 + (A2*TW4X - A1*TW3X)*TEMP4
      PMT11 = (B1*TW4Y - B2*TW3Y)*TEMP1 + (B1*TW4X - B2*TW3X)*TEMP3
      WMOMT = WMT1 + WMT11
      PMOMT = PMT1 + PMT11
      IF (TCTR - 1) 502,501,501
  502 CONTINUE
      DATT = 0.0
      WRITE (3,59)
      WRITE (3,58)
      WRITE (3,59)
      WRITE (3,55)
      WRITE (3,56)
      WRITE (3,57) L1,L2,L3,L4,PSI1D,PSI2D,PSI3D,PSI4D,TENS1,TENS2,TENS3
     1,TENS4
      GO TO 503
      END
```

APPENDIX B

COUPLED AERCAB (RIGID SUSPENSION) 3-PLANE MOTION COMPUTER PROGRAM

"AERCAB 5"

APPENDIX B

Coupled-AERCAB Motion in Three-Planes

The initial studies of the rigid body AERCAB were limited to motion only in the pitch-plane. To facilitate improved and more realistic investigations, a study of system motion in six degrees of freedom was undertaken. The model selected has certain definite limitations in that total coupling of all the motions is not included. It was felt that the preliminary information required under this program could be obtained from a model that included the more severe effects of coupling, but retained the economy of simplicity without incurring an intolerable loss in accuracy.

Two Cartesian coordinate systems are considered: an earth-fixed system with an arbitrary origin, and a moving coordinate system with origin at the center of gravity of the AERCAB. In the development of the equations, all moments are assumed to be mathematically positive and all forces and moments either act through or about the system center of gravity (or were transferred to meet this criterion).

Lift and drag were assumed to act normal to and along the relative wind vector. The weight acts through the system center of gravity and was allowed to vary as a function of time. The allowance was included to compensate for the fuel consumed. The thrust vector was permitted to be canted and/or displaced vertically in the pitch plane.

Figure B-1 indicates the moving coordinate system used as well as some of the symbols for ease in understanding the development of the equations.

Nomenclature

The aerodynamic data used in this investigation were taken from NASA TN D-1957 (Ref. 20). The argument used, in all cases, was the angle of attack (α). The damping moment used in the pitch-plane was developed at SAEC, while the expression used for the damping moments in the roll-and-yaw-planes were taken from Perkins and Hage (Ref. 22). All the coefficients obtained from Ref. 20 are based on the flat planform area of the wing; the reference length used in determination of the pitching moment coefficients was the keel length, and the reference length used in determination of the rolling moment and yawing moment was the flat planform span. Pitching, rolling, and yawing moments are referred to a moment center

FIGURE B-1

PITCH~ROLL~YAW COMPUTER MODEL

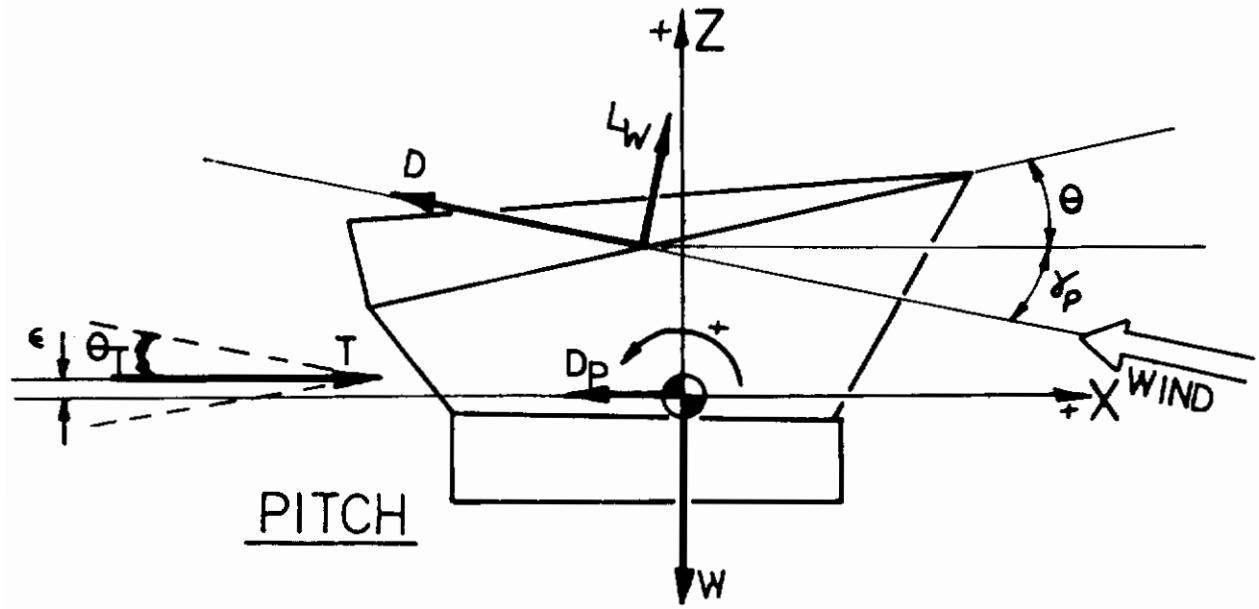

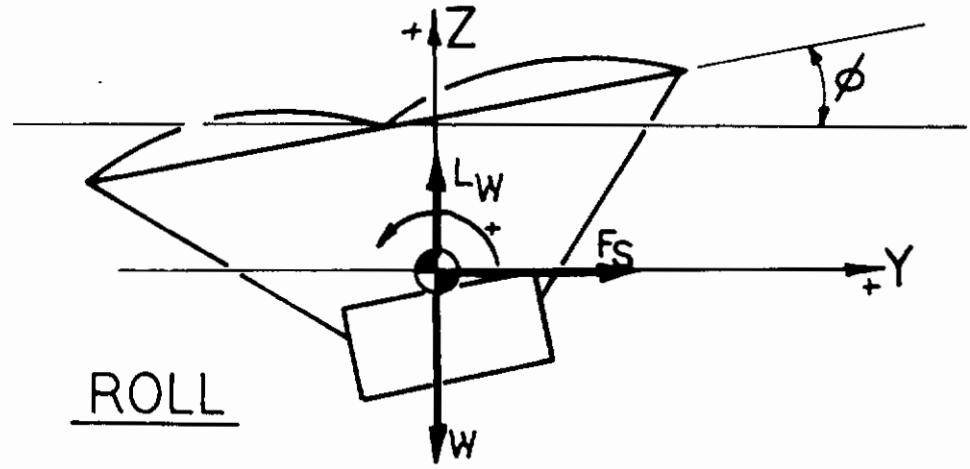

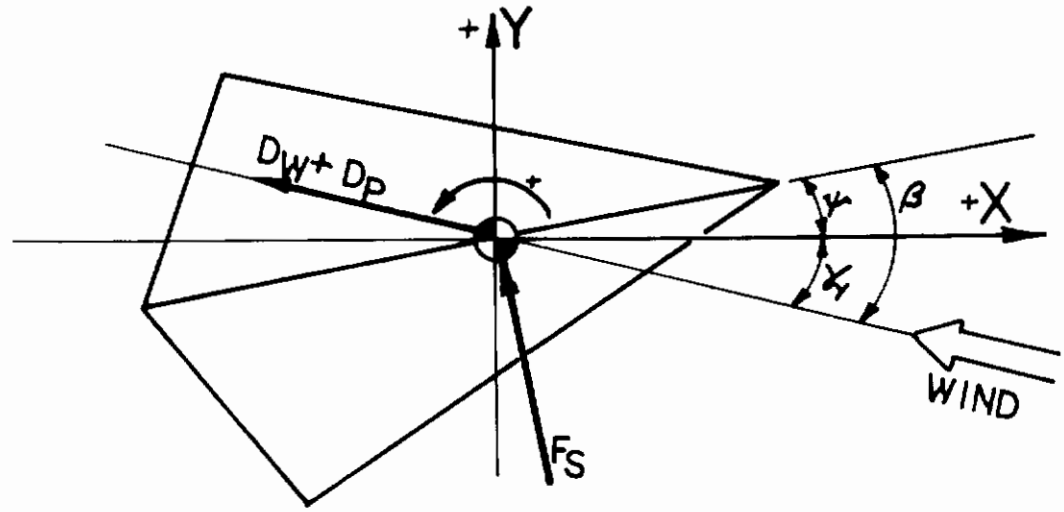

located at the CG of the system.

SYMBOL	DEFINITION, UNITS
A	reference area, sq. ft.
b	wing span, ft.
C_D	drag coefficient
C_L	lift coefficient
C_ℓ	rolling moment coefficient
C_m	pitching moment coefficient
C_n	yawing moment coefficient
C_Y	side force coefficient
C_{ℓ_β}	effective-dehedral parameter, $\frac{\delta C_\ell}{\delta \beta}$, per deg.
C_{n_β}	static directional-stability parameter, $\frac{\delta C_n}{\delta \beta}$, per deg.
C_{Y_β}	side-force parameter, $\frac{\delta C_Y}{\delta \beta}$, per deg.
D	drag, lb.
D_x	damping moment in roll, ft.lb.
D_Y	damping moment in pitch, ft.lb.
D_Z	damping moment in roll, ft.lb.
F_S	side force, lb.
F_t	thrust, lb.
F_{t_i}	idle thrust of engine, lb.
F_{t_c}	cruise thrust of engine, lb.
F	fuel weight, lb.
I_x	moment of inertia about roll axis; slugs-sq.ft.

SYMBOL	DEFINITION, UNITS
I_Y	moment of inertia about pitch axis, slugs-sq.ft.
I_Z	moment of inertia about yaw axis, slugs-sq.ft.
K_d	pitch damping coefficient
L	lift, lb.
l_k	keel length, ft.
m	mass, lb.-sec.^{2}/ft.
Max	aerodynamic moment in roll, ft.-lb.
May	aerodynamic moment pitch, ft.-lb.
Max	aerodynamic moment in yaw, ft.-lb.
Mx	total moment in roll, ft.-lb.
My	total moment in pitch, ft.-lb.
M_Z	total moment in yaw, ft.-lb,
q	free stream dynamic pressure, lb./sq.ft.
S_{FC}	specific fuel comsumption, lb./hr.
t	time, sec.
v	velocity, ft./sec.
w	weight, lb.
x	range, ft.'
X_ℓ	the distance from the leading edge of the keel of the intersection of a line normal to the of the keel and passing through the system C.G. ft.
Y	lateral displacement, ft.
Z	altitude, ft.

SYMBOL	DEFINITION, UNITS
Z_k	the perpendicular distance from the system C.G. to the $\mathcal{L}$ of the keel, ft.
α	$\theta + \gamma_p$, deg.
β	yaw angle with respect to relative wind, $\psi + \gamma_y$, deg.
θ	pitch angle, deg.
ϕ	roll angle, deg.
ψ	yaw angle with respect to ground axis system, deg.
γ_p	angle between local horizontal and the relative wind vector (γ_p = arc tan $\dot{z}/\dot{x}$), deg.
γ_y	angle between flight path and relative wind vector (γ_y = arc tan $\dot{y}/\dot{x}$), deg.
θ_T	angle of thrust cant, deg.
ρ	density of air at altitude, lb./sq.ft.
ϵ	vertical displacement of thrust vector in the pitch plane, ft.
δ	vertical displacement of the drag vector in the pitch plane, ft.
δ_t	time required for thrust buildup, sec.
Δt	increment of time (integration increment), sec.

NOTE: Subscripts w and p refer to parawing and payload respectively, a subscript of R relates to the earth fixed coordinate system.

The Equations of Motion

The thrust description is quite simple but may easily be changed in the computer program as required. As presently programmed, the thrust, F_t, is permitted to build up linearly from an idle thrust, F_{t_i}, to a constant cruise thrust

F_{t_c}, over a time period Δt.

$$F_t = \left[(F_{t_c} - F_{t_i})/\Delta t\right] t + F_{t_i};\ 0 \leq t \leq \delta_t \qquad \text{(B-1)}$$

$$F_t = F_{t_c} \qquad ;\ t > \delta_t \qquad \text{(B-2)}$$

Lift and drag were determined in the conventional manner, where,

$$V = (\dot{x}^2 + \dot{y}^2 + \dot{z}^2)^{\frac{1}{2}} \qquad \text{(B-3)}$$

$$\rho = 0.002377\ e^{-.0000415 Z_R} \qquad \text{(B-4)}$$

and where x, y, z are the horizontal, lateral, and vertical components of the velocity, ρ is the density of air, and Z_R is the altitude of the vehicle above the origin of the earth fixed system. Then

$$q = \tfrac{1}{2}\rho v^2 \qquad \text{(B-5)}$$

$$L_w = q\ A\ C_{L_W}(\alpha) \qquad \text{(B-6)}$$

$$D_w = q\ A\ C_{D_W}(\alpha) \qquad \text{(B-7)}$$

$$Lp = 0 \qquad \text{(B-8)}$$

$$Dp = q\ A\ C_{D_P}(\alpha) \qquad \text{(B-9)}$$

and,

$$L = L_W + L_P \qquad \text{(B-10)}$$

$$D = Dw + Dp \qquad \text{(B-11)}$$

where $C_{D_P}(\alpha)$ is assumed to be constant.

The parawing aerodynamic moment coefficients in Ref. 20 were compiled for moments about the midpoint of the keel of the parawing. In the system to be described these moments must be transferred to the system center of gravity. The moment transfer equations are

$$C_{m_w}(\alpha)^1 = C_{m_w}(\alpha) + \left(\frac{Xe}{lk} - 0.5\right)\left[C_{L_W}(\alpha) * \cos\alpha + \ldots\right.$$

$$\left. + \ldots C_{D_W}(\alpha) * \sin\alpha\right] + \ldots$$

$$\ldots + Z_\ell/lk\left[C_{D_W}(\alpha) * \cos\alpha - C_{L_W}(\alpha) * \sin\alpha\right] \qquad \text{(B-12)}$$

$$C_{n_\beta}(\alpha)^1 = C_{n_\beta}(\alpha) - (X_\ell/1k - 0.5)\, C_{Y_\beta}(\alpha) \ldots \quad \text{(B-13)}$$

The aerodynamic moments may then be written

$$M_{a_x} = q*A*b*C_{l_\beta}(\alpha) \quad \text{roll} \quad \text{(B-14)}$$

$$May = q\ A\ l_k\ C_{m_w}(\alpha) \quad \text{(B-15)}$$

$$M_{a_Z} = -q*A*b*C_{n_\beta}(\alpha) \quad \text{(B-16)}$$

Where C_{ℓ_β} as a function of α is taken from Ref. 20, and the damping moment coefficient in pitch was developed by SAEC, and the coefficients for the roll and yaw damping moments were obtained from Reference 22. The values used are:

$$C_{\ell_p} = -0.3 \text{ (from Ref. 22, Fig 9-14, page 357)} \quad \text{(B-17)}$$

$$C_{\ell_\gamma} = \frac{C_{L_W}}{4} \quad \text{(B-18)}$$

$$\dot{C}_{n_p} = -\frac{C_{L_W}}{8} \quad \text{(B-19)}$$

$$C_{n_\gamma} = -\frac{C_{D_W}}{4} \quad \text{(B-20)}$$

(see Ref. 22, pp. 428-429)

and the damping moments used are

$$D_x = (C_{\ell_p} * \dot{\phi} + C_{\ell_\gamma} * \dot{\psi}) * q*A*b \text{ , (Roll)} \quad \text{(B-21)}$$

$$D_Y = K_d * \dot{\theta} * |V \sin \theta| \text{ , (Pitch)} \quad \text{(B-22)}$$

$$D_Z = (C_{n_p} * \dot{\phi} + C_{n_\gamma} \dot{\psi}) * q*A*b \text{ , (Yaw)} \quad \text{(B-23)}$$

The side force, F_s, was determined by

$$F_s = q*A*C_{Y_\beta}(\alpha) * \beta \quad \text{(B-24)}$$

The sums of the forces and moments may now be written

$$\sum F_x = (L \sin \gamma_p) * \cos \phi - D\cos \gamma_p + F_t \cos (\theta + \theta_T) \cos \psi - \ldots$$
$$\ldots - F_s * \sin (-\psi) \ldots \quad \text{(B-25)}$$

$$\sum F_Y = F_t \cos (\theta + \theta_T) * \sin(-\psi) + D \sin \gamma_p + F_s \cos (-\psi) \ldots \quad \text{(B-26)}$$

$$\sum F_Z = (L \cos \gamma_p) * \cos \phi + D \sin \gamma_p + F_t \sin (\theta + \theta_T) - w(t) \ldots \quad \text{(B-27)}$$

$$\sum M_X = (M_{ax} + D_x) \cos \theta \qquad \text{(B-28)}$$

$$\sum M_Y = May + Dy - \epsilon * F_t * \cos(\theta + \theta_T) * \cos(-\psi) * \cos \theta + \delta * D_p \ldots \qquad \text{(B-29)}$$

$$\sum M_Z = (M_{aZ} + D_Z) \cos \theta \qquad \text{(B-30)}$$

Where θ is defined in equation B-58, below; and the accelerations are:

$$\ddot{X} = \sum F_x / m(t) \qquad \text{(B-31)}$$

$$\ddot{Y} = \sum F_y / m(t) \qquad \text{(B-32)}$$

$$\ddot{Z} = \sum F_z / m(t) \qquad \text{(B-33)}$$

$$\ddot{\phi} = \sum M_x / I_x \qquad \text{(B-34)}$$

$$\ddot{\theta} = \sum M_y / I_y \qquad \text{(B-35)}$$

$$\ddot{\psi} = \sum M_z / I_z \qquad \text{(B-36)}$$

The velocities and displacements may be obtained by successive integration. The method used is as follows:

$$\dot{X}_i = \dot{X}_{i-1} + \Delta t * \ddot{X}_i \qquad \text{(B-37)}$$

$$\dot{Y}_i = \dot{Y}_{i-1} + \Delta t * \ddot{Y}_i \qquad \text{(B-38)}$$

$$\dot{Z}_i = \dot{Z}_{i-1} + \Delta t * \ddot{Z}_i \qquad \text{(B-39)}$$

$$\dot{\theta}_i = \dot{\theta}_{i-1} + \Delta t * \ddot{\theta}_i \qquad \text{(B-40)}$$

$$\dot{\phi}_i = \dot{\phi}_{i-1} + \Delta t * \ddot{\phi}_i \qquad \text{(B-41)}$$

$$\dot{\psi}_i = \dot{\psi}_{i-1} + \Delta t * \ddot{\psi}_i \qquad \text{(B-42)}$$

$$\Delta X_i = \Delta t * \dot{X}_i - \tfrac{1}{2} \Delta t^2 * \ddot{X}_i \qquad \text{(B-43)}$$

$$\Delta Y_i = \Delta t * \dot{Y}_i - \tfrac{1}{2} \Delta t^2 * \ddot{Y}_i \qquad \text{(B-44)}$$

$$\Delta Z_i = \Delta t * \dot{Z}_i - \tfrac{1}{2} \Delta t^2 * \ddot{Z}_i \qquad \text{(B-45)}$$

$$\Delta \theta_i = \Delta t * \dot{\theta}_i - \tfrac{1}{2} \Delta t^2 * \ddot{\theta}_i \qquad \text{(B-46)}$$

$$\Delta \phi_i = \Delta t * \dot{\phi}_i - \tfrac{1}{2} \Delta t^2 * \ddot{\phi}_i \qquad \text{(B-47)}$$

$$\Delta \psi_i = \Delta t * \dot{\psi}_i - \tfrac{1}{2} \Delta t^2 * \ddot{\psi}_i \qquad \text{(B-48)}$$

then,

$$X = \sum \Delta X_i \tag{B-49}$$

$$Y = \sum \Delta Y_i \tag{B-50}$$

$$Z = \sum \Delta Z_i \tag{B-51}$$

$$\theta = \sum \Delta \theta_i \tag{B-52}$$

$$\phi = \sum \Delta \phi_i \tag{B-53}$$

$$\psi = \sum \Delta \psi_i \tag{B-54}$$

and,

$$X_R = X_{R_O} + \sum \Delta X_i \tag{B-55}$$

$$Y_R = Y_{R_O} + \sum \Delta Y_i \tag{B-56}$$

$$Z_R = Z_{R_O} + \sum \Delta Z_i \tag{B-57}$$

$$\theta_R = \theta_{R_O} + \sum \Delta \theta_i \tag{B-58}$$

$$\phi_R = \phi_{R_O} + \sum \Delta \phi_i \tag{B-59}$$

$$\psi_R = \psi_{R_O} + \sum \Delta \psi_i \tag{B-60}$$

then since,

$$\gamma_p = \arctan -\dot{Z}/\dot{X} \tag{B-61}$$

and,

$$\gamma_y = \arctan -\dot{Y}/\dot{X} \tag{B-62}$$

it follows that

$$\alpha = \theta_R + \gamma_p = \theta_R + \arctan -\dot{Z}/\dot{X} \tag{B-63}$$

$$\beta = \psi_R + \gamma_Y = \psi_R + \arctan -\dot{Y}/\dot{X} \tag{B-64}$$

The specific fuel consumption is computed as a function of velocity and altitude:

$$S_{F_C} = 0.0007466667V - 0.0000021\ Z_R + 0.673 \tag{B-65}$$

and, the amount of fuel consumed is expressed as:

$$FC_i = FC_{i-1} + S_{F_C} * \Delta t * F_t / 3600 \qquad \text{(B-66)}$$

The damping moment in pitch was changed from one developed at SAEC to a more useful aerodynamic damping moment

$$Dy = q * A * l_k * C_{M_D} \qquad \text{(B-67)}$$

$$C_{M_D} = \Delta\alpha \frac{\delta C_{M(\alpha)}}{\delta \alpha} \qquad \text{(B-68)}$$

where

$$\Delta\alpha = \frac{\dot{\theta} * \ell}{v} * \sin(\alpha - \beta) \qquad \text{(B-69)}$$

$$\beta = \arctan \left[\frac{\left(\frac{x}{lk}\right)_{CG} - \left(\frac{x}{lk}\right)_{CP}}{\left(\frac{z}{lk}\right)_{CG} - \left(\frac{z}{lk}\right)_{CP}} \right] \qquad \text{(B-70)}$$

$$\ell = \left\{ \left[\left(\frac{x}{lk}\right)_{CG} - \left(\frac{x}{lk}\right)_{CP} \right]^2 + \left[\left(\frac{z}{lk}\right)_{CG} - \left(\frac{z}{lk}\right)_{CP} \right]^2 \right\}^{\frac{1}{2}} * l_k \qquad \text{(B-71)}$$

$$\left(\frac{x}{lk}\right)_{CP} = \frac{1}{2} - \frac{Cm(\alpha) \quad \left\{ \text{for } \frac{x}{lk} = \frac{1}{2},\ \frac{z}{lk} = 0 \right\}}{C_{L_W} \cos \alpha_w + C_{D_W} \sin \alpha_w} \qquad \text{(B-72)}$$

$$\left(\frac{z}{lk}\right)_{CP} = 0 \qquad \text{(B-73)}$$

THE COMPUTER PROGRAM

A generous number of comment cards have been included in the program deck for ease in "setting up" the input, and understanding the output, and the major parts of the program. A few comments are included here to point out certain features examined.

1. Sense switch 5 controls the printout. An input constant (PCOT) specifies the number of integration steps to be performed between each print order. However at any time in the execution of the program every integration step may be printed out by turning SS5 to the "ON" position.

2. The coefficients of the equation used to determine the specific fuel consumption (SFC) are fixed in the program (i.e. they are not included in the input data). The equation appears only once (the forth statement prior to statement 891).

$$SFC = 0.001634 * V - 0.000004 * ZR + 0.480$$

If a change is desired in the specific fuel consumption it is necessary that the appropriate expression replace the one now used and the program be compiled.

3. A stop order has been included in the event the angle of attack in pitch (ALPHA) becomes negative. If this occurs the computer will print "ALPHA IS NEGATIVE", the time of occurrence, the value of ALPHA is degrees, and will then stop computing.

4. A stop order is included in the event of fuel depletion. If this occurs the computer will print "FUEL DEPLETION", and the time of occurrence. The thrust is made zero and the program will continue with AERCAB in a glide status.

5. A stop is included in the event the altitude becomes negative. If this occurs the computer will print "IMPACT" and the time.

6. A stop on time is also included, a final time "F TIME" is included in the input data if this is reached the computer will print "PROGRAM COMPLETED" and halt.

TABLE B-1

AERCAB 5

INPUT DEFINITIONS

Nomenclature	Definitions	Units
WGT	Total Weight	lbs.
IX	Moment of inertia about roll axis	sl.-ft.^{2}
IY	Moment of inertia about pitch axis	sl.-ft.^{2}
IZ	Moment of inertia about yaw axis	sl.-ft.^{2}
KD	Pitch-moment damping coefficient	lb.-sec.^{2}
AREA	Reference area	ft.^{2}
B	Wing span	ft.
LK	Keel length	ft.
XLK	Ratio (x - c.g. dist. from keel leading edge/keel length)	---
ZLK	Ratio (z - c.g. dist. from keel axis/keel length)	---
ITHR	Idle thrust	lbs.
CTHR	Cruise thrust	lbs.
DTIME	Time required for thrust buildup	sec.
THAD	Nozzle angle	degrees
FUEL	Fuel loading	lbs.
OTIME	Initial time	sec.
FTIME	Final time	sec.
DELT	Time increment	sec.
E	Vertical displacement of thrust vector from system c.g.	ft.
DELTA	Vertical displacement of payload drag	ft.
PCOT	Number of integration steps executed between printouts	---
XRO	Initial range	ft.
YRO	Initial lateral displacement	ft.
ZRO	Initial altitude	ft.
XD	Horizontal component of velocity	ft./sec.
YD	Vertical component of velocity	ft./sec.
ZD	Lateral component of velocity	ft./sec.
THETA	Pitch angle	degrees
PHI	Roll angle	degrees
PSI	Yaw angle	degrees
DTHD	Pitch angular velocity	deg./sec.
DPHID	Roll angular velocity	deg./sec.
DPSID	Yaw angular velocity	deg./sec.
CDP	Payload drag coefficient	deg./sec.
DEL1	Vertical displacement of strut drag vector from system c.g.	ft.
CDST	Strut drag coefficient	---

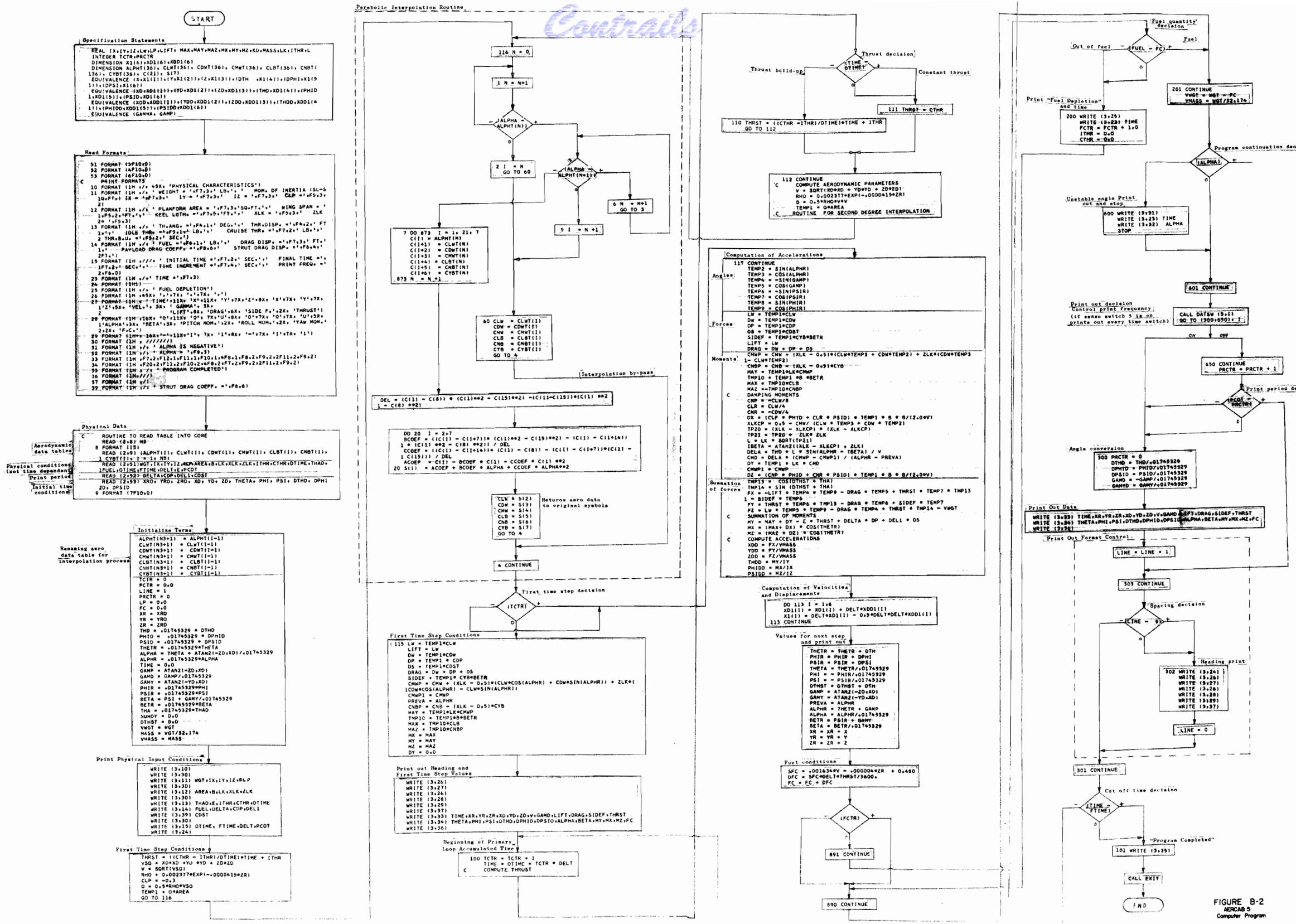

FIGURE B-2
AERCAB 5
Computer Program

```
// JOB
// FOR
*EXTENDED PRECISION
*ONE WORD INTEGERS
*IOCS (CARD, 1132 PRINTER, DISK)
* LIST SOURCE PROGRAM
*NAME ARCB5
C
C      INPUT DATA
C
C      THE FIRST 55 CARDS CONTAIN VALUES OF SIX AERODYNAMIC COEFFICIENTS.
C      A TABLE OF VALUES OF CL,CD,CM,CLBETA,CNBETA,CYBETA, AS FUNCTIONS
C      OF THE ANGLE OF ATTACK ALPHA ARE READ IN. A SECOND DEGREE INTERPOL
C      ATION IS USED.THE READ ORDER IS THE FIRST STATEMENT FOLLOWING STAT
C      EMENT NO. 8.
C
C                     ****************************************
C
C      PHYSICAL DATA
C
C      CARD NO. 1
C
C         1. TOTAL WEIGHT = WGT (LB.)
C         2. MOMENT OF INERTIA ABOUT ROLL AXIS = IX (SL-SQ.FT.)
C         3. MOMENT OF INERTIA ABOUT PITCH AXIS = (SL-SQ.FT.)
C         4. MOMENT OF INERTIA ABOUT YAW AXIS = IZ (SL-SQ.FT.)
C         5. ROLL - MOMENT DAMPING DERIVATIVE = CLP
C
C      CARD NO. 2
C
C         1. REFERENCE AREA = AREA (SQ.FT.)
C         2. WING SPAN = B (FT.)
C         3. KEEL LENGTH = LK (FT.)
C         4. RATIO(OF DIST. FROM LEADING EDGE OF KEEL TO INTERSECTION OF
C            LINE NORMAL TO KEEL AND PASSING THROUGH SYSTEM CG: TO (THE
C            KEEL LENGTH) = XLK
C         5. RATIO OF (PERPENDICULAR DISTANCE FROM SYSTEM C.G TO KEEL) TO
C            (THE KEEL LENGTH) = ZLK
C
C      CARD NO. 3
C
C         1. IDLE THRUST = ITHR (LB.)
C         2. CRUISE  THRUST = CTHR  (LB.)
C         3. TIME  REQUIRED FOR THRUST BUILDUP = DTIME (SEC.)
C         4. NOZZLE ANGLE = THAD (DEG.)
C         5. FUEL LOADING = FUEL (LB.)
C
C      CARD NO. 4
C
C         1. INITIAL TIME = OTIME (SEC.)
C         2. FINAL TIME = FTIME (SEC.)
C         3. TIME INCREMENT = DELT (SEC.)
C         4. VERTICAL DISPLACEMENT OF THRUST VECTOR FROM SYSTEM C.G. (FT.)
C         5. NUMBER OF INTEGRATION STEPS TO BE EXECUTED BETWEEN PRINTOUTS.
C
C      CARD NO. 5
C
C         1. VERTICAL DISPLACEMENT OF PAYLOAD DRAG VECTOR FROM SYSTEM
C            C.G. (FT.)
C         2. PAYLOAD DRAG COEFFICIENT
C         3. VERTICAL DISPLACEMENT OF STRUT DRAG VECTOR FROM SYSTEM C.G.
C            (FT.)
C         4. STRUT DRAG COEFFICIENT
C
```

```
C     CARD NO. 6
C
C
C     INITIAL CONDITIONS
C
C        1. INITIAL RANGE = XRO (FT.)
C        2. INITIAL LATERAL DISPLACEMENT = YRO (FT.)
C        3. INITIAL ALTITUDE = ZRO (FT.)
C        4. HORIZONTAL COMPONENT OF VELOCITY = XD (FT./SEC.)
C        5. LATERAL COMPONENT OF VELOCITY = YD (FT./SEC.)
C        6. VERTICAL COMPONENT OF VELOCITY = ZD (FT./SEC.)
C
C     CARD NO. 7
C
C        1. PITCH ANGLE = THETA (DEG.)
C        2. ROLL ANGLE = PHI (DEG.)
C        3. YAW ANGLE = PSI (DEG.)
C        4. PITCH ANGULAR VELOCITY = THD (DEG./SEC.)
C        5. ROLL ANGULAR VELOCITY = PHID (DEG./SEC.)
C        6. YAW ANGULAR VELOCITY = PSID (DEG./SEC.)
C
C                          OUTPUT DATA
C
C      THE FIRST PRINTOUTS EXECUTED WRITE THE INPUT DATA AND ARE SELF EX-
C      PLANATORY.
C
C      FOR EACH LINE OF PRINT THEREAFTER THE FOLLOWING ARE PRINTED IN TWO
C      LINES.  READING FIRST LINE FROM LEFT TO RIGHT.
C
C        1. TIME = TIME (SEC.).
C        2. RANGE = XR (FT.).
C        3. LATERAL DISPLACEMENT = YR (FT.).
C        4. ALTITUDE = ZR (FT.).
C        5. HORIZONTAL VELOCITY = XD (FT./SEC.).
C        6. LATERAL VELOCITY = YR (FT./SEC.).
C        7. VERTICAL VELOCITY = ZR (FT./SEC.).
C        8. RESULTANT VELOCITY = V (FT./SEC.).
C        9. ANGLE BETWEEN WIND VECTOR AND LOCAL HORIZ. = GAMD (DEG.)
C       10. LIFT = LIFT (LB.)
C       11. DRAG = DRAG (LB.)
C       12. SIDE FORCE = SIDEF (LB.).
C       13. THRUST LEVEL = THRST (LB.).
C
C      READING SECOND LINE FROM LEFT TO RIGHT.
C
C        1. PITCH ANGLE BETWEEN KEEL AND LOCAL HORIZ. (DEG.).
C        2. ROLL ANGLE = PHI (DEG.).
C        3. YAW ANGLE = PSI (DEG.).
C        4. ANGULAR VELOCITY IN PITCH = DTHD (DEG./SEC.).
C        5. ANGULAR VELOCITY IN ROLL = DPHID (DEG./SEC.).
C        6. ANGULAR VELOCITY IN YAW = DPSID (DEG./SEC.).
C        7. ANGLE OF ATTACK IN PITCH = ALPHA (DEG.).
C        8. ANGLE OF ATTACK IN YAW = BETA (DEG.).
C        9. PITCH MOMENT = MX (FT.-LB.).
C       10. ROLL MOMENT = MY (FT.-LB.).
C       11. YAW MOMENT = MZ (FT.-LB.).
C       12. AMOUNT OF FUEL CONSUMED (LB.).
C
C
C           NOTE--- EACH STEP MAY BE PRINTED OUT BY TURNING SS 5 ON.
C
C
      REAL IX,IY,IZ,LW,LP,LIFT, MAX,MAY,MAZ,MX,MY,MZ,   MASS,LK,ITHR,L
      REAL IBETA
```

```
      INTEGER TCTR,PRCTR
      DIMENSION X1(6),XD1(6),XDD1(6)
      DIMENSION ALPHT(60), CLWT(60), CDWT(60), CMWT(60), CLBT(60), CNBT(
     160), CYBT(60), C(21), S(7)
      EQUIVALENCE (X,X1(1)),(Y,X1(2)),(Z,X1(3)),(DTH  ,X1(4)),(DPHI,X1(5
     1)),(DPSI,X1(6))
      EQUIVALENCE (XD,XD1(1)),(YD,XD1(2)),(ZD,XD1(3)),(THD,XD1(4)),(PHID
     1,XD1(5)),(PSID,XD1(6))
      EQUIVALENCE (XDD,XDD1(1)),(YDD,XDD1(2)),(ZDD,XDD1(3)),(THDD,XDD1(4
     1)),(PHIDD,XDD1(5)),(PSIDD,XDD1(6))
      EQUIVALENCE (GAMMA, GAMP)
C     READ FORMATS
   51 FORMAT (5F10.0)
   52 FORMAT (4F10.0)
   53 FORMAT (6F10.0)
C     PRINT FORMATS
   10 FORMAT (1H ,/, 45X, 'PHYSICAL CHARACTERISTICS')
   11 FORMAT (1H ,/, ' WEIGHT = ',F7.3,' LB.', '   MOM. OF INERTIA (SL-S
     1Q.FT.) IX = ',F7.3,'   IY = ',F7.3,'   IZ = ',F7.3,'  CLP =',F5.3,
     2)
   12 FORMAT (1H ,/, ' PLANFORM AREA = ',F7.3,'SQ.FT.',',   WING SPAN = '
     1,F5.2,'FT.',',   KEEL LGTH. =',F7.5,'FT.',',   XLK = ',F5.3,'   ZLK
     2= ',F5.3)
   13 FORMAT (1H ,/, ' TH.ANG. =',F4.1,' DEG.',',  THR.DISP. =',F4.2,' FT
     1.',',   IDLE THR. =',F5.1,' LB.',',    CRUISE THR. =',F7.2,' LB.','
     2 THR.B.U. =',F5.2,' SEC.')
   14 FORMAT (1H ,/, ' FUEL =',F6.1,' LB.',',   DRAG DISP. =',F7.3,' FT.'
     1,',    PAYLOAD DRAG COEFF. =',F8.6,',    STRUT DRAG DISP. =',F6.4,'
     2FT.')
   15 FORMAT (1H ,///, ' INITIAL TIME =',F7.2,' SEC.',',   FINAL TIME =',
     1F7.2,' SEC.',',   TIME INCREMENT =',F7.4,' SEC.',',   PRINT FREQ. ='
     2,F6.0)
   23 FORMAT (1H ,/,' TIME =',F7.3)
   24 FORMAT (1H1)
   25 FORMAT (1H ,/, ' FUEL DEPLETION')
   26 FORMAT (1H ,45X, '.',7X, '.',7X, '.')
   27 FORMAT (1H , ' TIME',11X, 'X',11X, 'Y',7X,'Z',8X, 'X',7X, 'Y',7X,
     1'Z',5X, 'VEL.', 3X, ' GAMMA', 3X,
     2                    'LIFT',8X, 'DRAG',6X, 'SIDE F.',2X, 'THRUST')
   28 FORMAT (1H ,16X, '0',11X, '0', 7X,'U',8X, '0',7X, '0',7X, 'U',5X,
     1'ALPHA',3X, 'BETA',3X, 'PITCH MOM.',2X, 'ROLL MOM.',2X, 'YAW MOM.'
     2,2X, 'F.C.')
   29 FORMAT (1H+, 16X,'-',11X,'I', 7X, 'I',8X, '-',7X, 'I',7X, 'I')
   30 FORMAT (1H , ///////)
   31 FORMAT (1H ,/, ' ALPHA IS NEGATIVE')
   32 FORMAT (1H ,/, ' ALPHA = ',F9.3)
   33 FORMAT (1H ,F7.2,F12.1,F11.1,F10.1,4F8.1,F8.2,F9.2,2F11.2,F9.2)
   34 FORMAT (1H ,F20.2,F11.2,F10.2,4F8.2,F7.2,F9.2,2F11.2,F9.2)
   35 FORMAT (1H , /, ' PROGRAM COMPLETED')
   36 FORMAT (1H,///)
   37 FORMAT (1H ,/)
   39 FORMAT (1H ,/, ' STRUT DRAG COEFF. =',F8.6)
   40 FORMAT (1H , ' IMPACT')
C     PHYSICAL DATA
C     ROUTINE TO READ TABLE INTO CORE
      READ (2,8) N3
    8 FORMAT (I5)
      READ (2,9) (ALPHT(I), CLWT(I), CDWT(I), CMWT(I), CLBT(I), CNBT(I),
     1 CYBT(I), I = 1, N3)
      READ (2,51) WGT,IX,IY,IZ,CLP,AREA,B,LK,XLK,ZLK,ITHR,CTHR,DTIME,THA
     2D,FUEL,OTIME,FTIME,DELT,E,PCOT
      READ (2,52) DELTA,CDP,DEL1,CDST
      READ (2,53) XRO, YRO, ZRO, XD, YD, ZD, THETA, PHI, PSI, DTHD, DPHI
     2D, DPSID
```

```
  9 FORMAT (7F10.0)
    ALPHT(N3+1)  = ALPHT(I-1)
    CLWT(N3+1)   = CLWT(I-1)
    CDWT(N3+1)   =  CDWT(I-1)
    CMWT(N3+1)   = CMWT(I-1)
    CLBT(N3+1)   =  CLBT(I-1)
    CNBT(N3+1)   = CNBT(I-1)
    CYBT(N3+1)   =  CYBT(I-1)
    TCTR = 0
    FCTR = 0.0
    LINE = 1
    PRCTR = 0
    LP = 0.0
    FC = 0.0
    XR = XRO
    YR = YRO
    ZR = ZRO
    THD = .01745329 * DTHD
    PHID =  .01745329 * DPHID
    PSID = .01745329 * DPSID
    THETR = .01745329*THETA
    ALPHA = THETA + ATAN2(-ZD,XD)/.01745329
    ALPHR = .01745329*ALPHA
    TIME = 0.0
    GAMP = ATAN2(-ZD,XD)
    GAMD = GAMP/.01745329
    GAMY = ATAN2(-YD,XD)
    PHIR = .01745329*PHI
    PSIR = .01745329*PSI
    BETA = PSI + GAMY/.01745329
    BETR = .01745329*BETA
    THA = .01745329*THAD
    SUMDY = 0.0
    DTHST = 0.0
    VWGT = WGT
    MASS = WGT/32.174
    VMASS = MASS
    WRITE (3,10)
    WRITE (3,30)
    WRITE (3,11) WGT,IX,IY,IZ,CLP
    WRITE (3,30)
    WRITE (3,12) AREA,B,LK,XLK,ZLK
    WRITE (3,30)
    WRITE (3,13) THAD,E,ITHR,CTHR,DTIME
    WRITE (3,14) FUEL,DELTA,CDP,DEL1
    WRITE (3,39) CDST
    WRITE (3,30)
    WRITE (3,15) OTIME, FTIME,DELT,PCOT
    WRITE (3,24)
    THRST = ((CTHR - ITHR)/DTIME)*TIME + ITHR
    VSQ = XD*XD +YD *YD + ZD*ZD
    V = SQRT(VSQ)
    RHO = 0.002377*EXP(-.0000415*ZR)
    Q = 0.5*RHO*VSQ
    TEMP1 = Q*AREA
    GO TO 116
115 LW = TEMP1*CLW
    LIFT = LW
    DW = TEMP1*CDW
    DP = TEMP1 * CDP
    DS = TEMP1*CDST
    DRAG = DW + DP + DS
    CMWP = CMW + (XLK - 0.5)*(CLW*COS(ALPHR) + CDW*SIN(ALPHR)) + ZLK*(
   1CDW*COS(ALPHR) - CLW*SIN(ALPHR))
```

```
      CMWP1 = CMWP
      PREVA = ALPHR
      CNBP = CNB - (XLK - 0.5)*CYB
      SIDEF = TEMP1*CYB*BETR
      MAY = TEMP1*LK*CMWP
      TMP10 = TEMP1 * B
      MAX = TMP10*CLB*BETR
      MAZ = -TMP10*CNBP*BETR
      MX = MAX
      MY = MAY
      MZ = MAZ
      DY = 0.0
      WRITE (3,26)
      WRITE (3,27)
      WRITE (3,26)
      WRITE (3,28)
      WRITE (3,29)
      WRITE (3,37)
      WRITE (3,33) TIME,XR,YR,ZR,XD,YD,ZD,V,GAMD,LIFT,DRAG,SIDEF,THRST
      WRITE (3,34) THETA,PHI,PSI,DTHD,DPHID,DPSID,ALPHA,BETA,MY,MX,MZ,FC
      WRITE (3,36)
C     PRIMARY LOOP
  100 TCTR = TCTR + 1
      TIME = OTIME + TCTR * DELT
C     COMPUTE THRUST
      IF (TIME -DTIME) 110,111,111
  110 THRST = ((CTHR -ITHR)/DTIME)*TIME + ITHR
      GO TO 112
  111 THRST = CTHR
  112 CONTINUE
C     COMPUTE AERODYNAMIC PARAMETERS
      V = SQRT(XD*XD + YD*YD + ZD*ZD)
      RHO = 0.002377*EXP(-.0000415*ZR)
      Q = 0.5*RHO*V*V
      TEMP1 = Q*AREA
C    ROUTINE  FOR SECOND DEGREE INTERPOLATION
  116 N = 0
      CALL TSTOP
    1 N = N+1
      IF (ALPHA -ALPHT(N)) 1,2, 3
    3 IF (ALPHA -ALPHT(N+1)) 7, 5, 6
    5 I  = N +1
   60 CLW  = CLWT(I)
      CDW = CDWT(I)
      CMW  = CMWT(I)
      CLB  = CLBT(I)
      CNB  = CNBT(I)
      CYB  = CYBT(I)
      GO TO 4
    6 N  = N+1
      GO TO 3
    7 DO 873  I = 1, 21, 7
      C(I) = ALPHT(N)
      C(I+1)  = CLWT(N)
      C(I+2)  = CDWT(N)
      C(I+3)  = CMWT(N)
      C(I+4) = CLBT(N)
      C(I+5)  = CNBT(N)
      C(I+6)  = CYBT(N)
  873 N  = N +1
      DEL = (C(1) - C(8)) * (C(1)**2 - C(15)**2) -(C(1)-C(15))*(C(1) **2
     1 - C(8) **2)
      DO 20  I = 2,7
      BCOEF = ((C(I) - C(I+7))* (C(1)**2 - C(15)**2) - (C(I) - C(I+14))
```

```
     1 * (C(1) **2 - C(8) **2)) / DEL
      CCOEF = ((C(I) - C(I+14))* (C(1) - C(8)) - (C(I) - C(I+7))*(C(1) -
     1 C(15))) / DEL
      ACOEF  = C(I) - BCOEF * C(1) - CCOEF * C(1) **2
   20 S(I)  = ACOEF + BCOEF * ALPHA + CCOEF * ALPHA**2
      CALL TSTRT
      CLW = S(2)
      CDW = S(3)
      CMW = S(4)
      CLB = S(5)
      CNB = S(6)
      CYB = S(7)
      GO TO 4
    2 I  = N
      GO TO 60
    4 CONTINUE
      CALL TSTRT
      IF (TCTR) 117, 115, 117
  117 CONTINUE
      TEMP2 = SIN(ALPHR)
      TEMP3 = COS(ALPHR)
      TEMP4 = -SIN(GAMP)
      TEMP5 = COS(GAMP)
      TEMP6 = -SIN(PSIR)
      TEMP7 = COS(PSIR)
      TEMP8 = SIN(PHIR)
      TEMP9 = COS(PHIR)
      TMP50 = SIN(GAMY)
      LW = TEMP1*CLW
      DW = TEMP1*CDW
      DP = TEMP1*CDP
      DS = TEMP1*CDST
      LIFT = LW
      DRAG = DW + DP + DS
      CMWP = CMW + (XLK - 0.5)*(CLW*TEMP3 + CDW*TEMP2) + ZLK*(CDW*TEMP3
     1- CLW*TEMP2)
      CNBP = CNB - (XLK - 0.5)*CYB
      SIDEF = TEMP1*CYB*BETR
      MAY = TEMP1*LK*CMWP
      TMP10 = TEMP1 * B
      MAX = TMP10*CLB*BETR
      MAZ = -TMP10*CNBP*BETR
C     DAMPING MOMENTS
      CNP = -CLW/8
      CLR = CLW/4
      CNR = -CDW/4
      DX = (CLR * PSID - CLP *PHID) * TEMP1 * B * B/(2.0*V)
      XLKCP = 0.5 - CMW/ (CLW * TEMP3.+ CDW * TEMP2)
      TP20 = (XLK - XLKCP) * (XLK - XLKCP)
      TP21 = TP20 +  ZLK* ZLK
      L = LK * SQRT(TP21)
      IBETA = ATAN2((XLK - XLKCP) , ZLK)
      DELA = THD * L * SIN(ALPHR - IBETA) / V
      CMD = DELA * (CMWP - CMWP1) / (ALPHR - PREVA)
      DY = TEMP1 * LK * CMD
      CMWP1 = CMWP
      DZ = (CNP *.PHID + CNR * PSID) * TEMP1 * B * B/(2.0*V)
C     SUMMATION OF FORCES
      TMP13 =  COS(DTHST + THA)
      TMP14 = SIN (DTHST + THA)
      FX = -LIFT * TEMP4 * TEMP9 - DRAG * TEMP5 + THRST * TEMP7 * TMP13
     1 - SIDEF * TEMP6
      SF2 = 0.5*WGT*SIN(2.0*PHIR)
      FY = THRST*TEMP6*TMP13 + DRAG*TMP50 + SIDEF*TEMP7 - SF2
```

```
      FZ = LW * TEMP5 * TEMP9 - DRAG * TEMP4 + THRST * TMP14 - VWGT
C     SUMMATION OF MOMENTS
      MY = MAY + DY - E * THRST + DELTA * DP + DEL1 * DS
      MX = (MAX + DX) * COS(THETR)
      MZ = (MAZ + DZ) * COS(THETR)
C     COMPUTE ACCELERATIONS
      XDD = FX/VMASS
      YDD = FY/VMASS
      ZDD = FZ/VMASS
      THDD = MY/IY
      PHIDD = MX/IX
      PSIDD = MZ/IZ
      DO 113 I = 1,6
      XD1(I) = XD1(I) + DELT*XDD1(I)
      X1(I) = DELT*XD1(I) - 0.5*DELT*DELT*XDD1(I)
  113 CONTINUE
      THETR = THETR + DTH
      PHIR = PHIR + DPHI
      PSIR = PSIR + DPSI
      THETA = THETR/.01745329
      PHI = PHIR/.01745329
      PSI = PSIR/.01745329
      DTHST = DTHST + DTH
      GAMP = ATAN2(-ZD,XD)
      GAMY = ATAN2(-YD,XD)
      PREVA = ALPHR
      ALPHR = THETR + GAMP
      ALPHA = ALPHR/.01745329
      BETR = PSIR + GAMY
      BETA = BETR/.01745329
      XR = XR + X
      YR = YR + Y
      ZR = ZR + Z
      SFC = .001634*V - .000004*ZR  + 0.480
      DFC = SFC*DELT*THRST/3600.
      FC = FC + DFC
      IF (FCTR) 890,891,890
  891 CONTINUE
      IF (FUEL - FC) 200,200,201
  200 WRITE (3,25)
      WRITE (3,23) TIME
      FCTR = FCTR + 1.0
      ITHR = 0.0
      CTHR = 0.0
  890 CONTINUE
  201 CONTINUE
      VWGT = WGT - FC
      VMASS = WGT/32.174
      IF (ALPHA) 600, 601, 601
  600 WRITE (3,31)
      WRITE (3,23) TIME
      WRITE (3,32)  ALPHA
      STOP
  601 CONTINUE
      CALL DATSW (5,I)
      GO TO (300,650), I
  650 CONTINUE
      PRCTR = PRCTR + 1
      IF (PCOT - PRCTR) 300,300,303
  300 PRCTR = 0
      DTHD = THD/.01745329
      DPHID = PHID/.01745329
      DPSID = PSID/.01745329
      GAMD = -GAMP/.01745329
```

```
      GAMYD = GAMY/.01745329
      WRITE (3,33) TIME,XR,YR,ZR,XD,YD,ZD,V,GAMD,LIFT,DRAG,SIDEF,THRST
      WRITE (3,34) THETA,PHI,PSI,DTHD,DPHID,DPSID,ALPHA,BETA,MY,MX,MZ,FC
      WRITE (3,36)
      LINE = LINE + 1
  303 CONTINUE
      IF (LINE -  9) 301,302,302
  302 WRITE (3,24)
      WRITE (3,26)
      WRITE (3,27)
      WRITE (3,26)
      WRITE (3,28)
      WRITE (3,29)
      WRITE (3,37)
      LINE = 0
      IF (ZR) 331, 331, 301
  331 WRITE (3,40)
      WRITE (3,23) TIME
      STOP
  301 CONTINUE
      IF (TIME - FTIME) 100, 101, 101
  101 WRITE (3,35)
      CALL EXIT
      END
```

APPENDIX C

COUPLED AERCAB
FLIGHT PERFORMANCE PARAMETERS
COMPUTER PROGRAM

"PARAM"

APPENDIX C

"PARAM" COMPUTER PROGRAM

The purpose of the PARAM computer program was to provide a parametric analysis of steady flight performance. The program was used to find the effect of design cruise speed and the lift-to-drag ratio on the wing area. Results of computer runs were plotted on carpet plots of lift/drag and velocity versus wing area. They showed that, with a typical AERCAB arrangement, any increase in lift/drag did not appreciably improve performance. The high inherent drag generated by the man/seat payload over shadows any potential benefits that might have been expected through lift/drag increase.

The equations used in PARAM for the necessary relationships were:

$$S1 = \frac{WTC + \frac{R*SFC*CDSPL*Q}{2V}}{Q\left\{C_L - \left[\frac{CL}{(L/D)W} + CDST\right]\frac{R*SFC}{2V} - WTW\right\}} \qquad (C\text{-}1)$$

where,

...S1 is the wing area (sq.ft.) corresponding to an assigned value of lift/drag for the wing.

and

$$S2 = \frac{WTC}{CL * Q\left(1 - \frac{R*SFC}{2V*(L/D)T}\right) - WTW} \qquad (C\text{-}2)$$

where,

...S2 is the wing area (sq.ft.) corresponding to an assigned value of lift/drag for the total system.

SFC is the engine's specific fuel consumption calculated from:

$$SFC = 0.001634*V - 0.000004 * Z + 0.673$$

The specific fuel consumption is dependent on the engine selected The coefficients of the linear expression used are not entered as input data and any variation in the specific fuel consumption would require a modification of statement 100 + 008.

The other symbols and terms used in the equations are defined below. These equations were written and programmed for

application on the IBM 1130 computer. A flow chart of the complete program is included in Figure C-1.

The program is flexible enough to be applied to other lift/drag generators having the denoted lift-coefficient characteristics. It is not limited to parawing application.

Consider the equation (C-1) presented above,

where,

...S1 is the wing area (sq.ft.) corresponding to a certain value of (L/D)W

...WTC is the weight of items which have an invarient weight (man, seat, engine = 450 lbs.)

...R is the range in nautical miles (50 n.mi. constant)

...SFC is the engine's specific fuel consumption (lbs.-fuel per lb-thrust) has been calculated via the expression:

$$SFC = 0.0007466 * V - 0.0000021 * Z + 0.673 \qquad (C-3)$$

where,

...V = true airspeed, knots

...Z = pressure altitude, ft. (Z = 0 herein)

...CDSPL is the man/seat/engine effective drag area (CDSPL = 4.2 sq.ft.)

...Q is the dynamic pressure in lbs./sq.ft. and is equal to $1.42636\ \rho\ V^2$ where ρ is the mass density of the air in lb.-sec.^{2}/ft.^{4} (0.002377 @ S.L.), and 1.42636 is the conversion factor from knots to ft./sec.^{2} divided by 2

...CL is the wing lift coefficient

...(L/D)W is the wing's lift to drag ratio

...CDST is the drag coefficient of the suspension means (0.0334 used herein)

...WTW is the unit wing weight per unit wing area (1.337 lb./sq.ft. used herein)

...W_1 is the average cruise gross weight corresponding to wing area S_1 ($W = CL*Q*S_1$), lbs.

...FW_1 is the fuel weight corresponding to wing area S_1, ($FW_1 = 2 * \left[W_1 - WTW * S_1 - WTC\right]$, lbs.

...W_1T is the weight at mission onset corresponding to S_1($W_1T = W_1 + 1/2\ FW_1$), lbs.

...$(W/S)_1$ is the wing-loading, lbs./sq.ft. (W_1/S_1)

And now, considering the second equation (C-2) presented above, the terms therein are defined as:

...S_2 is the wing area, sq.ft., corresponding to a given (L/D)T

...(L/D)T is the total system lift to drag ratio

...W_2 is the average cruise gross weight, lbs., corresponding to S_2 ($W_2 = CL*Q*S_2$)

...FW2 is the fuel weight, lbs., corresponding to S_2 ($FW2 = 2\ \left[W_2 - WTW*S_2 - WTC\right]$)

...W2T is the weight at mission onset, lbs., corresponding to S_2(W2T = W_2 + 1/2 FW2)

...DT is the total drag of the system, lbs., corresponding to (L/D)T,

$$DT = \frac{W_2}{(L/D)T}$$

...$(W/S)_2$ is the wing-loading, lbs./sq.ft., (W_2/S_2)

TABLE C-1

"PARAM" COMPUTER PROGRAM

INPUT DEFINITIONS

Nomenclature	Definition	Units
DELCL	Variation in lift coefficient	---
DELV	Increment variation in velocity	knots
Y	Pressure altitude	ft.
RHO	Air density at altitude Y	lb./sec^2/ft^4
CDSPL	Man/seat/engine effective drag area	ft.^{2}
CDST	Strut drag coefficient	---
WTW	Unit wing weight per unit wing area	lb./sq.ft.
WTC	Weight of invarient items (man, seat, engine)	lbs.
R	Range	n.mi.
V1	True velocity (initial)	knots
CL1	Wing lift coefficient (initial)	---
NCL	Number of lift coefficient increments	---
NV	Number of velocity increments	---
LDW	Lift to drag ratio for wing	---
LDT	Lift to drag ratio for total systems	---

OUTPUT DEFINITIONS

V	Velocity	knots
Y	Altitude	ft.
CL	Wing lift coefficient	---
S1	Wing area corresponding to certain LDW	sq.ft.
W1	Ave. cruise gross weight corresponding to S1	lbs.
FW1	Fuel weight corresponding to S1	lbs.
W1T	Weight at mission onset corresponding to S1	lbs.
WS1	Wing loading (W/S)1	lb./sq.ft.
S2	Wing area corresponding to given LDT	sq.ft.
W2	Ave. cruise gross weight corresponding to S2	lbs.
FW2	Fuel weight corresponding to S2	lbs.
WST	Weight at mission onset corresponding to S2	lbs.
WS2	Wing loading $(W/S)_2$	lbs./sq.ft.
DT	Total drag of system corresponding to LDT	lbs.

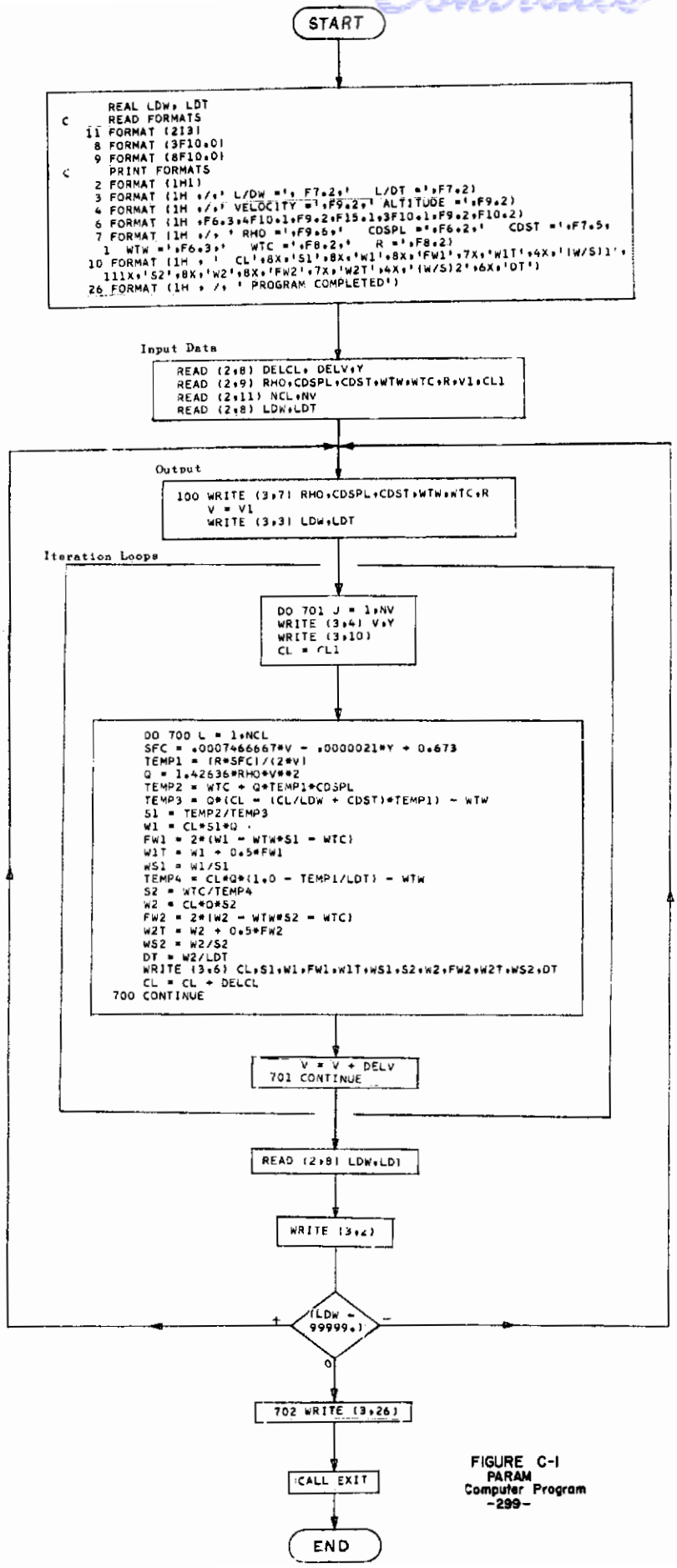

FIGURE C-I
PARAM
Computer Program

```
// JOB
// FOR
*EXTENDED PRECISION
* LIST SOURCE PROGRAM
*ONE WORD INTEGERS
*IOCS (CARD, 1132 PRINTER, DISK)
**NAME PARAM
C
C                          INPUT DATA
C
C     THE INPUT DATA IS READ IN BY MEANS OF FOUR DATA CARDS.  THE READ
C     ORDERS ARE THE FOUR STATEMENTS THAT FOLLOW STATEMENT NO. 26.
C
C     CARD NO. 1
C
C       1. DELCL = INCREMENT OF VARIATION IN AERO. LIFT COEFFICIENT.
C       2. DELV = INCREMENTAL VARIATION IN VELOCITY  (KNOTS).
C       3. Y = ALTITUDE (FT.).
C
C     CARD NO. 2
C
C       1. RHO = AIR DENSITY AT ALTITUDE Y (LB.-SECSQ/FT. TO FOURTH POWER).
C       2. CDSPL = MAN/SEAT/ENGINE EFFECTIVE DRAG AREA (SQ.FT.).
C       3. CDST = STRUT DRAG COEFFICIENT.
C       4. WTW = UNIT WING WEIGHT PER UNIT WING AREA (LB./SQ.FT.).
C       5. WTC = WEIGHT OF INVARIANT ITEMS, MAN, SEAT, ENGINE, ETC. (LB.).
C       6. R = RANGE (NAUT. MILES).
C       7. VI = TRUE INITIAL VELOCITY. (KNOTS).
C       8. CL1 = INITIAL WING LIFT COEFF.
C
C     CARD NO. 3
C
C       1. NCL = NO. OF LIFT COEFFICIENT INCREMENTS.
C       2. NV = NO. OF VELOCITY INCREMENTS.
C
C     CARD NO. 4
C
C       1. LDW = LIFT TO DRAG RATIO FOR WING.
C       2. LDT = LIFT TO DRAG RATIO FOR TOTAL SYSTEM.
C
C                          OUTPUT DATA
C
C     THE FIRST TWO LINES OF PRINTOUT ARE INPUT DATA AND/OR INITIAL COND.
C     THE FIRST LINE WRITES RHO,CDSPL,CDST,WTW,WTC,R, THE SECOND LINE IS
C     LDW AND LDT (SEE DEFINITIONS ABOVE).
C     SUCCESSIVELY THEREAFTER FOR A SPECIFIED ALTITUDE AND INCREMENTALLY
C     VARYING VELOCITY AND LIFT COEFFICIENT THE FOLLOWING ARE LISTED.
C
C       1. S1 = WING AREA CORRESPONDING TO A SPECIFIED L/DW (SQ. FT.).
C       2. W1 = AV CRUISE GROSS WEIGHT (LB.).
C       3. FW1 = FUEL WEIGHT CORRESPONDING TO S1 (LB.).
C       4. W1T = WEIGHT AT MISSION ONSET CORRESPONDING TO S1 (LB.).
C       5. WS1 = WING LOADING (LB./SQ.FT.)
C       6. S2 = WING AREA CORRESPONDING TO GIVEN LDT (SQ. FT.).
C       7. W2 = AV. CRUISE GROSS WEIGHT CORRESPONDING TO S2 (LB.).
C       8. FW2 = FUEL WEIGHT CORRESPONDING TO S2 (LB.).
C       9. WST = WEIGHT AT MISSION ONSET CORRESPONDING TO S2 (LB.).
C      10. SW2 = WING LOADING (LB./SQ.FT.).
C      11. DT = TOTAL DRAG OF SYSTEM CORRESPONDING TO LDT (LB.).
C
C
      REAL LDW, LDT
C     READ FORMATS
   11 FORMAT (2I3)
```

```
    8 FORMAT (3F10.0)
    9 FORMAT (8F10.0)
C     PRINT FORMATS
    2 FORMAT (1H1)
    3 FORMAT (1H ,/,' L/DW =', F7.2,'   L/DT =',F7.2)
    4 FORMAT (1H ,/,' VELOCITY =',F9.2,' ALTITUDE =',F9.2)
    6 FORMAT (1H ,F6.3,4F10.1,F9.2,F15.1,3F10.1,F9.2,F10.2)
    7 FORMAT (1H ,/, ' RHO =',F9.6,'   CDSPL =',F6.2,'   CDST =',F7.5,'
     1  WTW =',F6.3,'   WTC =',F8.2,'   R =',F8.2)
   10 FORMAT (1H , '  CL',8X,'S1',8X,'W1',8X,'FW1',7X,'W1T',4X,'(W/S)1',
     111X,'S2',8X,'W2',8X,'FW2',7X,'W2T',4X,'(W/S)2',6X,'DT')
   26 FORMAT (1H , /, ' PROGRAM COMPLETED')
      READ (2,8) DELCL, DELV,Y
      READ (2,9) RHO,CDSPL,CDST,WTW,WTC,R,V1,CL1
      READ (2,11) NCL,NV
      READ (2,8) LDW,LDT
  100 WRITE (3,7) RHO,CDSPL,CDST,WTW,WTC,R
      V = V1
      WRITE (3,3) LDW,LDT
      DO 701 J = 1,NV
      WRITE (3,4) V,Y
      WRITE (3,10)
      CL = CL1
      DO 700 L = 1,NCL
      SFC = .001634 * V -.000004 *Y + 0.673
      TEMP1 = (R*SFC)/(2*V)
      Q = 1.42636*RHO*V**2
      TEMP2 = WTC + Q*TEMP1*CDSPL
      TEMP3 = Q*(CL - (CL/LDW + CDST)*TEMP1) - WTW
      S1 = TEMP2/TEMP3
      W1 = CL*S1*Q
      FW1 = 2*(W1 - WTW*S1 - WTC)
      W1T = W1 + 0.5*FW1
      WS1 = W1/S1
      TEMP4 = CL*Q*(1.0 - TEMP1/LDT) - WTW
      S2 = WTC/TEMP4
      W2 = CL*Q*S2
      FW2 = 2*(W2 - WTW*S2 - WTC)
      W2T = W2 + 0.5*FW2
      WS2 = W2/S2
      DT = W2/LDT
      WRITE (3,6) CL,S1,W1,FW1,W1T,WS1,S2,W2,FW2,W2T,WS2,DT
      CL = CL + DELCL
  700 CONTINUE
      V = V + DELV
  701 CONTINUE
      READ (2,8) LDW,LDT
      WRITE (3,2)
      IF (LDW - 99999.) 100, 702, 100
  702 WRITE (3,26)
      CALL EXIT
      END
```

APPENDIX D

COUPLED AERCAB
(RIGID SUSPENSION)
FUEL WEIGHT AND SERVICE CEILING
COMPUTER PROGRAM

"LIMIT"

APPENDIX D

"LIMIT" COMPUTER PROGRAM

The LIMIT computer program was written to determine the limits on fuel weight and altitude service ceiling. The limit lines determined were included on the carpet plots made using data obtained from the PARAM computer program.

Equations programmed in the LIMIT computer program were derived from equations used in the PARAM program to achieve coordinated output. The equations used were:

$$(L/D)TL = \frac{CL*Q\left(WTC + \frac{T*R*SFC}{2V}\right)}{T(CL*Q-WTW) - \frac{R/C*CL*Q*WTC}{101.3 * \frac{V}{\sigma^{1/2}}}} \qquad (D\text{-}1)$$

where,

...(L/D)TL is the (L/D)T (i.e., total lift-to-drag ratio) corresponding to a rate of climb of 100 ft./min. at 10,000 ft. pressure altitude, with maximum thrust; and at a velocity corresponding to (L/D)TL

...T is the maximum thrust, lbs., at 10,000 ft. pressure altitude calculated from the expression

$$T = 0.00055VS^2 - 0.4VS + 356$$

where,

$VS=V/\sigma^{1/2}$ and $\sigma = \rho / \rho_0$, ρ is the standard density at 10,000 ft., and ρ_0 is the standard density at sea level ($\sigma^{1/2} = 0.8593$)

...R/C is the rate of climb (100 ft./min.)

$$(L/D)WL = \frac{GL}{\frac{CL}{(L/D)TL} - \frac{CDSPL}{S_2} - CDST} \qquad (D\text{-}2)$$

where,

...(L/D)WL is the (L/D)W (i.e., wing lift-to-drag characteristic) corresponding to (L/D)TL, and S_2 is computed from "PARAM" program, with (L/D)T = (L/D)TL

The equations above were used to determine the limiting line for the service ceiling on the PARAM carpet plots.

The final equations which were used to determine the limiting lines on the "PARAM" carpet plots for maximum fuel weight are:

$$(L/D)TF = \frac{(WTC + 1/2FW) * CL * Q * R * SFC}{FW(CL * Q - WTW) * V} \qquad (D\text{-}3)$$

where,

...(L/D)TF is the total lift to drag ratio corresponding to a fuel weight, FW, of 120 lbs. The 120 lbs. fuel weight is based on using total fuel over a 50 n.mi. range.

and,

$$(L/D)WF = \frac{CL}{\frac{CL}{(L/D)TF} - \frac{CDSPL}{S22} - CDST} \qquad (D\text{-}4)$$

where,

...(L/D)WF is the wing lift-to-drag ratio corresponding to a (L/D)TF and S22 is computed from the "PARAM" program, with S2 = S22 and (L/D)T = (L/D)TF.

Other symbols in the equations have been previously defined in this report; and a flow chart of the complete program is included in Figure D-1.

This program is also of a general nature and can be applied to other lift/drag generators having the denoted lift-coefficient characteristics.

TABLE D-1

LIMIT COMPUTER PROGRAM

INPUT DEFINITIONS

Nomenclature	Definition	Units
RC	Rate of climb	ft./min.
SQRS	Square root of sigma $\sigma = \frac{\text{Density at 10,000 ft.}}{\text{Density at sea level}} = \frac{\rho}{\rho_o}$	---
FW	Fuel weight	lbs.
RHO	Air density at altitude Y	lb.-sec.^{2}/ft.^{4}
CDSPL	Man/seat/engine drag area	sq.ft.
CDST	Strut drag coefficient	---
WTW	Unit wing weight per unit wing area	lbs./sq.ft.
WTC	Weight of invarient items (man, seat, engine)	lbs.
R	Range	nautical mi.
V1	True velocity (initial)	knots
CL1	Wing lift coefficient (initial)	---
DELCL	Increment variation in lift coefficient	---
DELV	Increment variation in velocity	---
Y	Pressure altitude	ft.
NCL	Number of lift coefficient increments	---
NV	Number of velocity increments	---
A,B,C	Constants in thrust equation	---

OUTPUT DEFINITIONS

V	Velocity	knots
Y	Altitude	ft.
T	Thrust	lbs.
CL	Wing lift coefficient	---
S2	Wing area corresponding to LDTL	sq.ft.
LDTL	Total lift to drag corresponding to RC = 100 ft./min., at 10,000 ft. pressure altitude with max, thrust	---
LDWL	Wing lift to drag corresponding to LDTL	---
S22	Wing area corresponding to LDTF	sq.ft.
LDTF	Total lift to drag corresponding to fuel weight (120 lbs.)	---
LDWF	Wing lift to drag corresponding to LDTF	---

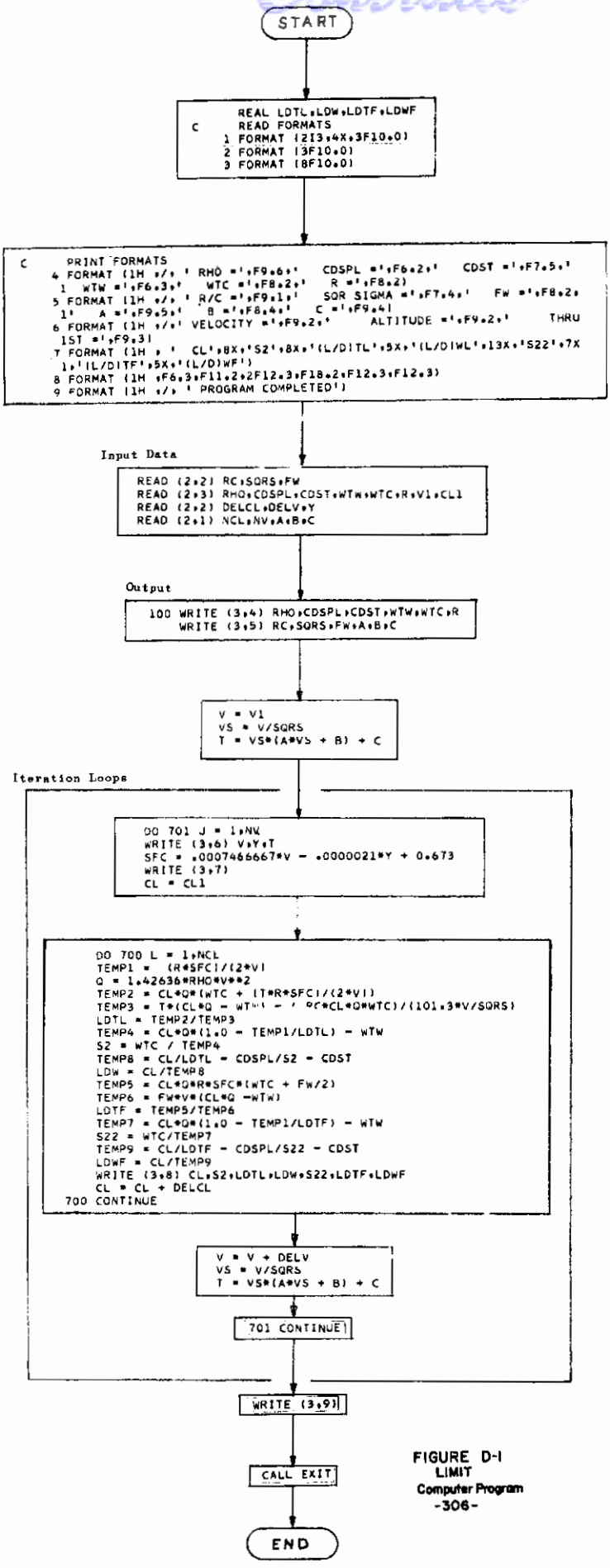

FIGURE D-I
LIMIT
Computer Program

```
// JOB
// FOR
*ARITHMETIC TRACE
*TRANSFER TRACE
* LIST SOURCE PROGRAM
*EXTENDED PRECISION
*ONE WORD INTEGERS
*IOCS (CARD, 1132 PRINTER)
**NAME LIMIT
C
C                          INPUT DATA
C
C     THE INPUT DATA IS READ IN BY MEANS OF FOUR DATA CARDS.  THE READ
C     ORDERS ARE THE FOUR STATEMENTS THAT FOLLOW STATEMENT NO. 9.
C
C     CARD NO. 1
C
C       1. RC = RATE OF CLIMB
C       2. SQRS = (SQUARE ROOT OF SIGMA), SIGMA = (DENSITY AT 10,000 FT.)/
C          (DENSITY AT SEA LEVEL).
C       3. FW = FUEL WEIGHT (LB.).
C
C     CARD NO. 2
C
C       1. RHO = AIR DENSITY AT ALTITUDE Y (LB.-SECSQ/FT. TO FOURTH POWER).
C       2. CDSPL = MAN/SEAT/ENGINE EFFECTIVE DRAG AREA (SQ.FT.).
C       3. CDST = STRUT DRAG COEFFICIENT.
C       4. WTW = UNIT WING WEIGHT PER UNIT WING AREA (LB./SQ.FT.).
C       5. WTC = WEIGHT OF INVARIANT ITEMS, MAN, SEAT, ENGINE, ETC. (LB.).
C       6. R = RANGE (NAUT. MILES).
C       7. VI = TRUE INITIAL VELOCITY. (KNOTS).
C       8. CL1 = INITIAL WING LIFT COEFF.
C
C     CARD NO. 3
C
C       1. DELCL = INCREMENT OF VARIATION IN AERO. LIFT COEFFICIENT.
C       2. DELV = INCREMENTAL VARIATION IN VELOCITY  (KNOTS).
C       3. Y = ALTITUDE (FT.).
C
C     CARD NO. 4
C
C       1. NCL = NO. OF LIFT COEFFICIENT INCREMENTS.
C       2. NV = NO. OF VELOCITY INCREMENTS.
C       3. A =
C       4. B = COFFFICIENTS OF THRUST EQUATION (QUADRATIC).
C       5. C =
C
C                          OUTPUT DATA
C
C
C     THE FIRST TWO LINES ARE INPUT DATA AND/OR INITIAL CONDITIONS.  THE
C     FIRST LINE WRITES RHO,CDSPL,CDST,WTW,WTC,R. THE SECOND LINE WRITES
C     RC,SQRS,FW,A,B,C  (SEE DEFINITIONS ABOVE).
C     SUCCESSIVELY THEREAFTER FOR A SPECIFIED ALTITUDE AND INCREMENTALLY
C     VARYING VELOCITY, THRUST, AND LIFT COEFFICIENT THE FOLLOWING ARE
C     LISTED.
C
C       1. CL = WING LIFT COEFFICIENT.
C       2. S2 = WING AREA CORRESPONDING TO LDTL (SQ.FT.).
C       3. LDTL = TOTAL LIFT TO DRAG RATIO CORRESPONDING TO RC = 100 FT./
C          MIN , AT 10,000 FT. ALTITUDE WITH MAX. THRUST.
C       4. LDWL = WING LIFT TO DRAG RATIO CORRESPONDING TO LDWL.
C       5. S22 = WING AREA CORRESPONDING TO LDTF (SQ.FT.).
C       6. LDTF = TOTAL LIFT TO DRAG RATIO CORRESPONDING TO FUEL WEIGHT
```

```
C       7. LDWF = WING LIFT TO DRAG RATIO CORRESPONDING TO LDTF.
C
C
      REAL LDTL,LDW,LDTF,LDWF
C     READ FORMATS
    1 FORMAT (2I3,4X,3F10.0)
    2 FORMAT (3F10.0)
    3 FORMAT (8F10.0)
C     PRINT FORMATS
    4 FORMAT (1H ,/, ' RHO =',F9.6,'   CDSPL =',F6.2,'   CDST =',F7.5,'
     1  WTW =',F6.3,'   WTC =',F8.2,'   R =',F8.2)
    5 FORMAT (1H ,/, ' R/C =',F9.1,'   SQR SIGMA =',F7.4,'   FW =',F8.2,
     1'   A =',F9.5,'   B =',F8.4,'   C =',F9.4)
    6 FORMAT (1H ,/,' VELOCITY =',F9.2,'     ALTITUDE =',F9.2,'     THRU
     1ST =',F9.3)
    7 FORMAT (1H , '  CL',8X,'S2',8X,'(L/D)TL',5X,'(L/D)WL',13X,'S22',7X
     1,'(L/D)TF',5X,'(L/D)WF')
    8 FORMAT (1H ,F6.3,F11.2,2F12.3,F18.2,F12.3,F12.3)
    9 FORMAT (1H ,/, ' PROGRAM COMPLETED')
      READ (2,2) RC,SQRS,FW
      READ (2,3) RHO,CDSPL,CDST,WTW,WTC,R,V1,CL1
      READ (2,2) DELCL,DELV,Y
      READ (2,1) NCL,NV,A,B,C
  100 WRITE (3,4) RHO,CDSPL,CDST,WTW,WTC,R
      WRITE (3,5) RC,SQRS,FW,A,B,C
      V = V1
      VS = V/SQRS
      T = VS*(A*VS + B) + C
      DO 701 J = 1,NV
      WRITE (3,6) V,Y,T
      SFC = .001634 * V - .000004 * Y + .480
      WRITE (3,7)
      CL = CL1
      DO 700 L = 1,NCL
      TEMP1 =  (R*SFC)/(2*V)
      Q = 1.42636*RHO*V**2
      TEMP2 = CL*Q*(WTC + (T*R*SFC)/(2*V))
      TEMP3 = T*(CL*Q - WTW) - ( RC*CL*Q*WTC)/(101.3*V/SQRS)
      LDTL = TEMP2/TEMP3
      TEMP4 = CL*Q*(1.0 - TEMP1/LDTL) - WTW
      S2 = WTC / TEMP4
      TEMP8 = CL/LDTL - CDSPL/S2 - CDST
      LDW = CL/TEMP8
      TEMP5 = CL*Q*R*SFC*(WTC + FW/2)
      TEMP6 = FW*V*(CL*Q -WTW)
      LDTF = TEMP5/TEMP6
      TEMP7 = CL*Q*(1.0 - TEMP1/LDTF) - WTW
      S22 = WTC/TEMP7
      TEMP9 = CL/LDTF - CDSPL/S22 - CDST
      LDWF = CL/TEMP9
      WRITE (3,8) CL,S2,LDTL,LDW,S22,LDTF,LDWF
      CL = CL + DELCL
  700 CONTINUE
      V = V + DELV
      VS = V/SQRS
      T = VS*(A*VS + B) + C
  701 CONTINUE
      WRITE (3,9)
      CALL EXIT
      END
```

APPENDIX E

AERCAB

WEIGHT OPTIMIZATION COMPUTER PROGRAM

"WEIGHT"

APPENDIX E

WEIGHT COMPUTER PROGRAM

The WEIGHT computer program was developed for optimizing system weight and volume against AERCAB performance. The program was used in trade-off analysis.

Basic criteria adopted for the program include:

$C_{l_w} = 0.6$

$(L/D)_w = 4.615$

$C_{D_{struts}} = 0.0334$

$(C_D S)$ payload = 4.2 sq.ft.

Inputs such as fuel weight, fuel tank weight, wing fabric weight, wing structure weight, suspension strut weight and engine weight were allowed to vary with cruise velocity.

The fuel weight was that needed to cruise 50 miles at the design cruise velocity, assuming fuel flow at the average cruise weight, (i.e. half fuel load) held constant for the entire mission.

Fuel tank weight was assumed to be 8 oz./sq.yd.

The wing structure weight was determined by assuming tubular sections for the keel and booms and spreader bars, exposed to a 6G ultimate load. It was assumed that each leading edge boom carried half the total load.

When aluminum structure was considered, a uniformly distributed load was assumed, and the spreader bar length varied proportionally to keel length. When steel structure was considered, an isosceles triangular load distribution was assumed, and a 64 inch constant length spreader bar was assumed. An extra 10% in length was allowed for telescoping and fittings. A rigid suspension strut-set weight was computed assuming the 6G ultimate load on aluminum tubes whose length was 75% that of the keel, loaded in tension; each of which carried 1/4 the ultimate load.

Engine weight was allowed to vary as the 3/2 power of the thrust. The thrust was that required to achieve a 100 ft./min. rate of climb at 10,000 ft. at the same equivalent airspeed as design cruise speed. Engine weight was ratioed from the then current design engine at the same airspeed as that for

which the thrust was computed.

All inputs are defined by the listing presented below. In the program a value for the first approximation of wing area was calculated using:

$$S_w = \frac{WTC + \frac{R*SFC*CDSPL*Q}{2V}}{Q\left\{C_L - \left(\frac{CL}{(L/D)W} + CDST\right)\frac{R*SFC}{2V} - WTWW\right\}} \qquad (E\text{-}1)$$

The iteration process follows this equation. The complete program is flow charted in Figure E-3.

Figures E-1 and E-2 show typical results of the weight trade-off studies, exemplifying the compromises paid in selecting steel versus aluminum wing structures.

First, an approximate value for the wing area, S_W(sq.ft.), was calculated from the equation (E-1), wherein:

...WTC is the approximate invariant weight, 450 lbs.

...R is the 50 nautical mile range

...SFC is the specific fuel consumption, where SFC = 0.0007466*V -0.0000021*Y + 0.673

...V is the true airspeed in knots

...Y is the pressure altitude (Y = 0 ft.)

...CDSPL is the payload drag area, 4.2 sq.ft.

...Q is the dynamic pressure in lbs./sq.ft., where $Q = 1.42636*RHO*V^2$

...RHO is the mass density of the air in lb.-sec.^{2}/ft.^{4} and $\rho = 0.002377$ for S.L. conditions

...1.42636 is the conversion factor from knots to (ft./sec.)^2 divided by 2.0

...CL is the lift coefficient, 0.6

...(L/D)W is the wing's lift-to-drag ratio, 4.615

...CDST is the strut drag coefficient, 0.0334

...WTWW is the parawing's weight per sq.ft.; 1.33 psf

MAXIMUM CRUISE WEIGHT
VS
DESIGN CRUISE SPEED

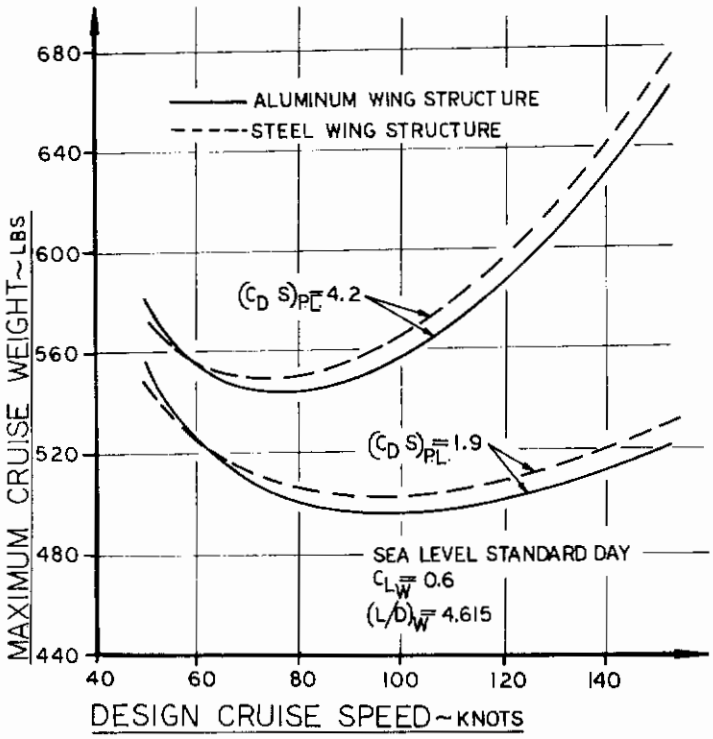

FIGURE E-2
WEIGHT OPTIMIZATION
WING AREA VS. DESIGN CRUISE SPEED

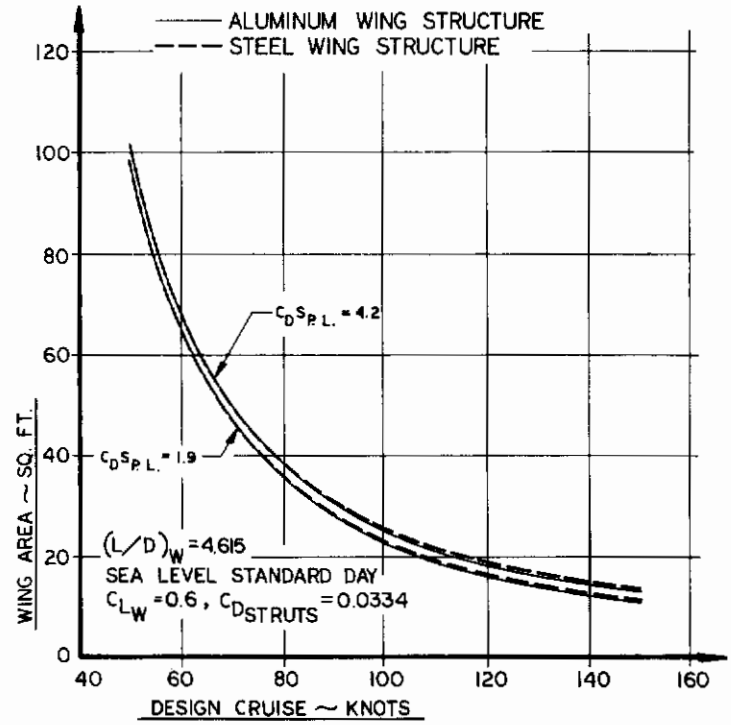

The wing area calculated from equation (E-1) is then used as the first estimate in the following iteration process:

From the equation

$$SW_{calc} = \frac{WT.AV.}{CL*Q} \text{ , where } WT.AV. = f\ (SW_{assumed}) \qquad (E\text{-}2)$$

where:

WT.AV. is the average cruise weight,

$$(WT.AV. = CW + FTW + \frac{FW}{2} + WW + BW + STW + EW) \qquad (E\text{-}3)$$

wherein:

CW is the invariant weight, 378.9 lbs.

FTW is the fuel tank weight, and is equal to

$$\frac{2*FTFW}{3*FD^{2/3}} \qquad (2*A + 2*B*SW)^{2/3}$$

FTFW is the fuel tank "fabric" density, 1.0 lb./sq.yd.

FD is the fuel density, 48.6 lbs./cu.ft.

$$A = \frac{R*SFC*CDSPL*Q}{2V}$$

$$B = \frac{R*SFC*F}{2V}$$

$$F = \left(\frac{CL}{(L/D)W} + CDST \right) *Q$$

FW is the fuel weight, 2*A + 2*B*SW, lbs.

WW is the wing fabric weight, $\frac{DF*SW}{144}$

DF is the wing fabric density, 8 oz./sq.yd.

BW is the wing structural member weights:

(aluminum): $BW = \frac{BW}{S^{3/2}} * SW^{3/2}$

where, $\frac{BW}{S^{3/2}}$ = f (W/S), i.e., a function of wing-loading

$W/S = CL*Q + B + \frac{A}{SW}$, which is the wing loading at start of cruise.

Now, $\frac{BW}{S^{3/2}}$ vs. SW was entered into the computer in tabular form and was calculated by:

Assuming values of R/t, where "R" is the average section radius (i.e., $\frac{ID + OD}{4}$), where ID is the tube inner diameter, and OD is the outer diameter) and "t" is the section thickness (i.e., $\frac{OD - ID}{2}$);

then,

$$W/S = \left(\frac{5000(55-0.42\ R/t)}{DEFL*24\ EA\sqrt{\cos\Lambda_o}}\right)^4 * \left\{\frac{2\ DEFL*6EA\ \cos\Lambda_o*144\pi\left[1-(d2/d1)\right]^4}{5N*SF}\right\} \quad (E-4)$$

Where, (55-0.42 R/t) is the nominal critical compressive stress for 6061-T6 aluminum alloy tubes in Kips/sq.in. (Ref. Alcoa Structural Handbook, P. 158).

and,

...DEFL is the maximum deflection of the L.E. boom divided by the boom length

...EA is the modulus of elasticity for aluminum; $10X10^6$ psi

... Λ_o is the wing planform sweepback angle, 45^o

...N is the limit load, 4 G's

...SF is a safety factor of 1.5

... d_2/d_1 is the ratio of ID to OD; i.e., $\frac{2R/t-1}{2R/t+1}$

and,

$$\frac{BW}{S^{3/2}} = \left[\frac{5000(55-0.42\ R/t)}{DEFL*24EA\sqrt{\cos\Lambda}}\right]^2 \left[1-\left(\frac{d_2}{d_1}\right)^2\right] \frac{\pi}{4} \frac{DA}{\sqrt{\cos\Lambda_o}} (3+\cot\Lambda) \quad (E-5)$$

where,

...DA is the density of aluminum; 169 lb./cu.ft.

... Λ is the inflight sweep angle, 55^{o}

Then, for

Steel :

$$BW = \frac{\pi}{4} d_1^2 \left[1 - \left(\frac{d_2}{d_1} \right)^2 \right] *(3.3\ LK + SBL)*\frac{DI}{1728}$$

where,

...d_1^2 is the squared tube section I.D., and $d_1^2 = 0.04 \frac{LK*FTU}{DEFL*EM}^2$

...LK is the keel length, $12*\left(\frac{SW}{\cos \Lambda_o} \right)^{1/2}$

...FTU is the ultimate tensile strength of steel; 125,000 psi

...EM is the modulus of elasticity for steel, $30X10^6$ psi

$$\left(\frac{d_2}{d_1} \right)^2 = \left(\frac{1 - 8N*SF*WTW*LK^2}{15 \quad d_1^4 \quad *DEFL*EM} \right)^{1/2}$$

where,

...WTW = W/S*SW, the weight at start of cruise

...SBL is the spreader bar length, 64 in.

...DI is steel's density, 487.5 lb./cu.ft.

...STW = $E \left[(CL*Q+B)* SW-A \right] SW^{1/2}$, which is the suspension strut weight, lbs.

...$\frac{E = N*SF*z/\ell_k * DA}{YSS*(\cos \Lambda_o)1/2*144}$

...z/ℓ_k is the ratio of the perpendicular distance from the CG to the keel, to the keel length; 0.75

...YSS is the yield strength of the struts; 35,000 psi

...EW = $\frac{EWD}{TW^{3/2}} \quad (C*SW + D)^{3/2}$, the engine weight

...EWD is design engine weight; 70 lbs.

...TW is the maximum thrust of the present engine design @ 10,000 ft. pressure altitude, where,

$$...TW = 0.00055\ VS^2 - 0.4VS + 356$$

$$...VS = V/\sqrt{\sigma}$$

$$...\ \sigma = \rho/\rho_o \quad = 0.8593 \text{ for } 10{,}000 \text{ ft. MSL}$$

$$...C = \frac{R/C\ (CL*Q+B)}{101.3*VS} + F$$

$$...D = \frac{R/C*A}{101.3*VS} + CDSPL*Q$$

...R/C is the rate of climb; 100 ft./min.

TABLE E-1

WEIGHT COMPUTER PROGRAM

INPUT DEFINITIONS

Nomenclature	Definition	Units
CL1	Lift coefficient	---
CD	Drag coefficient	---
CDST	Strut drag coefficient	---
R	Range	n.mi.
CDSPL	Payload drag area	sq.ft.
FTFW	Density of fuel tank fabric	lb./sq.yd.
FD	Fuel density	lb./cu.ft.
N	G loading	G's
SF	Safety factor	---
ZLK	Ratio: (Z-C.G. dist. from keel axis/keel length)	---
DA	Density of aluminum =	lb./cu.ft.
YSS	Yield strength of struts	lb./sq.in.
LAMDA	Sweep angle of flat wing planform	deg.
ROC	Rate of climb	ft./min.
SQRS	SQRT of air density at thrust reg. alt. to sea level standard	---
EWD	Engine design weight	lb.
VO	Initial velocity	knots
DELV	Increment variation in velocity	knots
DF	Density of wing fabric	oz./sq.yd.
CW	Weight of invarient items	lbs.
ALT	Altitude	ft.
WTWW	Approx. total weight of parawing per sq.ft.	lb./sq.ft.
WTC	Approx. weight of invarient items	lbs.
FTU	Ultimate tensile strength	lb./sq.in.
DEFL 1	Max. deflection of leading edge booms	---
EM	Modulus of elasticity	lb./sq.in.
SBL	Length of spreader bar	in.
DI	Density of steel	lb./cu.ft.
IDENT	Identification number for engine used	---
E1, F1, G1	Constants in SFC equation	---
NV	Number of velocity changes	---
A1, B1, C1	Constants in thrust equation	---
THETD	Inclination of thrust axis	deg.
PDTH	Preliminary design thrust at a selected vel. and alt.	lbs.
MBETH	Manuf. best estimate of thrust at selected vel. and alt.	lbs.

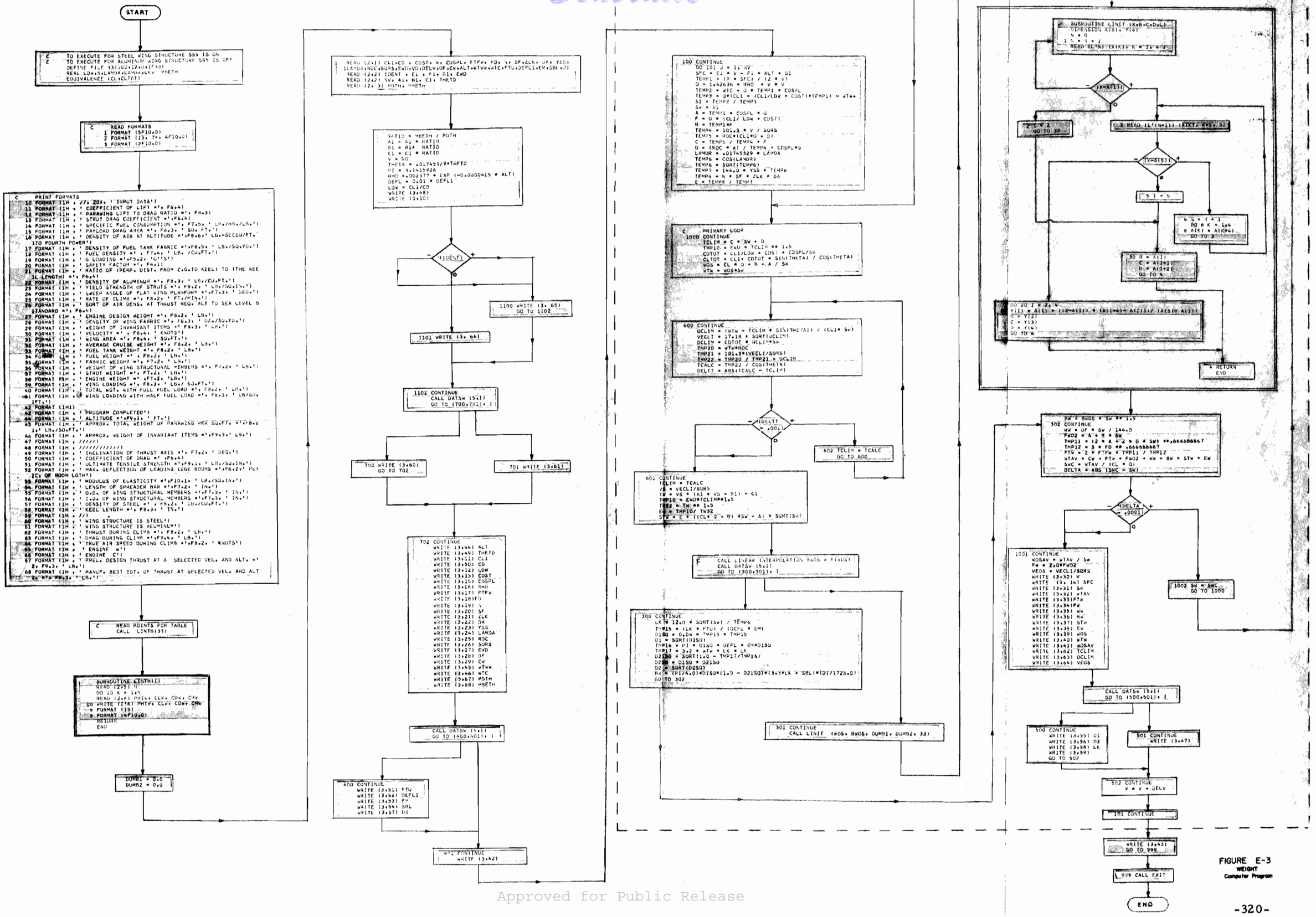

FIGURE E-3
WEIGHT
Computer Program

```
// JOB
// FOR
*ARITHMETIC TRACE
*TRANSFER TRACE
*EXTENDED PRECISION
*ONE WORD INTEGERS
*IOCS (CARD, 1132 PRINTER,DISK)
*LIST SOURCE PROGRAM
*NAME WEIGT
C
C                          INPUT DATA
C
C     THE FIRST 21 CARDS OF INPUT DATA ARE A TABLE OF BW/S(3/2) AS A
C     FUNCTION OF W/S WHERE
C
C           BW = WEIGHT OF WING STRUCTURAL MEMBERS IN LB.
C           S = WING AREA (SQ. FT.)
C           W/S = WING LOADING AT START OF CRUISE (LB./SQ.FT.)
C
C
C     THE INPUT DATA IS ENTERED ON 8 DATA CARDS. THE READ ORDERS ARE THE
C     FOUR STATEMENTS STARTING WITH STATEMENT 68 + 0005.
C
C     CARD NO. 1
C
C       1. CL1 = LIFT COEFFICIENT.
C       2. CD = DRAG COEFFICIENT.
C       3. CDST = STRUT DRAG COEFFICIENT.
C       4. R = RANGE (NAUT.MI.).
C       5. CDSPL = PAYLOAD DRAG AREA (SQ.FT.).
C
C     CARD NO. 2
C
C       1. FTFW = DENSITY OF FUEL TANK FABRIC (LB./SQ.YD.).
C       2. FD = FUEL DENSITY (LB./CU.FT.).
C       3. N = G LOADING (G'S).
C       4. SF = SAFETY FACTOR.
C       5. ZLK = RATIO OF (PERP. DIST. FROM C.G. TO KEEL) TO (KEEL LGTH.).
C
C     CARD NO. 3
C
C       1. DA = DENSITY OF ALUMINUM (LB./CU.FT.).
C       2. YSS = YIELD STRENGTH OF STRUTS (LB./SQ.IN.).
C       3. LAMDA = SWEEP ANGLE OF FLAT WING PLANFORM (DEG.).
C       4. ROC = RATE OF CLIMB (FT./MIN.).
C       5. SQRS = SQUARE ROOT OF AIR DENSITY AT THRUST REQUIRED, ALT. TO
C          SEA LEVEL STANDARD.
C
C     CARD NO. 4
C
C       1. EWD = ENGINE DESIGN WEIGHT (LB.).
C       2. VO = INITIAL VELOCITY (KNOTS).
C       3. DELV = INCREMENT OF VARIATION IN VELOCITY (KNOTS).
C       4. DF = DENSITY OF WING FABRIC (OZ./SQ.YD.).
C       5. CW = WEIGHT OF INVARIANT ITEMS (LB.)
C
C     CARD NO. 5
C
C       1. ALT = ALTITUDE (FT.).
C       2. WTWW = APPROX. WEIGHT OF PARAWING PER SQ. FT. (LB./SQ.FT.).
C       3. WTC = APPROX. WEIGHT OF INVARIANT ITEMS (LB.).
C       4. FTU = ULTIMATE TENSILE STRENGTH (LB./SQ.IN.).
C       5. DEFL1 = MAX DEFLECTION OF LEADING EDGE BOOMS (PERC. OF BOOM
C          LENGTH).
```

```
C     CARD NO. 6
C
C       1. EM = MODULUS OF ELASTICITY (LB./SQ.IN.).
C       2. SBL = LENGTH OF SPREADER BAR (IN.).
C       3. DI = DENSITY OF STEEL (LB./CU. FT.).
C       4. PDTH = PRELIMINARY DESIGN THRUST AT SELECTED VEL. AND ALT. (LB.).
C       5. MBETH = MANUF. BEST ESTIMATE OF THRUST AT ESLECTED VEL. AND
C          ALT. (LB.).
C
C     CARD NO. 7
C
C       1. E1 =
C       2. E2 = COEFFICIENTS FOR SPECIFIC FUEL CONSUMPTION EQUATION.
C       3. E3 =
C
C     CARD NO. 8
C
C       1. NV = NUMBER OF VELOCITY CHANGES.
C       2. A1
C       3. A2 = COEFFICIENTS IN THRUST EQUATION (QUADRATIC).
C       4. A3
C       5. THETD = INCLINATION OF THRUST AXIS (DEG.)
C
C                ***********************************
C
C                          OUTPUT DATA
C
C     ALL THE OUTPUT DATA IS WELL DOCUMENTED IN THE PRINTOUT WITH EACH
C     DATA ITEM CLEARLY EXPLAINED. THE APPROPRIATE UNITS ARE ATTACHED.
C     THE FIRST BLOCK OF DATA PRINTED IS THE INPUT DATA.
C
C                ***********************************
C
C                               NOTE
C
C     THE PROGRAM WILL CALCULATE THE INDICATED DATA FOR A STRUCTURE OF
C     ALUMINUM OR STEEL. CONTROL IS BY MEANS OF SENSE SWITCH 5. IF SENSE
C     SWITCH 5 IS IN THE ON POSITION THE WING STRUCTURE MUST BE STEEL.
C     IF SENSE SWITCH 5 IS IN THE OFF POSITION THE WING STRUCTURE MUST BE
C     ALUMINUM.
C
C
      DEFINE FILE 33(100,12,U,IF33)
      REAL LDW,N,LAMDA,LAMDR,LK,  MBETH
      EQUIVALENCE (CL,CLTOT)
C     READ FORMATS
    1 FORMAT (5F10.0)
    2 FORMAT (I3, 7X, 4F10.0)
    3 FORMAT (3F10.0)
C     PRINT FORMATS
   10 FORMAT (1H , //, 20X, ' INPUT DATA')
   11 FORMAT (1H , ' COEFFICIENT OF LIFT =', F6.4)
   12 FORMAT (1H , ' PARAWING LIFT TO DRAG RATIO =', F8.3)
   13 FORMAT (1H , ' STRUT DRAG COEFFICIENT =',F6.4)
   14 FORMAT (1H , ' SPECIFIC FUEL CONSUMPTION =', F7.5, ' LB./HR./LB.')
   15 FORMAT (1H , ' PAYLOAD DRAG AREA =', F8.3, ' SQ. FT.')
   16 FORMAT (1H , ' DENSITY OF AIR AT ALTITUDE =',F8.6,' LB.-SECSQ/FT.
     1TO FOURTH POWER')
   17 FORMAT (1H , ' DENSITY OF FUEL TANK FABRIC =',F8.5, ' LB./SQ.YD.')
   18 FORMAT (1H , ' FUEL DENSITY =' , F7.4, ' LB. /CU.FT.')
   19 FORMAT (1H , ' G LOADING =',F5.2, 'G''S')
   20 FORMAT (1H , ' SAFETY FACTOR =', F4.1)
   21 FORMAT (1H , ' RATIO OF (PERP. DIST. FROM C.G.TO KEEL) TO (THE KEE
```

```
     1L LENGTH) =', F6.4)
  22 FORMAT (1H , ' DENSITY OF ALUMINUM =', F8.3, ' LB./CU.FT.')
  23 FORMAT (1H , ' YIELD STRENGTH OF STRUTS =', F9.2, ' LB./SQ.IN.')
  24 FORMAT (1H , ' SWEEP ANGLE OF FLAT WING PLANFORM =',F7.3, ' DEG.')
  25 FORMAT (1H , ' RATE OF CLIMB =', F8.2, ' FT./MIN.')
  26 FORMAT (1H , ' SQRT OF AIR DENS. AT THRUST REQ. ALT TO SEA LEVEL S
     1TANDARD =', F6.4)
  27 FORMAT (1H , ' ENGINE DESIGN WEIGHT =', F8.2, ' LB.')
  28 FORMAT (1H , ' DENSITY OF WING FABRIC =', F6.3, ' OZ./SQ.YD.')
  29 FORMAT (1H , ' WEIGHT OF INVARIANT ITEMS =' F9.3, ' LB.')
  30 FORMAT (1H , ' VELOCITY =' , F8.4, ' KNOTS')
  31 FORMAT (1H , ' WING AREA =', F8.4, ' SQ.FT.')
  32 FORMAT (1H , ' AVERAGE CRUISE WEIGHT =', F8.2, ' LB.')
  33 FORMAT (1H , ' FUEL TANK WEIGHT =', F8.2, ' LB.')
  34 FORMAT (1H , ' FUEL WEIGHT =' , F8.2, ' LB.')
  35 FORMAT (1H , ' FABRIC WEIGHT =', F7.2, ' LB.')
  36 FORMAT (1H , ' WEIGHT OF WING STRUCTURAL MEMBERS =', F7.2, ' LB.')
  37 FORMAT (1H , ' STRUT WEIGHT =', F7.2, ' LB.')
  38 FORMAT (1H , ' ENGINE WEIGHT =' ,F7.2, 'LB.')
  39 FORMAT (1H , ' WING LOADING =', F8.3, ' LB./ SQ.FT.')
  40 FORMAT (1H , ' TOTAL WGT. WITH FULL FUEL LOAD =', F8.2, ' LB.')
  41 FORMAT (1H , ' WING LOADING WITH HALF FUEL LOAD =', F8.3, ' LB/SQ.
     1FT.')
  42 FORMAT (1H1)
  43 FORMAT (1H , ' PROGRAM COMPLETED')
  44 FORMAT (1H , ' ALTITUDE =',F9.1, ' FT.')
  45 FORMAT (1H , ' APPROX. TOTAL WEIGHT OF PARAWING PER SQ.FT. =',F8.2
     1,' LB./SQ.FT.')
  46 FORMAT (1H , ' APPROX. WEIGHT OF INVARIANT ITEMS =',F9.3,' LB.')
  47 FORMAT (1H , /////)
  48 FORMAT (1H , ////////////)
  49 FORMAT (1H , ' INCLINATION OF THRUST AXIS =', F7.2, ' DEG.')
  50 FORMAT (1H , ' COEFFICIENT OF DRAG =' ,F6.4)
  51 FORMAT (1H , ' ULTIMATE TENSILE STRENGTH =',F9.1, ' LB./SQ.IN.')
  52 FORMAT (1H , ' MAX. DEFLECTION OF LEADING EDGE BOOMS =',F6.2,' PER
     1C. OF BOOM LGTH')
  53 FORMAT (1H , ' MODULUS OF ELASTICITY =',F10.1, ' LB./SQ.IN.')
  54 FORMAT (1H , ' LENGTH OF SPREADER BAR =',F7.2, ' IN.')
  55 FORMAT (1H , ' O.D. OF WING STRUCTURAL MEMBERS =',F7.3, ' IN.')
  56 FORMAT (1H , ' I.D. OF WING STRUCTURAL MEMBERS =',F7.3, ' IN.')
  57 FORMAT (1H , ' DENSITY OF STEEL =' , F8.2, ' LB./CU.FT.')
  58 FORMAT (1H , ' KEEL LENGTH =', F8.3, ' IN.')
  59 FORMAT (1H , //)
  60 FORMAT (1H , ' WING STRUCTURE IS STEEL')
  61 FORMAT (1H , ' WING STRUCTURE IS ALUMINUM')
  62 FORMAT (1H , ' THRUST DURING CLIMB =', F8.2, ' LB.')
  63 FORMAT (1H , ' DRAG DURING CLIMB =',F9.4, ' LB.')
  64 FORMAT (1H , ' TRUE AIR SPEED DURING CLIMB =',F8.2, ' KNOTS')
  67 FORMAT (1H , ' PREL. DESIGN THRUST AT A  SELECTED VEL. AND ALT. ='
     2, F9.3, ' LB.')
  68 FORMAT (1H , ' MANUF. BEST EST. OF THRUST AT SELECTED VEL. AND ALT
     2. =', F9.3, ' LB.')
C      READ POINTS FOR TABLE
       CALL  LINTB(33)
       DUMB1 = 0.0
       DUMB2 = 0.0
       READ (2,1) CL1,CD , CDST, R, CDSPL, FTFW, FD, N, SF,ZLK, DA, YSS,
     1LAMDA,ROC,SQRS,EWD,VO,DELV,DF,CW,ALT,WTWW,WTC,FTU,DEFL1,EM,SBL,DI,
     2PDTH,MBETH
       READ (2,3) E1, F1, G1
       READ (2,2) NV, A1, B1, C1, THETD
       RATIO = MBETH / PDTH
       A1 = A1 * RATIO
       B1 = B1*  RATIO
```

```
      C1 = C1 * RATIO
      V = VO
      THETA = .01745329*THETD
      PI = 3.1415926
      RHO =.002377 * EXP (-0.0000415 * ALT)
      DEFL = 0.01 * DEFL1
      LDW = CL1/CD
      WRITE (3,48)
      WRITE (3,10)
      CALL DATSW (5,I)
      GO TO (700,701), I
  700 WRITE (3,60)
      GO TO 702
  701 WRITE (3,61)
  702 CONTINUE
      WRITE (3,44) ALT
      WRITE (3,49) THETD
      WRITE (3,11) CL1
      WRITE (3,50) CD
      WRITE (3,12) LDW
      WRITE (3,13) CDST
      WRITE (3,15) CDSPL
      WRITE (3,16) RHO
      WRITE (3,17) FTFW
      WRITE (3,18)FD
      WRITE (3,19) N
      WRITE (3,20) SF
      WRITE (3,21) ZLK
      WRITE (3,22) DA
      WRITE (3,23) YSS
      WRITE (3,24) LAMDA
      WRITE (3,25) ROC
      WRITE (3,26) SQRS
      WRITE (3,27) EWD
      WRITE (3,28) DF
      WRITE (3,29) CW
      WRITE (3,45) WTWW
      WRITE (3,46) WTC
      WRITE (3,67) PDTH
      WRITE (3,68) MBETH
      CALL DATSW (5,I)
      GO TO (400,401), I
  400 CONTINUE
      WRITE (3,51) FTU
      WRITE (3,52) DEFL1
      WRITE (3,53) EM
      WRITE (3,54) SBL
      WRITE (3,57) DI
  401 CONTINUE
      WRITE (3,42)
  100 CONTINUE
      DO 101 J = 1, NV
      SFC = E1 * V - F1 * ALT + G1
      TEMP1 = (R * SFC) / (2 * V)
      Q = 1.42636 * RHO  * V * V
      TEMP2 = WTC + Q * TEMP1 * CDSPL
      TEMP3 = Q*(CL1 - (CL1/LDW + CDST)*TEMP1) - WTWW
      S1 = TEMP2 / TEMP3
      SW = S1
      A = TEMP1 * CDSPL * Q
      F = Q * (CL1/ LDW + CDST)
      B = TEMP1*F
      TEMP4 = 101.3 * V / SQRS
      TEMP5 = ROC*(CL1*Q + B)
```

```
      C = TEMP5 / TEMP4 + F
      D = (ROC * A) / TEMP4 + CDSPL*Q
      LAMDR = .01745329 * LAMDA
      TEMP6 = COS(LAMDR)
      TEMP6 = SQRT(TEMP6)
      TEMP7 = 144.0 * YSS * TEMP6
      TEMP8 = N * SF * ZLK * DA
      E = TEMP8 / TEMP7
C     PRIMARY LOOP
 1000 CONTINUE
      TCLIM = C * SW + D
      TMP10 = EWD * TCLIM ** 1.5
      CDTOT = CL1/LDW + CDST + CDSPL/SW
      CLTOT = CL1+ CDTOT * SIN(THETA) / COS(THETA)
      WOS = CL * Q + B + A / SW
      WTW = WOS*SW
  600 CONTINUE
      QCLIM = (WTW - TCLIM * SIN(THETA)) / (CL1* SW)
      VECLI = 17.18 * SQRT(QCLIM)
      DCLIM = CDTOT * QCLIM*SW
      TMP20 = WTW*ROC
      TMP21 = 101.3*(VECLI/SQRS)
      TMP22 = TMP20 / TMP21 + DCLIM
      TCALC = TMP22 / COS(THETA)
      DELTT = ABS(TCALC - TCLIM)
      IF (DELTT - .001) 601, 601, 602
  602 TCLIM = TCALC
      GO TO 600
  601 CONTINUE
      TCLIM = TCALC
      VS = VECLI/SQRS
      TW = VS * (A1 * VS + B1) + C1
      TMP10 = EWD*TCLIM**1.5
      TW32 = TW ** 1.5
      EW = TMP10/ TW32
      STW = E * ((CL* Q + B) *SW + A) * SQRT(SW)
C     CALL LINEAR INTERPOLATION BWOS = F(WOS)
      CALL DATSW (5,I)
      GO TO (300,301), I
  301 CONTINUE
      CALL LINIT  (WOS, BWOS, DUMB1, DUMB2, 33)
      BW = BWOS * SW ** 1.5
  302 CONTINUE
      WW = DF * SW / 144.0
      FWO2 = A + B * SW
      TMP11 = (2 * A + 2 * B * SW) **.666666667
      TMP12 = 3 * FD ** .666666667
      FTW = 2 * FTFW * TMP11 / TMP12
      WTAV = CW + FTW + FWO2 + WW + BW + STW + EW
      SWC = WTAV / (CL * Q)
      DELTA = ABS (SWC - SW)
      IF (DELTA - .0001) 1001, 1001, 1002
 1002 SW = SWC
      GO TO 1000
 1001 CONTINUE
      WOSAV = WTAV / SW
      FW = 2.0*FWO2
      VEOS = VECLI/SQRS
      WRITE (3,30) V
      WRITE  (3, 14) SFC
      WRITE (3,31) SW
      WRITE (3,32) WTAV
      WRITE (3,33)FTW
      WRITE (3,34)FW
```

```
      WRITE (3,35) WW
      WRITE (3,36) BW
      WRITE (3,37) STW
      WRITE (3,38) EW
      WRITE (3,39) WOS
      WRITE (3,40) WTW
      WRITE (3,41) WOSAV
      WRITE (3,62) TCLIM
      WRITE (3,63) DCLIM
      WRITE (3,64) VEOS
      CALL DATSW (5,I)
      GO TO (500,501), I
  500 CONTINUE
      WRITE (3,55) D1
      WRITE (3,56) D2
      WRITE (3,58) LK
      WRITE (3,59)
      GO TO 502
  501 CONTINUE
      WRITE (3,47)
  502 CONTINUE
      V = V + DELV
  101 CONTINUE
      WRITE (3,43)
      GO TO 999
C
C
  300 CONTINUE
      LK = 12.0 * SQRT(SW) / TEMP6
      TMP15 = (LK * FTU) / (DEFL * EM)
      D1SQ = 0.04 * TMP15 * TMP15
      D1 = SQRT(D1SQ)
      TMP16 = PI * D1SQ * DEFL * EM*D1SQ
      TMP17 = 3.2 * WTW * LK * LK
      D21SQ = SQRT(1.0 - TMP17/TMP16)
      D2SQ = D1SQ * D21SQ
      D2 = SQRT(D2SQ)
      BW = (PI/4.0)*D1SQ*(1.0 - D21SQ)*(3.3*LK + SBL)*(DI/1728.0)
      GO TO 302
  303 CONTINUE
C
C
  999 CALL EXIT
      END
```

APPENDIX F

AERCAB
WEIGHT & BALANCE
AND
Mass Moment of Inertia
SUMMARY

(General Self-Rescue Flying Arrangement)

FIGURE F-1
COMPONENT & SYSTEM CG LOCATIONS
(FLIGHT ARRANGEMENT)

*Please refer to Table F-8 for identification of components whose centers of gravity are numbered hereon....

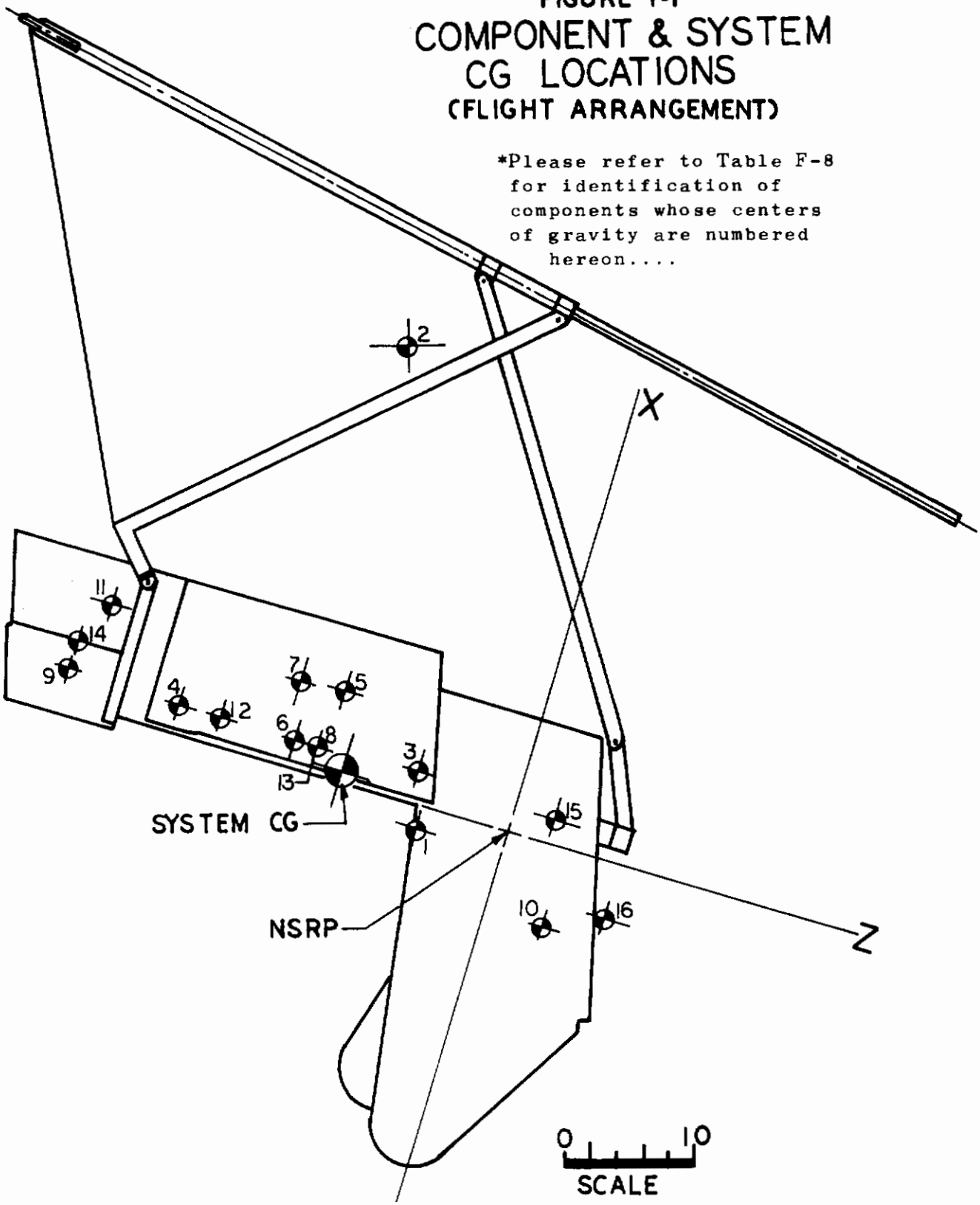

APPENDIX F

F.1 This Appendix is comprised of a summary of weight, balance and mass moment of inertia data related to the selected AERCAB design configuration shown in its general flying arrangement in Figure F-1.

F.1.a SEAT BUCKET ASSEMBLY

Figure F-2 shows the basic referenced structure of the bucket assembly comprised of the ejection handles, bucket side panels, front/back/and bottom panels, and upper support beam.

FIGURE F-2

SEAT BUCKET ASSEMBLY

(REFERENCE AXES PASS THRU NEUTRAL SEAT REFERENCE POINT)

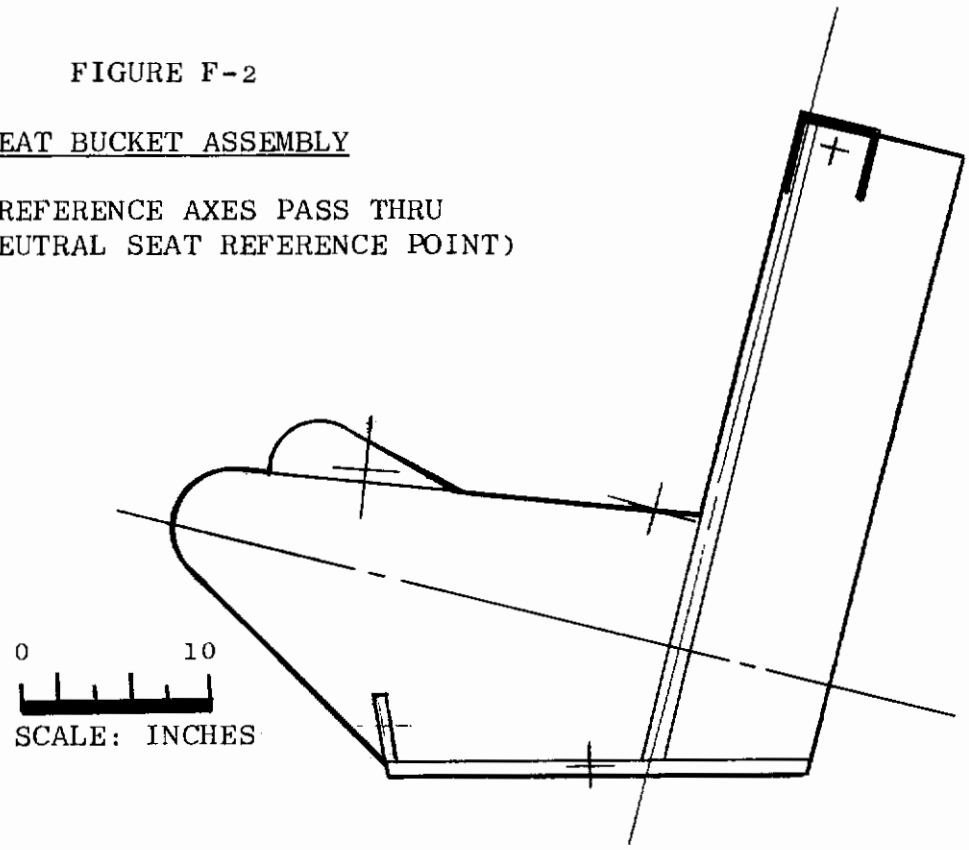

Table F-1 summarizes the calculated weight, balance and inertia data for the bucket assembly.

Figures F-3 through F-8 show the major bucket components, and the tables with each figure display the pertinent W, B & I data.

FIGURE F-3

SEAT BUCKET SIDE PANEL

FRAME X-SECTION IS .5 x .5
FACINGS ARE .032 THICK
CORE IS ALUMINUM HONEY COMB
} MAT'L IS ALUMINUM

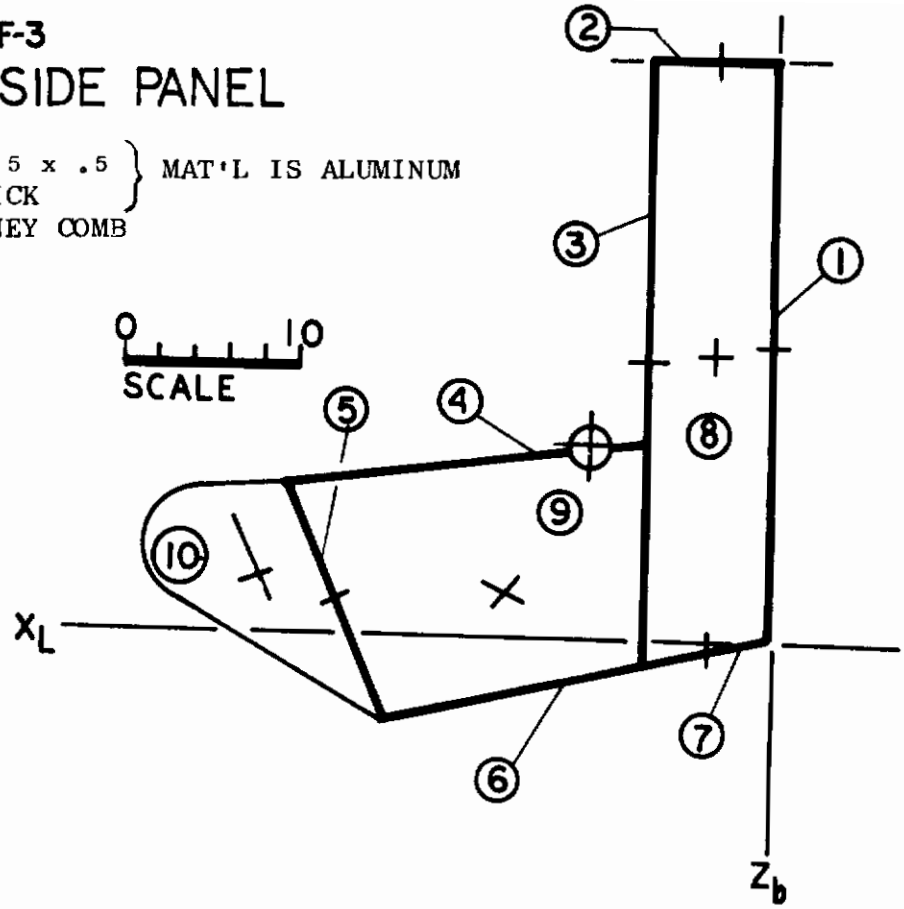

FIGURE F-4

SEAT BUCKET BACK PANEL

FRAME X-SECTION IS .5 x .5
FACINGS ARE .032 THICK
} MAT'L IS ALUMINUM

CORE IS ALUMINUM HONEYCOMB

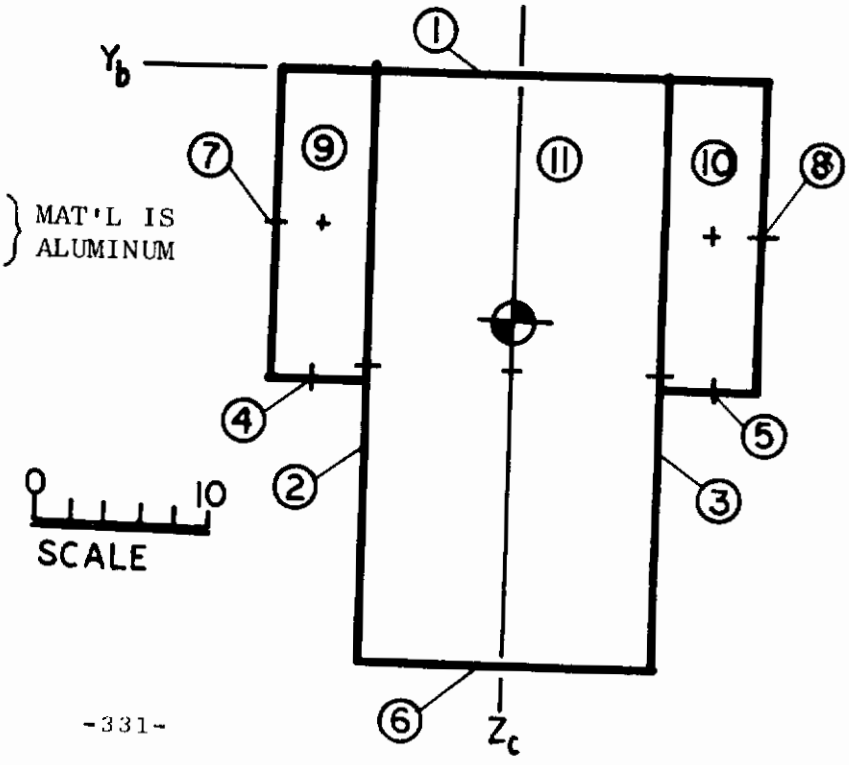

TABLE F-1
SEAT BUCKET DATA SUMMARY

COMPONENT	WEIGHT	X_b	Y_c	Z_b	WX	WZ	WX^2	WY^2	WZ^2	I_x	I_y	I_z
R.H. HANDLE	.82	17.70	8.75	5.50	14.50	4.51	256.5	62.8	24.8	.	.	.
L.H. HANDLE	.82	17.70	-8.75	5.50	14.50	4.51	256.5	62.8	24.8			
R.H. SIDE	6.26	1.70	8.75	6.80	10.62	42.60	18.2	479.0	290.0	726.0	1311.0	575.0
L.H. SIDE	6.26	1.70	-8.75	6.80	10.62	42.60	18.2	479.0	290.0	726.0	1311.0	575.0
FRONT PANEL	1.39	13.50	0	-7.70	18.75	-10.70	253.5	0	82.4	33.8	14.5	27.4
BACK PANEL	8.83	-.75	0	14.50	-6.62	128.00	5.0	0	1855.0	1206.4	986.7	605.8
BOTTOM PANEL	2.51	1.70	0	-7.00	4.26	-17.55	7.2	0	123.0	67.8	99.4	167.0
UPPER BEAM	3.81	-2.70	0	28.10	-10.30	107.00	27.8	0	3005.0	107.9	41.8	139.6
TOTALS	30.70				56.33	300.97	842.9	1083.6	5695.0	2867.9	3764.4	2089.8

$\bar{X} = \Sigma WX / \Sigma W = 56.33/30.70 = 1.84$ in

$\bar{Z} = \Sigma WZ / \Sigma W = 300.97/30.7 = 9.80$ in

$I_{x_b} = \Sigma I_{x_o} + \Sigma WY^2 + \Sigma WZ^2 = 2867.9 + 1083.6 + 5695.0 = 9655.5$ lb-in^2

$I_{y_b} = \Sigma I_y + \Sigma WX^2 + \Sigma WZ^2 = 3764.4 + 842.9 + 5695.0 = 10302.3$ lb-in^2

$I_{z_b} = \Sigma I_z + \Sigma WX^2 + \Sigma WY^2 = 2089.8 + 842.9 + 1083.6 = 4016.3$ lb-in^2

$I_{x_c} = I_{x_b} - W(\bar{Y}^2 + \bar{Z}^2) = 9655.5 - 30.7(0 + 9.8^2) = 9655.5 - 30.7(96.0) = 6705$ lb-in^2

$I_{y_c} = I_{y_b} - W(\bar{X}^2 + \bar{Z}^2) = 10{,}302 - 30.7\,(1.84^2 + 9.82) = 10302 - 3055 = 7247$ lb-in^2

$I_{z_c} = I_{z_b} - W(\bar{X}^2 + \bar{Y}^2) = 4016 - 30.7\,(1.84^2 + 0) = 4016 - 104 = 3912$ lb-in^2

$\Sigma WX_b Z_b = -256.3$ lb-in^2 $\Sigma WX_o Z_o = -843.4$ lb-in^2

$I_{x_c z_c} = -265.3 = 843.4 - 30.7\,(1.84)(9.80) = -1661.7$ lb-in^2

TABLE F-2
SEAT BUCKET SIDE PANEL SUMMARY

NO.	(LBS.) WEIGHT	(IN.) X	WX	WX^2	(IN) Z	WZ	WZ^2	I_x	I_y	I_z	WXZ
1	.825	.25	.21	.04	16.7	13.78	230.00	76.6	76.6	0	3.46
2	.160	3.50	.56	1.68	32.7	5.24	171.20	0	.6	.6	18.30
3	.875	7.00	6.12	42.80	15.7	13.75	216.00	88.2	88.2	0	96.10
4	.500	17.40	8.70	151.00	9.6	4.80	46.10	0	15.7	15.7	83.50
5	.380	24.80	9.42	234.00	2.0	.76	1.52	6.8	6.8	0	18.80
6	.360	14.60	5.25	76.60	-3.2	-1.15	3.68	0	5.9	5.9	-16.80
7	.165	3.50	.58	2.02	-.6	-.09	.05	0	.6	.6	-.35
8	1.650	3.50	5.77	20.20	16.1	26.60	429.00	159.0	165.0	7.9	92.80
9	.770	15.20	11.70	178.00	2.6	2.00	5.20	12.6	41.5	20.8	30.40
10	.575	29.00	16.70	485.00	3.3	1.90	6.27	5.0	20.0	10.0	55.10
	6.260		65.01	1191.34		67.59	1109.02	348.2	420.9	61.5	381.31

$\bar{X} = \Sigma WX / \Sigma W = 65.01/6.26 = 10.4$ in

$\bar{Z} = \Sigma WZ / \Sigma W = 67.59/6.26 = 10.8$

$I_{x_b} = \Sigma I_{x_o} + \Sigma WY_b^2 + \Sigma WZ_b^2 = 348.2 + 0 + 1109.02 = 1457.22$ lb-in^2

$I_{y_b} = \Sigma I_{y_o} + \Sigma WX_b^2 + \Sigma WZ_b^2 = 420.8 + 1191.34 + 1109.02 = 2721.16$ lb-in^2

$I_{z_b} = \Sigma I_{z_o} + \Sigma WX_b^2 + \Sigma WY_b^2 = 61.5 + 1191.34 + 0 = 1252.84$ lb-in^2

$I_{xz} = \Sigma WXZ - W\bar{X}\bar{Z} = 381.3 - 6.26(10.4)(10.8) = -421.7$ lb-in^2

$I_{x_c} = 1457.22 = 6.26(10.8)^2 = 726$ lb-in^2

$I_{y_c} = 2721 - 6.26\ (10.8^2 + 10.4^2) = 1311$ lb-in^2

$I_{z_c} = 1253 - 6.26(10.4)^2 = 575$ lb-in^2

TABLE F-3
SEAT BUCKET BACK PANEL SUMMARY

NO.	WEIGHT	(IN) Z	WZ	WZ^2	(IN) Y	WY^2	I_{x_o}	I_{y_o}	I_{z_o}	WYZ
1	.70	.25	.17	--	0	0	45.6	0	45.6	0
2	.82	17.00	13.95	237.0	8.3	56.5	74.4	74.4	0	118.0
3	.82	17.00	13.95	237.0	8.3	56.5	74.4	74.4	0	-118.0
4	.13	17.80	1.01	17.8	11.4	16.9	.3	0	.3	11.5
5	.13	17.80	1.01	17.8	11.4	16.9	.3	0	.3	-11.5
6	.43	33.75	14.50	488.0	0	0	10.3	0	10.3	0
7	.42	9.00	3.78	34.0	13.7	78.8	10.1	10.1	0	51.8
8	.42	9.00	3.78	34.0	13.7	78.8	10.1	10.1	0	-51.8
9	.63	9.00	5.66	51.0	11.0	76.3	1.5	17.0	1.5	62.3
10	.63	9.00	5.66	51.0	11.0	76.3	1.5	17.0	1.5	-62.3
11	3.70	17.00	62.90	1069.0	0	0	89.3	356.0	89.3	0
	8.83		126.37	2236.6		457.0	317.8	555.1	148.8	0

$\bar{Z} = \Sigma WZ/\Sigma W = 126.37/8.83 = 14.3$ IN

$I_{x_b} = \Sigma I_{x_o} + \Sigma WY_b^2 + \Sigma WZ_b^2 = 317.8 + 457.0 + 2236.6 = 3011.4$ LB-IN^2

$I_{y_b} = \Sigma I_{y_o} + \Sigma WX_b^2 + \Sigma WZ_b^2 = 555.1 + 0 + 2236.6 = 2791.7$ LB-IN^2

$I_{z_b} = \Sigma I_{z_o} + \Sigma WX_b^2 + \Sigma WY_b^2 = 148.8 + 457.0 = 605.8$ LB-IN^2

$I_{x_c} = 3011.4 - 8.83(14.3)^2 = 1206.4$ LB-IN^2

$I_{y_c} = 2791.7 - 8.83(14.3)^2 = 986.7$ LB-IN^2

$I_{z_c} = 605.8$ LB-IN^2

FIGURE F-5
SEAT BUCKET FRONT PANEL

FRAME X-SECTION IS .50 x .50

FACINGS ARE .032 THICK

CORE IS ALUMINUM HONEYCOMB

MATERIAL IS ALUMINUM

1/10 SCALE

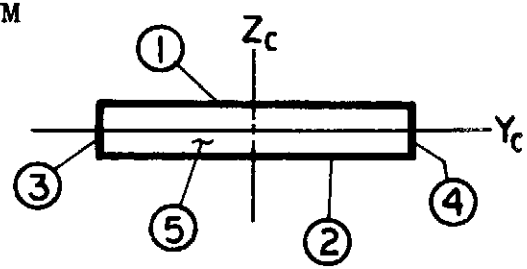

TABLE F-4
SEAT BUCKET FRONT PANEL SUMMARY

NO.	(LBS.) WEIGHT	Z	WZ^2	Y	WY^2	I_x	I_y	I_z
1	.39	0	0	1.5	.9	7.9	0	7.9
2	.39	0	0	1.5	.9	7.9	0	7.9
3	.10	8.3	6.9	0	0	.1	.1	0
4	.10	8.3	6.9	0	0	.1	.1	0
5	.41	0	0	0	0	2.2	.5	9.8
	1.39		13.8		1.8	18.2	.7	25.6

$$I_{x_c} = \Sigma I_{x_o} + \Sigma WZ^2 + \Sigma WY^2 = 18.2 + 13.8 + 1.8 = 33.8 \text{ lb-in}^2$$
$$I_{y_c} = \Sigma I_{y_o} + \Sigma WZ^2 + \Sigma WX^2 = .7 + 13.8 + 0 = 14.5 \text{ lb-in}^2$$
$$I_{z_c} = \Sigma I_{z_o} + \Sigma WX^2 + \Sigma WY^2 = 25.6 + 1.8 + 0 = 27.4 \text{ lb-in}^2$$

FIGURE F-6

SEAT BUCKET UPPER BEAM

MATERIEL IS ALUMINUM EXTRUSION
LENGTH ALONG Y AXIS IS 18 INCHES
WEB & FLANGES ARE .19 THICK

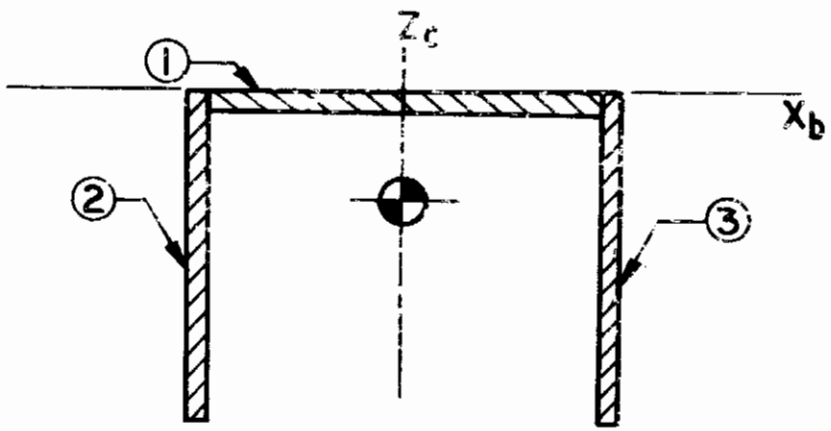

1/2 SCALE

TABLE F-5
SEAT BUCKET UPPER BEAM SUMMARY

NO.	(LBS.) WEIGHT	(IN) Z	X	WZ^2	WX^2	I_{x_o}	I_{y_o}	I_{z_o}
1	1.41	.09	0	---	0	38.1	2.0	40.0
2	1.20	1.75	2.14	3.8	17.4	33.6	1.2	32.4
3	1.20	1.75	-2.14	3.8	17.4	33.6	1.2	32.4
	3.81			7.6	34.8	105.3	4.4	104.8

$\bar{Z} = \Sigma WZ/\Sigma W = 4.34/3.81 = 1.14$ IN

$I_{x_b} = \Sigma I_{x_o} + \Sigma WY_b^2 + \Sigma WZ_b^2 = 105.3 + 7.6 = 112.9$ LB-IN^2

$I_{y_b} = \Sigma I_{y_o} + \Sigma WX_b^2 + \Sigma WZ_b^2 = 4.4 + 7.6 + 34.8 = 46.8$ LB-IN^2

$I_{z_b} = \Sigma I_{z_o} + \Sigma WX_b^2 + \Sigma WY_b^2 = 104.8 + 34.8 = 139.6$ LB-IN^2

$I_{x_c} = 112.9 - 3.81(1.14)^2 = 107.9$ LB-IN^2

$I_{y_c} = 46.8 - 3.81(1.14)^2 = 41.8$ LB-IN^2

$I_{z_c} = 139.6$ LB-IN^2

FIGURE F-7
SEAT BUCKET BOTTOM PANEL

½" ALUMINUM HONEYCOMB WITH
.032 THICK ALUMINUM FACINGS

1/10 SCALE

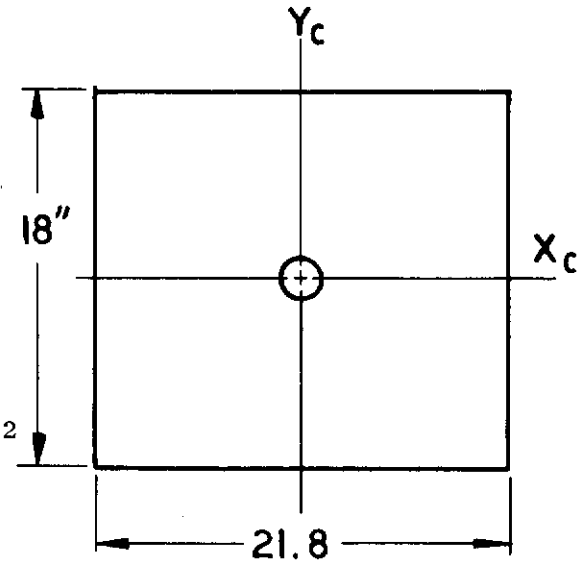

WEIGHT = 18 x 21.8 x .064 x .1 = 2.51
$I_x = 2.51\ (18)^2/12 = 67.8$ LB-IN^2
$I_y = 2.51\ (21.8)^2/12 = 99.4$ LB-IN^2
$I_z = 2.51\ (21.8^2 + 18^2)/12 = 167.0$ LB-IN^2

FIGURE F-8
EJECTION & FLIGHT CONTROL HANDLE

MATERIAL: .½ INCH THICK ALUMINUM

½ SCALE

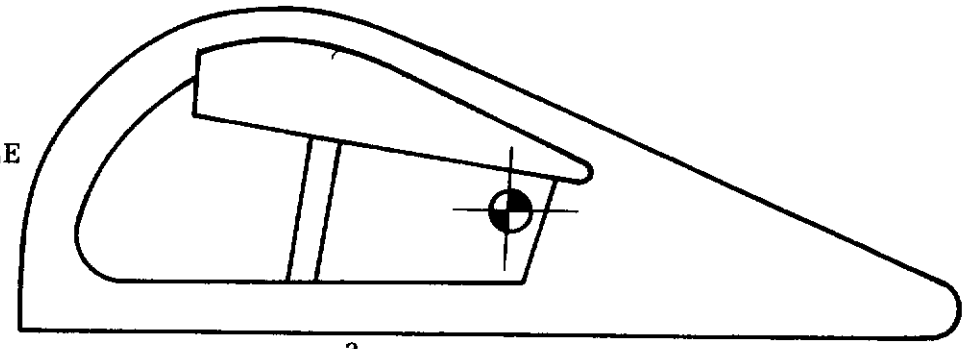

AREA = 16.4 IN^2 VOLUME = 8.2 IN^3 WEIGHT = .82 LBS
MOMENTS OF INERTIA ASSUMED TO BE NEGLIGABLE

F.1.b Parawing Assembly

Figure F-9 portrays the stowed parawing assembly, and Table F-6 summarizes the W, B & I data related thereto.

Figure F-10 shows that same assembly in its flying arrangement, and Table F-7 summarizes its characteristics in the deployed position.

F.1.c Rockets

Figure F-11 portrays the basic characteristics of the seat back rockets when both loaded and inert (or expended).

F.1.d Powered Inertia Reel

Figure F-12 shows the characteristics of a typical applicable reel which could be used in AERCAB.

F.1.e. Engine

The high bypass ratio turbofan engine's characteristics are described in Figure F-13.

F.1.f Fuel and Cells

Figure F-14 portrays the full and empty characteristics of the onboard fuel tanks.

F.1.g Seat Adjuster

Figure F-15 shows the characteristics of the hydraulic pump and electric motor which drives the seat adjustment mechanism.

F.1.h Catapults

The characteristics of the inert catapults remaining with AERCAB in flight are:

ASSUME 50 INCH LONG, 1.38 O.D. x 1.2 I.D. ALUMINUM TUBE
VOL = 50 $(\pi/4)(1.38^2 - 1.2^2) = 18.25$ IN^3
WT. = 1.8 LBS.
$I_x = I_y = 1.8\ (.69^2 + .6^2 + 50\ 2/3)/4 = 376$ LB-IN^2
I_z 0

FIGURE F-9

PARAWING IN STOWED POSITION

ALL MATERIAL IS ASSUMED TO BE
1 in. O.D. STEEL TUBING.
FABRIC WEIGHT — 8 oz. $yd.^2$

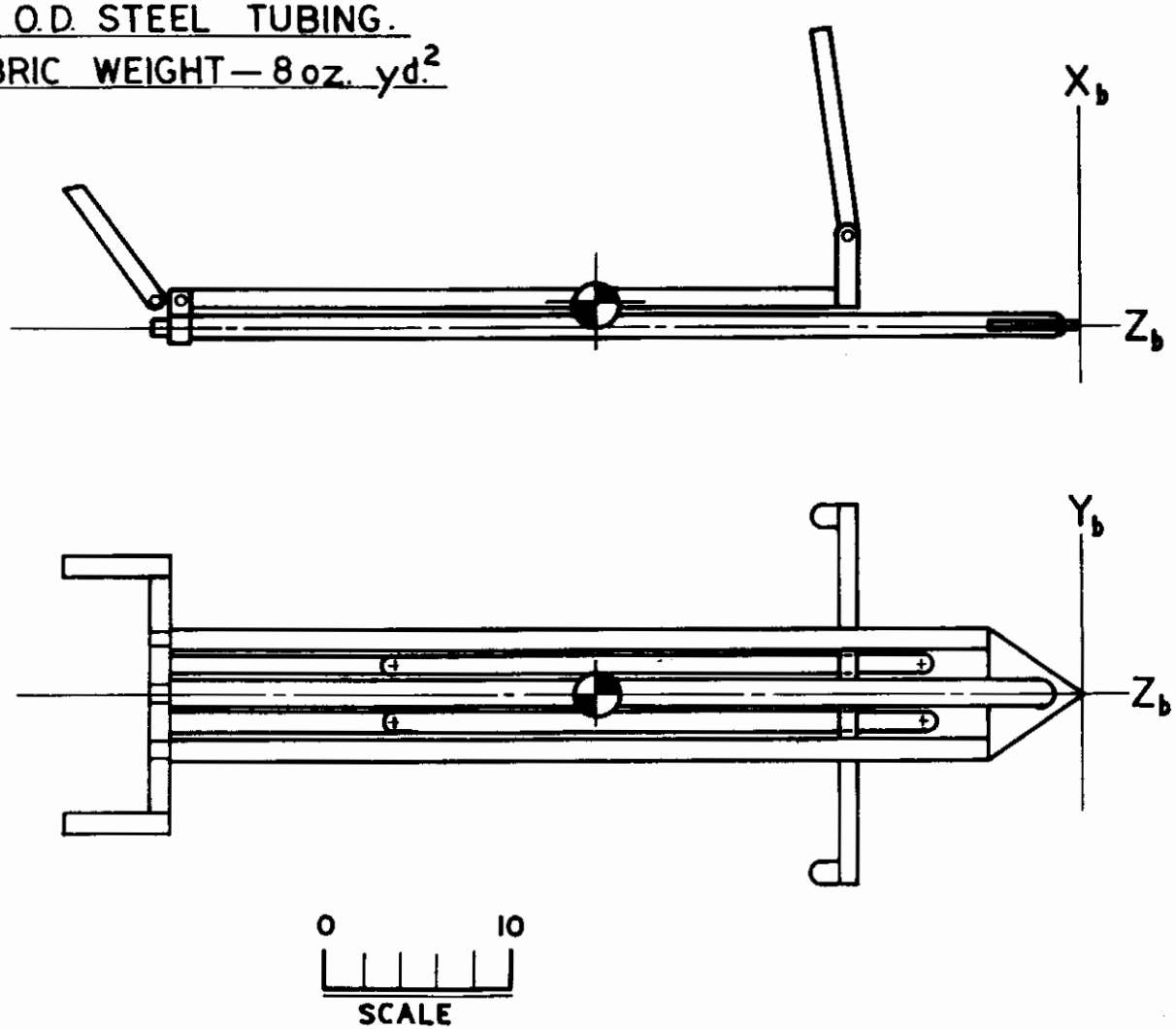

FIGURE F-10
PARAWING DEPLOYED POSITION

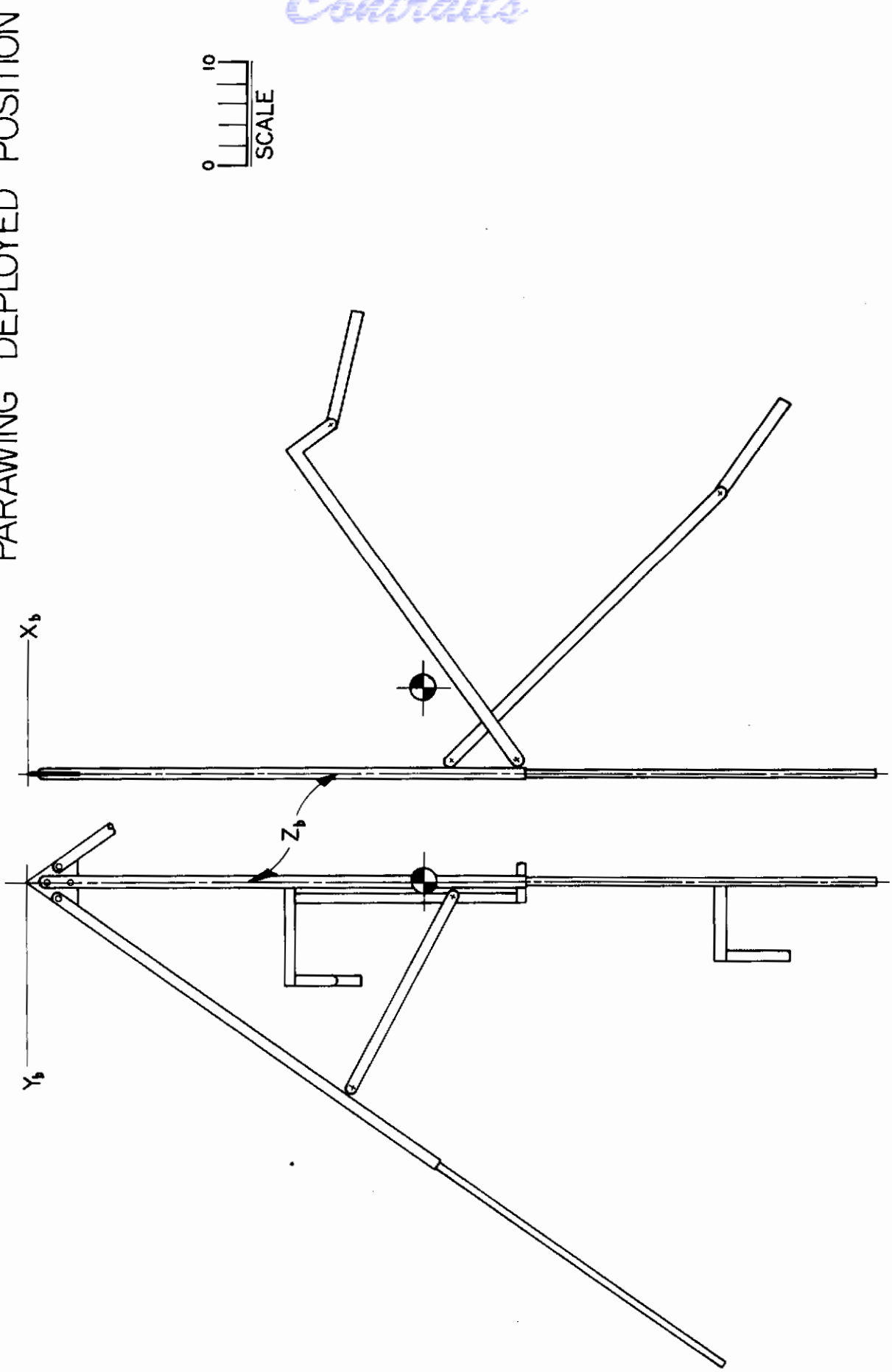

FIGURE F-11

SEAT BACK ROCKET CHARACTERISTICS

THE SEAT BACK ROCKETS ARE
SCALED UP FROM SPACE
ORDNANCE SYSTEMS, INC.
P/N S04-110961-1. IMPULSE,
WEIGHTS & LENGTH ARE SCALED UP 40%

TOTAL IMPULSE = 1.4 x 600 = 840 LB-SEC/EACH

a. LOADED CONDITION:

WEIGHT = 1.4 x 6.85 = 9.58 LBS
$I_x = 9.85 \ (3)(1.13^2) + 30.8^2)/12 = 782$ LB-IN^2
$I_y = 782$ LB-IN^2
$I_z = 0$

b. INERT CONDITION:

WEIGHT = 1.4 x 3.85 = 5.39 LBS
$I_x = 5.39 \ (1.12^2 + 30.8^2/6)/2 = 430$ LB-IN^2
$I_y = 430$ LB-IN^2
$I_z = 0$

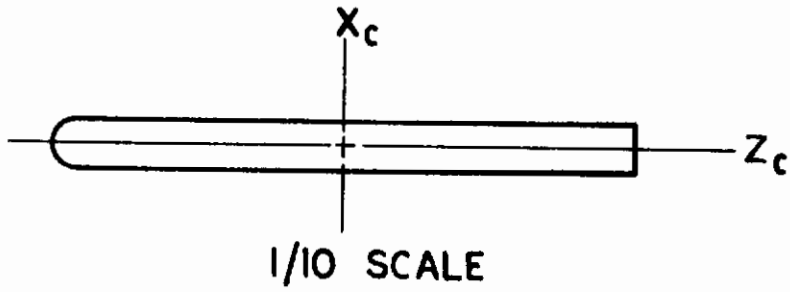

FIGURE F-12

POWERED INERTIA REEL CHARACTERISTICS

THE WEIGHT & VOLUME OF THE PACIFIC SCIENTIFIC CO. 0103 182-1 DEVICE IS SHOWN IN THE PRELIMINARY DESIGN. THIS DEVICE WOULD BE ALTERED TO INCORPORATE BALLISTIC SEVERING OF THE SHOULDER STRAPS.

WEIGHT (INCLUDING GAS GENERATOR) = 3.6 LBS

$I_x = 3.6(5.35^2 + 5.12^2)/12 = 16.5$ LB-IN^2

$I_y = 3.6(5.35^2 + 2^2)/12 = 9.8$ LB-IN^2

$I_z = 3.6(5.12^2 + 2^2)/12 = 9.1$ LB-IN^2

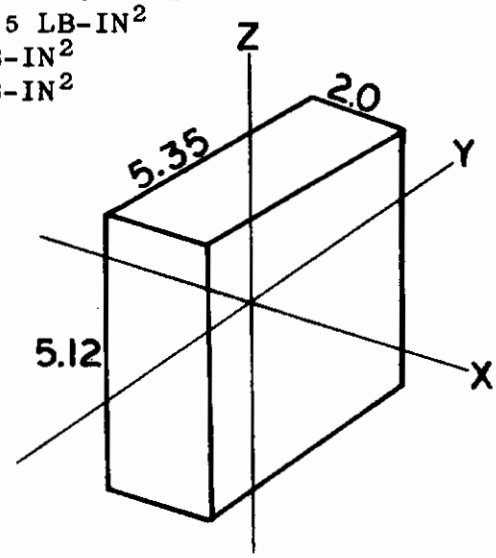

FIGURE F-13

TURBOFAN ENGINE CHARACTERISTICS

THE ENGINE IS PER CONTINENTAL DWG L8789

WEIGHT (INCLUDING GENERATOR, PUMPS & STARTER) = 54.0 LBS

$I_x = 6530$ LBS-IN^2

$I_y = 3500$ LBS-IN^2

$I_z = 1990$ LBS-IN^2

ANGULAR MOMENTUM = 34.4 LB-FT/RAD/SEC

(ABOVE VALUES PER TELECON WITH JOE SOMERS OF CONTINENTAL)

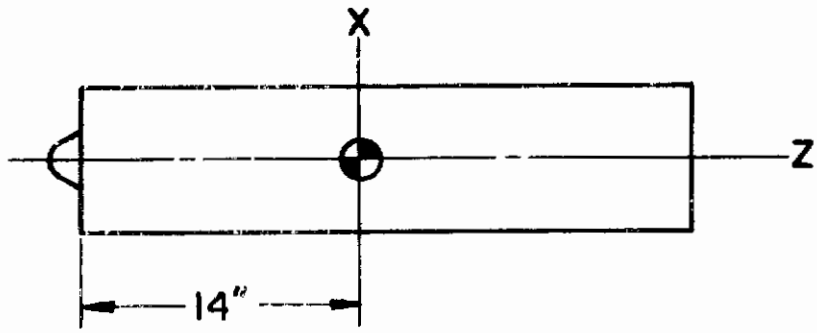

FIGURE F-14

FUEL & FUEL TANKS CHARACTERISTICS

TANK CONSTRUCTION IS CONSIDERED TO BE .032 ALUMINUM SHEET

FUEL IS ASSUMED TO BE JP-4 AT A DENSITY OF 6.5 LBS/U.S. GAL

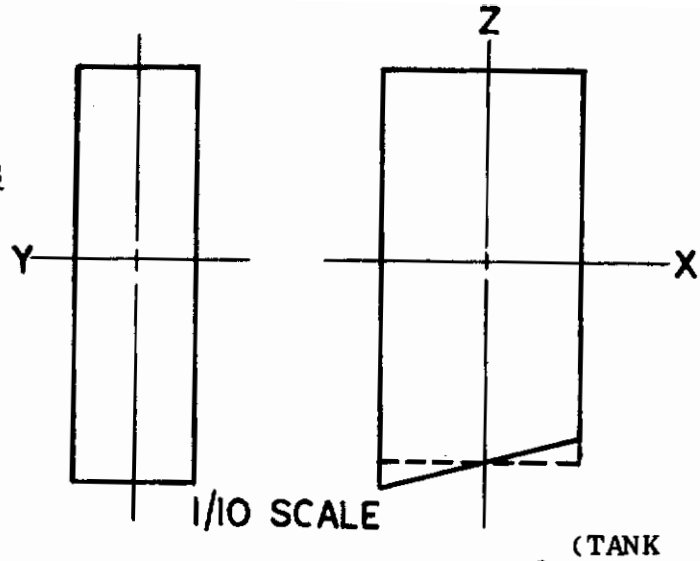

SHEET VOLUME = $2(22 \times 2 + 22 \times 6.5 + 6.5 \times 11)(.032) = 16.6\ IN^3$ (TANK SHELL)
3 VERTICAL BAFFLE PLATES = $3 \times 22 \times 6.5 \times .032 = 13.7\ IN^3$
6 HORIZONTAL BAFFLE PLATES = $6 \times 6.5 \times 11 \times .032 = 13.7\ IN^3$

$44.0\ IN^3$

TANK WT = 4.40 LBS
FUEL WT = 40.0 LBS
$I_x = 44.4(6.5^2 + 22^2)/12 = 1945\ LB\text{-}IN^2$
$I_y = 44.4\ (11^2 + 22^2)/12 = 2240\ LB\text{-}IN^2$ FULL TANK
$I_z = 44.4\ (11^2 + 6.5^2)/12 = 605\ LB\text{-}IN^2$

$I_x = 390\ LBS\text{-}IN^2$
$I_y = 448\ LBS\text{-}IN^2$ EMPTY TANK
$I_z = 122\ LBS\text{-}IN^2$

FIGURE-15

HYDRAULIC PUMP & MOTOR CHARACTERISTICS

UNIT SHOWN IS EASTERN INDUSTRIES P/N 310393
WEIGHT = 2.3 LBS
$I_x = I_z = 2.3(3 + 49)/12 = 10\ LBS\text{-}IN^2$
$I_y = 2.3/2 = 1.1\ LBS\text{-}IN^2$

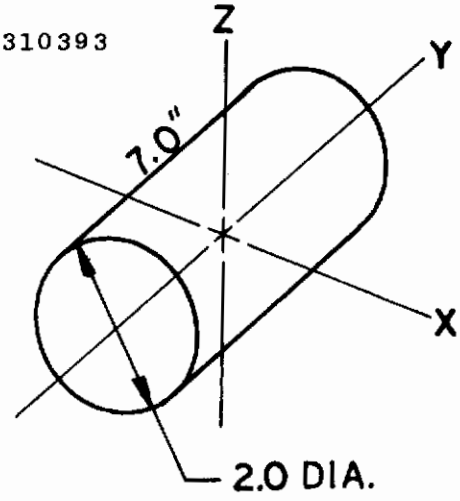

F.1.i Main Parachute

Figure F-16 shows the main recovery parachute and its container, the latter of which dually serves as the seat's headrest.

F.1.j Survival Kit

The survival kit's characteristics are portrayed in Figure F-17.

F.1.k Turn Control Mechanism

The turn control device is assumed to be an electrically driven drum of approximately the size and wt. of the hydraulic pump and motor.

WT = 2.3 LBS
I_x = 10 LBS-IN^2
I_y = 1.1 LBS-IN^2
I_z = 10 LBS-IN^2

F.1.l Hydraulic Selector Valve

The selector valve is a 3 position 4-way solenoid operated Sterer Co. P/N 40440.

WT = 1.0 LBS
Mass Moments of Inertia are Negligible

F.1.m Initiators

Assume six initiators at .5 lbs. each: WT = 3 LBS
Moments of Inertia are Negligible.

F.1.n Dart Brakes

Wt. of Dart Brake Assembly = 6.0 LBS
Moments of Inertia are Negligible

F.1.o Miscellaneous

Plumbing, control cables, etc. 10 LBS

F.1.p Instrumentation and Display Mirrors

Figure F-18 portrays the characteristics of the instrumentation subassembly.

F.1.q Engine Inlet

The characteristics of the inlet duct are shown in Figure F-19.

F.1.r Drogue

Figure F-20 shows the drogue stabilization parachute and its container as a package for W, B & I estimating purposes.

F.2 SYSTEM SUMMARY

Table F-8 summarizes the characteristics of the total system selected under the subject program.

FIGURE F-16

MAIN RECOVERY PARACHUTE & ITS CONTAINER

CONTAINER IS 1/8" FIBERGLAS & NYLON PACK CLOTH. PARACHUTE IS 28 FT DIA FLAT CIRCULAR WITH SAEC FAIL-SAFE SPREADER GUN

TOTAL WEIGHT = 30 LB (BY SIMILARITY TO NB-11)

$I_x = 30(9.5^2 + 16.5^2)/12 = 905$ LB-IN^2
$I_y = 30(9.5^2 + 5.75^2)/12 = 311$ LB-IN^2
$I_z = 30(5.75^2 + 16.5^2)/12 = 765$ LB-IN^2

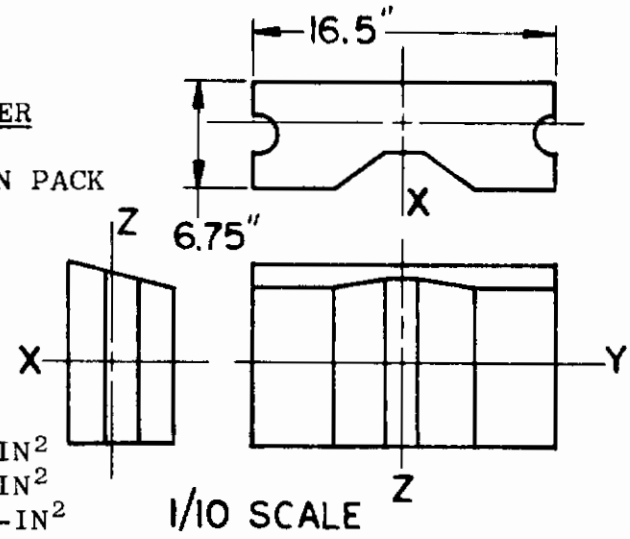

FIGURE F-17

SURVIVAL KIT

WEIGHT = 40 LBS
$I_x = 40(5.9^2 + 16^2)/12 = 970$ LB-IN^2
$I_y = 40(5.9^2 + 14.5^2)/12 = 816$ LB-IN^2
$I_z = 40(14.5^2 + 16^2)/12 = 1550$ LB-IN^2

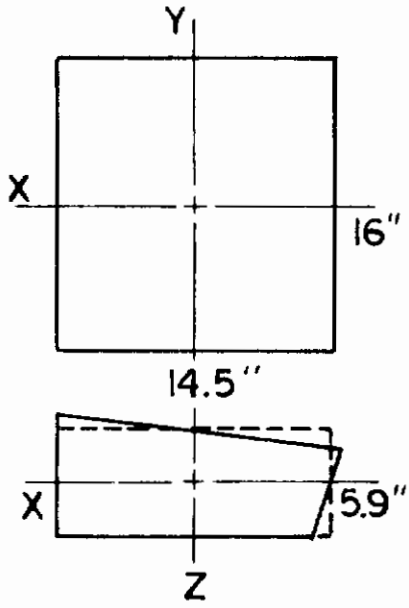

FIGURE F-18

INSTRUMENTATION & DISPLAY MIRRORS

TOTAL INSTRUMENT WT = 18.45 LBS OR 9.2 LBS/SIDE (REF: MSR 419-5)
INSTRUMENT BOX WT = (.1)(.030)(2) 10 x 7 + 7 x 3.5 + 3.5 x 10 = .78 LBS

DISPLAY MIRROR & SUPPORT STRUCTURE = .8 LBS
GROUP WT = 10.8 LBS/SIDE
$I_x = 10.8(7^2 + 3.5^2)/12 = 55$ LB-IN^2
$I_y = 10.8(10^2 + 7^2)/12 = 134$ LB-IN^2
$I_z = 10.8(10^2 + 3.5^2)/12 = 101$ LB-IN^2

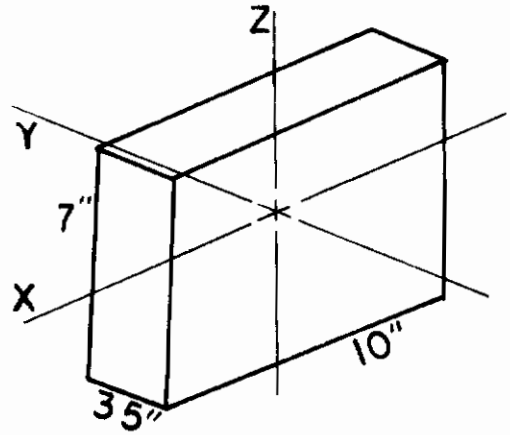

FIGURE F-19

ENGINE INLET DUCT

MAT'L: .040 THICK ALUMINUM
MAT'L VOL = (7) + 18 (15.4)(.04) = 24.6 IN^3
WEIGHT = 2.46 LBS
$I_x = 2.46(16^2 + 15.4^2)/6 = 202$ LB-IN^2
$I_y = 2.46(15.8^2 + 7^2)/6 = 117$ LB-IN^2
$I_z = 2.46(7^2 + 16^2)/6 = 125$ LB-IN^2

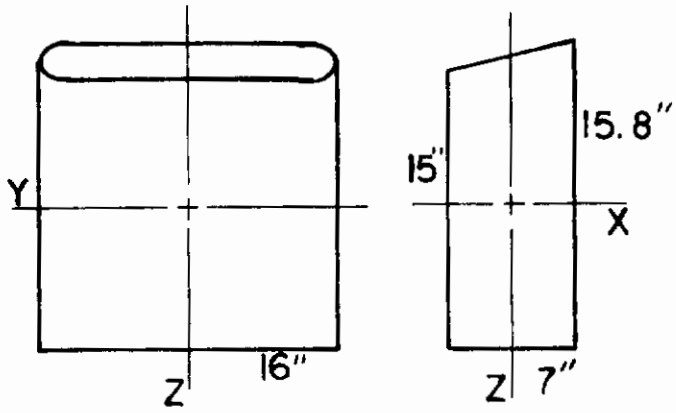

FIGURE F-20

DROGUE PARACHUTE & ITS CONTAINER

DROGUE IS A 5.0 FT DIA GUIDE SURFACE PARACHUTE OF MODERATELY HEAVY CONSTRUCTION. CONTAINER IS NYLON PACK CLOTH
DROGUE WT = 9.0 LBS (REF: PARACHUTE HANDBOOK)
PACK WT = 1.0 LBS
TOTAL WT = 10 LBS
$I_x = 10(3.5^2 + 16^2)/12 = 223$ LB-IN^2
$I_y = 10(3.5^2 + 8^2)/12 = 63$ LB-IN^2
$I_z = 10(8^2 + 16^2)/12 = 267$ LB-IN^2

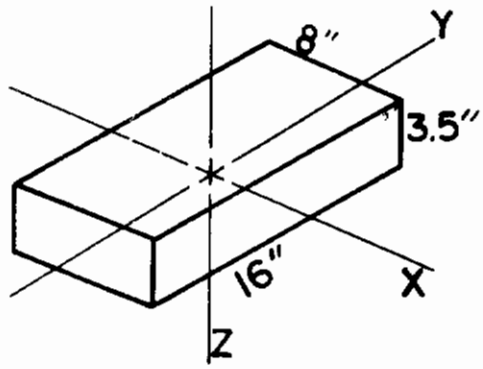

TABLE F-6

STOWED PARAWING SUMMARY

ELEMENT	WEIGHT	X	Y	Z	WX	WZ	WXZ	I_{x_o}	I_{y_o}	I_{z_o}	WX^2	WY^2	WZ^2
L.H. LEADING EDGE	4.00	0	-3.0	25.5	0	102.0	0	678.0	67.8	0	0	36.0	2600
R.H. LEADING EDGE	4.00	0	3.0	25.5	0	102.0	0	678.0	67.8	0	0	36.0	2600
L.H. SPREADER BAR	1.54	0	-2.0	23.0	0	35.4	0	112.0	112.0	0	0	6.1	815
R.H. SPREADER BAR	1.54	0	2.0	23.0	0	35.4	0	112.0	112.0	0	0	6.1	815
L.H. FWD SUPPORT	2.03	1.6	-2.0	31.3	3.25	63.6	101.5	245.0	245.0	0	5.2	8.1	1985
R.H. FWD SUPPORT	2.03	1.6	2.0	31.3	3.25	63.6	101.5	245.0	245.0	0	5.2	8.1	1985
AFT SUPPORT	2.08	1.6	0	29.3	3.33	61.0	98.5	306.0	0	0	5.3	0	1785
KEEL	4.00	0	0	25.5	0	102.0	0	678.0	678.0	0	0	0	2600
APEX PLATE	1.23	0	0	3.4	0	4.2	0	---	---	---	0	0	14
FWD CROSS BAR	1.54	3.0	0	12.6	4.62	19.4	58.2	54.0	0	54.0	13.9	0	245
LOWER CROSS BAR	.83	1.6	0	49.7	1.32	41.2	54.4	16.0	0	16.0	2.1	0	2050
L.H. FWD STUB	.61	10.7	-8.6	13.3	6.54	8.1	87.0	0	7.6	7.6	70.0	45.1	108
R.H. FWD STUB	.61	10.7	8.6	13.3	6.54	8.1	87.0	0	7.6	7.6	70.0	45.1	108
L.H. LWR STUB	.44	4.1	-7.0	52.0	1.80	22.9	93.5	0	2.0	2.0	7.4	21.6	1190
R.H. LWR STUB	.44	4.1	7.0	52.0	1.80	22.9	93.5	0	2.0	2.0	7.4	21.6	1190
FABRIC	2.00	0	0	33.5	0	67.0	0	0	0	0	0	0	2250
TOTALS	28.92				32.45	758.8	775.1	3124.0	1852.8	89.2	186.5	233.9	22340

$\bar{X} = \Sigma WX / \Sigma W = 32.45/28.92 = 1.12$ IN

$I_{x_o} = \Sigma I_{x_o} + \Sigma WY^2 + \Sigma WZ^2 = 3124 + 234 + 22340 = 25{,}698$

$I_{y_b} = I_{y_o} + WX^2 + WZ^2 = 1853 + 187 + 22340 = 24{,}380$

$I_{z_o} = \Sigma I_{z_o} + \Sigma WX^2 + \Sigma WY^2 = 89 + 187 + 234 = 510$

$I_{x_b z_b} = \Sigma WXZ = 775$

$\bar{Z} = \Sigma WZ / \Sigma W = 758.8/28.92 = 26.2$ IN

$I_{x_c} = 25{,}698 - 28.9(26.2)^2 = 5848$ LB-IN^2

$I_{y_c} = 24{,}380 - 28.9(1.12^2 + 26.2^2) = 4530$ LB-IN^2

$I_{z_c} = 510 - 28.9(1.12)^2 = 474$ LB-IN^2

$I_{xz_c} = 775 - 28.9(1.12)(26.2) = -71$ LB-IN^2

TABLE F-7

PARAWING IN DEPLOYED POSITION

ELEMENT	WT	X_b	Y_b	Z_b	WX	WZ	WX^2	WY^2	WZ^2	WXZ	I_{x_o}	I_{y_o}	I_{z_o}
L.H. LEADING EDGE	4.00	0	-23.2	33.5	0	134.0	0	2150.0	4480.0	0	1410.0	1410.0	675.0
R.H. LEADING EDGE	4.00	0	23.2	33.5	0	134.0	0	2150.0	4480.0	0	1410.0	1410.0	675.0
L.H. SPREADER BAR	1.54	0	-10.6	36.2	0	55.7	0	173.0	2010.0	0	12.0	12.0	51.3
R.H. SPREADER BAR	1.54	0	10.6	36.2	0	55.7	0	173.0	2010.0	0	12.0	12.0	54.3
L.H. FWD SUPPORT	2.03	16.3	- 1.6	36.3	33.1	73.6	540.0	5.2	2670.0	1200.0	91.0	152.0	152.0
R.H. FWD SUPPORT	2.03	16.3	1.6	36.3	33.1	73.6	540.0	5.2	2670.0	1200.0	91.0	152.0	152.0
AFT SUPPORT	2.08	14.5	0	53.8	30.1	112.0	436.0	0	6040.0	1620.0	126.5	126.0	126.0
KEEL	1.00	0	0	40.7	0	163.0	0	0	6640.0	0	2210.0	2210.0	0
APEX PLATE	1.23	0	0	3.1	0	3.8	0	0	11.4	0	0	0	0
FWD CROSS BAR	1.54	31.7	0	25.3	48.8	39.0	1545.0	0	987.0	1235.0	51.0	0	51.0
AFT CROSS BAR	.83	27.5	0	66.4	22.8	55.1	627.0	0	3660.0	1515.0	17.7	0	17.0
L.H. FWD STUB	.61	39.0	- 9.5	30.4	23.8	18.5	929.0	55.0	562.0	724.0	0	61.4	61.4
R.H. FWD STUB	.61	39.0	9.5	30.4	23.8	18.5	929.0	55.0	562.0	724.0	0	61.4	61.4
L.H. AFT STUB	.44	31.6	- 7.0	69.5	13.9	30.5	440.0	21.5	2120.0	966.0	2.5	1.8	2.5
R.H. AFT STUB	.44	31.6	7.0	69.5	13.9	30.5	440.0	21.5	2120.0	966.0	2.5	1.8	2.5
FABRIC	2.00	0	0	54.5	0	109.0	0	0	5950.0	0	0	0	0
TOTALS	28.92				243.3	1106.5	6426.0	4809.4	46972.4	10150.0	5436.2	5610.4	2078.4

$\bar{X} = \Sigma WX/\Sigma W = 243.3/28.92 = 8.42$ IN

$\bar{Z} = \Sigma WZ/\Sigma W = 1106.5/28.92 = 38.25$ IN

$I_{x_b} = \Sigma I_{x_o} + \Sigma WY^2 + \Sigma WZ^2 = 5,436 + 4,809 + 46,972 = 57,217$

$I_{y_b} = \Sigma I_{y_o} + \Sigma WX^2 + \Sigma WZ^2 = 5,610 + 6,426 + 46,972 = 59,008$

$I_{z_c} = \Sigma I_{z_o} + \Sigma WX^2 + \Sigma WY^2 = 2078 + 6426 + 4809 = 13,313$

$I_{xz} = 10,150$

$I_{x_c} = 57,217 - 28.92(38.25)^2 = 14,917$ LB-IN^2

$I_{y_c} = 59,008 - 28.92(38.25^2 + 8.42^2) = 14,808$ LB-IN^2

$I_{z_c} = 13,313 - 28.92(8.42)^2 = 11,263$ LB-IN^2

$I_{x_c z_c} = 10,150 - 28.92(8.42)(38.25) = +830$ LB-IN^2

TABLE F-8

SYSTEM IN FLYING CONFIGURATION

	COMPONENT	WEIGHT	X	Y	Z	WX	WZ	WX^2	WY^2	WZ^2	WXZ	I_{x_o}	I_{y_o}	I_{z_o}	$I_{x_oz_o}$
1	SEAT SHELL	30.70	-1.84	0	9.80	- 53.3	301.0	104	0	2,950	- 554	6,705	7,247	3,912	-1,662
2	PARAWING	28.92	31.50	0	18.00	910.0	520.0	28,700	0	9,360	16,400	14,917	14,808	11,263	830
3	L.H. ROCKET	5.39	2.50	- 7.00	8.00	13.5	43.1	33	264.0	344	- 320	430	430	0	0
3	R.H. ROCKET	5.39	2.50	7.00	8.00	13.5	43.1	33	264.0	344	320	430	430	0	0
4	INERTIA REEL	3.60	2.20	0	27.20	7.9	98.0	16	0	2,660	215	17	10	9	0
5	ENGINE	54.00	6.80	0	15.00	368.0	810.0	2,500	0	12,150	5,510	6,530	3,500	1,990	0
6	HYD. PUMP	2.30	2.20	0	17.80	5.1	41.0	11	0	728	90	10	1	10	0
7	L.H. FUEL	40.00	6.60	-12.00	18.60	264.0	743.0	2,590	5,750.0	13,830	4,910	1,945	2,240	605	0
7	L.H. TANK	4.40	6.60	-12.00	18.60	26.4	74.3	259	575.0	1,383	491	--	--	--	--
7	R.H. FUEL	40.00	6.60	12.00	18.60	264.0	743.0	2,590	5,750.0	13,830	4,910	1,945	2,240	605	0
7	R.H. TANK	4.40	6.60	12.00	18.60	26.4	74.3	259	575.0	1,383	491	--	--	--	--
8	L.H. CATAPULT	1.80	2.20	- 7.50	16.00	4.0	28.8	9	101.0	461	216	376	376	0	0
8	R.H. CATAPULT	1.80	2.20	7.50	16.00	4.0	28.8	9	101.0	461	216	376	376	0	0
9	MAIN 'CHUTE	30.00	2.60	0	36.10	78.0	1080.0	202	0	39,000	2,810	905	311	765	0
10	SURVIVAL KIT	40.00	-6.10	0	-4.60	-244.0	-184.0	1,490	0	847	1,120	970	816	1,550	0
11	ENGINE INLET	2.46	8.20	0	34.30	20.2	84.4	165	0	2,900	694	202	117	125	0
12	TURN MECH.	2.30	2220	0	23.80	5.1	54.7	12	0	1,300	122	10	1	10	0
13	SEL. VALVE	1.00	2.20	0	16.00	2.2	16.0	5	0	256	35	--	--	--	--
14	L.H. INSTR.	10.80	4.80	-10.00	36.00	51.9	389.0	249	1,080.0	14,000	1,870	55	134	101	0
14	R.H. INSTR.	10.80	4.80	10.00	36.00	51.9	389.0	249	1,080.0	14,000	1,870	55	134	101	0
15	INITIATORS	3.00	2.20	0	-3.20	6.6	- 9.6	15	0	31	- 21	--	--	--	--
16	DART BRAKES	6.00	-4.20	0	-9.10	- 25.2	- 54.6	106	0	496	229	--	--	--	--
17	MISCELL.	10.00	--	--	--	--	--		--	--	--	--	--	--	--
18	50% TILE	172.00	-7.90	0	9.50	-1360.0	1632.0	10,750	0	15,500	-12.900	23,600	25,700	12,900	
	TOTALS	511.06				440.2	6945.3	50,356	15,540.0	148,214	28,724	59,378	58,871	33,937	-832

$\bar{X} = \Sigma WX/\Sigma W = 440.2/511.06 = .86$ IN

$I_{x_b} = \Sigma I_{x_o} + \Sigma WY^2 + \Sigma WZ^2 = 223,132$ LBS-IN^2

$I_{y_b} = \Sigma I_{y_o} + \Sigma WX^2 + \Sigma WZ^2 = 257,441$ LBS-IN^2

$I_{z_o} = \Sigma I_{z_o} + \Sigma WX^2 + \Sigma WY^2 = 99,833$ LBS-IN^2

$I_{x_oz_b} = \Sigma I_{x_oz_o} + \Sigma WXZ = 27,892$ LBS-IN^2

$\bar{Z} = \Sigma WZ/\Sigma W = 6945/511.06 = 13.6$ IN

$I_{x_c} = I_{x_b} - W(Y^2 + Z^2) = 128,632$ LBS-IN^2

$I_{y_c} = I_{y_b} - W(X^2 + Z^2) = 162,941$ LBS-IN^2

$I_{z_c} = I_{z_b} - W(X^2 + Y^2) = 99,455$ LBS-IN^2

$I_{x_cz_c} = I_{x_oz_o} - W(X)(Z) = 22,302$ LBS-IN^2

NOTE: THESE CALCULATIONS WERE MADE WITH THE FOLLOWING ASSUMPTIONS:

50% TILE OCCUPANT WITH 10 LBS OF FLIGHT GEAR & CLOTHING
SEAT IN NEUTRAL POSITION
FULL FUEL
PARAWING DEPLOYED

LIST OF REFERENCES

1. Brinkley, J. W. — "Development of Aerospace Escape Systems", Air University Review, July-August 1968, Department of the Air Force, Vol. XIX, No. 5.

2. AFSCM 80-1 — Handbook of Instructions for Aircraft Design (HIAD); Hq., Air Force Systems Command, Andrews Air Force Base, Washington, D. C.; 1 July 1967.

3. AFSCM 80-3 — Handbook of Instructions for Aerospace Personnel Subsystems Design (HIAPSD); Hq., Air Force Systems Command, Andrews Air Force Base, Washington, D. C.; 15 April 1967.

4. MIL-S-9479A (USAF) — Seat System: Upward Ejection, Aircraft, General Specification for; 16 June 1967.

5. Manzuk, R. J. and Peck, W. R. — Building Blocks to Commonality; prepared for delivery at the USAF - Industry Life Support Systems Conference; November 1967 (not delivered); Stencel Aero Engineering Corporation, Asheville, North Carolina.

6. Duncan, J. W. — Pyrotechnic Initiators; U. S. Patent No. 3,356,025; 5 December 1967; assigned to Stencel Aero Engineering Corporation.

7. Stencel, F. B. and Duncan, J. W. — Adjustable Ejection Seat with Canopy Breakers; U. S. Patent Application No. 708,702; 27 February 1968; assigned to Stencel Aero Engineering Corporation.

8. Moy, H. R. — Advanced Stabilized Ejection Seat Development Program; SEG-TR-67-51; January 1968; Douglas Aircraft Company, McDonnell Douglas Corporation.

9. Chernowitz, G. and DeWeese, J. H. — USAF Parachute Handbook; ASD-TR-61-579. June 1963.

10. Stencel, F. B. — Parachute Deployment Device; U. S. Patent Application No. 744,134; 11 July 1968; assigned to Stencel Aero Engineering Corporation.

11. Stencel, F. B., et al — Fail-Safe Parachute Apparatus; U. S. Patent No. 3,281,098; 25 October 1966; assigned to Stencel Aero Engineering Corporation.

12. Bull, J. O.; Serochki, E. L.; McDowall, H. L., et al — Compilation of Data on Crew Emergency Escape Systems; AFFDL-TR-66-150; September 1966; The Boeing Company, Renton, Washington.

13. Eshbach, O. W. — Handbook of Engineering Fundamentals; Wiley and Sons, Inc.; March 1958.

14. Barte, G. R. — Flexible Wings for Maneuvering and Landing Application in the De-Coupled Concept; AIAA 5th Aerospace Sciences Meeting; New York, N. Y.; January 1967.

15. Sleeman, W. C.; Croom, D. R.; and Rogallo, F. M. — Resume of Research on Parawings; NASA Working Paper No. 164; University of Minnesota Aero Deceleration Course; July 1965.

16. Polhamus, E. C. and Naeseth, R. L. — Experimental and Theoretical Studies of the Effects of Camber and Twist on the Aerodynamic Characteristics of Parawings Having Nominal Aspect Ratios of 3 and 6; NASA TN-D-972, 1963.

17. Bugg, F. M. — Effects of Aspect Ratio and Canopy Shape on Low-Speed Aerodynamics of 50° Swept Parawings; NASA TN-D-2922, 1965.

18. Heilicer, B. J. — Non-linear Dispensing System; ATL TR-65-21; March 1965; Fairchild-Republic Corporation.

19. Final Report A Study to Select Optimum Altitude Sensing Devices; Sylvania Report No. A58-4-5.0-17; two volumes; May 1963; prepared under contract NAS 9-1098, Sylvania Electronic Laboratories; Williamsville, New York.

20. Naeseth, R. L. and Gainer, T. G. — Low-Speed Investigation of the Effects of Wing Sweep on the Aerodynamic Characteristics of Parawings Having Equal-Length Leading Edges and Keel; NASA TN-D-1957; 1963.

21. Etkin, B. — Dynamics of Flight-Stability and Control; John Wiley & Sons, Inc.; 1959.

22. Perkins, C. D. and Hage, R. E. — Airplane Performance, Stability and Control; Wiley & Sons, Inc.; printed June 1960.

23. Hoerner, S. F. — Fluid-Dynamic Drag; published by the author; 1965.

24. DH-1-6; AFSC Design Handbook-System Safety; Hq. Air Force Systems Command; First Edition; 25 July 1967; developed by Martin-Marietta Corp., Denver Division.

25. A-7 Crewstation Drawings; Vought Aeronautics Division, LTV Aerospace Corp., Dallas, Texas.

Dwg. No.	
216-21135	Sheets 1 and 2
216-00602	Sheets 2 and 3

26. F-4 Crewstation Drawings; McDonnell Aircraft Corporation St. Louis, Mo.

Dwg. No.	Title
32-82026, Rev. H	Seat Installation Pilots Ground Level Ejection
53-80003, Rev. C	Furnishings Instl-Aft Cockpit
53-61050, Rev. D	Controls Installation-Forward Fuselage, Primary

Dwg. No.	Title
53-80043, Rev. E	Seat Assy-Ground Level Ejection, P.S.O.
53-80044, Rev. E	Seat Assy-Ground Level Ejection, Pilot's
53-80002, Rev. A	Furnishings Instl.-Forward Cockpit
32-31145, Rev. G	Seat Rail Assy-Forward Cockpit

27. Bioastronautics Data Book; NASA SP-3006; August 1964; Webb Associates, Yellow Springs, Ohio.

28. A Descriptive Model for Determining Optimal Human Performance in Systems; NASA CR-878, Volume III; "An Approach for Determining the Optimal Role of Man and Allocation of Functions in an Aerospace System"; March 1968; Serendipity Associates, Chatsworth, California.

29. Seckel, E. Stability and Control of Airplanes and Helicopters; (Academic Press, New York, 1964).

30. Ribner, H. S. The Stability Derivatives of Low-Aspect-Ratio Triangular Wings at Subsonic and Supersonic Speeds; NACA-TN-1423, September 1947.

31. Johnson, J. L., Jr. and Hassell, J. L , Jr. Full-Scale Wind-Tunnel Investigation of a Flexible-Wing Manned Test Vehicle. NASA TN-D-1946, August 1963.

32. Chambers, J. R. and Bjisseau, P. C. A Theoretical Analysis of the Dynamic Lateral Stability and Control of a Parawing Vehicle; NASA TN-D-3461, June 1966.

UNCLASSIFIED
Security Classification

DOCUMENT CONTROL DATA - R & D

(Security classification of title, body of abstract and indexing annotation must be entered when the overall report is classified)

1. ORIGINATING ACTIVITY *(Corporate author)*
Stencel Aero Engineering Corporation
Asheville, North Carolina

2a. REPORT SECURITY CLASSIFICATION
Unclassified

2b. GROUP
N/A

3. REPORT TITLE
Investigation of an Integrated Aircrew Escape/Rescue System Capability . . ."AERCAB"

4. DESCRIPTIVE NOTES *(Type of report and inclusive dates)*
Final Report March 1968 - December 1968

5. AUTHOR(S) *(First name, middle initial, last name)*
Robert J. Manzuk, Charles A Yost, E.A. Braunlich, N.J. Bentzen, Walter R. Peck, James W. Duncan, L.A. Pond, Jr., E. Seckel, J.W. Olcott

6. REPORT DATE
1969

7a. TOTAL NO. OF PAGES
356

7b. NO. OF REFS
32

8a. CONTRACT OR GRANT NO.
F33615-68-C-1461

b. PROJECT NO.
6065

c. Task No.
606509

d.

9a. ORIGINATOR'S REPORT NUMBER(S)
SAEC No. FTR-419-1

9b. OTHER REPORT NO(S) *(Any other numbers that may be assigned this report)*
AFFDL-TR-68-159

10. DISTRIBUTION STATEMENT
This document is subject to special export controls and each transmittal to foreign governments or foreign nationals may be made only with prior approval of the Air Force Flight Dynamics Laboratory (FDF)(See block 12)

11. SUPPLEMENTARY NOTES
N/A

12. SPONSORING MILITARY ACTIVITY
AF Flight Dynamics Laboratory (FDF)
Wright-Patterson AFB, Ohio 45433

13. ABSTRACT
A concept was investigated whereby aircrewmembers are given a capability to aid in their own rescue subsequent to emergency ejection from their mission vehicle. The self-rescue capability was achieved by way of integrating a parawing into the ejection seat escape system to provide an aerodynamic-lift generating surface, and also a twin-turbofan jet engine to provide propulsion for gaining altitude and departing from the emergency site toward a safe area for liaison with allied force. The self-rescue AERCAB mode is capable of flight at 10,000 feet (MSL) over a distance of fifty nautical miles at airspeeds approaching 100 knots. The system is manually controllable in both powered and unpowered flight, and it appears feasible to incorporate an automatic homing flight control system. Under all emergency circumstances, the aircrewman using AERCAB retains the capability to descend to terrain level with his personnel parachute. A detailed preliminary design study was accomplished, and it is shown that the system is retrofitable in the existing crew stations of the A-7 and F-4 aircraft with only minor modifications thereto. The investigative program resulted in the generation of specific operational and design criteria for an integrated aircrew escape/rescue system capability; operational and performance limits thereof were defined; and it was analytically shown that the AERCAB concept is feasible and merits continued study, experimental testing, and development.

DD FORM 1 NOV 65 1473 (The Distribution of this Abstract is Unlimited)

UNCLASSIFIED
Security Classification

14. KEY WORDS	LINK A		LINK B		LINK C	
	ROLE	WT	ROLE	WT	ROLE	WT
Escape Systems						
Ejection Seats						
Life Support						
Rescue Systems						
Rescue Equipment						
Self-Rescue Capability						